CATALYSIS BY METAL COMPLEXES 35

**Series Editors** C. Bianchini · D.J. Cole-Hamilton
P.W.N.M. van Leeuwen
**Volume Editors** G. Giambastiani · J. Cámpora

# Olefin Upgrading Catalysis by Nitrogen-based Metal Complexes I

## State-of-the-art and Perspectives

Springer

Catalysis by Metal Complexes

Volume 35

For further volumes:
http://www.springer.com/series/5763

# Catalysis by Metal Complexes

This book series covers topics of interest to a wide range of academic and industrial chemists, and biochemists. Catalysis by metal complexes plays a prominent role in many processes. Developments in analytical and synthetic techniques and instrumentation, particularly over the last 30 years, have resulted in an increasingly sophisticated understanding of catalytic processes.

Industrial applications include the production of petrochemicals, fine chemicals and pharmaceuticals (particularly through asymmetric catalysis), hydrometallurgy, and waste-treatment processes. Many life processes are based on metallo-enzyme systems that catalyze redox and acid–base reactions.

Catalysis by metal complexes is an exciting, fast developing and challenging interdisciplinary topic which spans and embraces the three areas of catalysis: heterogeneous, homogeneous, and metallo-enzyme.

*Catalysis by Metal Complexes* deals with all aspects of catalysis which involve metal complexes and seeks to publish authoritative, state-of-the-art volumes which serve to document the progress being made in this interdisciplinary area of science.

*Series Editors*

Prof. Claudio Bianchini
Institute of Chemistry of Organometallic Compounds
Polo Scientific Area
Via Madonna del Piano 10
50019 Sesto Fiorentino
Italy

Prof. D. J. Cole-Hamilton
School of Chemistry
University of St Andrews
North Haugh
KY16 9ST St Andrews
UK

Prof. Piet W. N. M. van Leeuwen
Institute of Chemical Research of Catalonia
Av. Paisos Catalans 16
43007 Tarragona
Spain

---

**Volume 35:**
Olefin Upgrading Catalysis by Nitrogen-based Metal Complexes I
State-of-the-Art and Perspectives

*Volume Editors*

Giuliano Giambastiani
ICCOM, Florence Research Area
National Council of Research (CNR)
Via Madonna del Piano 10
50019 Florence
Italy

Juan Cámpora
Instituto de Investigaciones Químicas
CSIC - Universidad de Sevilla
C/ Americo Vespucio, 49
41092 Sevilla
Spain

Giuliano Giambastiani · Juan Cámpora
Editors

# Olefin Upgrading Catalysis by Nitrogen-based Metal Complexes I

## State-of-the-art and Perspectives

Springer

*Editors*
Giuliano Giambastiani
ICCOM, Florence Research Area
National Council of Research (CNR)
Via Madonna del Piano 10
50019 Florence
Italy
e-mail: giuliano.giambastiani@iccom.cnr.it

Juan Cámpora
Instituto de Investigaciones Químicas
CSIC - Universidad de Sevilla
C/ Americo Vespucio, 49
41092 Sevilla
Spain
e-mail: campora@iiq.csic.es

ISSN 0920-4652

ISBN 978-90-481-3814-2 e-ISBN 978-90-481-3815-9

DOI 10.1007/978-90-481-3815-9

Springer Dordrecht Heidelberg London New York



*Cover design:* eStudio Calamar, Berlin/Figueres

Printed on acid-free paper

Springer is part of Springer Science+Business Media (www.springer.com)

# Foreword

Olefin polymerization has remarkably progressed over the last two decades, mainly thanks to the contribution of organometallic chemistry to the design of innovative ligand systems and metal complexes. The irreversible decrease of fossil-resources requires continuous efforts to improve the selectivity and productivity of the industrial processes as well as to reduce the environmental impact, especially in terms of energy and waste. Due to the wealth of possible ligand structures and metal combinations, organometallic-based catalysis can indeed address many of the issues of the sustainable production of polymeric and composite materials.

These two volumes edited by Giambastiani and Cámpora cover a hot research subject such as that of post-metallocene nitrogen-containing complexes and their use in homogeneous catalysis for the efficient and selective olefin upgrading. These books cover the state-of-the-art of olefin polymerization by catalysts with **N**-donor ligands as well as hybrid ligands in conjunction with a wide range of metals across the periodic table. Particular attention has been devoted to important, still unresolved issues such as the efficient insertion polymerization of polar monomers. Advantages and limits of the known technologies have been discussed and critically addressed in the light of the most relevant contributions of the many thousand researchers active in the field.

Claudio Bianchini
Director ICCOM-CNR

# Preface

Millions of tons of polyolefin-based materials are produced yearly, in most cases under relatively mild conditions mediated by transition-metal catalysts. Through a simple insertion reaction, inexpensive and abundant olefins (such as ethylene and propene) are transformed into polymeric materials for a wide range of applications, including plastics, fibers, and elastomers. The discovery of the Ziegler–Natta catalysts and the seminal works at Phillips Petroleum in the 1950s not only revoluzionized polyolefin production, but also paved the way to the development of modern organometallic chemistry. Despite its long history, the polyolefin industry keeps growing steadily and remains technologically driven by the continuous discovery of new catalysts, processes, and applications.

Since Ziegler–Natta's time, important milestones in the field of homogeneous oligomerization/polymerization catalysis were set-up one after the other; from nickel complexes with phosphine donors (SHOP-type catalysts) for the highly selective and efficient production of α-olefins to Group IV metallocene polymerization catalysts and their subsequent industrial exploitation (in the early 1980s) due to the discovery of partially hydrolyzed organoaluminum compounds (MAOs) as co-catalysts/activators. All these scientific successes have shown how discrete "single-site" molecular catalysts could offer unmatched opportunities, compared with heterogeneous systems, towards the tailored synthesis of new polymeric architectures as well as the in-depth understanding of complex reaction mechanisms.

Until a few years ago there have been relatively few reports on late transition metal complexes capable of catalyzing the polymerization of ethylene and α-olefins efficiently. A distinct feature of the latter systems is a high rate of chain transfer which favors their application as oligomerization catalysts. The discovery of new ligands and activators has been fundamental to fill the gap and make late transition metal catalysts as efficient (and in some cases even more versatile) as metallocene-based systems for the oligomerization and polymerization catalysis.

In 1995, Brookhart and co-workers synthesized a new class of $Ni^{II}$and $Pd^{II}$ complexes stabilized by bulky α-diimine ligands (Schiff bases) which represented

a real breakthrough into the development of late transition metal catalysts for the efficient olefin polymerization/oligomerization.

Since then, an almost infinite variety of imine-based ligands or, more generally, nitrogen-containing ligands in combination with either *d*- and *f*- block metals have been explored as efficient and selective oligomerization and polymerization catalysts. The major advantages of this ligand class are represented by the facile control of their stereoelectronic properties, their simple preparation from available and cheap building blocks and their easy handling and storage. All these considerations, together with the capability of most of their metal derivatives to impart high activity and selectivity in olefin upgrading processes, have contributed to make nitrogen-containing catalysts highly desirable for industry and academy.

The aim of these books is to provide an overview on the state-of-the-art and the perspectives in the field of oligomerization/polymerization catalysis mediated by metal complexes (spanning from early to late and lanthanide series) stabilized by ligands containing nitrogen donor groups. Rather than a systematic revision of the major break throughs achieved over the last decades, these two volumes offer to the readership the critical point of view of researchers active in specific fields of polymerization catalysis. The amplitude and rigor of each contribution also provide an exhaustive account on the topic: from the synthesis of ligands and related complexes to mechanistic details, the investigation of the catalyst performance and future perspectives. Although the chapters' extension has made the book division into two separate volumes necessary, this partition is merely due to editorial reasons.

Finally, the editors are extremely grateful to all book co-authors for their enthusiasm in participating to this editorial project and for writing up their contribution at their best. A special thank is also due to Sonia Ojo, Claudia Culierat and Ilaria Tassistro from the London Springer office, whose precious assistance in facing technical and logistic details has been essential for the success of the Editors' efforts.

Giuliano Giambastiani
Juan Cámpora

# Contents

# List of Contributors

**Laura Boggioni**
Istituto per lo Studio delle Macromolecole (ISMAC), Consiglio Nazionale delle Ricerche (CNR), Via E. Bassini 15, 20133 Milano, Italy.

**Giuliano Giambastiani**
Institute of Chemistry of OrganoMetallic Compounds–ICCOM-CNR, Via Madonna del Piano, 10-Sesto Fiorentino, 50019 Florence, Italy.

**Phillip D. Hustad**
The Dow Chemical Company, 2301 N. Brazosport Blvd.-B-1603, Freeport, TX, 77541, USA.

**Roger L. Kuhlman**
The Dow Chemical Company, 2301 N. Brazosport Blvd.-B-1603, Freeport, TX, 77541, USA.

**Lapo Luconi**
Institute of Chemistry of OrganoMetallic Compounds–ICCOM-CNR, Via Madonna del Piano, 10-Sesto Fiorentino, 50019, Florence, Italy.

**David S. McGuinness**
School of Chemistry, University of Tasmania, Private Bag 75, Hobart 7000, Australia.

**Andrea Ravasio**
Istituto per lo Studio delle Macromolecole (ISMAC), Consiglio Nazionale delle Ricerche (CNR), Via E. Bassini 15, 20133 Milano, Italy.

**Carl Redshaw**
School of Chemistry, University of East Anglia, Norwich, NR4 7TJ, UK.

**Alexander A. Trifonov**
G.A. Razuvaev Institute of Organometallic Chemistry of Russian Academy of Sciences, Tropinina 49, GSP-445, 603950 Nizhny Novgorod, Russia.

**Incoronata Tritto**
Istituto per lo Studio delle Macromolecole (ISMAC), Consiglio Nazionale delle Ricerche (CNR), Via E. Bassini 15, 20133 Milano, Italy.

# Chapter 1
# Cr Complexes of Nitrogen Donor Ligands for Olefin Oligomerisation and Polymerisation

**David S. McGuinness**

**Abstract** Chromium complexes continue to play an important role as catalysts for olefin oligomerisation and polymerisation, with many of these catalysts supported by N-donor containing ligation. A number of highly active catalysts for ethylene polymerisation have been developed in recent years, as well as new catalysts for highly selective ethylene oligomerisation. New developments in this area since 2003, in which chromium complexes of N-donor ligands are utilized, are discussed in subsequent sections.

## 1.1 Introduction

The oligomerisation and polymerisation of olefins to higher oligomers and polymer continues to receive a high level of research interest, both within industry and academia [1, 2]. The most important industrial products resulting from these processes are ethylene oligomers (linear α-olefins) and polyethylene plastics, so it is of no surprise that the vast majority of studies detailed below make use of ethylene as the monomer. Chromium catalysts occupy an important position in this field. The heterogeneous Phillips catalyst ($Cr/SiO_2$) is used to produce a large proportion of global polyethylene supplies [3], while homogenous chromium catalysts have been utilized for selective production of 1-hexene and 1-octene from ethylene [4]. As such, there has been much interest in the development of new chromium based catalysts for oligomerisation and polymerisation, with many of these new systems supported by N-donor ligation. As can be seen below, the most common linkage is an imine donor, although examples of amine and amido donors are also detailed.

D. S. McGuinness (✉)
School of Chemistry, University of Tasmania, Private Bag 75, Hobart 7000, Australia
e-mail: David.mcguinness@utas.edu.au

G. Giambastiani and J. Cámpora (eds.), *Olefin Upgrading Catalysis by Nitrogen-based Metal Complexes I*, Catalysis by Metal Complexes, 35
DOI: 10.1007/978-90-481-3815-9_1, 

Non-metallocene polymerisation catalysts, including chromium systems, were reviewed in 2003 [1], while selective oligomerisation with chromium catalysts was reviewed in 2004 [4]. As such, the coverage herein focuses on developments which occurred after this period. Nonetheless, some reference to the older literature is made where required to provide a background to new work. The vast majority of systems described below are precatalysts which require activation with a cocatalyst; this is almost always MAO or another alkylaluminium reagent [5]. Wherever possible, activities for ethylene polymerisation have been calculated in terms of kg(product) mol(cat)$^{-1}$ bar(ethylene)$^{-1}$ h$^{-1}$ (kg mol$^{-1}$ bar$^{-1}$ h$^{-1}$). In keeping with previous reviews [1, 6], the following descriptors of activity have been used, bearing in mind the limitations of comparing different systems under different conditions and differing degrees of optimisation: very high (>1,000); high (1,000–100); moderate (100–10); low (10–1); very low (<1).

The catalysts have been grouped into two major divisions. Systems which produce a mathematical distribution of oligomer or polymer molecular weights (unselective catalysts) are detailed in Sects. 1.2–1.6. In most of these cases a Cossee mechanism is assumed (linear chain growth via migratory insertion), although this is rarely investigated and caution is warranted where the mechanism has not been studied. Recently the metallacycle mechanism of oligomerisation has been exploited for its selectivity benefits, and such systems are discussed in Sect. 1.7.

## 1.2 Cr Complexes of Cyclopentadienyl Ligands Containing Pendant N-donors

Much of the interest in chromium based polymerisation catalysts has revolved around constrained geometry systems, in which the Cp-based unit is bridged to an additional nitrogen donor group. The interest in these catalysts can be traced back to the work of Jolly, who demonstrated that complexes such as **1** and **2** give rise to highly active catalysts [7], and Enders, who introduced complexes such as **3** and **4** in combination with MAO [8–10]. Most of this work predates 2003 and had been covered in past reviews [1], so will not be discussed further here.

Various modifications of this theme have been investigated in the years since. Huang et al. prepared and tested complexes of general structure **5** and **6** for ethylene polymerisation in combination with MAO [11]. The effect of different bridge substitution and steric bulk on the Cp group was explored. Complex **5** with RCp = indenyl was the most active, and activities up to 2,000 kg mol Cr$^{-1}$ bar$^{-1}$ h$^{-1}$ were reported. Complexes of structure **6** displayed a much lower activity (ca. 200 kg mol Cr$^{-1}$ bar$^{-1}$ h$^{-1}$). Ethylene/1-hexene copolymerization was also studied, and some incorporation of the 1-hexene into the polymer was noted. Other researchers [12] subsequently also studied ethylene polymerization with complexes of structure **5**, with similar results to those of the original report. A structurally similar complex was disclosed in a patent from the Sumitomo Chemical Company, structure **7** [13]. Activation with MAO or $AlR_3$/fluorinated boranes led to ethylene polymerisation with very high activities up to 22, 000 kg mol Cr$^{-1}$ bar$^{-1}$ h$^{-1}$.

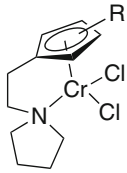


**1**

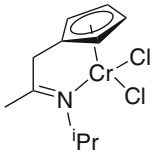


**2**

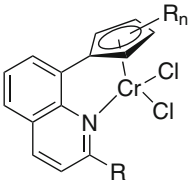


**3**

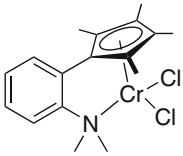


**4**

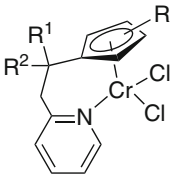


**5**

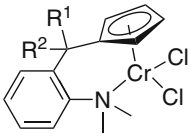


**6**

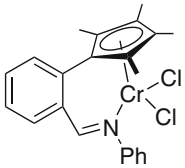


**7**

A broad range of related complexes, in which different pendant imine donors are bridged to cyclopentadienyl or indenyl groups, have been reported in a series of patents from Basell Polyolefine. In these patents structures **8** [14], **9** [15], **10** [16], **11** [17] and **12** [18] were evaluated for ethylene homopolymerisation and ethylene/1-hexene copolymerisation after MAO activation. The activities of these complexes range up to around 2,600 kg mol $Cr^{-1}$ $bar^{-1}$ $h^{-1}$ for complex **11**. Recently Derlin and Kaminsky evaluated a range of these catalysts for propylene polymerisation [19]. Interestingly, chain walking was observed to occur, which effectively results in 3,1 incorporation of propylene. This 'chain straightening' process, which removes methyl branching from a proportion of the polymer, give rise to a polyethylene like structure to much of the polymer. As such, the polymer produced had a structure more like ethylene/propylene copolymer. The most recent new Cp-imine system reported seems to be **13**, as prepared by Enders et al. [20]. The activity of this system for ethylene polymerisation (330 kg mol $Cr^{-1}$ $bar^{-1}$ $h^{-1}$) appears much lower than the original quinolyl functionalized complex **3**; however.

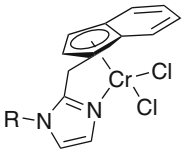


**8**

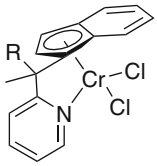


**9**

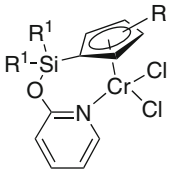


**10**

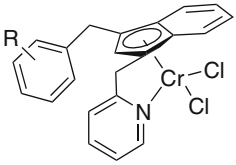


**11**

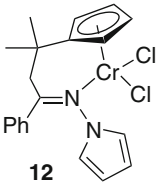


**12**

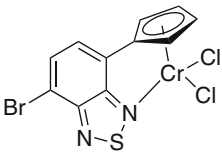


**13**

Following on from the development of group 4 cyclopentadienyl-amido constrained geometry catalysts, in 1996 Theopold et al. evaluated Cr analogues such as **14** for ethylene polymerisation [21]. The activities achieved with these complexes were very low; however. Tamm et al. have recently prepared a number of chromium complexes with amido-like donor coordination, structures **15** and **16** [22]. These complexes are regarded as closer analogues to group 4 Cp-amido catalysts. Complex **15**, after activation with MAO, leads to low molecular weight, polydisperse polyethylene with moderate activity (<50 kg mol $Cr^{-1}$ $bar^{-1}$ $h^{-1}$). Catalyst decomposition is suggested to occur, leading to more than one active site. The indenyl complex **16** is more active (730 kg mol $Cr^{-1}$ $bar^{-1}$ $h^{-1}$), but also suffers from catalyst deactivation.

It has been shown that a nitrogen donor bridged to cyclopentadiene leads to more active catalysts than is the case when an unbridged donor is present [23], hence the investigations detailed above. Nonetheless a number of cyclopentadienyl chromium complexes with an unbridged nitrogen donor have been studied with interesting results. Gabbaï showed that complex **17**, in the presence of $AlEt_3$, leads to a Poisson distribution of ethylene oligomers centered on aluminium [24]. The process probably involves an equilibrium of chain growth at chromium followed by rapid chain transfer with $AlEt_3$ (catalysed Aufbau reaction, Fig. 1.1). Complex **18**, with a chelated phenoxy-imine ligand, is also activated with $AlR_3$ but gives rise to linear polyethylene [25]. The attraction of this catalyst is the low levels of $AlR_3$ required for activation (as opposed to more expensive MAO); an activity of 810 kg mol $Cr^{-1}$ $bar^{-1}$ $h^{-1}$ was achieved with only 25 equivalents of $AlMe_3$. The activity is around half this with the more attractive activator $AlEt_3$, however. Complex **19** has also been reported to polymerise ethylene after treatment with $AlEt_3$, with activities up to 168 kg mol $Cr^{-1}$ $bar^{-1}$ $h^{-1}$ with 25 equivalents of $AlEt_3$ [26]. Closely related complexes **20** and **21** were reported by the same authors [27]. Both are inactive in the presence of MAO but lead to high molecular weight polyethylene with 25 equivalents of $AlEt_3$ (up to 153 kg mol $Cr^{-1}$ $bar^{-1}$ $h^{-1}$). Finally, activation of unbridged complexes with MAO has also been investigated. Complex **22** produced a bimodal distribution of polyethylene with an activity of around 40 kg mol $Cr^{-1}$ $bar^{-1}$ $h^{-1}$ [28].

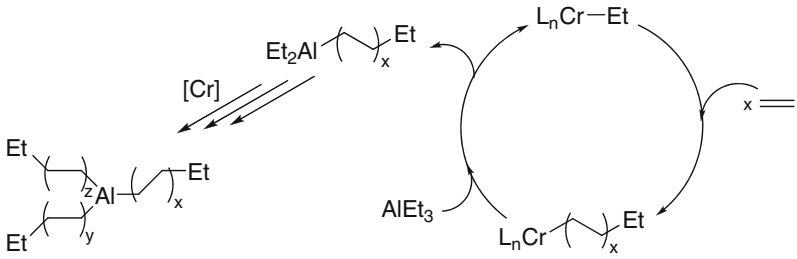


**Fig. 1.1** Mechanism of catalysed chain growth at aluminium with complex **17**

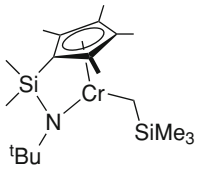


**14**

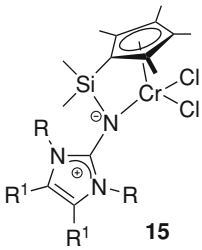


**15**

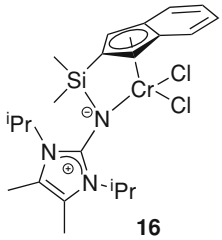


**16**

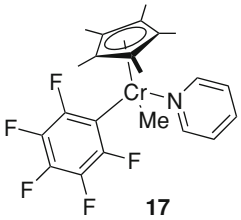


**17**

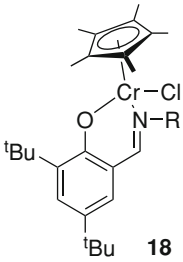


**18**

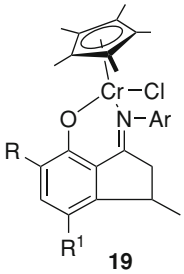


**19**

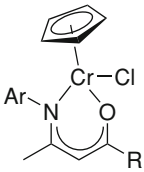


**20**

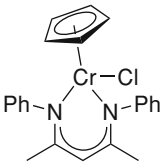


**21**

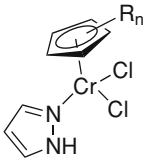


**22**

## 1.3 Chromium Complexes of *β*-diketiminate (NacNac) and *β*-ketoiminate (NacAc) Type Ligands

Chromium complexes of *β*-diketiminate (NacNac) ligands, both mono- and bis-ligand, were introduced by Theopold [29] and Gibson [30]. These complexes led to moderate activities for ethylene polymerisation upon activation with $Et_2AlCl$ or MAO (with $Et_2AlCl$ generally superior) [1]. More recently, Theopold has prepared the Cr-alkyl cation **23** which is active in the absence of co-catalyst [31]. Polyethylene is produced with an activity of around 20 kg mol $Cr^{-1}$ $bar^{-1}$ $h^{-1}$ and has a low polydispersity, indicative of a single site catalytic species. Copolymerisation with 1-hexene is also catalysed, and the complex is suggested to be a model for the heterogeneous Phillips catalyst. These complexes are also activated by MAO, with activities up to 40 kg mol $Cr^{-1}$ $bar^{-1}$ $h^{-1}$ [32]. Complexes in which the NacNac ligand is backbone substituted with a pendant pyridyl donor have also been disclosed in the patent literature, structure **24** [33]. Again MAO activation was employed, leading to a catalyst with low activity for ethylene polymerisation (ca. 6 kg mol $Cr^{-1}$ $bar^{-1}$ $h^{-1}$).

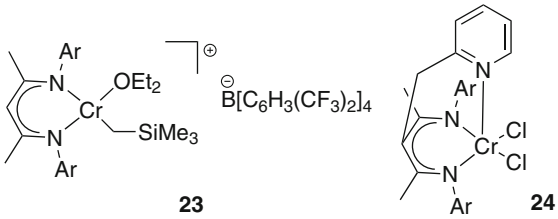


**23** **24**

Phenoxy-imine based chromium catalysts were again introduced by Gibson et al. [1], and have been developed into highly active systems. A high throughput screening approach was employed to optimize catalysts of general structure **25** in combination with MAO [34]. Catalysts in which the phenoxy substituent ($R^1$ in **25**) is an anthracenyl group lead to high molecular weight polyethylene with activities up to around 3,000 kg mol $Cr^{-1}$ $bar^{-1}$ $h^{-1}$. With even greater steric bulk at this position and a further pendant donor tethered to the imine, as in complex **26**, linear α-olefins and low molecular weight polyethylene is formed with activities up to 10,000 kg mol $Cr^{-1}$ $bar^{-1}$ $h^{-1}$. In the case of complex **26**, a metallacycle mechanism for oligomerisation has been established, see Sect. 1.7.4 [35]. Recently it was shown that substitution of the ligand with a bulky $–SiPh_3$ group is also effective [36]. Complex **27** also leads to oligomers and low molecular weight polyethylene ($M_n$ = 600–1,600 g $mol^{-1}$) with activities up to 2,500 kg mol $Cr^{-1}$ $bar^{-1}$ $h^{-1}$. The catalyst was reported to be tolerant to excess (4 equivalents) of additional donor ligands (MeCN, THF, pyridine). More unusual alterations to these catalysts include ferrocenyl substitution of the imine nitrogen (**28**, 130 kg mol $Cr^{-1}$ $bar^{-1}$ $h^{-1}$) [37], and imidazolium functionalisation as in complex **29** with two chelate ligands per chromium (ca. 1 kg mol $Cr^{-1}$ $bar^{-1}$ $h^{-1}$) [38].

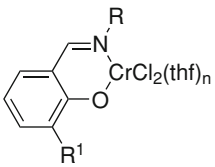


**25**

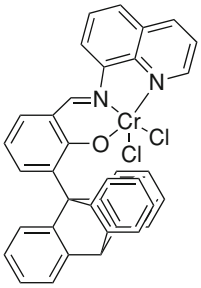


**26**

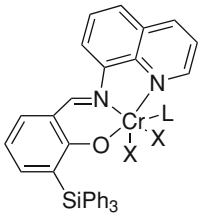


**27**

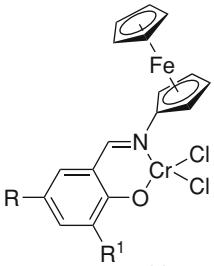


**28**

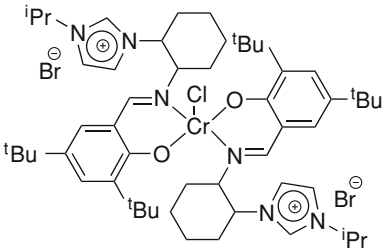


**29**

## 1.4 Chromium Complexes of Imidazole and Pyrazole Based Ligands

Chromium complexes containing multidenate ligands incorporating imidazole N-donors have been known for some time in olefin polymerisation [1]. Rüther and Cavell have prepared complexes of bidentate diimidazole ligands, general structure **30**, and tested these for ethylene oligomerisation following treatment with MMAO [39]. A mixture of both α-olefins and alkanes are formed, indicating a degree of chain transfer with $AlR_3$ (analogous to that shown in Fig. 1.1). The activities obtained range from low to moderate (1–10 kg mol $Cr^{-1}$ $bar^{-1}$ $h^{-1}$). In one instance these ligands have been shown to lead to polymer formation; complex **31**, albeit poorly characterized, appears in a patent from Exxon Mobil [40]. Bimodal distributions of polyethylene form after MAO activation, again with low to moderate activities. A tridentate tris(imidazole)phosphine complex, **32**, has also been tested for ethylene polymerisation, leading to low activity (2.7 kg mol $Cr^{-1}$ $bar^{-1}$ $h^{-1}$) [39]. A later patent; however, details very similar complexes but lacking the bulky *tert*-butyl substitution of **32**. This change leads to high activities (up to 400 kg mol $Cr^{-1}$ $bar^{-1}$ $h^{-1}$) for ethylene polymerisation [41].

Structurally similar complexes featuring tris(pyrazolyl)methane ligands have also been employed for olefin polymerisation. Complexes of structure **33** lead to very high activities, up to 2,500 kg mol $Cr^{-1}$ $bar^{-1}$ $h^{-1}$, following MAO activation [42]. A bimodal distribution of polyethylene is normally formed in which a low molecular weight fraction ($M_n$ = 1,500 g $mol^{-1}$) is predominant. This led the authors to propose two different active species. The molecular weight of the main fraction decreases with increasing loadings of MAO. This, together with the absence of terminal double bonds in the polymer, suggests that the main chain transfer process is alkyl exchange with MAO. Chromium complexes of this ligand have also been employed for selective ethylene trimerisation, see Sect. 1.7.2. A tris(pyrazolyl)borate complex, **34**, has also been evaluated, but leads only to moderate activity (to 18 kg mol $Cr^{-1}$ $bar^{-1}$ $h^{-1}$) after MAO activation [43]. Other researchers investigated tridenate pyrazole-containing ligands with an N, O or S central donor, general structure **35** [44]. With a central NH group high molecular weight polymer is formed (MAO activation); all other complexes led to distributions of linear α-olefin oligomers. The NON and NSN complexes displayed the highest activities, up to 97 kg mol $Cr^{-1}$ $bar^{-1}$ $h^{-1}$. A similar complex with flanking pyrazole groups is **36**, which was briefly reported to polymerise ethylene with activities up to 150 kg mol $Cr^{-1}$ $bar^{-1}$ $h^{-1}$ [45].

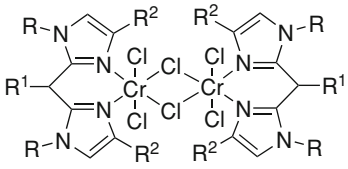

$R^1$ = H, $PPh_2$, =O, =NPh

**30**

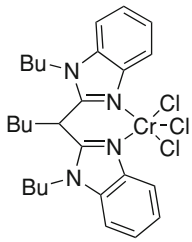

**31**

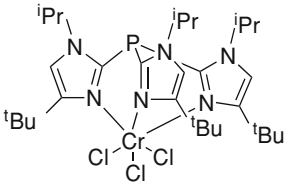

**32**

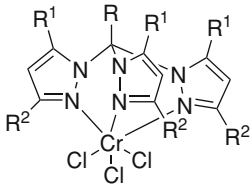

**33**

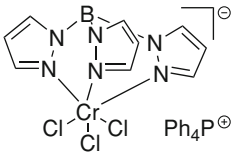

**34**

**35**

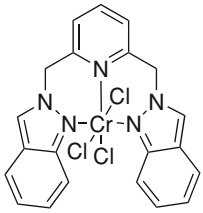

**36**

## 1.5 Chromium Complexes of Bis(imino)pyridine and Structurally Related Ligands

Transition metal complexes of bis(imino)pyridine ligands have attracted much interest over the past decade following the discovery that Fe, Co, V and Cr complexes of these ligands form very effective catalysts for olefin polymerisation [1]. Esteruelas [46] and Small [47] independently reported, and patented [48, 49], complexes of structure **37**. In combination with MAO these lead to very high activity for ethylene oligomerisation or polymerisation (Esteruelas reported an activity of 41,000 kg mol $Cr^{-1}$ $bar^{-1}$ $h^{-1}$). The steric bulk of the N-substitution has a controlling influence on both activity and product molecular weight. Bulky *ortho*-aryl substitution leads to higher molecular weight polymer at the expense of activity [46], while lower steric bulk on nitrogen leads to 1-butene or a distribution of α-olefins and wax [47]. Both groups noted the active catalysts were robust with respect to temperature, and also found evidence for chain transfer with aluminium. These catalysts also copolymerize

1-hexene and ethylene to afford branched polymers. Ethyl-branched polymer is also produced by aryl-fluorinated analogues of **37** [50]. In this case this was thought to be due to ethylene/1-butene copolymerisation, with the 1-butene formed by a second active site. A comparison of Fe, Co, V and Cr bis(imino)pyridines under the same conditions has been made, which allows direct comparison of the catalysts [51]. This work reveals that the chromium based system is one of the most active and thermally robust catalysts.

A wide range of alterations to the general ligand structure have been investigated for this class of catalyst. Bis(benzimidazolyl)pyridine complexes (structure **38**, R = H) lead to a Schulz–Flory distribution of ethylene oligomers following MAO activation, with an activity of over 5,000 kg mol $Cr^{-1}$ $bar^{-1}$ $h^{-1}$ being demonstrated [35, 52]. In one report it was conclusively demonstrated that ethylene oligomerization with this catalyst proceeds via a metallacycle mechanism, see Sect. 1.7.4 [53]. When the N substituent, R on **38**, is an alkyl group the activity is lower and 1-butene is the major product [52]. Sun et al. have studied a wide range of similar complexes in a series of reports, structures **39** [54], **40** [55], **41** [56, 57], **42** [58], and **43** [59]. The behavior of all of these complexes is similar following activation with MAO or MMAO. A Schulz–Flory distribution of ethylene oligomers along with some polyethylene is formed with activities ranging from 200 to 1,600 kg mol $Cr^{-1}$ $bar^{-1}$ $h^{-1}$.

Chromium complexes based upon two very similar bis(oxazoline)pyridine ligands seem to lead to starkly different products to one another. Complex **44** in which R = $^{i}$Pr yields linear high molecular weight polyethylene with only moderate activity (6 kg mol $Cr^{-1}$ $bar^{-1}$ $h^{-1}$) [60]. The authors noted; however, that the catalyst is very stable, with a 16 h run showing no deactivation. A more recent patent reports that ethylene is dimerised to 1-butene with very high activity (ca. 1,900 kg mol $Cr^{-1}$ $bar^{-1}$ $h^{-1}$) when R = Ph, although the precatalyst was not characterized in this work [61].

A number of researchers have also replaced the imino group or central pyridine in these ligands with alternate donor groups. The ONN chromium complexes **45** also lead to high activity in ethylene oligomerisation once activated with MAO [47, 62]. Polyethylene is produced when this complex is activated with $Et_2AlCl$ (66 kg mol $Cr^{-1}$ $bar^{-1}$ $h^{-1}$) [62]. Complexes such as **46** and **47** have also been reported recently, leading to mixtures of polyethylene and soluble oligomers with activities up to 2,600 kg mol $Cr^{-1}$ $bar^{-1}$ $h^{-1}$ [63]. Again, a metallacycle mechanism (Sect. 1.7.4) for oligomerisation was proposed for complex **46**.

Gambarotta et al. have studied the reaction chemistry of Cr(II) and Cr(III) catalyst precursors, and have prepared the formally Cr(I) complex **48** through reduction and alkylation of a Cr(II) precursor [64]. Upon treatment with MAO, complex **48** is highly active for ethylene polymerization, suggesting that activation of the typical Cr(III) precursors involves metal reduction to Cr(I). The identity of the active species still remains unknown however.

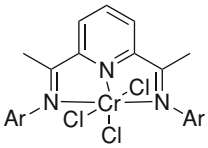

**37**

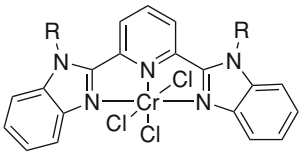

**38**

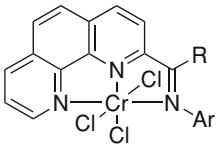

**39**

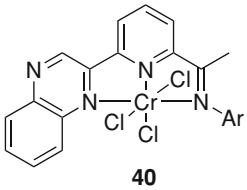

**40**

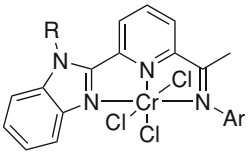

**41**

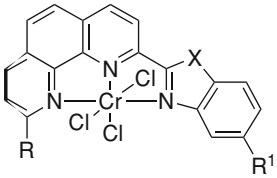

X = NH, NEt, O, S

**42**

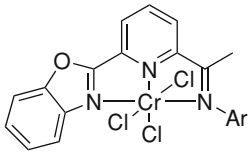

**43**

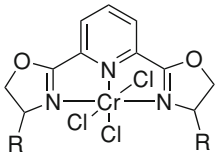

**44**

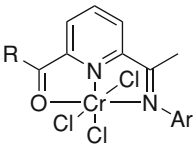

**45**

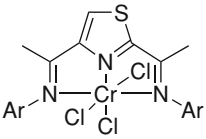

**46**

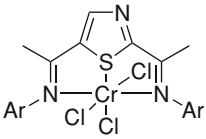

**47**

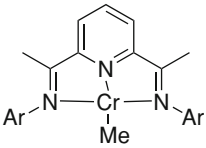

**48**

## 1.6 Chromium Complexes of Other N-donor Ligands

A number of complexes have been trialled which do not easily fit within the above classifications. The ligands in these are typically mixed-donor multidentates, in which the nitrogen donor is either neutral (imine-type) or anionic (amido). Carney et al. have prepared and tested complexes of structure **49**, which display either *fac* or *mer* geometry depending on the pyridyl substituents ($R^1$ = H *fac*; $R^1$ = Me *mer*) [65]. It was demonstrated that the precatalysts with a *fac* geometry are approximately 30–40 times more active (24 kg mol $Cr^{-1}$ $bar^{-1}$ $h^{-1}$) than *mer* complexes following MAO activation. The *fac* complexes also produce mainly low molecular weight polyethylene, while the *mer* complexes yield a higher molecular weight polymer. The same authors also tested the tetradenate ligand in complex **50** and derivatives [66]. A similar activity in ethylene polymerisation was observed, ca 10–20 kg mol $Cr^{-1}$ $bar^{-1}$ $h^{-1}$. A complex containing a tetradentate $N_2P_2$ ligand has also been reported to oligomerise ethylene with

around the same activity, complex **51** [67]. Higher activities have been reported for complexes containing tridenate ligands, for instance **52** (190 kg mol $Cr^{-1}$ $bar^{-1}$ $h^{-1}$) [68] and **53** (80 kg mol $Cr^{-1}$ $bar^{-1}$ $h^{-1}$) [69].

Functionalised pyrrole ligands have also received some attention (see also Sect. 1.7.1). Complex **54**, containing a $\pi$-bound neutral pyrrole as well as $\sigma$-bound anionic pyrroles, leads to moderate activity for ethylene oligomerisation with MAO and polymerisation with isobutylaluminoxane [70]. Complex **55** was reported by Theopold to lead to low activity for ethylene polymerisation (7 kg mol $Cr^{-1}$ $bar^{-1}$ $h^{-1}$, $EtAlCl_2$ activation) and a bimodal polymer distribution [71]. In contrast, a recent report shows that addition of a soft phosphine donor to a similar ligand, as shown in structure **56**, leads to very high activity to produce low molecular weight polyethylene (5,800 kg mol $Cr^{-1}$ $bar^{-1}$ $h^{-1}$) [72].

While the vast majority of chromium precatalysts are based upon Cr(II) or Cr(III) in combination with multidenate ligands, simple Cr(IV) amido complexes such as **57** have also been evaluated. Activation of this complex with MAO or $Et_2AlCl$ led to ethylene polymerisation with an activity of around 50 kg mol $Cr^{-1}$ $bar^{-1}$ $h^{-1}$ [73].

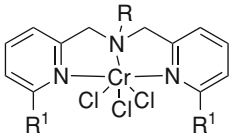

**49**

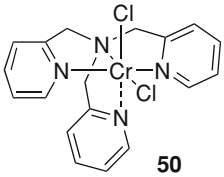

**50**

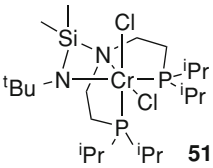

**51**

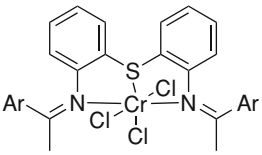

**52**

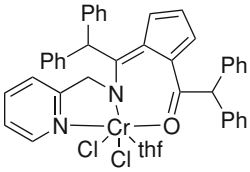

**53**

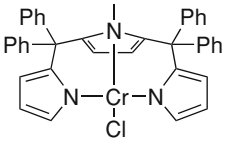

**54**

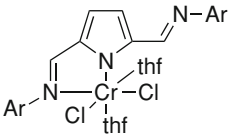

**55**

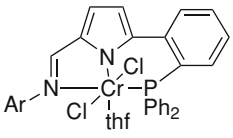

**56**

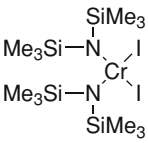

**57**

## 1.7 Selective Oligomerisation via Metallacycle Intermediates

A generalised mechanism for ethylene oligomerisation via metallacycles is shown in Fig. 1.2. The process begins with oxidative (with respect to the metal) coupling of two ethylene units to produce a metallacyclopentane complex. From here, insertion of further ethylene into the metallacyclopentane produces larger ring metallacycles, while decomposition of the metallacycle at any point can produce

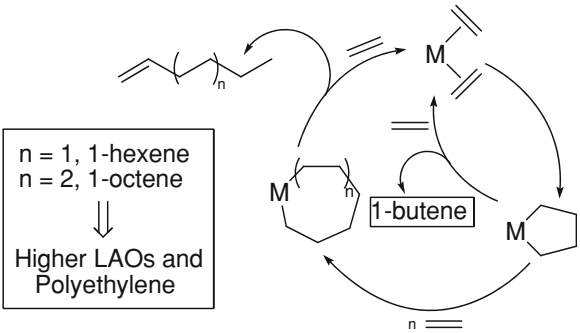


**Fig. 1.2** Metallacycle mechanism for ethylene oligomerisation

linear α-olefins. The selectivity of the process is thus controlled by the relative stability of the different sized metallacycles, in particular their propensity to either decompose or grow via ethylene insertion. The ability of certain catalysts, particularly those based on chromium, to selectively produce ethylene trimer (1-hexene) via this process has been extensively studied, due to the high demand for 1-hexene as a polyethylene comonomer [4]. Selective trimerisation can result when olefin insertion (metallacycle growth) into the metallacyclopentane is more facile than elimination of 1-butene, according to Fig. 1.2. This is normally the case due to the stability of metallacyclopentanes, while the instability of metallacycloheptanes leads to selectivity to 1-hexene (as opposed to further metallacycle growth). A range of trimerisation systems incorporating N-donor ligands have been developed, and are discussed in the following sections.

### *1.7.1 The Phillips Trimerisation Catalyst*

The Phillips trimerisation catalyst (not to be confused with the Phillips catalyst for ethylene polymerisation, Sect. 1.1) is thus far the only ethylene trimerisation system to be commercialised. A detailed background to this catalyst is provided in a published review [4]. The system is employed by Chevron–Phillips to produce ca. 47,000 ton per annum of 1-hexene. The catalyst is composed of a chromium source, 2,5-dimethylpyrrole and an alkylating agent such at $AlEt_3$, and has been proposed to operate via a Cr(II)/Cr(IV) mechanism starting from a chromium complex such as **58** [74]. The pyrrole ligand is thought to flip between $\eta^1$ and $\eta^5$ coordination throughout the catalytic cycle, effectively compensating for changes in the coordination environment at chromium. Recent reports from Gambarotta et al. provide good evidence for a Cr(I)/Cr(III) mechanism however [75, 76]. By utilizing more bulky pyrrole ligands, single site self activating catalaysts such as **59** could be isolated. This chromium(I) complex behaves similarly to the Phillips trimerisation catalyst, and a catalytic cycle proceeding through an intermediate such as **60** was proposed, in which the chloro group acts in a hemilabile fashion. It is noteworthy that

the proposed interaction between chromium and a chloro group is in general agreement with the known ability of chloro compounds to improve both activity and selectivity in this system [4, 77]. Armed with these experimental insights, Budzelaar has revisited the theoretical treatment of the Phillips system and found that such a Cr(I)/Cr(II) mechanism is quite feasible [78]. As such, the mechanistic details surrounding this catalyst remain uncertain, despite its importance to the field.

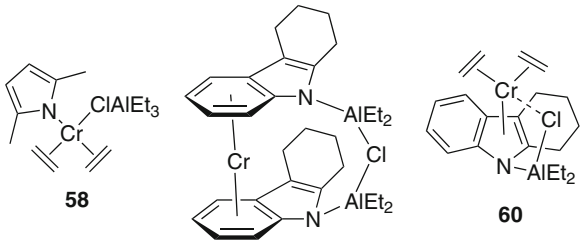


## 1.7.2 Trimerisation Catalysts Based on Chromium Complexes of Tridentate Ligands

McGuinness and Wasserscheid prepared precatalysts of structure **61**, which upon activation with MAO, formed highly selective catalysts for 1-hexene production [79]. Second-generation catalysts of structure **62** were later reported which represented an improvement in terms of ease of ligand preparation and cost [80]. Optimisation of catalysts **62** by researchers at Sasol Technology showed that they could be operated with very low levels of MAO (30–100 equivalents), and that very high overall 1-hexene selectivities (>97%) were achievable. Activities up to around 280 kg mol $Cr^{-1}$ $bar^{-1}$ $h^{-1}$ were reported.

Recent studies on these systems have focused on elucidating the structure and oxidation state of the active catalyst, and the precise role of MAO. Precatalysts **61** and **62** contain N–H functionality, and there is interest in ascertaining whether or not this is preserved in the active species. Direct analogues of **61** containing N-alkyl functionality (**63**) were prepared and tested following activation with MAO [81]. These complexes displayed very low activity and 1-hexene selectivity, instead generating between 30 and 70% polyethylene. The authors concluded that N–H functionality is essential for high activity and selectivity with this ligand class. This led to speculation that the N–H group is deprotonated during activation, leading to a monoanionic tridentate ligand.

Follow up studies concentrated again on the N–H functionality, as well as the Cr oxidation state and role of MAO [82]. Chromium(II) complexes **64** and **65** were prepared and it was found that activities and selectivities to 1-hexene were broadly similar to the original Cr(III) complexes. This led to the conclusion that Cr(III) precursors are reduced to Cr(II) or lower upon activation

with MAO, assuming that MAO is not able to oxidize Cr(II) back up to a higher oxidation state (it was subsequently found by other researchers that this is not always a safe assumption, below). Deprotonation of complex **64** with the organic base DABCO (1,4-diazabicyclo(2.2.2)octane) led to the amido complex **66**, while reaction of $LiN(CH_2CH_2S^tBu)_2$ with $CrCl_2(thf)_2$ led to complex **67**. Both dimer complexes feature N–H deprotonated ligands, and importantly both were active catalysts for ethylene trimerization. The activity of **67** was greatly attenuated relative to monomeric precursors; however, the catalytic relevance of such a structure is uncertain. Its formation may result more from the absence of other ligating compounds (ethylene, MAO, $AlMe_3$), and under catalytic conditions it may not form. Nonetheless, the fact that both deprotonated complexes, particularly **66**, were active for ethylene trimerisation was taken as significant evidence that these ligands are deprotonated under the conditions of catalysis.

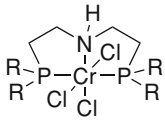
**61**

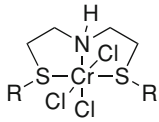
**62**

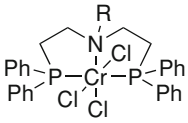
**63** R = Me, Bz

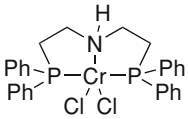
**64**

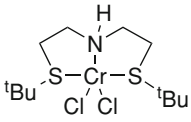
**65**

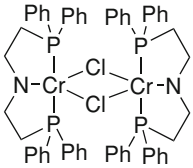
**66**

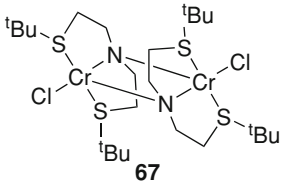
**67**

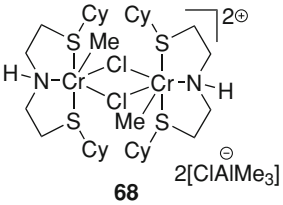
**68**

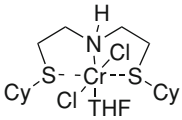
**69**

Independent but closely related studies of Gambarotta and Duchateau [83, 84] led to somewhat different conclusions on the issue of ligand deprotonation. When complex **62** with R = cyclohexyl was reacted with $AlMe_3$, the Cr(III) cationic dimer **68** was isolated [83]. When MAO was employed an undefined complex was formed, thought also to be a Cr(III) cation of similar structure. When isobutylalumoxane was employed, instead a Cr(II) dimer was isolated (the same structure as **68** but without Cr–Me groups). In each case the N–H group remains intact, and the authors suggested this as proof that deprotonation does not occur during catalysis. A potential problem here; however, is that these model reactions are done at room temperature, whereas this class of catalysts are not active for trimerisation under these conditions, requiring temperatures of 80–110 °C before good activity and selectivity result [79, 80]. Furthermore,

the complexes are not effectively activated with the amounts of $AlMe_3$ or MAO utilised in these studies (ca. 5 equivalents). It is thus difficult to draw concrete conclusions from studies that are not conducted under catalytically relevant conditions, particularly when elevated temperature and the amount of cocatalyst are so crucial to the operation of these catalysts. The authors also prepared an analogue of complex **67** with cyclohexyl substitution at sulfur, and found this to be inactive in combination with MAO. This was interpreted as further evidence that the N–H group is not deprotonated, but here again caution is required as the temperature of catalysis may be responsible for this observation. As discussed above, complexes **66** and **67** are in fact active at 80 °C, whereas the cyclohexyl analogue of **67** was tested at 50 °C. It was demonstrated in the original reports of these systems that at 50 °C the catalysts produce a high percentage of polymer and the activities are over an order of magnitude lower than at 80 °C.

Similarly to the work discussed above [82], these authors also compared Cr(III) and Cr(II) precatalysts (including complex **69**), and again found that both oxidation states behave similarly once activated with MAO [83]. This was again taken as evidence for reduction to Cr(II) or lower during catalysis. Later work by the same authors; however, raises some doubt over this [84]. When the Cr(II) precursor $CrCl_2(thf)_2$, SNS ligand and 10 equivalents of $AlMe_3$ were reacted, the Cr(III) dimer **68** was again isolated, along with Cr(0) resulting from a disproportionation reaction. This result clearly shows that the action of $AlMe_3$ on Cr(II) precursors can result in oxidation of the Cr center, and thus a Cr(III) active species remains a possibility.

The work of both research groups supports the notion of a cationic active species, as might be expected from MAO activation. McGuinness showed that more well defined perfluoroborane activators, known to generate cationic metal centers, are effective cocatalysts [82]. Gamborotta and Duchateau showed that reaction with alkyl aluminium reagents almost invariably led to cationic complexes [83, 84]. Given this conclusion, two possible mechanistic cycles can be proposed (Fig. 1.3). That shown in Fig. 1.3a involves a Cr(II)/Cr(IV) redox couple and a monoanionic ligand resulting from deprotonation. The alternative in Fig. 1.3b involves a Cr(I)/Cr(III) couple in which the ligand remains neutral. It is clear that further work is required to definitively elucidate which of these mechanisms, or another, is operating.

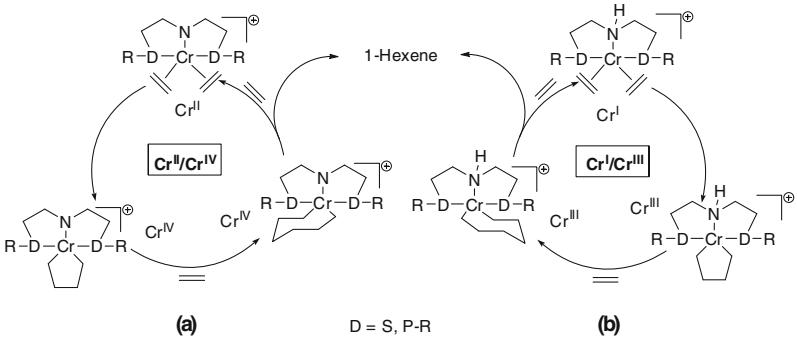


**Fig. 1.3** Possible mechanisms for ethylene trimerisation with Cr–SNS and Cr–PNP complexes

The development of SNS–Cr catalysts spawned interest in alternative sulfur-based tridentates; however, thus far none of these seem to have matched the original bis(sulfanyl)amine catalysts in terms of activity or selectivity. The effect of chelate ring size in these systems was explored through preparation of complex **70**, in which an extra methylene spacer group has been added to one side of the ligand [81]. While this complex did give rise to an active trimerisation catalyst (MAO activation), the productivity was around half that of the symmetrical analogue **62** and the selectivity to 1-hexene lower. Bluhm et al. [85] tested a large range of tridentates with central imine or amine donors. The best catalysts from a trimerisation perspective were those of structure **71**. When activated with MAO and run at 24–30 °C, around 82–86% 1-hexene was formed with the remainder being polyethylene (productivities up to ca. 5 kg mol $Cr^{-1}$ $bar^{-1}$ $h^{-1}$). Increasing the temperature seemed to shift the selectivity more toward polymer. A wide variety of other complexes, of general structure **72**, were also tested. Most of these gave mainly polyethylene (60 + %), but the only other significant product in the majority of cases was 1-hexene, indicating high selectivity within the oligomeric products. Also tested were the amine complexes of structure **73**. These similarly produced 60–70% polyethylene with the remainder being 1-hexene.

Somewhat related Cr–SNS complexes with a central pyridine donor, **74**, were later prepared and tested [86]. Activation with MAO produced catalysts with activities up to 8 kg mol $Cr^{-1}$ $bar^{-1}$ $h^{-1}$ and liquid product selectivities of 99% 1-hexene. The amount of polyethylene produced relative to 1-hexene was not explicitly given, but can be estimated as 5–22% from the data provided. A number of Cr(II) complexes of the ligand were also tested and found to produce more higher α-olefins at the expense of 1-hexene. The authors therefore suggested the possibility of a number of catalytic active species; Cr(II) leading to a Schulz–Flory distribution and Cr(III) generating 1-hexene. A Cr(I)/Cr(III) cycle analogous to that shown in Fig. 1.3b can be envisaged for these systems, along with the other neutral tridentate ligands discussed above; however, this has hitherto not been studied (although has been for Cr–triazacyclohexane catalysts, see below).

While the tridentate ligands hitherto discussed display *mer* coordination (at least in the precatalysts), a number of systems are known which force a *fac* coordination geometry. Around a decade ago, the Tosoh Corporation developed catalysts based upon chromium in combination with the ubiquitous tris(pyrazolyl) methane ligands [4]. These are covered in a past review [4]; however, in more recent studies Hor et al. have investigated related heteroscorpionate systems [87–89]. Complexes in which the third donor is oxygen or sulfur, of general structure **75**, were the first to be prepared and tested [87]. Both the thioether and ether complexes were selective for ethylene trimerisation in combination with MAO. The ether analogues were; however, superior, and the best catalyst (L = O, R = hexyl, R′= Me) led to an overall 1-hexene selectivity of 97.6% at 44 kg mol $Cr^{-1}$ $bar^{-1}$ $h^{-1}$. In recent follow up studies, a broad range of complexes, **76**, were investigated in which the third donor group altered between pyrazolyl

(Tosoh system), imidazolyl, pyridyl and amine [88, 89]. All of these systems trimerise ethylene upon MAO activation. The complex with an imidazolyl moiety (R = H) was most active and selective (92 kg mol $Cr^{-1}$ $bar^{-1}$ $h^{-1}$; 97.6% 1-hexene), while the amine group was the worst performer.

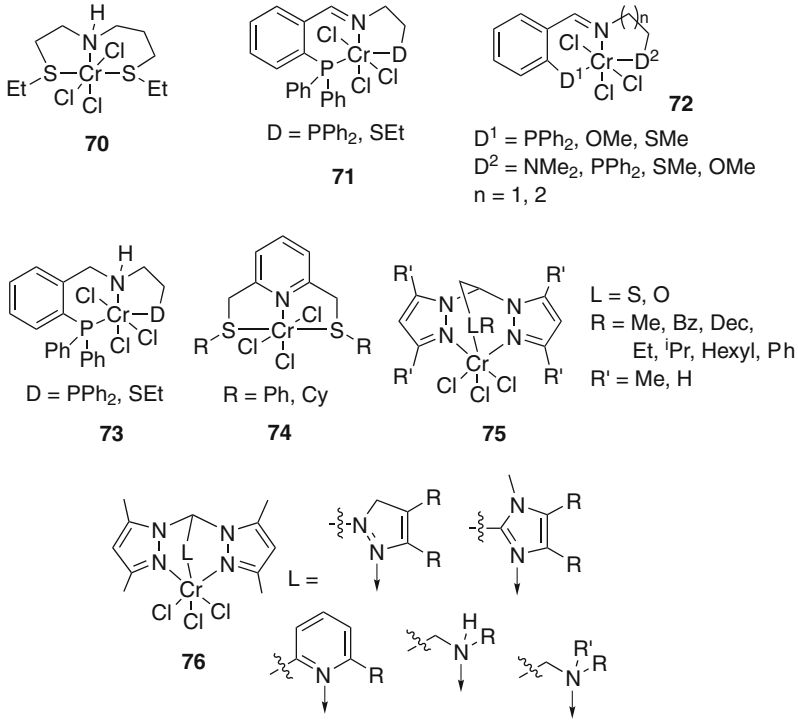


Köhn et al. developed chromium complexes of triazacyclohexane ligands, and showed that these convert ethylene to mixtures of 1-hexene and polyethylene when activated with MAO or $[Me_2PhNH][B(C_6F_5)_4]/Al^iBu_3$ [4, 90]. When higher α-olefin monomers were employed, the catalyst was highly selective for trimers, and mechanistic studies supported a Cr(I)/Cr(III) metallacycle mechanism [91]. These researchers have subsequently studied the activation process with $[Me_2PhNH][B(C_6F_5)_4]/Al^iBu_3$ in more detail, and their observations provide insight into the likely mode of catalyst deactivation [92]. Treatment of the triazacyclohexane complex **77** with $[Me_2PhNH][B(C_6F_5)_4]/Al^iBu_3$ firstly produces a more soluble anilinium adduct (Fig. 1.4). Treatment of this complex with triisobutylaluminium results in formation of a Cr(III) dialkyl cation. Reductive elimination from here is thought to produce a Cr(I) triazacyclohexane cation which is active for α-olefin trimerisation. However, reduction also leads to $[(arene)_2Cr]^+$ and an aluminium–triazacyclohexane complex, which represent products of catalyst deactivation. The arene here is sourced from the solvent, and both the bis(benzene) and bis(toluene) complexes were characterised by X-ray crystallography.

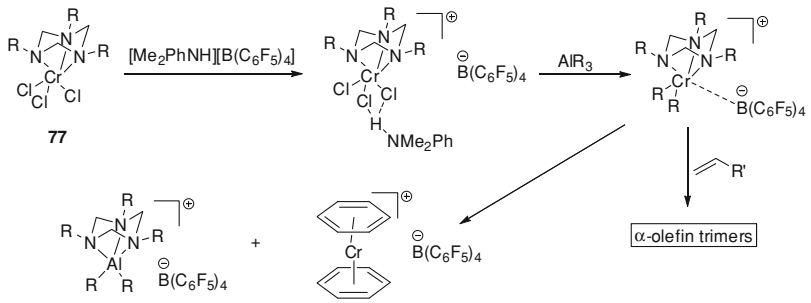


**Fig. 1.4** Activation and decomposition of Cr-triazacyclohexane catalysts

## *1.7.3 Chromium Complexes of Bidentate Ligands*

A large range of N,N-, N,O-, N,P- and N,S-bidentates have been disclosed in a series of patents from Exxon-Mobil. High throughput screening of ligands of general structure **78** and **79** [93], **80** and **81** [94], **82** [95], **83** [96], **84** [97] and **85** [98], in combination with various chromium sources and MAO, led to mixed results for ethylene trimerisation and tetramerisation. The α-olefin selectivities presented in these patents are somewhat misleading, as polyethylene formation is not factored into these numbers. In some cases for instance, 1-hexene selectivity is reported as 98 + % while well over 50% of the formed product constitutes polyethylene. The most active catalysts are formed when ligands **78** and **79** are employed (up to ca. 2,900 kg mol $Cr^{-1}$ $bar^{-1}$ $h^{-1}$), and there is no doubt in this case that the catalysts are truly selective towards 1-hexene (up to ca. 98% 1-hexene inclusive of polymer). Ligands of structure **80** and **81** produced 1-hexene and 1-octene (upto ca. 50% 1-octene), but displayed a much lower activity. The results with the remaining ligands **82**–**85** seemed much less impressive. 1-Hexene is formed with very low activities (<500 turnovers) and the product is in most cases mainly polyethylene.

Gambarotta et al. have prepared Cr(II) complexes of NPN monoanionic ligands (structure **86**) and found these to be selective ethylene trimerisation catalysts after activation with excess $Al^iBu_3$ [99–101]. Activities up to around 20 kg mol $Cr^{-1}$ $bar^{-1}$ $h^{-1}$ were achieved. Addition of MAO led to unselective oligomerisation and polymerisation. It was shown that the ligand in **86** is not innocent and that alkylaluminium reagents result in alkylation of the phosphorus atom and aluminium coordination. One of the intermediates isolated and which shows the final(?) ligand assembly is **87**, which resulted when **86** was treated with 10 equivalents of $Al^iBu_3$. The final identity of the active catalyst remains unclear; however, further addition of excess $Al^iBu_3$ is required before **87** becomes selective for trimerisation.

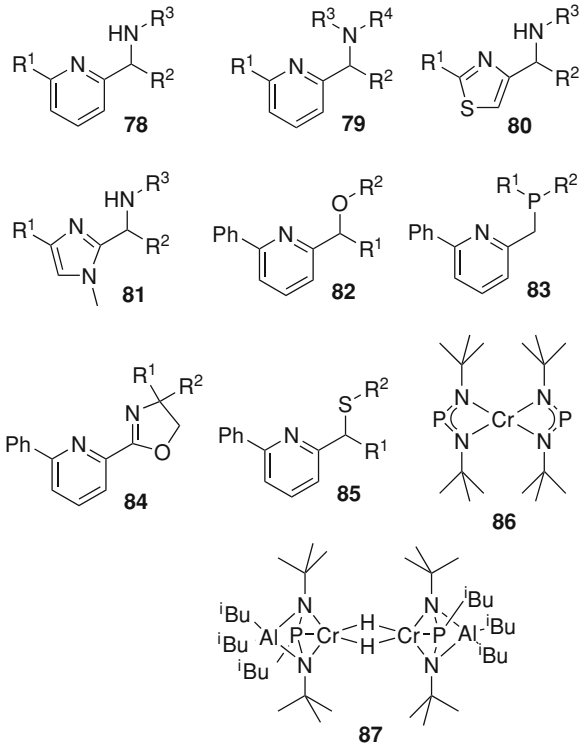


### *1.7.4 Oligomerisation and Polymerisation via Extended Metallacycles*

Selective oligomerisation via metallacycles occurs when metallacycle decomposition (α-olefin formation) is more facile than further ethylene insertion at various metallacycle ring sizes. When this condition breaks down the growth of large ring metallacycles can be envisaged, which can be termed an extended metallacycle mechanism. The question then becomes how far can this process progress, and is it possible for high molecular weight polyethylene to form via metallacycles? This question is of fundamental importance, as such a process has long been proposed as one model for polyethylene formation with the commercial Phillips catalyst (Cr on silica) [3, 102]. This catalyst has been used on great industrial scale for over half a century; however, despite this the mechanism of chain growth is still uncertain. There is no doubt some evidence for a metallacycle mechanism [3, 103–105]. There seems to be no obvious reason why large ring metallacycles could not grow to high molecular weight polymer. Following the formation of the metallacyclopentane, the subsequent steps involve only migratory insertion of ethylene. As such, the growth process differs little from a conventional Cossee mechanism.

Over recent years a number of reports have appeared which unequivocally demonstrate an extended metallacycle mechanism for the formation of higher α-olefins. All of these involve chromium catalysts. In the first such study, Gibson et al. described ethylene oligomerisation and polymerisation with catalysts **26** (Sect. 1.3) and **38** (R = H, Sect. 1.5) in combination with MAO [35, 53]. A Schulz–Flory distribution of α-olefins and low molecular weight polymer is formed, and deuterium labeling experiments ($CH_2CH_2/CD_2CD_2$ copolymerization) indicate a metallacycle mechanism. Gibson's group later reported the catalyst system composed of **88**/MAO, which converts ethylene to higher α-olefins and low molecular weight polyethylene ($M_n$ = 800–900) with exceptional activity (in excess of 100,000 kg mol $Cr^{-1}$ $bar^{-1}$ $h^{-1}$) [106]. An unprecedented α-olefin distribution was observed in which the $C_{4n}$ products ($C_8$, $C_{12}$, $C_{16}$, etc.) were more abundant than the $C_{4n+2}$ products ($C_{10}$, $C_{14}$, $C_{18}$, etc.). This was explained by a metallacycle mechanism in which the metallacycle can occupy two distinct sites, arising from the non-planarity of the central nitrogen donor. In the proposed model the metallacycle prefers one of these sites, and elimination occurs preferentially from one of the two sites. More recently, researchers from Sasol have reported a similar catalyst (**46**, Sect. 1.5) which behaves likewise [63]. Again a model involving two different metallacycle sites provided the best explanation.

A further example of higher olefins and low polymer being produced by metallacycles is provided by complex **89** [107]. In this instance the distribution of α-olefins showed another type of deviation from Schulz–Flory behavior. Depending upon the ligand substitution, the distribution was depleted in 1-butene or both 1-butene and 1-hexene. This revealed that metallacycle decomposition is retarded relative to further growth at the Cr–$C_4$ (±Cr–$C_6$) stage. This represents a qualitatively similar bias to that which must exist for ethylene tetramerisation catalysts [108], except in this case higher metallacycle formation is competitive with Cr–$C_8$ product release. Again these catalysts displayed exceptional activities, in excess of 40,000 kg mol $Cr^{-1}$ $bar^{-1}$ $h^{-1}$ [109, 110].

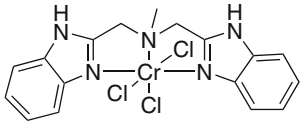


**88**

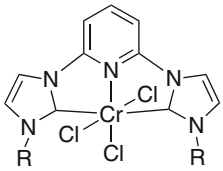


**89**

## 1.8 Summary and Outlook

Chromium is one of the most intensively studied metals for the development of new olefin polymerisation and oligomerisation catalysts. This is due to the use of this metal for commercial production of both polyethylene and liner α-olefins. Homogenous catalysts ligated by N-donor ligands account for a large proportion of

new generation catalysts, and represent some of the most active systems know to date. The development of new chromium-based catalysts in general, and those containing N-donor ligands specifically, is likely to continue to be an area of rapid development going forward.

## References


1. Gibson VC, Spitzmesser SK (2003) Advances in non-metallocene olefin polymerization catalysis. Chem Rev 103:283–315
2. Forestière A, Olivier-Bourbigou H, Saussine L (2009) Oligomerization of monoolefins by homogeneous catalysts. Oil Gas Sci Tech Rev IFP 64:649–667
3. Groppo E, Lamberti C, Bordiga S, Spoto G, Zecchina A (2005) The structure of active centers and the ethylene polymerization mechanism on the $Cr/SiO_2$ catalyst: A frontier for the characterization methods. Chem Rev 105:115–183
4. Dixon JT, Green MJ, Hess FM, Morgan DH (2004) Advances in selective ethylene trimerisation—a critical overview. J Organomet Chem 689:3641–3669
5. Chen EY-X, Marks TJ (2000) Cocatalysts for metal-catalyzed olefin polymerization: activator, activation processes, and structure–activity relationships. Chem Rev 100: 1391–1434
6. Britovsek GJP, Gibson VC, Wass DF (1999) The search for new-generation olefin polymerization catalysts: life beyond metallocenes. Angew Chem Int Ed 38:428–447
7. Döhring A, Göhre J, Jolly PW, Kryger B, Rust J, Verhovnik GPJ (2000) Donor-ligand-substituted cyclopentadienylchromium(III) complexes: a new class of alkene polymerization catalysts. 1. Amino-substituted systems. Organometallics 19:388–402
8. Enders M, Fernández P, Ludwig G, Pritzkow H (2001) New chromium(III) complexes as highly active catalysts for olefin polymerization. Organometallics 20:5005–5007
9. Enders M, Fernández P, Mihan S, Pritzkow H (2003) Quinolyl-functionalised Cp-chromium polymerisation catalysts: synthesis and crystal structures of alkylation products. J Organomet Chem 687:125–130
10. Enders M, Kohl G, Pritzkow H (2004) Synthesis of main group and transition metal complexes with the (8-quinolyl)cyclopentadienyl ligand and their application in the polymerization of ethylene. Organometallics 23:3832–3839
11. Zhang H, Ma J, Qian Y, Huang J (2004) Synthesis and characterization of nitrogen-functionalized cyclopentadienylchromium complexes and their use as catalysts for olefin polymerization. Organometallics 23:5681–5688
12. Cheng Z, Sun J, Li Y, Xu S, Wang B (2006) Synthesis and characterization of novel chromium catalyst and polyethylene with high molecular weight. J Wuhan Univ Technol Mater Sci Ed 21:50–55
13. Yoshikawa E, Hanaoka H (2004) Transition metal complexes as catalysts for olefin polymerization and production of polyolefins using them. JP 2004189690 (Sumitomo Chem Co)
14. Mihan S, Enders M, Nifant'ev I, Nicoara C (2004) Monocyclopentadienyl complexes. WO 2004/056481 (Basell Polyolefine)
15. Mihan S, Nifant'ev I (2004) Monocyclopentadienyl complexes. WO 2004/056482 (Basell Polyolefine)
16. Mihan S, Enders M, Fernandez P (2005) Monocyclopentadienyl complexes. WO 2005/058983 (Basell Polyolefine)
17. Mihan S (2006) Monocyclopentadienyl complexes. WO 2006/063826 (Basell Polyolefine)
18. Mihan S, Bildstein B, Steiner G (2006) Monocyclopentadienyl complexes. WO 2006/100004 (Basell Polyolefine)

19. Derlin S, Kaminsky W (2008) Chain-walking olefin polymerizations with donor-substituted half-sandwich chromium complexes: ethylene/propylene copolymer look-alikes by polymerization of propylene. Macromolecules 41:6280–6288
20. Schuhen K, Sieb D, Wadepohl H, Enders M (2009) New donor-functionalized Cp ligands: synthesis and complexation behaviour of quinoxalyl and benzothiadiazolyl systems. Z Anorg Allg Chem 635:1560–1567
21. Liang Y, Yap GPA, Rheingold AL, Theopold KH (1996) Constrained geometry chromium catalysts for olefin polymerization. Organometallics 15:5284–5286
22. Randoll S, Jones PG, Tamm M (2008) Chromium complexes with $Me_2Si$-bridged cyclopentadienyl-imidazolin-2-imine ligands: synthesis, structure, and use in ethylene polymerization catalysis. Organometallics 27:3232–3239
23. Jensen VR, Angermund K, Jolly PW, Børve KJ (2000) Activity of homogeneous chromium(III)-based alkene polymerization catalysts: lack of importance of the barrier to ethylene insertion. Organometallics 19:403–410
24. Ganesan M, Gabbaï FP (2004) [Cp*Cr($C_6F_5$)(Me)(py)] as a living chromium(III) catalyst for the 'Aufbaureaktion'. Organometallics 23:4608–4613
25. Xu T, Mu Y, Gao W, Ni J, Ye L, Tao Y (2007) Highly active half-metallocene chromium(III) catalysts for ethylene polymerization activated by trialkylaluminum. J Am Chem Soc 129:2236–2237
26. Huang Y-B, Yu W-B, Jin G-X (2009) Half-sandwich chromium(III) catalysts bearing hydroxyindanimine ligands for ethylene polymerization. Organometallics 28:4170–4174
27. Huang Y-B, Jin G-X (2009) Half-sandwich chromium(III) complexes bearing $\beta$-diketiminate ligands as catalysts for ethylene polymerization. Dalton Trans 767–769
28. Rojas R, Valderrama M, Garland MT (2004) Substituted cyclopentadienylchromium(III) complexes containing neutral donor ligands. Synthesis, crystal structures and reactivity in ethylene polymerization. J Organomet Chem 293–301
29. Kim W-K, Fevola MJ, Liable-Sands LM, Rheingold AL, Theopold KH (1998) [$(Ph)_2$nacnac]$MCl_2(thf)_2$ (M = Ti, V, Cr): a new class of homogeneous olefin polymerization catalysts featuring $\beta$-diiminate ligands. Organometallics 17:4541–4543
30. Gibson VC, Newton C, Redshaw C, Solan GA, White AJP, Williams DJ (2001) Synthesis, structures and ethylene polymerisation behaviour of low valent $\beta$-diketiminato chromium complexes. Eur J Inorg Chem 2001:1895–1903
31. MacAdams LA, Buffone GP, Incarvito CD, Rheingold AL, Theopold KH (2005) A chromium catalyst for the polymerization of ethylene as a homogenous model for the Phillips catalyst. J Am Chem Soc 127:1082–1083
32. Theopold KH, Kim W-K, MacAdams LA, Power JM, Mora JM, Masino AP (2003) Catalyst compounds with $\beta$-diiminate anionic ligands and processes for polymerizing olefins. US 6511936 (Chevron Chem Co)
33. Michaud G, Hillairet C, Sirol S (2008) Polymerisation of ethylene and alpha olefins with single site catalysts having an anionic scorpion-like ligand. EP 1925620 (Total Petrochemicals)
34. Jones DJ, Gibson VC, Green SM, Maddox PJ, White AJP, Williams DJ (2005) Discovery and optimization of new chromium catalysts for ethylene oligomerization and polymerization aided by high-throughput screening. J Am Chem Soc 127:11037–11046
35. Tomov AK, Chirinos JJ, Jones DJ, Long RJ, Gibson VC (2005) Experimental evidence for large ring metallacycle intermediates in polyethylene chain growth using homogeneous chromium catalysts. J Am Chem Soc 127:10166–10167
36. Kirillov E, Roisnel T, Razavi A, Carpentier J-F (2009) Chromium(III) complexes of sterically crowded bidentate $ON^R$ and tridentate $ONN^R$ naphthoxy-imine ligands: Synthesis, structures, and use in ethylene oligomerization. Organometallics 28:2401–2409
37. Gibson VC, Gregson CKA, Halliwell CM, Long NJ, Oxford PJ, White AJP, Williams DJ (2005) The synthesis, coordination chemistry and ethylene polymerisation activity of ferrocenediyl nitrogen-substituted ligand and their metal complexes. J Organomet Chem 609:6271–6283

38. Houghton J, Simonovic S, Whitwood AC, Douthwaite RE, Carabineiro SA, Yuan J-C, Marques MM, Gomes PT (2008) Transition-metal complexes of phenoxy-imine ligands modified with pendant imidazolium salts: synthesis, characterisation and testing as ethylene polymerisation catalysts. J Organomet Chem 693:717–724
39. Rüther T, Cavell KJ, Braussaud NC, Skelton BW, White AH (2002) Synthesis, characterisation and catalytic behaviour of a novel class of chromium(III) and vanadium(III) complexes containing bi- and tri-denate imidazole chelating ligands: a comparative study. J Chem Soc Dalton Trans 4684–4693
40. Kacker S, Berluche E, Stibrany RT, Sissano JA, Baugh LS (2006) Chromium complexes and their use in olefin polymerization. WO 2006/012327 (Exxon-Mobil)
41. Mihan S, Enders M, Fritz O (2004) Transition-metal complexes with tridenate, nitrogen-containing ligands. WO 2004/104052 (Basell Polyolefine)
42. García-Orozco I, Quijada R, Vera K, Valderrama M (2006) Tris(pyrazolyl)methane-chromium(III) complexes as highly active catalysts for ethylene polymerization. J Molec Catal A Chem 260:70–76
43. Rojas R, Valderrama M, Wu G (2004) Synthesis, structural characterization and ethylene polymerization behavior of complex $[Ph_4P][CrCl_3\{HB(pz)_3\}]$ [$HB(pz)_3$ = hydrotris (1-pyrazolyl)borate]. Inorg Chem Commun 7:1295–1297
44. Junges F, Kuhn MCA, dos Santos AHDP, Rabello CRK, Thomas CM, Carpentier J-F, Casagrande OL (2007) Chromium catalysts based on tridentate pyrozolyl ligands for ethylene oligomerization. Organometallics 26:4010–4014
45. Hurtado J, MacLeod Carey D, Muñoz-Castro A, Arratia-Pérez R, Quijada R, Wu G, Rojas R, Valderrama M (2009) Chromium(III) complexes with terdenate 2, 6-bis(azolylmethyl)pyridine ligands: synthesis, structures and ethylene polymerization behavior. J Organomet Chem 694:2636–2641
46. Esteruelas MA, López AM, Méndez L, Oliván M, Oñate E (2003) Preparation, structure, and ethylene polymerization behavior of bis(imino)pyridyl chromium(III) complexes. Organometallics 22:395–406
47. Small BL, Carney MJ, Holman DM, O'Rourke CE, Halfen JA (2004) New chromium complexes for ethylene olgomerization: extended use of tridenate ligands in metal-catalyzed olefin polymerization. Macromolecules 37:4375–4386
48. Mendez L, Sanz E, Sancho J, Esteruelas MA, Olivan M, Onate E (2004) Chromium catalysts active in olefin polymerization. US 2004/0087434
49. Small BL, Marcucci AJ (2003) Catalyst composition and olefin polymerization using same. WO 03/054038 (Chevron Phillips)
50. Nakayama Y, Sogo K, Yasuda H, Shiono T (2005) Unique catalytic behavior of chromium complexes having halogenated bis(imino)pyridine ligands for ethylene polymerization. J Polym Sci A 43:3368–3375
51. Semikolenova NV, Zakharov VA, Echevskaja LG, Matsko MA, Bryliakov KP, Talsi EP (2009) Homogeneous catalysts for ethylene polymerization based on bis(imino)pyridine complexes of iron, cobalt, vanadium and chromium. Catal Today 144:334–340
52. Zhang W, Sun W-H, Zhang S, Hou J, Wedeking K, Schultz S, Fröhlich R, Song H (2006) Synthesis, characterization, and ethylene oliogomerization and polymerization of [2, 6-bis(2-benzimidazolyl)pyridyl)chromium chlorides. Organometallics 25:1961–1969
53. Tomov AK, Gibson VC, Britovsek GJP, Long RJ, van Meurs M, Jones DJ, Tellmann KP, Chirinos JJ (2009) Distinguishing chain growth mechanisms in metal-catalyzed olefin oligomerization and polymerization systems: $C_2H_4/C_2D_4$ co-oligomerization/polymerization experiments using chromium, iron, and cobalt catalysts. Organometallics 28:7033–7040
54. Zhang S, Ji S, Shi Q, Sun W-H (2007) Chromium(III) complexes bearing 2-imino-1, 10-phenanthrolines: synthesis, molecular structures and ethylene oligomerization and polymerization. J Mol Catal A Chem 276:174–183
55. Amolegbe SA, Asma M, Zhang M, Li G, Sun W-H (2008) Synthesis, characterization, and ethylene oligomerization and polymerization by 2-quinoxalinyl-6-iminopyridine chromium chlorides. Aust J Chem 61:397–403

56. Chen Y, Zuo W, Hao P, Zhang S, Gao K, Sun W-H (2008) Chromium(III) complexes ligated by 2-(1-isopropyl-2-benzimidazolyl)-6-(1-(arylimino)ethyl)pyridines: synthesis, characterization and their ethylene oligomerization and polymerization. J Organomet Chem 693:750–762
57. Xiao L, Zhang M, Sun W-H (2010) Synthesis, characterization and ethylene oligomerization and polymerization of 2-(1H–2-benzimidazolyl)-6-(1(arylimino)ethyl)pyridinechromium chlorides. Polyhedron 29:142–147
58. Zhang M, Wang K, Sun W-H (2009) Chromium(III) complexes bearing 2-benzazole-1,10-phenanthrolines: synthesis, molecular structures and ethylene oligomerization and polymerization. Dalton Trans 6354–6363
59. Gao R, Liang T, Wang F, Sun W-H (2009) Chromium(III) complexes bearing 2-benzoxazolyl-6-arylimino-pyridines: synthesis and their ethylene reactivity. J Organomet Chem 694: 3701–3707
60. Esteruelas MA, López AM, Méndez L, Oliván M, Oñate E (2002) Synthesis, X-ray structure, and polymerisation activity of a bis(oxazolinyl)pyridine chromium(III) complex. New J Chem 26:1542–1544
61. Ackerman LJ, Diamond GM, Hall KA, Longmire JM, Micklatcher M (2008) Chromium complexes of pyridine bis (oxazoline)-ligands for ethylene dimerization. WO 2008/085657 (Exxon-Mobil)
62. Zhang W, Sun W-H, Tang X, Gao T, Zhang S, Hao P, Chen J (2007) Chromium complexes ligated by 2-carbethoxy-6-iminopyridines: synthesis, characterization and their catalytic behavior toward ethylene polymerization. J Mol Catal A Chem 265:159–166
63. Tenza K, Hanton MJ, Slawin AMZ (2009) Ethylene oligomerization using first-row transition metal complexes featuring heterocyclic variants of bis(imino)pyridine ligands. Organometallics 28:4852–4867
64. Vidyaratne I, Scott J, Gambarotta S, Duchateau R (2007) Reactivity of chromium complexes of a bis(imino)pyridine ligand: highly active ethylene polymerization catalysts carrying the metal in a formally low oxidation state. Organometallics 26:3201–3211
65. Carney MJ, Robertson NJ, Halfen JA, Zakharov LN, Rheingold AL (2004) Octahedral chromium(III) complexes supported by bis(2-pyridylmethyl)amines: ligand influence on coordination geometry and ethylene polymerization activity. Organometallics 23:6184–6190
66. Robertson NJ, Carney MJ, Halfen JA (2003) Chromium(II) and chromium(III) complexes supported by tris(2-pyridylmethyl)amine: synthesis, structures, and reactivity. Inorg Chem 42:6876–6885
67. Rozenel SS, Chomitz WA, Arnold J (2009) Chromium complexes supported by the multidentate monoanionic $N_2P_2$ ligand: reduction chemistry and reactivity with ethylene. Organometallics 28:6243–6253
68. Liu J-Y, Li Y-S, Liu J-Y, Li Z-S (2006) Synthesis and chromium(III) complexes with schiff-base ligands and their catalytic behaviors for ethylene polymerization. J Mol Catal A Chem 244:99–104
69. Lansalot-Matras C, Lavastre O, Sirol S (2009) Catalysts systems based on carbonylamino fulvenes. WO 2009/013196 (Total Petrochemicals)
70. Crewdson P, Gambarotta S, Djoman M-C, Korobkov I, Duchateau R (2005) Switchable chromium(II) ethylene oligomerization/polymerization catalyst. Organometallics 24: 5214–5216
71. Salisbury BA, Young JF, Yap GPA, Theopold KH (2007) Synthesis and reactivity of pyrrolide-diimine complexes of chromium. Collect Czech Chem Commun 72:637–648
72. He L-P, Liu J-Y, Pan L, Wu J-Q, Xu B-C, Li Y-S (2009) Ethylene polymerization by the new chromium catalysts based on amino-pyrrolide ligands. J Polym Sci A Polym Chem 47:713–721
73. Ballem KHD, Shetty V, Etkin N, Patrick BO, Smith KM (2004) Chromium(III) and chromium(IV) bis(trimethylsilyl)amido complexes as ethylene polymerisation catalysts. Dalton Trans 3431–3433

74. Janse van Rensburg W, Grove C, Steynberg JP, Stark KB, Huyser JJ, Steynberg PJ (2004) A DFT study toward the mechanism of chromium-catalyzed ethylene trimerization. Organometallics 23:1207
75. Jabri A, Mason CB, Sim Y, Gambarotta S, Burchell TJ, Duchateau R (2008) Isolation of single-component trimerization and polymerization chromium catalysts: the role of the metal oxidation state. Angew Chem Int Ed 47:9717–9721
76. Vidyaratne I, Nikiforov GB, Gorelsky SI, Gambarotta S, Duchateau R, Korobkov I (2009) Isolation of a self activating ethylene trimerisation catalyst. Angew Chem Int Ed 2009:6552–6556
77. Luo H-K, Li D-G, Li S (2004) The effect of halide and the coordination geometry of chromium center in homogeneous catalyst system for ethylene trimerization. J Mol Catal A Chem 221:9–17
78. Budzelaar PHM (2009) Ethene trimerization at $Cr^{I}/Cr^{III}$—a density functional theory study. Can J Chem 87:832–837
79. McGuinness DS, Wasserscheid P, Keim W, Hu C, Englert U, Dixon JT, Grove C (2003) Novel Cr-PNP complexes as catalysts for the trimerisation of ethylene. Chem Commun 334–335
80. McGuinness DS, Wasserscheid P, Keim W, Morgan DH, Dixon JT, Bollmann A, Maumela H, Hess F, Englert U (2003) First Cr(III)-SNS complexes and their use as highly efficient catalysts for the trimerization of ethylene to 1-hexene. J Am Chem Soc 125:5272–5273
81. McGuinness DS, Wasserscheid P, Morgan DH, Dixon JT (2005) Ethylene trimerization with mixed-donor ligand (N, P, S) chromium complexes: effect of ligand structure on activity and selectivity. Organometallics 24:552–556
82. McGuinness DS, Brown DB, Tooze RP, Hess FM, Dixon JT, Slawin AMZ (2006) Ethylene trimerization with Cr-PNP and Cr-SNS complexes: effect of ligand structure, metal oxidation state, and role of activator on catalysis. Organometallics 25:3605–3610
83. Jabri A, Temple C, Crewdson P, Gambarotta S, Korobkov I, Duchateau R (2006) Role of the metal oxidation state in the SNS-Cr catalyst for ethylene trimerization: isolation of di- and trivalent cationic intermediates. J Am Chem Soc 128:9238–9247
84. Temple C, Jabri A, Crewdson P, Gambarotta S, Korobkov I, Duchateau R (2006) The question of the Cr oxidation state in the Cr(SNS) catalyst for selective ethylene trimerization: an unanticipated re-oxidation pathway. Angew Chem 118:7208–7211
85. Bluhm ME, Walter O, Döring M (2005) Chromium imine and amine complexes as homogeneous catalysts for the trimerisation and polymerisation of ethylene. J Organomet Chem 690:713–721
86. Temple CN, Gambarotta S, Korobkov I, Duchateau R (2007) New insight into the role of the metal oxidation state in controlling the selectivity of the Cr-(SNS) ethylene trimerization catalyst. Organometallics 26:4598–4603
87. Zhang J, Braunstein P, Hor TSA (2008) Highly selective chromium(III) ethylene trimerization catalysts with [NON] and [NSN] heteroscorpionate ligands. Organometallics 27:4277–4280
88. Zhang J, Li A, Hor TSA (2009) Crystallographic revelation of the role of $AlMe_3$ (in MAO) in Cr [NNN] pyrozolyl catalyzed ethylene trimerization. Organometallics 28:2935–2937
89. Zhang J, Li A, Hor TSA (2009) Ligand effect on ethylene trimerisation with [NNN]-heteroscorpionate pyrazolyl Cr(III) catalysts. Dalton Trans 9327–9333
90. Köhn RD, Haufe M, Mihan S, Lilge D (2000) Triazacyclohexane complexes of chromium as highly active homogeneous model systems for the Phillips catalyst. Chem Comm 1927–1928
91. Köhn RD, Haufe M, Kociok-Köhn G, Grimm S, Wasserscheid P, Keim W (2000) Selective trimerization of alpha-olefins with triazacyclohexane complexes of chromium as catalysts. Angew Chem Int Ed 39:4337–4339
92. Köhn RD, Smith D, Mahon MF, Prinz M, Mihan S, Kociok-Köhn G (2003) Coordination chemistry of the activation of [(triazacyclohexane)CrCl3] with [PhNMe2H][$B(C_6F_5)_4$] and $AlR_3$. J Organomet Chem 683:200

93. Ackerman LJ, Bei X, Boussie TR, Diamond GM, Hall KA, Lapointe AM, Longmire JM, Murphy VJ, Sun P, Verdugo D, Schofer S, Dias E, McConville DH, Li RT, Walzer J, Rix F, Kuchta M (2006) Methods for oligomerizing olefins. WO 2006/096881 (Exxon-Mobil)
94. McConville DH, Ackerman LJ, Li RT, Bei X, Kuchta M, Boussie TR, Walzer JF, Diamond GM, Rix FC, Hall KA, La Pointe AM, Longmire JM, Murphy VJ, Sun P, Verdugo D, Schofer S, Dias E (2006) Methods for oligomerizing olefins. WO 2006/099053 (Exxon-Mobil)
95. Ackerman LJ, Diamond GM, Hall KA, Longmire JM, Murphy VJ, Verdugo D (2008) Methods for oligomerizing olefins with chromium pyridine ether catalysts. WO 2008/085659 (Exxon-Mobil)
96. Ackerman LJ, Diamond GM, Hall KA, Longmire JM, Murphy VJ, Nava-Salgado VO (2008) Methods for oligomerizing olefins with chromium pyridine phosphino catalysts. WO 2008/085653 (Exxon-Mobil)
97. Ackerman LJ, Diamond GM, Hall KA, Longmire JM, Micklatcher M (2008) Methods for oligomerizing olefins with chromium pyridine mono-oxazoline catalysts. WO 2008/085655 (Exxon-Mobil)
98. Ackerman LJ, Diamond GM, Hall KA, Longmire JM, Murphy VJ, Verdugo D (2008) Methods for oligomerizing olefins with chromium pyridine thioether catalysts. WO 2008/085658 (Exxon-Mobil)
99. Albahily K, Koç E, Al-Baldawi D, Savard D, Gambarotta S, Burchell TJ, Duchateau R (2008) Chromium catalysts supported by a nonspectator NPN ligand: isolation of single-component chromium polymerization catalysts. Angew Chem Int Ed 47:5816–5819
100. Albahily K, Al-Baldawi D, Gambarotta S, Duchateau R, Koç E, Burchell TJ (2008) Preparation and characterization of a switchable single-component chromium trimerization catalyst. Organometallics 27:5708–5711
101. Albahily K, Al-Baldawi D, Gambarotta S, Koç E, Duchateau R (2008) Isolation of a chromium hydride single-component ethylene polymerization catalyst. Organometallics 27:5943–5947
102. McDaniel MP (1985) Supported chromium catalysts for ethylene polymerization. Adv Catal 33:47–98
103. Ruddick VJ, Badyal JPS (1998) Early stages of ethylene polymerization using the phillips $CrO_x$/silica catalyst. J Phys Chem B 102:2991–2994
104. Espelid Ø, Børve KJ (2002) Molecular-level insight into Cr/silica Phillips-type catalysts: polymerization-active dinuclear chromium sites. J Catal 206:331–338
105. Groppo E, Lamberti C, Bordiga S, Spoto G, Zecchina A (2006) In situ FTIR spectroscopy of key intermediates in the first stages of ethylene polymerization on the Cr/$SiO_2$ phillips catalyst: solving the puzzle of the initiation mechanism? J Catal 240:172–181
106. Tomov AK, Chirinos JJ, Long RJ, Gibson VC, Elsegood MRJ (2006) An unprecedented α-olefin distribution arising from a homogeneous ethylene oligomerization catalyst. J Am Chem Soc 128:7704–7705
107. McGuinness DS, Suttil JA, Gardiner MG, Davies NW (2008) Ethylene oligomerization with Cr-NHC catalysts: further insights into the extended metallacycle mechanism of chain growth. Organometallics 27:4238–4247
108. Bollmann A, Blann K, Dixon JT, Hess FM, Killian E, Maumela H, McGuinness DS, Morgan DH, Neveling A, Otto S, Overett M, Slawin AMZ, Wasserscheid P, Kuhlmann S (2004) Ethylene tetramerization: a new route to produce 1-octene in exceptionally high selectivities. J Am Chem Soc 126:14712–14713
109. McGuinness DS, Gibson VC, Steed JW (2004) Bis(cabene)pyridine complexes of the early to middle transition metals: survey of ethylene oligomerization and polymerization capability. Organometallics 23:6288–6292
110. McGuinness DS, Gibson VC, Wass DF, Steed JW (2003) Bis(carbene)pyridine complexes of Cr(III): exceptionally active catalysts for the oligomerization of ethylene. J Am Chem Soc 125:12716–12717

# Chapter 2
# Late-Transition Metal Complexes with Mixed $N^O$, $N^S$, $N^P$ Chelating Ligands for Olefin Polymerization Catalysis

**Andrea Ravasio, Laura Boggioni and Incoronata Tritto**

**Abstract** Mixed chelating ligands which contain a nitrogen donor atom in combination with P, O, or S are a novel class of frameworks for generating complexes of unusual reactivity. Complexes of group X metals (Ni and Pd) supported by these ligands are currently exploited as homogeneous catalysts for: olefin polymerization, copolymerization of olefins with functionalized monomers, olefin polymerization in uncommon solvent such as water. This chapter covers the literature on the subject.

## 2.1 Introduction

Polyolefins, namely produced by heterogenous early transition metal catalysts, are a multibillion dollar a year industry [1]. It has been more than half a century since polyethylene's commercialization, still enormous progresses have been made in the past 30 years in the polymerization with homogeneous and well defined catalysts, which lead to well controlled polymer architectures and to novel materials [2–6]. Despite these successes, the controlled copolymerization of simple olefins with polar functional monomers via the coordination–insertion mechanism has remained a challenge in the polyolefin field [7, 8]. The high oxophilicity of early transition metal catalysts (titanium, zirconium, or chromium) causes them to be poisoned by polar comonomers. Thus, great interest in late transition metal catalysts arises from their tolerance to polar molecules, which can lead to the

A. Ravasio · L. Boggioni · I. Tritto (✉)
Istituto per lo Studio delle Macromolecole (ISMAC), Consiglio Nazionale delle Ricerche (CNR), Via E. Bassini 15, 20133 Milano, Italy
e-mail: tritto@ismac.cnr.it

G. Giambastiani and J. Cámpora (eds.), *Olefin Upgrading Catalysis by Nitrogen-based Metal Complexes I*, Catalysis by Metal Complexes, 35
DOI: 10.1007/978-90-481-3815-9_2, 

copolymerization of polar vinyl monomers with non polar olefins and the copolymerization of olefins with carbon monoxide [9–13].

In the mid-1990s the first example of copolymerization of ethylene with methylacrylate by cationic Pd(II) α-diimine complexes was reported by Brookhart [14–20]. This constituted a major breakthrough that generated a great interest in this field. Now, organometallic complexes of group X metals (Ni and Pd) used as catalyst precursors in homogeneous olefin (co)polymerization are conventionally supported by nitrogen containing chelating ligands. Noteworthy are the cationic Ni- and Pd-based diimine catalysts which serve as catalysts for the polymerization of ethylene and α-olefins to high molar mass materials, with turnover frequencies (TOFs) as high as those of traditional homogeneous metallocene catalysts based on early transition metals. The key features of these systems are: (1) the highly electrophilic and cationic Ni and Pd metal centers; (2) the use of sterically encumbered diimine ligands; (3) the use of noncoordinating counterions or the use of reagents thought to produce noncoordinating counterions. Nevertheless and exactly for the same features α-diimine Ni and Pd catalysts suffer from some shortcomings in copolymerization of α-olefins with polar vinyl monomers. The cationic nature of metal center favours the coordination of polar vinyl monomers by polar functional group rather than by double bond. In addition, activators such as $AlR_3$ or methylaluminoxane (MAO) can react with the polar vinyl comonomers, leading to protected and high encumbered species or starting their homopolymerization by other mechanisms than coordination polymerization [21]. A relevant review appeared describing late transition metal catalysts containing N–N ligands [9].

Neutral hydrocarbyl Ni and Pd active species, which bear anionic chelating ancillary ligands, are proving to be the effective candidates for copolymerization reactions of olefins with polar vinyl monomers for both electronic and structural reasons which result in high functional group tolerance and easy activation. Attempts to introduce negative charge in N–N ligands resulted in poor activity and prompted the interest in the mixed ligand concept. Mixed ligands which have different chemical donor functions, such as hard and soft donor atoms or groups, find increasing use in chemistry, mainly because they often exhibit a hemilabile character in the coordination sphere of a metal complex. First and successfully applied in olefin oligomerization the mixed ligand concept is the base of Shell higher olefin process (SHOP) which exploits Ni and Pd complexes with anionic P–O ligands to produce linear olefins ($C_6$–$C_{20}$) [22–24].

Herein, we focus on nitrogen containing mixed ligands as building blocks of catalysts for olefin polymerization. We particularly focus on some notable developments on mixed N–O, N–P, and N–S supporting ligands and their uses in late transition-metal-catalyzed polymerization. Thus, this review covers families of catalysts based on mixed chelating ligands, containing nitrogen, that are active for the homopolymerization of ethylene and the copolymerization of ethylene with α-olefins and polar comonomers. Late metal catalysts not active for ethylene polymerization are not included. Catalyst syntheses, activities, and chain-growth mechanisms and the influence of these factors on the structures of the resulting polymers are discussed.

## 2.2 Mixed Ligand Concept

Mixed ligands are bi- or polydentate ligands that contain at least two different types of chemical functionality capable of binding to metal centers. There is an increasing interest in the development of these ligands, as the different features associated with each donor atom confer unique reactivity to their metal complexes [25–32]. In homogeneous catalysis these functionalities are often chosen to be very different from each other to increase the differentiation between their interactions with the metal center(s). In turn, these functionalities will influence the bonding/reactivity of the other ligands bound to the metal. Ligands containing both hard and soft donors have often been synthesized, the hope being that different and contrasting reactivity associated within the same molecule would lead to novel and unprecedented properties for the resulting metal complexes.

The greater the $\sigma$-donor ability is, the greater the $\pi$-acceptor ($\pi$-back donation from metal to ligand) capacity is in the metal complexes and thus hard in the HSAB Pearson's scale [33]. When coordinated to transition metal ions, N-ligands are generally strong $\sigma$-donors, while the $\pi$-character depends on the frameworks. Also oxygen ligands are hard while P- and S-ligands are soft. The sulfur donor ligands, which are poor $\sigma$-donor and poor $\pi$-acceptor ligands, are the softest. Phosphine ligands are generally regarded as $\sigma$-donors and $\pi$-acceptors. Mixed N–O, N–P, or N–S ligands can display quite different coordination modes compared to N–N ligands. Of particular interest is that modification of the steric and electronic properties of either the phosphine or the nitrogen donor function is expected to influence the coordination chemistry and catalysis with these systems.

Over the past 15 years, much effort has been dedicated to the development of mixed donor ligands for Ni and Pd complexes as olefin polymerization catalysts [6–10]. This class of ligands is particularly interesting because of the different *trans*-effect, as a result of different donor and acceptor properties of the two coordinating groups in the ligand. The differences of these donor atoms would offer an effective tool in targeting particular catalytic activity and comonomer discrimination even though the influence of a ligand on catalytic properties of a transition metal complex is still hard to predict. For example, complexes with P–N ligands can have the advantage of improved thermal stability in catalysis with respect to those with N–N ligands, as nickel complexes with P–N ligands showed much higher thermal stability than related diimime complexes [34, 35]. This might overcome the problem of fast catalyst deactivation at high temperatures that diimine-based catalysts suffer [36]. Alternating the donor atom on the ligand scaffold to adjust the catalyst activity, selectivity, and reactivity towards different monomers can play an important role in achieving polymers with high molar masses and novel architectures. This kind of versatility is of interest both in basic research and for catalytic applications.

Nickel and palladium complexes with mixed ligands have been used in the oligomerization [37] and polymerization of ethylene [9–11]. We will limit ourselves to the presentation of ligands which form complexes that after activation

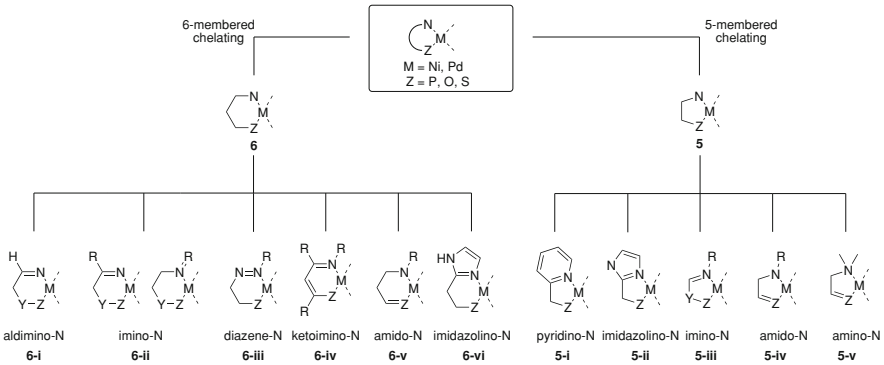


**Fig. 2.1** Organization of Ni and Pd complexes with nitrogen-based mixed ligands according to the number of terms involved in metallacycle and the nature of nitrogen donor

give polymers with relatively high molar masses. We anticipate that great part of this chapter will regard Ni and Pd transition-metal complexes with N–O ligands and their catalytic properties since those with N–P and especially with N–S mixed donor ligands have been relatively unexplored for olefin polymerization. This review organizes ligands in two main categories according to the number of terms involved in the forming metallacycles, 5- and 6-membered (Fig. 2.1), in general 4-membered rings are strained, whereas 7- or longer membered rings are not so much geometrically favoured.

### *2.2.1* N–O *Ligands*

Imino nitrogen is the most common donor function involved in 6-membered ring complexes especially for the high versatility as well as the simple synthesis that exploits conventional Schiff-base chemistry; both aldimino- (6-i) and imino-based (6-ii) complexes are of interest.

The most popular types are salicylaldimines (Fig. 2.2) on which N-aryl groups are installed via condensation reaction of proper aniline with aldehyde affording the corresponding bidentate ligand **A1**–**43**.

As carbonyl building blocks, the most studied are the salicylaldehydes [38–51], though also salicylketones appeared [52]. These scaffolds possess many sites of substitution allowing for the evaluation of both electronic and steric effects. Generally, electronic effects are investigated by introducing electron-withdrawing groups ($NO_2$, $CF_3$), electron-donating groups (OMe, $^t$Bu), or halogen atoms in both *o*- and *p*-position ($R^{1-2}$). In addition, the *o*-position ($R^1$) allows to take into account the steric effect of introducing bulky substituents such as anthracene or phenanthrene near to oxygen donor. In principle, basicity of imino-N can be directly tuned through imine backbone or indirectly by substitutes ($R^{3-4-5}$) on N-aryl moiety. These groups also play a crucial role by their steric hindrance.

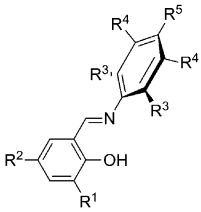

**A1**: $R^1 = R^2 = R^4 = R^5 = H$; $R^3 = {}^iPr$
**A2**: $R^1 = {}^tBu$; $R^2 = R^4 = R^5 = H$; $R^3 = {}^iPr$
**A3**: $R^1 = Ph$; $R^2 = R^4 = R^5 = H$; $R^3 = {}^iPr$
**A4**: $R^1$ = 9-phen; $R^2 = R^4 = R^5 = H$; $R^3 = {}^iPr$
**A5**: $R^1$ = 9-anth; $R^2 = R^4 = R^5 = H$; $R^3 = {}^iPr$
**A6**: $R^1 = R^4 = R^5 = H$; $R^2 = MeO$; $R^3 = {}^iPr$
**A7**: $R^1 = R^4 = R^5 = H$; $R^2 = NO_2$; $R^3 = {}^iPr$
**A8**: $R^1$ = trityl; $R^2 = R^4 = R^5 = H$; $R^3 = {}^iPr$
**A9**: $R^1$ = m-terp; $R^2 = R^4 = R^5 = H$; $R^3 = {}^iPr$
**A10**: $R^1 = R^2 = I$; $R^3 = {}^iPr$; $R^4 = R^5 = H$
**A11**: $R^1 = {}^tBu$; $R^2 = Me$; $R^3 = {}^iPr$; $R^4 = R^5 = H$
**A12**: $R^1 = R^2 = NO_2$; $R^3 = {}^iPr$; $R^4 = R^5 = H$
**A13**: $R^1 = R^2 = NO_2$; $R^3 = R^4 = R^5 = H$
**A14**: $R^1 = R^2 = I$; $R^3 = 3,5\text{-}(CF_3)_2C_6H_3$; $R^4 = R^5 = H$
**A15**: $R^1 = R^2 = I$; $R^3 = 3\text{-}NO_2C_6H_4$; $R^4 = R^5 = H$
**A16**: $R^1 = R^2 = I$; $R^3 = C_6H_5$; $R^4 = R^5 = H$
**A17**: $R^1 = R^2 = I$; $R^3 = 3,5\text{-}Me_2C_6H_3$; $R^4 = R^5 = H$
**A18**: $R^1 = R^2 = I$; $R^3 = 3,5\text{-}(MeO)_2C_6H_3$; $R^4 = R^5 = H$
**A19**: $R^1$ = Cy; $R^2$ = Me; $R^3 = {}^iPr$; $R^4 = R^5 = H$
**A20**: $R^1$ = Cy; $R^2$ = Cl; $R^3 = {}^iPr$; $R^4 = R^5 = H$
**A21**: $R^1 = R^2 = I$; $R^3 = 4\text{-}C_8F_{17}C_6H_4$; $R^4 = R^5 = H$
**A22**: $R^1 = R^2 = I$; $R^3 = 4\text{-}CF_3C_6H_4$; $R^4 = R^5 = H$
**A23**: $R^1 = R^2 = R^3 = 3,5\text{-}Me_2C_6H_3$; $R^4 = R^5 = H$
**A24**: $R^1 = R^2 = 3,5\text{-}Me_2C_6H_3$; $R^3 = 4\text{-}C_8F_{17}C_6H_4$; $R^4 = R^5 = H$
**A25**: $R^1 = R^2 = I$; $R^3 = 3,5\text{-}{}^tBu_2C_6H_3$; $R^4 = R^5 = H$
**A26**: $R^1 = R^2 = I$; $R^3 = 3,5\text{-}{}^tBu_2\text{-}4\text{-}OHC_6H_2$; $R^4 = R^5 = H$
**A27**: $R^1 = R^2 = I$; $R^3 = 3,5\text{-}Me_2\text{-}4\text{-}MeOC_6H_2$; $R^4 = R^5 = H$
**A28**: $R^1$ = 9-anth; $R^2 = R^4 = R^5 = H$; $R^3 = 3,5\text{-}(CF_3)_2C_6H_3$
**A29**: $R^1$ = 9-anth; $R^2 = R^4 = R^5 = H$; $R^3 = 3,5\text{-}{}^tBu_2C_6H_3$
**A30**: $R^1$ = 9-anth; $R^2 = R^4 = R^5 = H$; $R^3 = 3,5\text{-}{}^tBu_2\text{-}4\text{-}OHC_6H_2$
**A31**: $R^1$ = 9-anth; $R^2 = R^4 = R^5 = H$; $R^3 = 3,5\text{-}Me_2C_6H_3$
**A32**: $R^1$ = 9-anth; $R^2 = R^4 = R^5 = H$; $R^3 = 3,5\text{-}Me_2\text{-}4\text{-}MeOC_6H_2$
**A33**: $R^1$ = 9-anth; $R^2 = R^4 = R^5 = H$; $R^3 = 3,5\text{-}(MeO)_2C_6H_3$
**A34**: $R^1$ = 9-anth; $R^2 = R^4 = R^5 = H$; $R^3 = 3,4,5\text{-}(MeO)_3C_6H_2$
**A35**: $R^1 = R^4 = R^5 = H$; $R^2 = NO_2$; $R^3 = 3,5\text{-}(CF_3)_2C_6H_3$
**A36**: $R^1 = {}^tBu$; $R^2 = R^4 = R^5 = H$; $R^3 = 3,5\text{-}(CF_3)_2C_6H_3$
**A37**: $R^1 = R^2 = I$; $R^3 = 4\text{-}FC_6H_4$; $R^4 = R^5 = H$
**A38**: $R^1 = R^2 = I$; $R^3 = 4\text{-}MeC_6H_4$; $R^4 = R^5 = H$
**A39**: $R^1 = R^2 = I$; $R^3 = 4\text{-}MeOC_6H_4$; $R^4 = R^5 = H$
**A40**: $R^1 = R^2 = I$; $R^3 = 4\text{-}{}^tBuC_6H_4$; $R^4 = R^5 = H$
**A41**: $R^1 = R^2 = I$; $R^3 = 4\text{-}Me_2NC_6H_4$; $R^4 = R^5 = H$
**A42**: $R^1 = R^2 = R^3 = R^5 = R^3 = 3,5\text{-}(CF_3)_2C_6H_3$ ; $R^4 = H$
**A43**: $R^1 = NO_2$; $R^2 = R^4 = R^5 = H$; $R^3 = {}^iPr$

**Fig. 2.2** Salicylaldimine ligands reported in academic articles

Recently, another possible way to influence electronic properties of oxygen donor was introduced by replacing the anionic aryloxide moiety by a neutral pyridine N-oxide fragment affording ligands **B1-6** [53] (Fig. 2.3).

In addition, different approaches were proposed to incorporate two phenoxyimine chelating units affording binucleating ligands. Properly designed spacing units such as bisamines or bisaldehydes can be used for the purpose. Several bisamines were prepared and used as building blocks to prepare ditopic ligands [54–60]. A first class (**C1–12**) bears two amino moieties onto the same phenyl ring [54, 55]. Other spacers bearing two amino groups onto different phenyl rings were designed onto biphenyl (**C13–14**, **C17**), benzylphenyl (**C15–16**, **C18–20**), and terphenyl fragments (**C21–22**) [56]. In the bis-salicylaldimine ligand **C23** [59], which derives from the 3,3'-bisalicylaldimine scaffold, the two *o*-positions of oxygen donors are mutually hindered allowing for skipping synthetic steps to introduce bulky groups in such a crucial position. Ideally, naphthyloxy dialdehyde can be considered as constituted by two condensed salicylaldehydes. The corresponding N-aryl naphthyloxydiimine ligand **C24** possesses the unique feature of having two adjacent crabs [60] (Fig. 2.4).

Another strategy for generating imino groups in conjugation with an oxygen donor, specifically a carboxylic group, consists in reacting anthranilic acid with ketones yielding iminocarboxylato ligands **D1–3** [61] (Fig. 2.5).

**Fig. 2.3** Selected 2-iminopyridine *N*-oxides ligands

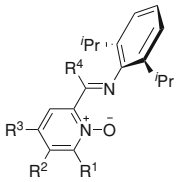

**B1**: $R^1$ = H; $R^2$ = H; $R^3$ = H; $R^4$ = Me
**B2**: $R^1$ = H; $R^2$ = H; $R^3$ = H; $R^4$ = H
**B3**: $R^1$, $R^2$ = $C_6H_4$; $R^3$ = H; $R^4$ = H
**B4**: $R^1$ = Ph; $R^2$ = H; $R^3$ = H; $R^4$ = H
**B5**: $R^1$ = H; $R^2$ = H; $R^3$ = $NO_2$; $R^4$ = H
**B6**: $R^1$ = H; $R^2$ = H; $R^3$ = MeO; $R^4$ = H

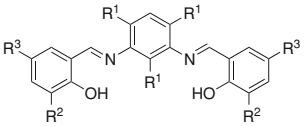

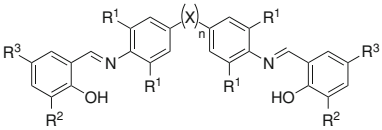

**C1**: $R^1$ = Me; $R^2$ = $^t$Bu; $R^3$ = Me
**C2**: $R^1$ = Me; $R^2$ = Ph; $R^3$ = H
**C3**: $R^1$ = Me; $R^2$ = Me; $R^3$ = H
**C4**: $R^1$ = Me; $R^2$ = $^t$Bu; $R^3$ = H
**C5**: $R^1$ = Et; $R^2$ = Me; $R^3$ = H
**C6**: $R^1$ = Et; $R^2$ = $^t$Bu; $R^3$ = H
**C7**: $R^1$ = $^i$Pr; $R^2$ = H; $R^3$ = H
**C8**: $R^1$ = $^i$Pr; $R^2$ = Me; $R^3$ = H
**C9**: $R^1$ = $^i$Pr; $R^2$ = $^t$Bu; $R^3$ = H
**C10**: $R^1$ = $^i$Pr; $R^2$ = Ph; $R^3$ = H
**C11**: $R^1$ = $^i$Pr; $R^2$ = $NO_2$; $R^3$ = $NO_2$
**C12**: $R^1$ = $^i$Pr; $R^2$ = H; $R^3$ = $NO_2$

**C13**: n = 0; $R^1$ = $^i$Pr; $R^2$ = $R^3$ = I
**C14**: n = 0; $R^1$ = 3,5-$(CF_3)_2C_6H_3$; $R^2$ = $R^3$ = I
**C15**: n = 1; X = $CH_2$; $R^1$ = $^i$Pr; $R^2$ = $R^3$ = I
**C16**: n = 1; X = $CH_2$; $R^1$ = 3,5-$(CF_3)_2C_6H_3$; $R^2$ = $R^3$ = I
**C17**: n = 0; $R^1$ = $R^2$ = $R^3$ = 3,5-$(CF_3)C_6H_3$
**C18**: n = 1; X = $CH_2$; $R^1$ = $R^2$ = $R^3$ = 3,5-$(CF_3)_2C_6H_3$
**C19**: n = 1; X = $C(CF_3)_2$; $R^1$ = $R^2$ = $R^3$ = 3,5-$(CF_3)_2C_6H_3$
**C20**: n = 1; X = $CH_2$; $R^1$ = $^i$Pr; $R^2$ = 9-Anthryl; $R^3$ = H
**C21**: n = 1; X = *o*-$C_6H_4$; $R^1$ = $^i$Pr; $R^2$ = 9-Anthryl; $R^3$ = H
**C22**: n = 1; X = *o*-$C_6H_4(C_6H_4)_2$; $R^1$ = $^i$Pr; $R^2$ = 9-Anthryl; $R^3$ = H

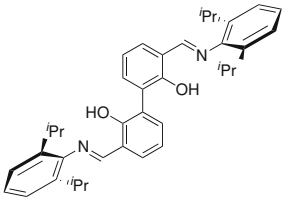

**C23**

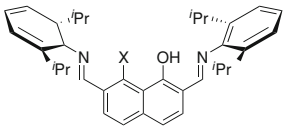

**C24**: X = OH
**C24**: X = OTMS

**Fig. 2.4** Ditopic aldimine ligands

**Fig. 2.5** Iminocarboxylic ligands

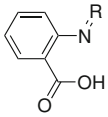

**D1**: R = cyclohexylidene
**D2**: R = $CEt_2$
**D3**: R = $CH^tBu$

Alternatively, in ligands **E1–3** the imine fragment is replaced by a diazene (-N=N-) donor function. This family of ligands can be prepared via azo coupling of aniline with aromatic alcohols. Though little explored, these scaffolds offer, at least in principle, the same versatility and availability of substitution sites of salicylaldehydes [62] (Fig. 2.6).

Also enamines, which are the tautomeric form of imines, can be considered as practical building blocks in N–O ligand synthesis. Stabilization offered by conjugated ketones affords $\beta$-ketoimines **F1–17**, that is the conjugated acid of the monoanionic chelating $\beta$-ketoiminato ligand (6-iv). Similarly to salicylaldimine,

these strong $\pi$ ligands allow for selectively tuning electronic properties and steric demand. Electron-withdrawing substituents such as $CF_3$, and $CF_3C{=}O$ are commonly added to the ketoimino backbone to reduce $\pi$-donation and enhance $\pi$-accepting abilities of the ligand, in order to increase the electrophilicity of the chelated metal. Steric bulk of the ligand can be amplified through both N-aryl moiety and $R^1$ fragment. According to the chemistry of enamines, methods of synthesis are somewhat more sophisticated than the usual Schiff condensation exploited in imine preparation and harsh conditions or activated synthones are required, especially when electron poor reagents are involved [63–68] (Fig. 2.7).

Other rare examples of 6-membered chelating ligands bear: (1) amino nitrogen in combination with an aldheyde oxygen donor (**G1**) [69]; (2) imidazole-based nitrogen donor in combination with a charged phenolato donor (**G2**) [70] (Fig. 2.8).

The length of the connecting bridge between two donor atoms in bidentate ligands plays a pivotal role in catalysis and it is tightly connected with the preferential coordination mode. The flexibility (elsewhere referred as plasticity) of a ligand can influence a catalytic reaction by stabilizing or destabilizing initial, transition, or final states and different coordination modes. In catalytic polymerization side reactions such as chain transfers, chain releasing, and displacements

**Fig. 2.6** Diazene-naphthol ligands

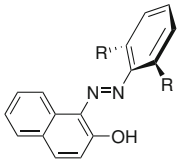


**E1**: R = H
**E2**: R = Me
**E3**: R = $^i$Pr

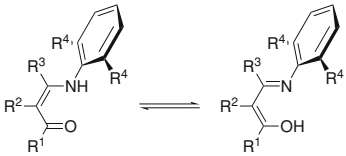


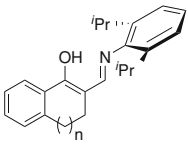


**F1**: $R^1$ = Ph; $R^2$ = H; $R^3$ = $CF_3$; $R^4$ = $^i$Pr
**F2**: $R^1$ = Ph; $R^2$ = H; $R^3$ = Me; $R^4$ = $^i$Pr
**F3**: $R^1$ = $CF_3$; $R^2$ = H; $R^3$ = Me; $R^4$ = $^i$Pr
**F4**: $R^1$ = $CF_3$; $R^2$ = $COCF_3$; $R^3$ = H; $R^4$ = $^i$Pr
**F5**: $R^1$ = $CF_3$; $R^2$ = $COCF_3$; $R^3$ = Me; $R^4$ = $^i$Pr
**F6**: $R^1$ = $CF_3$; $R^2$ = H; $R^3$ = Me; $R^4$ = $^i$Pr
**F7**: $R^1$ = $CF_3$; $R^2$ = $COCF_3$; $R^3$ = Me; $R^4$ = Me
**F8**: $R^1$ = Ph; $R^2$ = H; $R^3$ = H; $R^4$ = $^i$Pr
**F9**: $R^1$ = 2-$PhC_6H_4$; $R^2$ = H; $R^3$ = H; $R^4$ = $^i$Pr
**F10**: $R^1$ = 2-Naphtyl-$C_6H_4$; $R^2$ = H; $R^3$ = H; $R^4$ = $^i$Pr
**F11**: $R^1$ = 2-$PhC_6H_4$; $R^2$ = H; $R^3$ = Me; $R^4$ = $^i$Pr
**F12**: $R^1$ = 2-$PhC_6H_4$; $R^2$ = H; $R^3$ = $CF_3$; $R^4$ = $^i$Pr
**F13**: $R^1$ = $CF_3$; $R^2$ = $COCF_3$; $R^3$ = H; $R^4$ = 3,5-$(CF_3)_2C_6H_3$
**F14**: $R^1$ = Me; $R^2$ = CN; $R^3$ = Me; $R^4$ = $^i$Pr

**F15**: n = 0
**F16**: n = 1
**F17**: n = 2

**Fig. 2.7** Selected $\beta$-ketoimine ligands

can involve changes in catalyst geometry. Hence a limited flexibility in chelating ligand can in principle prevent side reactions and in turn increase TOF.

As a general rule, 5-membered chelated complexes are significantly more stable than the 6-membered homologs, especially for square-planar and octahedral complexes. The shorter spacer between the two donor atoms in pro-5-membered chelating ligands best meets the L-M-L angle of 90° preferred by square-planar (and octahedral) complexes. A higher thermodynamical stability prevents ligand displacement involved in catalyst deactivation pathways. Therefore, there is a strong interest in developing catalysts with N–O mixed ligands which possess a 5-membered chelate ring.

Indeed, early research on mixed N–O chelating ligands as components in polymerization catalysts refer to the very simple pyridine carboxylate ligands **H1–4** (5-i) [71, 72]. By introducing electron withdrawing or donating group onto aryl unit of ancillary chelating ligands electronic effects were considered. In any case, both the simple scaffold and the not modifiable carboxylato ligand did not allow an evaluation of steric effects. Other heterocycle-based ligands involve imidazole in combination with carboxylic (**H5–6**) and alcoholic (**H7**) donors [70] (Fig. 2.9).

While imine nitrogen donors dominate the field of 6-membered chelating ligands there are only few cases of the smaller 5-membered ring ligands involving imine as donor. A special case is represented by α-iminocarboxamide ligand **I1–9** [73–75] in which the imine donor is supported by an amide fragment. A number of these ligands was prepared by combining pyruvamides or other 2-oxo-substituted amides analogous with proper aniline. Binding mode of the ligand (N–N or N–O) depends upon the steric hindrance of aryl moieties and tends to N–O when it is sufficiently large (Fig. 2.10).

A rare neutral example of imino-based ligands is designed on the backbone of O-alkyl ester of iminohydroxamic acid. By iminoacylation of N,O-bisalkyl-hydroxylamines the corresponding bidentate ligands **L1–4** can be readily obtained [76] (Fig. 2.11).

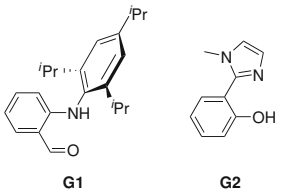


**Fig. 2.8** Aminoketone (**G1**) and 2-imidazolinophenol (**G2**) ligands

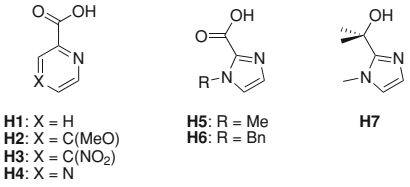


**Fig. 2.9** 5-membered chelating ligands containing N-heterocycles

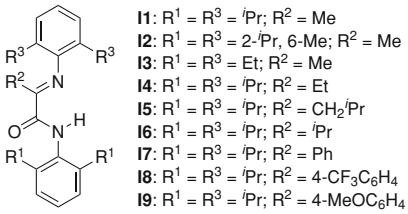


**Fig. 2.10** α-imino-carboxamide ligands

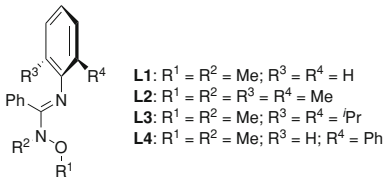


**Fig. 2.11** Bisalkyl-hydroxylamines ligands

More frequent are the ligands that bear vinylogous amido nitrogen donors (5-iii). This family includes 2-anilinotropone-based ligands **M1–14** whose synthesis exploits the palladium catalyzed cross-coupling of aniline with 2-triflatotropone [77–79]. Several variations can be introduced by using hindered or electron poor N-aryl group and modified tropone skeleton. A similar synthetic approach was reported for the preparation of anilinoperinaphthenone-based ligands **N1-2** [80]. These ligands possess as additional feature the impossibility of delocalizing a negative charge onto oxygen donor upon deprotonation (Fig. 2.12).

Similar ligands can be prepared by using hydroxyquinones as carbonyl building blocks. Reaction with proper amine by vinylogous nucleophilic substitution readily affords the mono **O1–4** [81, 82] or binucleating **P1–5** ligands [83]. Also classical α-amino carboxylates can be in principle used as N–O-chelate ligands **Q1–4** (Fig. 2.13).

### *2.2.2* N–P *and* N–S *Ligands*

Imino groups can be tethered to a phosphine-based donor function affording bidentate iminophosphine ligands **R1–9**. They constitute important chiral P–N bidentate ligands for asymmetric catalysis by metal complexes [37] and appear in patents regarding olefin polymerization [85, 86]. These ligands are readily prepared by Schiff condensation of the corresponding amine and the aldehyde bearing the phosphine group. Besides sites of substitution on aromatic scaffold of the ligand also substituents at the phosphorus atom are accessible [87–89]. Alternatively the P donor can be combined with an amide fragment affording the diphenylphosphanylbenzamide ligand **S1–5** [90] (Fig. 2.14).

Pyridine-based 5-membered chelating ligands **T1–2** were prepared by Suzuki coupling of chloropicoline with mesitylboronic acid followed by diarylphospinylation at the α-position (Fig. 2.15).

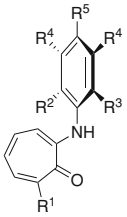

**M1**: $R^1 = R^4 = R^5 = H$; $R^2 = R^3 = Me$
**M2**: $R^1 = R^4 = R^5 = H$; $R^2 = R^3 = {}^iPr$
**M3**: $R^1 = R^2 = R^4 = R^5 = H$; $R^3 = {}^tBu$
**M4**: $R^1 = R^4 = R^5 = H$; $R^2 = Me$; $R^3 = {}^tBu$
**M5**: $R^1 = R^4 = R^5 = H$; $R^2 = R^3 = Ph$
**M6**: $R^1 = R^4 = R^5 = H$; $R^2 = R^3 = Cl$
**M7**: $R^1 = R^4 = R^5 = H$; $R^2 = R^3 = Br$
**M8**: $R^1 = H$; $R^2 = R^3 = R^4 = R^5 = F$
**M9**: $R^1 = R^2 = R^3 = R^5 = H$; $R^4 = CF_3$
**M10**: $R^1 = R^3 = R^4 = R^5 = H$; $R^2 = Me$
**M11**: $R^1 = R^4 = R^5 = H$; $R^2 = Me$; $R^3 = CF_3$
**M12**: $R^1 = R^4 = R^5 = H$; $R^2 = R^3 = F$
**M13**: $R^1 = Ph$; $R^2 = R^3 = {}^iPr$; $R^4 = R^5 = H$
**M14**: $R^1$ = 1-Naphtyl; $R^2 = R^3 = {}^iPr$; $R^4 = R^5 = H$

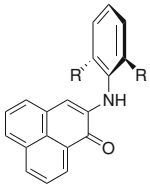

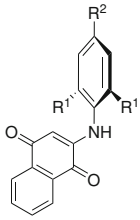

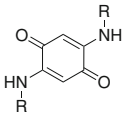

**N1**: R = Me
**N2**: R = ${}^iPr$

**O1**: $R^1 = {}^iPr$; $R^2 = H$
**O2**: $R^1 = Me$; $R^2 = H$
**O3**: $R^1 = Me$; $R^2 = Me$
**O4**: $R^1 = Et$; $R^2 = H$

**P1**: R = 2,6-${}^iPr_2C_6H_3$
**P2**: R = 2,6-$Me_2C_6H_3$
**P3**: R = 1-Naphtyl
**P4**: R = Ph
**P5**: R = Cy

**Fig. 2.12** Vinylogous amido-based ligands

**Q1**: R = H
**Q2**: R = ${}^tBu$
**Q3**: R = Ph
**Q4**: R = $CH_2$(3-Indolyl)

**Fig. 2.13** α-aminoacids investigated as ligands for catalysts for ethylene polymerization

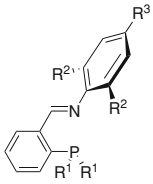

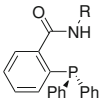

**R1**: $R^1 = Ph$; $R^2 = R^3 = H$
**R2**: $R^1 = Ph$; $R^2 = Me$; $R^3 = H$
**R3**: $R^1 = Ph$; $R^2 = {}^iPr$; $R^3 = H$
**R4**: $R^1 = 4\text{-}MeOC_6H_4$; $R^2 = {}^iPr$; $R^3 = H$
**R5**: $R^1 = 3\text{-}MeOC_6H_4$; $R^2 = {}^iPr$; $R^3 = H$
**R6**: $R^1 = 2\text{-}MeOC_6H_4$; $R^2 = H$; $R^3 = Cl$
**R7**: $R^1 = 2\text{-}MeOC_6H_4$; $R^2 = H$; $R^3 = H$
**R8**: $R^1 = 2\text{-}MeOC_6H_4$; $R^2 = H$; $R^3 = OMe$
**R9**: $R^1 = 2\text{-}MeOC_6H_4$; $R^2 = {}^iPr$; $R^3 = H$

**S1**: R = Ph
**S2**: R = ${}^tBu$
**S3**: R = H
**S4**: R = Pr
**S5**: R = ${}^iPr$

**Fig. 2.14** Iminophosphine (**R1-9**) and diphenylphosphanylbenzamide (**S1-5**) ligands

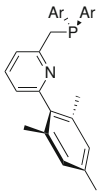


**T1**: Ar = 2,4,6-$Me_3C_6H_2$
**T2**: Ar = 2-$MeC_6H_4$

**Fig. 2.15** Selected pyridinophosphine ligands

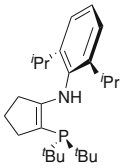


**U1**

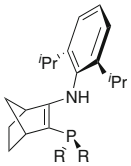


**U2**: R = $^t$Bu
**U3**: R = Ph

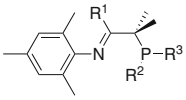


**V1**: $R^1$ = Ph; $R^2$ = $R^3$ = Me
**V2**: $R^1$ = $R^2$ = $R^3$ = Ph
**V3**: $R^1$ = H; $R^2$ = Me; $R^3$ = 2,4,5-$Me_3C_6H_2$
**V4**: $R^1$ = Ph; $R^2$ = Me; $R^3$ = 2,4,5-$Me_3C_6H_2$
**V5**: $R^1$ = Ph; $R^2$ = $R^3$ = 2-$MeC_6H_4$

**Fig. 2.16** R-phosphine enamines (**U1-3**) and phosphinoimine (**V1-5**) ligands

Imino nitrogen can be also tethered to a phosphine moiety through a bridging group in 5-membered chelating ligands. A family of ligands, which exists as R-phosphine enamines before complexation to Ni(II) or Pd(II) and affords phosphine imine by tautomerization, was successfully prepared by nucleophilic substitution of bisalkylchlorophosphine by imine anions [91]. Monocyclic (**U1**) and bicyclic (**U2–3**) backbones were used to enhance the conformational rigidity and prevent ligand displacement [34]. Both bulky *ortho* substituents on the aniline moieties and bulky phosphines were introduced to supply the steric requirement that is crucial for obtaining high molar mass polymers.

Nonenolizable bulky phosphine imine bidentate ligands **V1–5** [35] can be prepared by installing a *gem*-dimethyl group $\alpha$ to phosphorus. Ligands can be obtained by direct nucleophilic attack of the azaenolate to the phosphorus electrophiles $R_2PCl$ (R = Me, Ph). In the case of higher hindered mesityl-substituted-P compounds the azaenolate was reacted with $MesPCl_2$ followed by the Grignard reagent MeMgBr to introduce other substituents on phosphorous. Otherwise, reaction occurred at both carbon and nitrogen of the azaenolate, yielding a mixture of isomers. The purity and yield of the ligands can be estimated from the $^{31}P$ NMR spectra (Fig. 2.16).

Ideally, the most straightforward modification of diimine ligands consists in replacing one imine moiety with a phosphinidine. Nucleophilic attack of deprotonated imine to mesityl-$PCl_2$ followed by elimination of HCl affords ligands **W1–2** (Fig. 2.17) [92] .

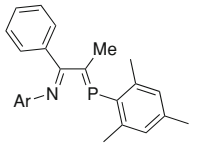


**W1**: Ar = 2,6-$^{i}Pr_2C_6H_3$
**W2**: Ar = 2,4,6-$Me_3C_6H_2$

**Fig. 2.17** Phosphinidine-imine-based ligands

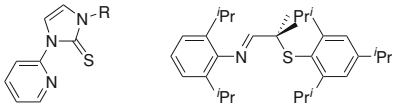


**X1**: R = $^{t}Bu$
**X2**: R = 2,6-$^{i}PrC_6H_3$

**Y1**

**Fig. 2.18** Imidazole-2-thione (**X1-2**) and imine-sulfide (**Y1**) ligands

Despite the intensive research on catalysts with hard-and-soft mixed ligands for olefin oligomerization or polymerization, examples of N–S ligands remain scarce (Fig. 2.18. A family of 6-membered chelating ligands combines pyridine donor with imidazole-2-thione moieties affording the corresponding bidentate N–S ligands **X1–2** [93].

The single case of a 5-membered chelating ligand refers to the imine-sulfide ligand **Y1**, which is prepared from the condensation of the corresponding $\alpha$-thioaldehyde with 2,6-diisopropylaniline [92].

## 2.3 Group X Metal Complexes

Ni and Pd compounds with mixed ligands (N–Z) exploited as catalysts for olefin (co)polymerization are generally 16 electron square planar complexes. Asymmetry of the chelating mixed ligand as well as diversity of the ligands completing the coordination sphere of the metal cause distortion of complexes from ideal square planar geometry ($D_{4h}$). Definitely, one of the key features of these complexes is *trans*-effect, and in turn *trans*-influence. The former drives their synthesis and final structure, the latter deeply influences their reactivity. Different synthetic approaches are used to prepare Ni and Pd complexes with mixed ligands depending on the nature of the ligand as well as the features of the final complex (Fig. 2.19).

Even dihalide complexes are seldom achieved by direct ligand addition to dihalide metal salt (I). They are in general synthesized by ligand displacement reaction between the chelating ligand and a proper metal precursor, containing an isoelectronic labile bidentate ligand such as dme or tmeda (IIa). The major driving force is the higher stability furnished by $\pi$-accepting frameworks in chelating ligand with respect to the pure $\sigma$-donors in the ligand precursors.

Hydrocarbyl complexes are generally prepared by using alkyl-containing metal sources rather than converting the dihalo-compounds into the corresponding metal

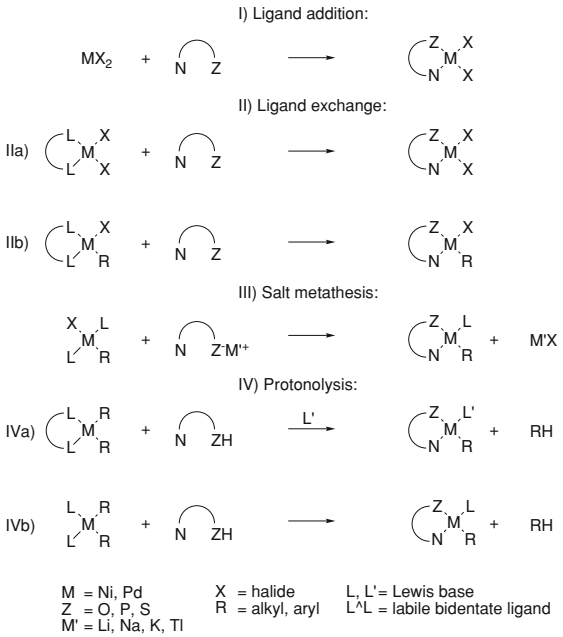


**Fig. 2.19** General synthetic routes to Ni and Pd complexes with N–Z ligands

alkyls by nucleophilic attack. This avoids the partial reduction of metal with consequent loss of mixed chelating ligand or undesired reactions of mixed ligand with the alkylating agent.

The selection of the metal precursor depends on the charge of mixed chelating ligand, which influences the method of synthesis employed. Thus, neutral mixed ligands can be installed by ligand exchange on metal precursors (IIb) built with an alkyl fragment (R), an anionic donor such as halide (X), and a leaving neutral chelating ligand (L–L). In the resulting hydrocarbyl complexes the alkyl fragment will possess a *cis*-anionic donor.

Most commonly, the installing mixed ligands are anionic ($N–Z^{-}$) and synthesis occurs via salt metathesis (III) or protonolysis (IV).

Salt metathesis (III) between precursor and the salt of anionic ligand, which is commonly obtained by deprotonation with alkali hydride, is the most used synthesis for complexes containing mixed ligands, one alkyl group, and a Lewis base. In this case the precursor should be able to lose one anionic ligand ($X^{-}$), which is eliminated as salt, commonly an alkaline halide salt, and a neutral ligand that is replaced by the mixed chelating ligand. Trans labilizing effect of the alkyl group drives the synthesis and the resulting complex contains the nitrogen ligand trans to the Lewis base, with few exceptions, due to high steric hindrance.

Alternatively, the protonolysis approach uses acid ligands and bis-hydrocarbyl precursors affording the desired organometallic complexes by sacrificing one hydrocarbyl ligand. This strategy is frequently accomplished by a concomitant ligand exchange to substitute a bidentate Lewis base with a monodentate ligand

(IVa). Otherwise, Lewis bases can be already present in the precursor and displaced by the neutral fragment of the mixed ligand (IVb). Again, trans effect affords complexes with nitrogen ligands trans to the Lewis bases.

The reported methods for the synthesis of Ni and Pd complexes are summarized in Fig. 2.19 and they will be referred with the corresponding keys in Table 2.1.

## 2.4 Application in Homogeneous Catalyzed Polymerization

### *2.4.1 Activation*

The Ni and Pd complexes with mixed N–O, N–S, and N–P chelating ligands listed in Table 2.1 are catalyst precursors which need to be activated to yield the species active for the polymerization. Such N–Z ligands must be coordinated to the metal also in the active species to effectively control catalyst selectivity and activity via steric and electronic interactions.

In general, it is the cationic form of organometallic complexes that is of interest in polymerizations, generated from catalyst precursors by activation with a cocatalyst. The most frequently used cocatalysts are aluminoxanes such as MAO or derivatives (MMAO) [94, 95]. The role of MAO includes alkylation of dihalides, subsequent abstraction of a ligand to form the cationic complex, and the scavenging of impurities. Other important cocatalysts for precursors containing alkyl or aryl ligands are perfluorinated boranes, such as $B(C_6F_5)_3$ and $[Ph_3C][B(C_6F_5)_4]$. Often aluminum alkyls ($AlR_3$ with R = $^{i}$Bu, $n$-$C_6H_{13}$) are employed together with the cocatalyst.

All Ni and Pd dihalide catalyst precursors with neutral N–Z ligands and in some case even the more sophisticated precursors bearing anionic N–Z ligands, which are already alkylated, can be activated by aluminum-based cocatalysts (Fig. 2.20). Discrete cationic alkyl complexes of palladium and nickel are synthesized by reaction with a variety of salts of noncoordinating anions to yield cationic organometallic species.

In the general structure the 'stabilizing' ligands L allows for facile removal from the metal center, e.g. by displacement by coordination of olefin monomer; L is most often neutral, while the ligand R bound to the metal via a carbon atom enables facile entry into the catalytic cycle. When the cationic species is generated in situ in the presence of the olefin, the L′ may also be a solvent molecule or the olefin monomer. $Y^-$ is very weakly or non-coordinating to avoid interactions with the metal center, leading e.g. to displacement of labile ligands L′ or to strong coordination blocking the sites during catalysis. As alkyl complexes of late transition metals easily give $\beta$-hydride elimination, often R alkyl substituents do not have $\beta$-H atoms, or for steric reasons do not allow $\beta$-H eliminations. Anyhow, among the listed precursors halo and alkyl complexes activated as metallocenes and diimine catalysts are rare.

**Table 2.1** Synthetic routes to Ni and Pd complexes with N–O, N–P, and N–S ligands

| Metal precursor | | Ligand | Method | Catalyst | No. | References |
|---|---|---|---|---|---|---|
| *6-membered chelated complexes with N–O ligands* | | | | | | |
| | | 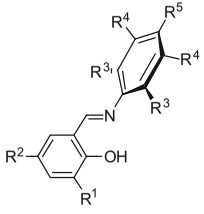 | | 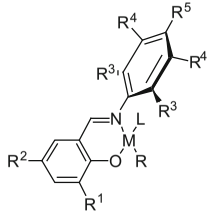 | | |
| $[NiCl(Ph)(PPh_3)_2]$ | **A1** | $R^1 = R^2 = R^4 = R^5 = H$; $R^3 = {}^iPr$ | III | [Ni(**A1**)Ph($PPh_3$)] | **1** | [38] |
| | **A2** | $R^1 = {}^tBu$; $R^2 = R^4 = R^5 = H$; $R^3 = {}^iPr$ | | [Ni(**A2**)Ph($PPh_3$)] | **2** | |
| | **A3** | $R^1 = Ph$; $R^2 = R^4 = R^5 = H$; $R^3 = {}^iPr$ | | [Ni(**A3**)Ph($PPh_3$)] | **3** | |
| | **A4** | $R^1$ = 9-phen; $R^2 = R^4 = R^5 = H$; $R^3 = {}^iPr$ | | [Ni(**A4**)Ph($PPh_3$)] | **4** | |
| | **A5** | $R^1$ = 9-anth; $R^2 = R^4 = R^5 = H$; $R^3 = {}^iPr$ | | [Ni(**A5**)Ph($PPh_3$)] | **5** | |
| | **A6** | $R^1 = R^4 = R^5 = H$; $R^2 = MeO$; $R^3 = {}^iPr$ | | [Ni(**A6**)Ph($PPh_3$)] | **6** | |
| | **A7** | $R^1 = R^4 = R^5 = H$; $R^2 = NO_2$; $R^3 = {}^iPr$ | | [Ni(**A7**)Ph($PPh_3$)] | **7** | |
| $[Ni(tmeda)Me_2]$ | **A5** | $R^1$ = 9-anth; $R^2 = R^4 = R^5 = H$; $R^3 = {}^iPr$ | IVa | [Ni(**A5**)Me(MeCN)] | **8** | [39] |
| | **A8** | $R^1$ = trityl; $R^2 = R^4 = R^5 = H$; $R^3 = {}^iPr$ | | [Ni(**A8**)Me(MeCN)] | **9** | |
| | **A9** | $R^1$ = *m*-terp; $R^2 = R^4 = R^5 = H$; $R^3 = {}^iPr$ | | [Ni(**A9**)Me(MeCN)] | **10** | |
| $[NiCl(Ph)(PPh_3)_2]$ | **A10** | $R^1 = R^2 = I$; $R^3 = {}^iPr$; $R^4 = R^5 = H$ | II | [Ni(**A10**)Ph($PPh_3$)] | **11** | [40] |
| $[Ni(tmeda)Me_2]$ | **A10** | | IVa | [Ni(**A10**)Me(py)] | **12** | |

(continued)

**Table 2.1** (continued)

| Metal precursor | | Ligand | Method | Catalyst | No. | References |
|---|---|---|---|---|---|---|
| $[Ni(\eta^3\text{-}C_3H_5)Br]_2$ | **A11** | $R^1 = {}^t$Bu; $R^2$ = Me; $R^3 = {}^i$Pr; $R^4 = R^5$ = H | a | $[Ni_2(\mathbf{A11})_2(\mu\text{-}OH)_2]$ | **13** | [41] |
| $NiBr_2*6H_2O$ | **A11** | | I | $[Ni_2(\mathbf{A11})_2(\mu\text{-}OH)_2]$ | **13** | |
| $[Ni(acac)_2]$ | **A11** | | IIa | [Ni(**A11**)(acac)] | **14** | |
| $[Ni(dme)Br_2]$ | **A11** | | b | $[Ni(\mathbf{A11})_2]$ | **15** | |
| $[Ni(dme)Cl_2]$ | **A11** | | c | $[Ni(\mathbf{A11})Me]^+$ (in situ) | **16** | |
| $[Ni(cod)_2]$ | **A3** | $R^1$ = Ph; $R^2 = R^4 = R^5$ = H; $R^3 = {}^i$Pr | d | [Ni(**A3**)(cod)] | **17** | [42] |
| | **A7** | $R^1 = R^4 = R^5$ = H; $R^2 = NO_2$; $R^3 = {}^i$Pr | | [Ni(**A7**)(cod)] | **18** | |
| | **A12** | $R^1 = R^2 = NO_2$; $R^3 = {}^i$Pr; $R^4 = R^5$ = H | | [Ni(**A12**)(cod)] | **19** | |
| | **A13** | $R^1 = R^2 = NO_2$; $R^3 = R^4 = R^5$ = H | | [Ni(**A13**)(cod)] | **20** | |
| $[Ni(tmeda)Me_2]$ | **A14** | $R^1 = R^2$ = I; $R^3 = 3,5\text{-}(CF_3)_2C_6H_3$; $R^4 = R^5$ = H | IVa | [Ni(**A14**)Me(py)] | **21** | [44] |
| | **A15** | $R^1 = R^2$ = I; $R^3 = 3\text{-}NO_2C_6H_4$; $R^4 = R^5$ = H | | [Ni(**A15**)Me(py)] | **22** | |
| | **A16** | $R^1 = R^2$ = I; $R^3$ = Ph; $R^4 = R^5$ = H | | [Ni(**A16**)Me(py)] | **23** | |
| | **A17** | $R^1 = R^2$ = I; $R^3 = 3,5\text{-}Me_2C_6H_3$; $R^4 = R^5$ = H | | [Ni(**A17**)Me(py)] | **24** | |
| | **A18** | $R^1 = R^2$ = I; $R^3 = 3,5\text{-}(MeO)_2C_6H_3$; $R^4 = R^5$ = H | | [Ni(**A18**)Me(py)] | **25** | |
| $[NiCl(Ph)(PPh_3)_2]$ | **A19** | $R^1$ = Cy; $R^2$ = Me; $R^3 = {}^i$Pr; $R^4 = R^5$ = H | III | [Ni(**A19**)Ph($PPh_3$)] | **26** | [45] |
| $[NiCl(Ph)(PPh_3)_2]$ | **A20** | $R^1$ = Cy; $R^2$ = Cl; $R^3 = {}^i$Pr; $R^4 = R^5$ = H | III | [Ni(**A20**)Ph($PPh_3$)] | **27** | [46] |
| $[Ni(tmeda)Me_2]$ | **A21** | $R^1 = R^2$ = I; $R^3 = 4\text{-}C_8F_{17}C_6H_4$; $R^4 = R^5$ = H | IVa | [Ni(**A21**)Me(py)] | **28** | [47] |

(continued)

**Table 2.1** (continued)

| Metal precursor | | Ligand | Method | Catalyst | No. | References |
|---|---|---|---|---|---|---|
| | **A22** | $R^1 = R^2 = I$; $R^3 = 4\text{-}CF_3C_6H_4$; $R^4 = R^5 = H$ | | [Ni(**A22**)Me(py)] | **29** | |
| | **A23** | $R^1 = R^2 = R^3 = 3,5\text{-}Me_2C_6H_3$; $R^4 = R^5 = H$ | | [Ni(**A23**)Me(py)] | **30** | |
| | **A24** | $R^1 = R^2 = 3,5\text{-}Me_2C_6H_3$; $R^3 = 4\text{-}C_8F_{17}C_6H_4$; $R^4 = R^5 = H$ | | [Ni(**A24**)Me(py)] | **31** | |
| [Ni(tmeda)$Me_2$] | **A5** | $R^1$ = 9-anth; $R^2 = R^4 = R^5 = H$; $R^3 = {}^iPr$ | IVa | [Ni(**A5**)Me(py)] | **32** | [48] |
| | **A25** | $R^1 = R^2 = I$; $R^3 = 3,5\text{-}{}^tBu_2C_6H_3$; $R^4 = R^5 = H$ | | [Ni(**A25**)Me(py)] | **33** | |
| | **A26** | $R^1 = R^2 = I$; $R^3 = 3,5\text{-}{}^tBu_2\text{-}4\text{-}OHC_6H_2$; $R^4 = R^5 = H$ | | [Ni(**A26**)Me(py)] | **34** | |
| | **A27** | $R^1 = R^2 = I$; $R^3 = 3,5\text{-}Me_2\text{-}4\text{-}MeOC_6H_2$; $R^4 = R^5 = H$ | | [Ni(**A27**)Me(py)] | **35** | |
| | **A28** | $R^1$ = 9-anth; $R^2 = R^4 = R^5 = H$; $R^3 = 3,5\text{-}(CF_3)_2C_6H_3$ | | [Ni(**A28**)Me(py)] | **36** | |
| | **A29** | $R^1$ = 9-anth; $R^2 = R^4 = R^5 = H$; $R^3 = 3,5\text{-}{}^tBu_2C_6H_3$ | | [Ni(**A29**)Me(py)] | **37** | |
| | **A30** | $R^1$ = 9-anth; $R^2 = R^4 = R^5 = H$; $R^3 = 3,5\text{-}{}^tBu_2\text{-}4\text{-}OHC_6H_2$ | | [Ni(**A30**)Me(py)] | **38** | |
| | **A31** | $R^1$ = 9-anth; $R^2 = R^4 = R^5 = H$; $R^3 = 3,5\text{-}Me_2C_6H_3$ | | [Ni(**A31**)Me(py)] | **39** | |
| | **A32** | $R^1$ = 9-anth; $R^2 = R^4 = R^5 = H$; $R^3 = 3,5\text{-}Me_2\text{-}4\text{-}MeOC_6H_2$ | | [Ni(**A32**)Me(py)] | **40** | |

(continued)

**Table 2.1** (continued)

| Metal precursor | Ligand | Method | Catalyst | No. | References |
|---|---|---|---|---|---|
| | **A33** $R^1$ = 9-anth; $R^2 = R^4 = R^5$ = H; $R^3$ = 3,5-$(MeO)_2C_6H_3$ | | [Ni(**A33**)Me(py)] | **41** | |
| | **A34** $R^1$ = 9-anth; $R^2 = R^4 = R^5$ = H; $R^3$ = 3,4,5-$(MeO)_3C_6H_2$ | | [Ni(**A34**)Me(py)] | **42** | |
| | **A35** $R^1 = R^4 = R^5$ = H; $R^2 = NO_2$; $R^3$ = 3,5-$(CF_3)_2C_6H_3$ | | [Ni(**A35**)Me(py)] | **43** | |
| | **A36** $R^1 = {}^t$Bu; $R^2 = R^4 = R^5$ = H; $R^3$ = 3,5-$(CF_3)_2C_6H_3$ | | [Ni(**A36**)Me(py)] | **44** | |
| $[Ni(py)_2Me_2]$ | **A25** $R^1 = R^2$ = I; $R^3$ = 3,5-${}^t$Bu$_2$C$_6$H$_3$; $R^4 = R^5$ = H | IVb | [Ni(**A25**)Me(py)] | **33** | |
| | **A26** $R^1 = R^2$ = I; $R^3$ = 3,5-${}^t$Bu$_2$-4-OHC$_6$H$_2$; $R^4 = R^5$ = H | | [Ni(**A26**)Me(py)] | **34** | |
| | **A27** $R^1 = R^2$ = I; $R^3$ = 3,5-Me$_2$-4-MeOC$_6$H$_2$; $R^4 = R^5$ = H | | [Ni(**A27**)Me(py)] | **35** | |
| | **A28** $R^1$ = 9-anth; $R^2 = R^4 = R^5$ = H; $R^3$ = 3,5-$(CF_3)_2C_6H_3$ | | [Ni(**A28**)Me(py)] | **36** | |
| | **A29** $R^1$ = 9-anth; $R^2 = R^4 = R^5$ = H; $R^3$ = 3,5-${}^t$Bu$_2$C$_6$H$_3$ | | [Ni(**A29**)Me(py)] | **37** | |
| | **A30** $R^1$ = 9-anth; $R^2 = R^4 = R^5$ = H; $R^3$ = 3,5-${}^t$Bu$_2$-4-OHC$_6$H$_2$ | | [Ni(**A30**)Me(py)] | **38** | |
| | **A32** $R^1$ = 9-anth; $R^2 = R^4 = R^5$ = H; $R^3$ = 3,5-Me$_2$-4-MeOC$_6$H$_2$ | | [Ni(**A32**)Me(py)] | **40** | |

(continued)

**Table 2.1** (continued)

| Metal precursor | | Ligand | Method | Catalyst | No. | References |
|---|---|---|---|---|---|---|
| | **A33** | $R^1$ = 9-anth; $R^2 = R^4 = R^5$ = H; $R^3$ = 3,5-$(MeO)_2C_6H_3$ | | [Ni(**A33**)Me(py)] | **41** | |
| | **A34** | $R^1$ = 9-anth; $R^2 = R^4 = R^5$ = H; $R^3$ = 3,4,5-$(MeO)_3C_6H_2$ | | [Ni(**A34**)Me(py)] | **42** | |
| [Ni(tmeda)$Me_2$] | **A37** | $R^1 = R^2$ = I; $R^3$ = 4-$FC_6H_4$; $R^4 = R^5$ = H | IVa | [Ni(**A37**)Me(py)] | **45** | [49] |
| | **A38** | $R^1 = R^2$ = I; $R^3$ = 4-$MeC_6H_4$; $R^4 = R^5$ = H | IVa | [Ni(**A38**)Me(py)] | **46** | |
| | **A39** | $R^1 = R^2$ = I; $R^3$ = 4-$MeOC_6H_4$; $R^4 = R^5$ = H | | [Ni(**A39**)Me(py)] | **47** | |
| | **A40** | $R^1 = R^2$ = I; $R^3$ = 4-$^t$Bu$C_6H_4$; $R^4 = R^5$ = H | | [Ni(**A40**)Me(py)] | **48** | |
| | **A41** | $R^1 = R^2$ = I; $R^3$ = 4-$Me_2NC_6H_4$; $R^4 = R^5$ = H | | [Ni(**A41**)Me(py)] | **49** | |
| [Ni(tmeda)$Me_2$] | **A42** | $R^1 = R^2 = R^3 = R^5$ = 3,5-$(CF_3)_2C_6H_3$; $R^4$ = H | IVa | [Ni(**A42**)Me(py)] | **50** | [50] |
| [Ni(tmeda)$Me_2$] | **A5** | $R^1$ = 9-anth; $R^2 = R^4 = R^5$ = H; $R^3$ = $^i$Pr | IVb | [Ni(**A5**)Me(tmeda)] | **51** | |
| | **A14** | $R^1 = R^2$ = I; $R^3$ = 3,5-$(CF_3)_2C_6H_3$; $R^4 = R^5$ = H | | [Ni(**A14**)Me(tmeda)] | **52** | |
| | **A23** | $R^1 = R^2 = R^3$ = 3,5-$Me_2C_6H_3$; $R^4 = R^5$ = H | | [Ni(**A23**)Me(tmeda)] | **53** | |
| | **A42** | $R^1 = R^2 = R^3$ = 3,5-$Me_2C_6H_3$; $R^4 = R^5$ = H | | [Ni(**A42**)Me(tmeda)] | **54** | |
| [NiCl(Ph)$(PPh_3)_2$] | **A43** | $R^1 = NO_2$; $R^2 = R^4 = R^5$ = H; $R^3$ = $^i$Pr | III | [Ni(**A43**)Ph$(PPh_3)$] | **55** | [51] |
| [NiCl($\eta^1$-$CH_2$Ph)$(PMe_3)_2$] | **A5** | $R^1$ = 9-anth; $R^2 = R^4 = R^5$ = H; $R^3$ = $^i$Pr | III | [Ni(**A5**)($\eta^1$-$CH_2$Ph)$(PMe_3)$] | **56** | [58] |
| [NiCl(Me)$(PMe_3)_2$] | **A2** | $R^1$ = $^t$Bu; $R^2 = R^4 = R^5$ = H; $R^3$ = $^i$Pr | III | [Ni(**A2**)(Me)$(PMe_3)$] | **57** | [60] |

(continued)

**Table 2.1** (continued)

| Metal precursor | Ligand | | Method | Catalyst | No. | References |
|---|---|---|---|---|---|---|
| $[NiCl(1\text{-naph})(PPh_3)_2]$ | **A2** | | III | [Ni(**A2**)(1-naph)($PPh_3$)] | **58** | |
| $[Ni(tmeda)Me_2]$ | **A14** | $R^1 = R^2 = I$; $R^3 = 3,5\text{-}(CF_3)_2C_6H_3$; $R^4 = R^5 = H$ | IVa | [Ni(**A14**)Me(tppts)] | **59** | [103] |
| | **A14** | | | [Ni(**A14**)Me(tppds)] | **60** | |
| | **A14** | | | [Ni(**A14**)Me($H_2N$-PEG-OMe)] | **61** | |
| | **A26** | $R^1 = R^2 = I$; $R^3 = 3,5\text{-}^tBu_2\text{-}4\text{-}OHC_6H_2$; $R^4 = R^5 = H$ | | [Ni(**A26**)Me(tppts)] | **61** | |
| | **A26** | | | [Ni(**A26**)Me(tppds)] | **62** | |
| | **A28** | $R^1$ = 9-anth; $R^2 = R^4 = R^5 = H$; $R^3 = 3,5\text{-}(CF_3)_2C_6H_3$ | | [Ni(**A28**)Me(tppts)] | **63** | |
| | **A28** | | | [Ni(**A28**)Me($H_2N$-PEG-OMe)] | **64** | |
| | **A30** | $R^1$ = 9-anth; $R^2 = R^4 = R^5 = H$; $R^3 = 3,5\text{-}^tBu_2\text{-}4\text{-}OHC_6H_2$ | | [Ni(**A30**)Me(tppts)] | **65** | |
| | **A30** | | | [Ni(**A30**)Me($H_2N$-PEG-OMe)] | **66** | |
| $[Ni(tmeda)Me_2]$ | **A14** | $R^1 = R^2 = I$; $R^3 = 3,5\text{-}(CF_3)_2C_6H_3$; $R^4 = R^5 = H$ | IVa | [Ni(**A14**)Me(pta)] | **67** | [104] |
| | **A14** | | | [Ni(**A14**)Me(hmta)] | **68** | |
| | **A14** | | | [Ni(**A14**)Me(3-$Et_4NO_3S\text{-}C_5H_4N$)] | **69** | |
| $[Ni(tmeda)Me_2]$ | **A14** | $R^1 = R^2 = I$; $R^3 = 3,5\text{-}(CF_3)_2C_6H_3$; $R^4 = R^5 = H$ | IVa | [Ni(**A14**)Me(dmso)] | **70** | [107] |
| [Ni(**A14**)Cl($PMe_3$)] | **A14** | | e | [Ni(**A14**)H($PMe_3$)] | **71** | |

(continued)

**Table 2.1** (continued)

| Metal precursor | | Ligand | Method | Catalyst | No. | References |
|---|---|---|---|---|---|---|
| [Ni(**A14**)Me(dmso)] | **A14** | 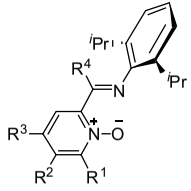 | f | [Ni(**A14**)Et(dmso)] 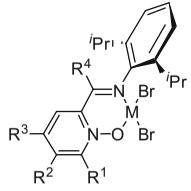 | **72** | |
| [Ni(dme)$Br_2$] | **B1** | $R^1 = R^2 = R^3 = H$; $R^4 = Me$ | IIa | [Ni(**B1**)$Br_2$] | **73** | [53] |
| | **B2** | $R^1 = R^2 = R^3 = R^4 = H$ | | [Ni(**B2**)$Br_2$] | **74** | |
| | **B3** | $R^1,R^2 = C_6H_4$; $R^3 = R^4 = H$ | | [Ni(**B3**)$Br_2$] | **75** | |
| | **B4** | $R^1 = Ph$; $R^2 = R^3 = R^4 = H$ | | [Ni(**B4**)$Br_2$] | **76** | |
| | **B5** | $R^1 = R^2 = R^4 = H$; $R^3 = NO_2$ | | [Ni(**B5**)$Br_2$] | **77** | |
| | **B6** | $R^1 = R^2 = R^4 = H$; $R^3 = MeO$ | | [Ni(**B6**)$Br_2$] | **78** | |
| $PdBr_2$ | **B4** | $R^1 = Ph$; $R^2 = R^3 = R^4 = H$ 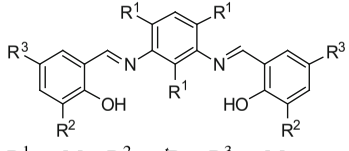 | I | [Pd(**B4**)$Br_2$] 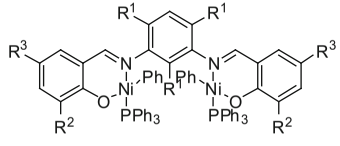 | **79** | [53] |
| [NiCl(Ph)($PPh_3$)$_2$] | **C1** | $R^1 = Me$; $R^2 = {}^tBu$; $R^3 = Me$ | III | [$Ni_2$(**C1**)(Ph)$_2$($PPh_3$)$_2$] | **80** | [54] |

(continued)

**Table 2.1** (continued)

| Metal precursor | | Ligand | Method | Catalyst | No. | References |
|---|---|---|---|---|---|---|
| | **C2** | $R^1$ = Me; $R^2$ = Ph; $R^3$ = H | | [$Ni_2$(**C2**)$(Ph)_2(PPh_3)_2$] | **81** | |
| [$NiCl(Ph)(PPh_3)_2$] | **C3** | $R^1$ = Me; $R^2$ = Me; $R^3$ = H | III | [$Ni_2$(**C3**)$(Ph)_2(PPh_3)_2$] | **82** | [55] |
| | **C4** | $R^1$ = Me; $R^2$ = $^t$Bu; $R^3$ = H | | [$Ni_2$(**C4**)$(Ph)_2(PPh_3)_2$] | **83** | |
| | **C5** | $R^1$ = Et; $R^2$ = Me; $R^3$ = H | | [$Ni_2$(**C5**)$(Ph)_2(PPh_3)_2$] | **84** | |
| | **C6** | $R^1$ = Et; $R^2$ = $^t$Bu; $R^3$ = H | | [$Ni_2$(**C6**)$(Ph)_2(PPh_3)_2$] | **85** | |
| | **C7** | $R^1$ = $^i$Pr; $R^2$ = $R^3$ = H | | [$Ni_2$(**C7**)$(Ph)_2(PPh_3)_2$] | **86** | |
| | **C8** | $R^1$ = $^i$Pr; $R^2$ = Me; $R^3$ = H | | [$Ni_2$(**C8**)$(Ph)_2(PPh_3)_2$] | **87** | |
| | **C9** | $R^1$ = $^i$Pr; $R^2$ = $^t$Bu; $R^3$ = H | | [$Ni_2$(**C9**)$(Ph)_2(PPh_3)_2$] | **88** | |
| | **C10** | $R^1$ = $^i$Pr; $R^2$ = Ph; $R^3$ = H | | [$Ni_2$(**C10**)$(Ph)_2(PPh_3)_2$] | **89** | |
| | **C11** | $R^1$ = $^i$Pr; $R^2$ = $R^3$ = $NO_2$ | | [$Ni_2$(**C11**)$(Ph)_2(PPh_3)_2$] | **90** | |
| | **C12** | $R^1$ = $^i$Pr; $R^2$ = H; $R^3$ = $NO_2$ | | [$Ni_2$(**C12**)$(Ph)_2(PPh_3)_2$] | **91** | |
| | | 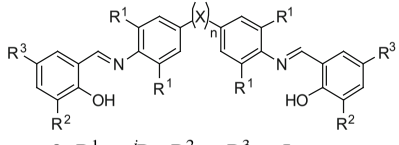 | | 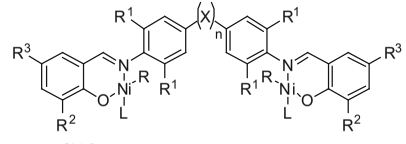 | | |
| [$Ni(py)_2Me_2$] | **C13** | n = 0; $R^1$ = $^i$Pr; $R^2$ = $R^3$ = I | IVb | [$Ni_2$(**C13**)$Me_2(py)_2$] | **92** | [56] |
| | **C14** | n = 0; $R^1$ = 3,5-$(CF_3)_2C_6H_3$; $R^2$ = $R^3$ = I | | [$Ni_2$(**C14**)$Me_2(py)_2$] | **93** | |
| | **C15** | n = 1; X = $CH_2$; $R^1$ = $^i$Pr; $R^2$ = $R^3$ = I | | [$Ni_2$(**C15**)$Me_2(py)_2$] | **94** | |
| | **C16** | n = 1; X = $CH_2$; $R^1$ = 3,5-$(CF_3)_2C_6H_3$; $R^2$ = $R^3$ = I | | [$Ni_2$(**C16**)$Me_2(py)_2$] | **95** | |

(continued)

**Table 2.1** (continued)

| Metal precursor | | Ligand | Method | Catalyst | No. | References |
|---|---|---|---|---|---|---|
| $[Ni(tmeda)Me_2]$ | **C14** | n = 0; $R^1$ = 3,5-$(CF_3)_2C_6H_3$; $R^2 = R^3$ = I | IVb | $[Ni_2(\mathbf{C14})Me_2(tmeda)_2]$ | **96** | [56] |
| $[Ni(py)_2Me_2]$ | **C17** | n = 0; $R^1 = R^2 = R^3$ = 3,5-$(CF_3)C_6H_3$ | IVb | $[Ni_2(\mathbf{C17})Me_2(py)_2]$ | **97** | [57] |
| | **C18** | n = 1; X = $CH_2$; $R^1 = R^2 = R^3$ = 3,5-$(CF_3)_2C_6H_3$ | | $[Ni_2(\mathbf{C18})Me_2(py)_2]$ | **98** | |
| | **C19** | n = 1; X = $C(CF_3)_2$; $R^1 = R^2 = R^3$ = 3,5-$(CF_3)_2C_6H_3$ | | $[Ni_2(\mathbf{C19})Me_2(py)_2]$ | **99** | |
| $[Ni(\eta^3\text{-}CH_2Ph)Cl(PMe_3)]$ | **C20** | n = 1; X = $CH_2$; $R^1$ = $^i$Pr; $R^2$ = 9-Anth; $R^3$ = H | III | $[Ni_2(\mathbf{C20})(\eta^1\text{-}CH_2Ph)(PMe_3)_2]$ | **100** | [58] |
| | **C21** | n = 1; X = o-$C_6H_4$; $R^1$ = $^i$Pr; $R^2$ = 9-Anth; $R^3$ = H | | $[Ni_2(\mathbf{C21})(\eta^1\text{-}CH_2Ph)(PMe_3)_2]$ | **101** | |
| | **C22** | n = 1; X = o-$C_6H_4(C_6H_4)_2$; $R^1$ = $^i$Pr; $R^2$ = 9-Anth; $R^3$ = H | | $[Ni_2(\mathbf{C22})(\eta^1\text{-}CH_2Ph)(PMe_3)_2]$ | **102** | |
| | | 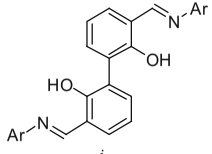 | | 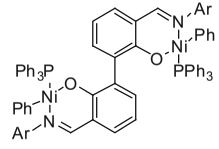 | | |
| $[NiCl(Ph)(PPh_3)_2]$ | **C23** | Ar = 2,6-$^i$Pr$C_6H_3$ | III | $[Ni_2(\mathbf{C23})(Ph)_2(PPh_3)_2]$ | **103** | [59] |
| | | 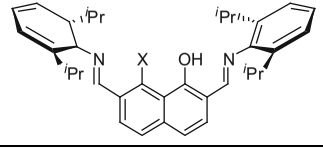 | | 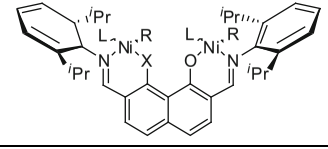 | | |

(continued)

**Table 2.1** (continued)

| Metal precursor | | Ligand | Method | Catalyst | No. | References |
|---|---|---|---|---|---|---|
| $[NiClMe(PMe_3)_2]$ | **C24** | X = OH | III | $[Ni_2(\mathbf{C24})Me_2(PMe_3)_2]$ | **104** | [60] |
| $[NiClMe(PPh_3)_2]$ | **C24** | X = OH | | $[Ni_2(\mathbf{C24})Me_2(PPh_3)_2]$ | **105** | |
| $[NiCl(1\text{-naph})(PPh_3)_2]$ | **C24** | X = OH | | $[Ni_2(\mathbf{C24})(1\text{-naph})_2(PPh_3)_2]$ | **106** | |
| | **C25** | X = OTMS | | $[Ni(\mathbf{C25})(1\text{-naph})(PPh_3)]$ | **107** | |
| | | 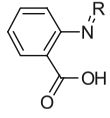 | | 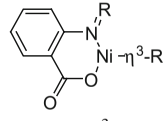 | | |
| $[Ni(\eta^3\text{-}CH_2CMeCH_2)Cl]_2$ | **D1** | R = cyclohexylidene | III | $[Ni(\mathbf{D1})(\eta^3\text{-}CH_2CMeCH_2)]$ | **108** | [61] |
| $[Ni(\eta^3\text{-}CH_2Ph)Cl(PMe_3)]$ | **D1** | | | $[Ni(\mathbf{D1})(\eta^3\text{-}CH_2Ph)]$ | **109** | |
| | **D2** | R = $CEt_2$ | | $[Ni(\mathbf{D2})(\eta^3\text{-}CH_2Ph)]$ | **110** | |
| | | 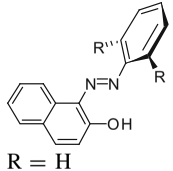 | | 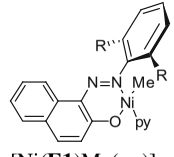 | | |
| $[Ni(tmeda)Me_2]$ | **E1** | R = H | IVa | $[Ni(\mathbf{E1})Me(py)]$ | **111** | [62] |
| | **E2** | R = Me | | $[Ni(\mathbf{E2})Me(py)]$ | **112** | |
| | **E3** | R = $^i$Pr | | $[Ni(\mathbf{E3})Me(py)]$ | **113** | |
| | | 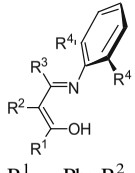 | | 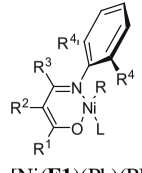 | | |
| $[NiCl(Ph)(PPh_3)_2]$ | **F1** | $R^1$ = Ph; $R^2$ = H; $R^3$ = $CF_3$; $R^4$ = $^i$Pr | III | $[Ni(\mathbf{F1})(Ph)(PPh_3)]$ | **114** | [63] |
| | **F2** | $R^1$ = Ph; $R^2$ = H; $R^3$ = Me; $R^4$ = $^i$Pr | | $[Ni(\mathbf{F2})(Ph)(PPh_3)]$ | **115** | |

(continued)

**Table 2.1** (continued)

| Metal precursor | | Ligand | Method | Catalyst | No. | References |
|---|---|---|---|---|---|---|
| | **F3** | $R^1 = CF_3$; $R^2 = H$; $R^3 = Me$; $R^4 = {}^iPr$ | | [Ni(**F3**)(Ph)($PPh_3$)] | **116** | |
| [NiCl(Ph)($PPh_3$)$_2$] | **F4** | $R^1 = CF_3$; $R^2 = COCF_3$; $R^3 = H$; $R^4 = {}^iPr$ | III | [Ni(**F4**)(Ph)($PPh_3$)] | **117** | [64] |
| | **F5** | $R^1 = CF_3$; $R^2 = COCF_3$; $R^3 = Me$; $R^4 = {}^iPr$ | | [Ni(**F5**)(Ph)($PPh_3$)] | **118** | |
| | **F6** | $R^1 = CF_3$; $R^2 = H$; $R^3 = Me$; $R^4 = {}^iPr$ | | [Ni(**F6**)(Ph)($PPh_3$)] | **119** | |
| | **F7** | $R^1 = CF_3$; $R^2 = COCF_3$; $R^3 = Me$; $R^4 = Me$ | | [Ni(**F7**)(Ph)($PPh_3$)] | **120** | |
| [NiCl(Ph)($PPh_3$)$_2$] | **F8** | $R^1 = Ph$; $R^2 = H$; $R^3 = H$; $R^4 = {}^iPr$ | III | [Ni(**F8**)(Ph)($PPh_3$)] | **121** | [65] |
| | **F9** | $R^1 = 2\text{-}PhC_6H_4$; $R^2 = H$; $R^3 = H$; $R^4 = {}^iPr$ | | [Ni(**F9**)(Ph)($PPh_3$)] | **122** | |
| | **F10** | $R^1 = 2\text{-}Naph\text{-}C_6H_4$; $R^2 = H$; $R^3 = H$; $R^4 = {}^iPr$ | | [Ni(**F10**)(Ph)($PPh_3$)] | **123** | |
| | **F11** | $R^1 = 2\text{-}PhC_6H_4$; $R^2 = H$; $R^3 = Me$; $R^4 = {}^iPr$ | | [Ni(**F11**)(Ph)($PPh_3$)] | **124** | |
| | **F12** | $R^1 = 2\text{-}PhC_6H_4$; $R^2 = H$; $R^3 = CF_3$; $R^4 = {}^iPr$ | | [Ni(**F12**)(Ph)($PPh_3$)] | **125** | |
| [Ni(tmeda)$Me_2$] | **F4** | $R^1 = CF_3$; $R^2 = COCF_3$; $R^3 = H$; $R^4 = {}^iPr$ | IVa | [Ni(**F4**)Me(py)] | **126** | [66] |
| | **F13** | $R^1 = CF_3$; $R^2 = COCF_3$; $R^3 = H$; $R^4 = 3,5\text{-}(CF_3)_2C_6H_3$ | | [Ni(**F13**)Me(py)] | **127** | |
| [Ni(**F13**)Me(py)] | **F13** | | g | [Ni(**F13**)Me($PPh_3$)$_2$] | **128** | |
| [Ni($\eta^1$-$CH_2Ph$)Cl($PMe_3$)$_2$] | **F14** | $R^1 = Me$; $R^2 = CN$; $R^3 = Me$; $R^4 = {}^iPr$ | III | [$Ni_2$(**F14**)($\eta^1$-$CH_2Ph$)($PMe_3$)$_2$] | **129** | [67] |

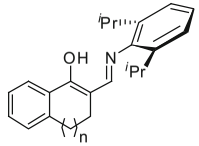


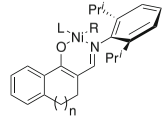


(continued)

**Table 2.1** (continued)

| Metal precursor | | Ligand | Method | Catalyst | No. | References |
|---|---|---|---|---|---|---|
| $[NiCl(Ph)(PPh_3)_2]$ | **F15** | $n = 0$ | III | [Ni(**F15**)(Ph)(PPh$_3$)] | **130** | [68] |
| | **F16** | $n = 1$ | II | [Ni(**F16**)(Ph)(PPh$_3$)] | **131** | |
| | **F17** | $n = 2$ | | [Ni(**F17**)(Ph)(PPh$_3$)] | **132** | |
| $[Ni(py)_2Me_2]$ | **F15** | $n = 0$ | IVb | [Ni(**F15**)Me(py)] | **133** | [68] |
| | **F16** | $n = 1$ | | [Ni(**F16**)Me(py)] | **134** | |
| | **F17** | $n = 2$ | | [Ni(**F17**)Me(py)] | **135** | |
| | | 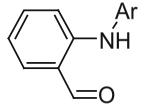 | | 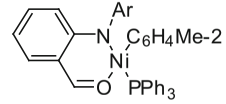 | | |
| $[NiCl(2\text{-}MeC_6H_4)(PPh_3)_2]$ | **G1** | Ar = 2,4,6-$^i$Pr$_3$C$_6$H$_2$ | III | [Ni(**G1**)(2-MeC$_6$H$_4$)(PPh$_3$)] | **136** | [69] |
| | | 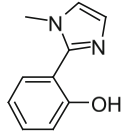 | | 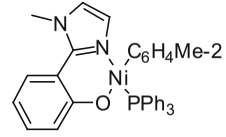 | | |
| $[NiBr(2\text{-}MeC_6H_4)(PPh_3)_2]$ | **G2** | | II | [Ni(**G2**)(2-MeC$_6$H$_4$)(PPh$_3$)] | **137** | [70] |
| *5-membered chelated complexes with N–O ligands* | | | | | | |
| | | 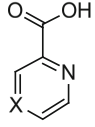 | | 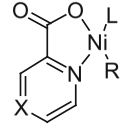 | | |
| $[NiX(2\text{-}MeC_6H_4)(PPh_3)_2]$ | **H1** | X = H | III | [Ni(**H1**)(2-MeC$_6$H$_4$)(PPh$_3$)] | **138** | [71] |

(continued)

**Table 2.1** (continued)

| Metal precursor | | Ligand | Method | Catalyst | No. | References |
|---|---|---|---|---|---|---|
| [NiX(2-MeC$_6$H$_4$)(P{CH$_2$Ph}$_3$)$_2$] | **H1** | | | [Ni(**H1**)(2-MeC$_6$H$_4$)(P{CH$_2$Ph}$_3$)] | **139** | |
| [NiX(2-MeC$_6$H$_4$)(PMePh$_2$)$_2$] | **H1** | | | [Ni(**H1**)(2-MeC$_6$H$_4$)(PMePh$_2$)] | **140** | |
| [NiX(2-MeC$_6$H$_4$)(PMe$_2$Ph)$_2$] | **H1** | | | [Ni(**H1**)(2-MeC$_6$H$_4$)(PMe$_2$Ph)] | **141** | |
| [NiX(2-MeC$_6$H$_4$)(PCy$_3$)$_2$] | **H1** | | | [Ni(**H1**)(2-MeC$_6$H$_4$)(PCy$_3$)] | **142** | |
| [NiX(4-MeC$_6$H$_4$)(PPh$_3$)$_2$] | **H1** | | | [Ni(**H1**)(4-MeC$_6$H$_4$)(PPh$_3$)] | **143** | |
| [NiX(Ph)(PPh$_3$)$_2$] | **H1** | | | [Ni(**H1**)(Ph)(PPh$_3$)] | **144** | |
| [NiX(2,4,6-Me$_3$C$_6$H$_4$)(PPh$_3$)$_2$] | **H1** | | | [Ni(**H1**)(2-MeC$_6$H$_4$)(PPh$_3$)] | **145** | |
| [NiX(2-MeC$_6$H$_4$)(PPh$_3$)$_2$] | **H2** | X = C(OMe) | III | [Ni(**H2**)(2-MeC$_6$H$_4$)(PPh$_3$)] | **146** | [72] |
| [NiX(2-MeC$_6$H$_4$)(PPh$_3$)$_2$] | **H3** | X = C(NO$_2$) | | [Ni(**H3**)(2-MeC$_6$H$_4$)(PPh$_3$)] | **147** | |
| [NiX(2-MeC$_6$H$_4$)(PPh$_3$)$_2$] | **H4** | X = N | | [Ni(**H4**)(2-MeC$_6$H$_4$)(PPh$_3$)] | **148** | |
| | | 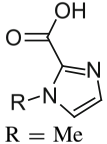 | | 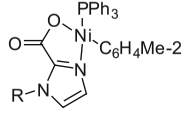 | | |
| [NiBr(2-MeC$_6$H$_4$)(PPh$_3$)$_2$] | **H5** | R = Me | III | [Ni(**H5**)(2-MeC$_6$H$_4$)(PPh$_3$)] | **149** | [70] |
| | **H6** | R = Bn | | [Ni(**H6**)(2-MeC$_6$H$_4$)(PPh$_3$)] | **150** | |
| | | 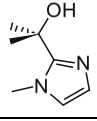 | | 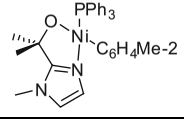 | | |

(continued)

**Table 2.1** (continued)

| Metal precursor | | Ligand | Method | Catalyst | No. | References |
|---|---|---|---|---|---|---|
| $[NiBr(2\text{-}MeC_6H_4)(PPh_3)_2]$ | **H7** | 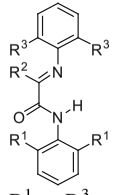 | II | $[Ni(\mathbf{H7})(2\text{-}MeC_6H_4)(PPh_3)]$ 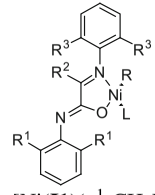 | **151** | [70] |
| $[Ni(\eta^1\text{-}CH_2Ph)Cl(PMe_3)_2]$ | **I1** | $R^1 = R^3 = {}^iPr$; $R^2 = Me$ | III | $[Ni(\mathbf{I1})(\eta^1\text{-}CH_2Ph)(PMe_3)]$ | **152** | [73] |
| $[Ni(\eta^1\text{-}CH_2Ph)Cl(PMe_3)_2]$ | **I2** | $R^1 = R^3 = 2\text{-}{}^iPr,6\text{-}Me$; $R^2 = Me$ | III | $[Ni(\mathbf{I2})(\eta^1\text{-}CH_2Ph)(PMe_3)]$ | **153** | [74] |
| | **I3** | $R^1 = R^3 = Et$; $R^2 = Me$ | | $[Ni(\mathbf{I3})(\eta^1\text{-}CH_2Ph)(PMe_3)]$ | **154** | |
| $[Ni(\eta^1\text{-}CH_2Ph)Cl(py)_2]$ | **I1** | $R^1 = R^3 = {}^iPr$; $R^2 = Me$ | III | $[Ni(\mathbf{I1})(\eta^1\text{-}CH_2Ph)(py)]$ | **155** | [96] |
| $[Ni(\eta^1\text{-}CH_2Ph)Cl(2,6\text{-}lu))_2]$ | **I1** | | | $[Ni(\mathbf{I1})(\eta^1\text{-}CH_2Ph)(2,6\text{-}lu)]$ | **156** | |
| $[Ni(\eta^1\text{-}C{=}OPh)Cl(py)_2]$ | **I1** | | | $[Ni(\mathbf{I1})(\eta^1\text{-}C{=}OPh)(py)]$ | **157** | |
| $[Ni(\eta^1\text{-}CH_2Ph)Cl(PMe_3)_2]$ | **I4** | $R^1 = R^3 = {}^iPr$; $R^2 = Et$ | III | $[Ni(\mathbf{I4})(\eta^1\text{-}CH_2Ph)(PMe_3)]$ | **158** | [75] |
| | **I5** | $R^1 = R^3 = {}^iPr$; $R^2 = CH_2{}^iPr$ | | $[Ni(\mathbf{I5})(\eta^1\text{-}CH_2Ph)(PMe_3)]$ | **159** | |
| | **I6** | $R^1 = R^2 = R^3 = {}^iPr$ | | $[Ni(\mathbf{I6})(\eta^1\text{-}CH_2Ph)(PMe_3)]$ | **160** | |
| | **I7** | $R^1 = R^3 = {}^iPr$; $R^2 = Ph$ | | $[Ni(\mathbf{I7})(\eta^1\text{-}CH_2Ph)(PMe_3)]$ | **161** | |
| | **I8** | $R^1 = R^3 = {}^iPr$; $R^2 = 4\text{-}CF_3C_6H_4$ | | $[Ni(\mathbf{I8})(\eta^1\text{-}CH_2Ph)(PMe_3)]$ | **162** | |

(continued)

**Table 2.1** (continued)

| Metal precursor | | Ligand | Method | Catalyst | No. | References |
|---|---|---|---|---|---|---|
| | **I9** | $R^1 = R^3 = {}^i$Pr; $R^2 = 4\text{-MeOC}_6H_4$ | | [Ni(**I9**)($\eta^1$-$CH_2Ph$)($PMe_3$)] | **163** | |
| | | 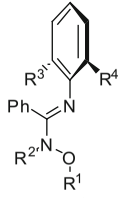 | | 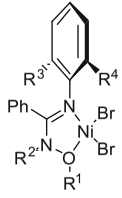 | | |
| [Ni(dme)$Br_2$] | **L1** | $R^1 = R^2 = $ Me; $R^3 = R^4 = $ H | IIa | [Ni(**L1**)$Br_2$] | **164** | [76] |
| | **L2** | $R^1 = R^2 = R^3 = R^4 = $ Me | | [Ni(**L2**)$Br_2$] | **165** | |
| | **L3** | $R^1 = R^2 = $ Me; $R^3 = R^4 = {}^i$Pr | | [Ni(**L3**)$Br_2$] | **166** | |
| | **L4** | $R^1 = R^2 = $ Me; $R^3 = $ H; $R^4 = $ Ph | | [Ni(**L4**)$Br_2$] | **167** | |
| | | 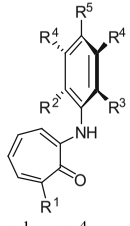 | | 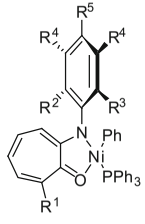 | | |
| [NiCl(Ph)($PPh_3$)$_2$] | **M1** | $R^1 = R^4 = R^5 = $ H; $R^2 = R^3 = $ Me | III | [Ni(**M1**)(Ph)($PPh_3$)] | **168** | [79] |
| | **M2** | $R^1 = R^4 = R^5 = $ H; $R^2 = R^3 = {}^i$Pr | | [Ni(**M2**)(Ph)($PPh_3$)] | **169** | [78] |
| | **M3** | $R^1 = R^4 = R^5 = $ H; $R^2 = R^3 = {}^t$Bu | | [Ni(**M3**)(Ph)($PPh_3$)] | **170** | [79] |
| | **M4** | $R^1 = R^4 = R^5 = $ H; $R^2 = $ Me; $R^3 = {}^t$Bu | | [Ni(**M4**)(Ph)($PPh_3$)] | **171** | |

(continued)

**Table 2.1** (continued)

| Metal precursor | | Ligand | Method | Catalyst | No. | References |
|---|---|---|---|---|---|---|
| | **M5** | $R^1 = R^4 = R^5 = H$; $R^2 = R^3 = Ph$ | | [Ni(**M5**)(Ph)($PPh_3$)] | **172** | |
| | **M6** | $R^1 = R^4 = R^5 = H$; $R^2 = R^3 = Cl$ | | [Ni(**M6**)(Ph)($PPh_3$)] | **173** | |
| | **M7** | $R^1 = R^4 = R^5 = H$; $R^2 = R^3 = Br$ | | [Ni(**M7**)(Ph)($PPh_3$)] | **174** | |
| | **M8** | $R^1 = H$; $R^2 = R^3 = R^4 = R^5 = F$ | | [Ni(**M8**)(Ph)($PPh_3$)] | **175** | |
| | **M9** | $R^1 = R^2 = R^3 = R^5 = H$; $R^4 = CF_3$ | | [Ni(**M9**)(Ph)($PPh_3$)] | **176** | |
| | **M10** | $R^1 = R^3 = R^4 = R^5 = H$; $R^2 = Me$ | | [Ni(**M10**)(Ph)($PPh_3$)] | **177** | |
| | **M11** | $R^1 = R^4 = R^5 = H$; $R^2 = Me$; $R^3 = CF_3$ | | [Ni(**M11**)(Ph)($PPh_3$)] | **178** | |
| | **M12** | $R^1 = R^4 = R^5 = H$; $R^2 = R^3 = F$ | | [Ni(**M12**)(Ph)($PPh_3$)] | **179** | |
| | **M13** | $R^1 = Ph$; $R^2 = R^3 = {}^iPr$; $R^4 = R^5 = H$ | | [Ni(**M13**)(Ph)($PPh_3$)] | **180** | |
| | **M14** | $R^1$ = 1-naph; $R^2 = R^3 = {}^iPr$; $R^4 = R^5 = H$ | | [Ni(**M14**)(Ph)($PPh_3$)] | **181** | |
| [Ni(M2)Cl($PPh_3$)] | **M2** | $R^1 = R^4 = R^5 = H$; $R^2 = R^3 = {}^iPr$ | h | [Ni(**M2**)($\eta^1$-$C_6H_{13}$)($PPh_3$)] | **182** | [107] |
| | | 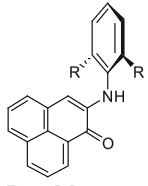 | | 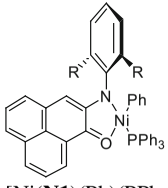 | | |
| [NiCl(Ph)($PPh_3$)$_2$] | **N1** | R = Me | III | [Ni(**N1**)(Ph)($PPh_3$)] | **183** | [80] |
| | **N2** | R = ${}^iPr$ | | [Ni(**N2**)(Ph)($PPh_3$)] | **184** | |
| | | 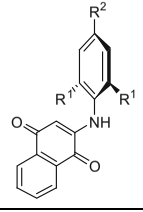 | | 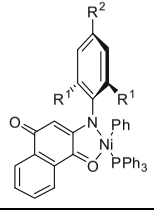 | | |

(continued)

**Table 2.1** (continued)

| Metal precursor | | Ligand | Method | Catalyst | No. | References |
|---|---|---|---|---|---|---|
| $[NiCl(Ph)(PPh_3)_2]$ | **O1** | $R^1 = {}^iPr$; $R^2 = H$ | III | $[Ni(\mathbf{O1})(Ph)(PPh_3)]$ | **185** | [81] |
| $[NiCl(Ph)(PPh_3)_2]$ | **O2** | $R^1 = Me$; $R^2 = H$ | III | $[Ni(\mathbf{O2})(Ph)(PPh_3)]$ | **186** | [82] |
| | **O3** | $R^1 = R^2 = Me$ | | $[Ni(\mathbf{O3})(Ph)(PPh_3)]$ | **187** | |
| | **O4** | $R^1 = Et$; $R^2 = H$ | | $[Ni(\mathbf{O4})(Ph)(PPh_3)]$ | **188** | |
| | | 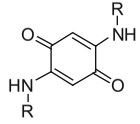 | | 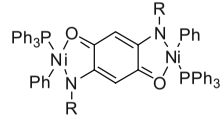 | | |
| $[NiCl(Ph)(PPh_3)_2]$ | **P1** | $R = 2,6\text{-}{}^iPr_2C_6H_3$ | III | $[Ni_2(\mathbf{P1})(Ph)_2(PPh_3)_2]$ | **189** | [83] |
| | **P2** | $R = 2,6\text{-}Me_2C_6H_3$ | | $[Ni_2(\mathbf{P2})(Ph)_2(PPh_3)_2]$ | **190** | |
| | **P3** | R = 1-naph | | $[Ni_2(\mathbf{P3})(Ph)_2(PPh_3)_2]$ | **191** | |
| | **P4** | R = Ph | | $[Ni_2(\mathbf{P4})(Ph)_2(PPh_3)_2]$ | **192** | |
| | **P5** | R = Cy | | $[Ni_2(\mathbf{P5})(Ph)_2(PPh_3)_2]$ | **193** | |
| | |  | | 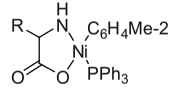 | | |
| $[NiBr(2\text{-}MeC_6H_4)(PPh_3)_2]$ | **Q1** | R = H | III | $[Ni(\mathbf{Q1})(2\text{-}MeC_6H_4)(PPh_3)]$ | **194** | [84] |
| | **Q2** | R = ${}^tBu$ | | $[Ni(\mathbf{Q2})(2\text{-}MeC_6H_4)(PPh_3)]$ | **195** | |
| | **Q3** | R = Ph | | $[Ni(\mathbf{Q3})(2\text{-}MeC_6H_4)(PPh_3)]$ | **196** | |
| | **Q4** | $R = CH_2(3\text{-Indolyl})$ | | $[Ni(\mathbf{Q4})(2\text{-}MeC_6H_4)(PPh_3)]$ | **197** | |

(continued)

**Table 2.1** (continued)

| Metal precursor | | Ligand | Method | Catalyst | No. | References |
|---|---|---|---|---|---|---|
| *6-membered chelated complexes with N–P ligands* | | | | | | |
| | | 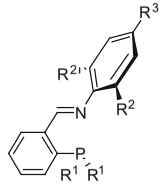 | | 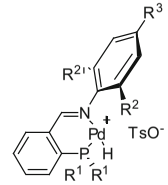 | | |
| $Pd(OAc)_2$ | **R1** | $R^1$ = Ph; $R^2$ = $R^3$ = H | i | [Pd(**R1**)H(TsO)] (in situ) | **198** | [89] |
| | **R2** | $R^1$ = Ph; $R^2$ = Me; $R^3$ = H | | [Pd(**R2**)H(TsO)] (in situ) | **199** | |
| | **R3** | $R^1$ = Ph; $R^2$ = $^i$Pr; $R^3$ = H | | [Pd(**R3**)H(TsO)] (in situ) | **200** | |
| | **R4** | $R^1$ = 4-$MeOC_6H_4$; $R^2$ = $^i$Pr; $R^3$ = H | | [Pd(**R4**)H(TsO)] (in situ) | **201** | |
| | **R5** | $R^1$ = 3-$MeOC_6H_4$; $R^2$ = $^i$Pr; $R^3$ = H | | [Pd(**R5**)H(TsO)] (in situ) | **202** | |
| | **R6** | $R^1$ = 2-$MeOC_6H_4$; $R^2$ = H; $R^3$ = Cl | | [Pd(**R6**)H(TsO)] (in situ) | **203** | |
| | **R7** | $R^1$ = 2-$MeOC_6H_4$; $R^2$ = H; $R^3$ = H | | [Pd(**R7**)H(TsO)] (in situ) | **204** | |
| | **R8** | $R^1$ = 2-$MeOC_6H_4$; $R^2$ = H; $R^3$ = OMe | | [Pd(**R8**)H(TsO)] (in situ) | **205** | |
| | **R9** | $R^1$ = 2-$MeOC_6H_4$; $R^2$ = $^i$Pr; $R^3$ = H | | [Pd(**R9**)H(TsO)] (in situ) | **206** | |
| [Pd(cod)MeCl] | **R9** | $R^1$ = 2-$MeOC_6H_4$; $R^2$ = $^i$Pr; $R^3$ = H | IIb | [Pd(**R9**)MeCl] | **207** | [89] |
| | | 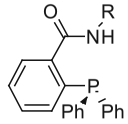 | | 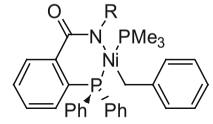 | | |

(continued)

**Table 2.1** (continued)

| Metal precursor | | Ligand | Method | Catalyst | No. | References |
|---|---|---|---|---|---|---|
| $[Ni(\eta^1\text{-}CH_2Ph)Cl(PMe_3)_2]$ | **S1** | R = Ph | III | $[Ni(\mathbf{S1})(\eta^1\text{-}CH_2Ph)(PMe_3)]$ | **208** | [90] |
| | **S2** | R = $^t$Bu | | $[Ni(\mathbf{S2})(\eta^1\text{-}CH_2Ph)(PMe_3)]$ | **209** | |
| | **S3** | R = H | | $[Ni(\mathbf{S3})(\eta^1\text{-}CH_2Ph)(PMe_3)]$ | **210** | |
| | **S4** | R = Pr | | $[Ni(\mathbf{S4})(\eta^1\text{-}CH_2Ph)(PMe_3)]$ | **211** | |
| | **S5** | R = $^i$Pr | | $[Ni(\mathbf{S5})(\eta^1\text{-}CH_2Ph)(PMe_3)]$ | **212** | |
| *5-membered chelated complexes with N–P ligands* | | | | | | |
| | | 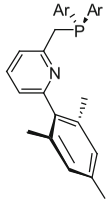 | | 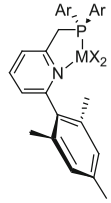 | | |
| $[Ni(dme)Br_2]$ | **T1** | Ar = 2,4,6-$Me_3C_6H_2$ | IIa | $[Ni(\mathbf{T1})Br_2]$ | **213** | [91] |
| | **T2** | Ar = 2-$MeC_6H_4$ | | $[Ni(\mathbf{T2})Br_2]$ | **214** | |
| [Pd(cod)MeCl] | **T1** | Ar = 2,4,6-$Me_3C_6H_2$ | IIb | [Pd(**T1**)MeCl] | **215** | [91] |
| | **T2** | Ar = 2-$MeC_6H_4$ | | [Pd(**T2**)MeCl] | **216** | |
| | | 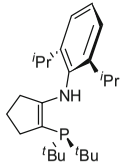 | | 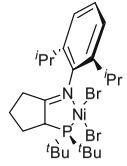 | | |

(continued)

**Table 2.1** (continued)

| Metal precursor | | Ligand | Method | Catalyst | No. | References |
|---|---|---|---|---|---|---|
| [Ni(dme)$Br_2$] | **U1** | 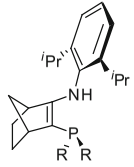 | IIa | [Ni(**U1**)$Br_2$] 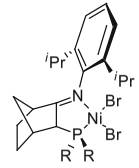 | **217** | [34] |
| [Ni(dme)$Br_2$] | **U2** | R = $^t$Bu | IIa | [Ni(**U2**)$Br_2$] | **218** | [34] |
| | **U3** | R = Ph | | [Ni(**U3**)$Br_2$] | **219** | |
| [Pd(cod)$Cl_2$] | **U1** | | IIa | [Pd(**U1**)$Cl_2$] | **220** | [34] |
| | **U2** | R = $^t$Bu | | [Pd(**U2**)$Cl_2$] | **221** | |
| | **U3** | R = Ph | | [Pd(**U3**)$Cl_2$] | **222** | |
| | | 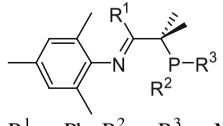 | | 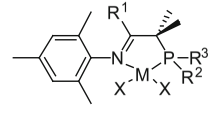 | | |
| [Ni(dme)$Br_2$] | **V1** | $R^1$ = Ph; $R^2$ = $R^3$ = Me | IIa | [Ni(**V1**)$Br_2$] | **223** | [35] |
| | **V2** | $R^1$ = $R^2$ = $R^3$ = Ph | | [Ni(**V2**)$Br_2$] | **224** | |
| | **V3** | $R^1$ = H; $R^2$ = Me; $R^3$ = 2,4,5-$Me_3C_6H_2$ | | [Ni(**V3**)$Br_2$] | **225** | |
| | **V4** | $R^1$ = Ph; $R^2$ = Me; $R^3$ = 2,4,5-$Me_3C_6H_2$ | | [Ni(**V4**)$Br_2$] | **226** | |
| | **V5** | $R^1$ = Ph; $R^2$ = $R^3$ = 2-$MeC_6H_4$ | | [Ni(**V5**)$Br_2$] | **227** | |
| [Pd(cod)MeCl] | **V1** | $R^1$ = Ph; $R^2$ = $R^3$ = Me | IIb | [Pd(**V1**)MeCl] | **228** | [35] |
| [Pd(cod)MeCl] | **V2** | $R^1$ = $R^2$ = $R^3$ = Ph | | [Pd(**V2**)MeCl] | **229** | |

(continued)

**Table 2.1** (continued)

| Metal precursor | | Ligand | Method | Catalyst | No. | References |
|---|---|---|---|---|---|---|
| [Pd(cod)MeCl] | **V3** | $R^1$ = H; $R^2$ = Me; $R^3$ = 2,4,5-$Me_3C_6H_2$ | | [Pd(**V3**)MeCl] | **230** | |
| [Pd(cod)MeCl] | **V4** | $R^1$ = Ph; $R^2$ = Me; $R^3$ = 2,4,5-$Me_3C_6H_2$ | | [Pd(**V4**)MeCl] | **231** | |
| | | 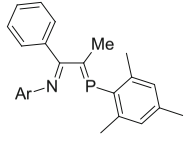 | | 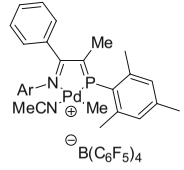 | | |
| [Pd(cod)MeCl] | **W1** | Ar = 2,6-$^i$Pr$_2$C$_6$H$_3$ | IIb[j] | [Pd(**W1**)Me(MeCN)][B($C_6F_5$)$_4$] | **232** | |
| | **W2** | Ar = 2,4,6-$Me_3C_6H_2$ | | [Pd(**W2**)Me(MeCN)][B($C_6F_5$)$_4$] | **233** | |
| *6-membered chelated complexes with N–S ligands* | | | | | | |
| | | 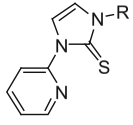 | | 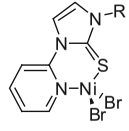 | | |
| [Ni(dme)$Br_2$] | **X1** | R = $^t$Bu | IIa | [Ni(**X1**)$Br_2$] | **234** | [93] |
| | **X2** | R = 2,6-$^i$Pr$_2$C$_6$H$_3$ | | [Ni(**X2**)$Br_2$] | **235** | |

(continued)

**Table 2.1** (continued)

| Metal precursor | Ligand | Method | Catalyst | No. | References |
|---|---|---|---|---|---|
| *5-membered chelated complexes wth N–S ligands* | | | | | |
| [Pd(cod)MeCl] | **Y1** 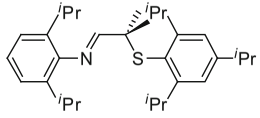 | IIb | [Pd(**Y1**)MeCl] 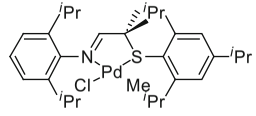 | **236** | [92] |

*Abbreviations 9-phen* 9-phenantrenyl; *9-anth* 9-anthryl; *m-terp m*-terphenyl; *tmeda* tetramethyletylendiamine; *acac* acetylacetonate; *dme* dimethoxyethane; *cod* cyclooctadiene; *1-naph* 1-naphthyl; *tppts* tri(*m*-sulfonylphenyl)phosphine; *tppds* di(*m*-sulfonylphenyl)phenylphosphine; $H_2N$-PEG-OMe, amino-terminated poly(ethylene glycol)monomethoxy ether; *pta* 1,3,5-triaza-7-phosphaadamantane; *hmta* hexamethylenetetramine; *dmso* dimethylsolfoxide; *2,6-lu* 2,6-lutidine

[a]Unspecified mechanism

[b]Multiple ligand exchange

[c]In situ alkylation with MeLi

[d]Cod displacement followed by oxidative addition

[e]Reaction with $NaHB(OMe)_3$

[f]From catalytic process involving: (i) E insertion in Ni-Me; (ii) $\beta$-H elimination with propylene releasing and Ni–H formation; (iii) insertion of E into Ni–H bond

[g]Ligand exchange between py and $PPh_3$

[h]Alkylation with *n*-hexyl magnesium bromide

[i]In situ generation of catalyst by addition of TsOH probably involving oxidative addition

[j]Followed by reaction with NaB $(C_6F_5)_4$

The novelty and the interest in these Ni and Pd complexes with mixed N–O, N–P, and N–S chelating ligands resides in that most bear anionic ligands and thus catalysts are neutral. They include primarily alkyl and aryl nickel complexes with salicylaldimine, anilinotropone, enolatoimine derivatives, and others developed afterwards. Besides the hydrocarbyl ligands, which effectively trigger the polymerization, they are also characterized by the presence of bulky groups on the ancillary ligand, and a neutral monodentate ligand such as $PR_3$ or more labile ligands, such as MeCN, pyridine, lutidine, etc. Their activation requires the removal of the neutral ligand (L) to form the coordination vacancy for the incoming olefin. Depending on the relative binding strength of L to the metal center the activation can require or not a scavenger, such as $[Ni(cod)_2]$ or $B(C_6F_5)$. The strength of the interaction is connected with structural and electronic features of the complex as well as with steric and electronic properties of L.

Relating to Ni-salicylaldimine (Fig. 2.21) the need to use a scavenger to extract L can be avoided by selective introduction of bulky groups in *ortho*-position ($R^1$) to O-donor, by introducing EWGs in *para*-position ($R^2$) to O-donor, and by using more labile L such as py or MeCN. All these modifications on original catalyst skeleton promote activation by simple thermal dissociation by decreasing the strength of phosphine-nickel bond.

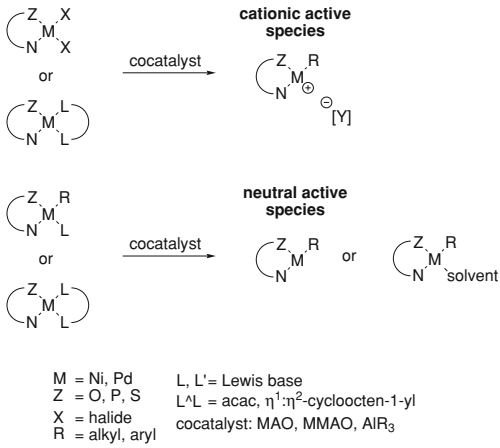


**Fig. 2.20** Activation by aluminium-based cocatalysts

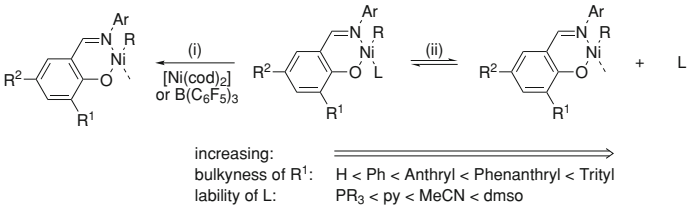


**Fig. 2.21** Examples of the effect of ligands on activation of salicylaldiminato Ni complexes

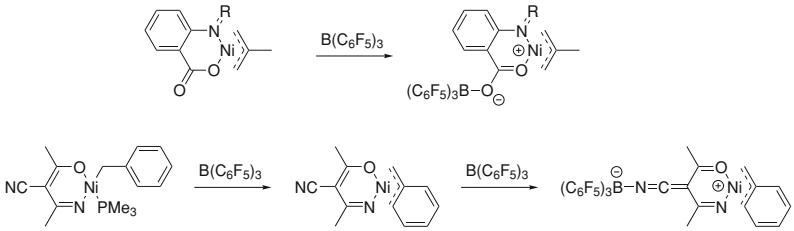


**Fig. 2.22** Examples of remote activation generating zwitterionic catalysts

Interestingly, what influences activation has also a strong impact on the whole catalytic process. Indeed, the decreasing energy in Ni–L bond is effective also in intermediates involved in propagation, such as metal-growing chain and hydrido species, demonstrated to be resting states. Moreover, the presence of a bulky group in $R^1$ position prevents the formation of bischelate complexes $[Ni(\kappa^2\text{-N,O})_2]$, recognized as deactivation route for these systems.

Differently, anilinotropone- and anilinoperinaphtenone-based systems with the strong $\sigma$-donor $PPh_3$ and a scaffold without EWGs or particularly bulky substituents act as single component catalysts. The easy removal of the phosphine donor can be explained in terms of trans-influence of amido ligand. Nevertheless, *ortho*-aryl effect has an influence on productivity, catalyst lifetime, and polymer properties also in these systems.

Similarly, the family of complexes with enolatoimine ligands behave as single component catalysts thanks to the highly negative nitrogen, which enhances the rate of dissociation of phosphine or pyridine. As a general rule, the substitution of phosphine with more labile ligands, such as pyridine or lutidine ligands prevents the use of activators. This is true for a variety of catalysts including diazene- and $\alpha$-iminocarboxamide-based systems.

A novel activation concept, sometimes referred as remote activation, was reported in the frame of zwitterionic catalysts. This type of activation places the Lewis acid away from the trajectory of monomer insertion and eliminates the complexities associated with the use of MAO derivatives and the equilibria of complexes where anion decoordination or displacement required for monomer insertion. Essentially, remote activation requires a ligand with an available basic functionality for the Lewis acid attachment, often a carbonyl group, which acts as an electronically delocalized canal towards the metal center. Generation of zwitterionic species is often accomplished by reorganization of the coordination sphere surrounding the metal. Examples of this activation are reported in Fig. 2.22 for iminobenzoato- and ketoimino-based ligands containing catalysts **108** and **128**.

## *2.4.2 Ethylene Polymerization*

The development of electron-rich catalyst systems compatible with polar functionality would satisfy the desire to include polar functionalities into linear

(Fig. 2.23) polyolefins with precise control over polymer characteristics such as mechanical toughness, rheology, and surface functionalization properties, as well as avoid the need for rigorous drying of monomers and polymerization solvents. Such interest turned the attention towards the cationic (N–N) group 10 systems pioneered by Brookhart and to cationic and neutrally charged (N–Z) group 10 systems reviewed in this chapter. The need to reach a rational design of catalysts which allows to control activity, molar masses, and branching, in addition to tolerance to functional groups led to much research studies on α-olefin polymerization pioneered by Grubbs [38] and Johnson [85]. New families of complexes were introduced, the main results in ethylene polymerization are reviewed following the ligand organization in Fig. 2.1. Selected polymerization data of the main (N–Z)Ni catalysts are reported in Table 2.2.

Independently Grubbs at Caltech [38] and Johnson at Dupont [85] rationalized to replace the P–O chelate of the neutral SHOP system [24] with a ligand based on the harder nitrogen and a scaffold containing increased steric demand to have polymers with high molecular weight; both selected salicylaldimine complexes. The DuPont group reported use of allyl complexes, while the Caltech group used the phosphine complexes. Grubbs reported that neutral Ni(II) salicylaldiminato complexes are highly active catalysts for the polymerization of ethylene to high molecular weight polymers under moderate conditions [38]. The introduction of bulkier substituents on the imine nitrogen and the phenolic ring blocks the axial faces of the metal center, retarding the rate of associative displacement (Fig. 2.23). Moreover, bulky groups might decrease the rate of catalyst deactivation, which was shown to occur by ligand disproportionation and dimerization as in the analogous SHOP system.

The polymerization of ethylene by complexes **1**–**7** were performed in toluene by injection of a toluene solution of the appropriate phosphine scavenger ($[Ni(cod)_2]$ or $B(C_6F_5)_3$) to the catalyst solution. Attempts to polymerize ethylene without the phosphine scavenger did not yield polyethylene [38]. However, when the catalyst **1** was combined with a phosphine scavenger, after a 5–8 min induction period, there was a rapid ethylene uptake. Increasing the ethylene pressure yields polyethylene with higher $M_w$. Bulky substituents in the *ortho*-position to O donor suppress the chain migratory process and also the chain termination reactions. In fact, catalysts **2**–**5** produced higher molecular weight than **1** and a slight decrease of total number of branches. Moreover, no induction period was observed. Best results were obtained with an electron deficient system (**7**), bearing the $NO_2$ substituent in *p*-position to O donor ($R^2$) of the salicylaldiminato, while catalyst

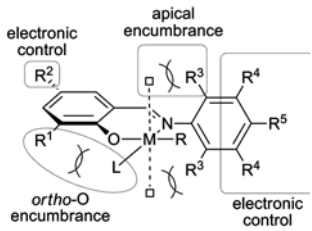


**Fig. 2.23** Examples of the effect of substituent variation in salicylaldiminato catalysts

**Table 2.2** Selected ethylene polymerization data of the main (N–Z) Ni catalysts

*6-membered chelated complexes with N–O ligands*

| | $R^1$ | $R^2$ | $R^3$ | $R^4$ | $R^5$ | L | Cat. no. | *p*E (bar) | T (°C) | TOF[a] | $M_w$ (kg mol$^{-1}$) | $M_w/M_n$ | Br/1000 C | References |
|---|---|---|---|---|---|---|---|---|---|---|---|---|---|---|
| 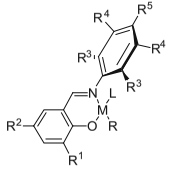 | H | H | $^i$Pr | H | H | $PPh_3$ | **1**/Ni(cod)$_2$ | 14.18 | 50 | 48 | 10.0 | 1.4 | 20 | [38] |
| | $^t$Bu | H | $^i$Pr | H | H | $PPh_3$ | **2**/Ni(cod)$_2$ | 6.89 | 50 | 71 | 11.4 | 1.8 | 55 | [38] |
| | Ph | H | $^i$Pr | H | H | $PPh_3$ | **3** | 6.89 | 50 | 100 | 207.0 | 2.2 | 10 | [39] |
| | 9-phen | H | $^i$Pr | H | H | $PPh_3$ | **4** | 6.89 | 50 | 300 | 207.0 | 2.4 | 8 | [39] |
| | 9-anth | H | $^i$Pr | H | H | $PPh_3$ | **5** | 6.89 | 50 | 940 | 236.0 | 2.2 | 5 | [39] |
| | Ph | H | $^i$Pr | H | H | $PPh_3$ | **3**/Ni(cod)$_2$ | 14.18 | 50 | 198 | 242.0 | 2.1 | 5 | [38] |
| | H | $NO_2$ | $^i$Pr | H | H | $PPh_3$ | **7**/Ni(cod)$_2$ | 14.18 | 50 | 380 | 360.0 | 12.4 | 22 | [38] |
| | 9-anth | H | $^i$Pr | H | H | MeCN | **8** | 17.23 | 50 | 6,400 | 120.0 | 3.0 | 20 | [39] |
| | *m*-terp | H | $^i$Pr | H | H | MeCN | **10** | 6.89 | 50 | 960 | 532.0 | 2.1 | 7 | [39] |
| | I | I | $^i$Pr | H | H | Py | **12** | 40 | 50 | 210 | 30.0 | 2.5 | 5 | [44] |
| | I | I | 3,5-$(CF_3)_2C_6H_3$ | H | H | Py | **21** | 40 | 50 | 1,170 | 96.9 | 5.1 | 10 | [44] |
| | I | I | 3-$NO_2C_6H_4$ | H | H | Py | **22** | 40 | 50 | 150 | 28.6 | 2.6 | 26 | [44] |
| | I | I | Ph | H | H | Py | **23** | 40 | 50 | 450 | 6.7 | 2.3 | 52 | [44] |
| | I | I | 3,5-$Me_2C_6H_3$ | H | H | Py | **24** | 40 | 50 | 1,200 | 2.3 | 2.1 | 76 | [44] |
| | I | I | 3,5-$(MeO)_2C_6H_3$ | H | H | Py | **25** | 40 | 50 | 1,250 | 4.7 | 2.5 | 79 | [44] |
| | I | I | 3,5-$^t$Bu$_2C_6H_3$ | H | H | Py | **33** | 40 | 50 | 1,411 | 29.7 | 2.7 | 38 | [48] |
| | I | I | 3,5-$^t$Bu$_2$-4-$OHC_6H_2$ | H | H | Py | **34** | 40 | 50 | 1,477 | 28.0 | 2.0 | 32 | [48] |
| | I | I | 3,5-$Me_2$-4-$MeOC_6H_2$ | H | H | Py | **35** | 40 | 50 | 671 | 1.7 | 2.1 | 81 | [48] |
| | 9-anth | H | 3,5-$(CF_3)_2C_6H_3$ | H | H | Py | **36** | 40 | 50 | 1,195 | 129.0 | 3.0 | 13 | [48] |
| | 9-anth | H | 3,5-$^t$Bu$_2C_6H_3$ | H | H | Py | **37** | 40 | 50 | 1,860 | 30.8 | 2.8 | 31 | [48] |

(continued)

**Table 2.2** continued

*6-membered chelated complexes with N–O ligands*

| | $R^1$ | $R^2$ | $R^3$ | $R^4$ | $R^5$ | L | Cat. no. | *p*E (bar) | T (°C) | TOF[a] | $M_w$(kg mol$^{-1}$) | $M_w/M_n$ | Br/1000 C | References |
|---|---|---|---|---|---|---|---|---|---|---|---|---|---|---|
| 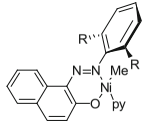 | 9-anth | H | 3,5-$^t$Bu$_2$-4-OHC$_6$H$_2$ | H | H | Py | **38** | 40 | 50 | 1,242 | 44.8 | 2.8 | 30 | [48] |
| | 9-anth | H | 3,5-Me$_2$C$_6$H$_3$ | H | H | Py | **39** | 40 | 50 | 1,374 | 12.5 | 3.9 | 92 | [48] |
| | 9-anth | H | 3,5-Me$_2$-4-MeOC$_6$H$_2$ | H | H | Py | **40** | 40 | 50 | 707 | 2.4 | 2.7 | 88 | [48] |
| | 9-anth | H | 3,5-(MeO)$_2$C$_6$H$_3$ | H | H | Py | **41** | 40 | 50 | 538 | 17.2 | 4.3 | 80 | [48] |
| | 9-anth | H | 3,4,5-(MeO)$_3$C$_6$H$_2$ | H | H | Py | **42** | 40 | 50 | 641 | 53.0 | 5.3 | 78 | [48] |
| | H | $NO_2$ | 3,5-(CF$_3$)$_2$C$_6$H$_3$ | H | H | Py | **43** | 40 | 50 | 750 | 20.4 | 2.4 | 15 | [48] |
| | $^t$Bu | H | 3,5-(CF$_3$)$_2$C$_6$H$_3$ | H | H | Py | **44** | 40 | 50 | 100 | 21.1 | 2.2 | 14 | [48] |

*6-membered chelated complexes with N–O ligands*

| | $R^1$ | $R^2$ | $R^3$ | $R^4$ | L | Cat. no. | *p*E (bar) | T (°C) | TOF[a] | $M_w$ (kg mol$^{-1}$) | $M_w/M_n$ | Br/1000 C | References |
|---|---|---|---|---|---|---|---|---|---|---|---|---|---|
| 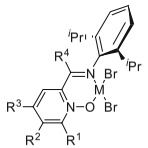 | H | H | H | Me | – | **73**/MMAO | 5 | 30 | 556 | 3.0 | 1.7 | 87 | [53] |
| | H | H | H | H | – | **74**/MMAO | 5 | 30 | 836 | 1.7 | 1.7 | 65 | [53] |
| | Ph | H | H | H | – | **76**/MMAO | 5 | 30 | 3,084 | 57.2 | 2.8 | 30 | [53] |
| | H | H | MeO | H | – | **78**/MMAO | 5 | 30 | 476 | 2.8 | 1.2 | 70 | [53] |
| 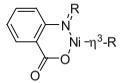 | cyclohexylidene | – | – | – | $\eta^3$-CH$_2$CMeCH$_2$ | **108** | 3.4 | 50 | 1,700 | 7.3 | 2.0 | 43 | [61] |
| | CEt$_2$ | – | – | – | $\eta^3$-CH$_2$Ph | **110** | 5.2 | 50 | 4,100 | 12.0 | 2.3 | 47 | [61] |

(continued)

**Table 2.2** continued

*6-membered chelated complexes with N–O ligands*

| | $R^1$ | $R^2$ | $R^3$ | $R^4$ | L | Cat. no. | *p*E (bar) | T (°C) | TOF[a] | $M_w$(kg mol$^{-1}$) | $M_w/M_n$ | Br/1,000 C | References |
|---|---|---|---|---|---|---|---|---|---|---|---|---|---|
| 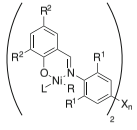 | n = 0; $^i$Pr | I | I | – | py | **92** | 40 | 50 | 770 | 381.6 | 5.3 | 4 | [56] |
| | n = 0; 3,5-$(CF_3)_2C_6H_3$ | I | I | – | py | **93** | 40 | 50 | 3,400 | 236.8 | 3.2 | 4 | [56] |
| | n = 1; X = $CH_2$; $^i$Pr | I | I | – | py | **94** | 40 | 50 | 480 | 437.0 | 4.6 | 4 | [56] |
| | n = 1; X = $CH_2$; 3,5-$(CF_3)_2C_6H_3$ | I | I | – | py | **95** | 40 | 50 | 5,040 | 249.0 | 3.0 | 4 | [56] |
| | n = 0; 3,5-$(CF_3)_2C_6H_3$ | I | I | | tmeda | **96** | 40 | 50 | 9,520 | 920 | 3.3 | 2 | [56] |
| 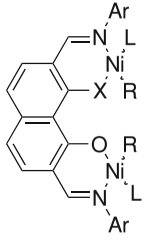 | X = O | – | – | – | $PMe_3$ | **104**/ $Ni(cod)_2$ | 7 | 25 | 99 | 10.3 | 2.6 | 80 | [60] |
| | X = O | – | – | – | $PPh_3$ | **106**/ $Ni(cod)_2$ | 7 | 25 | 102 | 10.1 | 2.6 | 93 | [60] |

*6-membered chelated complexes with N–O ligands*

| | $R^1$ | $R^2$ | $R^3$ | $R^4$ | $R^5$ | L | Cat. no. | *p*E (bar) | T (°C) | TOF[a] | $M_w$ (kg mol$^{-1}$) | $M_w/M_n$ | Br/1000 C | References |
|---|---|---|---|---|---|---|---|---|---|---|---|---|---|---|
| 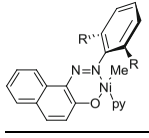 | / | / | $^i$Pr | H | H | py | **113** | 50 | 70 | 80 | 52.0 | 1.9 | – | [62] |

(continued)

**Table 2.2** continued

*6-membered chelated complexes with N–O ligands*

| | $R^1$ | $R^2$ | $R^3$ | $R^4$ | $R^5$ | L | Cat. no. | *p*E (bar) | T(°C) | TOF [a] | $M_w$(kg mol$^{-1}$) | $M_w/M_n$ | Br/1000 C | References |
|---|---|---|---|---|---|---|---|---|---|---|---|---|---|---|
| 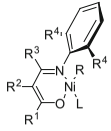 | $CF_3$ | $COCF_3$ | H | $^iPr$ | – | $PPh_3$ | **117** | 13.78 | 60 | 14,168 | 25.0 | 3.7 | 41 | [64] |
| | $CF_3$ | $COCF_3$ | Me | $^iPr$ | – | $PPh_3$ | **118** | 13.78 | 50 | 2,968 | 27.0 | 3.3 | 58 | [64] |
| | $CF_3$ | H | Me | $^iPr$ | – | $PPh_3$ | **119** | 13.78 | 50 | 896 | 17.0 | – | – | [64] |
| | Ph | H | H | $^iPr$ | – | $PPh_3$ | **121**/ $B(C_6F_5)_3$ | 25 | 60 | 345 | 27.3 | 2.2 | 25 | [65] |
| | 2-$PhC_6H_4$ | H | H | $^iPr$ | – | $PPh_3$ | **122**/ $B(C_6F_5)_3$ | 25 | 60 | 3,420 | 17.0 | 1.8 | 22 | [65] |
| | 2-Naph-$C_6H_4$ | H | H | $^iPr$ | – | $PPh_3$ | **123**/ $B(C_6F_5)_3$ | 25 | 60 | 2,625 | 9.0 | 2.0 | 39 | [65] |
| | $CF_3$ | $COCF_3$ | H | $^iPr$ | – | py | **126** | 40 | 60 | 3,864 | 24.0 | 3.0 | – | [66] |
| | $CF_3$ | $COCF_3$ | H | 3,5-$(CF_3)_2C_6H_3$ | – | py | **127** | 40 | 60 | 687 | 38.0 | 2.3 | – | [66] |
| | $CF_3$ | $COCF_3$ | H | 3,5-$(CF_3)_2C_6H_3$ | – | $PPh_3$ | **128** | 40 | 70 | 2,280 | 32.0 | 2.1 | – | [66] |
| | $CF_3$ | $COCF_3$ | H | 3,5-$(CF_3)_2C_6H_3$ | – | $PPh_3$ | **128**/$Ni(cod)_2$ | 40 | 70/100 | 4,680 | 21.0 | 5.1 | – | [66] |
| 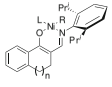 | n = 0 | – | – | – | – | $PPh_3$ | **130** | 50 | 63 | 1,760 | 9.8 | 1.9 | 54 | [68] |
| | n = 1 | – | – | – | – | $PPh_3$ | **131** | 50 | 63 | 1,875 | 46.8 | 2.0 | 26 | [68] |
| | n = 2 | – | – | – | – | $PPh_3$ | **132** | 50 | 63 | 3,570 | 46.5 | 2.1 | 27 | [68] |
| | n = 0 | – | – | – | – | py | **133** | 25 | 63 | 1,005 | 8.2 | 2.1 | 77 | [68] |
| | n = 1 | – | – | – | – | py | **134** | 50 | 63 | 1,791 | 56.9 | 1.9 | 28 | [68] |
| | n = 2 | – | – | – | – | py | **135** | 25 | 63 | 960 | 41.6 | 2.1 | 47 | [68] |

(continued)

**Table 2.2** (continued)

*5-membered chelated complexes with N–O ligands*

| | $R^1$ | $R^2$ | $R^3$ | R | L | Cat. no. | *p*E (bar) | T (°C) | TOF[a] | $M_w$ (kgmol$^{-1}$) | $M_w/M_n$ | Br/1000 C | References |
|---|---|---|---|---|---|---|---|---|---|---|---|---|---|
| 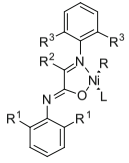 | $^i$Pr | Me | $^i$Pr | $\eta^1$-$CH_2Ph$ | $PMe_3$ | **152**/$B(C_6F_5)_3$ | 6.89 | 20 | 350 | 349.0 | 2.3 | 104 | [73] |
| | $^i$Pr | Me | $^i$Pr | $\eta^1$-$CH_2Ph$ | Py | **155** | 6.89 | 20 | 60 | 63.0 | 1.8 | – | [96] |
| | $^i$Pr | Me | $^i$Pr | $\eta^1$-$CH_2Ph$ | 2,6-lu | **156** | 6.89 | 40 | 304 | 143.0 | 2.2 | – | [96] |
| | $^i$Pr | Me | $^i$Pr | $\eta^1$-C=OPh | Py | **157** | 27.57 | 50 | 301 | 160.0 | 2.0 | – | [96] |
| | $^i$Pr | Et | $^i$Pr | $\eta^1$-$CH_2Ph$ | $PMe_3$ | **158**/$Ni(cod)_2$ | 6.89 | 20 | 255 | 111.8 | 1.3 | – | [75] |
| | $^i$Pr | $CH_2{}^iPr$ | $^i$Pr | $\eta^1$-$CH_2Ph$ | $PMe_3$ | **159**/$Ni(cod)_2$ | 6.89 | 20 | 420 | 169.4 | 1.4 | – | [75] |
| | $^i$Pr | $^i$Pr | $^i$Pr | $\eta^1$-$CH_2Ph$ | $PMe_3$ | **160**/$Ni(cod)_2$ | 6.89 | 20 | 534 | 218.4 | 1.2 | – | [75] |
| | $^i$Pr | Ph | $^i$Pr | $\eta^1$-$CH_2Ph$ | $PMe_3$ | **161**/$Ni(cod)_2$ | 6.89 | 20 | 259 | 122.4 | 1.2 | – | [75] |
| | $^i$Pr | 4-$CF_3C_6H_4$ | $^i$Pr | $\eta^1$-$CH_2Ph$ | $PMe_3$ | **162**/$Ni(cod)_2$ | 6.89 | 20 | 280 | 124.3 | 1.1 | – | [75] |
| | $^i$Pr | 4-$MeOC_6H_4$ | $^i$Pr | $\eta^1$-$CH_2Ph$ | $PMe_3$ | **163**/$Ni(cod)_2$ | 6.89 | 20 | 180 | 109.2 | 1.2 | – | [75] |

| | $R^1$ | $R^2$ | $R^3$ | $R^4$ | $R^5$ | No. | *p*E (bar) | T (°C) | TOF[a] | $M_w$ (kg mol$^{-1}$) | $M_w/M_n$ | Br /1000 C | Referencces |
|---|---|---|---|---|---|---|---|---|---|---|---|---|---|
| 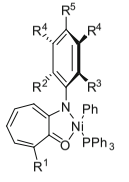 | H | Me | Me | H | H | **168** | 13.78 | 80 | 5,424[b] | 73.1 | 1.7 | 61 | [79] |
| | H | $^i$Pr | $^i$Pr | H | H | **169** | 13.78 | 80 | 8,800[b] | 165.6 | 1.8 | 61 | [79] |
| | H | Me | $^t$Bu | H | H | **171** | 13.78 | 80 | 1,014[b] | 230.0 | 2.0 | 73 | [79] |
| | H | Ph | Ph | H | H | **172** | 13.78 | 80 | 10,038[b] | 171.0 | 1.8 | 53 | [79] |
| | H | Cl | Cl | H | H | **173** | 13.78 | 80 | 3,924 [b] | 20.0 | 2.0 | 53 | [79] |
| | H | Br | Br | H | H | **174** | 13.78 | 80 | 4,152 [b] | 41.8 | 1.9 | 56 | [79] |

(continued)

**Table 2.2** (continued)

| | $R^1$ | $R^2$ | $R^3$ | $R^4$ | $R^5$ | No. | *p*E (bar) | T (°C) | TOF[a] | $M_w$ (kg mol$^{-1}$) | $M_w/M_n$ | Br/1000 C | Referencces |
|---|---|---|---|---|---|---|---|---|---|---|---|---|---|
| 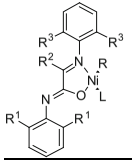 | H | F | F | F | F | **175** | 13.78 | 80 | 1,152[b] | 4.8 | 3.0 | 49 | [79] |
| | H | Me | H | H | H | **176** | 13.78 | 80 | 936[b] | 112.8 | 2.4 | 57 | [79] |
| | H | Me | $CF_3$ | H | H | **178** | 13.78 | 80 | 6,924[b] | 167.2 | 1.9 | 59 | [79] |
| | Ph | $^i$Pr | $^i$Pr | H | H | **180** | 13.78 | 80 | 2,338 | 184.8 | 2.1 | 63 | [79] |
| | 1-Naph | $^i$Pr | $^i$Pr | H | H | **181** | 13.78 | 80 | 2,461 | 151.2 | 2.7 | 62 | [79] |

*5-membered chelated complexes with N–O ligands*

| | $R^1$ | $R^2$ | Cat. no. | *p*E (bar) | T (°C) | TOF[a] | $M_w$ (kg mol$^{-1}$) | $M_w/M_n$ | Br/1000 C | References |
|---|---|---|---|---|---|---|---|---|---|---|
| 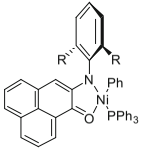 | $^i$Pr | / | **184** | 13.78 | 80 | 1,749 | 144.0 | 1.6 | 44 | [80] |
| 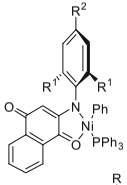 | $^i$Pr | H | **185** | 1.01 | 40 | 1,460 | 150.9 | 3.3 | 22 | [81] |
| | Me | H | **186** | 1.01 | 40 | 363 | 11.4 | 2.2 | 41 | [82] |
| | Me | H | **186** | 1.01 | 20 | 39 | 105.0 | 2.2 | 5 | [82] |
| | Me | Me | **187** | 1.01 | 20 | 176 | 255.0 | 2.4 | 9 | [82] |
| | Et | H | **188** | 1.01 | 40 | 394 | 185.6 | 2.0 | 12 | [82] |
| 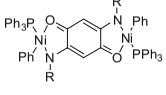 | 2,6-$^i$Pr$C_6H_3$ | – | **189** | 4 | 40 | 104 | 43.1 | 3.5 | – | [82] |
| | 2,6-Me$C_6H_3$ | – | **190** | 4 | 80 | 64 | 53.5 | 8.2 | – | [83] |

(continued)

**Table 2.2** (continued)

*5-membered chelated complexes with N–O ligands*

| | $R^1$ | $R^2$ | Cat. no. | *p*E(bar) | T(°C) | TOF[a] | $M_w$(kg mol$^{-1}$) | $M_w/M_n$ | Br/1000 C | References |
|---|---|---|---|---|---|---|---|---|---|---|
| 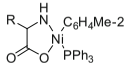 | H | – | **194** | 40 | 100 | 1,756 | 900.0 | – | 1.8 | [84] |

*6-membered chelated complexes with N–P ligands*

| | $R^1$ | $R^2$ | $R^3$ | Cat. no. | *p*E (bar) | T (°C) | TOF[a] | $M_w$ (kg mol$^{-1}$) | $M_w/M_n$ | Br/ 1000 C | References |
|---|---|---|---|---|---|---|---|---|---|---|---|
| 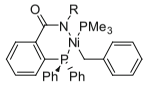 | $^i$Pr | – | – | **212** | 6.89 | 50 | 5,300 | 1,070.0 | 3.7 | 60 | [90] |
| 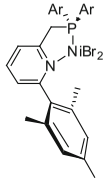 | 2,4,6-$Me_3C_6H_2$ | – | – | **213**/MAO | 34.47 | 30 | 15 | 9.2 | 2.1 | 76 | [91] |
| 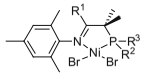 | Ph | Me | Me | **223**/MMAO-3A | 27.57 | 35 | 1,000 | 2.8 | – | 66 | [35] |
| | Ph | Ph | Ph | **224**/MMAO-3A | 27.57 | 29 | 667 | 140.0 | 1.9 | 64 | [35] |
| | H | Me | 2,4,5-$Me_3C_6H_2$ | **225**/MMAO-3A | 27.57 | 60 | 960 | 37.0 | n.d. | 57 | [35] |
| | Ph | 2-$MeC_6H_4$ | 2-$MeC_6H_4$ | **226**/MMAO-3A | 27.57 | 29 | 1,386 | 75.0 | 1.8 | 67 | [35] |

[a] Kg PE mol cat$^{-1}$ h$^{-1}$
[b] Polymerization time = 10 min

activity diminishes with electron rich catalyst such as **6**. However, complex **7**, with greatest activity, gave a broad molecular weight distribution ($M_w/M_n > 12.4$) [38]. Salicylaldimines with sufficient bulk in the *ortho*-position to O donor constitute a new family of neutral, single component catalysts [39]. In the absence of cocatalysts, catalysts **3–5** have an indefinite lifetime and are capable of producing TOFs from $0.5 \times 10^3$ to $3.0 \times 10^3$ kg PE mol $Ni^{-1}$ $h^{-1}$ at low temperatures and pressures. Grubbs did not observe a dissociated phosphine in NMR spectroscopic studies of the polymerization reaction suggesting that the resting state of these systems is the phosphine complex. Activity of the catalysts containing phosphine was reduced by additional amounts of phosphine and increased with temperature up to 80 °C.

In order to further enhance the activity of the catalyst, Grubbs et al. [39] prepared complexes containing the acetonitrile ligand, more labile than triphenylphosphine. This family of catalysts (**8–10**) exhibits a 2- to 3-fold increase in catalytic activity as compared with catalysts **3–5**. Complexes **13–16**, easily prepared from readily available Ni complexes and salts, were synthesized by Chen [41] and activated by near-stoichiometric amounts of almost any metal-alkyl or hydride (BuLi, MAO, $BH_3$·THF, or MeLi) for the polymerization of ethylene (at 1–75 bars of ethylene). Catalyst productivity was found to depend on ethylene pressure and similar for all three complexes with all the activators except for complex **13** that shows at $p$E = 75 bar a turnover number (TON = mol PE mol $Ni^{-1}$) of over $10^5$. The catalyst showed a long lifetime and the polymer produced was highly linear.

Carlini et al. [42] reported the synthesis of monochelate nickel (II) catalysts **17–20**, obtained by in situ oxidative addition of salicylaldimine ligands to $[Ni(cod)_2]$, for the polymerization of ethylene. Almost stoichiometric amounts of MAO as cocatalyst are necessary to activate these systems, the productivity being dependent on the Al/Ni molar ratio. Both activity and molecular weight of the resulting PE are influenced by the nature of the substituent on both the phenolate moiety and on the N-aryl ring. In particular, when two nitro groups are present on the 3,5-positions of phenolate moiety (**19**, **20**) activities are higher than 120 (kg PE mol $Ni^{-1}$ $h^{-1}$). The PE obtained showed a high linearity and $M_w$ was in the 100–500 kg $mol^{-1}$ range.

Further studies on the effect of free trimethylaluminum (TMA) content in MAO on performances of catalyst **19** [43] led to conclude that TMA alone is not able to activate the catalyst in the polymerization of ethylene and MAO appears necessary. When a large excess of TMA with respect to the amount of catalyst was used, independently of the relative amount of MAO and hence of the $Al_{tot}$/Ni molar ratio, a significant detrimental effect on both the activity and PE molecular weight was generally obtained. For TMA/Ni molar ratio = 15 high molecular weight linear PE was obtained with the maximum of activity (1,920 kg PE mol $Ni^{-1}$ $h^{-1}$) when a proper amount of MAO was also present ($Al_{tot}$/Ni = 150).

The interest in the synthesis of latexes of high-molecular-weight polyethylene prompted Mecking et al. to design novel Ni(II) salicylaldiminato complexes. Based on the interesting results with **11** they reasoned that an $R^3$ aryl substituent

with strongly electron-withdrawing groups could provide steric bulk and electron withdrawing properties at the same time [44]. A series of salicylaldimine ligands with systematically varied electronic properties were synthesized and employed as precursors for ethylene polymerization (**21**–**25**). They are characterized from having a nickel bound methyl group in the trans position to the O donor, a pyridine as labile ligand, and a strong steric shielding of the apical positions of the metal center by the $R^3$ aryl groups of the N-aryl moiety. This series of well-defined catalyst precursors with a systematically varied substitution pattern revealed a surprising and unprecedent effect of remote substituents on polymer branching and molecular weight, despite their spatial remoteness from the catalytically active center.

Performances of complexes **21**–**25** were compared with those of complex **12**. The activity of all catalysts with 3,5-substituted aryl moieties ($R^3$ = 3,5-$(CF_3)_2C_6H_3$ (**21**), 3,5-$(Me)_2C_6H_3$ (**24**) and 3,5-$(OMe)_2C_6H_3$ (**25**) is much higher than that of **12** with the isopropyl substitution pattern. Catalysts which do not bear substituents in the 3,5-position ($R^3$ = Ph (**23**)) or are only monosubstituted ($R^3$ = 3-$NO_2C_6H_4$ (**22**)) appeared much less active. Studies of catalyst stability over time revealed that **21, 24**, **25**, and **12** remain active for hours at 60 °C and 10 bar ethylene pressure, **22** and **23** are deactivated completely within 20 min.

Surprisingly, despite their spatial distance from the metal center the nature of the substituents on the aryl moiety has a dramatic effect on branching and thus crystallinity, and on polymer molecular weight. With $R^3$ = 3,5-$(CF_3)_2C_6H_3$ (**21**) a semicrystalline (50% crystalline) stiff polymer was obtained. Complexes with $R^3$ = 3-$NO_2C_6H_4$ (**22**) and $R^3$ = 3,5-$(CF_3)_2C_6H_3$ (**21**) afford polyethylenes with a considerably higher degree of branching, and correspondingly low crystallinities (18 and < 10%, respectively), and from those with $R^3$ = 3,5-$(Me)_2C_6H_3$ (**24**) and $R^3$ = 3,5-$(OMe)_2C_6H_3$ (**25**) an entirely amorphous material is obtained. At the same time, the molecular weight of the polymer decreases by more than an order of magnitude going from **21** to **25**. Given the similar intrinsic activities of all catalysts, the lower molecular weight obtained must indeed result from a higher rate of chain transfer rather than from a lower rate of chain growth.

The methyl branching originates from a $\beta$-H transfer and a subsequent 2,1-reinsertion of the resulting metal-bound 1-olefin. Whereas the steric requirements of the substituents are similar in **21**, **24** and **25** ($R^3$ = 3,5-$(CF_3)_2C_6H_3$ (**21**), $R^3$ = 3,5-$(Me)_2C_6H_3$ (**24**), and $R^3$ = 3,5-$(OMe)_2C_6H_3$ (**25**)) and higher than in **23** ($R^3$ = $C_6H_5$), their electron withdrawing character increases in the sequence **25** ~ **24** < **23** < **22** ~ **21**. Both the molecular weights and the branching of the polymers obtained with these different catalyst precursors vary systematically with the electronic nature of R rather than their steric requirements. This indicates that the effect of these remote substituents is related to their electronic properties.

Catalytic performances of complexes **21**, **24**, and **25** were compared to those of two other series of ($\kappa^2$-N,O)-salicylaldiminato Ni(II)-methyl pyridine complexes **33**–**35** and **36**–**42** [48], the former have two iodine substituents in *ortho*- and *para*-positions of the phenolate moiety, the latter and **32** have an anthryl substituent in *ortho* and triphenyl with different substitutions in 3 and 5 ($R^3$ = 3,5-$(CF_3)_2C_6H_3$

(**36**), $R^3 = 3,5\text{-}^tBu_2C_6H_3$ (**37**), $R^3 = 3,5\text{-}^tBu_2\text{-}4\text{-}OHC_6H_2$ (**38**) etc.) [47]. All behave as single component ethylene polymerization catalysts at temperatures above 15 °C, reaching their highest productivities in the range between 40 and 75 °C. The anthryl-substituted complex **37** is the most active precatalyst under these polymerization conditions (1,860 kg PE mol $Ni^{-1}$ $h^{-1}$), while all diiodo-substituted complexes **21**, **24**, **25**, and **33**–**35** perform similarly well when compared to the respective anthryl-substituted complexes **32, 36**–**42**. Further, the anthryl versus diiodo substitution does not exert a major influence on the degree of branching of the obtained polyethylenes.

As already found for complexes **21**, **24**, and **25**, [44] the degree of branching of obtained polyethylenes is highly sensitive to the 3,5-substitution pattern of the terminal arene rings of the terphenyl moieties in both diiodo- and anthryl-substituted complexes. More electron-deficient N-aryl substituents result in higher molecular weights and lower degrees of branching probably by suppressing chain walking and chain transfer relative to ethylene insertion.

At 50 °C all catalysts are quite stable. In more detail, complexes **32**, **21**, and **44** derived from 2,6-diisopropylaniline or terphenylamine appeared to exhibit constant polymerization activities over time and polymer yields in 40 and 60 min (for **21**: 120 min) polymerization runs. Further, complexes **33**, **34**, **37**, and **38** showed a slight decrease in polymerization activity over time reaching one-half of the initial activity after ca. 1.5–2.0 h, while one-half of the initial activities after ca. 1 h were observed with complexes **24**, **25**, **39**, and **43**. At 70 °C, the decrease in polymerization activities over time is more pronounced with precatalysts **37** and **38**. It was concluded that the positive effect on the stability of the anthryl substituent in **5** observed by Grubbs [38] is not valid when anthryl and terphenyl substituents are combined in the same catalyst. Probably deactivation mechanisms are different.

Moreover, Mecking [49] synthesized another series of ($k^2$-N,*O*)salicylaldiminato nickel methyl pyridine complexes as precatalysts varying the remote substituents of 2,6-di-(4-R-phenyl)phenyl groups on the imine nitrogen [$R = C_8F_{17}$ (**28**), $CF_3$ (**29**), F (**48**), H (**23**), Me (**46**), $^t$Bu (**48**), OMe (**47**), and $NMe_2$ (**49**)] to complete the studies on the electronic effects of remote substituents.

Also these complexes behave as single component catalysts but catalyze the polymerization of ethylene to low molecular weight polyethylene. Decreasing molecular weight and increasing degrees of branching are observed in the order $R = C_8F_{17} \sim CF_3 > F > H > Me > MeO > {}^tBu > NMe_2$. They are less active and decompose faster, under the polymerization conditions employed, than complexes 2,6-di-(3,5-$R'_2$-phenyl)phenyl substituted. X-ray diffraction analysis of complex **45** ($R^2 = I$; $R^3 = 4\text{-}FC_6H_4$) and polymerization results indicated that it is not the sterics but the electronics of the R′ group that controls the polymer microstructure.

The cyclohexyl-substituted salicylaldiminato-Ni(II) complex **26** was tested by Sun et al. [45] in the ethylene polymerization. As a single component catalyst, complex **26** shows no activity in the polymerization of ethylene. Then, $[Ni(cod)_2]$ was used as cocatalyst to trap the triphenylphosphine. The catalytic activity of **26** and the molecular weight of PE are in relation to the amount of $[Ni(cod)_2]$ added

as a cocatalyst. The catalytic activity increases as the [Ni(cod)$_2$]/**26** molar ratio increases and 3 or 4 equiv. of the cocatalyst are sufficient for the whole polymerization time. The activity increases with increasing temperature during the initial stage and reaches the maximum values at 45–55 °C. A polymerization activity of $3.62 \times 10^2$ kg PE mol Ni$^{-1}$ h$^{-1}$ and a $M_n$ of 57.3 kg mol$^{-1}$ have been found for 10 μmol of **26** and a [Ni(cod)$_2$]/**26** ratio of 3 at 45 °C and 12 bar of ethylene. The polydispersity index of the resulting polyethylene is 2.04. Moreover, the aluminum alkyls AlEt$_3$ and Al$^i$Bu$_3$ were tested as cocatalyst. The activity of the catalyst and $M_\eta$ of PE are lower than those produced with [Ni(cod)$_2$].

There is an increasing interest in the field of single-site bimetallic olefin polymerization catalysis since these systems may exhibit increased activity, branch formation, and comonomer enchainment versus their mononuclear analogues. The origin of these bimetallic cooperativity effects is proposed to include non-negligible comonomer secondary binding to weakly basic groups on the olefin which modifies relative chain transfer rates and facilitates comonomer enchainment at the second, proximate metal center.

The first example of neutral binuclear nickel(II) catalysts are the bimetallic salicylaldimine–nickel complexes with *tert*-butyl (**80**) or Ph (**81**) substituents in R$^2$ were prepared by Zhang [54]. At 10 atm of ethylene pressure complex **80** was catalytically less active toward ethylene polymerization with ca. 2–3 equiv. of [Ni(cod)$_2$] as phosphine scavenging agent, while complex **81** comprising a phenyl group was demonstrated to have high potential for ethylene polymerization without any cocatalyst. Although $^t$Bu groups are generally considered to be bulkier than unsubstituted phenyl group, phenyl is more electron-withdrawing than $^t$Bu. Complex **81** (R$^2$ = Ph), therefore, revealed a marked increase from 37 kg PE mol Ni$^{-1}$ h$^{-1}$ for **80** (R$^2$ = $^t$Bu) to 110 kg PE mol Ni$^{-1}$ h$^{-1}$. This electron-deficient effect is consistent with the electronic effect of mononuclear Grubbs catalysts. It is notable that the polymerization temperature greatly influences the activity of the binuclear nickel catalyst. For **81**, lower temperature (30 °C) represents the optimum and at an increased temperature of 50 °C or 70 °C, catalytic performance quickly decreased from 290 kg PE mol Ni$^{-1}$ h$^{-1}$ to be 64 and 21 kg PE mol Ni$^{-1}$ h$^{-1}$, respectively.

Polyethylene obtained employing binuclear **81** revealed higher $M_w = 141$ kg mol$^{-1}$ and relatively broader molecular weight distribution ($M_w/M_n = 6.1$) than PE from the mononuclear one ($M_w = 18.6$ kg mol$^{-1}$, $M_w/M_n = 2.8$). The broad polydispersity was supposed to arise from the interactions of the metal centers, electronically coupled through the ligand, which may create more than one active species. $^{13}$C NMR showed that the polymers produced by **81** are moderately branched, with methyl branches predominating (ca. 20 methyl branches per 1,000 carbon atoms).

High catalytic activities for ethylene polymerization with a series of novel *m*-arene-bridged salicylaldimine-based binuclear neutral nickel(II) complexes (**82–91**) in the presence or absence of the phosphine scavenger [Ni(cod)$_2$] were also obtained by Huang et al. [55]. The introduction of an electron-withdrawing group to the ligand framework improves the catalytic activity significantly.

Highly branched polyethylenes (46–127 branches per 1,000 carbon atoms) with moderate molecular weights ($M_\eta$ = 10–169 kg mol$^{-1}$) and narrow molecular weight distributions ($M_w/M_n$ = 2.3–2.4) were obtained. In the presence of a polar solvent such as THF or $Et_2O$, complex **89** polymerizes ethylene as a single-component catalyst. The variation of substituents on the *ortho*-positions of the phenyl rings and arene bridge of the ligand dramatically influences the polymerization behavior of these binuclear nickel complexes. The introduction of an electron-withdrawing group to the ligand framework improves the catalytic activity significantly, and very high molecular weight polyethylenes can be obtained by complexes **90** and **91** with nitro groups. In comparison to the corresponding mononuclear Ni catalysts, the binuclear Ni catalysts showed higher thermal stability, and complexes **82**, **84**, **86**, and **87**, which feature small $R^2$ substituents, are capable of acting as single-component ethylene polymerization catalysts showing much higher thermal stability and can tolerate polar functional groups.

Recently, novel binuclear Ni(II) methylpyridine complexes (**92–95**) of di (salicylaldimines) bridged in the *p*-position of the N-aryl moiety were prepared and characterized by Mecking [56], and studied for ethylene polymerization. No activators were used with the pyridine complexes. They are active between 20 and 70 °C as single-component catalyst precursors. Maximum productivities were observed at 50 °C, while at higher temperatures some deactivation occurs. Mecking compared the performances of pyridine complexes to those of the complex with the less strongly coordinating tertiary amine tmeda (**96**). A high activity was observed at low polymerization temperature (20 °C). In both cases the substitution in the 2, 2′, 6, and 6′ positions of the N-aryl moieties with 3,5-bis(trifluoromethyl)phenyl groups results in more active catalysts than isopropyl substitution.

Polymerization activities of all binuclear complexes are substantially higher than those of mononuclear analogues. A maximum activity of 9,520 kg PE mol Ni$^{-1}$ h$^{-1}$ was observed for **96**, with formation of high molecular weight polymers of $M_w$ 920 kg mol$^{-1}$ and $M_n$ 280 kg mol$^{-1}$. The increase in polymerization activity of the binuclear complexes, compared to the mononuclear analogues, appears to be due to an intrinsically higher rate of chain growth rather than to a more efficient dissociation of pyridine as activator of the catalyst precursors. Polymer microstructure is affected by chain walking only to a small extent. Linear polyethylenes with, for example, two methyl branches per 1,000 carbon atoms (polymerization temperature 30 °C) have been obtained.

Binuclear neutral nickel(II) complex (**103**) based on the 3,3′-bisalicylaldimine ligand, was synthesized in high yield by Li [63]. Interestingly, this complex, which may be treated as the product of the two **1** molecules coupled at the *ortho* position of the phenoxy group, is capable of polymerizing ethylene without any cocatalyst with an activity of up to 455 kg PE mol Ni$^{-1}$ h$^{-1}$ and with $M_w$ up to 487.7 kg mol$^{-1}$ and relatively broad molecular weight distribution ($M_w/M_n$ = 2.8–3.8) were produced. In contrast in the absence of other added activators, complex **1** exhibited no activity for ethylene polymerization. Even when $[Ni(cod)_2]$ or $B(C_6F_5)_3$ was used as a phosphine acceptor, only a low catalytic activity was observed.

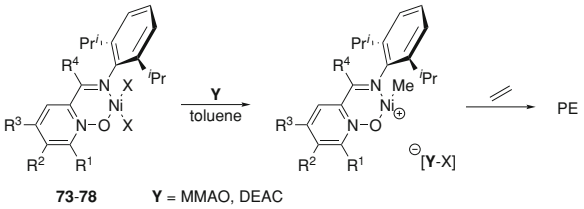


**Fig. 2.24** Ethylene homopolymerization by iminopyridine *N*-oxides-based catalysts

Marks [60] reported the synthesis and characterization of novel bimetallic, neutrally charged dinickel 2,7-diimino-1,8-dioxynaphthalene polymerization catalysts. Room-temperature ethylene homopolymerizations were carried out in the presence of the phosphine scavenger/cocatalyst [Ni(cod)$_2$]. Bimetallic **104**, **105**, and **106** afforded polyethylenes with molecular weights comparable to those produced by the mononuclear analogue **107** and with polydispersities consistent with single-site processes ($M_w \sim 10$ kg mol$^{-1}$, $M_w/M_n = 2.5$). Moreover, the bimetallic catalysts exhibit a 2-fold greater polymerization activity along with increased methyl branching.

In addition to the nature of the copolymer microstructures produced, the mechanism by which the cooperative effects take place was investigated. Low temperature 1 and 2D $^1$H NMR spectroscopy of the thermally labile [Ni$_2$(**C24**)-Bu$_2$(PPh$_3$)$_2$] derivative provides evidence for agostic species in the bimetallic complex. Results evidenced also an agostic interaction of an alkyl group coordinated to one Ni communicating with the second Ni. Such agostic interactions which span both metal centers contribute to Ni ⋯ Ni cooperation. Thus, bimetallic catalysts evidence significant active center-active center cooperative effects in ethylene homopolymerization versus their mononuclear analogues. This cooperativity doubtless arises from the rigidity of the ligands that binds the two Ni centers in close enough proximity (Fig. 2.24).

Recently, Campora devised to replace the anionic aryloxide of salicylaldiminate systems with a neutral pyridine N-oxide to attain highly active catalysts. Nickel catalysts with 2-iminopyridine N-oxides (PymNox) as ligand constitute a promising class of complexes that lead to cationic equivalent of the well-known salicylaldiminate system. The electrically neutral N-oxide fragment effectively delocalizes the positive charge on the ligand. A series of nickel PymNox complexes with different substitution patterns in the ligand were synthesized [53]. They (**73–79**) are active catalysts for the ethylene polymerization or oligomerization when activated with alumoxanes or diethylaluminum chloride (DEAC). Actually, PymNox nickel catalysts are more active than their neutral salicylaldiminato-based analogues, but the two systems give rise to similar polymers in terms of both molecular weights and branching degree. Electronic effects modulate the activity. An electron–donor group ($R^3$ = OMe) in the remote position 4 of the pyridine ring causes a modest decrease of the catalytic activity and increase of the polyethylene molecular weight, a strong electron-withdrawing group ($NO_2$) in the same position shifts the catalyst selectivity from ethylene polymerization to oligomerization. More importantly, the introduction of a phenyl substituent in

*ortho*-position causes a significant increase of the catalytic activity and the polymer molecular weight. Thus, performances of PymNox catalytic systems are strongly reminiscent of those of nickel salicylaldiminates.

The $\eta^3$-benzyl (2-(alkylideneamino)benzoato)nickel complexes in the presence of $B(C_6F_5)_3$ give the zwitterionic $\eta^3$-benzyl complexes active in the polymerization of ethylene (Fig. 2.25). NMR studies with a methallyl complex **108** [61] showed no consumption of ethylene. However, after the mixture standed overnight, the appearance of polymer particles along with the disappearance of the ethylene signal was observed, but signals of the end vinyl group were not detected, which implies that even the molecular weight of the soluble part of the obtained poly(ethylene) was fairly high. In contrast the $\eta^3$-benzyl analogue **109**, which displays faster initiation rates, gave high activity (3,200 kg PE mol $Ni^{-1}$ $h^{-1}$) when the polymerization was initiated at 50 °C, while the activity of the zwitterionic species of **110** is 4,100 kg PE mol $Ni^{-1}$ $h^{-1}$ under the same conditions. The obtained polyethylenes are branched in the range of 35–50 branches/1,000 carbons. The branch number decreases slightly with increase of the pressure. Molecular weights of polyethylene are rather low ($M_w \sim 10$ kg $mol^{-1}$) while the molecular weight distribution is narrow ($M_w/M_n = 2.0$–$2.7$), indicating that a single active species is present in the polymerization solution. Even though molecular weights are rather low this result is interesting when considering that the corresponding (2-(diphenylphosphino)benzoato)- and (2-(diphenylamino)benzoato)nickel complexes give mainly butene by a rapid chain transfer reaction.

The chain transfer process is usually reduced by an increase of steric bulkiness on the axial sites, but no increase of the steric bulkiness on the axial sites is observed when the solid structure of the (2-(cyclohexylideneamino)benzoato)nickel complex is compared with that of the (2-(diphenylamino)benzoato)nickel complex. Thus, reduction of the chain transfer process in (2-(alkylideneamino)benzoato)nickel complexes might be explained by a change of electronic effect.

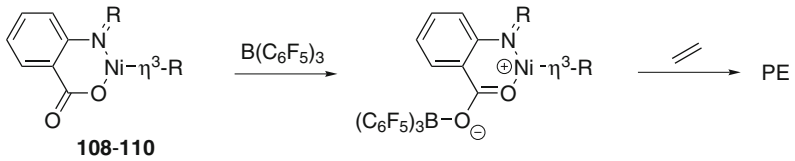


**Fig. 2.25** Ethylene homopolymerization by $\eta^3$-R (2-(alkylideneamino)benzoato)nickel catalysts

**Fig. 2.26** Ethylene homopolymerization by nickel diazene-naphtholato-based catalysts

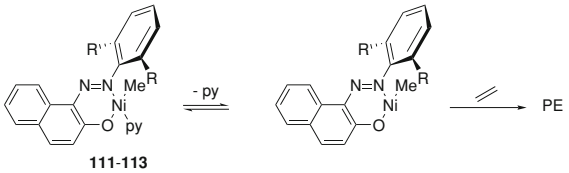

The search for new ligand structures with other donor functions, empirical to a large extent, though developments had provided some guidelines for catalyst design lead to the synthesis of another class of neutral nickel(II) complexes with chelating diazene ligands [62] as ethylene polymerization catalysts (Fig. 2.26). Well-defined complexes are available as precursors to activator-free catalysts. All complexes **111**–**113** are moderately active for ethylene oligo- or polymerization, depending on the steric bulk of the substituent on the aryl group. The catalyst bearing the bulky substituted aryl group (R = $^{i}$Pr) (**113**) bound to the diazene function give polymeric materials while a reduction in steric bulk results in a marked decrease in product molecular weight (oligomers). This dependence of the catalytic behavior on the ligand substitution pattern clearly demonstrates coordination of the diazene moiety to the metal center throughout the catalytic reaction. Polymerization requires somewhat elevated temperatures (70–80 °C). The temperature stability is increased by bulky substituents (**113** > **112** > **111**), the catalyst with the less sterically demanding R = H (**111**) decomposing to a significant extent already at temperatures above 50 °C. The polyethylenes obtained by the complex with the bulky substituted diazene ligand (**113**) has typically $M_w > 50$ kg mol$^{-1}$ and $M_w/M_n = 1.8$–$2.3$, indicative of a well-behaved single site catalyst.

Brookhart [64] to further enhance the activity of neutral Ni(II) catalysts synthesized new neutral (N–O) chelated Ni(II) complexes, derived from anilino-substituted enone ligands bearing strongly electron withdrawing $-CF_3$ and $-C(O)CF_3$ [51] in the ligand backbone, and utilized in ethylene polymerization in the presence of an activator as $[Ni(cod)_2]$ or $B(C_6F_5)_3$ (Fig. 2.27). Polymerizations were generally carried out at ethylene pressures between 7.09 and 28.37 bar and temperatures from 25 to 80 °C. Without the addition of an activator to sequester $PPh_3$, that drives the equilibrium toward the Ni(ethylene)(alkyl) complex, low productivities were observed for complexes **117**, **118** and no polymer was obtained for **119**, **120** even at 14.18 bar of ethylene. This implies, that even at high ethylene pressures the equilibrium lies in favor of the $PPh_3$ complexes. The productivity under standard conditions (13.78 bar, 60 °C, $[Ni(cod)_2]$ activator) follows the order **117** > **118** > **119** ~ **120**. The spread in productivities was modest but significant (14,168 kg PE mol Ni$^{-1}$ h$^{-1}$ for **117** to 840 kg PE mol Ni$^{-1}$ h$^{-1}$ for **120**). Moderately branched polyethylenes, generally in the range of 35–55 branches per 1,000 carbons, were produced, consistent with expectations based on the presence of *ortho*-disubstituted aryl groups on nitrogen. It is worth noting that **117**, the most productive and with long lifetime catalyst, is the only one which bears no methyl substituent $R^3$ to nitrogen.

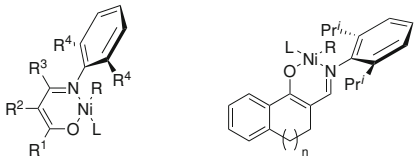


**Fig. 2.27** Catalysts with *β*-ketoimine frameworks

Neutral $\beta$-ketoiminato nickel complexes **121–125**, bearing a bulky substituent at the $R^1$ position of the ligand, were designed by Li [63–65] et al. This design was based on Grubbs's results that introduction of a bulky substituent at the ortho position of the phenoxy group not only blocks the axial faces of the nickel center and retards the rate of chain termination but also enhances the catalytic activity by accelerating triphenylphosphine dissociation and decreases the rate of catalyst deactivation. Neutral nickel complexes **121–125** were investigated as the catalysts for ethylene polymerization in toluene. The ligand structure significantly affects catalytic activity and polymer microstructure along with properties. Catalyst **121** shows an activity of 13.86 kg PE mol $Ni^{-1}$ $h^{-1}$ $bar^{-1}$ using $B(C_6F_5)_3$ as phosphine scavenger (T = 60 °C, $p$E = 25.33 bar, and B/Ni molar ratio = 1). It is noteworthy that catalyst **122** shows a much higher activity of up to 135.6 kg PE mol $Ni^{-1}$ $h^{-1}$ $bar^{-1}$ under the same conditions, which is about 10 times more than the unsubstituted catalyst **121**. Under the same conditions, a comparable catalytic activity of 106 kg PE mol $Ni^{-1}$ $h^{-1}$ $atm^{-1}$ was observed for catalyst **123**. These results confirmed that an aryl group in the $R^1$ position greatly enhances the catalytic activity for ethylene polymerization of the $\beta$-ketoiminato neutral nickel catalyst, just like salicylaldiminato neutral nickel catalysts. Probably also with these systems the aryl in the $R^1$ position plays a key role in protecting the active nickel species from the formation of bis-ligated analogues, proven in salicylaldiminato nickel catalysis to be inactive toward ethylene polymerization. **124** is the catalyst with intrinsically low activity toward ethylene polymerization 5.54 kg PE mol $Ni^{-1}$ $h^{-1}$ $bar^{-1}$ while catalyst **125** showed a higher activity of 21.38 kg PE mol $Ni^{-1}$ $h^{-1}$ $bar^{-1}$ relative to catalyst **124**, but the activity is still much lower than that of **122**.

The variation of the $R^2$ group also had a remarkable influence on the branch content and microstructure of the polymer produced, allowing access to the polyethylene whose structure varies from a relatively linear semicrystalline material (with catalyst **122**) to a highly branched (with catalyst **125**) and completely amorphous material.

Moreover, Li [68] succeeded in the synthesis of easily accessible complexes, which are highly active catalysts (**130–135**) for ethylene polymerization without an activator. Under the optimized conditions ($p$E = 50.66 bar, T = 63 °C) an activity of 70.69 kg of PE mol $Ni^{-1}$ $h^{-1}$ $bar^{-1}$ and $M_w$ of 46.5 kg $mol^{-1}$ were observed using **132** as a catalyst. Particularly, it is of great interest that a bulky substituent proximate to the oxygen atom of the $\beta$-ketiminato complex is no longer a prerequisite to attain high catalytic efficiency, which is much different from the case for salicylaldiminato neutral nickel catalysts. Moreover, the degree of conjugation between the phenylene ring and the corresponding nickel chelate of the complex can be tuned via changes in the ligand structure, which remarkably influences the molecular weights and the microstructures of the resulting polyethylenes. The less conjugated complexes **131**, **132** and **134**, **135** produced polyethylenes with much higher molecular weights and lower branching numbers relative to those from the rigid, highly conjugated complexes **130** and **133**.

DFT methods gave a rationale of the main difference between these and the salicylaldiminato complexes, that is the high catalytic efficiency of complexes without a bulky substituent at the close position of the coordinating oxygen atom originates from the lower activation energies of these complexes relative to the typical salicylaldiminato complexes.

The synthesis of a new organometallic nickel complexes supported by the 3-cyano-4-(2,6-diisopropylphenylimino)pent-2-en-2-olate ligand **129** [67] allowed for the investigation of remote activation through an exocyclic CN functionality. The binding of $B(C_6F_5)_3$ to the carbonitrile nitrogen results in a redistribution of electron density within the electronically delocalized ligand framework and initiates the homopolymerization of ethylene. The resulting polymers are described by monomodal molecular weight distributions. This complex, activated via an exocyclic CN functionality, opens new ways to design of appropriate ligands for zwitterionic ethylene polymerization initiators.

Aryl nickel phosphine complexes containing pyridine carboxylate ligands represent the first example of single component catalysts for oligo- or polymerization of ethylene [71, 72]. Electronic effects on nickel-catalyzed oligomerizations/polymerizations were delineated through the use of a series of substituted pyridine carboxylate complexes (**138**–**145**). Lower basicity of the substituted pyca ligand facilitated migratory insertion and therefore chain growth. At 80 °C and 40 bar, the electron-rich methoxy substituted catalyst (**146**) gave mostly linear olefins (56%) with only 10–20 % of the product consisting of higher molecular weight polyethylene. The electron deficient nitro-substituted catalyst (**147**) produced between 80 and 100% of high molecular weight PE under similar conditions. In addition, the nitro-substituted catalyst gave the highest activities of all these complexes.

The α-iminocarboxamide ligands were selected by Bazan who first thought that metal activation by formation of carbonyl adducts could form the basis of a new strategy for designing novel nickel olefin polymerization catalysts (Fig. 2.28) [73]. It was disclosed that the activation of **152** with $[Ni(cod)_2]$ results in an active olefin polymerization catalyst which is capable of catalyzing the quasi-living homopolymerization of ethylene. Polymerizations were conducted at 7.09 bar, 20 °C and for 20 min. No polyethylene was formed when **152** was used alone. There is a sharp increase in reactivity when the $[Ni(cod)_2]$/**152** ratio increases from 1 to ca. 2.5, followed by a slower increase in activity as this ratio approaches. NMR spectroscopy showed that the polyethylene has a relatively low branching content

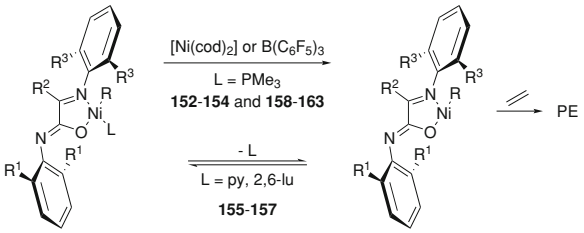


**Fig. 2.28** Ethylene homopolymerization by α-iminocarboxamide nickel catalysts

(10–20 Me branches per 1,000 C). The molecular weight distributions are monomodal but not as narrow as those of a truly living system; the authors proposed this results from an initiation step considerably slower than the propagation and from the precipitation of the polymer.

The α-iminocarboxamide species **155** and **156**, [96] that take advantage of pyridine ligand instead of $PMe_3$ as **152**, are single-component initiators for the polymerization of ethylene. There is no need to use $[Ni(cod)_2]$ for activation, as is the case for the $PMe_3$ analogues. However, the thermal activation required for dissociation of py or 2,6-lu probably reduces the control over the polymer structure; that is, it was not possible to find polymerization conditions with quasi-living characteristics. The polymerizations with **156** can be accomplished under milder reaction conditions, relative to **155**. Best results in activity (304 kg PE mol $Ni^{-1}$ $h^{-1}$) and molecular weight ($M_w$ 143 kg $mol^{-1}$, $M_w/M_n = 2.2$) were obtained in the presence of **156** at $p$E = 6.89 bar and $T = 40$ °C.

More recently, neutral nickel complexes containing α-iminocarboxamide, $\eta^1$-$CH_2Ph$, and $PMe_3$ ligands were synthesized by Bazan [75] and used in the homopolymerization of ethylene. In particular, the effect of steric and electronic variations at the site adjacent to the imine functionality was studied. Ethylene homopolymerization reactions were performed using complexes **154**, **158–163** and $[Ni(cod)_2]$ as activator. Polymerizations were carried in toluene at an ethylene pressure of 7.09 bar at 20 °C. The polymerization activity increases as the bulk on the ligand framework increases i.e. **154** < **158** ~ **161** < **159** < **160**. The isopropyl derivative **160** exhibits an activity > 2-fold as compared to the parent methyl species **152**. The $M_n$ of the polymer products also increases proportionally with the increase in activity. Compound **160** exhibits the lowest molecular weight distribution ($M_w/M_n \sim 1.2$) when compared to the other alkyl variants.

In the case of **161**, the activity and molecular weight observed are higher than those obtained with the parent species **152**. The molecular weight and activity are higher for compound **162** and lower for **163** relative to **161**. This trend suggests that as electron density is removed from the metal center, the catalytic species becomes more active in ethylene polymerization reactions (i.e., reactivity: **162** > **161** > **163**). Polyethylene made with compounds **161–163** exhibits the narrowest polydispersities, between 1.1 and 1.2 in all cases.

A new family of ligands based iminohydroxamate backbone and their transition metal halide complexes were proposed by Bildstein [76] as new precatalysts for MAO activated olefin polymerizations. Ethylene polymerizations were performed in toluene, at a temperature of 70 °C at $p$E of 40 bar. In terms of activity, only compound **164** truly stands out as a precatalyst with a high activity of 302.8 kg PE mol $Ni^{-1}$ $h^{-1}$ $bar^{-1}$ but in short polymerization time. Indeed, the stability of the $[N,O]NiBr_2$ complexes **164-167** in their MAO-activated form has not yet been optimized, indicating fast deactivation pathways. PE samples obtained from nickel complexes **164–167** were of the HDPE type with no detectable branches and molar masses ($M_v$) of 1.0 to 250 kg $mol^{-1}$.

Brookhart [77, 78] designed a ligand which incorporated the key elements of the six-membered chelate salicylaldimine ligand but which would lead instead to a

five-membered chelate. He chose for this purpose the 2-anilinotropone moiety because it contained the desired anionic N,O chelate, a hindered N-aryl group, and complete conjugation between the N and O. The corresponding highly neutral nickel catalyst is active in ethylene polymerization and it does not require an activator (Fig. 2.29).

Under optimized conditions, catalyst **169** can produce PE, without the addition of a cocatalyst, with a TOF of $8.8 \times 10^3$ kg of PE mol $Ni^{-1}$ $h^{-1}$ in a 10 min run. Additionally, **169** produced PE with a substantially higher $M_n$ when compared with the salicylaldimino type bearing the anthryl substituent in the *ortho* position (89.6 vs. 54 kg $mol^{-1}$). Nevertheless **169** shows a short lifetime when compared to 2-salicylaldimino type bearing the anthryl substituent. Ethylene pressure has also been shown to have dramatic effects on the resultant PE. Increasing the pressure from 1.01 to 40.53 bar at 80 °C causes a decrease in the branching number from 113 to 41 branches per 1,000 C.

Moreover, a series of anilinotropone ligands and corresponding nickel complexes was synthesized in an effort to determine the effects of varying the *ortho*-aryl substituents on ethylene polymerization. Catalysts incorporating alkyl substituents at the 2- and 6-positions of the N-aryl ring generated high-molecular-weight polyethylenes with monomodal molecular weight distributions of ca. 2 (or less at low temperatures). Total turnover numbers of ca. 60,000 were observed in 10 min at 80 °C, but catalyst lifetimes are short at this temperature. Branching increases with increasing temperature and decreasing pressure, consistent with earlier observations using aryl-substituted diimine catalysts.

Replacement of the standard 2,6-diisopropyl substituents on the aryl group with 2,6-dimethyl (**168**), 2,6-dichloro (**173**), 2,6-dibromo (**174**), and 2-methyl-6-trifluoromethyl (**178**) substituents had little effect on productivity. A slight increase in TON was observed for the 2,6-diphenyl-substituted catalyst (**172**). Significant reduction in TON was observed for the 2-methyl-6-tert-butyl-(**171**), 2-methyl-(**177**), 2-tert-butyl-(**170**), and 2,3,4,5,6-pentafluoro-substituted (**175**) catalysts. Molecular weights generally increase with increasing steric bulk of the *ortho* substituents.

Substitution of the 2-(2,6-diisopropylanilino)tropone ligand with either phenyl (**180**) or naphthyl (**181**) groups resulted in a small increase in productivities and lifetimes at 80 °C and 14.18 bar. However, at 40 °C these catalysts exhibited much longer lifetimes ($t_{1/2} > 1$ h) and higher total turnover numbers

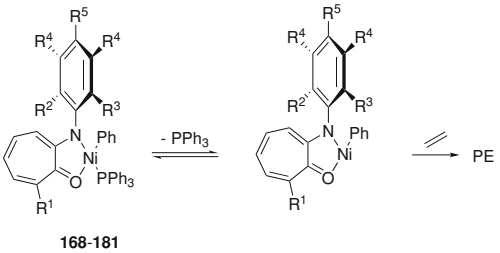


**Fig. 2.29** Anilinotropone-based catalysts for ethylene polymerization

could be achieved relative to 80 °C polymerizations. Molecular weights of the polyethylenes increased with pressure, which suggests that chain transfer at least in part occurs through classical $\beta$-H elimination rather than chain transfer to monomer. The catalyst decay product is the Ni(II) bis-ligand complex, whose formation must be initiated by reductive elimination of the ligand from a Ni(II) species.

The anilinoperinaphthenone nickel complexes **183**, **184** [80] are active ethylene polymerization catalysts and **184** is significantly more reactive than **183** with turnover numbers of 47,000 and 8,000, respectively, under identical reaction conditions (14 atm ethylene, 80 °C). The number average molecular weight under these conditions is 99,000 with a $M_w/M_n = 1.9$ and significantly increases with ethylene pressure (e.g., $M_n$ = 37 kg mol$^{-1}$ at 3.04 bar, 80 °C; 54 kg mol$^{-1}$at 7.09 bar, 80 °C) suggesting that chain transfer to monomer is not the major chain transfer mechanism. As temperature increased from 40 to 100 °C, with pressure held constant at 14 atm ethylene, the number average molecular weight of the polymer decreased and the branching number increased from 17 to 66 branches per 1,000 carbon atoms. The catalyst half-life is ca. 20–30 min. In conclusion, these catalysts have an activity that is similar to the previously reported anilinotropone based neutral nickel(II) ethylene polymerization catalysts. The similarity in overall activity suggests that the lack of delocalization of electron density onto the oxygen atom has little effect on catalyst performance.

A novel nickel complex ligated with 2-(2,6-diisopropylanilino)-1,4-naphthoquinone (**185**) was synthesized by Shiono [81]. This complex polymerized ethylene at 40 °C to give linear polyethylene in low yield. On the other hand, **185** when activated with 4 eq of $B(C_6F_5)_3$ was highly active for ethylene polymerization and gave a polymer possessing short methyl, ethyl, and propyl chain branches formed by a chain walking mechanism, as well as long chain branches, the content of long chain branches was almost the same as that of all short chain branches. Thus, the macromonomer formed via $\beta$-H elimination were effectively copolymerized with ethylene to give the long chain branches.

Later on, a series of nickel complexes (**186–188**) bearing anilinonaphthoquinone derivatives possessing different substituents were synthesized [82]. Decreasing the bulkiness of 2,6-substitution on anilines lowered the polymerization activity as well as the molecular weight of the polymer produced. In contrast, the methyl substitution at 4-position of aniline increased the polymerization activity and the molecular weight of the products. This indicates that polymerization activity and molecular weight depended on the electronic state of the metal center as well as the bulkiness of 2,6-substitution on anilines. The molecular weight of the obtained polymer increased lowering the temperature, indicating that the $\beta$-H elimination is more suppressed than propagation at low temperature. This trend is more notable with the complex with the less bulky substituent on aniline 2,6-position. These complexes produce short chain branches such as methyl, ethyl, and propyl as well as long chain branches. The branching amounts decreased in the more bulky systems, indicating that chain migration was suppressed by introducing bulky substituent at 2,6-position of aniline.

New, neutral binuclear nickel(II) complexes with bridging ligands comprising 2,5-disubstituted amino-*p*-benzoquinones (**189**–**193**) have been synthesized and tested in the ethylene polymerization without any cocatalysts [83]. The complexes are catalytically active in ethylene polymerization. Particularly, complex **189**, comprising a bulky substituted aryl group bound to the anilino function, has activity comparable to that of the Grubbs catalyst **3** under the same conditions. A reduction in steric bulk resulted in a marked activity decrease while the optimum polymerization temperature seems to be 80 °C. Polyethylene obtained employing complexes **189**–**191** revealed molecular weights of $M_w = 4.31$, 535, and 60.3 kg mol$^{-1}$, respectively. The molecular weight distribution is quite wide (3.21–48.24) and quite different from those of well-behaved single-site catalysts. Methyl branches predominate with ca. 10 methyl branches per 1,000 carbon atoms but additional higher branches, such as butyl, are also present.

In the course of their studies on metal complexes of amino acids and their derivatives Beck et al. [84] reported the synthesis of aryl complexes of nickel and palladium with the "classical" α-amino carboxylates as N–O-chelate ligands which may have catalytic activity. The complex **194** is, in the presence of $AlEt_3$, a highly active catalyst for the polymerization of ethylene (up to 1,800 kg PE mol Ni$^{-1}$ h$^{-1}$). The polymerization started with a high activity peak. Polymers with high molecular weights (up to 900 kg mol$^{-1}$) were obtained. In comparison with the related nickel complexes by Cavell (**147**), Keim and Grubbs (**1–10**) and their co-workers complex **194** affords polymers with remarkably high molecular weights and with much less branching.

The quest for identifying novel Ni(II) and Pd(II) catalysts bearing bulky bidentate ligands which would expand the scope of utility of such catalysts encouraged considerable efforts. The interest to have catalysts with higher thermal stability than bisimine Ni(II) and Pd(II) catalysts which decompose rapidly at about 70 and 50 °C, respectively prompted towards the synthesis of late transition metal complexes with various phosphine nitrogen (P–N) ligands (Fig. 2.30).

Ni(II) and Pd(II) complexes (**217**–**219**) with phosphine imine hybrid ligands were successfully synthesized by Guan [34]. The Ni(P–N) complexes assume a tetrahedral coordination geometry, while the Pd(P–N) complexes are all square planar. The Ni complexes, upon activation with MAO, were active for ethylene polymerization and significantly more stable than the corresponding Ni-diimine complexes, whereas the activities of these catalysts are lower than those of the Ni-diimine complexes. Complex **219** was much more active than **217**–**218** and this is presumably due to differences in the electronic structure. The phosphine in **217**–**218** is much more electron rich than the phosphine in **219** because the $^t$Bu group has stronger electron donating ability than the phenyl group. On the other hand, the lower molecular weight of polyethylene obtained with complex **219** is attributed to the decreased steric bulkiness of the diphenylphosphine as compared to the di-*tert*-butylphosphine in **217**–**218**. In complex **217** the chain transfer process should be reduced by the orientation of both the $^t$Bu groups from phosphine and the isopropyl groups of aniline towards the axial positions. However, the asymmetry of the steric bulkiness for **217**, the top axial face being much more

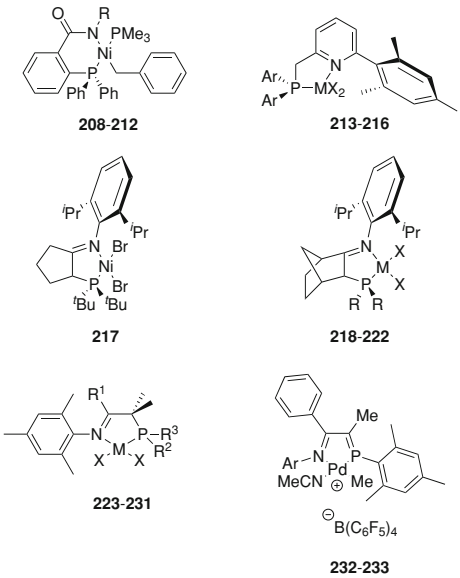


**Fig. 2.30** Catalysts with N–P mixed chelating ligands

open than the bottom one, makes the metal center susceptible to chain transfer. This is presumably the cause for the formation of polyethylenes with relatively low molecular weight in the ethylene polymerization catalyzed by the Ni(P–N) complexes. Another remarkable feature of ethylene polymerization by the Ni(P–N) complexes is that the polyethylenes formed contain much more branches (50–60 total branches per 1,000 C) than the polyethylenes by diimine complexes under similar conditions. Significant amounts of relatively long branches (such as amyl and hexyl) are formed. The presence of ethyl in isobutyl groups reveals the existence of short branch on-branches. Thus, chain walking is more competitive with complexes **217–219** than in the Ni-diimine system. In contrast, all the Pd(P–N) complexes **220–222** upon activation with MAO were inactive to polymerize ethylene probably due to their electronic structure. The major fraction of the polyethylene obtained by Guan had low $M_w$ in the range of a few thousands, but the minor fraction consisted of very high molecular weight polymer ($M_w$ up to $10^3$ kg mol$^{-1}$). Brookhart hypothesized that at high temperatures used by Guan the catalyst backbone is easily enolizable which is partially chemically modified, and this modification is responsible for the low molecular weight fraction in the polymer.

Thus, bulky nonenolizable phosphineimine Ni(II) (**223–227**) and Pd(II) (**228–231**) complexes from bidentate ligands were prepared by Brookhart [35] with the hope of obtaining thermally stable polymerization catalysts which would produce high molecular weight, branched polyethylene. They did show improved temperature stability with respect to the corresponding diimine complexes.

At 80 °C the palladium catalysts oligomerize ethylene giving branched oligomers with $M_n$ up to 0.66 kg mol$^{-1}$. Reaction of **229** with $NaB(C_6F_5)_4$ generates

the ion-pair [Pd(**V2**)Me][B($C_6F_5$)$_4$] that is unable to polymerize ethylene. In the iminephosphine palladium complexes the situation is unfavorable for migratory insertion since in the more stable isomer of [Pd(**V2**)Me]$^+$ the Pd–Me bond is expected to be stronger than the Pd–Me bond in diphosphine while the Pd–ethylene interaction is stronger than that in the diimine ligands. Thus, the stability of the methyl ethylene "unit" is greatest in [Pd(**V2**)($h^2$-$C_2H_4$)Me][B($C_6F_5$)$_4$]. The migratory insertion barrier of ethylene into the Pd–Me bond was shown to be 24.8(3) kcal mol$^{-1}$, which is ca. 8 kcal mol$^{-1}$ higher than the corresponding barriers in diimine and diphosphine palladium complexes.

The nickel dimethyl-substituted complex **223** was used to screen the behavior and efficiency of several aluminum alkyl derived activators. The use of ethylaluminum dichloride led to the production of butenes with TO h$^{-1}$ > 10$^6$ in an exothermic reaction. Activation with DEAC resulted in the production of butenes and only polymer traces. Polymethylaluminoxane (PMAO–IP) afforded both butenes and polymer while the use of MMAO-3A under 27.86 bar of ethylene at room temperature gave exclusively polymer with $M_n = 2.4$ kg mol$^{-1}$ and 1,000 kg PE mol Ni$^{-1}$ h$^{-1}$.

Catalyst **225** would be more reactive than dimethyl-substituted complex **223** and give high molecular weight product. Unexpectedly, only a small amount of polymer with a bimodal molecular weight distribution ($M_p = 37.2$; 3.1 kg mol$^{-1}$) was obtained while diphenyl-substituted precatalyst **224** was found to be more effective producing an elastomeric material with $M_n = 72$ kg mol$^{-1}$ and $M_w = 133$ kg mol$^{-1}$. Increase of steric bulk at phosphorus, as in **227**, gives rise to lower molecular weight material ($M_w = 75$ vs. 140 kg mol$^{-1}$ for diphenyl-substituted precatalyst).

The polymer produced by **224** has almost exclusively methyl branches while that formed by **227** at 60 °C contains a great amount of higher branches. In general, polyethylenes obtained using catalysts **223–227** are substantially more branched than polymers obtained by Ni-diimine catalysts under similar conditions.

Finally, nickel imine-phosphine precatalysts containing gemdimethyl substituent α to phosphorus produce substantially higher molecular weight polyethylene compared to the corresponding enolizable complexes.

Pd(II) catalysts incorporating phosphinidine-imine ligands were also synthesized by Brookhart [92]. Complexes **232–233** proved to be ethylene oligomerization catalysts and were studied at 26 °C and 400 psi ethylene. They exhibit very low turnover rates, the more hindered catalyst **232** in a 3 h run yielded 23 kg PE mol Pd$^{-1}$. Higher turnover numbers (94 kg PE mol Pd$^{-1}$) were observed with decreased hindrance in **233** along with a drop of oligomer molecular weight from 0.67 to 0.3 kg mol$^{-1}$. The catalysts are more stable than Pd–diimine complexes at room temperature; they do not significantly deactivate in 15 h. Ethylene insertion barriers were measured for the less hindered mesitylimine system **233** by generating the cationic ethylene complex with NaB($C_6F_5$)$_4$ under excess olefin (20 eq). Insertion of ethylene into Pd–alkyl bonds was measured 18.7 kcal mol$^{-1}$. For comparison, typical migratory insertion barriers in (diimine)palladium(methyl)(ethylene)

complexes are ca. 17 kcal $mol^{-1}$, that is 2 kcal higher than the insertion into barriers in Pd(diimine)Me(ethylene) complexes.

Ni and Pd complexes **213–216** [91] with P–N ligands linked by a nonenolizable rigid carbon framework were designed. The steric bulk was created by introducing substituents at the 6-position of pyridine and a mesityl or tolyl group on the phosphorus atom. The palladium complexes are inactive in the polymerization of ethylene. In fact, palladium black was obtained in most instances, indicating the instability of these palladium complexes under the reaction conditions. The behaviour of nickel complexes in oligo- or polymerization of ethylene is quite different from that of the palladium species. With a molar ratio of MAO to complex of 150:1, complex **213** catalyzed the polymerization of ethylene to form PE in poor yields with a bimodal molecular weight distribution. Butenes and hexenes were obtained in high conversions when a larger quantity of MAO (Al/Ni = 500) is used. The nickel(II) dibromo complexes were highly active in the presence of MAO. With a lower Al/Ni ratio, the nickel complexes catalyzed the polymerization of ethylene, yielding an orthorhombic form.

Zwitterionic 2-diphenylphosphanylbenzamido nickel(II) complexes $[Ph_2PC_6H_4C(O)NR\text{-}\kappa^2\text{-}N,P]Ni(\eta^3\text{-}CH_2Ph)$ (R = $C_6H_5$, (**208**); R = $^t$Bu, (**209**); R = H, (**210**); R = Pr, (**211**); R = $^i$Pr, (**212**) were prepared by Lee [73] and tested in the ethylene polymerization. Generally, in both N–N and N–O late transition metal complexes, steric factors regulate the balance between the chain propagation and the chain transfers. High molecular-weight polyethylene is obtained by sterically congested complexes. However, there are some examples showing that electronic effects of the ligand also may play an important role in determining polymer molecular weight.

Slight changes in the ligand frame of complexes **208–212** result in big differences on the products [90]. Phenylamido complex **208** is unable to oligomerize ethylene under the pressure of 6.89 bar, at room temperature and gives 1-butene. Additions of ethylene gas to complexes **209–212** give mainly butene with relatively low activities (230–300 kg PE mol $Ni^{-1}$ $h^{-1}$). However, isopropylamido complex **212** gives excellent activity at room temperature (2,300 kg PE mol $Ni^{-1}$ $h^{-1}$). When the polymerization temperature is raised to 50 °C, the activity increases to 5,200 kg PE mol $Ni^{-1}$ $h^{-1}$, which is a quite high value among the activities observed for similar-type zwitterionic nickel complexes. The molecular weight of the polymers is considerably high ($M_w \sim 1{,}300$ kg $mol^{-1}$) but rather broad molecular weight distributions ($M_w/M_n \sim 2.8$–$3.7$) were observed, most probably for the difficulty to keep the polymerization under control for the very high activity.

The enormous differences in molar masses could not be easily explained since the two solid structures of **208** and **212** are quite similar. Since a big difference is observed on the angles between the square plane and the benzamide benzene ring it was suggested that, probably, when the angle is steep as observed for **212**, there is a shielding of the other axial site by $\pi$-electrons on the benzamide ring.

Only very few reports are in the literature of attempts to substitute one imine with sulphide groups. The results reported below explain such scarcity.

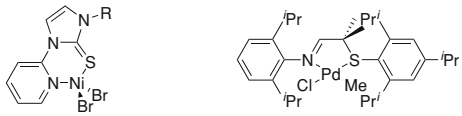


234-235 236

**Fig. 2.31** Rare examples of catalysts with N–S ligands

Brookhart prepared the imine-sulfide palladium(II) complex **236** [92] in an effort to increase the molecular weight of the oligomer/polymer produced with a phosphinidine-imine catalysts (see above). It was expected that geminal dimethyl groups on the chelate backbone of **236** should impart a more restricted conformation to the S-aryl group, thus leading to more effective blocking of the axial sites.

In an NMR experiment **236** activated with $NaB(C_6F_5)_4$ completely consumed ethylene, but in a preparative run under 1.01 bar of ethylene afforded small amount of polyethylene with $M_n = 2.8$ kg mol$^{-1}$ in 44 h. Under 27.86 bar of ethylene, only a small amount (54 mg/3 h; 72 mg/15 h) of polyethylene with $M_n =$ 1.8 kg mol$^{-1}$ was obtained. Since the high pressure experiment afforded less polyethylene than the 1 atm run, probably under high pressure of ethylene the ligand is displaced from the palladium and thus the catalyst decomposes as confirmed by the precipitation of palladium black (Fig. 2.31).

More recently, the nickel complexes **234**–**235** [93] bearing bulky N-substituents were synthesized, they possess potentially reactive sites for the ethylene polymerization. However, unfortunately, after activation with MAO, nickel complex **235** with the bulkier N-2,6-diisopropylphenyl substituent catalyzed ethylene to waxes with low activity at atmosphere pressure. By increasing ethylene pressure to 7 bar only small amount of high molecular weight PE was obtained, while the complex **235** bearing N-$^t$butyl substituent gave only waxes under the same condition. The catalyst activity of **235** to high molecular weight PE was lower than those of the pyridylimine nickel complexes and α-diimine nickel catalysts. Probably steric bulky at only one arm side (imidazole N-substituent) resulted in chain propagation slower than chain transfer in contrast to the α-diimine nickel catalysts with two bulky arm sides. Additional possible reasons for the low activity to high molecular weight PE are in non square planar arrangement of the pyridine and the imidazole rings which lead to deviation of the steric bulk introduced from the axial sites.

### *2.4.3 Copolymerization of Ethylene with Monomers with Functional Groups*

The selective introduction of functional groups into aliphatic poyolefin backbones represents a pivotal and overdue issue in polyolefin technology. Since they can

significantly control surface material properties, such as adhesion, wettability, dyeability, and printability as well as compatibility. Despite the tremendous advances in organometallic-catalyzed olefin polymerization, industrial incorporation of polar monomers in polyolefins still exploits radical polymerization. Radical polymerization provides branched polymers and highly-functionalized copolymers having physical properties not comparable to those of linear polyolefins.

Catalysts based on Ni and Pd, with respect to those based on early transition metals employed in industry, are intrinsically less sensitive to functional groups, as a result of their less oxophilic nature. Certainly they are well far away to be unfailing and any functionalized monomer represents a specific issue in terms of productivity, degree of functionalization, molar mass, etc. Specifically, for any monomer the possible interactions between the main-group functionality and the metal center before and after insertion should be considered. The recent advances in olefin-polymerization catalysts based on late transition metals allow for incorporating most of polar functionalities. For example, N–N Pd-based systems tolerate acrylates, vinyl ketones, and silyl vinyl ethers, they fail with others such as vinyl acetate, vinyl chloride, and acrylonitrile; in any case they afford hyperbranched copolymers with functionalities located mainly at the end of ramifications. Differently, Ni-based systems were reported to afford linear copolymers of ethylene and MA but with extremely low productivity.

Some promising results were reported by catalysts with nitrogen-based mixed chelating ligands. The functionalized monomers so far copolymerized with ethylene by Ni and Pd catalysts bearing nitrogen-based mixed ligands are listed in Fig. 2.32. The monomers are namely functionalized norbornenes, functionalized α-olefins, and polar vinyl monomers, whose C–C double bond is directly substituted by polar functional groups. The norbornene derivatives have the functional group distant from the double bond and are more easily incorporated than functionalized α-olefins. Incorporation of 2–4 mol% of functionalized norbornenes would be enough for depressing the polyethylene melting point and serves as a

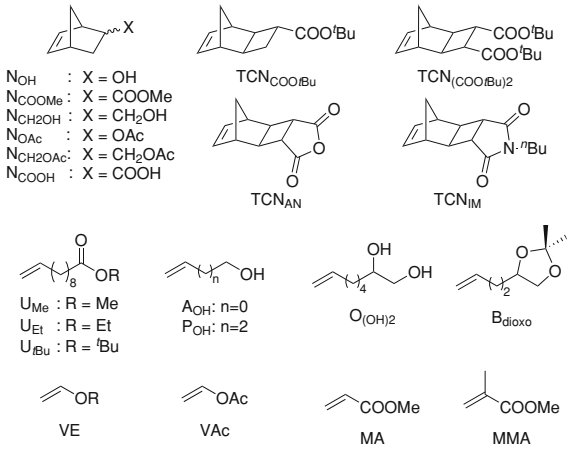


**Fig. 2.32** Functionalized norbornenes, functionalized α-olefins, and polar vinyl monomers copolymerized with ethylene by N–Z-containing catalysts

starting point for testing comonomers that can be incorporated and to what extent. Their features will be discussed in detail in the text along with the behavior with catalysts involved.

Copolymerization reactions of ethylene with functionalized monomers catalyzed by nickel (salicylaldiminato)-based catalysts are summarized in Fig. 2.33.

Complexes **5** and **8** were early reported as single-component catalysts for the copolymerization of ethylene with functionalized norbornene derivatives $N_{OH}$ and $N_{COOMe}$ affording P(E-*co*-$N_{OH}$) with the $N_{OH}$ incorporation of 22 wt%, $M_w = 17.2$ kg mol$^{-1}$, and $M_w/M_n = 1.6$ and P(E-*co*-$N_{COOMe}$) with the $N_{COOMe}$ incorporation of 12 wt% and $M_w = 73.8$ kg mol$^{-1}$, respectively [2]. In the pioneer report the authors pointed out polar group tolerance and effective incorporation of functionalized monomers while neither activities nor difference in catalytic behaviour were discussed. A more exhaustive investigation revealed that acetonitrile-containing catalyst **8** demonstrated a higher activity than the phosphine-containing analogous **5** due to the easier activation, in analogy with ethylene homopolymerization [97].

Copolymerization of ethylene with functionalized norbornene derivatives was extended to monomers $N_{CH2OH}$ and $N_{OAc}$. As expected monomers $N_{COOMe}$ and $N_{OAc}$ bearing ester groups resulted less poisoning than the protic $N_{CH2OH}$ as showed by productivities and molar masses. In addition, the higher the steric demand of substituent onto the comonomer the lower the incorporation (in the

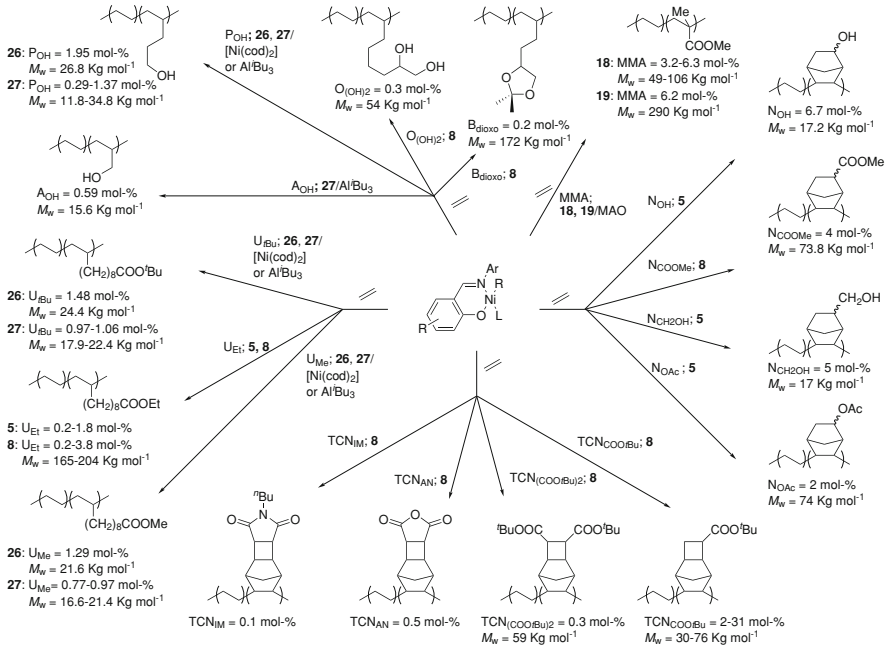


**Fig. 2.33** Functionalized ethylene copolymers obtained by salicylaldiminato complexes

order $N_{COOMe} < N_{OAc} < N_{CH2OH}$). Since starting monomers were used as isomer mixture, this trend is ascribable to *endo* isomers, which after insertion are prone to give chelated intermediates, that block the vacant coordination site of catalyst. In this regard, tricyclononene-based functionalized monomers ($TCN_{COOtBu}$, $TCN_{(COOtBu)2}$, $TCN_{AN}$, $TCN_{IM}$) were expected to be more readily incorporated than bicyclic analogues for the higher distance of polar functionality from olefin double bond. Indeed, catalyst **8** showed a 3.5-fold higher TON in copolymerization of ethylene with monomer $TCN_{COOtBu}$ than with the monomer $N_{COOMe}$ in similar experiment. Interestingly, incorporation of monomer $TCN_{COOtBu}$ could be tuned from 2 to 31 mol% through $TCN_{COOtBu}$/E feed ratio, though productivity dropped down with decreasing E concentration. Other interesting aspects of these uncommon tricyclic monomers were discussed on the basis of their chemical diversity.

Functionalized α-olefins such as alkyl undecylenoate esters $U_{Me}$, $U_{Et}$, and $U_{tBu}$ were successfully copolymerized with ethylene by catalysts **5**, **8** [39, 97], **26** [45], and **27** [46]. Activities of these reactions are approximately one order of magnitude lower than in E homopolymerization in non-coordinating medium (toluene, benzene) but resemble those obtained in more coordinating solvents (ether, esters) [2]. Again, acetonitrile-containing catalyst **8** exhibited higher activities than phosphine-containing **5**, **26**, and **27**. Though to some extent less active, catalyst **26** bearing the cyclohexyl substituent at the ortho position of the phenoxy group showed a slightly higher incorporation of functionalized monomers than anthracenyl-substituted analogous **5** and **8**.

A series of copolymers containing monomer $U_{Et}$ in different concentration was prepared by catalysts **5** and **8**. The resulting materials moved from HDPE to LLDPE domain ($U_{Et} = 10$ mol%). $T_m$ values reflected the composition and decrease with comonomer incorporation as expected.

Interestingly, the ester-functionalized olefins significantly reduce the formation of short alkyl branches (Me, Et, Pr, and Bu) compared to those in ethylene homopolymerization and copolymerization with α-olefins such as 1-octene. This suggests that coordination of polar functionalities competes with β-H agostic interaction, preventing elimination side reactions.

More problematical was the copolymerization of ethylene with free alcoholic monomers $A_{OH}$ and $P_{OH}$ that can hydrolyze Ni-polymeryl bond, protonate the N–O ligand, and favor the displacement. The approach of protecting the alcoholic monomer with $Al^iBu_3$ was exploited for the copolymerization of ethylene with monomers $A_{OH}$ and $P_{OH}$ by catalyst **26–27** that furnished P(E-*co*-$A_{OH}$) in good yield ($M_w = 26.8$ kg mol$^{-1}$, $M_w/M_n = 2.29$, $A_{OH} = 1.95$ mol%). On the other hand, catalyst **8** gave a poor yield and a polymer with low $M_w$ without protecting the diol-containing monomer $O_{(OH)2}$ whereas furnished activity and $M_w$ values as good as in the reactions involving the ester-based monomer $U_{Et}$ when the similar dioxolane $B_{dioxo}$ was copolymerized.

A different and challenging task is represented by (co)polymerization of electron-deficient vinyl monomers such as acrylates. Modification of the energy of frontier orbitals as well as proximity of polar functionality to olefinic double bond

had made the coordination polymerization of these monomers elusive for a long time. A prerequisite for the incorporation of polar vinyl monomers is that $\pi$-coordination of the olefin double bond is competitive with the heteroatom $\sigma$-coordination.

Indeed, attempts to copolymerize ethylene with MA, VAC, and VE by catalyst **5** and **8** failed. An in-depth NMR investigation of organometallic species and decomposition product originating from interaction of more sophisticated salicylaldimino-based catalysts and MA revealed that after the first insertion of MA no further E or MA insertion occurs; VA behaves similarly [97].

MMA is definitely one of the most challenging functionalized monomer to be copolymerized with ethylene because besides the aforementioned features of electron-deficient vinyl monomers it possesses a *gem*-disubstituted olefinic carbon.

Preliminary trials, which exploited bischelated complexes activated by MAO, produced high MMA content materials ($61 < \text{MMA} < 81$ mol%) but molar masses, polydispersities, and microstructure of MMA sequences suggest the cooperation of radical and coordinative mechanism [99]. Conversely, copolymerization by complexes **18** and **19**, which contain nitro groups onto phenoxy ring, activated by MAO (Al/Ni = 15/1) in the presence of ethylene atmosphere ($p$E = 50 atm) afforded high molar mass P(E-*co*-MMA) with an incorporation of MMA of 3–7 mol% and $T_m$ values of about 130 °C, indicating the high linearity of the products.

Iminopyridine *N*-oxide-based complexes **73–78** activated by MMAO were investigated as catalysts for the copolymerization of ethylene with MA (Fig. 2.34). Except for **73**, which effectively furnished P(E-*co*-MA) in low yield and molar mass ($M_n = 1.9$ kg mol$^{-1}$) with low incorporation of comonomer (0.7 mol%), the addition of MA resulted in a complete deactivation of the catalysts.

Copolymerization of ethylene with polar monomers by bimetallic catalysts, which are generally and intrinsically more active than their monometallic analogous, can profit from cooperative effects arising from the close proximity of two metal centers [100].

Indeed, a clear and positive effect of dinuclearity was demonstrated by catalysts **100–102**/$B(C_6F_5)_3$ in copolymerization of ethylene with functionalized norbornene derivatives $N_{COOMe}$ and $N_{CH2OAc}$ (Fig. 2.35) [58].

A series of E-*co*-$N_{CH2OAc}$ copolymerizations by the three catalysts revealed a 2-fold higher activity as well as higher incorporation of functionalized monomer than mononuclear **56** analogous in the same conditions. Complex **102**, which possesses the terphenyl *o*-$C_6H_4(C_6H_4)_2$ group as bridging unit between the two salicylaldimine cores, exhibited the highest incorporation (14–42 mol%). Effect of dinuclearity on activity, incorporation, and best performance of catalyst **102** was


**Fig. 2.34** Linear ethylene copolymers with MA by iminopyridine *N*-oxides-based catalysts

confirmed also for monomer $N_{COOMe}$. Experimental evidence and theoretical calculations suggested the effective action of a cooperative effect between the two metal centers.

Binuclear naphthyloxydiiminato nickel catalysts **104** and **106** activated by $[Ni(cod)_2]$ efficiently copolymerize a variety of functionalized monomers ranging from norbonene derivatives to acrylates (Fig. 2.36) [100].

The effective occurrence of eventual cooperative effects in copolymerization of ethylene with monomers $N_{OH}$, $N_{COOMe}$, $N_{CH2OH}$ was demonstrated by comparing bimetallic systems with monometallic **57** and **58**. Activities as well as incorporation of functionalized monomers of bimetallic catalysts 3–4-fold higher than monometallic analogue in identical conditions confirmed the higher selectivity for the enchainment of polar components. Interestingly, molar masses of copolymers are similar to those of copolymers of ethylene with norbornene. Attempts to enchain $N_{COOH}$ failed because the high acidity of the comonomer leads to catalyst deactivation by protonation of hydroxyl ligands with consequent ligand displacement as confirmed by $^1H$ NMR experiments.

In addition to norbornene derivatives, catalysts **104** and **106** were also exploited for the copolymerization of ethylene with MA and MMA. Here, the effect of binuclearity is even more evident since monometallic analogous are only minimally responsive to these monomers. Indeed, both catalysts afforded in good yield

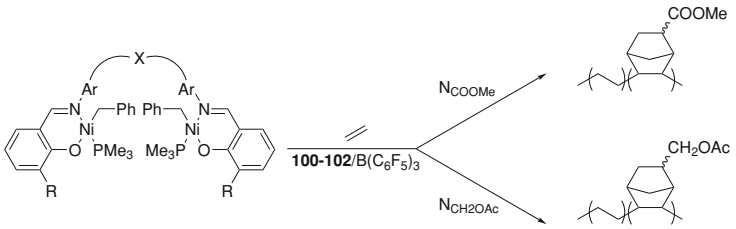


**Fig. 2.35** Ethylene copolymers with functionalized norbornenes by binuclear bis-salicylaldiminato nickel catalysts

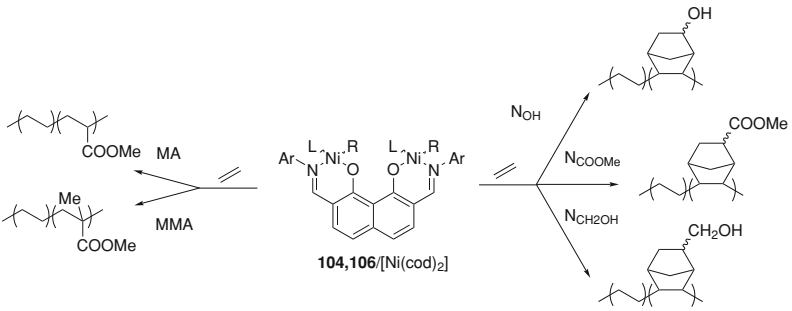


**Fig. 2.36** Ethylene copolymers with MA, MMA, and functionalized norbornenes by naphthyloxydiiminato Ni(II) catalysts

P(E-*co*-MA) ($M_w$ = 6.3–6.7 kg mol$^{-1}$, $M_w/M_n$ = 1.6–1.7, $T_m$ = 108 °C) with an excellent incorporation of MA (11 mol%) and P(E-*co*-MMA) ($M_w$ = 7.9–8 kg mol$^{-1}$, $M_w/M_n$ = 1.4–1.7, $T_m$ = 106 °C) with MMA content of 8–9 mol%. The effective random copolymerization of E and (meth)acrylates was confirmed by fractionation, SEC, $^{13}$C NMR, FT-IR, and DSC data.

The neutral nickel complexes **114–116** with asymmetric $\beta$-ketoiminato ligands activated by MMAO were reported to efficiently copolymerize ethylene with MMA (Fig. 2.37), though they behave as ethylene oligomerization catalysts in absence of MMA. As for ethylene homopolymerization substituents on N–O ligand strongly affect catalytic behaviour. Specifically strong EWG such as $CF_3$ allow for preparing P(E-*co*-MMA) copolymers with considerably high incorporation of MMA (until 17 mol%). Conversely, activity resulted higher when ancillary ligand was less electron deficient ($R^1$ = Ph; $R^2$ = Me). These copolymers possessed interestingly high molar masses, although polydispersity resulted somewhat broad.

Five membered chelated complexes **146–148** were investigated as catalysts for the copolymerization of ethylene with carbon monoxide (Fig. 2.38). Interestingly, the presence of EWG on the pyridyl ring on the N–O chelate ligand not only converts oligomerization catalysts into polymerization catalysts but also allow for obtaining polyketon-based material.

Catalyst **147** with the strong EWG nitro afforded the perfectly alternating P(E-*al*-CO) whereas the pyrazine-containing complex **148** yielded the blocky PE-*b*-P(E-*alt*-CO). By contrast, a weak donor group such as MeO promoted E oligomerization rather than E-*co*-CO copolymerization.

Nickel complexes with $\alpha$-iminocarboxamide ligands were intensively investigated in the copolymerization of ethylene with functionalized norbornene derivatives $N_{OH}$ and $N_{OAc}$ [101] (Fig. 2.39).

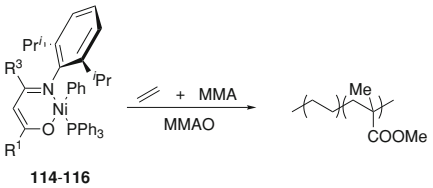


**Fig. 2.37** P(E-*co*-MMA) copolymers by $\beta$-ketoiminato Ni(II) complexes

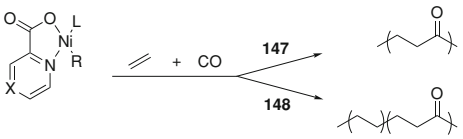


**Fig. 2.38** Copolymerization of ethylene with carbon monoxide by pyridine carboxylato Ni(II) complexes

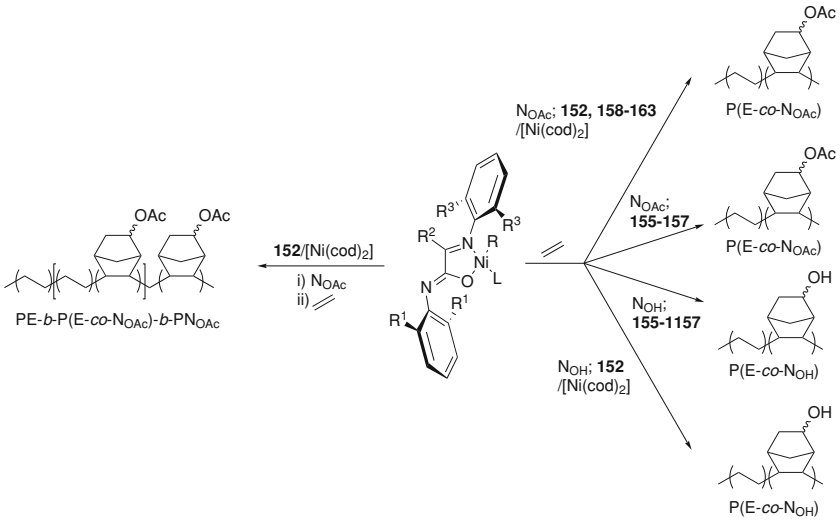


**Fig. 2.39** Ethylene copolymerization with functionalized norbornenes by α-iminocarboxamide nickel catalysts

Complex **152** activated by $[Ni(cod)_2]$ as scavenger of $PMe_3$ yielded P(E-*co*-$N_{AC}$) copolymers containing 4–17 mol% of $N_{AC}$ with excellent molar masses ($M_n$ = 30–110 kg $mol^{-1}$). Very interestingly, catalyst **152** preserved the ability to promote the controlled polymerization of ethylene even in presence of $N_{AC}$ as confirmed by linear time dependence of molar mass, that keep molar mass distribution somewhat narrow even after 90 min of reaction.

Also the hydroxyl-functionalized $N_{OH}$ is readily incorporated in polyethylene backbone affording P(E-*co*-$N_{OH}$) copolymers with an incorporation of $N_{OH}$ ranging from 5 to 18 mol% and possessing $M_n$ = 11–56 kg $mol^{-1}$. Since hydroxyl functionality resulted more poisoning than acetyl group molar masses and activities were lower than those observed in E-*co*-$N_{AC}$ copolymerization. In addition controlled nature of copolymerization is absent, as revealed by the non-linear increase of molar masses with increasing reaction time as well as by the broader molar mass distributions.

Very interestingly, catalyst **152**/$[Ni(cod)_2]$ was exploited to prepare P(E-*co*-$N_{AC}$) copolymers with decreasing content of polar monomer. Thanks to the controlled nature of copolymerization and through complete conversion of $N_{AC}$ "polar–apolar" block-copolymers that show microphase separation were prepared [102].

Complexes **152**, **158–163**/$[Ni(cod)_2]$ were exploited as catalysts for the copolymerization of ethylene with $N_{AC}$ to investigate eventual steric and perturbative effects of group adjacent to imine ($R^2$), by keeping the same bulky 2,6-$^iPrC_6H_4$ as aryl frameworks. Interestingly both activity and incorporation of comonomer are sensitive to this modification. Productivity increased with the increasing of the

bulkyness of alkyl groups as $^{i}$Pr (**160**) > $^{i}$Bu (**159**) > Et (**158**) > Me, whereas incorporation behaved oppositely. In the series of aromatic substituents, that is complexes **161–163** the higher electron withdrawing power the lower activity. Incorporation was less influenced though lower than the alkyl-substituted analogous.

Also complexes **156–157** with 2,6-lutidine and pyridine as neutral ligand, were demonstrated to act as single component catalysts for the copolymerization of ethylene with $N_{OH}$ and $N_{AC}$ yielding comparable results to phosphine-based analogous apart from molar mass distribution which was evidently affected by a less efficient activation [96].

### *2.4.4 Aqueous Olefin Polymerization*

Neutral late transition metal complexes are more tolerant toward polar media than their cationic counterparts. Soon after their introduction, Ni(II) polymerization catalysts **1** and **2** were noted to display a certain stability toward small amounts of added water [39]. The use of water as a dispersing medium offers a unique combination of features, such as effective transfer of the heat of reaction, high polarity and formation of micelles. Moreover, polymerizations that can be carried out in aqueous emulsion give dispersions of submicron polymer particles (Fig. 2.40).

In 2001 Mecking gave the first full account on aqueous coordination polymerization of ethylene by neutral nickel(II) complexes **11**, **12** and by using $[Rh(C_2H_4)_2(acac)]$ as a phosphine scavenger [40]. A small amount of water or acetone was utilized to effectively add the water insoluble Ni(II) catalyst precursors or the phosphine scavenger, respectively. Polymer yields are lowered in water by comparison to conventional polymerization in organic solvents, while polymer molecular weights are noticeably higher compared to aqueous polymerization reactions with P–O chelate catalysts [103] (Table 2.3).

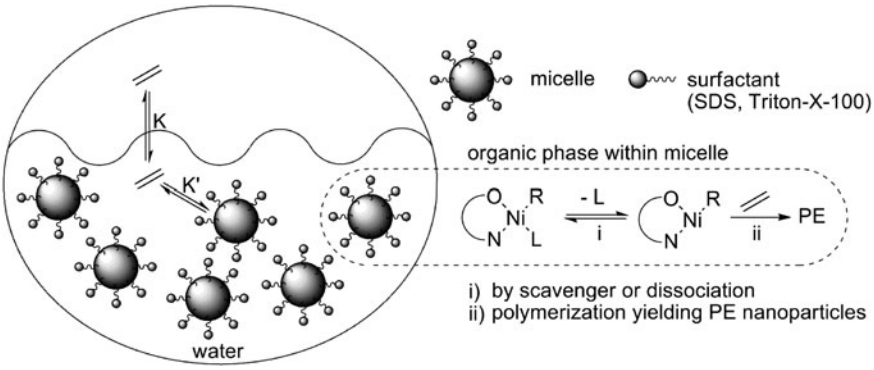


**Fig. 2.40** Catalytic aqueous emulsion polymerization

**Table 2.3** Aqueous polymerization by catalyst **11**

| Cat. no. | L | Reaction medium | *p*E (bar) | Solvent used for addition of cat. | T (°C) | TOF[a] | $M_w$ (kg mol$^{-1}$) | $M_w/M_n$ |
|---|---|---|---|---|---|---|---|---|
| **11** | $PPh_3$ | $H_2O$ | 50 | Pentane (10%) | 70 | 50 | 410 | 4.1 |
| **11** | $PPh_3$ | $H_2O$/acetone 50:50 | 50 | / | 50 | 40 | 18 | 1.5 |
| **11** | $PPh_3$ | pentane | 50 | / | 70 | 144 | 410 | 3.7 |
| **11** | $PPh_3$ | Acetone | 50 | / | 50 | 143 | n.d. | n.d. |
| **11** | $PPh_3$ | Toluene | 8 | / | 50 | 11 | 43 | 2.3 |
| **11** | $PPh_3$ | Toluene | 50 | / | 50 | 228 | n.d. | n.d. |
| **12** | py | $H_2O$ | 50 | Acetone (5%) | 50 | 36 | 310 | 2.6 |

[a] Kg PE mol cat$^{-1}$ h$^{-1}$

Water soluble complexes suited as catalysts precursors, which simplify the dispersions by removing the organic solvent in the initial catalyst system, are desirable for studies of the processes and of particle formation [104]. Four Ni-salicylaldiminato methyl complexes [(N–O)NiMe(L)], **61** and **67–69**, with various P- and N-coordinating water soluble ligands L (Fig. 2.41) were prepared by Mecking [105].

All complexes are soluble in toluene whereas **67–69** are insoluble in water; however, **69** is soluble in 2-propanol. In contrast, **61** is soluble in water. Polymerizations in aqueous systems were carried out in the presence of sodium dodecylsulfate (SDS) as a surfactant to stabilize polymer particles formed. Complex **67** with the water-soluble alkylphosphine PTA was inactive in aqueous suspension as well as in toluene solution due to the strong coordination of phosphine. Exposure of suspensions of the water-insoluble **68** to ethylene pressure (in the presence of surfactant to potentially stabilize polymer particles formed)

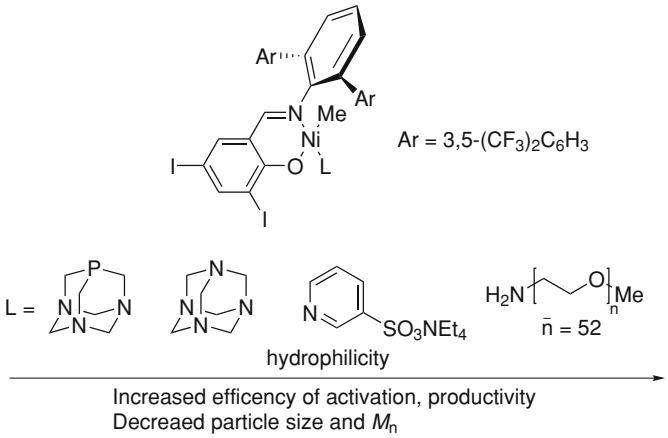


**Fig. 2.41** Effect of the stabilizing ligand on the efficiency and polymer particles in aqueous polymerization with salicylaldiminato nickel catalysts

afforded polymer suspensions. When **69** was introduced to an aqueous surfactant solution as a solution in 2-propanol, no visible precipitate was formed. Exposure to ethylene resulted in formation of polymer particles in the form of a latex, with large particle size.

These findings highlight that the size of polyethylene particles obtained by aqueous catalytic polymerization depends on the degree of dispersion of the catalyst in the initial reaction mixture. Catalyst **61** revealed to be a very performing catalyst producing in 3.5 h, at T = 20 °C and $p$E = 40 bar, 9.4 g of PE in form of latex ($M_n$ = 8.8 kg mol$^{-1}$) with particle size of 230 nm.

Electron-withdrawing substituents in the bidentate N, O- or P, O-coordinating ligand, substantially increased the polymerization rates of Ni(II) complexes as shown by Brookhart et al. for enolatoimine complexes **117–120**, while electron-poor phosphinoenolate complexes afforded higher molecular weight polymer. Even though with increasing electrophilicity of the metal center, an increased reactivity and sensitivity toward water was anticipated in 2007 Mecking synthesized a series of neutral Ni(II) complexes based on enolatoimine ligands with strongly electron-withdrawing trifluoromethyl and trifluoroacetyl groups that were studied as catalyst precursors for ethylene polymerization [66]. Despite the electron-deficient nature of the metal centers, which can enhance deactivation processes such as hydrolysis or coordination of water, they were very active in aqueous emulsions affording polyethylene dispersions. Studies of different catalyst precursors, [(N–O)NiMe(L)] with L = pyridine or $PPh_3$, or in situ prepared catalysts [(tmeda)-$NiMe_2$]/ketoenamine, show that exchange of the coordinating ligand L is a critical step for the electron-poor Ni(II) complexes studied and likely is one limiting factor for catalyst activities.

The pyridine complexes **126** and **127** were dissolved in a small amount of toluene and the solution miniemulsified in aqueous SDS solution. Exposure to ethylene in a pressure reactor afforded stable dispersions. This demonstrates that in spite of the strongly electron-withdrawing nature of the enolatoimine ligands in the catalysts studied, catalyst stability toward water is sufficient to carry out polymerization in aqueous systems. Catalyst **127** at 70 °C gives an average activity of $1.9 \times 10^4$ mol $C_2H_4$ mol Ni$^{-1}$. This competes with the highest activities reported for neutral Ni(II) salicylaldiminato complexes, the only ones reported before to afford polyethylene dispersions of high molecular weight material ($M_n$ = 10 kg mol$^{-1}$) [106]. Also the phosphine complex **128** is suited for polymerization in aqueous medium by using [Ni(cod)$_2$] as a phosphine scavenger with a TOF of 9,500 mol $C_2H_4$ mol Ni$^{-1}$ h$^{-1}$and $M_w$ = 24 kg mol$^{-1}$. The phosphine complex **128** is active in the absence of a phosphine scavenger in non aqueous systems. Thus, by comparison to polymerizations in nonaqueous systems, activity is reduced 5–10-fold probably due to the disactivation of a part of the catalyst precursor upon preparation of the miniemulsion or in the early stages of the polymerization experiment. TEM micrographs show the particles to be spherical with particle size ranging from 91 to 544 nm.

The substituents on the N-bound aryl group (N-$C_6H_3R_2$) affect the degree of branching of the polymer formed and in turn its crystallinity and melt temperature.

For R = $^{i}$Pr a total degree of branching of 40–50 is observed ($T_m \sim 97$ °C, crystallinity $\sim$ 35%), while for R = 3,5-$(F_3C)_2C_6H_3$ ca. 25 branches/1,000 carbon atoms ($T_m \sim 110$ °C, crystallinity $\sim$ 45%) are found.

There is a strong interest in developing more active neutral Ni(II) complexes, being catalyst activity an issue in polymerization with these systems in general and in aqueous systems in particular. Since binuclear complexes can afford greater activity, higher molar masses and comonomer incorporation than the mononuclear analogue Mecking tested the binuclear complexes **96–99** in the ethylene polymerization in aqueous emulsion obtaining polyethylene dispersions. These binuclear pyridine complexes are very robust, in fact they are active over the entire temperature range studied, 20–70 °C, as single-component catalyst precursors, without the necessity of an activator and with a maximum of productivities up to $184 \times 10^3$ $C_2H_4$ mol $Ni^{-1}$ $h^{-1}$ at 50 °C and pE = 40 bar. A broad distribution of polymer particle size with approximately a circular circumference was obtained. In addition to the pyridine complexes, the complex **96** of the less strongly coordinating tertiary amine tmeda was studied. In this case an activity was observed at a low polymerization temperature of 25 °C with a productivity of 2,500 mol $C_2H_4$ mol $Ni^{-1}$ $h^{-1}$ and a very high ($M_n = 232$ kg $mol^{-1}$) molecular weight and linear polyethylene. Polymer molecular weights and melting points are similar to those obtained in nonaqueous polymerizations under identical conditions. However, as for mononuclear complexes, productivities in aqueous emulsions are decreased by comparison to polymerization in organic solvents.

## 2.5 Mechanistic Aspects

### *2.5.1 Mechanism of Ethylene Homopolymerization*

Fundamental steps involved in ethylene polymerization catalyzed by N–Z containing Ni and Pd catalysts are depicted in Fig. 2.42. Generation of the active species, previously discussed, yields the hydrocarbyl complex with a vacant coordination site for the incoming olefin. Polymerization propagates via chain migration through four-centered transition state and product of insertion resembles the starting active species with a new vacant coordination site available for the further olefin coordination and insertion. Frequent termination pathways involve $\beta$-H elimination and $\beta$-H transfer to the monomer. Both lead to chain releasing with generation of a new active species. A feature of these catalysts is the formation of chain branches as a result of consecutive $\beta$-H elimination, rotation, and reinsertion reactions; the longer the chain walks the longer the branches.

In-depth mechanistic and theoretical works were focused on the cationic diimine complexes of nickel and palladium. NMR studies revealed a unique feature of these systems, the catalyst resting state is the alkyl ethylene complex. This is in clear contrast with early transition metal catalysts whereby such species are

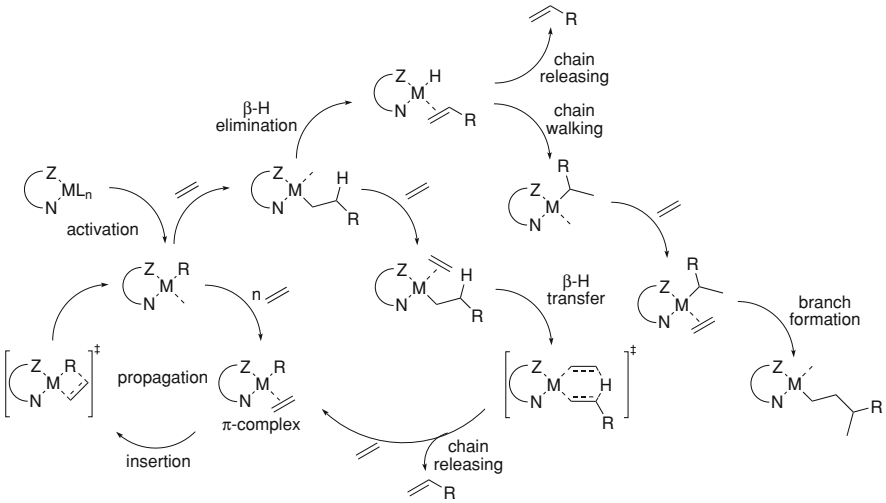


**Fig. 2.42** Mechanism for ethylene polymerization and branch formation with $[M(N–Z)L_n]$ complexes

generally not detected. Thus, the turnover limiting step is the migratory insertion reaction of the alkyl ethylene complex. Other remarkable insights originate from determination of the barriers to migratory insertions measured by low temperature NMR spectroscopy. For the palladium catalysts barriers lie in the range of 17–18 kcal $mol^{-1}$; systems bearing the bulkiest ligands exhibit the lowest insertion barriers. Barriers for the insertions in the nickel complexes are substantially lower and in the range of 13–14 kcal $mol^{-1}$. Such expected difference between first-row and second-row insertion accounts for the much higher activities of the nickel complexes. Increase in steric bulk of aryl substituents of diimine ligands leads to an increase in the ground-state energy of the resting-state species relative to the migratory insertion transition state in nickel species As a consequence, lower migratory insertion barriers were expected with bulkier diimine substituents.

In contrast, neutral Ni complexes are less amenable to mechanistic studies via direct observation with NMR spectroscopy than cationic Pd complexes. Thus, there is relatively little mechanistic information available regarding neutral nickel ethylene polymerization systems.

A number of salicylaldiminato nickel complexes were studied at DFT level to gain insights into polymerization mechanism adopted by these systems as well as to clarify various experimental evidences [118]. The influence of substituents on the ligand scaffold on phosphine dissociation, that is on catalyst activation, was previously discussed. Very interesting was the detailed investigation of species involved in propagation. The reduced symmetry introduced by the mixed ligand is reflected in the doubling of the number of geometric isomers of $\pi$ complexes, transition states, and insertion products (Fig. 2.43). As a result of trans-influence the barriers associated with the olefin insertion into sites having the alkyl located

trans to the nitrogen donor are lower. Since the insertion of an ethylene unit changes the configuration of the chain with respect to the salicylaldiminato ligand, isomerization occurs at the $\pi$-complex stage so that insertion could proceed through the lower energy transition state. Accordingly, the lowest energy pathway for insertion proposed is depicted here with continuous arrows.

Interestingly, the $\beta$-H transfer mechanism for the termination was found to be energetically more favorable than the $\beta$-H elimination mechanism. The termination barriers found were generally higher than the insertion barriers. A comparison of the results obtained by varying the substituents on the catalyst backbone led to the conclusion that while influence of electronics on catalyst activity could not be easily predicted the addition of bulky substituents on the catalyst backbone should enhance catalyst activity.

Subsequently, combined DFT/stochastic studies were undertaken on the mechanism of ethylene polymerization catalyzed by a neutral Ni-anilinotropone catalysts. Chain propagation and isomerization as well as influence of reaction conditions on the branching formation were investigated. Similarly to the case of nickel-salicylaldiminato catalysts the activation barriers for the insertion of ethylene in complexes with the alkyl group trans to the oxygen donor were found higher than those encountered in *cis*/*trans* isomerization. Interestingly, stochastic simulation allowed for establishing temperature and pressure dependence of the polymer microstructure. In agreement with experimental evidences the model predicts a decrease with the number of branches with the increase of pressure. Temperature dependence behaves oppositely as a result of an increase in secondary insertions with the temperature.

To get a full mechanistic picture of a typical neutral catalyst system an elegant and in-depth NMR study of ethylene polymerizations catalyzed by the anilinotropone complexes was reported by Jenkins and Brookhart [107]. Detailed information concerning the chain propagation process, the barrier to ethylene insertion, the nature, and dynamics of the intermediate Ni alkyl complexes, and the chain transfer and catalyst decay processes were obtained.

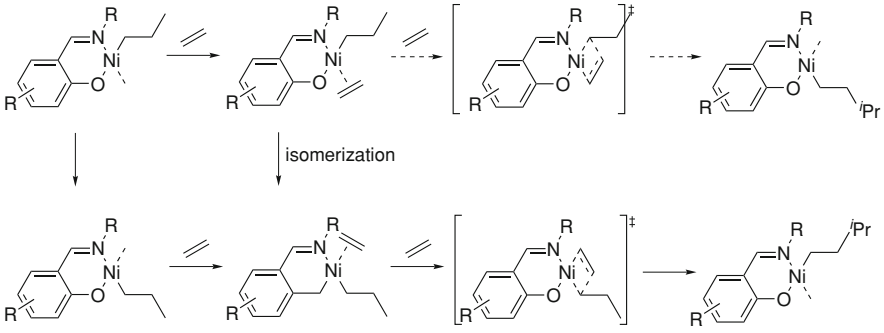


**Fig. 2.43** The lowest (continuous) and highest (dashed) energy pathways for the insertion of ethylene at nickel center in salicylaldiminato catalysts calculated by DFT

The rate of insertion of ethylene into the Ni-phenyl bonds of both unsubstituted and aryl-substituted of anilinotropone nickel(II) complexes was monitored by low-temperature NMR spectroscopy. The ethylene chain growth to form, initially, the corresponding [Ni(**L**)($PPh_3$)($CH_2CH_2Ph$)] (**L = M2, M13–16)** complexes, was determined by monitoring the change in concentrations of starting complexes. First-order rate constants were measured as a function of temperature and ethylene concentration.

Even at high ethylene concentrations, only $PPh_3$ complexes were observed (no ethylene complexes were detected). As expected, rates accelerate with temperature, increasing about an order of magnitude between −10 and 10 °C. Insertion is dramatically inhibited by phosphine concentration. Thus, it was concluded that for these systems, the catalyst resting state(s) are an equilibrium mixture of phosphine and ethylene complexes (Fig. 2.44). Nevertheless, at high ethylene pressures, the equilibrium is shifted nearly completely to the side of the ethylene complex and TOF becomes independent of ethylene pressure (saturation conditions).

The barriers to migratory insertion in (N–O)Ni(R)-($C_2H_4$) complexes, from measurements of TOFs under saturation conditions, were determined to lie in the range of 16–17 kcal $mol^{-1}$, that is only about 2–3 kcal $mol^{-1}$ greater than those observed for cationic diimine complexes.

The intermediate alkyl complexes have $\alpha$-agostic interactions with dynamic behavior similar to the cationic alkyl diimine complexes. The barrier to $\beta$-H elimination and reinsertion is estimated in ca. 17 kcal $mol^{-1}$. Free energy barrier to nickel–carbon bond rotation in these complexes occurs with a barrier of 11.1 kcal $mol^{-1}$. These isomerization processes account for branched polyethylenes generated from these catalysts and resemble those previously observed with diimine catalysts.

Thermolysis of hexyl complex **182** generates the nickel hydride complex and 1-hexene via $\beta$-H elimination, through two pathways, one (dominant) independent of phosphine concentration and one involving reversible loss of phosphine, and thus inhibited by $PPh_3$. This process is a model for chain transfer and clearly explains why polymer molecular weights decrease with increasing phosphine

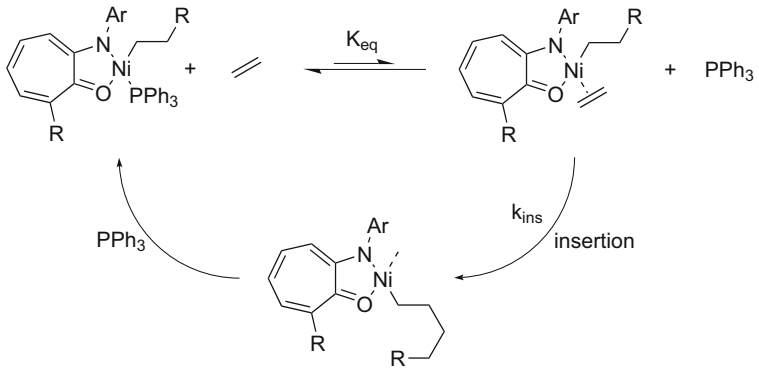


**Fig. 2.44** Ethylene polymerization catalyzed by Ni-anilinotropone catalysts

concentration. The rate of propagation is retarded by increasing [$PPh_3$], while the rate of chain transfer is unchanged, resulting in an increase in $R_{ct}/R_{prop}$. Since chain transfer to monomer would exhibit a rate inhibition equal to that for $R_{prop}$ with added $PPh_3$ it was concluded that the major chain transfer route is a simple $\beta$-elimination process, and not chain transfer to monomer.

At much slower rates, reductive elimination of the free ligand occurred from the hydride complex, (Fig. 2.45) and is inhibited by added phosphine. Catalyst decay under polymerization conditions was shown to occur by a similar process to generate free ligand and a bis-ligand complex formed by reaction of free ligand with an active catalyst species (Fig. 2.46).

Recently, Mecking [108] reported in depth mechanistic studies of the novel (dmso)-coordinated complex **70**. Such complex resulted to be a suitable precursor for mechanistic studies of deactivation routes of neutral Ni(II) catalysts. Activation of **70** could be directly observed using dmso as a solvent, by $^1$H NMR spectroscopy. Interestingly, a minor but sufficient portion of **70** was transformed into the hydride containing active species by insertion of ethylene and subsequent elimination of propylene.

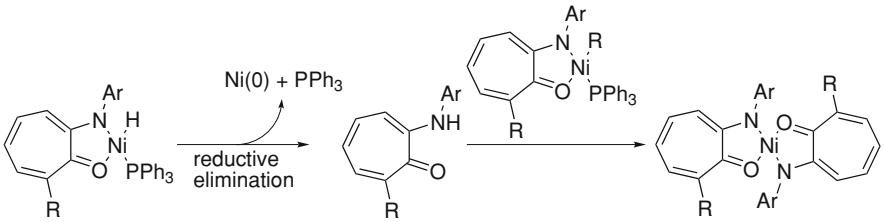


**Fig. 2.45** Catalysts deactivation for anilinotropone nickel catalysts

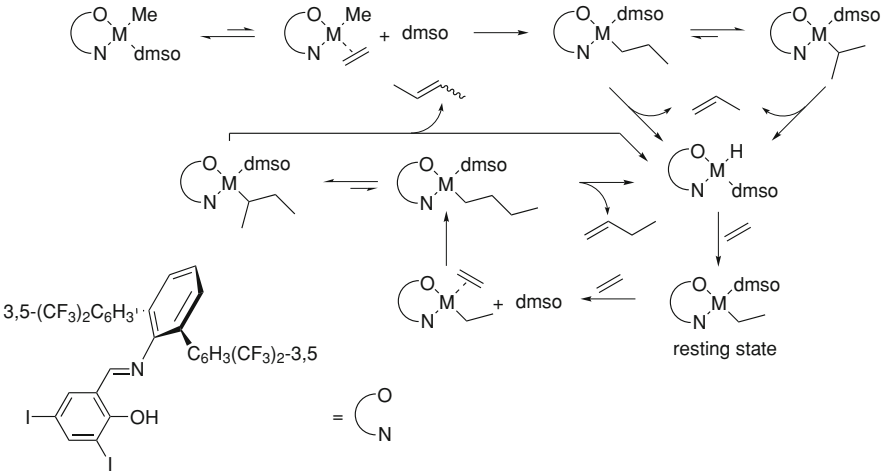


**Fig. 2.46** Mechanism for ethylene polymerization from NMR studies of neutral [Ni(**A14**)R(dmso)] species

Surprisingly, catalyst resting state is the ethyl complex **72** that can undergo two different processes: (1) *cis*/*trans* isomerization of alkyl and dmso in respect to the position of donors in salicylaldiminato ligand and (2) exchange of α- and *β*-carbon of ethyl group *β*-H, rotation, and reinsertion. Catalytic dimerization of ethylene to 1- (15%) and 2-butenes (85%) was observed. Isomer ratio suggests secondary butyl-Ni complex as thermodynamically favoured.

To get insights on how this system behaves in presence of polar reagents, the reactivity toward water was examined. Added $D_2O$ revealed that water does not significantly coordinate to the metal center. Hydrolysis of the Ni–Me bond of the catalyst precursor is evidenced by the formation of $CH_3D$. Conversely, no hydrolysis of the higher Ni-$C_nH_{2n+1}$ ($n > 1$) occurring during chain growth was observed, suggesting that hydrolysis of Ni-alkyl species is a minor decomposition pathway. More remarkably, the significant deactivation was found to be the reductive elimination of alkanes by reaction between alkyl and hydride containing species as well as by reaction of two Ni–Me catalyst precursors yielding ethane. This is in line with the previous Grubbs' suggestion that bulky substituted salicylaldiminato ligands hinder catalyst decomposition [109]. These studies demonstrated for the first time that bimolecular elimination of alkane from reaction of Ni-alkyl and Ni-hydride species is a possible deactivation route for neutral nickel catalysts. This provides a rationale for catalyst design and for an appropriate choice of reaction conditions that provide site isolation.

### 2.5.2 Mechanism of Copolymerization of Ethylene with Polar Monomers

Neutral nickel(II) catalysts are attractive for their functional group tolerance and potential in copolymerization of vinyl polar monomers. As already pointed out, cationic Pd-diimine catalysts pioneered by Brookhart, allow the coordination–insertion copolymerization of ethylene with polar vinyl monomers such as MA and VA. Low-temperature NMR studies of reactions of cationic palladium R-diimine complexes with ethylene and methyl acrylate revealed all of the critical intermediates spectroscopically and allowed in depth mechanistic understanding. They are formed by chelating coordination of the carbonyl group of an inserted MA unit. Acrylate insertion occurs predominantly in a 2,1-fashion, yielding chelate species of general formula [Pd(N–N)($\kappa^2$-*C*,*O*-CHRC(= O)OMe] in which the carbonyl group of the inserted MA is coordinated to Pd yielding a strained four-membered chelate ring. Subsequent *β*-H eliminations and readditions expand the ring stepwise to the six membered chelate complex, which is the catalyst resting state. Opening of these chelates by coordination of incoming monomer to form the corresponding olefin complexes is the turnover-limiting step during copolymer chain-growth [110, 111].

The relative E/MA ratios of incorporation into the copolymers are governed by both the equilibrium ratio of the alkyl ethylene and alkyl MA complexes and their relative rates of migratory insertion. Even if the rate of migratory insertion of MA

is somewhat faster than that of ethylene at low temperature, there is a great preference for ethylene binding to the electrophilic Pd center is over that of the electron-deficient olefin, MA. This implies use of very large [MA]/[E] ratios to achieve significant incorporation of MA into the copolymer. As a consequence, the overall rate of polymerization decreases due to increased concentrations of the chelate complex.

Conversely, most attempts to copolymerize ethylene with MA with Ni-diimine catalysts were unsuccessful. Theoretical investigations by gradient-corrected DFT theory revealed that the main difference between Ni and Pd is that *O*-bonding mode of MA due to the higher oxophilicity of Ni, owed namely to steric reasons rather than to the orbital interaction [112]. They suggested that copolymerization would be possible under harsh conditions. Indeed some Ni-diimine-based systems were reported to effectively copolymerize E with MA at high temperatures (120 °C) and very high pressure (340 bar). These conditions appeared to favour the dissociation of the carbonyl coordination of MA from the electrophilic nickel centre. Very interestingly while ethylene-MA copolymers obtained with cationic Pd diimine catalysts are highly branched due to extensive chain walking, Ni complexes give linear ethylene-MA copolymers.

It was foreseen that to avoid problem of the *O*-binding of MA to oxophilic cationic Ni catalysts the use of anionic ligands would enhance the preference for the $\pi$-coordination and favour the ethylene MA copolymerization [112, 113].

These results encouraged extensive studies of novel neutral nickel(II) olefin polymerization catalysts [97, 114, 115]. They are much more stable to protic and aqueous media and the variety of catalysts developed with different ligands allows to vary the microstructures and crystallinities of resulting polymers in a controlled fashion over a wide range. However, although the numerous polymerization studies, copolymerization of ethylene (or 1-olefins) with polar vinyl monomers, like MA, to high-molecular-weight copolymers employing neutral Ni(II) precatalysts is limited from either low activity or rapid catalyst deactivation.

Recently, a comprehensive NMR study of two neutral nickel complexes **71** and **72** provided insights into the reactivity of active neutral Ni(II) species toward polymerization of polar vinyl monomers (Fig. 2.47). The two complexes were found to be well-defined model compounds for these studies and allowed direct observations of organometallic species and decomposition products originating from insertion of polar vinyl monomer into the key intermediates.

MA insertion into the Ni–H bond of **71** was monitored at $T \geq -40$ °C by NMR spectroscopy. MA readily inserts into Ni–H bond as well as into Ni-alkyl species with exclusively regiospecific 2,1-insertions even at low temperature (−30 °C). A weak, but distinct, chelating interaction of the O-atom of the carbonyl group with the metal center after insertion was demonstrated at low temperature, in agreement with a geometry-optimized structure calculated by DFT.

Exposure of the hydride **71** to equal amounts of ethylene and MA resulted in the formation of MA and ethylene insertion products in a 9:1 ratio, which demonstrated that both monomers can effectively compete with each other for coordination and insertion. Thus, a prerequisite for their copolymerization was fulfilled.

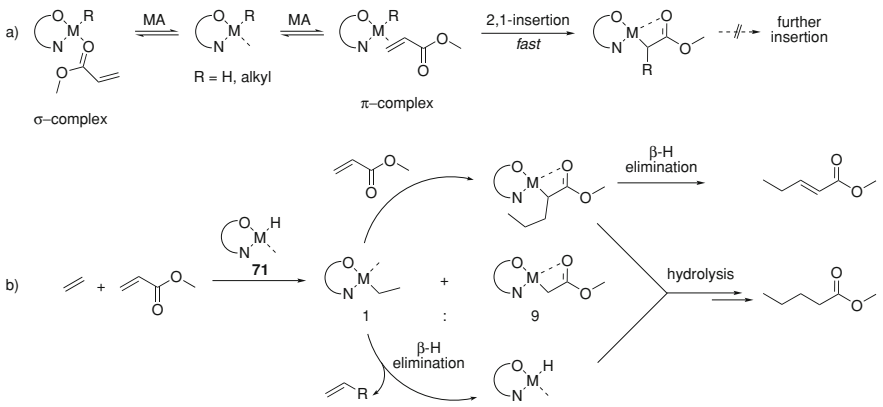


**Fig. 2.47** Reactions of complex **71** with ethylene and MA

However, although the product of insertion is stable in the absence of residual Ni–H species at low temperatures, it is subject to rapid bimolecular elimination of the functionalized alkyl moiety in the presence of free **71**. Moreover, at 0 °C $\beta$-H elimination occurs to such an extent and decomposition from solutions initially not containing the hydride takes place. Exposure of the higher Ni-alkyl complex to MA in the presence of excess ethylene results in the immediate formation of methyl pentanoate as the ultimate decomposition product.

Interestingly, while the Ni-Et species is practically stable toward hydrolysis at 55 °C [107, 108] the analogous R-carbonyl substituted metal alkyl originating from 2,1-insertion of MA is subject to rapid hydrolysis at room temperature in agreement with the previous studies on the organic decomposition products of the reaction of a Ni-phenyl complex **5** with MA [116].

VA inserts less readily than MA into the hydride complex **71**. Insertion occurs at 0 °C, yielding both the kinetic 1,2-insertion product and the thermodynamically favored 2,1-insertion product. NMR data and a theoretical study indicate an interaction of the carbonyl O-atom with the nickel atom, structurally similar to the MA insertion product. Decomposition occurs by $\beta$-acetate elimination even at low temperatures.

Qualitatively, the observed reactivity of VA toward the neutral hydride and alkyls complexes studied parallels observations with cationic Ni(II) diimine complexes [117].

## 2.6 Summary and Conclusions

Group 10 metal complexes with mixed ligands based on nitrogen (N–Z) for olefin polymerization catalysis in academic articles have been comprehensively reviewed. Olefin, namely ethylene, homopolymerization and copolymerization of

ethylene with functionalized norbornenes, functionalized α-olefins, and polar vinyl monomers have been considered. It is clear that while palladium and P–O ligands were discovered first and dominate ethylene copolymerization with CO and the SHOP process, nickel and N–O chelates prevail in the new classes of late-transition metal complexes with mixed chelating ligands for olefin polymerization catalysis. This is related to the higher insertion barrier in palladium diimine catalysts when compared to the analogous nickel complexes. The nickel P–N based catalysts reported so far reveal a greater stability and a greater tendency to chain walking (branches on branches) than diimine catalysts, but there is no clear tendency in the few examples since small changes in the substituents or subtle variations in the structure give dramatic differences in the catalytic behaviour. Palladium catalysts with P–N ligands are low active and tend to decompose, as they seem to do those with N–S ligands.

Most ligands in nickel complexes such as salicylaldimine, anilinotropone, enolatoimine, and other ligands are anionic and feature steric bulk to achieve high molecular weights. Thanks to the combination of steric and electronic factors on the substituents and the dissociation ability of the stabilizing ligand (dmso > MeCN > py > $PR_3$) most behave as single component catalysts. Addition of a cocatalyst or of a scavenger as $B(C_6F_5)_3$ or $[Ni(cod)_2]$ enhances the activity. In phosphine complexes insertion is inhibited by phosphine concentration since the resting state of these systems is the phosphine complex. In NMR studies of anilinotropone catalyst in the presence of ethylene the resting state(s) was demonstrated to be an equilibrium mixture of phosphine and ethylene complexes.

Regarding the olefin polymerization there is a temperature and pressure dependence of the polymer microstructure, namely the degree of branches. A decrease of branching occurs with the increase of pressure, while the temperature dependence is opposite, due to an increase in secondary insertions with the temperature.

More relevant for the design of catalysts is the selection of the substituent on the chelate scaffold. The salicylaldiminato complexes of Ni(II) are the best studied of these systems since, having many sites available for substitution, they allow appropriate tailoring of the catalyst. Depending on substituent variation it is possible to tune activities, molar masses, and branching. High activity can be reached.

The N-aryl ring lies roughly perpendicular to the square plane of the molecule, increasing the steric bulk of ortho substituents on this ring increases the catalyst productivity, $M_w$, and linearity of PE. Electron withdrawing or donating substituents on N-terphenyl moieties have remote dramatic effects on branching, crystallinity and molar masses: linear, semicrystalline or highly branched, amorphous polymers can be prepared. Often branches increase at the expense of molecular weight. Electron withdrawing substituents on the phenoxide ring also increase the productivity. Thus, an increased electrophilicity of the Ni center, brought about by electron withdrawing groups in the N–O ligand increases the polymerization rates. Bulky substituents adjacent to the phenoxide group increase catalyst lifetime by slowing or preventing decomposition to the corresponding bis(salicylaldiminato)

Ni complexes. The design and synthesis of binuclear Ni(II) aldiminato complexes showed cooperativity effects leading to more linear PE with very high activity and molar masses.

Similar effects of substituents adjacent the oxygen of the chelate ring or on the N aryl groups are observable in other families of six membered ring ligands as PymNox and enolatoimine complexes, which are also very active for ethylene polymerization.

Steric and electronic effects have similar influence also in complexes with five membered ring ligands. In particular the anilinotropone complexes feature PE with highest activity and very high molar masses, while those based on α-iminocarboxamide allow to obtain living systems at 20 °C, when activated with $[Ni(cod)_2]$.

Thus, these Ni catalyst systems are capable of introducing over 50 branches/1,000 C into the polymer chain, yielding polymers with lower melting points than those produced by their group 4 catalysts. A controlled degree of branching is desirable in polyolefins to depress the glass transition and melting temperatures, thus improving processability. However, they typically exhibit PE with lower molecular weight than catalysts industrially used.

The high activity of some of these neutral late transition metal catalysts, which are active in the presence of polar additives with only minor reduction in activity, makes them interesting for the synthesis of polymer dispersions by polymerization in aqueous systems. Although, with increasing electrophilicity of the metal center also reactivity and sensitivity toward water increase. Very interesting results were achieved with the most active complexes, especially those based on enolatoimine and ditopic salyciladimines. Very high TOF and molar masses were obtained even though productivities in aqueous emulsions are decreased by comparison to non aqueous polymerization.

The main interest in these systems arise from the need to incorporate small amount of monomers containing polar groups to endow polyolefins with additional physical and chemical characteristics. Indeed, the neutral salicylaldiminato based nickel catalysts copolymerize ethylene with a variety of functionalized norbornenes such as 5-norbornen-2-ol and 5-norbornene-2-yl acetate, and functionalized α-olefins, showing the functional-group tolerance of these neutral catalysts. Incorporation of functionalized norbornenes with bimetallic complexes is four times that with mononuclear analogues. Random and block copolymers between ethylene and functionalized norbornenes have been achieved with α-iminocarboxamide complexes.

More challenging still is copolymerization with polar vinyl monomers. There are few examples of linear copolymers with acrylates by mononuclear (N–O)Ni complexes. Recent studies have demonstrated that the challenging nature of these copolymerizations arises from the low reactivity towards olefin insertion of an α-carbonyl substituted metal alkyl combined to the particular susceptibility of functionalized olefin insertion products to specific bimolecular deactivation reactions and hydrolytic pathways. Site isolation (and strictly inert conditions), however, enhancing the reactivity of the functionalized olefin insertion product for following insertions seems to be necessary.

More interesting are the results with binuclear (N–O)Ni complexes. The cooperative bimetallic catalytic interactions lead to increased polar comonomer enchainment selectivity for functionalized monomers and especially for acrylates (ten, one hundred times that from monometallic complexes). The selectivity of the bimetallic systems for higher comonomer incorporation, as well as different branch content, affords substantially altered polymer microstructures, with lowered melting points and greater solubility. Furthermore, the bimetallic catalysts exhibit significantly higher activities than the monometallic catalysts in the presence of polar solvents, while concurrently achieving higher molecular weights. This feature permits using less rigorously dried media for polymerization while preserving the desired product microstructure. Finally, the cooperative effects between group 10 catalytic centers, not only substantially enhance the catalyst/polymer properties that have made the monometallic analogues of interest, but also expand the range of polymerizations possible.

In conclusions, progress in design and synthesis of neutral nickel catalysts and understanding of the factors that regulate the reactivity towards olefin and polar monomers give promise to address the issue of introducing functional groups into aliphatic polyolefin backbones. It is expected that even though modern palladium complexes based on P–O ligands give very attractive copolymers with polar monomers, economical and environmental concerns related to palladium catalysts will encourage further efforts in the design and developments of nickel and other more environmental friendly catalysts.

**Acknowledgments** Financial support from Regione Lombardia in the frame of the International Scientific Cooperation AQUA project (ID 17163 e Rif.n° EN-18) is acknowledged.

## References

1. Polyolefins Planning Service: Executive Report (2010) Global commercial analysis March 2010, Nexant, Inc, London
2. Pino P, Mülhaupt R (1980) Stereospecific polymerization of propylene: an outlook 25 years after its discovery. Angew Chem Int Ed 19:857–875. doi:10.1002/anie.198008571
3. Brintzinger HH, Fischer D, Mülhaupt R, Rieger B, Waymouth RM (1995) Stereospecific olefin polymerization with chiral metallocene catalysts. Angew Chem Int Ed 34:1143–1170. doi:10.1002/anie.199511431
4. Coates GW (2000) Precise control of polyolefin stereochemistry using single-site metal catalysts. Chem Rev 100:1223–1252. doi:10.1021/cr990286u
5. Resconi L, Cavallo L, Fait A, Piemontesi F (2000) Selectivity in propene polymerization with metallocene catalysts. Chem Rev 100:1253–1346. doi:10.1021/cr9804691
6. Gibson VC, Spitzmesser SK (2003) Advances in non-metallocene olefin polymerization catalysis. Chem Rev 103:283–315. doi:10.1021/cr980461r
7. Boffa LS, Novak BM (2000) Copolymerization of polar monomers with olefins using transition-metal complexes. Chem Rev 100:1479–1494. doi:10.1021/cr990251u
8. Nakamura A, Ito S, Nozaki K (2009) Coordination-insertion copolymerization of fundamental polar monomers. Chem Rev 109:5215–5244. doi:101021/cr900079r

9. Ittel SD, Johnson LK, Brookhart M (2000) Late-metal catalysts for ethylene homo- and copolymerization. Chem Rev 100:1169–1204. doi:10.1021/cr9804644
10. Rieger B, Saunders Baugh L, Kacker S, Striegler S (eds) (2003) Late transition metal polymerization catalysis. Wiley, Weinheim
11. Mecking S (2001) Olefin polymerization by late transition metal complexes. A root of Ziegler catalysts gains new ground. Angew Chem Int Ed 40:534–540. doi:10.1002/1521-3773(20010202)40:3<534:AID-ANIE534>3.0.CO;2-C
12. Drent E, Budzelaar PHM (1996) Palladium-catalyzed alternating copolymerization of alkenes and carbon monoxide. Chem Rev 96:663–682. doi:10.1021/cr940282j
13. Bianchini C, Meli A (2002) Alternating copolymerization of carbon monoxide and olefins by single-site metal catalysis. Coord Chem Rev 225:35–66. doi:10.1016/S0010-8545(01)00405-2
14. Johnson LK, Killian CM, Brookhart M (1995) New Pd(II)- and Ni(II)-based catalysts for polymerization of ethylene and α-olefins. J Am Chem Soc 117:6414–6415. doi:10.1021/ja00128a054
15. Johnson LK, Mecking S, Brookhart M (1996) Copolymerization of ethylene and propylene with functionalized vinyl monomers by palladium(II) catalysts. J Am Chem Soc 118:267–268. doi:10.1021/ja953247i
16. Killian CM, Tempel DJ, Johnson LK, Brookhart M (1996) Living polymerization of α-olefins using $Ni^{II}$-α-diimine catalysts. Synthesis of new block polymers based on α-olefins. J Am Chem Soc 118:11664–11665. doi:10.1021/ja962516h
17. Killian CM, Johnson LK, Brookhart M (1997) Preparation of linear α-olefins using cationic nickel(II) α-diimine catalysts. Organometallics 16:2005–2007. doi:10.1021/om961057q
18. Mecking S, Johnson LK, Wang L, Brookhart M (1998) Mechanistic studies of the palladium-catalyzed copolymerization of ethylene and α-olefins with methyl acrylate. J Am Chem Soc 120:888–899. doi:10.1021/ja964144i
19. Svejda SA, Johnson LK, Brookhart M (1999) Low-temperature spectroscopic observation of chain growth and migratory insertion barriers in (α-diimine)Ni(II) olefin polymerization catalysts. J Am Chem Soc 121:10634–10635. doi:10.1021/ja991931h
20. Gates DP, Svejda SA, Onate E, Killian CM, Johnson LK, White PS, Brookhart M (2000) Synthesis of branched polyethylene using (α-diimine)nickel(II) catalysts: influence of temperature, ethylene pressure, and ligand structure on polymer properties. Macromolecules 33:2320–2334. doi:10.1021/ma991234+
21. Chen EYX (2009) Coordination polymerization of polar vinyl monomers by single-site metal catalysts. Chem Rev 109:5157–5214. doi:10.1021/cr9000258
22. Keim W, Kowaldt FH, Goddard R, Krüger C (1978) Novel coordination of (Benzoylmethylene) triphenylphosphorane in a nickel oligomerization catalyst. Angew Chem Int Ed 17:466–467. doi:10.1002/anie.197804661
23. Keim W, Behr A, Gruber B, Hoffmann B, Kowaldt FH, Kuerschner U, Limbaecker B, Sistig FP (1986) Reactions of chelate ylides with nickel(0) complexes. Organometallics 5:2356–2359. doi:10.1021/om00142a031
24. Keim W (1990) Nickel: an element with wide application in industrial homogeneous catalysis. Angew Chem Int Ed 29:235–244. doi:10.1002/anie.199002351
25. Newkome GR (1993) Pyridylphosphines. Chem Rev 93:2067–2089. doi:10.1021/cr00022a006
26. Espinet P, Soulantica K (1999) Phosphine-pyridyl and related ligands in synthesis and catalysis. Coord Chem Rev 193–195:499–556. doi:10.1016/S0010-8545(99)00140-X
27. Gómeza M, Muller G, Rocamora M (1999) Coordination chemistry of oxazoline ligands. Coord Chem Rev 193–195:769–835. doi:10.1016/S0010-8545(99)00086-7
28. Helmchen G, Pfaltz A (2000) Phosphinooxazolines a new class of versatile, modular P, N-ligands for asymmetric catalysis. Acc Chem Res 33:336–345. doi:10.1021/ar9900865
29. Braunstein P, Naud F (2001) Hemilability of hybrid ligands and the coordination chemistry of oxazoline-based systems. Angew Chem Int Ed 40:680–699. doi:10.1002/1521-3773(20010216)40:4<680:AID-ANIE6800>3.0.CO;2-0

30. Chelucci G, Orru G, Pinna GA, Chiral P (2003) N-ligands with pyridine-nitrogen, phosphorus donor atoms. Syntheses, applications in asymmetric catalysis. Tetrahedron 59:9471–9515. doi:10.1016/j.tet.2003.09.066
31. Braunstein P (2004) Functional ligands and complexes for new structures, homogeneous catalysts, and nanomaterials. J Organomet Chem 689:3953–3967. doi:10.1016/j.jorganchem.2004.06.024
32. Guiry PJ, Saunders CP (2004) The development of bidentate P, N ligands for asymmetric catalysis. Adv Synth Catal 346:497–537. doi:10.1002/adsc.200303138
33. Yamamoto A (1986) Organotransition metal chemistry. Wiley, New York
34. Guan Z, Marshall WJ (2002) Synthesis of new phosphine imine ligands and their effects on the thermal stability of late-transition-metal olefin polymerization catalysts. Organometallics 21:3580–3586. doi:10.1021/om020240i
35. Brookhart M, Daugulis O (2002) Polymerization of ethylene with cationic palladium and nickel catalysts containing bulky nonenolizable imine-phosphine ligands. Organometallics 21:5926–5934. doi:10.1021/om0206305
36. Tempel DJ, Johnson LK, Huff RL, White PS, Brookhart M (2000) Mechanistic studies of Pd(II)-$\alpha$-diimine catalyzed olefin polymerizations. J Am Chem Soc 122:6686–6700. doi:10.1021/ja000893v
37. Speiser F, Braunstein P, Saussine L (2005) Catalytic ethylene dimerization and oligomerization: recent developments with nickel complexes containing P, N-chelating ligands. Acc Chem Res 38:784–793. doi:10.1021/ar050040d
38. Wang C, Friedrich S, Younkin TR, Li RT, Grubbs RH, Bansleben DA, Day MW (1998) Neutral nickel(II)-based catalysts for ethylene polymerization. Organometallics 17:3149–3151. doi:10.1021/om980176y
39. Younkin TR, Connor EF, Henderson JI, Friedrich SK, Grubbs RH, Bansleben DA (2000) Neutral, single-component nickel (II) polyolefin catalysts that tolerate heteroatoms. Science 287:460–462. doi:10.1126/science.287.5452.460
40. Bauers FM, Mecking S (2001) Aqueous homo- and copolymerization of ethylene by neutral nickel(II) complexes. Macromolecules 34:1165–1171. doi:10.1021/ma001704w
41. Pickel M, Casper T, Rahm A, Dambouwy C, Chen P (2002) Facile preparation and activation of high-productivity single-site nickel catalysts for highly linear polyethylene. Helv Chim Acta 85:4337–4352
42. Carlini C, Raspolli Galletti AM, Sbrana G (2003) Ethylene homopolymerization by novel Ziegler Natta-type catalytic systems obtained by oxidative addition of salicylaldimine ligands to bis(1, 5-cyclooctadiene)nickel(0) and methylalumoxane. Polymer 44:1995–2003. doi:10.1016/S0032-3861(03)00078-8
43. Carlini C, De Luise V, Grillo Fernandes E, Martinelli M, Raspolli Galletti AM, Sbrana G (2005) Effect of free trimethylaluminum content in methylaluminoxane on performances of bis(salicylaldiminate)nickel(ii)-based catalysts for ethylene polymerization. Macromol Rapid Comm 26:808–812. doi:10.1002/marc.200500005
44. Zuideveld MA, Wehrmann P, Röhr C, Mecking S (2004) Remote substituents controlling catalytic polymerization by very active and robust neutral nickel(ii) complexes. Angew Chem Int Ed 43:869–869. doi:10.1002/anie.200352062
45. Sun JQ, Shan YH, Xu YJ, Cui YG, Schumann H, Hummert M (2004) Novel cyclohexyl-substituted salicylaldiminato–nickel(II) complex as a catalyst for ethylene homopolymerization and copolymerization. J Polym Sci Part A Polym Chem 42:6071–6080. doi:10.1002/pola.20458
46. Shan YH, Sun JQ, Xu YJ, Cui YG, Lin F (2005) Ethylene polymerization and copolymerization with polar monomers by a neutral nickel catalyst combined with co-catalyst of $Ni(COD)_2$ or $Al(i\text{-}Bu)_3$. Chin J Polym Sci 23:301–310. doi:10.1142/S0256767905000436
47. Bastero A, Franciò G, Leitner W, Mecking S (2006) Catalytic ethylene polymerisation in carbon dioxide as a reaction medium with soluble nickel(II) catalysts. Chem Eur J 12:6110–6116. doi:10.1002/chem.200600499
48. Göttker-Schnetmann I, Wehrmann P, Röhr C, Mecking S (2007) Substituent effects in [($\kappa^2$-N, O)salicylaldiminato nickel(II)-methyl pyridine polymerization catalysts: terphenyls

controlling polyethylene microstructures. Organometallics 26:2348–2362. doi: 10.1021/om0611498
49. Bastero A, Göttker-Schnetmann I, Röhr C, Mecking S (2007) Polymer microstructure control in catalytic polymerization exclusively by electronic effects of remote substituents. Adv Sinth Catal 349:2307–2316
50. Guironnet D, Göttker-Schnetmann I, Mecking S (2009) Catalytic polymerization in dense $CO_2$ to controlled microstructure polyethylenes. Macromolecules 42:8157–8164. doi: 10.1021/ma901397q
51. Zhang D, Weng L, Jin GX (2010) Structural characterization of nitro-substituted phenoxyiminato nickel complexes; inter-molecular $\pi$-$\pi$ interactions in the solid states and effect of the electron drawing groups on catalytic activity. J Organomet Chem 695:643–647. doi:10.1016/j.jorganchem.2009.11.033
52. Kettunen M, Abu-Surrah AS, Abdel-Halim HM, Repo T, Leskela M, Laine M, Mutikainen I, Ahlgren M (2004) Synthesis, spectroscopy and molecular structures of new salicylketiminato nickel(II) complexes. Polyhedron 23:1649–1656. doi:10.1016/j.poly.2004.03.018
53. Brasse M, Campora J, Palma P, Alvarez E, Cruz V, Ramos J, Reyes ML (2008) Nickel 2-iminopyridine N-oxide (PymNox) complexes: cationic counterparts of salicylaldiminate-based neutral ethylene polymerization catalysts. Organometallics 27:4711–4723. doi: 10.1021/om800548y
54. Zhang D, Jin GX (2006) Bimetallic nickel complexes of trimethyl phenyl linked salicylaldimine ligands: synthesis, structure and their ethylene polymerization behaviors. Inorg Chem Commun 9:322–1325. doi:10.1016/j.inoche.2006.08.017
55. Chen Q, Yu J, Huang J (2007) Arene-bridged salicylaldimine-based binuclear neutral nickel(II) complexes: synthesis and ethylene polymerization activities. Organometallics 26:617–625. doi:10.1021/om060778e
56. Wehrmann P, Mecking S (2008) Highly active binuclear neutral nickel(II) catalysts affording high molecular weight polyethylene. Organometallics 27:1399–1408. doi:10.1021/om700942z
57. Guironnet D, Friedberger T, Mecking S (2009) Ethylene polymerization in supercritical carbon dioxide with binuclear nickel(II) catalysts. Dalton Trans 8929–8934. doi: 10.1039/b912883b
58. Sujith S, Dae JJ, Na SJ, Park YW, Choi JH, Lee BY (2005) Ethylene/polar norbornene copolymerizations by bimetallic salicylaldimine-nickel catalysts. Macromolecules 38:10027–10033. doi:10.1021/ma051344i
59. Hu T, Tang LM, Li XF, Li YS, Hu NH (2005) Synthesis and ethylene polymerization activity of a novel, highly active single-component binuclear neutral nickel(II) catalyst. Organometallics 24:2628–2632. doi:10.1021/om049223e
60. Rodriguez BA, Del ferro M, Marks TJ (2008) Neutral bimetallic nickel(II) phenoxyiminato catalysts for highly branched polyethylenes and ethylene-norbornene copolymerizations. Organometallics 27:2166–2168. doi:10.1021/om800208f
61. Shim CB, Kim YH, Lee BY, Dong Y, Yun H (2003) [2-(alkylideneamino)benzoato]nickel(II) complexes: active catalysts for ethylene polymerization. Organometallics 22:4272–4280. doi: 10.1021/om0303303
62. Schroder DL, Keim W, Zuideveld MA, Mecking S (2002) Ethylene polymerization by novel, easily accessible catalysts based on nickel(II) diazene complexes. Macromolecules 35:6071–6073. doi:10.1021/ma012171
63. Li XF, Li YG, Li YS, Chen YX, Hu NH (2005) Copolymerization of ethylene with methyl methacrylate with neutral nickel(II) complexes bearing $\alpha$-ketoiminato chelate ligands. Organometallics 24:2502–2510. doi:10.1021/om049080w
64. Zhang L, Brookhart M, White PS (2006) Synthesis, characterization, and ethylene polymerization activities of neutral nickel(II) complexes derived from anilino-substituted enone ligands bearing trifluoromethyl and trifluoroacetyl substituents. Organometallics 25:1868–1874. doi:10.1021/om050931p
65. Song DP, Ye WP, Wang YX, Liu JY, Li YS (2009) Highly active neutral nickel(II) catalysts for ethylene polymerization bearing modified $\beta$-ketoiminato ligands. Organometallics 28:5697–5704. doi:10.1021/om900477k

66. Yu SM, Berkefeld A, Göttker-Schnetmann I, Mulller G, Mecking S (2007) Synthesis of aqueous polyethylene dispersions with electron-deficient neutral nickel(II) catalysts with enolatoimine ligands. Macromolecules 40:421–428. doi:10.1021/ma061804n
67. Boardman BM, Valderrama JM, Muñoz F, Wu G, Bazan GC, Rojas R (2008) Remote activation of nickel complexes by coordination of $B(C_6F_5)_3$ to an exocyclic carbonitrile functionality. Organometallics 27:1671–1674. doi:10.1021/om700933y
68. Song DP, Wu Jq, Ye WP, Mu HL, Li YS (2010) accessible, highly active single-component $\beta$-ketoiminato neutral nickel(II) catalysts for ethylene polymerization. Organometallics 29:2306–2314. doi:10.1021/om100075u
69. Nodono M, Novak BM, Boyle PT (2004) Ethylene polymerization catalyzed by neutral nickel(II) complex with O–N-chelating ligand. Polymer J 36:140–145. doi:10.1295/polymj.36.140
70. Batten MP, Canty AJ, Cavell KJ, Ruther T, Skelton BW, White AH (2006) Synthesis of nickel(II) complexes containing neutral N, N- and anionic N, O- bidentate ligands, and their behaviour as chain-growth catalysts; structural characterization of complexes containing (mim)2CO, mimCO2-, and mimCPh2O- (mim = 1-methylimidazol-2-yl). Inorg Chim Acta 359:1710–1724. doi:10.1016/j.ica.2004.06.069
71. Desjardins SY, Cavell KJ, Jin H, Skelton BW, White AH (1996) Insertion into the nickel-carbon bond of N-O chelated arylnickel(II) complexes. The development of single component catalysts for the oligomerisation of ethylene. J Organomet Chem 515:233–243. doi:10.1016/0022-328X(95)06105-6
72. Desjardins SY, Cavell KJ, Hoare JL, Skelton BW, Sobolev AN, White AH, Keim W (1997) Single component N-O chelated arylnickel(II) complexes as ethane polymerisation and CO/ethene copolymerisation catalysts. Examples of ligand induced changes to the reaction pathway. J Organomet Chem 554:163–174. doi:10.1016/S0022-328X(96)06953-7
73. Lee BY, Bazan GC, Vela J, Komon ZJA, Bu X (2001) $\alpha$-Iminocarboxamidato-nickel(II) ethylene polymerization catalysts. J Am Chem Soc 123:5352–5353. doi:10.1021/ja004191h
74. Rojas RS, Wasilke JS, Wu G, Ziller JW, Bazan GC (2005) $\alpha$-Iminocarboxamide nickel complexes: synthesis and uses in ethylene polymerization. Organometallics 24:5644–5653. doi:10.1021/om050640g
75. Azoulay JD, Itigaki K, Wu G, Bazan GC (2008) Influence of steric and electronic perturbations on the polymerization activities of $\alpha$-iminocarboxamide nickel complexes. Organometallics 27:2273–2280. doi:101021/om8000263
76. Krajete A, Steiner G, Kopacka H, Ongania KH, Wurst K, Kristen MO, Preishuber-Pflügl P, Bildstein B (2004) Iminohydroxamato early and late transition metal halide complexes—new precatalysts for aluminoxane-cocatalyzed olefin insertion polymerization. Eur J Inorg Chem 1740–1752. doi: 10.1002/ejic.200300405
77. Hicks FA, Brookhart M (2000) Synthesis of 2-anilinotropones via palladium-catalyzed amination of 2-triflatotropone. Org Lett 2:219–221. doi:10.1021/ol991310t
78. Hicks FA, Brookhart M (2001) A highly active anilinotropone-based neutral nickel(II) catalyst for ethylene polymerization. Organometallics 20:3217–3219. doi:10.1021/om010211s
79. Hicks FA, Jenkins JC, Brookhart M (2003) Synthesis and ethylene polymerization activity of a series of 2-anilinotropone-based neutral nickel(II) catalysts. Organometallics 22:3533–3545. doi:10.1021/om030142c
80. Jenkins JC, Brookhart M (2003) A highly active anilinoperinaphthenone-based neutral nickel(II) catalyst for ethylene polymerization. Organometallics 22:250–256. doi:10.1021/om020648f
81. Okada M, Nakayama Y, Ikeda T, Shiono T (2006) Synthesis of uniquely branched polyethylene by anilinonaphthoquinone ligated nickel complex activated with tris(pentafluorophenyl)borane. Macromol Rapid Commun 27:1418–1423. doi:10.1002/marc.200600335

82. Okada M, Nakayama Y, Shiono T (2007) Synthesis of anilinonaphthoquinone-based nickel complexes and their application for olefin polymerization. J Organomet Chem 692:5183–5189. doi:10.1016/j.jorganchem.2007.07.049
83. Zhang D, Jin GX (2003) Novel, highly active binuclear 2, 5-disubstituted amino-p-benzoquinone-nickel(II) ethylene polymerization catalysts. Organometallics 22:2851–2854. doi:10.1021/om030068y
84. Ponikwar W, Mihan S, Sünkel K, Beck W (2006) Aryl Phosphine Nickel(II) and Palladium(II) Complexes with N, O-Aminocarboxylate Chelate Ligands [(Aryl)($R_3P$)M(N, O-α-aminocarboxylate)] (M = Ni, Pd). Catalysts for the polymerization of olefins. Z Anorg Allg Chem 632:2299–2304. doi:10.1002/zaac.200600174
85. Johnson LK, Bennett AMA, Ittel SD, Wang L, Parthasarathy A, Hauptman E, Simpson RD, Feldman J, Coughlin EB (1997) WO Patent Application 9830609 to DuPont, Priority date 4 January 1997
86. Killian CM, MacKenzie PB, McDevitt JP, Moody LS, Ponasik JA (1998) WO Patent Application 9840420 to Eastman, Priority date 10 December 1998
87. Drent E, Arnoldy P, Budzelaar PHM (1993) Efficient palladium catalysts for the carbonylation of alkynes. J Organomet Chem 455:247–253. doi:10.1016/0022-328X(93)80406-2
88. Dekker GPCM, Buijs A, Elsevier J, van Leeuwen PWNM, Smeets WJJ, Spek AL, Wang YF, Stam CH (1992) New neutral and ionic methyl and chloro palladium and platinum complexes containing hemilabile phosphorus-nitrogen ligands. Study of the insertion of carbon monoxide into the metal-methyl bond. Organometallics 11:1937–1948. doi:10.1021/om00041a028
89. van den Beuken EK, Smeets WJJ, Spek AL, Feringa BL (1998) Oligomerisation of ethene by new palladium iminophosphine catalysts. Chem Commun 2:223–224. doi:10.1039/A707495F
90. Kwon HY, Lee SY, Lee BY, Shin DM, Chung YK (2004) Synthesis, characterization and ethylene reactivity of 2-diphenylphosphanylbenzamido nickel complexes. Dalton Trans 921–928. doi:10.1039/b317033k
91. Chen HP, Liu YH, Peng SM, Liu ST (2003) New bulky phosphino-pyridine ligands. Palladium and nickel complexes for the catalytic polymerization and oligomerization of ethylene. Organometallics 22:4893–4899. doi:10.1021/om030242i
92. Daugulis O, Brookhart M, White PS (2002) Phosphinidine-palladium complexes for the polymerization and oligomerization of ethylene. Organometallics 21:5935–5943. doi:10.1021/om020631x
93. Huang YB, Jia WG, Jin GX (2009) Synthesis, characterization and olefin polymerization of the nickel catalysts supported by [N, S] ligands. J Organomet Chem 694:86–90. doi:10.1016/j.jorganchem.2008.10.009
94. Tritto I, Donetti R, Sacchi MC, Locatelli P, Zannoni G (1997) Evidence of zircononium-polymeryl ion pairs from $^{13}C$ NMR in situ $^{13}C$-$_2H_4$ polymerization with $Cp_2Zr(^{13}CH_3)_2$-based catalysts. Macromolecules 32:264–269. doi:10.1021/ma981164r
95. Chen Y-X, Marks TJ (2000) Cocatalysts for metal-catalyzed olefin polymerization: activators, activation processes, and structure-activity relationships. Chem Rev 100:1391–1434. doi:10.1021/cr980462j
96. Rojas RS, Galland GB, Wu G, Bazan GC (2007) Single-component α-iminocarboxamide nickel ethylene polymerization and copolymerization initiators. Organometallics 26:5339–5345. doi:10.1021/om070155g
97. Connor EF, Younkin TR, Henderson JI, Hwang S, Grubbs RH, Roberts WP, Litzau JJ (2002) Linear functionalized polyethylene prepared with highly active neutral Ni(II) complexes. J Polym Sci Part A Polym Chem 40:2842–2854. doi:10.1002/pola.10370
98. Berkefeld A, Drexler M, Möller HM, Mecking S (2009) Mechanistic insights on the copolymerization of polar vinyl monomers with neutral Ni(II) catalysts. J Am Chem Soc 131:12613–12622. doi:10.1021/ja901360b

99. Carlini C, Martinelli M, Raspolli Galletti AM, Sbrana G (2002) Copolymerization of ethylene with methacrylate by Ziegler-Natta-type catalysts based on nickel salicylaldiminate/methylalumoxane systems. Macromol Chem Phys 203:1606–1613
100. Li H, Marks TJ (2006) Nuclearity and cooperative effects in binuclear catalysts and cocatalysts for olefin polymerization. J Proc Natl Acad Sci USA 103:15295–15302. doi:10.1073/pnas.0603396103
101. Diamanti SJ, Ghosh P, Shimizu F, Bazan GC (2003) Ethylene homopolymerization and copolymerization with functionalized 5-Norbornen-2-yl monomers by a novel nickel catalyst system. Macromolecules 36:9731–9735. doi:10.1021/ma035102z
102. Diamanti SJ, Khanna V, Hotta A, Coffin RC, Yamakawa D, Kramer EJ, Fredrickson GH, Bazan GC (2006) Tapered block copolymers containing ethylene and a functionalized comonomer. Macromolecules 39:3270–3274. doi:10.1021/ma052456c
103. Soula R, Novat C, Tomov A, Spitz R, Claverie J, Drujon X, Malinge J, Saudemont T (2001) Catalytic polymerization of ethylene in emulsion. Macromolecules 34:2022–2026. doi:10.1021/ma0017135
104. Göttker-Schnetmann I, Korthals B, Mecking S (2006) Water-soluble salicylaldiminato Ni(II)-methyl complexes: enhanced dissociative activation for ethylene polymerization with unprecedented nanoparticle formation. J Am Chem Soc 128:7708–7709. doi:10.1021/ja0619962
105. Korthals B, Göttker-Schnetmann I, Mecking S (2007) Nickel(II)-methyl complexes with water-soluble ligands L [(salicylaldiminato-$\kappa^2$ N, O)NiMe(L)] and their catalytic properties in disperse aqueous systems. Organometallics 26:1311–1316. doi:10.1021/om0607191
106. Bastero A, Kolb L, Wehrmann P, Bauers F, Göttker-Schnetmann I, Monteil V, Thomann R, Chowdhry M, Mecking S (2004) Catalytic ethylene polymerization in aqueous emulsion: catalyst tailoring and synthesis of very small latex particles. Polym Mater Sci Eng 90:740–741
107. Jenkins JC, Brookhart M (2004) A mechanistic investigation of the polymerization of ethylene catalyzed by neutral Ni(II) complexes derived from bulky anilinotropone ligands. J Am Chem Soc 126:5827–5842. doi:10.1021/ja030634g
108. Berkefeld A, Mecking S (2009) Deactivation pathways of neutral Ni(II) polymerization catalysts. J Am Chem Soc 131:1565–1574. doi:10.1021/ja808855v
109. Connor EF, Younkin TR, Henderson JI, Waltman AW, Grubbs RH (2003) Synthesis of neutral nickel catalysts for ethylene polymerization—the influence of ligand size on catalyst stability. Chem Commun 2272–2273. doi:10.1039/b306701g
110. Braunstein P, Frison C, Morise X (2000) Stepwise ethene and/or methyl acrylate/CO insertions into the Pd−C bond of cationic palladium(II) complexes stabilized by a (P, O) chelate. Angew Chem Int Ed 39:2867–9870. doi:10.1002/1521-3773(20000818)39:16<2867:AID-ANIE2867>3.0.CO;2-X
111. Braunstein P, Agostinho M (2007) Structurally characterized intermediates in the stepwise insertion of CO-ethylene or CO-methyl acrylate into the metal-carbon bond of Pd(II) complexes stabilized by (phosphinomethyl)oxazoline ligands. Chem Commun 58–60. doi:10.1039/b613865a
112. Michalak A, Ziegler T (2003) Comparison of Ni- and Pd-diimine complexes as catalysts for ethylene/methyl acrylate copolymerization. A static and dynamic density functional theory study. Organometallics 22:2660–2669. doi:10.1021/om021044e
113. Michalak A, Ziegler T (2003) Polymerization of ethylene catalyzed by a nickel(+2) anilinotropone-based catalyst: DFT and stochastic studies on the elementary reactions and the mechanism of polyethylene branching. Organometallics 22:2069–2079. doi:10.1021/om030072+
114. Rodriguez BA, Delferro M, Marks TJ (2009) Bimetallic effects for enhanced polar comonomer enchainment selectivity in catalytic ethylene polymerization. J Am Chem Soc 131:5902–5919. doi:10.1021/ja900257k
115. Gibson VC, Tomov A (2001) Functionalised polyolefin synthesis using [P,O]Ni catalysts. Chem Commun 1964–1965. doi:10.1039/B106475D

116. Waltman AW, Younkin TR, Grubbs RH (2004) Insights into the deactivation of neutral nickel ethylene polymerization catalysts in the presence of functionalized olefins. Organometallics 23:5121–5123. doi:10.1021/om049360b
117. Williams BS, Leatherman MD, White PS, Brookhart M (2005) Reactions of vinyl acetate and vinyl trifluoroacetate with cationic diimine Pd(II) and Ni(II) alkyl complexes: identification of problems connected with copolymerizations of these monomers with ethylene. J Am Chem Soc 127:5132–5146. doi:10.1021/ja045969s
118. Chan MSW, Deng L, Ziegler T (2000) Density functional study of neutral salicylaldiminato nickel(II) complexes as olefin polymerization catalysts. Organometallics 19:2741–2750. doi:10.1021/om000055+

# Chapter 3
# Rare-Earth Metal Complexes Supported by Nitrogen-Containing Ligands in Olefin Polymerization

**Alexander A. Trifonov**

**Abstract** In this review the recent developments in the synthesis of rare-earth metal complexes active in catalysis of olefin polymerization are summarized. Alkyl (neutral and ate), cationic alkyl and hydrido complexes supported by nitrogen-containing ligands are considered. The polymerization-active complexes are classified according to monomer (ethylene, α-olefin, styrene), type of compound (neutral alkyl, cationic alkyl, ate-alkyl, hydrido) and the number of nitrogen atoms in supporting ligands. The properties of obtained polyolefins are discussed.

## 3.1 Introduction

As isoelectronic analogues of the group 4 metallocenium alkyl and hydride cations, neutral rare-earth metallocene alkyls and hydrides have received much attention during past three decades as olefin polymerization catalysts [1–5]. The combination in one molecule of Lewis acidity and of high reactivity of M–H and M–C bonds which undergo facile multiple carbon–carbon bond insertions [6–14] sets up a basis for high potential of rare-earth alkyl and hydrido complexes in olefin polymerization. The main advantage of rare-earth metal complexes is the fact that neutral low-coordinate alkyl and hydrido species are highly reactive towards ethylene, and unlike the group 4 metal compounds are able to act as one-component catalytic systems in the absence of activator or co-catalyst.

A. A. Trifonov (✉)
G.A. Razuvaev Institute of Organometallic Chemistry of Russian Academy of Sciences, Tropinina 49, GSP-445, 603950 Nizhny Novgorod, Russia
e-mail: trif@iomc.ras.ru

G. Giambastiani and J. Cámpora (eds.), *Olefin Upgrading Catalysis by Nitrogen-based Metal Complexes I*, Catalysis by Metal Complexes, 35
DOI: 10.1007/978-90-481-3815-9_3, 

The absence of co-catalyst in polymerization system allows to diminish side-processes like chain-transfer or chain-termination and to run polymerization in a 'controlled-living' fashion and to obtain polyolefinic materials with narrow molecular weight distributions. Also the capability of complexes of rare-earth metals to initiate polymerization of polar monomers (methacrylates, lactones, lactides) enables the sequential diblock polymerization of olefins with these monomers and their functionalization. The remarkable activity (and selectivity) of lanthanide-based catalysts in diene polymerization makes them promising candidates for development of efficient catalysts for diene-olefin copolymerization and production of new high performance resins. Another important feature relevant to catalytic applications is gradual variation of the ionic radius within the rare-earth metals series in the range from 0.89E (Sc3+) to 1.17E (La3+) [15] when the redox and chemical properties remain substantially similar. This affords a unique opportunity for tuning the activity and selectivity of metal complex by designing the metal coordination sphere and selecting the central atom with appropriate radius according to specific requirements of the catalyzed reaction.

A significant breakthrough in development of olefin polymerization catalysts is related to the beginning of post-metallocene era, which allowed to establish correlations between catalyst structure and polymer microstructure [16]. A significant progress has been done in understanding of the factors that are crucial for stabilizing polymerization-active metal centres and controlling their activity and selectivity. The supporting ligands play an important role since they should provide control over the metal coordination number and coordination geometry, steric protection of the active site in order to influence over stereoselectivity. The development of new supporting ligand environments for rare-earth metals which would allow to overcome the limitations inherent to the cyclopentadienyl system and to extend the means for design of metal coordination sphere [17–19] is currently in focus.

According to the MLX scheme [20, 21] polymerization-active rare-earth metal complex should contain "actor" M–C (preferably alkyl) or M–H groups which easily undergo C=C bond insertion and "spectator" supporting coordination environment. Electropositivity of rare-earth metals, high energy of their d-orbitals [22] and predominantly ionic character of the metal–ligand interactions in their organic derivatives have favoured employment of supporting ligands forming stable anions like cyclopentadienyl [23–25]. The ancillary ligand destined for synthesis of polymerization-active "one-site" alkyl or hydrido species of rare-earth metals should be completely inert to nucleophilic attack, non-labile and bulky enough to provide steric saturation of the metal atom coordination sphere and therefore the kinetic stability of the metal complex. In order to prevent ligand redistribution process typical for rare-earth metal complexes multidentate ligands containing donor sites that do not tend to form bridging bonds are preferable.

In this review the recent developments in the synthesis and catalysis of olefin polymerization by alkyl, cationic alkyl and hydrido rare-earth complexes supported by nitrogen containing ligands will be considered. The polymerization-active

complexes are classified according to monomer (ethylene, α-olefin, styrene), type of compound (neutral alkyl, cationic alkyl, ate-alkyl, hydrido) and the number of nitrogen atoms in supporting ligands.

## Neutral dialkyl lanthanide complexes

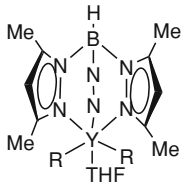


R = Me (**1**), Ph (**2**), $CMe_3$ (**3**), $CH_2SiMe_3$ (**4**)

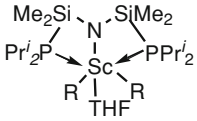


R = Me (**5**), Et (**6**), $CH_2SiMe_3$ (**7**)

## Cationic alkyl complexes

### $N_1$

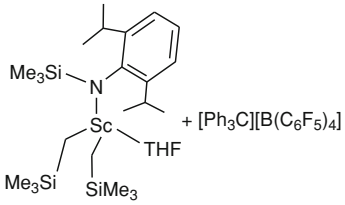


**(8)**

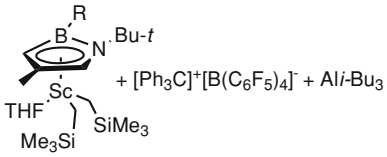


R = Ph (**9**), $N^iPr_2$ (**10**), Me (**11**)

### $N_2$

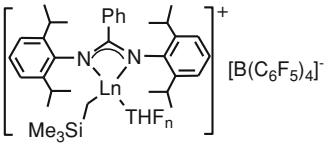


Ln = Sc, n = 2 (**12**); Y, 3 (**13**)
Gd, 3 (**14**), Lu, 3, (**15**)
La, 4 (**16**), Nd, 4 (**17**)

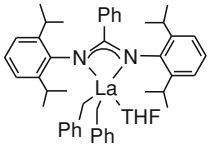


+ $[PhNMe_2H]^+[B(C_6F_5)_4]^-$
(**18**)

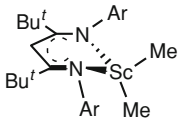


Ar = 2,6-$^iPr_2C_6H_3$ (**19**)

## $N_2$

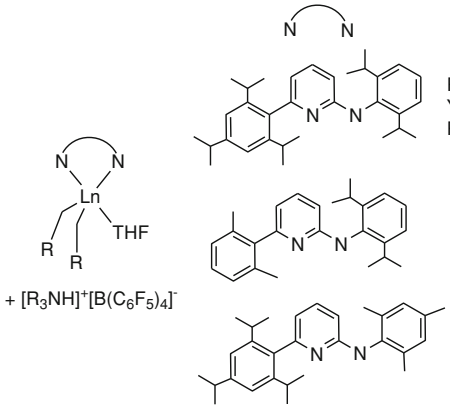

R = $SiMe_3$; Ln = Sc (**20**); Y (**21**); Er (**22**); Yb (**23**); Lu (**24**)
R = Ph; Sc (**25**); Y (**26**); Er (**27**); Lu (**28**)

R = $SiMe_3$; Ln = Sc (**29**); Y ( **30**);

R = $SiMe_3$; Ln = Sc (**31**); Y (**32**)

+ $[R_3NH]^+[B(C_6F_5)_4]^-$

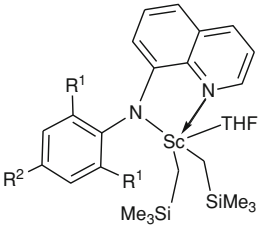

+ Borate + $AlR_3$

$R^1$ = Me, $R^2$ = H (**33**);$R^1$ = $R^2$ = Me (**34**);
$R^1$ =Et, $R^2$ = H (**35**); $R^1$ = *i*-Pr, $R^2$ = H (**36**);
$R^1$ = $R^2$ = H (**37**);

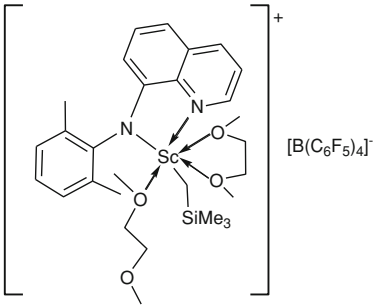

$[B(C_6F_5)_4]^-$

(**38**)

## $N_3$

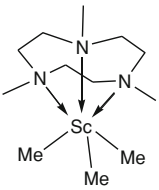

+ $[PhNMe_2H]^+[B(C_6F_5)_4]^-$

(**39**)

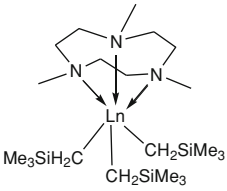

+ $B(C_6F_5)_3$ + Al*i*-$Bu_3$

Ln = Sc (**40**), Y (**41**)

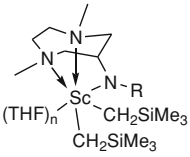

+ $[PhNMe_2H]^+[B(C_6F_5)_4]^-$

n = 1, R = Me (**42**); R = $PhMe_2Si$ (**43**)
n = 0, R = $PhMe_2Si$ (**44**)

## $N_3$

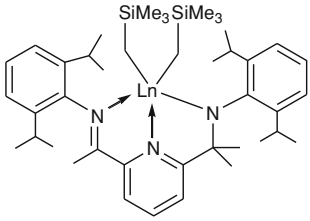


+ $[Ph_3C]^+[B(C_6F_5)_4]^-$ or $[PhNMe_2H]^+[B(C_6F_5)_4]^-$
or N-[tris(pentafluorophenyl)borane]-3H-indole

Ln = Sc (**45**), Y (**46**), Lu (**47**)

## $N_4$


+ $[PhNMe_2H]^+[B(C_6F_5)_4]^-$

R = *i*-Pr (**48**), Me (**49**)

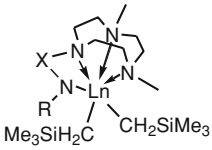


+ $[PhNMe_2H]^+[B(C_6F_5)_4]^-$
or $[Ph_3C]^+[B(C_6F_5)_4]^-$

| | | | |
|---|---|---|---|
| Ln = Sc, | R = *t*-Bu, | X = $Me_2Si$ | (**50**) |
| Sc | *sec*-Bu | $Me_2Si$ | (**51**) |
| Y | *sec*-Bu | $(CH_2)_2$ | (**52**) |
| Y | *n*-Bu | $(CH_2)_2$ | (**53**) |
| Y | *t*-Bu | $Me_2Si$ | (**54**) |
| Y | *sec*-Bu | $Me_2Si$ | (**55**) |
| La | *t*-Bu | $(CH_2)_2$ | (**56**) |
| Nd | *t*-Bu | $(CH_2)_2$ | (**57**) |
| Nd | *sec*-Bu | $(CH_2)_2$ | (**58**) |
| Nd | *t*-Bu | $Me_2Si$ | (**59**) |
| Nd | *sec*-Bu | $Me_2Si$ | (**60**) |

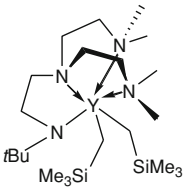


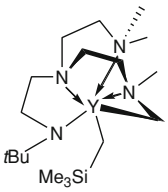


+$[Ph_3C]^+[B(C_6F_5)_4]^-$

(**61**) (**62**)

## $N_5$

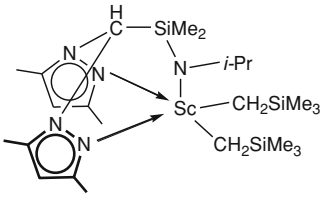


+ $[Ph_3C]^+[B(C_6F_5)_4]^-$

(**63**)

## $N_6$

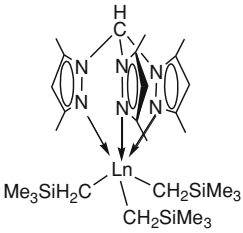


+ $B(C_6F_5)_3$ + Al*i*-$Bu_3$

Ln = Sc (**64**), Y (**65**)

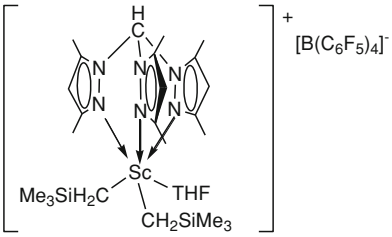


(**66**)

## NO

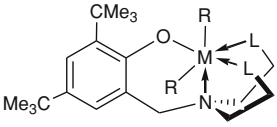


+ MAO

R = $CH_2SiMe_2Ph$
Ln = Y, L = $NEt_2$ (**67**)

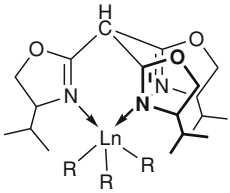


R = $CH_2SiMe_3$, Ln = Sc (**68**), Y (**69**),
Er (**70**), Ho (**71**), Dy (**72**), Tm (**73**), Lu (**74**)
R = $CH_2SiMe_2Ph$, Ln = Lu ( **75**)

## Alkyl ate-complexes

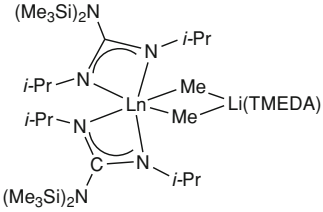


Ln = Nd (**76**), Yb (**77**)

**Hydrido complexes**

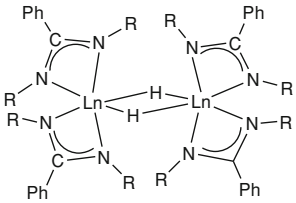

R = $SiMe_3$; Ln = Y (**78**), Sc (**79**)

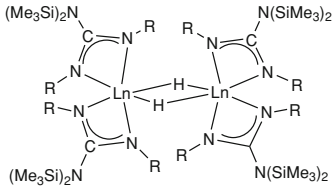

R = *i*-Pr, Ln = Y (**80**), Nd (**81**), Sm (**82**), Gd (**83**), Yb (**84**), Lu (**85**)
R = Cy, Ln = Y (**86**), Lu (**87**)

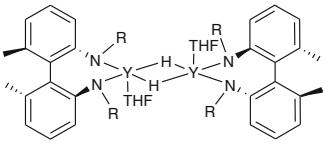

R = $SiMe_2$*t*-Bu (**88**)

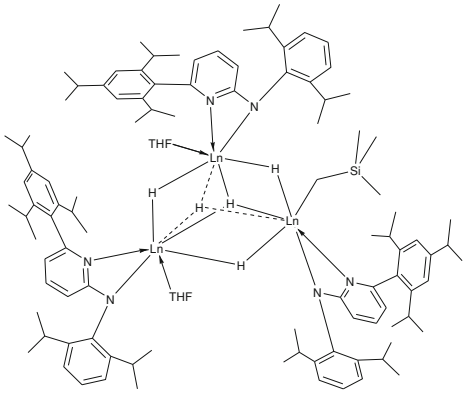

Ln = Y (**89**), Lu (**90**)

**Hydrido complexes**

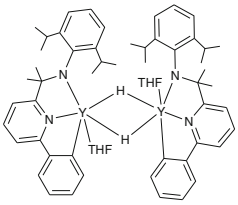

(**91**)

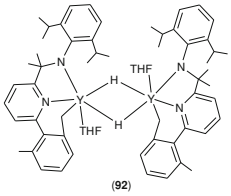

(**92**)

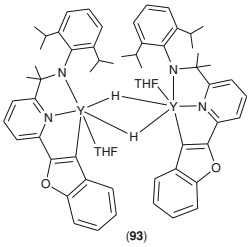

(**93**)

**Chart 3.1** Rare-earth metal complexes supported by nitrogen-containing ligands

## 3.2 Ethylene Polymerization

### *3.2.1 Neutral Alkyl Rare-Earth Metal Complexes*

The reports on catalytic activity of neutral alkyl rare-earth species in olefin polymerization still remain scarce. Bianconi et al. in 1996 reported on the

synthesis and in situ preparation of a series of bis(alkyl) yttrium complexes supported by monoanionic tris(pyrazolyl)borate ligands (Chart 3.1, **1**–**4**). Complexes **2** and **4** were synthesized by the salt metathesis reactions of $LYCl_2(THF)$ with two equivalents of the appropriate alkyl(aryl)lithium reagent and were isolated in 70% yield [26]. The di(methyl) derivative was found to be highly unstable even at low temperatures that is why 1 and tert-butyl species were generated in situ. All the alkyl complexes demonstrated catalytic activity in ethylene polymerization yielding highly linear polyethylene with $M_w$ in some cases exceeding $2 \times 10^6$. Unlike the metallocene-type rare-earth complexes even the species containing bulky Ph and $CH_2SiMe_3$ ligands and coordinated THF molecule turned out to be polymerization-active indicating the greater steric unsaturation in **1**–**4**. The in situ generated di(tert-butyl) complex has shown the highest activity ($N_t = 1{,}932$; Table 3.1, entry 4). Dissociation of coordinated THF molecules appears to be a controlling factor in the initiation of polymerization since no reaction occurs in THF-solutions. Overall catalytic activity is rather low with $N_t$ (mole of PE/mole of Y) 1,200–3,000. Molecular weights ($M_w$) of the obtained polymers range from $1.0 \times 10^5$ to $>2 \times 10^6$ with polydispersities ranging from 2.5 to 4.1.

Five-coordinate scandium dialkyl complexes containing amido diphospine ligand (Chart 3.1, **5**–**7**) are able to initiate ethylene polymerization, but no data on their activity and polymer properties are available [27].

### *3.2.2 Cationic Alkyl Rare-Earth Metal Complexes*

In the past decade an impressive progress has been done in the field of synthesis and characterization of organo rare-earth cationic species. In contrast to the neutral and anionic complexes which are known since 80th regular publications on this matter started to appear in the literature very recently [28–30]. Cationic species should possess an enhanced Lewis acidity compared to that of neutral alkyl complexes and provide stronger affinity of the metal centre to electron density of the C=C bond of olefin and also strongly bind main group alkyls.

### *3.2.3 Cationic Alkyl Rare-Earth Metal Complexes Supported by $N_2$-Ligands*

Bulky amidinate ligands were successfully employed in the research of Teuben–Hessen group and allowed the synthesis and isolation of a new family of highly reactive cationic alkyl species of rare-earth metals with various ionic radii (Sc, Lu, Y, Gd, Nd, La) [31–33]. Neutral dialkyl species $LM(CH_2SiMe_3)_2(THF)_n$ were converted to their cationic monoalkyl derivatives $LM(CH_2SiMe_3)(THF)_n[BPh_4]$ ($M$ = Sc, $n = 2$; $M$ = Lu, Y, $n = 3$; $M$ = Nd, La, $n = 4$) by protonolysis with

**Table 3.1** Lanthanide complexes supported by N-containing ligands in ethylene polymerization

| Type of catalyst | Entry | Catalyst | T(°C) | P | t(h) | Activity[a] | $N_t$ | $M_w \times 10^{-3}$ | $M_w/M_n$ | References |
|---|---|---|---|---|---|---|---|---|---|---|
| Neutral alkyl complex | 1 | **1** | 25 | 120 psi | 6 | – | 29.5 | – | – | [26] |
| | 2 | **2** | 25 | 120 psi | 6 | – | 1,096 | 100 | 2.50 | [26] |
| | 3 | **2** | 25 | 120 psi | 18 | – | 1,688 | 1,200 | 4.14 | [26] |
| | 4 | **3** | 25 | 120 psi | 6 | – | 1,932 | – | – | [26] |
| | 5 | **4** | 25 | 120 psi | 6 | – | 15.1 | – | – | [26] |
| | 6 | **5** | – | – | – | – | – | – | – | [27] |
| | 7 | **6** | – | – | – | – | – | – | – | [27] |
| | 8 | **7** | – | – | – | – | – | – | – | [27] |
| Cationic alkyl complexes | 9 | **12** + $[PhNMe_2H]$ $H[B(C_6F_5)_4]^-$ + TIBAO | 30 | 5 bar | 0.33 | 24 | – | 93 | 1.6 | [32] |
| | 10 | **13** + $[PhNMe_2H]$ $H[B(C_6F_5)_4]^-$ + TIBAO | 30 | 5 bar | 0.33 | 3,006 | – | 1,666 | 2.0 | [32] |
| | 11 | **14** + $[PhNMe_2H]$ $H[B(C_6F_5)_4]^-$ + TIBAO | 30 | 5 bar | 0.33 | 2,848 | – | 1,753 | 2.1 | [32] |
| | 12 | **15** + $[PhNMe_2H]$ $H[B(C_6F_5)_4]^-$ + TIBAO | 30 | 5 bar | 0.33 | 342 | – | 496 | 1.4 | [32] |
| | 13 | **16** + $[PhNMe_2H]$ $H[B(C_6F_5)_4]^-$ + TIBAO | 30 | 5 bar | 0.33 | 14 | – | 470 | 2.5 | [32] |
| | 14 | **17** + $[PhNMe_2H]$ $H[B(C_6F_5)_4]^-$ + TIBAO | 30 | 5 bar | 0.33 | 1,988 | – | 1,596 | 2.2 | [32] |
| | 15 | **18** + $[PhNMe_2H]^-$ $[B(C_6F_5)_4]^-$ + TIBAO | 50 | 5 bar | 0.25 | 59 | – | 89.5 | 14.6 | [33] |
| | 16 | **18** + TIBAO | 50 | 5 bar | 0.25 | 0 | – | 0 | | [33] |
| | 17 | **19** + PMAO-IP | 50 | 300 psi | – | $1.2 \times 10^6$ g(mol of catalyst)$^{-1}$ h$^{-1}$ | – | 1,866 | 1.98 | [34] |

(continued)

**Table 3.1** (continued)

| Type of catalyst | Entry | Catalyst | T(°C) | P | t(h) | Activity[a] | $N_t$ | $M_w \times 10^{-3}$ | $M_w/M_n$ | References |
|---|---|---|---|---|---|---|---|---|---|---|
| | 18 | **19** + $B(C_6F_5)_3$ + PMAO-IP | 50 | 300 psi | – | $3.0 \times 10^5$ g(mol of catalyst)$^{-1}$ h$^{-1}$ | – | 1,051 | 1.7 | [34] |
| | 19 | **19** + $[Ph_3C]^+$ $[B(C_6F_5)_4]^-$ + PMAO-IP | 50 | 300 psi | – | $4.8 \times 10^5$ g(mol of catalyst)$^{-1}$ h$^{-1}$ | – | 851 | 2.48 | [34] |
| | 20 | **21** + $[R_2NMeH]^-$ $[B(C_6F_5)_4]^-$ + TIBAO | 80 | 5 bar | 0.25 | 1,072 kg(mol of catalyst)$^{-1}$ h$^{-1}$ bar$^{-1}$ | – | 66.5 bimodal | 3.2 | [35] |
| | 21 | **30** + $[R_2NMeH]^-$ $[B(C_6F_5)_4]^-$ + TIBAO | 80 | 5 bar | 0.25 | 400 kg(mol of catalyst)$^{-1}$ h$^{-1}$ bar$^{-1}$ | – | 46.1(10.8) bimodal | 4.3(1.5) | [35] |
| Cationic alkyl complexes | 22 | **32** + $[R_2NMeH]^-$ $[B(C_6F_5)_4]^-$ + TIBAO | 80 | 5 bar | 0.25 | 432 kg(mol of catalyst)$^{-1}$ h$^{-1}$ bar$^{-1}$ | – | 263.9(16.3) bimodal | 28.8(2.4) | [35] |
| | 23 | **21** + $[R_2NMeH]^-$ $[B(C_6F_5)_4]^-$ + TIBAO | 30 | 5 bar | 0.25 | 40 kg(mol of catalyst)$^{-1}$ h$^{-1}$ bar$^{-1}$ | – | 67.9(1,950) bimodal | 43.0(1.3) | [35] |
| | 24 | **21** + $[R_2NMeH]^-$ $[B(C_6F_5)_4]^-$ + TIBAO | 50 | 5 bar | 0.25 | 200 kg(mol of catalyst)$^{-1}$ h$^{-1}$ bar$^{-1}$ | – | 76.4 | 19.1 | [35] |
| | 25 | **21** + $[R_2NMeH]^-$ $[B(C_6F_5)_4]^-$ + TIBAO | 100 | 5 bar | 0.25 | 808 kg(mol of catalyst)$^{-1}$ h$^{-1}$ bar$^{-1}$ | – | 15.6 | 1.4 | [35] |
| | 26 | **22** + $[R_2NMeH]^-$ $[B(C_6F_5)_4]^-$ + TIBAO | 80 | 5 bar | 0.25 | 1,616 kg(mol of catalyst)$^{-1}$ h$^{-1}$ bar$^{-1}$ | – | $M_n = 29.6$ | 2.0 | [37] |
| | 27 | **23** + $[R_2NMeH]^-$ $[B(C_6F_5)_4]^-$ + TIBAO | 80 | 5 bar | 0.25 | 2 kg(mol of catalyst)$^{-1}$ h$^{-1}$ bar$^{-1}$ | – | – | – | [37] |
| | 28 | **24** + $[R_2NMeH]^-$ $[B(C_6F_5)_4]^-$ + TIBAO | 80 | 5 bar | 0.25 | 128 kg(mol of catalyst)$^{-1}$ h$^{-1}$ bar$^{-1}$ | – | $M_n = 6$ | 1.5 | [37] |
| | 29 | **20** + $[R_2NMeH]^-$ $[B(C_6F_5)_4]^-$ + TIBAO | 80 | 5 bar | 0.25 | 536 kg(mol of catalyst)$^{-1}$ h$^{-1}$ bar$^{-1}$ | – | 607.1(13.1) bimodal | 3.33(1.62) | [37] |
| | 30 | **31** + $[R_2NMeH]^-$ $[B(C_6F_5)_4]^-$ + TIBAO | 80 | 5 bar | 0.25 | 384 kg(mol of catalyst)$^{-1}$ h$^{-1}$ bar$^{-1}$ | – | 373.5(4.28) bimodal | 16.1(1.56) | [37] |
| | 31 | **29** + $[R_2NMeH]^-$ $[B(C_6F_5)_4]^-$ + TIBAO | 80 | 5 bar | 0.25 | 312 kg(mol of catalyst)$^{-1}$ h$^{-1}$ bar$^{-1}$ | – | 39.6 | 2.56 | [37] |

(continued)

**Table 3.1** (continued)

| Type of catalyst | Entry | Catalyst | T(°C) | P | t(h) | Activity[a] | $N_t$ | $M_w \times 10^{-3}$ | $M_w/M_n$ | References |
|---|---|---|---|---|---|---|---|---|---|---|
| | 32 | **45** + $[Ph_3C]^+$ $[B(C_6F_5)_4]^-$ | 25 | 150 psi | 1 | 25 kg(mol of catalyst)$^{-1}$ h$^{-1}$ bar$^{-1}$ | – | 827.9 | 3.21 | [38] |
| | 33 | **47** + $[Ph_3C]^+$ $[B(C_6F_5)_4]^-$ | 25 | 150 psi | 1 | 15 kg(mol of catalyst)$^{-1}$ h$^{-1}$ bar$^{-1}$ | – | 434.8 | 2.04 | [38] |
| Cationic alkyl complexes | 34 | **45** + $[PhNMe_2H]^+$ $[B(C_6F_5)_4]^-$ | 25 | 150 psi | 1 | 33 kg(mol of catalyst)$^{-1}$ h$^{-1}$ bar$^{-1}$ | – | 822.6 | 3.69 | [38] |
| | 35 | **47** + $[PhNMe_2H]^+$ $[B(C_6F_5)_4]^-$ | 25 | 150 psi | 1 | 13 kg(mol of catalyst)$^{-1}$ h$^{-1}$ bar$^{-1}$ | – | 325.2 | 1.97 | [38] |
| | 36 | **40** + $B(C_6F_5)_3$ + Al*i*-$Bu_3$ | 21 | 5 bar | 1 | 220 kg(mol of catalyst)$^{-1}$ h$^{-1}$ bar$^{-1}$ | – | 847 | – | [39] |
| | 37 | **41** + $B(C_6F_5)_3$ + Al*i*-$Bu_3$ | 33 | 5 bar | 1 | 240 kg(mol of catalyst)$^{-1}$ h$^{-1}$ bar$^{-1}$ | – | 353 | – | [39] |
| | 38 | **66** + $B(C_6F_5)_3$ + Al*i*-$Bu_3$ | 33 | 5 bar | 1 | 290 kg(mol of catalyst)$^{-1}$ h$^{-1}$ bar$^{-1}$ | – | 192 | – | [39] |
| | 39 | **42** + $[PhNMe_2H]^+$ $[B(C_6F_5)_4]^-$ | 50 | 5 bar | 0.16 | 0 | – | 0 | 0 | [40] |
| | 40 | **43** + $[PhNMe_2H]^+$ $[B(C_6F_5)_4]^-$ | 50 | 5 bar | 0.16 | 0 | – | 0 | 0 | [40] |
| | 41 | **44** + $[PhNMe_2H]^+$ $[B(C_6F_5)_4]^-$ | 50 | 5 bar | 0.16 | 584 kg(mol of catalyst)$^{-1}$ h$^{-1}$ bar$^{-1}$ | – | 1,200 | 1.9 | [40] |
| | 42 | **48** + $[PhNMe_2H]^+$ $[B(C_6F_5)_4]^-$ | 30 | 5 bar | 0.16 | 960 kg(mol of catalyst)$^{-1}$ h$^{-1}$ bar$^{-1}$ | – | – | – | [41] |
| | 43 | **49** + $[PhNMe_2H]^+$ $[B(C_6F_5)_4]^-$ | 30 | 5 bar | 0.16 | 700 kg(mol of catalyst)$^{-1}$ h$^{-1}$ bar$^{-1}$ | – | 471 | 4.0 | [41] |
| | 44 | **49** + $[PhNMe_2H]^+$ $[B(C_6F_5)_4]^-$ | 50 | 5 bar | 0.16 | 1,180 kg(mol of catalyst)$^{-1}$ h$^{-1}$ bar$^{-1}$ | – | 325 | 4.9 | [41] |

(continued)

**Table 3.1** (continued)

| Type of catalyst | Entry | Catalyst | T(°C) | P | t(h) | Activity[a] | $N_t$ | $M_w \times 10^{-3}$ | $M_w/M_n$ | References |
|---|---|---|---|---|---|---|---|---|---|---|
| | 45 | **49** + $[PhNMe_2H]^+$ $[B(C_6F_5)_4]^-$ | 80 | 5 bar | 0.16 | 1,790 kg(mol of catalyst)$^{-1}$h$^{-1}$bar$^{-1}$ | – | 98 | 6.0 | [41] |
| | 46 | **50** + $[PhNMe_2H]^+$ $[B(C_6F_5)_4]^-$ | 50 | 5 bar | 0.16 | 75 kg(mol of catalyst)$^{-1}$ h$^{-1}$bar$^{-1}$ | – | 690 | 2.2 | [42] |
| Cationic alkyl complexes | 47 | **50** + $[PhNMe_2H]^+$ $[B(C_6F_5)_4]^-$ | 80 | 5 bar | 0.16 | 376 kg(mol of catalyst)$^{-1}$ h$^{-1}$ bar$^{-1}$ | – | 128 | 1.9 | [42] |
| | 48 | **50** $[Ph_3C]^+$ $[B(C_6F_5)_4]^-$ | 50 | 5 bar | 0.16 | 145 kg(mol of catalyst)$^{-1}$ h$^{-1}$ bar$^{-1}$ | – | 939 | 1.7 | [42] |
| | 49 | **50** + $[Ph_3C]^+$ $[B(C_6F_5)_4]^-$ | 80 | 5 bar | 0.16 | 541 kg(mol of catalyst)$^{-1}$ h$^{-1}$ bar$^{-1}$ | – | 138 | 2.1 | [42] |
| | 50 | **54** + $[PhNMe_2H]^+$ $[B(C_6F_5)_4]^-$ | 50 | 5 bar | 0.16 | 1,343 kg(mol of catalyst)$^{-1}$h$^{-1}$bar$^{-1}$ | – | 127 | 6.6 | [42] |
| | 51 | **54** + $[PhNMe_2H]^+$ $[B(C_6F_5)_4]^-$ | 80 | 5 bar | 0.16 | 1,132 kg(mol of catalyst)$^{-1}$ h$^{-1}$ bar$^{-1}$ | – | 72 | 6.2 | [42] |
| | 52 | **54** + $[Ph_3C]^+$ $[B(C_6F_5)_4]^-$ | 50 | 5 bar | 0.16 | 1,280 kg(mol of catalyst)$^{-1}$ h$^{-1}$ bar$^{-1}$ | – | 139 | 10.5 | [42] |
| | 53 | **54** + $[Ph_3C]^+$ $[B(C_6F_5)_4]^-$ | 80 | 5 bar | 0.16 | 1,571 kg(mol of catalyst)$^{-1}$ h$^{-1}$ bar$^{-1}$ | – | 60 | 5.1 | [42] |
| | 54 | **59** + $[PhNMe_2H]^+$ $[B(C_6F_5)_4]^-$ | 50 | 5 bar | 0.16 | 743 kg(mol of catalyst)$^{-1}$ h$^{-1}$ bar$^{-1}$ | – | 358 | 2.4 | [42] |
| | 55 | **59** + $[PhNMe_2H]^+$ $[B(C_6F_5)_4]^-$ | 80 | 5 bar | 0.16 | 243 kg(mol of catalyst)$^{-1}$ h$^{-1}$ bar$^{-1}$ | – | 65 | 2.2 | [42] |
| | 56 | **59** + $[Ph_3C]^+$ $[B(C_6F_5)_4]^-$ | 50 | 5 bar | 0.16 | 788 kg(mol of catalyst)$^{-1}$ h$^{-1}$ bar$^{-1}$ | – | 503 | 2.1 | [42] |
| | 57 | **59** + $[Ph_3C]^+$ $[B(C_6F_5)_4]^-$ | 80 | 5 bar | 0.16 | 325 kg(mol of catalyst)$^{-1}$ h$^{-1}$ bar$^{-1}$ | – | 71 | 1.7 | [42] |

(continued)

**Table 3.1** (continued)

| Type of catalyst | Entry | Catalyst | T(°C) | P | t(h) | Activity[a] | $N_t$ | $M_w \times 10^{-3}$ | $M_w/M_n$ | References |
|---|---|---|---|---|---|---|---|---|---|---|
| | 58 | **49** + $[PhNMe_2H]^+$ $[B(C_6F_5)_4]^-$ | 80 | 5 bar | 0.16 | 1,787 kg(mol of catalyst)$^{-1}$ h$^{-1}$ bar$^{-1}$ | – | 98 | 6.0 | [42] |
| | 59 | **49** + $[Ph_3C]^+$ $[B(C_6F_5)_4]^-$ | 50 | 5 bar | 0.16 | 1,811 kg(mol of catalyst)$^{-1}$ h$^{-1}$ bar$^{-1}$ | – | 130 | 7.2 | [42] |
| Cationic alkyl complexes | 60 | **49** + $[Ph_3C]^+$ $[B(C_6F_5)_4]^-$ | 80 | 5 bar | 0.16 | 2,200 kg(mol of catalyst)$^{-1}$ h$^{-1}$ bar$^{-1}$ | – | 72 | 3.8 | [42] |
| | 61 | **57** + $[PhNMe_2H]^+$ $[B(C_6F_5)_4]^-$ | 50 | 5 bar | 0.16 | 807 kg(mol of catalyst)$^{-1}$ h$^{-1}$ bar$^{-1}$ | – | 56 | 2.2 | [42] |
| | 62 | **57** + $[PhNMe_2H]^+$ $[B(C_6F_5)_4]^-$ | 80 | 5 bar | 0.16 | 625 kg(mol of catalyst)$^{-1}$ h$^{-1}$ bar$^{-1}$ | – | 35 | 1.8 | [42] |
| | 63 | **57** + $[Ph_3C]^+$ $[B(C_6F_5)_4]^-$ | 50 | 5 bar | 0.16 | 1,233 kg(mol of catalyst)$^{-1}$ h$^{-1}$ bar$^{-1}$ | – | 69 | 2.3 | [42] |
| | 64 | **57** + $[Ph_3C]^+$ $[B(C_6F_5)_4]^-$ | 80 | 5 bar | 0.16 | 482 kg(mol of catalyst)$^{-1}$ h$^{-1}$ bar$^{-1}$ | – | 38 | 1.9 | [42] |
| | 65 | **56** + $[PhNMe_2H]^+$ $[B(C_6F_5)_4]^-$ or $[Ph_3C]^+$ $[B(C_6F_5)_4]^-$ | 50 or 80 | 5 bar | 0.16 | 0 | – | 0 | 0 | [42] |
| | 66 | **51** + $[PhNMe_2H]^+$ $[B(C_6F_5)_4]^-$ | 50 | 5 bar | 0.16 | 203 kg(mol of catalyst)$^{-1}$ h$^{-1}$ bar$^{-1}$ | – | 350 | 1.4 | [42] |
| | 67 | **51** + $[PhNMe_2H]^+$ $[B(C_6F_5)_4]^-$ | 80 | 5 bar | 0.16 | 245 kg(mol of catalyst)$^{-1}$ h$^{-1}$ bar$^{-1}$ | – | 157 | 3.5 | [42] |
| | 68 | **51** + $[Ph_3C]^+$ $[B(C_6F_5)_4]^-$ | 50 | 5 bar | 0.16 | 340 kg(mol of catalyst)$^{-1}$ h$^{-1}$ bar$^{-1}$ | – | 484 | 1.8 | [42] |
| | 69 | **51** + $[Ph_3C]^+$ $[B(C_6F_5)_4]^-$ | 80 | 5 bar | 0.16 | 362 kg(mol of catalyst)$^{-1}$ h$^{-1}$ bar$^{-1}$ | – | 132 | 2.7 | [42] |
| | 70 | **55** + $[PhNMe_2H]^+$ $[B(C_6F_5)_4]^-$ | 50 | 5 bar | 0.16 | 562 kg(mol of catalyst)$^{-1}$h$^{-1}$bar$^{-1}$ | – | 778 | 2.0 | [42] |

(continued)

**Table 3.1** (continued)

| Type of catalyst | Entry | Catalyst | T(°C) | P | t(h) | Activity[a] | $N_t$ | $M_w \times 10^{-3}$ | $M_w/M_n$ | References |
|---|---|---|---|---|---|---|---|---|---|---|
| | 71 | **55** + $[PhNMe_2H]^+$ $[B(C_6F_5)_4]^-$ | 80 | 5 bar | 0.16 | 1,067 kg(mol of catalyst)$^{-1}$ h$^{-1}$ bar$^{-1}$ | – | 91 | 3.6 | [42] |
| Cationic alkyl complexes | 72 | **55** + $[Ph_3C]^+$ $[B(C_6F_5)_4]^-$ | 50 | 5 bar | 0.16 | 1,278 kg(mol of catalyst)$^{-1}$ h$^{-1}$ bar$^{-1}$ | – | 547 | 1.6 | [42] |
| | 73 | **55** + $[Ph_3C]^+$ $[B(C_6F_5)_4]^-$ | 80 | 5 bar | 0.16 | 1,942 kg(mol of catalyst)$^{-1}$ h$^{-1}$ bar$^{-1}$ | – | 53 | 2.6 | [42] |
| | 74 | **60** + $[PhNMe_2H]^+$ $[B(C_6F_5)_4]^-$ | 50 | 5 bar | 0.16 | 287 kg(mol of catalyst)$^{-1}$ h$^{-1}$ bar$^{-1}$ | – | 391 | 1.8 | [42] |
| | 75 | **60** + $[PhNMe_2H]^+$ $[B(C_6F_5)_4]^-$ | 80 | 5 bar | 0.16 | 187 kg(mol of catalyst)$^{-1}$ h$^{-1}$ bar$^{-1}$ | – | 61 | 2.0 | [42] |
| | 76 | **60** + $[Ph_3C]^+$ $[B(C_6F_5)_4]^-$ | 50 | 5 bar | 0.16 | 145 kg(mol of catalyst)$^{-1}$ h$^{-1}$ bar$^{-1}$ | – | 293 | 2.0 | [42] |
| | 77 | **52** + $[PhNMe_2H]^+$ $[B(C_6F_5)_4]^-$ | 50 | 5 bar | 0.16 | 1,331 kg(mol of catalyst)$^{-1}$ h$^{-1}$ bar$^{-1}$ | – | 90 | 3.8 | [42] |
| | 78 | **52** + $[PhNMe_2H]^+$ $[B(C_6F_5)_4]^-$ | 80 | 5 bar | 0.16 | 2,016 kg(mol of catalyst)$^{-1}$h$^{-1}$bar$^{-1}$ | – | 54 | 2.3 | [42] |
| | 79 | **52** + $[Ph_3C]^+$ $[B(C_6F_5)_4]^-$ | 50 | 5 bar | 0.16 | 1,303 kg(mol of catalyst)$^{-1}$ h$^{-1}$ bar$^{-1}$ | – | 135 | 4.3 | [42] |
| | 80 | **52** + $[Ph_3C]^+$ $[B(C_6F_5)_4]^-$ | 80 | 5 bar | 0.16 | 2,027 kg(mol of catalyst)$^{-1}$h$^{-1}$bar$^{-1}$ | – | 77 | 3.4 | [42] |
| | 81 | **53** + $[PhNMe_2H]^+$ $[B(C_6F_5)_4]^-$ | 50 | 5 bar | 0.16 | 285 kg(mol of catalyst)$^{-1}$ h$^{-1}$ bar$^{-1}$ | – | 294 | 2.6 | [42] |
| | 82 | **53** + $[PhNMe_2H]^+$ $[B(C_6F_5)_4]^-$ | 80 | 5 bar | 0.16 | 488 kg(mol of catalyst)$^{-1}$h$^{-1}$bar$^{-1}$ | – | 92 | 1.8 | [42] |
| | 83 | **53** + $[Ph_3C]^+$ $[B(C_6F_5)_4]^-$ | 50 | 5 bar | 0.16 | 638 kg(mol of catalyst)$^{-1}$ h$^{-1}$ bar$^{-1}$ | – | 703 | 2.4 | [42] |

(continued)

**Table 3.1** (continued)

| Type of catalyst | Entry | Catalyst | T(°C) | P | t(h) | Activity[a] | $N_t$ | $M_w \times 10^{-3}$ | $M_w/M_n$ | References |
|---|---|---|---|---|---|---|---|---|---|---|
| | 84 | **53** + $[Ph_3C]^+$ $[B(C_6F_5)_4]^-$ | 80 | 5 bar | 0.16 | 1,157 kg(mol of catalyst)$^{-1}$ h$^{-1}$ bar$^{-1}$ | – | 151 | 3.1 | [42] |
| | 85 | **61** + $[PhNMe_2H]^+$ $[B(C_6F_5)_4]^-$ | 50 | 5 bar | 0.25 | 0 | – | 0 | 0 | [43] |
| | 86 | **61** + $[Ph_3C]^+$ $[B(C_6F_5)_4]^-$ | 50 | 5 bar | 0.25 | 20 kg(mol Y)$^{-1}$ desactivation in 4 min | – | 55 | 2.2 | [43] |
| Hydrido complexes | 87 | **4** + $H_2$ | 25 | 120 psi | 2 | – | 3,000 | 1,900 | 15.86 | [26] |
| | 88 | **78** | 55 | 70 atm | – | 4 g(mmol of catalyst)$^{-1}$ h$^{-1}$ | – | – | – | [58] |
| | 89 | **79** | 60 | – | – | sluggishly | – | – | – | [59] |
| | 90 | **85** | 20 | 0.48 bar | 72 h | 83 g(mmol of catalyst)$^{-1}$ h$^{-1}$ atm$^{-1}$ | – | – | – | [61] |
| | 91 | **82** | 20 | 0.5 atm | – | 1,268 g(mmol of catalyst)$^{-1}$ h$^{-1}$ atm$^{-1}$ | – | – | – | [61] |
| | 92 | **80** | 20 | 0.5 atm | – | 442 g(mmol of catalyst)$^{-1}$ h$^{-1}$ atm$^{-1}$ | | | | [61] |
| | 93 | **84** | 20 | 0.5 atm | – | 77 g(mmol of catalyst)$^{-1}$ h$^{-1}$ atm$^{-1}$ | – | – | – | [61] |
| | 94 | **86** | 20 | 0.5 atm | – | 65 g(mmol of catalyst)$^{-1}$ h$^{-1}$ atm$^{-1}$ | – | – | – | [62] |
| | 95 | **87** | 20 | 0.5 | – | 76 g(mmol of catalyst)$^{-1}$ h$^{-1}$ atm$^{-1}$ | – | – | – | [62] |
| | 96 | **89** | 20 | 0.5 | – | 560 g(mmol of catalyst)$^{-1}$ h$^{-1}$ atm$^{-1}$ | – | – | – | [64] |
| | 97 | **90** | 20 | 0.5 | – | 168 g(mmol of catalyst)$^{-1}$ h$^{-1}$ atm$^{-1}$ | – | – | – | [64] |

[a] *Activity* kg(mol of catalyst)$^{-1}$ h$^{-1}$ atm$^{-1}$, otherwise stated
[b] *Overall turnover numbers* moles of PE/moles of Ln

$[PhNMe_2H][BPh_4]$ in THF. The complexes were isolated in good yields and crystal structures were established for the derivatives of Sc, Y, Gd, Nd, La [32]. Noteworthy the remaining alkyl group in all these complexes occupies an axial position relative to amidinate-metal plane. Ethylene polymerization tests were performed in toluene solvent (Chart 3.1, Table 3.1, entries 9–14), the catalytically active species were generated by reacting the dialkyls with an equimolar amount of the activator $[PhNMe_2H][B(C_6F_5)_4]$ in the presence of 20 equivalents of isobutylalumoxane (TIBAO) scavenger. The catalytic activity was shown to be highly dependent on the metal ionic radius. The smallest (Sc) and the largest (La) metals in the series demonstrate very low activities, the metals of intermediate size (Y, Gd) allow to reach activities of 3,006 and 2,848 kg PE $mol^{-1}$ $h^{-1}$ $bar^{-1}$, respectively.

The values of molecular weight ($M_w \approx 1.5 \times 10^6$) of polyethylene obtained in these experiments and low polydispersity ($M_w/M_n = 2$) are indicative of a single-site catalyst behaviour. For the Y-containing system in the absence of scavenger the polymerization process was found to have living character ($M_w/M_n = 1.1$–$1.2$). The authors conclude that the alkyl transfer to Al is the main chain transfer mechanism operating in this catalytic system. When $LY(CH_2SiMe_3)_2(THF)$ activated in toluene by $[PhNMe_2H][B(C_6F_5)_4]$ in the absence of alkylaluminium scavenger (50 °C) readily polymerises ethylene. The $M_w$ of polymer increases from $430 \times 10^3$ (5 min) to $1{,}211 \times 10^3$ (30 min) with a remarkably low polydispersity $M_w/M_n \approx 1.2$, thus indicating living character of polymerization.

The catalyst productivity noticeably decreases with increasing run time from 1,037 kg PE $mol^{-1}$ $h^{-1}$ $bar^{-1}$ over 5 min to 400 over 30 min [31].

Dibenzyl lanthanum complex supported by bulky amidinate ligand **18** (Chart 3.1) was inactive in ethylene polymerization, but when treated with 1 equivalent of $[PhNMe_2H][B(C_6F_5)_4]$ in the presence of TIBAO (La/Al = 1: 10) at 50 °C in toluene an activity of 59 kg PE $mol^{-1}$ $h^{-1}$ $bar^{-1}$ was reached (Table 3.1, entry 15) [33]. The activity of the cationic amidinate benzyl species is higher than that observed previously for the cation generated from $LLa(CH_2SiMe_3)_2(THF)_2$ [32] which may be attributed to the presence of one additional THF molecule coordinated to the metal centre.

Dimethyl scandium complex coordinated by $\beta$-diketiminato ligand **19** (Chart 3.1) reported by Piers et al. when activated with $B(C_6F_5)_3$, $[Ph_3C][B(C_6F_5)_4]$ or PMAO-IP is active in catalysis of ethylene polymerization [34] (Table 3.1, entries 17–19). Molecular weights of the obtained polymers are relatively high and the polydispersities are in the range 1.7–2.48. The activities are quite high ($3.0 \times 10^5$–$1.2 \times 10^6$ g(mol of catalyst)$^{-1}$ $h^{-1}$) and approach those reported for metallocene group 4 based catalysts. When the dichloro precursor $LScCl_2$ was used under MAO activation activity was noticeably lower indicating slow rate of the scandium centre activation by organoaluminium reagent.

Catalytic behaviour of a series of organoyttrium cationic species supported by amidopyridinato ligands in the presence of aluminium trialkyls and aluminoxanes at various temperatures was described in [35–37]. Neutral dialkyl complexes **21**, **30**, **32** (Chart 3.1) were obtained using the alkane elimination reaction

of the parent aminopyridines (LH) with $Y(CH_2SiMe_3)_2(THF)_2$ and characterized by NMR spectroscopy. The reactions of the dialkyl species with ammonium borates lead to selective elimination of one alkyl group and afford alkyl cationic species. Treatment of complexes **21** and **32** with $[PhNMe_2H][BPh_4]$ in THF-toluene mixture allowed isolation of cationic complexes $[LY(CH_2SiMe_3)(THF)_3][BPh_4]$, whose structures were established by X-ray diffraction study [35]. The catalytic tests in ethylene polymerization were run at 80 °C in the presence of one equivalent of $[R_2NHMe][B(C_6F_5)_4]$ (R = $C_{16}$–$H_{31}$, $C_{18}H_{35}$] and 20 equivalents of TIBAO. The presence of aluminium alkyl was found to be essential for polymerization activity. To reach high activity very bulky amidopyridinato ligands should be used (Table 3.1, entries 20–22). Investigation of temperature dependence of catalytic activity of the system **21** -$[R_2NHMe][B(C_6F_5)_4]$ (R = $C_{16}$–$H_{31}$, $C_{18}H_{35}$] in the temperature range 30–80 °C showed an unusual increase in activity together with an increase in molecular weight. This observation was explained by the authors as a result of a reversible chain transfer between the organoyttrium cation responsible for chain growth and the aluminium centre responsible for the chain storage [35]. The stability of the organoyttrium cations in combination with a nearly suppressed $\beta$-hydrido elimination at T up to 100 °C allows for synthesis of long-chain polymers (up to 4,000 g $mol^{-1}$) with a polydispersity below 1.1. In the synthesis of higher molecular polyethylene (15,600 g $mol^{-1}$) some increase in polydispersity (1.4) is observed. Both alumoxanes and aluminium alkyls can be used in these catalytic systems, but alkyl aluminium compounds demonstrate lower activities.

Dialkyl and cationic alkyl species supported by amidopyridinato ligands of rare-earth metals of various ionic radii (Sc, Er, Yb, Lu) **20**, **22–29**, **31** (Chart 3.1) were described in [37]. Dialkyl compounds were prepared by reacting $Ln(CH_2SiMe_3)_3(THF)_2$ (Ln = Er, Yb, Lu) and $Ln(CH_2Ph)_3(THF)_3$ (Ln = Y, Er, Lu) with an equimolar amount of aminopyridine. Protonolysis of dialkyl compounds with 1 equivalent of $[PhNMe_2H][BPh_4]$ in THF affords cationic species $[LLn(CH_2R)(THF)_n][BPh_4]$ (R = $SiMe_3$, Ln = Sc, Y; R = Ph, Ln = Sc, Er; n = 2,3) [37]. Complexes **20**, **22–24**, **29**, **31** were estimated as precatalysts for ethylene polymerization under activation with 1.1 equivalent of $[R_2NHMe][B(C_6F_5)_4]$ (R = $C_{16}H_{31}$, $C_{18}H_{35}$) and in the presence of TIBAO (20-equiv) at 80 °C (15 min). Dialkyl complexes of Er and Lu demonstrated low to good activities (40–1,616 kg(mol of catalyst)$^{-1}$ $h^{-1}$ $bar^{-1}$, Table 3.1, entries 26–31), while Yb-containing analogue showed very low activity (2 kg(mol of catalyst)$^{-1}$ $h^{-1}$ $bar^{-1}$. The polymerization activities of Y and Er, which have similar values of ionic radii [15] are much higher compared to those of smaller Lu and Yb, thus indicating the influence of the metal ion radius. The average number molecular weight (Mn) of the polymer obtained with the erbium complex (29,600 and 14,500 g $mol^{-1}$) is higher compared to that of the polymer obtained with yttrium compound (20,800 and 3,610 g $mol^{-1}$). For lutetium compound the molecular weight of obtained polymer is 6,000 g $mol^{-1}$. The activities of Er and Lu compounds were found to decrease when the concentration of TIBAO increases. In the case of scandium compound 20 which has the smallest ionic radius in the family of rare-earth metals

good activity in ethylene polymerization was observed. In contrast to the derivatives of yttrium, erbium and lutetium no dependence of the activity and molecular weight on the TIBAO concentration was observed for scandium. The authors suppose that the scandium ion size is too small for the coordination of alkylaluminium compounds which is necessary for the polyethylene chain transfer. Reduction of the steric bulk of the amidopyridinato ligand coordinated to the scandium centre decreases the catalytic activity.

### 3.2.4 Cationic Alkyl Rare-Earth Metal Complexes Supported by $N_3$-Ligands

The synthesis and structures of amido-pyridine-supported dialkyl complexes of Sc, Lu and Y (**45**–**47**, Chart 3.1) were reported in [38]. Activation of these complexes by $[Ph_3C][B(C_6F_5)_4]$, $[PhNMe_2H][B(C_6F_5)_4]$ or N-[tris(pentafluorophenyl)borane]-3H-indole leads to formation of polymerization-active species (Table 3.1, entries 32–35). The highest activities were observed for scandium-containing complex (25 and 33 kg(mol of catalyst)$^{-1}$ h$^{-1}$ bar$^{-1}$), while the lutetium analogue demonstrated lower activity (15 and 13 kg(mol of catalyst)$^{-1}$ h$^{-1}$ bar$^{-1}$).

Neutral 1,4,7-trimethyl-1,4,7-triazacyclonane ligand was successfully employed for the synthesis of tris(alkyl) $LLn(CH_2SiMe_3)_3$ (Ln = Sc, Y) (**40**, **41**, Chart 3.1) complexes [39]. Activation of complexes **40** and **41** by $B(C_6F_5)_3$ in the presence of 250 equivalents of *i*-$Bu_3Al$ allows ethylene polymerization (21 or 33 °C, 5 bar) with activities of 220–240 kg(mol of catalyst)$^{-1}$ h$^{-1}$ bar$^{-1}$ for Sc, while for the Y compound the activity was much lower (10 kg(mol of catalyst)$^{-1}$ h$^{-1}$ bar$^{-1}$) (Table 3.1, entries 36, 37).

Dialkyl scandium complexes $LSc(CH_2SiMe_3)(THF)n$ ($n$ = 0, 1) coordinated by monoanionic *fac*-k$^3$ tridentate [6-RN-1,4,6-trimethyl-1,4-diazepine] (R = Me, $PhMe_2Si$) ligands (**42**–**44**, Chart 3.1) were synthesized by Hessen et al. using the alkane elimination approach [40]. In THF complexes readily react with $[PhNMe_2H][BPh_4]$ to generate the ionic monoalkyl species $[LSc(CH_2SiMe_3)(THF)_2][BPh_4]$. Only the THF-free complex **44** after activation with $[PhNMe_2H][B(C_6F_5)_4]$ in toluene afforded an active single-site ethylene polymerization catalyst (activity 584 kg(mol of catalyst)$^{-1}$ h$^{-1}$ bar$^{-1}$, Table 3.1, entry 41). One THF molecule turned out to be sufficient to shut down the catalytic activity.

### 3.2.5 Cationic Alkyl Rare-Earth Metal Complexes Supported by $N_4$-Ligands

A series of dialkyl rare-earth metal (Sc, Y, La, Nd) complexes supported by monoanionic tetradentate linked 1,4,7-triazacyclononane (TACN) ligands bearing various substituents at the nitrogen atoms of the cycle (Me, *i*-Pr) and amido

nitrogen (*n*-Bu, *sec*-Bu, *t*-Bu) and having different length of backbone between neutral cyclic and monoanionic amido fragments ($(CH_2)_2$, $SiMe_2$) were described by Hessen et al. (**48–60**, Chart 3.1) [41, 42]. The complexes were synthesized by using alkane elimination approach. For the larger lanthanide metals such as La and Nd for which the neutral homoleptic trisalkyls $M(CHY_2SiMe_3)_3(THF)_n$ are not available, in situ generated trisalkyl species were used. The X-ray diffraction studies were performed for complexes **48**, **54**, **55–57**, **59** and proved their structures. The dialkyl complexes cleanly react with Brønsted acid $[PhNMe_2H][B(C_6F_5)_4]$ in $C_6D_5Br$ to give cationic alkyl species. The cationic alkyl complexes coordinated by the ligand containing Me-substituents at the endocyclic nitrogen atoms are sufficiently stable at ambient temperature. This is in contrast to the cationic species with the *i*-Pr-substituted ligand which in the absence of coordinating solvent (THF) undergoes rapidly intramolecular metallation of the *i*-Pr-fragments. Activities of obtained dialkyl complexes as precatalysts of ethylene polymerization were evaluated in toluene solvent at the temperature range of 30–80 °C under 5 bar of ethylene pressure (Table 3.1, entries 42–83). $[PhNMe_2H][B(C_6F_5)_4]$ or $[CPh_3][B(C_6F_5)_4]$ were used as activators without additional use of alkylaluminium scavengers. The catalytic activity was demonstrated to be strongly influenced by the metal ionic radius, while the variations of the ligand backbone and substituents on nitrogen atoms do influence catalyst stability and polymer molecular weight. Catalysts based on rare-earth metals of intermediate size like Y showed higher activities, but some of these catalytic systems yield the polymer with broad molecular weight distribution, thus indicating multisite behaviour. The yttrium complexes **48** and **49** when activated with $[PhNMe_2H][B(C_6F_5)_4]$ yield active polymerization catalysts with productivities $0.70 \times 10^3$–$1.79 \times 10^3$ kg(mol of catalyst)$^{-1}$ h$^{-1}$ bar$^{-1}$ [41]. The productivity of the system based on Y complex containing $(CH_2)_2$-linker is enhanced by increasing the reaction temperature, but the polydispersity of the polyethylene also increases noticeably (Table 3.1, entries 42–45). In the family of complexes supported by $Me_2$TACN-$SiMe_2$-N*t*-Bu ligand strangely Sc complexes demonstrated modest activity, which increases with increasing temperature. The trityl counter ion appears to be slightly more effective as activator. The Y derivative **54** showed high activity 1,500 kg(mol of catalyst)$^{-1}$ h$^{-1}$ bar$^{-1}$, but the obtained polymer had a broad polydispersity ($M_w/M_n = 5$–10). Molecular weights are significantly lower compared to those of polymers produced with Sc catalyst. The variations in ligand substitution pattern and ligand geometric constrain proved to be essential to effect on catalysts performance. Thus the Sc complex **51** containing $SiMe_2$-bridged ligand with *sec*-Bu substituent on amido nitrogen demonstrated enhanced activity compared to *t*-Bu-substituted analogue. For Y the catalyst **55** is highly active (activity up to 2,000 kg(mol of catalyst)$^{-1}$ h$^{-1}$ bar$^{-1}$) and obtained polymer has lower polydispersity 2.5. For Nd (complexes **59** and **60**) the activity is lower than for *t*-Bu-substituted analogue obviously due to decrease of thermal stability of catalyst. The pronounced effect of the size of the substituent at amido nitrogen was observed in the Y systems, where the small *n*-Bu group caused a strong differentiation in performance for two activators, possibly due to reversible coordination

of aniline formed in the course of activation to the metal ion (Table 3.1, entries 81–84). Replacement of the $SiMe_2$-linker by longer $(CH_2)_2$ in the case of Y (Chart 3.1, **49** and **54**) gives a catalyst with improved activity at higher temperature, but increase of polydispersity was also observed. For the largest Nd metal (Chart 3.1, **57**) this more sterically demanding ligand gives the best activity especially when combined with trityl cation as activator (Table 3.1, entry 63; 1,233 kg(mol of catalyst)$^{-1}$ h$^{-1}$ bar$^{-1}$). The analogous system based on La metal is absolutely inactive in ethylene polymerization, what on the authors' opinion can be associated with toluene coordination to the large metallic centre. Noteworthy that despite of the absence of alkylaluminium co-catalyst in the reaction system none of the obtained complexes allowed to perform living ethylene polymerization. The authors suggest that this is indicative of facile $\beta$-hydrogen elimination process in these complexes compared to the more electron-poor compounds supported by amidinate ligands.

Monoanionic tetradentate triamino-amido ligand based on linear triamine moiety and being less conformationally constrained was employed for the synthesis of yttrium dialkyl species (Chart 3.1, **61**) [43] using alkane elimination pathway. Upon standing in solution **61** cleanly undergoes intramolecular metallation with liberation of TMS and formation of **62** (Chart 3.1). The system **61**-$[PhNMe_2H][B(C_6F_5)_4]$ did not show any activity in ethylene polymerization, while the combination of **61** with $[Ph_3C][B(C_6F_5)_4]$ showed initial polymerization activity, but rapid catalyst deactivation took place (Table 3.1, entries 85–86).

### 3.2.6 Cationic Alkyl Rare-Earth Metal Complexes Supported by $N_5$-Ligands

The sole example of rare-earth metal cationic alkyl complex containing $N_5$-ligand is presented by the five-coordinate Sc derivative coordinated by monoanionic tridentate heteroscorpionate ligand (Chart 3.1, **63**) [44]. The dialkyl complex was obtained by reacting $Sc(CH_2SiMe_3)_3(THF)_2$ with protio ligand. Treatment of **63** with $[Ph_3C][B(C_6F_5)_4]$ in the presence of THF yields the stable monoalkyl species $[LSc(CH_2SiMe_3)(THF)][B(C_6F_5)_4]$, which was mentioned to be active in catalysis of ethylene polymerization. No details were provided.

### 3.2.7 Cationic Alkyl Rare-Earth Metal Complexes Supported by $N_6$-Ligands

Neutral *fac*-k$^3$ coordinated tris(pyrazolyl)methane ligand was used for stabilization of cationic scandium and yttrium species (Chart 3.1, **64**, **65**) which were generated by reacting $LLn(CH_2SiMe_3)_3$ with $[Ph_3C][B(C_6F_5)_4]$ in $CD_2Cl_2$ or in the presence

of THF [39]. The catalytic tests were carried out in toluene under the pressure of ethylene of 5 bar in the presence of 250 equivalents of $i$Bu$_3$Al. For the scandium catalyst an activity of 290 kg(mol of catalyst)$^{-1}$ h$^{-1}$ bar$^{-1}$ was reported, while in the case of the yttrium-containing analogue no solid polymer formation was observed.

### *3.2.8 Cationic Alkyl Complexes Supported by N,O-Ligands*

The synthesis of dialkyl yttrium complex supported by monoanionic tetradentate aminophenolate ligand (Chart 3.1, **67**) was reported by Bercawet al. [45]. Polymerization test upon activation with excess MAO showed very low activity.

## 3.3 Hydrido Rare-Earth Metal Complexes Supported by Nitrogen-Containing Ligands

Rare-earth metal hydrides demonstrate a variety of unique structural and chemical properties [46]. The impetuous development of this area, stimulated by promising catalytic activity of hydrido complexes, has considerably contributed in organolanthanide chemistry (For example see, hydrogenation: [47, 48]; polymerization: [49–52]; hydrosilylation: [53]; hydroboration: [54, 55]). Despite of the progress which has been done in this field until recently rare-earth metals hydrides were represented exclusively by sandwich- [46] and half-sandwich type ("constrained geometry") [24, 25] complexes and very few classes of their non-cyclopentadienyl analogues are known [18, 19, 56].

The first example of structurally characterized non-cyclopentadienyl rare-earth metal hydride, yttrium complex stabilized by benzamidinate ligands (78, Chart 3.1) was published by Teuben in 1996 [57]. Hydride **78** was prepared by the hydrogenolysis of the parent alkyl $L_2YCH(SiMe_3)_2$ at 3 atm of $H_2$ and 40 °C in benzene and was proved to have a dimeric structure in both crystalline state and in solutions in non-coordinating solvents. When heated at 55 °C and 70 atm of ethylene complex **78** showed activity of 4 g(mmol of catalyst)$^{-1}$ h$^{-1}$ (Table 3.1, entry 88). With propylene and 1-hexene complex **78** does not react [58]. The scandium analogue **79** (Chart 3.1) was also synthesized by the hydrogenolysis of alkyl complex $L_2ScCH_2SiMe_3$ but at milder conditions (ambient temperature, 1 atm) [59]. Complex **79** does not catalyze polymerizations of ethylene or propylene at room temperature; however, at 60 °C ethylene is sluggishly polymerized while propylene appeared to undergo multiple insertions.

A family of hydrido complexes of rare-earth metals of large (Nd, Sm), intermediate (Y, Gd) and small (Yb, Lu) ion size **80–87** (Chart 3.1) supported by guanidinate ligands of various steric bulk $[(Me_2Si)_2NC(NR)_2]^-$ (R = $i$-Pr, Cy) was described in articles [60–62]. The catalytic tests of complexes **80–87** in ethylene

polymerization were carried out at 20 °C, and ethylene pressure 0.5 atm. Even under such very mild conditions Sm complex **82**, containing isopropyl-substituted guanidinate ligands showed very high polymerization efficiency: 1,268 g(mmol of catalyst)$^{-1}$ h$^{-1}$ atm$^{-1}$. Noteworthy by the end of 24 h the complex was still active without loss of the reaction rate. In the case of the yttrium derivative **80** the catalyst activity was noticeably lower, but nevertheless high −442 g(mmol of catalyst)$^{-1}$ h$^{-1}$ atm$^{-1}$ and no loss of the reaction rate was observed during 3 days. The neodymium analogue **81** sluggishly polymerized ethylene and after 1 h the reaction stopped. Complexes of gadolinium, ytterbium and lutetium demonstrated modest activities (281, 77 and 83 g(mmol of catalyst)$^{-1}$ h$^{-1}$ atm$^{-1}$, respectively). Replacement of isopropyl fragments in guanidinate ligands by cyclohexyl ones resulted in considerable decrease of polymerization activity of yttrium complex **86** (65 g(mmol of catalyst)$^{-1}$ h$^{-1}$ atm$^{-1}$), while the activity of lutetium catalyst **87** (83 g(mmol of catalyst)$^{-1}$ h$^{-1}$ atm$^{-1}$) is close to the value observed for isopropyl-substituted analogue.

Don Tilley et al. reported on the synthesis and structure of yttrium hydride coordinated by dianionic $C_2$-symmetric bis(silylamido)biphenyl ligand **88** (Chart 3.1). Complex **88** does not show noticeable activity in ethylene or 1-hexene polymerization ($C_6D_6$, 80 °C, 5 psi, 2 h). The reaction resulted in the hydride decomposition and precipitation of a small amount of polyethylene [63]. When dissolved in THF at room temperature **88** undergoes rapid ethylene insertion into the Y–H bonds affording related ethyl complex. The insertion of the second ethylene molecule occurs slowly and is accompanied by the complex decomposition. No polyethylene formation was observed even at elevated ethylene pressure (80 psi, 48 h). The reaction of parent alkyl complex $LYCH(SiMe_3)_2(Et_2O)_2$ with ethylene ($C_6D_6$, 5 psi) results in the very slow formation of small amounts of polyethylene.

The hydrogenolysis of dialkyl yttrium complex **4** (Chart 3.1) containing tris(pyrazolyl)borate ligand (8 atm, 0 °C, toluene) leads to generation of the hydrido species which was characterized spectroscopically and was found to be able to catalyze ethylene polymerization ($N_t$ = 3,000, $M_w$ = 1.9 × 106, $M_w/M_n$ = 15.86) [26].

Trinuclear alkyl-hydrido clusters of yttrium and lutetium coordinated by bulky amidopyridinate ligands (Chart 3.1, **89**, **90**) and containing three $\mu^2$-bridging hydrido ligands situated in the equatorial plane and two $\mu^3$-hydrido ligands occupying the apical positions catalyze ethylene polymerization under very mild conditions (20 °C, 0.5 atm) [64]. The activity of yttrium complex **89** was found to be 560 g(mmol of catalyst)$^{-1}$ h$^{-1}$ atm$^{-1}$ but the catalyst was deactivated in 3 h. The lutetium derivative **90** showed lower activity (168 g(mmol of catalyst)$^{-1}$ h$^{-1}$ atm$^{-1}$) but no loss of the reaction rate was observed over 1 day (Table 3.1, entries 96, 97).

The catalytic performances of the dinuclear yttrium aryl-hydrido, benzyl-hydrido and benzofuryl-hydrido complexes **91–93** (Chart 3.1) have been systematically scrutinized for ethylene polymerization, but no polymerization activity has been observed [65, 66].

## 3.4 α-Olefin Polymerization

### *3.4.1 Cationic Alkyl Complexes*

Cationic alkyl amido complex of scandium in situ generated by reacting dialkyl scandium complex $LSc(CH_2SiMe_3)_2(THF)$ (**8**, Chart 3.1) with an equimolar amount of $[Ph_3C][B(C_6F_5)_4]$ (toluene, room temperature) is able to convert 650 equivalents of 1-hexene into atactic poly(1-hexene) with $M_n = 7{,}300$ and $M_w/M_n = 2.65$ (Table 3.2, entry 2). The Y, Ho and Lu analogues were found to be inreactive under the similar conditions [67].

Activation of scandium trimethyl complex coordinated by neutral 1,4,7-trimethyl-1,4,7-triazacyclononane ligand (Chart 3.1, **39**) with $B(C_6F_5)_3$ or $[PhNMe_2H][B(C_6F_5)_4]$ leads to formation of cationic alkyl species which catalyze polymerization of 1-pentene affording oligo(1-pentene) ($M_w = 4{,}000$, $M_w/M_n = 1.32$) [68].

In order to provide tacticity control of α-olefin polymerization scandium tris-alkyl complex coordinated by $C_3$-chiral trisoxazoline ligand binding the catalytically active site in facial manner **68** (Chart 3.1) was prepared by reacting free ligand with $Sc(CH_2SiMe_3)_3(THF)_2$ [69]. The reaction of **68** with one equivalent of $[Ph_3C][B(C_6F_5)_4]$ in $CD_2Cl_2$ or $C_6D_5Br$ resulted in the formation of monocationic species $[LSc(CH_2SiMe_3)_2][B(C_6F_5)_4]$ which demonstrated low catalytic activity in polymerization of 1-hexene (30 kg(mol of catalyst)$^{-1}$ h$^{-1}$) and somewhat variable reproducibility with respect to tacticity control. GPC analysis of the polymer revealed bimodal molecular-mass distributions, indicating the presence of at least two catalytically active species. Dicationic compound $[LSc(CH_2SiMe_3)][B(C_6F_5)_4]_2$ which was obtained in situ by reacting **68** with two equivalents of $[Ph_3C][B(C_6F_5)_4]$ in contrast to monoanionic species turned out to be highly active in 1-hexene polymerization (21 °C). The activity (36,200 kg(mol of catalyst)$^{-1}$ h$^{-1}$) is greater by three orders of magnitude compared to that of the monocationic complex. However, the tacticity of the poly(1-hexene) was relatively low and GPC analysis revealed a bimodal molecular mass distribution with rather high value of PDI ($M_w/M_n = 2.22$). Decrease of the polymerization temperature resulted in the activity decrease (2,030 kg(mol of catalyst)$^{-1}$ h$^{-1}$) but provided high isotacticity (*mmmm* = 90%) and narrow molecular weight distribution ($M_w = 750{,}000$, $M_w/M_n = 1.18$) of the obtained poly(1-hexene) (Table 3.2, entries 8–11).

The effect of the ionic radius of the metal centre on the catalyst activity and ability of tacticity control was investigated for the series of dicationic alkyl complexes generated in situ by reacting $LM(CH_2SiRMe_2)_3$ (Chart 3.1, **69–75**) with two equivalents of $[Ph_3C][B(C_6F_5)_4]$ [70, 71]. The obtained dicationic species are proved to be active catalysts for α-olefin polymerization (1-hexene, 1-heptene, 1-octene) which allow to obtain polyolefins with $M_w/M_n$ values in the range 1.58–12.08 and isotacticities of 80–95%. The polymerization activity increases from Lu to Tm and then subsequently decreases with increasing ionic radius of the

**Table 3.2** Lanthanide complexes supported by N-containing ligands in α-olefin polymerization

| Type of catalyst | Entry | Monomer | Catalyst | T(°C)/pressure of propylene | t(h) | Activity[a] | $M_n \times 10^{-3}$ | $M_w/M_n$ | Tacticity | References |
|---|---|---|---|---|---|---|---|---|---|---|
| Cationic alkyl complexes | 1 | 1-pentene | **39** + $B(C_6F_5)_3$ | rt | – | – | $M_w = 4$ | 1.32 | – | [68] |
| | 2 | 1-hexene | **8** + $[Ph_3C]^+$ $[B(C_6F_5)_4]^-$ | rt | 0.5 | – | 7.3 | 2.65 | atactic | [67] |
| | 3 | 1-hexene | **73** + $2[Ph_3C]^+$ $[B(C_6F_5)_4]^-$ | −5 | 0.25 | 165 | $M_n = 126$ $M_w = 246$ | 1.95 | isotactic *%mmmm* = 90 | [70] |
| | 4 | 1-hexene | **74** + $2[Ph_3C]^+$ $[B(C_6F_5)_4]^-$ | −5 | 0.25 | 137 | $M_n = 90.1$ $M_w = 149$ | 1.65 | isotactic *%mmmm* = 88 | [71] |
| | 5 | 1-hexene | **70** + $2[Ph_3C]^+$ $[B(C_6F_5)_4]^-$ | −5 | 0.25 | 122 | $M_n = 102$ $M_w = 165$ | 1.65 | isotactic *%mmmm* = 88 | [71] |
| | 6 | 1-hexene | **71** + $2[Ph_3C]^+$ $[B(C_6F_5)_4]^-$ | −5 | 0.25 | 65.8 | $M_n = 81.8$ $M_w = 138$ | 1.69 | isotactic *%mmmm* = 85 | [71] |
| | 7 | 1-hexene | **72** + $2[Ph_3C]^+$ $[B(C_6F_5)_4]^-$ | −5 | 0.25 | 66 | $M_n = 67.5$ $M_w = 10.7$ | 1.58 | isotactic *%mmmm* = 85 | [71] |
| | 8 | 1-hexene | **68** + $2[Ph_3C]^+$ $[B(C_6F_5)_4]^-$ | −30 | 0.05 | 2,030 | $M_w = 750$ | 1.18 | isotactic *%mmmm* = 90 | [69] |
| | 9 | 1-hexene | **68** + $2[Ph_3C]^+$ $[B(C_6F_5)_4]^-$ | 20 | 0.05 | 7,600 | $M_w = 552$ | 1.87 | – | [69] |
| | 10 | 1-hexene | **68** + $2[Ph_3C]^+$ $[B(C_6F_5)_4]^-$ | 0 | 0.05 | 13,080 | $M_w = 354$ | 2.36 | – | [69] |
| | 11 | 1-hexene | **68** + $2[Ph_3C]^+$ $[B(C_6F_5)_4]^-$ | 21 | 0.05 | 36,230 | $M_w = 227$ | 2.22 | – | [69] |
| | 12 | 1-heptene | **73** + $2[Ph_3C]^+$ $[B(C_6F_5)_4]^-$ | −5 | 0.25 | 120 | $M_n = 99$ $M_w = 206$ | 2.06 | isotactic *%mmmm* = 83 | [70] |
| | 13 | 1-heptene | **74** + $2[Ph_3C]^+$ $[B(C_6F_5)_4]^-$ | −5 | 0.25 | 74.2 | $M_n = 99$ $M_w = 206$ | 1.91 | isotactic *%mmmm* = 89 | [71] |

(continued)

**Table 3.2** (continued)

| Type of catalyst | Entry | Monomer | Catalyst | T(°C)/pressure of propylene | t(h) | Activity[a] | $M_n \times 10^{-3}$ | $M_w/M_n$ | Tacticity | References |
|---|---|---|---|---|---|---|---|---|---|---|
| | 14 | 1-heptene | **70** + 2[$Ph_3C]^+$ [$B(C_6F_5)_4]^-$ | −5 | 0.25 | 49.4 | $M_n = 99 M_w = 206$ | 2.01 | isotactic %mmmm = 80 | [71] |
| | 15 | 1-heptene | **71** + 2[$Ph_3C]^+$ [$B(C_6F_5)_4]^-$ | −5 | 0.25 | 33.3 | $M_n = 56.1$ $M_w = 16{,}110$ | 1.95 | isotactic %mmmm = 80 | [71] |
| | 16 | 1-heptene | **72** + 2[$Ph_3C]^+$ [$B(C_6F_5)_4]^-$ | −5 | 0.25 | 48.4 | $M_n = 55.1$ $M_w = 88.8$ | 1.61 | isotactic %mmmm = 80 | [71] |
| | 17 | 1-octene | **73** + 2[$Ph_3C]^+$ [$B(C_6F_5)_4]^-$ | −5 | 0.5 | 30 | $M_n = 103$ $M_w = 208$ | 1.8 | isotactic %mmmm = 95 | [70] |
| | 18 | 1-octene | **74** + 2[$Ph_3C]^+$ [$B(C_6F_5)_4]^-$ | −5 | 0.5 | 38.9 | $M_n = 164$ $M_w = 278$ | 1.69 | isotactic %mmmm = 80 | [71] |
| | 19 | 1-octene | **70** + 2[$Ph_3C]^+$ [$B(C_6F_5)_4]^-$ | −5 | 0.5 | 31.4 | $M_n = 165$ $M_w = 102$ | 1.69 | isotactic %mmmm = 90 | [71] |
| | 20 | 1-octene | **71** + 2[$Ph_3C]^+$ [$B(C_6F_5)_4]^-$ | −5 | 0.5 | 30.9 | $M_n = 77.8$ $M_w = 148$ | 1.90 | isotactic %mmmm = 80 | [71] |
| | 21 | 1-octene | **72** + 2[$Ph_3C]^+$ [$B(C_6F_5)_4]^-$ | −5 | 0.5 | 28.9 | $M_n = 72.2$ $M_w = 114$ | 1.58 | isotactic %mmmm = 80 | [71] |
| Hydrido complexes | 22 | propylene | **78** | – | – | 0 | – | – | – | [58] |
| | 23 | 1-hexene | **78** | | | 0 | – | – | – | [58] |
| | 24 | propylene | **79** | 60 | – | – | – | – | – | [59] |
| | 25 | propylene | **86** | 0/0.75 bar | 1 | 3.9 g(mmol of catalyst)$^{-1}$ h$^{-1}$ bar$^{-1}$ | – | – | – | [60] |

[a] kg(mol of catalyst)$^{-1}$ h$^{-1}$

metal (Table 3.2, entries 3–7 and 12–21); however, remains incomparable to the activity observed for the scandium complex **68**. At room temperature low activities were observed because of thermal decomposition of the cationic species. The decomposition was circumvented by carrying out the process at −5 °C. For all catalysts the polymerization activity decreases in the order 1-hexene > 1-heptene > 1-octene, which was explained by the increased steric demands imposed by the longer alkyl chain of the olefin. The difference in the activity was more pronounced between 1-hexene and 1-heptene whereas the difference between 1-heptene and 1-octene was less noticeable. The polymerization activities for 1-octene were in the range of 30–40 kg(mol of catalyst)$^{-1}$ h$^{-1}$. Generally higher molecular weights were obtained with the smaller lanthanides Lu and Tm.

### *3.4.2 Hydrido Complexes*

Hydrido lutetium complex stabilized by bulky guanidinate ligands (Chart 3.1, **87**) catalyzes propylene polymerization, but with low activity (3.9 g(mmol of catalyst)$^{-1}$ h$^{-1}$ atm$^{-1}$). The catalyst loses activity in 1 h [60].

## 3.5 Styrene Polymerization

Bisalkyl complex **8** (Chart 3.1) did not show activity for styrene polymerization, while when activated with $[Ph_3C][B(C_6F_5)_4]$ in toluene at room temperature was able to convert in 5 min 34% of monomer (Table 3.3, entry 3) in predominantly syndiotactic (*rrrr* > 99%) polystyrene ($M_n$ = 45.1 × 103, $M_w/M_n$ = 1.96) [67].

Scandium bisalkyl complexes coordinated by 1,2-azaborolyl ligands bearing various substituents at the boron atom (Chart 3.1, **9**–**11**) were synthesized by the salt metathesis reactions of cationic bisalkyl species $[Sc(CH_2SiMe_3)_2(THF)_3]^+$ $[BPh_4]^-$ with 1,2-azaborolyl lithium [72]. Activation of complexes **9**–**11** by 1 equivalent of $[Ph_3C]^+[B(C_6F_5)_4]^-$ in the presence of $i$Bu$_3$Al afforded species active for the syndiospecific polymerization of styrene which allow to obtain exclusively syndiotactic polymers (Table 3.3, entries 4–10). Complexes **9** and **11** convert 2,000–3,000 equivalents of styrene in polystyrene quantitatively within 10 min, yielding polymers with $M_n$ in the range 5.7–16.3 × 10$^5$ and moderate molecular weight distributions ($M_w/M_n$ = 1.5–3.5). Under the similar conditions ([M]:[Sc] = 2,000), complex **10** showed lower activity and afforded polystyrene with a bimodal molecular weight distribution, suggesting the presence of two active species in this system. The Lu complex [$i$-Pr$_2$NBC$_3$(Me)N$t$-Bu)]Lu(CH$_2$-SiMe$_3$)$_2$(THF) showed even lower activity. Its polymerization was unaffected by the monomer-catalyst ratio, but was significantly influenced by the amount of $i$-Bu$_3$Al added in the reaction mixture. For both complexes **9** and **11** the molecular weight of the resultant polymers has been significantly increased with decreased

**Table 3.3** Lanthanide complexes supported by N-containing ligands in styrene polymerization

| Type of catalyst | Entry | Catalyst | Monomer/catalyst | T(°C) | t(h) | Activity[a] | Yield (%) | $N_t$ | $M_n \times 10^{-3}$ | $M_w/M_n$ | Tacticity | $T_m$ | References |
|---|---|---|---|---|---|---|---|---|---|---|---|---|---|
| Alkyl ate-complex | 1 | **76** | 470 | 100 | 0.16 | 197 | 67 | | 20.2 | 1.84 | *rr* 31% | – | [74] |
| | 2 | **77** | 470 | 100 | 0.16 | 168 | 57 | | 40.8 | 2.01 | – | – | [74] |
| Cationic alkyl complexes | 3 | **8** + $[Ph_3C]^+$ $[B(C_6F_5)_4]^-$ | 1,000 | rt | 0.08 | | 34 | | 45.1 | 1.96 | syndiotactic *rrrr* > 99% | 267 | [67] |
| | 4 | **9** + $[Ph_3C]^+$ $[B(C_6F_5)_4]^-$ + $Al^iBu_3$ | 2,000 | 25 | 0.16 | | 100 | | 680 | 2.2 | syndiotactic 100% | 270 | [72] |
| | 5 | **9** + $[Ph_3C]^+$ $[B(C_6F_5)_4]^-$ + Al*i*-$Bu_3$ | 2,500 | 25 | 0.16 | | 100 | | 910 | 2.1 | syndiotactic 100% | 270 | [72] |
| | 6 | **9** + $[Ph_3C]^+$ $[B(C_6F_5)_4]^-$ + Al*i*-$Bu_3$ | 3,000 | 25 | 0.16 | | 94 | | 1,350 | 1.9 | syndiotactic 100% | 270 | [72] |
| | 7 | **10** + $[Ph_3C]^+$ $[B(C_6F_5)_4]^-$ + Al*i*-$Bu_3$ | 2,000 | 25 | 0.16 | | 27 | | 3,120/220 | 1.5/2.5 | syndiotactic 100% | 271 | [72] |
| | 8 | **11** + $[Ph_3C]^+$ $[B(C_6F_5)_4]^-$ + Al*i*-$Bu_3$ | 2,000 | 25 | 0.16 | | 100 | | 570 | 2.5 | syndiotactic 100% | 271 | [72] |
| | 9 | **11** + $[Ph_3C]^+$ $[B(C_6F_5)_4]^-$ + Al*i*-$Bu_3$ | 2,500 | 25 | 0.16 | | 100 | | 1,050 | 1.7 | syndiotactic 100% | 271 | [72] |
| | 10 | **11** + $[Ph_3C]^+$ $[B(C_6F_5)_4]^-$ + Al*i*-$Bu_3$ | 3,000 | 25 | 0.16 | | 95 | | 1,630 | 1.5 | syndiotactic 100% | 271 | [72] |
| | 11 | **33** + $[Ph_3C]^+$ $[B(C_6F_5)_4]^-$ | 500 | 25 | 0.5 | 104 | – | | 38 | 1.75 | $r = 0.72$ | – | [73] |
| | 12 | **33** + $[PhNMe_2H]$ $H[B(C_6F_5)_4]^-$ | 500 | 25 | 0.5 | 70 | – | | 29 | 1.70 | $r = 0.71$ | – | [73] |
| | 13 | **34** + $[Ph_3C]^+$ $[B(C_6F_5)_4]^-$ | 500 | 25 | 0.5 | 90 | – | | 35 | 1.68 | $r = 0.70$ | – | [73] |
| | 14 | **35** + $[Ph_3C]^+$ $[B(C_6F_5)_4]^-$ | 500 | 25 | 0.5 | 80 | – | | 30 | 1.59 | $r = 0.68$ | – | [73] |

(continued)

**Table 3.3** (continued)

| Type of catalyst | Entry | Catalyst | Monomer/ catalyst | T(°C) | t(h) | Activity[a] | Yield (%) | $N_t$ | $M_n \times 10^{-3}$ | $M_w/M_n$ | Tacticity | $T_m$ | References |
|---|---|---|---|---|---|---|---|---|---|---|---|---|---|
| | 15 | **36** + $[Ph_3C]^+$ $[B(C_6F_5)_4]^-$ | 500 | 25 | 0.5 | 46 | – | | 23 | 1.61 | $r = 0.56$ | – | [73] |
| | 16 | **33** + $[Ph_3C]^+$ $[B(C_6F_5)_4]^-$ + Al*i*-$Bu_3$ | 500 | 25 | 0.5 | 1,560 | – | | 23 | 1.87 | $r = 0.94$ | – | [73] |
| | 17 | **34** + $[Ph_3C]^+$ $[B(C_6F_5)_4]^-$ + Al*i*-$Bu_3$ | 500 | 25 | 0.5 | 624 | – | | 20 | 2.06 | $r = 0.93$ | – | [73] |
| Cationic alkyl complexes | 17 | **35** + $[Ph_3C]^+$ $[B(C_6F_5)_4]^-$ + Al*i*-$Bu_3$ | 500 | 25 | 0.5 | 624 | – | | 15 | 1.96 | $r = 0.93$ | – | [73] |
| Hydrido complexes | 19 | **85** | neat styrene, 5% of **86** | 20 | 144 | – | 90 | | $M_n = 811$ | 1.54 | – | – | [60] |
| | 20 | **84** | neat styrene, 5% of **84** | 20 | 72 | – | 100 | | $M_n = 90$ | 2.6 | – | – | [60] |

[a] kg(mol of catalyst)$^{-1}$ h$^{-1}$

polydispersity as the monomer-to-catalyst ratio is raised. The ratio Sc:*i*-$Bu_3Al$ also influences both catalyst activity and polymer molecular mass distribution. For complex **11** in the presence of $[Ph_3C]^+[B(C_6F_5)_4]^-$, an increase of concentration of alkylaluminium led to a higher yield of polystyrene but also to lower molecular weight and broader molecular weight distribution.

New monoanionic bidentate quinolyl amido ligand system developed by Cui et al. allowed synthesis of a series of dialkyl scandium complexes **33–37** (Chart 3.1) [73]. Compounds **33–37** or their combinations with *i*-$Bu_3Al$ do not initiate styrene polymerization, while the ternary systems based on complexes **33–35** after addition of $[Ph_3C][B(C_6F_5)_4]$ or $[PhMe_2NH][B(C_6F_5)_4]$ showed high activity at room temperature and allow to reach complete conversion within half an hour (Table 3.3, entries 11–18). The resultant polystyrenes have a relatively narrow polydispersity ($M_w/M_n = 1.59–1.75$), indicative of the single-site nature of these systems. Complex **36**, containing a ligand bearing bulky o-isopropyl groups at the N-aryl ring, demonstrated lower activity, what can be caused by excessive steric hindrance around the catalytic centre. Complex **37** coordinated by the less sterically demanding amido ligand was almost inert in polymerization due to its instability at room temperature. Catalytic activities proved to be dependent on the Sc:*i*-$Bu_3Al$ ratio. The catalytic activity increased stepwise with the amount of *i*-$Bu_3Al$ and reaches a peak value when five equivalents of *i*-$Bu_3Al$ were loaded. The type of alkyl aluminium component was found to play a significant role in adjusting the activity. When $Me_3Al$ was added the system **33**-$[Ph_3C][B(C_6F_5)_4]$ exhibited low activity, which might be attributed to the formation of less active aluminate species. When $Et_3Al$ was used the activity of the corresponding system increased, and the highest activity was obtained in the case of *i*-$Bu_3Al$. The catalytic activity also turned out to be significantly influenced by fluorinated borate/borane component. It decreases in the order $[Ph_3C][B(C_6F_5)_4] > [PhMe_2NH][B(C_6F_5)_4] > B(C_6F_5)_3$. The system **33**-*i*-$Bu_3Al$-$[Ph_3C][B(C_6F_5)_4]$ allows to carry out the polymerization in a controllable rather than in a living manner. Cationic complex 38 in the presence of *i*-$Bu_3Al$ intended to extrude the coordinated DME molecules from the scandium centre catalyzes the polymerization of styrene with moderate activity. The ternary systems exhibited high stereoselectivity to afford syndiotactic polystyrenes with *r* diad up to 0.94 in high yield.

Complexes **45–47** (Chart 3.1) activated with $[Ph_3C][B(C_6F_5)_4]$ were inactive neither in styrene homopolymerization nor in copolymerization of styrene and ethylene [38].

Ionic ate-complexes **76** and **77** (Chart 3.1) containing two methyl groups $\mu$-bridging Ln (Nd, Yb) and Li ions demonstrated high catalytic activity for styrene polymerization at elevated temperatures (70–100 °C, 10 min), while MeLi under the similar conditions was found to be inert [74]. At 55 °C both complexes showed very low activity, whereas at 100 °C the polymer yield reached 67% for **76** and 57% for **77**. The polymers obtained have molecular weights in the range $1.72–5.89 \times 10^4$ and rather narrow molecular weight distribution $M_w/M_n < 2$ (Table 3.3, entries 1, 2). The molecular weight distribution becomes broader when polymerization temperature increases. The polystyrenes formed in the presence of

complexes **76** and **77** have atactic/syndiotactic-enriched structures. The syndiotacticity decreases with increase of polymerization temperature (For complex **77**: $T = 70$ °C, $rr = 53\%$; $T = 85$ °C, $rr = 28\%$).

In the family of bis(guanidinate) hydrido rare-earth complexes **80–87** (Chart 3.1) only derivatives of smallest Yb (**84**) and Lu (**85**) metals coordinated by isopropyl-substituted guanidinate ligands turned out to be active in styrene polymerization at ambient temperature. In the case of complex **85** 90% conversion was reached in 6 days. The polystyrene obtained has a high molecular weight ($M_n = 811{,}000$ g mol$^{-1}$, $M_w = 1{,}250{,}000$ g mol$^{-1}$), narrow molecular weight distribution ($M_w/M_n = 1.54$), and melting temperature 255–260 °C. When complex **84** was used the reaction rate was higher and total conversion was reached in 3 days. The obtained polymer had higher molecular weight distribution $M_w/M_n = 2.6$ ($M_n = 90{,}000$ g mol$^{-1}$, $M_w = 237{,}700$ g mol$^{-1}$; melting temperature 289–293 °C). The $^{13}$C NMR spectra of both polystyrenes indicated their high syndiotactisity [61].

## 3.6 Outlook

A remarkable progress has been done in the field of olefin polymerization catalysts based on rare-earth metal post-metallocene complexes in the past decade. The development of new types of supporting ligation systems (mainly nitrogen-containing) for rare-earth metals gave an impact on increased understanding of ligand structure–catalyst property relationships and overcoming the limitations inherent to the cyclopentadienyl ligand. The design of multidentate systems allowed to achieve new geometries, to increase stabilities of catalytic centres and in some cases to gain control over polymerization process. The synthesis of mono- and dicationic rare-earth species demonstrating catalytic activities comparable to those of the group 4 metal complexes and able to polymerize not only ethylene but also bulkier α-olefins has highlighted the direction for further development of efficient and selective catalysts. Unfortunately little is done so far in co-polymerization of olefins with dienes and polar monomers, the field where rare-earth metals especially are likely to demonstrate high catalytic potential due to their unique properties and provide production of materials with improved and novel properties. The rare-earth metals also offer the attractive prospect for controlled functionalization of polyolefins. Another challenge which still remains actual is development of systems capable of catalysing the living polymerization of olefinic monomers.

## References

1. Watson PL, Parshall GW (1985) Organolanthanides in catalysis. Acc Chem Res 18:51–56
2. Yasuda H (2000) Organo transition metal initiated living polymerizations. Prog Polym Sci 25:573–626

3. Hou Z, Wakatsuki Y (2002) Recent developments in organolanthanide polymerization catalysts. Coord Chem Rev 231:1–22
4. Yasuda H (2002) Organo-rare-earth-metal initiated living polymerization of polar and non-polar monomers. J Organomet Chem 647:128–138
5. Gromada J, Carpentier J-F, Mortreux A (2004) Group 3 metalcatalysts for ethylene and α-olefin polymerization. Coord Chem Rev 248:397–410
6. Evans WJ, Meadows JH, Hunter WE, Atwood JL (1984) Organolanthanide and organoyttrium hydride chemistry. 5. Improved synthesis of $[(C_5H_4R)_2YH(THF)]_2$ complexes and their reactivity with alkenes, alkynes, 1,2-propadiene, nitriles, and pyridine, including structural characterization of an alkylideneamido product. J Am Chem Soc 106:1291–1300
7. Stern D, Sabat M, Marks TJ (1990) Manipulation of organolanthanide coordinative unsaturation. Synthesis, structures, structural dynamics, comparative reactivity, and comparative thermochemistry of dinuclear $\mu$-hydrides and $\mu$-alkyls with $[\mu\text{-}R_2Si(Me_4C_5)(C_5H_4)]_2$ supporting ligation. J Am Chem Soc 112:9558–9575
8. Shapiro PJ, Cotter WD, Schaefer WP, Labinger JA, Bercaw JE (1994) Model Ziegler-Natta α-olefin polymerization catalysts derived from$[\{(\eta^5\text{-}C_5Me_4)SiMe_2(\eta^1\text{-}NCMe_3)\}(PMe_3)Sc(\mu_2\text{-}H)]_2$ and$[\{(\eta^5\text{-}C_5Me_4)SiMe_2(\eta^1\text{-}NCMe_3)\}Sc(\mu^2\text{-}CH_2CH_2CH_3)]_2$. Synthesis, structures, and kinetic and equilibrium investigations of the catalytically active species in solution. J Am Chem Soc 116:4623–4640
9. Hulzsch KC, Voth V, Beckerle K, Spaniol TP, Okuda J (2000) Single-component polymerization catalysts for ethylene and styrene: synthesis, characterization, and reactivity of alkyl and hydrido yttrium complexes containing a linked amido—cyclopentadienyl ligand. Organometallics 19:228–243
10. Trifonov AA, Spaniol TP, Okuda J (2001) Yttrium hydrido complexes that contain a less "constrained geometry" ligand: synthesis, structure, and efficient hydrosilylation catalysis. Organometallics 20:4869–4874
11. Casey CP, Tunge JA, Lee T-Y, Carpenetti DW (2002) Kinetics and mechanism of formation of yttrium alkyl complexes from $(Cp^*_2YH)_2$ and alkenes. Organometallics 21:389–396
12. Casey CP, Tunge JA, Lee TY, Fagan MA (2003) Structural dependence of thermodynamics of alkene binding to yttrium alkyl complexes and of kinetics of alkyl migration to coordinated alkenes. J Am Chem Soc 125:2641–2651
13. Trifonov AA, Spaniol TP, Okuda J (2004) Hydrosilylation of dienes by yttrium hydrido complexes containing a linked amido-cyclopentadienyl ligand. Dalton Trans 2245–2250
14. Luo Y, Hou Z (2007) Computational study of ethylene insertion into the metal—hydrogen bond of the tetranuclear yttrium polyhydrido complex [(η5–C5Me4SiMe3)YH2]4. Organometallics 26:2941–2944
15. Shannon RD (1976) Revised effective ionic radii and systematic studies of interatomic distances in halides and chalcogenides. Acta Crystallogr Sect A 32:751–767
16. Gibson VC, Spitzmesser SK (2003) Advances in non-metallocene olefin polymerization catalysis. Chem Rev 103:283–316
17. Edelmann FT, Freckmann DMM, Schumann H (2002) Synthesis and structural chemistry of non-cyclopentadienyl organolanthanide complexes. Chem Rev 102:1851–1896
18. Piers WE, Emslie DJH (2002) Non-cyclopentadienyl ancillaries in organogroup 3 metal chemistry: a fine balance in ligand design. Coord Chem Rev 131:233–255
19. Trifonov AA (2007) Non-metallocene rare-earth organometallic derivatives: synthesis, structure and application in the catalysis of transformations of unsaturated substrates. Russ Chem Rev 76:1051–1072
20. Green MLH (1995) A new approach to the formal classification of covalent compounds of the elements. J Organomet Chem 500:127–148
21. Parkin G (2007) Classification of organotransition metal compounds. In: Crabtree RH, Mingos MD (eds) Comprehensive organometallic chemistry 3rd edn vol 1. Elsevier, Amsterdam
22. Morss LR (1976) Thermochemical properties of yttrium, lanthanum, and the lanthanide elements and ions. Chem Rev 76:827–841

23. Schumann H, Meese-Marktscheffel JA, Esser L (1995) Synthesis, structure, and reactivity of organometallic $\pi$-complexes of the rare earths in the oxidation state $Ln^{3+}$ with aromatic ligands. Chem Rev 95:865–986
24. Arndt S, Okuda J (2002) Mono(cyclopentadienyl) complexes of the rare-earth metals. Chem Rev 102:1953–1976
25. Okuda J (2003) Rare earth metal complexes that contain linked amido-cyclopentadienyl ligands: ansa-metallocene mimics and "constrained geometry" catalysts. Dalton Trans 2367–2378
26. Long DP, Bianconi PA (1996) A catalytic system for ethylene polymerization based on group III and lanthanide complexes of tris(pyrazolyl)borate ligands. J Am Chem Soc 118:12453–12454
27. Fryzuk MD, Giesbrecht G, Rettig SJ (1996) Synthesis and characterization of the five-coordinate scandium dialkyl complexes $ScR_2[N(SiMe_2CH_2PPr\textit{i}_2)_2]$ (R = Me, Et, $CH_2SiMe_3$). Organometallics 15:3329–3336
28. Arndt S, Okuda J (2005) Cationic alkyl complexes of rare-earth metals: synthesis, structure, and reactivity. Adv Synth Catal 347:339–354
29. Zeimentz PM, Arndt S, Elvidge BR, Okuda J (2006) Cationic organometallic complexes of scandium, yttrium, and the lanthanoids. Chem Rev 106:2404–2433
30. Hou Z, Luo Y, Li X (2006) Cationic rare earth metal alkyls as novel catalysts for olefin polymerization and copolymerization. J Organomet Chem 691:3114–3121
31. Bambirra S, Bouwkamp MW, Meetsma A, Hessen B (2004) One ligand fits all: cationic mono(amidinate) alkyl catalysts over the full size range of the group 3 and lanthanide metals. J Am Chem Soc 126:9182–9183
32. Bambirra S, Van Leusen D, Meetsma A, Hessen B, Teuben JH (2003) Yttrium alkyl complexes with a sterically demanding benzamidinate ligand: synthesis, structure and catalytic ethane polymerization. Chem Commun 522–523
33. Bambirra S, Meetsma A, Hessen B (2006) Lanthanum tribenzyl complexes as convenient starting materials for organolanthanum chemistry. Organometallics 25:3454–3462
34. Hayes PG, Piers WE (2002) Cationic scandium methyl complexes supported by a $\beta$-diketiminato ("nacnac") ligand framework. J Am Chem Soc 124:2132–2133
35. Kretschmer WP, Meetsma A, Hessen B, Schmalz T, Qayyum S, Kempe R (2006) Reversible chain transfer between organoyttrium cations and aluminium: synthesis of aluminium-terminated polyethylene with extremely narrow molecular-weight distribution. Chem Eur J 12:8969–8978
36. Kempe R (2007) Coordinative chain transfer polymerization (CCTP). Chem Eur J 13:2764–2773
37. Döring C, Kretschmer WP, Kempe R (2010) Aminopyridinate-stabilized lanthanoid complexes: synthesis, structure and polymerization of ethylene and isoprene. Eur J Inorg Chem 2853–2860
38. Zimmermann M, Törnroos KW, Waymouth RM, Anwander R (2008) Structure—reactivity relationships of amido-pyridine-supported rare-earth-metal alkyl complexes. Organometallics 27:4310–4317
39. Lawrence SC, Ward BD, Dubberley SR, Kozak CM, Mountford P (2003) Chem Commun 2880–2881
40. Ge S, Meetsma A, Hessen B (2007) Monoanionic *fac*-$\kappa^3$ ligands derived from 6-amino-1, 4-diazepine: ligand dependence of stability and catalytic activity of their scandium alkyl derivatives. Organometallics 26:5278–5284
41. Bambirra S, Van Leusen D, Meetsma A, Hessen B, Teuben JH (2001) Neutral and cationic yttrium alkyl complexes with linked 1, 4, 7-triazacyclononane-amide monoanionic ancillary ligands: synthesis and catalytic ethene polymerization. Chem Comm 637–638
42. Bambirra S, Van Leusen D, Tazelaar CGJ, Meetsma A, Hessen B (2007) Rare earth metal alkyl complexes with methyl-substituted triazacyclononane-amide ligands: ligand variation and ethylene polymerization catalysis. Organometallics 26:1014–1023
43. Bambirra S, Boot SJ, Van Leusen D, Meetsma A, Hessen B (2004) Yttrium alkyl complexes with triamino—amide ligands. Organometallics 23:1891–1898

44. Howe RG, Tredget CS, Lawrence SC, Subongkoj S, Cowley AR, Mountford P (2006) A novel transformation of a zirconium imido compound and the development of a new class of N3 donor heteroscorpionate Ligand. Chem Commun :223–225
45. Marinescu SC, Agapie T, Day MW, Bercaw JE (2007) Group 3 dialkyl complexes with tetradentate (L, L, N, O; L = N, O, S) monoanionic ligands: synthesis and reactivity. Organometallics 26:1178–1190
46. Ephritikhine M (1997) Synthesis, structure, and reactions of hydride, borohydride, and aluminohydride compounds of the f-elements. Chem Rev 97:2193–2242
47. Jeske G, Lauke H, Mauermann H, Schumann H, Marks TJ (1985) Highly reactive organolanthanides. A mechanistic study of catalytic olefin hydrogenation by bis(pentamethylcyclopentadienyl) and related 4f complexes. J Am Chem Soc 107:8111–8118
48. Conticello VP, Brard L, Giardello MA, Tsyji Y, Sabat M, Stern CL, Marks TJ (1992) Chiral organolanthanide complexes for enantioselective olefin hydrogenation. J Am Chem Soc 114:2761–2762
49. Jeske G, Lauke H, Mauermann H, Swepston PN, Schumann H, Marks TJ (1985) Highly reactive organolanthanides. Systematic routes to and olefin chemistry of early and late bis(pentamethylcyclopentadienyl) 4f hydrocarbyl and hydride complexes. J Am Chem Soc 107:8091–8103
50. Mauermann H, Swepston PN, Marks TJ (1985) The $5f^3$ vs. $4f^3$. Routes to and properties of highly reactive neodymium(III) hydrocarbyl and hydride complexes. Organometallics 4:200–2002
51. Jeske G, Schock LE, Swepston PN, Schumann H, Marks TJ (1985) Highly reactive organolanthanides. Synthesis, chemistry, and structures of 4f hydrocarbyls and hydrides with chelating bis(polymethylcyclopentadienyl) ligands. J Am Chem Soc 107:8103–8110
52. Desurmont G, Li Y, Yasuda H, Maruo T, Kanehisha N, Kai Y (2000) Reaction pathway for the formation of binuclear samarocene hydride from monomeric alkyl samarocene derivative and the effective catalysis of samarocene hydride for the block copolymerization of ethylene with polar monomers. Organometallics 19:1811–1813
53. Molander GA, Romero JAC (2002) Lanthanocene catalysts in selective organic synthesis. Chem Rev 102:2161–2186
54. Harrison KN, Marks TJ (1992) Organolanthanide-catalyzed hydroboration of olefins. J Am Chem Soc 114:9220–9221
55. Bijpost EA, Duchateau R, Teuben JH (1995) J Mol Catal 95:121
56. Konkol M, Okuda J (2008) Non-metallocene hydride complexes of rare-earth metals. Coord Chem Rev 252:1577–1591
57. Duchateau R, van Wee CT, Meetsma A, van Duijnen PT, Teuben JH (1996) Ancillary ligand effects in organoyttrium chemistry: synthesis, characterization, and electronic structure of bis(benzamidinato)yttrium compounds. Organometallics 15:2279–2290
58. Duchateau R, van Wee CT, Teuben JH (1996) Insertion and C − H bond activation of unsaturated substrates by bis(benzamidinato)yttrium alkyl, $[PhC(NSiMe_3)_2]_2YR$ (R = $CH_2$ Ph·THF, $CH(SiMe_3)_2$), and hydrido, $\{[PhC(NSiMe_3)_2]_2Y(\mu\text{-}H)\}_2$, compounds. Organometallics 15:2291–2302
59. Hagadorn JR, Arnold J (1996) Preparation of scandium complexes with benzamidinate ligands: synthesis and reactivity of alkyl and hydrido derivatives. Organometallics 15:984–991
60. Trifonov AA, Fedorova EA, Fukin GK, Bochkarev MN (2004) Post-metallocene hydridolanthanide chemistry: $[\{Lu\{(Me_3Si)_2NC(Ni\text{-}Pr)_2\}_2(\mu\text{-}H)\}]$—a novel lanthanide hydride in a non-cyclopentadienyl coordination environment; synthesis, structure and catalytic activity in olefin polymerization. Eur J Inorg Chem 4396–4401
61. Trifonov AA, Skvortsov GG, Lyubov DM, Skorodumova NA, Fukin GK, Baranov EV, Glushakova VN (2006) Post-metallocene lanthanide-hydrido chemistry: a new family of complexes $[\{Ln\{(Me_3Si)_2NC(Ni\text{-}Pr)_2\}_2(\mu\text{-}H)\}_2]$. Chem Eur J 12:5320–5327
62. Lyubov DM, Bubnov AM, Fukin GK, Dolgushin FM, Yu Antipin M, Pelcé O, Schappacher M, Guillaume SM, Trifonov AA (2008) Hydrido complexes of yttrium and lutetium

supported by bulky guanidinato ligands [{Ln($\mu$-H){($Me_3Si)_2NC(N$i$-Pr)$_2$}$_2$}$_2$]. Eur J Inorg Chem 2090–2098
63. Gountchev TI, Don Tilley T (1999) Yttrium complexes of the chelating, $C_2$-Symmetric, bis(silylamido)biphenyl ligand $[DADMB]^{2-}$ (= $\{[6,6'\text{-}Me_2\text{-}(C_6H_3)_2](2,2'\text{-}NSiMe_2tBu)_2\}^{2-}$). Organometallics 18:2896–2905
64. Lyubov DM, Döring C, Fukin GK, Cherkasov AV, Shavyrin AS, Kempe R, Trifonov AA (2008) Selective assembly of trinuclear rare-earth alkyl hydrido clusters supported by amidopyridinate ligands. Organometallics 27:2905–2907
65. Lyubov DM, Fukin GK, Cherkasov AV, Shavyrin AS, Trifonov AA, Luconi L, Bianchini C, Meli A, Giambastiani G (2009) Selective $\sigma$-bond metathesis in alkyl–Aryl and alkyl–benzyl yttrium complexes. New aryl–and benzyl–hydrido yttrium derivatives supported byamido-pyridinate ligands. Organometallics 28:1227–1232
66. Luconi L, Lyubov DM, Bianchini C, Rossin A, Faggi C, Fukin GK, Cherkasov AV, Shavyrin AV, Trifonov AA, Giambastiani G (2010) Yttrium-amidopyridinate complexes: synthesis and characterization of yttrium-alkyl and yttrium-hydrido derivatives. Eur J Inorg Chem 608–620
67. Luo Y, Nishiura M, Hou Z (2007) Rare earth metal bis(alkyl) complexes bearing a monodentate arylamido ancillary ligand: Synthesis, structure, and Olefin polymerization catalysis. J Organomet Chem 692:536–544
68. Hajela S, Schaefer WP, Bercaw JE (1997) Highly electron deficient group 3 organometallic complexes based on the 1, 4, 7-trimethyl-1, 4, 7-triazacyclononane ligand system. J Organomet Chem 532:45–53
69. Ward BD, Bellemin-Laponnaz S, Gade LH (2005) C3 chirality in polymerization catalysis: a highly active dicationic scandium(III) catalyst for the isoselective polymerization of 1-hexene. Angew Chem Int Ed 44:1668–1671
70. Lukešová L, Ward BD, Bellemin-Lapoonaz S, Wadepohl H, Gade LH (2007) High activity control in organolanthanide polymerization catalysis: formation of isotactic poly($\alpha$-oalkenes) with chiral $C_3$-symmetric thullium complex. Dalton Trans 920–922
71. Lukešová L, Ward BD, Bellemin-Lapoonaz S, Wadepohl H, Gade LH (2007) C3-Symmetric chiral organolanthanide complexes: synthesis, characterization, and stereospecific polymerization of $\alpha$-olefins. Organometallics 26:4652–4657
72. Fang X, Li X, Hou Z, Assoud J, Zhao R (2009) 1, 2-Azaborolyl-ligated half-sandwich complexes of scandium(III) and lutetium(III): synthesis, structures, and syndiotactic polymerization of styrene. Organometallics 28:517–522
73. Liu D, Luo Y, Gao W, Cui D (2010) Stereoselective polymerization of styrene with cationic scandium precursors bearing quinolyl aniline ligands. Organometallics 29:1916–1923
74. Luo Y, Yao Y, Shen Q (2002) [($Me_3Si)_2NC(Ni\text{-}Pr)_2]_2Ln(\mu\text{-}Me)_2Li(TMEDA)$ (Ln = Nd, Yb) as effective single-component initiators for styrene polymerization. Macromolecules 35:8670–8671

# Chapter 4
# Imine-Based Vanadium Catalysts for α-Olefin Polymerization

**Carl Redshaw**

**Abstract** Advances over the last decade in the development of vanadium-based pro-catalysts bearing ligands containing the imine functionality are discussed in terms of their synthesis, characterization and their ability to oligmerize/polymerize α-olefins. The chapter is organized by ligand type, considering initially ligands which chelate (bi- and tri-dentate) only through nitrogen centres, before discussing those binding via nitrogen and oxygen (bi-, tri- and tetra-dentate), those with nitrogen, oxygen and sulfur donors (penta- and hexa-dentate) and finally a number of ligand systems which are either mono-dentate or for which the term imine can be more loosely applied, such as the heterocycle pyridine.

**List of Abbreviations**

| | |
|---|---|
| Ar | Aryl |
| *i*Bu | Isobutyl |
| *t*Bu | *tert*-butyl |
| DMAC | Dimethylaluminum chloride |
| DSC | Differential scanning calorimetry |
| EPR | Electron paramagnetic resonance |
| Et | Ethyl |
| ETA | Ethyltrichloroacetate |
| FTIR | Fourier transform infrared |
| g/mmol h bar | Grams per millimole (of pro-catalyst) per hour per bar |
| *i*Pr | Isopropyl |
| MAO | Methylaluminoxane |
| Me | Methyl |

C. Redshaw (✉)
School of Chemistry, University of East Anglia, Norwich, NR4 7TJ, UK
e-mail: carl.redshaw@uea.ac.uk

G. Giambastiani and J. Cámpora (eds.), *Olefin Upgrading Catalysis by Nitrogen-based Metal Complexes I*, Catalysis by Metal Complexes, 35
DOI: 10.1007/978-90-481-3815-9_4, 

| | |
|---|---|
| MLCT | Metal to ligand charge transfer |
| MMAO | Modified or methylisobutylaluminoxane |
| $M_n$ | Number average molecular weight |
| $M_w$ | Weight average molecular weight |
| Nacnac | 2,4-pentanediimine anion |
| NBE | Norbornene |
| NMR | Nuclear magnetic resonance |
| *n*Pr | *n*-propyl |
| PDI | Polydispersity index |
| Ph | Phenyl |
| Py | Pyridine |
| THF | Tetrahydrofuran |
| TIBA | Triisobutylaluminum |
| TMEDA | Tetramethylethylenediamine |
| TOF | Turn over frequency |
| Tp′ | Tris(3,5-dimethylpyrazolyl)methane |
| Tp* | Tris(3,5-dimethylpyrazolyl)borato |
| TTPB | Trityl tetrakis(pentafluorophenyl)borate |
| UV–Vis | Ultraviolet-visible |
| XRF | X-ray fluorescence |

## 4.1 Introduction

Amongst the early transition metals deployed for α-olefin polymerization catalysis, the group 5 metals have existed very much in the shadows. To the left are the likes of titanium and zirconium, whilst to the right is chromium, all of which have formed the bedrock of the polyolefin industry for a number of years [1, 2]. Facile reduction to inactive, paramagnetic oxidation states and/or unfavourable olefin association/dissociation kinetics, have been at the centre of many of the problems associated with the use of the group 5 metals [3]. Only in the last decade has the use of vanadium-based catalytic systems for α-olefin polymerization (particularly ethylene) met with results which suggest it has the potential to compete with the more established metals [4]. Of particular note have been catalysts resulting from systems incorporating a vanadium pro-catalyst bearing a chelating ligand, a co-catalyst comprising a dialkylaluminum halide and a re-activator such as ethyltrichloroacetate [5]. This combination seems to overcome to some degree the problems associated with the ease of reduction of the metal centre to the inactive divalent state, and has led to a number of thermally robust, highly active systems. The results achieved to-date are even more impressive when one considers the polymerization behaviour of pro-catalysts based on the heavier congeners niobium and tantalum [3, 6]. In the case of imine-containing systems, it

is clear from the systems described herein that the stabilization brought about by the coordination of an imino nitrogen at vanadium is highly beneficial to the polymerization catalysis. Other donors too, such as sulfur, have been shown to have an impressive impact on catalytic performance, and the combination of such functionality and the imine moiety will also be discussed in this chapter. Initially, we will consider ligands which chelate (bi- and tri-dentate) only through nitrogen centres, before discussing those binding via nitrogen and oxygen (bi-, tri- and tetra-dentate), via nitrogen, oxygen and sulfur (penta- and hexa-dentate) and finally a number of ligand systems which are either mono-dentate or for which the term imine can be more loosely applied, such as the heterocycle pyridine.

## 4.2 *N,N*–Bi-Dentate Ligands

### *4.2.1 α-Diimines*

The α-dimine vanadium(III) complexes **1** and **2** (Fig. 4.1) are readily available in isolated yields of 60–70% from the ligand exchange reaction of $[VCl_3(THF)_3]$ and one equivalent of the corresponding parent α-diimine ligand. In the FTIR, the $\nu$(C = N) stretches are shifted somewhat to lower wave-numbers than those found in the free ligands, viz 1,590 $cm^{-1}$ in **1**, and 1,580 $cm^{-1}$ in **2**. Both EPR measurements and effective magnetic moments (as measured by Evans NMR method) were indicative of the additional presence of small amounts of vanadium(IV) species. Complex **1** produces a sharp, well-resolved $^1H$ NMR spectrum in $CH_2Cl_2$ in the range 0–110 ppm (Fig. 4.2). Variable temperature studies in tetrachloroethane-$d_2$ revealed reversible temperature dependence (up to 100 °C), with a linear relationship between the chemical shifts and the reciprocal of the temperature in accordance with the Curie law. By contrast, complex **2** exhibits a broad featureless spectrum.

When screened for ethylene polymerization at either −40 or 50 °C, using either MAO or $Et_2AlCl$ as co-catalyst ([Al]:[V] = 5 or 20), only moderate activities (<40 g/mmol h bar) were observed. The productivity of **2** appeared to be independent of temperature, whereas that of **1** significantly increased with temperature,

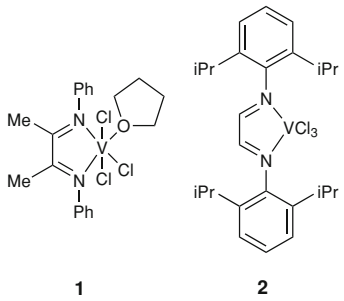


**Fig. 4.1** α-diimine vanadium(III) pro-catalysts **1** and **2**

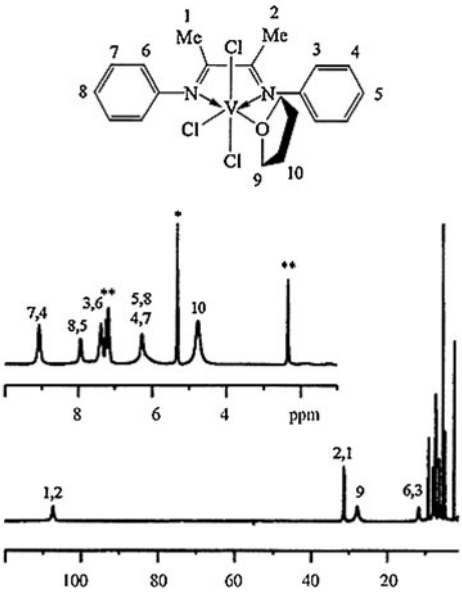


**Fig. 4.2** $^1$H NMR spectrum of **1**. Reproduced with permission from Ref [7]

and also with co-catalyst concentration. In both cases, activities were superior when using $Et_2AlCl$ over MAO. The concentration of active species was roughly calculated to be 12 and 18% for the catalyst systems derived from **1** and **2**, respectively [7].

### *4.2.2 Iminopyrrolide*

The vanadium complexes **3a–e** (Fig. 4.3) were prepared in moderate to good yields (45–75%) by reaction of $[VCl_3(THF)_3]$ with one equivalent of the lithium salt of the corresponding pyrrolide imine in THF [8]. These paramagnetic red or brown solids were screened for ethylene polymerization using a range of organoaluminum co-catalysts including MAO, $Me_3Al$, $Et_3Al$, $iBu_3Al$ and $Et_2AlCl$ together with the re-activator ETA. Highest activities were obtained using the $Et_2AlCl$/ETA combination. Increases in the [Al]:[V] molar ratio (of up to 2,000:1) led to significant increases in activity, but decreases in the polymer molecular weight. At elevated temperatures, increases in the [Al]:[V] molar ratio (of up to 4,000:1) further decreased the molecular weight, whilst the associated PDIs became much narrower. Best activities were achievable at temperatures of about 50 °C. Use of $[VCl_3(THF)_3]$ as a pro-catalyst standard revealed the beneficial role played by the iminopyrrolide ligand set in controlling the single-site behaviour, even at elevated temperatures. As is the case in most vanadium-based

**Fig. 4.3** Iminopyrrolide vanadium(III) pro-catalysts **3a–e**

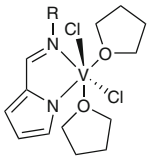


**3**: R = $C_6H_{11}$ (**a**), $C_6H_5$ (**b**), 2,6-*i*$Pr_2C_6H_3$ (**c**), 4-$CF_3C_6H_4$ (**d**), $C_6F_5$ (**e**).

systems, there was a considerable drop-off in activity over time. For example, over 30 min, there was an almost 60% reduction in activity, which occurred along with an increase in polymer molecular weight but with little change in associated PDIs. Increases in the steric bulk of the ancillary iminopyrrolide ligand or the use of electron withdrawing groups, led to enhanced activity, whereas the use of a non-conjugated cyclohexyl substituent over the similarly sized phenyl grouping led to a reduction in activity. In general, these vanadium(III) catalysts performed better (in terms of activity for ethylene polymerization) than related pro-catalysts of the type **31** (see Sect. 4.4.1.1, Fig. 4.19), bearing a single salicylaldiminato ligand. It also proved possible to co-polymerize ethylene and 10-undecen-1-ol, provided that the alcohol was pre-treated with an equimolar amount of an alkylaluminum reagent. Best results were obtained when using $Et_2AlCl$, yielding a co-monomer incorporation of 3.5 mol%. This incorporation could be increased by upward adjustment (ten-fold increase) of the co-monomer concentration in the feed; however, this occurred at the expense of activity (drops by ca. 90%). The microstructure of the co-polymer, as determined by $^{13}C$ NMR, revealed the presence of UU and UUU sequences for co-polymers containing the higher mol% incorporation.

### *4.2.3 β-Diiminate/Amidinate*

Theopold et al. isolated the octahedral vanadium(III) complex {$VCl_2(THF)_2$ [$(Ph)_2$nacnac]} (**4**, Fig. 4.4) from the reaction of [$VCl_3(THF)_3$] and the lithium salt of *N*,*N*-diphenyl-2,4-pentanediimine in THF [9]. Ethylene polymerization was conducted in the presence of 130 equivalents of MAO, and led to the isolation of ultra-high molecular weight ($M_w$ ca. 2,000,000) polymer. Polymerization was accompanied by an exotherm, but the use of ice-water kept temperatures below 60 °C. This system was also capable of the co-polymerization of ethylene with propylene, affording a polymer with $M_w$ 1,659,000 and with 14.9 branches per 1,000 carbon atoms. $^2H$ NMR experiments were consistent with retention of the $(Ph)_2$nacnac ligand by vanadium, i.e there was no supporting ligand transfer to aluminum. Treatment of **4** with two equivalents of methyllithium led to the complex [$(Ph)_2$nacnac$VMe_2$] (**5**), which on further treatment with [$H(Et_2O)_2$]-$BAr^f_4$ led to the salt [$(Ph)_2$nacnac$V(OEt_2)Me(THF)$][$B(3,5\text{-}(CF_3)_2C_6H_3)_4$] (**6**).

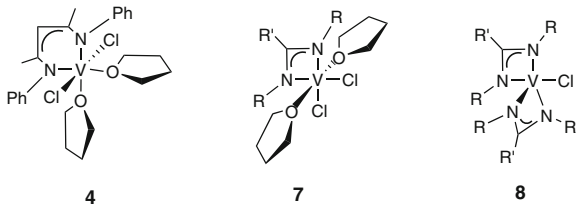


**Fig. 4.4** $\beta$-diiminate **4** and amidinate vanadium(III) pro-catalysts **7** and **8**

Salt **6**, presumably following loss of diethyl ether, was capable of ethylene polymerization in the absence of co-catalyst.

Amidinate vanadium(III) complexes of the type **7** (Fig. 4.4, middle; R = $CHMe_2$, $SiMe_3$) were readily accessible from $[VCl_3(THF)_3]$. Subsequent treatment with methyl Grignard reagent affords the corresponding mono-methyl complexes [10]. In the case of R = $SiMe_3$, NMR experiments at 80 °C revealed ethylene oligomerization with a Schultz–Flory distribution of linear 1- and 2-alkenes with $[C_n]/[C_{n-2}] = 0.6$. The ratio of 1-alkene:*Z*-2-alkene:*E*-2-alkene was 1:0.38:0.14. Although the majority of metal centers were involved in the catalysis, the process was slow with typically only 24 equivalents of ethylene being consumed over 24 h.

The vanadium center can be made more reactive by the use of electron withdrawing fluorinated amidinate ligands. In view of this, Hessen et al. prepared the pentafluorobenzamidinate ligand set $[C_6F_5C(NSiMe_3)_2]^-$ [11], by addition of one equivalent of $C_6F_5CN$ to $Li[N(SiMe_3)_2]$ in diethyl ether; the use of THF as solvent resulted in unwanted C–F activation of the nitrile [12]. Further reaction of the pentafluorobenzamidinate with $[VCl_3(THF)_3]$ led to the bis(amidinate) complex **8**, which can be heated *in-vacuo* at 120 °C (5 h) to afford base-free **9**. Both **8** and **9** can be readily reacted with methyl Grignard reagent in THF (**8**) or diethyl ether (**9**) to afford the methyl complexes $\{[C_6F_5C(NSiMe_3)_2]_2VMe(THF)\}$ (**10**) and $\{[C_6F_5C(NSiMe_3)_2]_2VMe\}$ (**11**), respectively. Autoclave screening (80 °C, 4 or 8 bar ethylene) of **11** and its non-fluorinated analogue revealed that **11** was more than five times more productive (8 g/mmol h) and formed a product of higher molecular weight ($M_n = 1{,}780$). One drawback of using such fluorinated ligation was that it appeared to promote deactivation to V(II), which presumably was one of the main factors accounting for the poor activities observed.

The vanadyl(V) amidinates **12** and **13** (Fig. 4.5), prepared via $VOCl_3$, are dimeric with Cl bridges. A crystal structure determination (Fig. 4.6) of **12** revealed the mono-dentate nature of the amidinate ligand, with the second nitrogen at a distance of 2.385(2) Å from the vanadium. The geometry at the metal can thus be either described as severely distorted octahedral or square-pyramidal. Both pro-catalysts behaved in a similar fashion towards propylene and 1,3-butadiene polymerization with a variety of co-catalysts. At −60 °C, **12** and **13** in the presence alkylaluminum chlorides, polymerized propylene to afford predominantly syndiotactic polymer. Use of $Me_2AlCl$ rather than $Et_2AlCl$ increased productivity with a slight reduction in syndiotacticity, whereas with the sesquichloride $Me_3Al_2Cl_3$, the increased productivity was achieved without loss of syndiotacticity. The use of

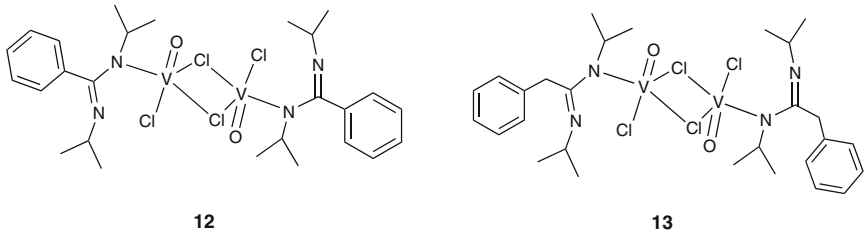


**Fig. 4.5** Amidinate vanadium(V) pro-catalysts **12** and **13**

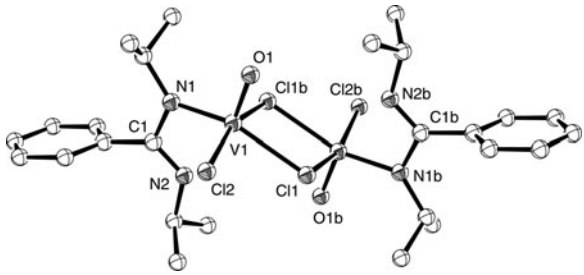


**Fig. 4.6** X-ray crystal structure of **12**. Reproduced with permission from Ref[13]

MAO as co-catalyst, even at low temperatures, resulted in stereo-irregular polymer. At ambient temperature, use of $Et_2AlCl$ with **13** resulted in a dramatic drop-off in activity and formation of a blue species thought to be due to decomposition; only trace amounts of polymer formed.

For the polymerization of 1,3-butadiene, use of $Et_2AlCl$ resulted in highly 1,4-*trans*-butadiene regardless of temperature, whereas the MAO containing system results in 1,4-*cis*-butadiene polymer [13]. Polymerization yields were somewhat higher at 25 °C than at −60 °C. The behavior of **12** and **13** resembled that of $[VOCl_3]$ (and other 'simple' vanadium-based pro-catalysts), and it was thought that the mono-dentate nature of the amidinate ligand allowed for its facile removal from the metal centre under the conditions employed during the polymerization catalysis. As a consequence, the active species was thought to contain two chlorines, a growing polymer chain, a vanadium centre in the +3 oxidation state, and was thought to resemble that resulting from the use of $[VCl_4]$.

The (dimethylamino)ethyl functionalized benzamidinate ligand $Li[Me_3SiNC(Ph)NCH_2CH_2NMe_2]$ was prepared by reaction of $Me_3SiCl$ and $Et_3N$ with $Me_2NCH_2CH_2NH_2$, followed by subsequent treatment with *n*BuLi and benzonitrile. On reaction with an equimolar amount of $[VCl_3(THF)_3]$, the green paramagnetic mono(amidinate) complex $\{Me_3SiNC(Ph)NCH_2CH_2NMe_2]VCl_2(THF)\}$ (**14**, Fig. 4.7, left) was formed in *ca* 60% yield [14]. A structure determination revealed that the amidinate adopted a *facial* coordination mode at the distorted octahedral vanadium(III) centre. Using $Et_2AlCl$ as co-catalyst, an activity of *ca* 450 g/mmol h bar was achievable at 30 °C, with $M_w$ 760,000 and $M_w/M_n$ 2.1.

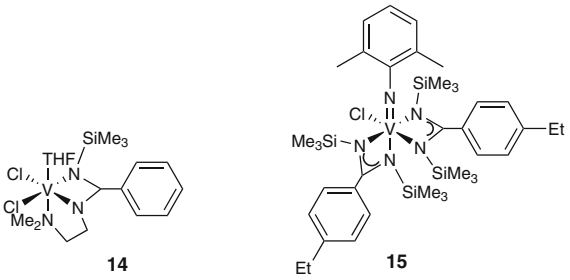


**Fig. 4.7** Benzamidinate vanadium pro-catalysts **14** and **15**

On increasing the temperature to 50 °C, the activity nearly halved, whilst at 80 °C, the activity fell below 50 g/mmol h bar, whilst the molecular weight distribution was found to be bimodal.

Immobilization of the vanadium(III) pro-catalysts **7** and **14** on magnesium chloride ($Et_3Al/MgCl_2 \cdot 2.1$ethanol—spherical adduct) led to enhanced performance. Quantitative immobilization could be achieved at low catalyst loadings (ca. 10 μmol). Conducting polymerizations in light petroleum to which had been added a small amount of $i$Bu$_3$Al led to activities as high as 31,200 and 14,200 g/mmol h bar for **7** and **14**, respectively. In the case of **7**, the activity at 1 h had fallen by around 50%, whereas **14** managed to maintain its' albeit lower activity over the same period. The polyethylene produced was linear (melting points 136–137 °C) with $M_w/M_n$ ca. 2, and with retention of the spherical morphology (advantageous in terms of reactor fouling) [15].

Salt metathesis of vanadium(2,4-xylylimido)trichloride [V(2,4-$Me_2C_6H_3N$)$Cl_3$] with two equivalents of lithium $p$-ethylbenzamidinate (or the TMEDA complex thereof) afforded the dark brown bis(amidinate) complex {2,6-$Me_2C_6H_3NVCl$ [$p$-$EtC_6H_4C(NSiMe_3)_2]_2$} (**15**, Fig. 4.7 right) in 80% yield [16]. In the solid-state structure, the chloride and the imido ligands are *cis*, and there was good evidence of a strong *trans* influence exerted by the imido group, which resulted in very different V–N(amidinate) bond lengths. Use of MAO ([Al]:[V] = 1:1,000) or a mixture comprising either MAO or TIBA (triisobutylaluminum) plus TTPB (trityl tetrakis(pentafluorophenyl)borate) ([V]:[Al]:[B] = 1:50:1), resulted in only negligible activity at 10 bar ethylene.

## 4.3 *N,N,N*-Tri-Dentate Ligands

### *4.3.1 Bis(imino)pyridines*

Given the catalytic successes of this ligand set with a variety of metals [17], it is not surprising that a considerable amount of work on vanadium has and continues to be carried out by a number of research group active in the olefin polymerization area.

The sparingly soluble paramagnetic red complex $VCl_3\{2,6\text{-bis}[2,6\text{-}(i\text{Pr})_2C_6H_3N = C(Me)]_2C_5H_3N\}$ (**16**, Fig. 4.8) is available in yields of ca. 90% from the reaction of $[VCl_3(THF)_3]$ and 2,6-bis(2,6-diisopropylphenyl)ethylpyridine. Despite the paramagnetic nature of **16**, the $^1H$ NMR spectrum recorded in $CD_2Cl_2$ is well-resolved. Peaks are assignable in the 10–60 ppm region based on their integration and proximity to the paramagnetic vanadium centre (see Fig. 4.9) [7].

Complex **16** and its 2,6-$Me_2$ and 2,4,6-$Me_3$ analogues have been characterised by FTIR, and it was found that the imine peak shifts to 1,575 $cm^{-1}$ (from 1,640 $cm^{-1}$) upon complexation. In the UV–Vis spectra, there are two bands at 270 and 440 nm, due to ligand-based $\pi$–$\pi^*$ transitions, and a broad MLCT absorption in the visible region at 570 nm. When activated with MAO, an emerald-green coloration occurred, and the system was capable of rapid initial ethylene uptake, which occurred with a concomitant exotherm. For example, in a typical run at 50 °C, the temperature rises to 80 °C within 20 s. The catalyst remained active (a typical activity is 1,416 g/mmol h) for about 15 min, although ethylene uptake diminished somewhat after 2 min. At 140 °C, the catalyst was deactivated within a minute, whilst GPC traces at this temperature were bimodal, suggesting more than one active species. Experiments revealed that high temperatures and/or high [Al]/[V] ratios favoured the formation of the high molecular weight fragment, whereas in situ alkylation (by MAO) followed by addition of $B(C_6F_5)_3$ (co-catalyst) disfavoured formation of the high molecular weight product (and this was also detrimental to the overall observed catalytic activity). Lower productivity was also noted for co-polymerization runs involving ethylene and 1-octene, with the poorer performance here thought to be due to the result of unfavourable steric congestion. Higher temperatures and co-catalyst molar ratios also promoted higher activities when $Et_2AlCl$ was employed as the co-catalyst. Activities observed at 50 °C were higher for deployment of $Et_2AlCl$ than for MAO as co-catalyst; the reverse trend was observed at −40 °C.

The activity of this type of pro-catalyst can be increased if combined with $Et_3Al/[Ph_3C][Al(O\mathit{t}Bu^f)_4]$ ($O\mathit{t}Bu^f$ = fluorinated *tert*-butoxide) as co-catalyst. However, screening of the Ar = phenyl and *o*-tolyl derivatives for ethylene oligomerization revealed that the increase in activity comes at a cost to the productivity (based on vanadium), which is lower than when these pro-catalysts are screened using MMAO as co-catalyst (MMAO is a modified aluminoxane, which was obtained from Akzo Nobel and has the general formula $[\text{-Al(R)-O-}]_n$, where R = Me (75%) and *t*Bu (25%)) [18].

**Fig. 4.8** Pro-catalyst **16**

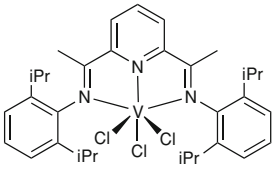


**16**

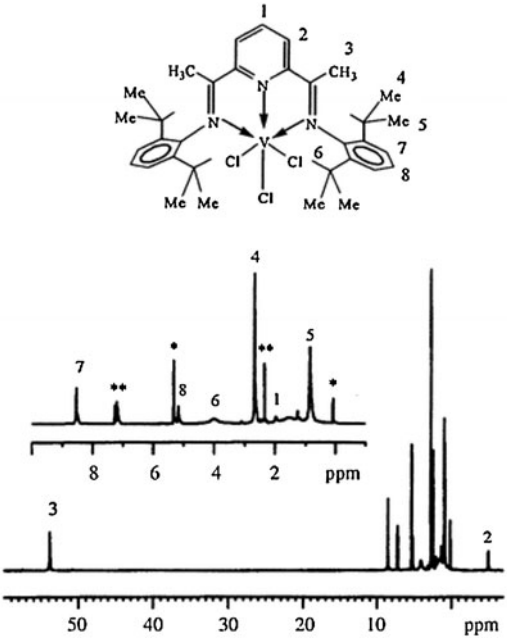


**Fig. 4.9** $^{1}$H NMR spectrum of pro-catalyst **16**. Reproduced with permission from Ref S[7]

Complex **16** has been screened with various co-catalysts, namely $Et_2AlCl$, $Et_3Al_2Cl_3$ and MAO, for butadiene polymerization and ethylene/butadiene co-polymerization. The $Et_3Al_2Cl_3$ activated system produced the highest activity (4,150 g/mmol h), particularly at [Al]:[V] ratios approaching 40:1, though after 1 h, the activity had fallen off dramatically. $^{13}$C NMR spectra were consistent with a predominantly *trans*-1,4 structure with 1–3 mol% isolated *cis*-1,4 units. Use of MAO as co-catalyst, led to lower activities as well as temperature dependent chemo-selectivity (decreasing *cis*-1,4 content with increasing temperature). Use of either of these co-catalysts led to PDIs in excess of 10 [19].

Interestingly, for ethylene/1,3-butadiene co-polymerization, the $Et_3Al_2Cl_3$ activated system was ineffective, whereas with MAO, activities as high as 186 g/mmol h (with PDI $\approx$ 50) were achievable at 50 °C and 5 bar ethylene. Butadiene incorporation of up to 44 mol% was possible with a block distribution of the two monomers. Saturated co-polymers were accessible via hydrogenation with *cis*-diimide.

The parent bis(imino)pyridine ligand has been shown to react with $Et_2AlCl$ to afford organoaluminum complexes of the type **17** and **18** (Fig. 4.10) in yields of 44 and 56%, respectively [7]. However, under the conditions employed for the polymerization screening, it has been shown that the parent ligand can be retrieved after hydrolysis in near quantitative yield. In other words, the diimine nature of the ligand was preserved and no alkylation of the backbone had taken place.

Attempts were made to identify the nature of the species responsible for the emerald green color formed on addition of MAO [20]. On a preparative scale,

complex **16** was reacted with two equivalents of MAO, and following work-up, dark green crystals of $VCl_2\{2,6\text{-bis}[2,6\text{-}(i\text{Pr})_2C_6H_3N = C(Me)]_2(2\text{-}MeC_5H_3N)\}\cdot 0.5$ toluene (**19**, Fig. 4.11 left) formed in ca. 30% yield; further crops were obtainable from the mother-liquor (overall yield 65%). Spectroscopic studies (UV–Vis) suggested that this was the only vanadium-containing product present. Reaction of **16** with an equimolar amount of MeLi also led to the formation of **19** in similar yield. In both cases, the alkylating reagent had promoted alkylation of one of the *ortho* carbons of the pyridine ring, whilst also removing a chloride from the metal center. The overall result was the creation of a vacant site at the now 5-coordinate, trigonal bipyramidal vanadium center. Furthermore, the previously neutral bis(imino)pyridine had been converted to an anionic amide. Wavefunction calculations (generating the electron density distribution) revealed that the *ortho* carbon atom positions of the pyridine ring were associated with increased positive charge and were therefore most likely to be susceptible to nucleophilic attack. The shorter $V\text{–}N_{pyridine}$ distance [1.886(6) Å] in **19** versus that observed in **16** [2.067(3) Å] was indicative of an increase in the V–N π-bonding, which was thought to go someway towards off-setting the loss of aromaticity.

Interestingly, both **16** and **19** possessed the same observed catalytic activity (and resultant polymer properties), but only when using MAO as co-catalyst; use of MeLi or $Me_3Al$ afforded no appreciable catalytic activity. Despite being unable to isolate species by interacting **19** with excess MAO under various conditions, it seemed reasonable to assume that **19** was the precursor to the catalytically active species. However, the need for the presence of further MAO to bring about the observed activity, discounted the involvement of a reversible alkylation of the pyridine ring and subsequent methyl transfer to the vanadium.

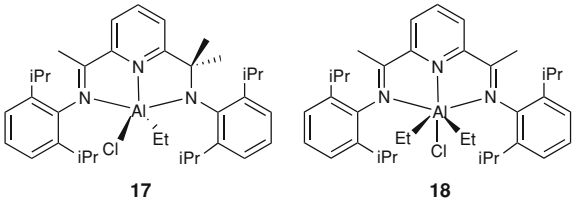


**Fig. 4.10** Organoaluminium complexes **17** and **18**

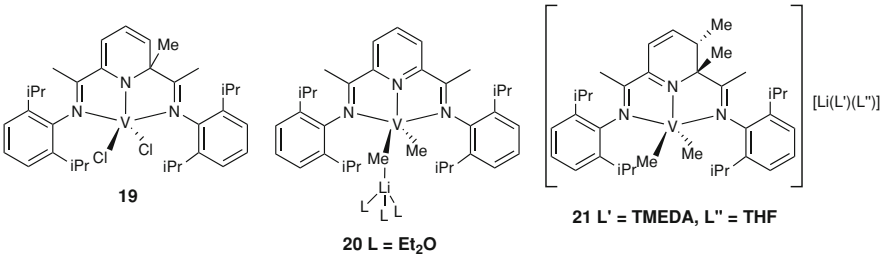


**Fig. 4.11** Products resulting from the alkylation of **16**

Interaction of excess MeLi (four equivalents) with **16** (or three equivalents with **19**) led to a dark brown dialkyl complex $V(CH_3)(\mu\text{-}CH_3)Li(Et_2O)_3\{2,6\text{-bis}[2,6\text{-}(i\text{Pr})_2C_6H_3N = C(Me)]_2C_5H_3N\}$ (**20**, Fig. 4.11 middle) in ca. 50% yield. The methyl group bound to the *ortho* carbon of the pyridine in **19** was no longer present in **20**, and the backbone of the tridentate ligand had reverted back to the bis(imino)pyridine form. The vanadium of **20** is further coordinated by two methyl groups, and given one of these is involved in bridging to a lithium cation, the oxidation state of the vanadium is now +1. Addition of TMEDA to the reaction mixture afforded the vanadium(I) complex $[V(CH_3)_2\{2,6\text{-bis}[2,6\text{-}(i\text{Pr})_2C_6H_3N = C(Me)]_2(2,3\text{-}Me_2C_5H_3N)\}][Li(THF)_2(TMEDA)_2]\cdot 0.5Et_2O$ (**21**, Fig. 4.11 right), which now contains a second methyl group at pyridine, this time in the *meta* position adjacent to the methylated *ortho* carbon. The role of the TMEDA here was thought to be one of promoting crystallization of **21** over **20**, as both species were likely to be present in the reaction mixture. The lithium cation in **21** is not directly bound to the anion. Both **20** and **21** were inactive towards ethylene polymerization, with or without co-catalyst present. The isolation and structural characterization of species such as **19–21** provided a plausible reduction pathway; however, given that the tri-dentate ligand remained firmly bound to the metal centre throughout, ligand transfer to the aluminum co-catalyst and resultant deactivation, was improbable.

The family of type **16** pro-catalysts has been extended by Schmidt et al. to include the variations shown in Fig. 4.12 [21]. A series of screening experiments were conducted using MAO as co-catalyst, with variation of the substituents at positions R. R′, X, Y and Z. It was found that variation of the substituents around the aniline had a dramatic effect on the observed activity. Typically, on increasing the bulk of the alkyl group at the *ortho* (2-) position, there was a decrease in activity, which was accompanied by an increase (from 2 to 55 wt%) in the amount of solid product formed (at the expense of the oligomers). Indeed, the bulkiest pro-catalyst afforded the least amount of 1-hexene of all. Interestingly, the pro-catalyst derived from unsubstituted aniline $PhNH_2$, proved to be the exception. It is well documented that in the related iron(II) systems, such a ligand set results in the formation of the inactive bis(chelate) salt $[FeL_2][FeCl_4]$ [17]. In the case of vanadium; however this ligand set led to a pro-catalyst exhibiting an activity of 196 g/mmol h, which was somewhat higher than that observed for a number of other members of this pro-catalyst family, e.g. for R = *i*Pr; R′= X = Y = X = H,

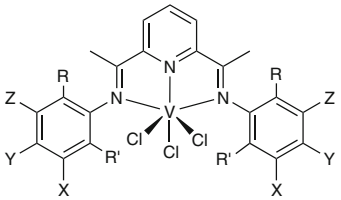


**16** R, R' = H, alkyl
X, Y, Z = H, alkyl, Cl, Br

**Fig. 4.12** Pro-catalyst **16** variations reported by Schmidt et al

activity = 63 g/mmol h. Although the presence of a second substituent at the other *ortho*-(6-) position had little effect on activity, it had a pronounced effect on the product distribution, with a shift occurring from mostly oligomers to low molecular weight solids. Use of a methyl group at the *meta*-(5-) position also led to enhanced polymer formation. Solid formation could be suppressed by deployment of either a substituent at the *meta*-(3-) position or a chloro group at the *meta*-(5-) position. Both substituent patterns also produced enhanced α-olefin purity as well as favoring productivity. Of all the pro-catalysts screened, the highest observed activity was achieved when the substituents involved were *ortho*-(2-) methyl in combination with *meta*-(3-) chloro, i.e. R = Me; X = Cl; R′= Y = Z = H. By contrast, substitution patterns involving a combination of *ortho* (2-) and *para*-(4-) substituents proved to be unfavourable to the observed catalytic activity.

Using the pro-catalyst with R = methyl; R′= X = Y = Z = H, the influence of various reaction parameters, such as co-catalyst concentration, temperature, pressure and the presence of hydrogen, were investigated and their influence on activity studied [22]. Over the range 0–5,000 for the [Al]:[V] molar ratio, maximum activity was observed at a ratio of 300:1. The molar ratio also had an impact on the α-olefin purity in the $C_6$–$C_{10}$ range. Optimum purity was achieved at about the same molar ratio as that used for achieving the highest activity. The α-olefins produced followed a Schulz–Flory distribution independent of the [Al]/[V] molar ratio. The Schulz–Flory constant value α ranged between 0.36 and 0.40. At low molar ratios, low levels of solids (1–4 wt%) were evident. However, an increase in the molar ratio beyond 2,000:1, led to an escalation in the amounts of solids present (>20 wt%). In the case of temperature variation, productivity was inversely proportional to reactor temperature (at constant ethylene pressure). The loss of activity at higher temperature was not reversible, likely due to decomposition of the active species. Increasing the temperature was only slightly detrimental to the purity (>96% linear 1-hexene) of the α-olefins. Larger α-olefins were favored at higher temperatures as evidenced by a decrease in the slope of the Schulz–Flory plot. The amount of solid (polymer) in the product increased with temperature, and at 90 °C, the product was almost entirely solid. Increasing the pressure from 150 (10.34 bar) to 400 psig (27.58 bar) led to an increase in activity, although any further increase in pressure beyond this point had little impact. Over this pressure range, the amount of solid in the product remained constant at about 1.5 wt%. The addition of hydrogen had little influence on activity (a slight decrease only was noted) or product distribution/purity. Similarly, the presence of other α-olefins (co-monomers) did little to effect the product distribution.

It proved difficult to support this type of vanadium pro-catalyst, despite the use of the methodologies that had been successfully applied to the analogous iron(II) systems [23]. The resulting heterogenized systems displayed only negligible activity.

The final paper of this series by Schmidt et al. employed UV–Vis spectroscopy in an attempt to identify the products formed on the addition of MAO at various concentrations [24]. It was noted that the spectra showed a remarkable dependence on the time elapsed prior to the addition of MAO, as well as temperature and the

MAO concentration. Observations were best conducted using the 2,6-diisopropylphenyl derivative, primarily due to its favorable solubility. The observed spectra ($\lambda_{max}$ 325 and 640 nm with a shoulder at 330 nm), using a low molar ratio of [V]:[Al] of the order of 1:10, were remarkably similar to that observed on addition of methyllithium to the vanadium precursor. Given that Rearden et al. had previously structurally characterized the product resulting from the addition of MeLi (see **20**) [20], it was proposed that the MAO product, at such low molar ratios, was indeed **20**. Scrutiny of the spectra also suggested that **20** was formed via an intermediate of unknown structure, but which possessed a prominent band at 370–460 nm. With excess MAO, **20** was thought to be rapidly converted to a dimethide complex related to **21**, which over time converted into an active charge-separated species with an absorption max at 390 nm. In contrast to the analogous iron(II) system, the activity of this vanadium(III) pro-catalyst did not rapidly decrease with MAO mixing time.

More recent observations by Carrillo–Hermosilla and Antiñolo et al. described orange colorations (rather than emerald green) on addition of MAO ([Al]:[V] 100:1) in toluene to **16** and its 2,6-$Me_2$ and 2,4,6-$Me_3$ analogues [25]. The UV–Vis spectra for all three systems were similar, though in the case of **16**, there was an additional band at 830 nm. Higher [Al]:[V] ratios essentially led to identical spectra. As in earlier work, such pro-catalysts were highly active for ethylene polymerization when combined with MAO, but yielded only oily residues when TIBA was employed as co-catalyst. For the MAO runs, little variation of activity was observed when changes were made to the [Al]:[V] ratio (for values <500:1), but significant decreases in activity were evident with time. Results using different solvents for UV–Vis studies of pro-catalyst **16** (Ar = mesityl)/MAO at [Al]:[V] ratios of >100 led to shifts to higher wavelengths with increasing polarity, an observation which was consistent with the formation of an ion-pair of the type **22** (Fig. 4.13, left).

Partially dehydroxylated silica pre-treated with MAO could be used to support such vanadium complexes; however, additional MAO or TIBA was necessary to bring about catalytic activity. Typical results over 30 min using 500 equivalents of MAO and 100 mg of supported catalyst in toluene at 70 °C comprised an observed

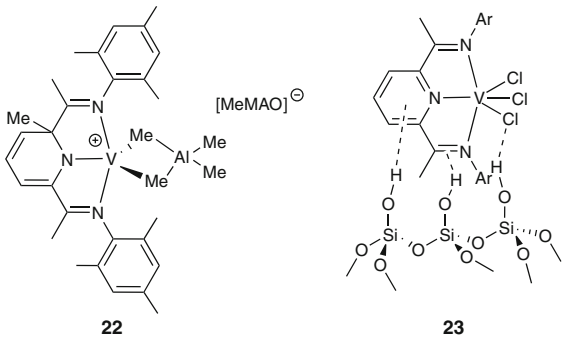


**Fig. 4.13** Proposed active species **22** and surface species **23**

activity of 185 g/mmol h bar and a resultant polymer molecular weight ($M_n$) of 95,600.

These complexes could be directly supported on unmodified partially dehydroxylated silica, with loadings in the region of 1.5% as measured by adsorption isotherms. IR spectra for these supported systems possessed slight modifications to the stretching bands, and given this, a number of interactions have been proposed for the possible active species (see Fig. 4.13, right). Unlike the MAO-modified supported systems, the activities associated with the unmodified silica surface bound species showed a dependence of co-catalyst on the nature of the original vanadium complex.

The derivatives shown in Fig. 4.14 were screened, in the presence of MAO (500 equivalents), for the dimerization of propylene. Activities were in the range 95–215 g/mmol h, whilst the product was greatly influenced by the bulk associated with the *ortho* substituents on the aryl rings. Bulkier groups favored a 1,2-insertion as the initial step resulting in 2-methyl-1-pentene; smaller substituents afforded 4-methyl-1-pentene. The use of *para* halides led to increased selectivity for 4-methyl-1-pentene, whilst for *meta* halides, selectivity was enhanced in the order F > Cl > Br. Addition of $PPh_3$ (two equivalents) to the system improved dimer selectivity. Varying the amount of $PPh_3$ added influenced the product distribution [26].

### *4.3.2 2,6-Bis(aryliminophosphoranyl)pyridine*

2,6-bis(aryliminophosphoranyl)pyridines formed red colored adducts of the type **24** (Fig. 4.15) when stirred with $[VCl_3(THF)_3]$ at ambient temperature in dichloromethane, the product being isolated in yields of 69% (Ar = 2,4,6-$Me_3C_6H_2$) and 35% (Ar = 2,6-*i*$Pr_2C_6H_3$). These octahedral pro-catalysts when activated with MAO ([Al]:[V] = 500–1,400:1) exhibited activities of up to 140 g/mmol h bar, affording high molecular weight polyethylene ($M_w \approx 1{,}300{,}000$) with wide polydispersity ($M_w/M_n$ = 9–15) [27].

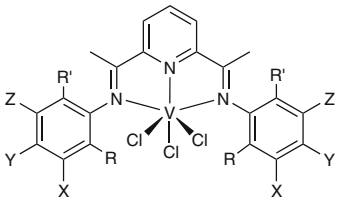


R = R' = Z = H, X = F, Y = Me
R = R' = Z = H, X = Cl, Y = Me
R = R' = Z = H, X = Br, Y = Me
R = R' = H, X = Z = Br, Y = Me

**Fig. 4.14** Pro-catalyst **16** and the variations reported by Alt et al

### 4.3.3 Bis(pyrazolyl)pyridine

The bis(pyrazolyl)pyridine vanadium(III) complexes **25** and **26** (Fig. 4.16) were accessible via the reaction of $VCl_3$ with the parent bis(pyrazolyl)pyridine ligands in THF in yields of 57 and 89%, respectively. Screening with $EtAlCl_2$ (500 equivalents) as co-catalyst at 25 °C and 10 bar ethylene, led to observed activities of 580(**25**) and 940(**26**) g/mmol h, which fell to 160 (**25**) and 422(**26**) g/mmol h at 1 bar. At 50 °C, although higher molecular weight polyethylene was formed, there was a substantial drop-off in productivity. A reduction in the [Al]:[V] ratio down to 250:1, led at 50 °C to an improvement in productivity for **26**, but not for **25**. All polymers produced were essentially linear high density polyethylene [28].

### 4.3.4 Bis(benzimidazole)amine

The vanadium(III) procatalyst **27** and vanadium(V) pro-catalyst **28** (Fig. 4.17) are readily available from the parent ligand on reaction with $[VCl_3(THF)_3]$ or $[VO(OnPr)_3]$, respectively. Complex **27** containing the neutral tridentate donor ligand set is insoluble in common organic solvents, whereas **28**, which as a result of deprotonation of one of the benzimidazole nitrogen atoms contains a mono anionic tri-dentate ligand, is readily soluble in the likes of dichloromethane.

Screening of **27** for ethylene polymerization in the presence of $Et_2AlCl$/ETA was hampered by mass transport problems. Use of hydrogen (which lowered the resulting polymer molecular weights) and conducting the screening using sub-micromole concentrations of pro-catalyst enabled runs of up to 1 h to be conducted. The thermal stability was highlighted by kinetic profiles (ethylene uptake versus time), and activities in excess of 30,000 g/mmol h bar were achievable at 60 °C. The catalyst exhibits single-site behavior (PDIs 2.4–3.3), with

**Fig. 4.15** Pro-catalyst **24**

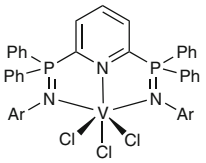


**24**

**Fig. 4.16** Pro-catalysts **25** and **26**

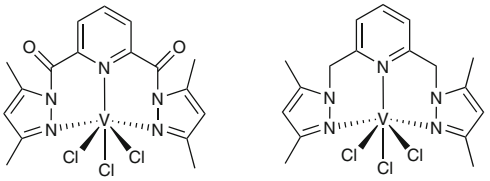


**25** **26**

polymer molecular weights in the range 248,300–992,900, for which $^{13}C$ NMR spectroscopy indicated little branching.

Use of **28** led to similar activities and polymer properties consistent with the generation of the same active species as for **27**. Both **27** and **28** were also capable of co-polymerization of ethylene with propylene or norbornene. In the case of propylene, activities as high as 16,670 g/mmol h bar were recorded with 2.4 mol% propylene incorporation. For norbornene, incorporation levels reached 32.5 mol% [29].

## 4.4 *N,O*–Bi-Dentate Ligands

### *4.4.1 Salicylaldiminato/Phenoxyimines*

#### 4.4.1.1 Bi-Dentate

The use of Schiff-base functionalized phenoxides of the type [(2-PhN = CH) $C_6R_4OH$] (R = H, *t*Bu) allowed access to the first highly active, thermally stable vanadium-based olefin polymerization catalysts, for example see **29** and **30** (Fig. 4.18). The catalyst group at the Mitsui Chemicals Corporation, having had great success with the group 4 metals, turned their attention to vanadium [30–32]. Use of $MgCl_2$ supports of the type $MgCl_2/Et_mAl(OR)_n$, synthesized via the de-alcoholysis of $MgCl_2$/2-ethyl-1-hexanol with $Et_3Al$, [33] led to the formation of well-defined polyethylene particles, which contrasts with the formation of a stringy product formed in the absence of the support. The polymer products formed by these supported catalysts were all of ultra-high molecular weight ($M_w > 5{,}000{,}000$). Analysis of this product proved to be troublesome, whereas

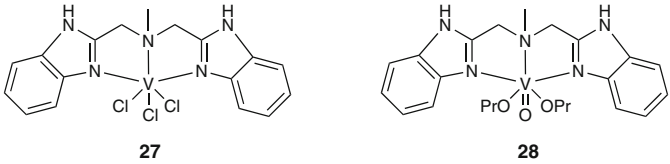


**Fig. 4.17** Pro-catalysts **27** and **28**

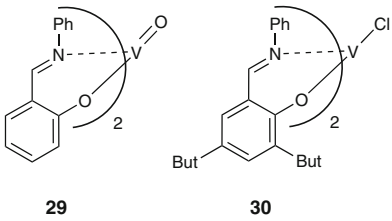


**Fig. 4.18** Pro-catalysts **29** and **30**

that formed in the presence of $H_2$ was shown to have a narrower molecular weight distribution ($M_w/M_n$ 2.3).

In the absence of the support, such phenoxyimine-based pro-catalysts proved to be poor at high temperature (75 °C), behaving in a similar fashion to $VOCl_3$-based systems. By contrast, in the presence of the support, these pro-catalysts proved to be thermally stable and highly active. For example, the system **29**/$MgCl_2$/$Et_mAl(OR)_n$ showed a steady increase in activity from 18,700 g/mmol h bar at 25 °C rising to 65,100 g/mmol h bar at 75 °C. It is noteworthy that use of $V(acac)_3$ with the same support afforded a much lower activity at 75 cf. 25 °C, which highlighted the important stabilizing role imparted by the phenoxyimine ligands. For the **29**/$MgCl_2$/$Et_mAl(OR)_n$ system, there was steady ethylene uptake with time, suggesting negligible catalyst deactivation. This is in stark contrast to $VOCl_3$-based systems, where there was rapid deactivation with or without the support present.

The system **29**/$MgCl_2$/$Et_mAl(OR)_n$ was also shown to be capable of ethylene/propylene co-polymerization at 75 °C. The amorphous co-polymer formed was of high molecular weight ($M_w$ 697,000) with $M_w/M_n$ 4.72. It possessed a propylene content of 21.3 mol%, and a random distribution of monomeric units, namely PPP 1.75%, PPE 4.80%, EPE 14.16%, PEP 50.81%, EEP 24.10% and EEE 4.58%, plus 3.4% inverted propylene units. GPC-IR measurements showed that longer co-polymer chains possessed higher co-monomer content.

A number of complexes of the type **31** (Fig. 4.19, left) have been obtained via reaction of $[VCl_3(THF)_3]$ in THF with one equivalent of the corresponding phenoxyimine ligand in the presence of triethylamine [34]. Depending on the steric requirements of the ligands present, similar use of only half an equivalent of $[VCl_3(THF)_3]$ led to the vanadium(III) complexes **32** (Fig. 4.19, right) or the THF-free version of **32**. Ethylene polymerization screening using $Et_2AlCl$ as co-catalyst gave highest activities when using 3,000–4,000 molar equivalents of co-catalyst. However, higher molar ratios led to decreases in polymer molecular weights. Pro-catalyst structure–activity studies revealed little variation in activity of resultant polymer molecular weight for those pro-catalysts derived from unsubstituted phenols, with only that bearing an *N*-bound cyclohexyl grouping behaving somewhat differently. This 'cyclohexyl' pro-catalyst displayed a much lower activity at 25 °C, yet the highest activity at 70 °C. For those systems where the phenolic part of the ligand contained bulky *tert*-butyl groups, activities were much lower. Further reduction in activity followed the introduction of bromo substituents.

The bis(phenoxyimine) complexes **32** were all less active than type **31** systems, but were able to maintain their activities over longer periods. More pronounced structure–activity relationships were also observed for these complexes.

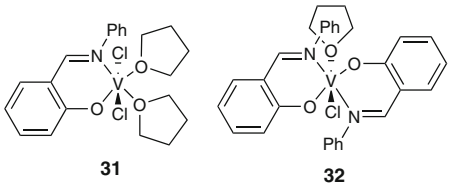


**Fig. 4.19** Pro-catalysts **31** and **32**

In particular, higher activities were favored by the presence of electron-withdrawing substituents as well as by increased steric bulk at either the *N*- or *O*-bound function. However, when both the *O*- and *N*-bound moieties contained bulky substituents, this proved to be detrimental to ethylene insertion (or catalyst activation), and as a consequence lower activities resulted. Use of an *N*-bound cyclohexyl substituent was found to be more favorable to performance than an *N*-bound phenyl group. These bis(phenoxyimine) pro-catalysts in general displayed higher activities at higher temperatures, with little change to the polydispersity indices of the resulting polymers.

Using a similar synthetic procedure, *N*-bound heteroatom containing substituents can be incorporated, and a number (see **33a–d**, Fig. 4.20) of these have been isolated in yields of 45–65%, and have also been screened for ethylene polymerization and ethylene/1-hexene co-polymerization using $Et_2AlCl$ and ETA [35]. Screening results were compared against pro-catalyst **31** as standard, and it was found that at elevated temperatures (70 °C), those possessing the *N*-bound hetero-substituents exhibited higher activities; at room temperature (25 °C) **31** displayed a higher activity. The presence of bulky *tert*-butyl groups on the phenoxy part of the ligand frame was detrimental in terms of activity. Notable electronic effects were observed for the *N*-bound hetero groups. In particular, highest activities were achievable when using the 'c' motif. With these systems, polymer molecular weights decreased sharply with increasing temperature, whereas associated PDIs changed only slightly over the initial 5 min period. Optimum catalytic activity for type 'c' catalyst systems was achieved using an [Al]:[V] ratio of 4,000:1, and increases in co-catalyst concentration also led to decreases in the PDIs. Use of other co-catalysts such as MAO, $Me_3Al$ or $Et_3Al$ afforded only trace or no polymer. Use of $Et_2AlCl$ in the absence of ETA also led to lower yields of polymer. Lifetime studies revealed that 'a' and 'c' (and the standard **31**) maintained some productivity over the 30 min run time, whereas 'b' and 'd' were virtually inactive after 10 min. All of these systems yielded a bi-modal molecular weight distribution, attributed to the presence of two types of active species. For 'a' and 'c', high molecular weight fractions dominate, whereas for 'b' and 'd', low molecular weight fractions make up greater than 90% of the product. For 'c', whilst 5 min runs resulted in a uni-modal molecular weight distribution, at 15 or 30 min, bi-modal distributions are observed for which the molecular weight of the lower fraction is close to that observed at 5 min.

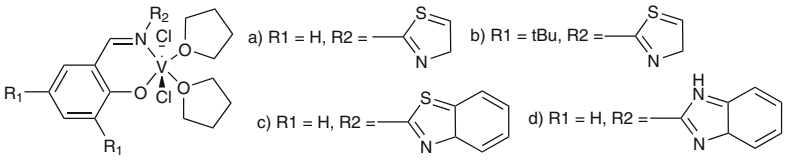


**33**

**Fig. 4.20** Pro-catalysts of type **33a–d**

For ethylene/1-hexene co-polymerizations, the observed catalytic activities followed the trend **c** > **a** > **b** ≫ **d**. The resulting high molecular weight co-polymers possessed uni-modal molecular weight distributions, with the 1-hexene incorporation falling in the range 2.69–3.71 mol%. For '**c**', increasing the 1-hexene feed led to decreased activity and molecular weights, but an increase in incorporation, for example 26.7 mol% at 2.70 mol/L 1-hexene. Again when using '**c**', at 10 min, highest activities were achievable at 50 °C, whereas at 30 min, 25 °C was preferable. Molecular weights of the co-polymers decreased upon increasing temperature of the run, the PDIs remained unaffected, whilst the 1-hexene incorporation increased. Molecular weights also increased with time. Analysis of the microstructure using $^{13}C$ NMR revealed the presence of HEH and EHH triads for the 10.7 mol% 1-hexene incorporated co-polymer, and HHH triads in the copolymer with 26.7 mol% 1-hexene incorporation.

## Imidazolium Bearing Phenoxyimines

The imidazolium salt **34** (Fig. 4.21) was isolated from the reaction of $[VCl_3(THF)_3]$ with the parent phenoxyimine in the presence of sodium bis(trimethylsilylamide) in 92% yield. In the presence of MAO, **34** exhibited low activity (0.18–6.20 g/mmol h bar) towards ethylene polymerization at temperatures ≤75 °C; the system peaked at ambient temperature (22 °C), but was essentially inactive above 80 °C. The [Al]:[V] molar ratio was varied between 250 and 1,000:1, and the best activity at 22 °C was observed for 500 equivalents of co-catalyst. The system was multi-modal, with a narrow mono-modal low molecular oligomeric fraction ($M_n$ = 390–450), and a multi-modal higher molecular weight fraction. MAO deprotonation of the imidazolium grouping to give an aluminum adduct, typically an imidazolium-aluminate zwitterionic species, was put forward as a possible reason for the multiple active species present [36].

## Imido Phenoxyimines

Reaction of $[V(NC_6H_3Me_2\text{-}2,6)Cl_3]$ with the lithium salts of the phenoxyimines LiO-2-R-6-$[(2,6\text{-}iPr_2C_6H_3)N = CH]C_6H_3$ led to the imido complexes **35** (Fig. 4.22, left)

**Fig. 4.21** Pro-catalyst **34**

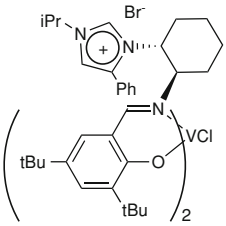


**34**

in yields of 64–78%. The imido group occupies the apical site of the distorted squared-based pyramidal geometry at vanadium (see Fig. 4.23 for the *t*Bu derivative); the imino nitrogen was also coordinated to the vanadium centre as a π donor. Screening (25 °C, 8 atm ethylene, 10 min) in the presence of MAO revealed that the *ortho* substituent in the aryloxo ligand had a strong affect on the ethylene polymerization activity, with an observed order of *t*Bu (2,150) > Me (680) > H (380 g/mmol h). From analysis of the crystallographic data, in-particular the Cl–V–Cl bond angle, it was postulated that the *ortho* substituent affected the bond angle between the alkyl and the olefin in the proposed cationic alkyl active species. The overall result being more facile insertion. The beneficial affect of the presence of the imine could also be inferred from comparison with the aryloxide pro-catalyst **36** (Fig. 4.22, right). Screening under the same conditions as for **35** resulted in an activity somewhat lower (880 g/mmol h) than that observed for **35** (*t*Bu). The enhanced electron donation from the imino nitrogen was assumed to stabilize the active species at temperatures below 50 °C. The resulting polymers were of high molecular weight and uni-modal molecular weight distributions ($M_w/M_n$ = 2.8–3.1). Above 50 °C, the active species is thought to decompose leading to less control and poorer activity [37].

## '*C*-capped' Phenoxyimines

An arylimine arm can readily be appended to the parent formyl-bearing *C*-capped ligand system by using the method of Scott et al. (Fig. 4.24) yielding phenoxyimines of the type $\mathbf{L^1H_3}$ [38]. Such an approach allowed for the facile introduction of a wide variety of aryl groups and as a consequence allows both the electronics and sterics of the system to be controlled by requisite choice of aniline. In our laboratory, the aryl derivatives $C_6H_5$, $C_6H_4Me$-4, $C_6H_2Me_3$-2,4,6 and $C_6H_3iPr_2$-2,6 were prepared, and subsequently treated with $[VO(OnPr)_3]$ to afford bis-chelate vanadium(IV) complexes of the form $[VO(L^1H_2)_2]$ (**37**, Fig. 4.25), in which each '*C*-capped' ligand binds in phenoxyimine fashion [39].

Using such pro-catalysts for ethylene polymerization afforded little or no polymer when MAO or $Me_3Al$, with or without ETA present, were employed as

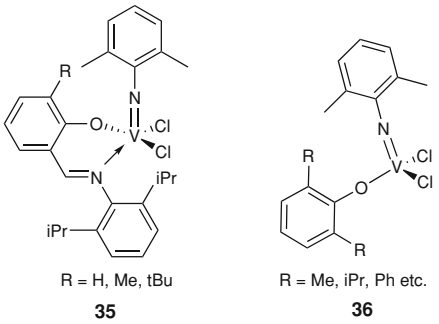


**Fig. 4.22** Imido phenoxyimine pro-catalyst **35** and imido aryloxide **36**

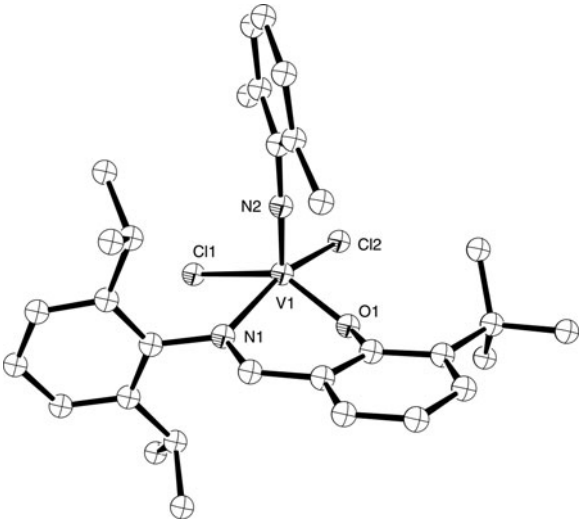


**Fig. 4.23** Crystal structures of pro-catalysts of type **35** (R = *t*Bu). Reproduced with permission from Ref [37]

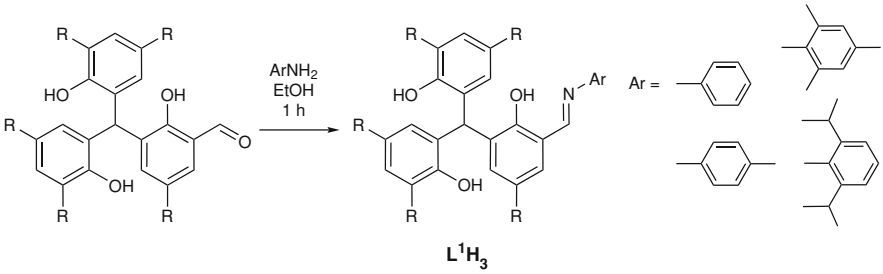


**Fig. 4.24** Synthesis of 'Scott-imine' ligands (R = tert-butyl)

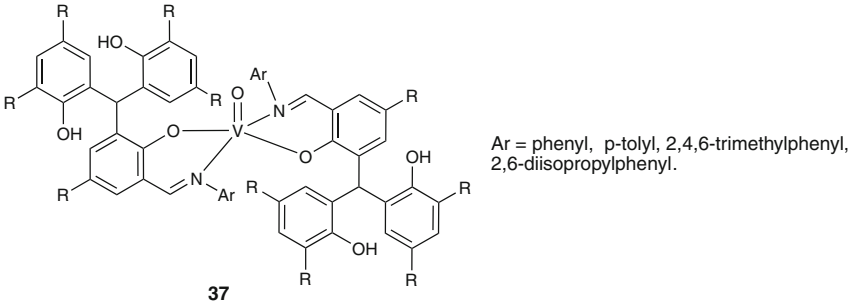


**Fig. 4.25** Pro-catalysts of the type **37**

co-catalysts. However, the use of DMAC did produce a system with appreciable activity. The catalytic system exhibited good thermal stability, whereby the activity was seen to increase over the temperature range 0–80 °C. The activity

increased from around about 2,000 to an activity in the region of 25,000 g/mmol h bar, but this was accompanied by a dramatic fall off in polymer molecular weight, down from 524,000 at 0 °C to 59,400 at 80 °C ($M_w/M_n$ remained relatively constant ≤4.8). Increases in the [Al]:[V] ratio beyond 16,000 led to big increases in the $M_w/M_n$ value (≥10), suggesting that completing processes were taking place leading to loss of single-site catalysis. A value of [Al]:[V] of 8,000:1 was found to be optimum for catalytic performance. It proved important to maintain the value of the [Al]:[V] ratio above 2,000:1 presumably so that the co-catalyst was able to carrying out its function as a scavenger. Changing the aniline precursor had an effect upon the catalytic activity, with bulkier anilines producing higher observed activities.

EPR studies were conducted on pro-catalyst **37** (where Ar = 2,6-*i*$Pr_2C_6H_3$) when mixed with $AlR_3$ or $AlR_2Cl$ (R = Me, Et) with and without ETA present. Initially at temperatures around −60 to −70 °C, signals interpreted as adducts of the form $[(L^{/})_2V(O)(AlR_3)]$ and $[(L^{/})_2V(O)(AlR_2Cl)]$ were found (see for example Fig. 4.26). At 20 °C, it was proposed that with $AlR_3$ (±ETA), complexes of the form $[L^{/}V(O)(R)(AlR_3)]$ ($L^{/}$= modified '*C*-capped' ligand) were formed. In the case of $AlR_2Cl$ (±ETA), complexes of the form $[L^{/}V(O)(R)(AlR_2Cl)]$ were proposed. It was shown that systems of the type **37**/$AlR_3$/ETA were inactive, whereas **37**/$AlR_2Cl$/ETA was moderately active, and there was a correlation between the concentration of vanadium(IV) alkyl halide present and the observed activity; however, most vanadium present was thought to exist as EPR silent vanadium(III) species. The observed drop in activity with time was accompanied by a loss in

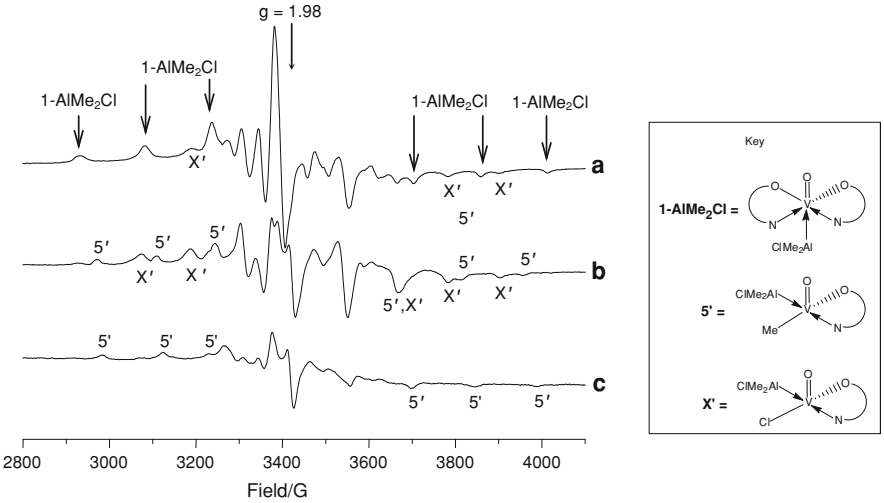


**Fig. 4.26** EPR spectra (−196 °C) of a sample of **37**/$AlMe_2Cl$/ETA (1:100:100; [1] = 5 × $10^{-3}$M) in toluene **a** 10 min after mixing at −60 °C; **b** a further 10 min at −20 °C; **c** a further 10 min at 20 °C. Reproduced with permission from Ref [40]

activity and reduction of V(IV) to V(III), which suggested V(IV) species were the active species. There was no evidence of the formation of V(II) complexes [40].

Use of the imido precursor [V(N*p*-tolyl)(O*n*Pr)$_3$] and the ligand $\mathbf{L^1H_3}$ bearing the aryl group $C_6H_3$*i*Pr$_2$-2,6 led, following work-up in acetonitrile, to the poorly soluble dimeric complex [{V(N*p*-tolyl)($\mathbf{L^1H}$)}$_2$($\mu$-O*n*Pr)$_2$] (**38**, Fig. 4.27, left). Both vanadium centres are distorted trigonal bipyramidal with the '*C*-capped' ligand binding in chelating aryloxide fashion. The phenoxyimine motif is not part of the metal coordination sphere, but rather is involved in intramolecular hydrogen bonding. The activity of this pro-catalyst, in the presence of DMAC (5,000 equivalents) as co-catalyst and with ETA as re-activator, was found to be 6,800 g/mmol h bar; $M_w$ 236,000 and poly-dispersity index 2.4.

It proved possible to isolate a second complex **39** from the acetonitrile mother liquor. This second complex turned out to be bi-metallic (Fig. 4.27, right) and possessed two very different vanadyl centres, each linked via a bridging oxo ligand. The coordination geometry at the near tetrahedral vanadyl centre was completed by mono-dentate aryloxo ligation from each of the '*C*-capped' ligands present. In the case of the distorted octahedral centre, the coordination was completed by two phenoxyimine groups. Interestingly, whilst there were no *p*-tolyl groups present, an exchange had occurred such that the imine aryl groups were now *p*-tolyl as opposed to the original $C_6H_3$*i*Pr$_2$-2,6. Screening of the complex using DMAC/ETA led to an observed activity of 5,200 g/mmol h bar, with $M_w$ 262,000 and $M_w/M_n$ 2.5.

Use of an excess of diamine in the equation shown in Fig. 4.24 led to the formation of a *C*-capped ligand $\mathbf{L^2H_3}$ bearing a pendant benzimidazolyl group (as in Fig. 4.28). On treatment with half an equivalent of [VO(O*n*Pr)$_3$], the bis(phenoxyimine) vanadium(IV) complex **40** (Fig. 4.29) was isolated. Screening of this

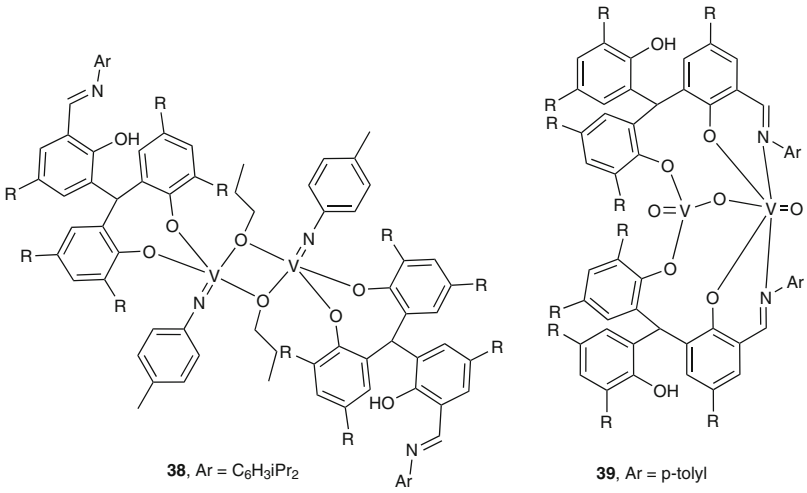


**Fig. 4.27** Pro-catalysts **38** and **39**

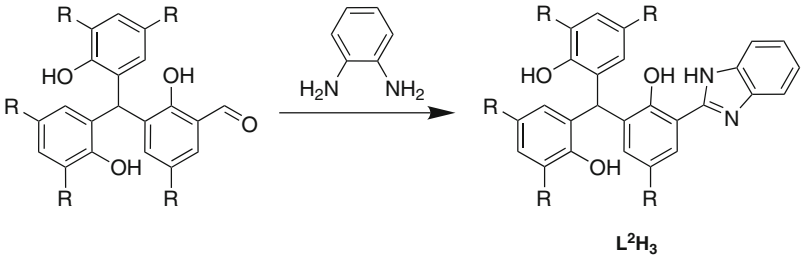


**Fig. 4.28** Synthesis of the benzimidazolyl containing ligand $\mathbf{L^2H_3}$

**Fig. 4.29** Pro-catalyst **40**

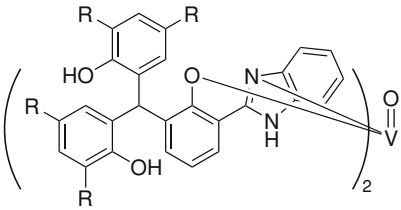


**40**

pro-catalyst for ethylene polymerization using DMAC/ETA at 45 °C, produced an observed catalytic activity of 3,000 g/mmol h bar and polymer molecular weight ($M_w$) of 230,000 ($M_w/M_n$ 2.3).

### 4.4.1.2 Tri-Dentate Salicylaldiminato/Phenoxyimines

A number of tri-dentate Schiff-base ligands were deprotonated using NaH and subsequently treated with $[VCl_3(THF)_3]$ at room temperature to afford vanadium(III) complexes of type **41** (Fig. 4.30). Similar procedures were used to prepare the complexes **42** and **43** (Fig. 4.31). In all of these complexes, the tri-dentate ligand binds in *meridional* fashion, with the chlorides in mutually *trans* positions. In the presence of $Et_2AlCl$ and ETA, these pro-catalysts proved to be thermally stable and highly active. Both the nature of the pendant donor group and the screening temperature had an influence on the observed catalytic activity. In the series of type **41**, phosphorus, nitrogen or sulfur donors performed better than do oxygen donors. Within the nitrogen series, that bearing a pyridylmethyl function possessed the highest activity (15,600 g/mmol h bar). Overall the best activity was achieved using pro-catalyst **43** at 50 °C (20,640 g/mmol h bar). Increasing the temperature led to reductions in polymer molecular weight, but did little to affect the PDIs, which remained in the range 1.9–3.0. Such behavior is in stark contrast to that of the bi-dentate Schiff-base systems described previously (Sect. 4.4.1.1), which suggests that the donor groups are helping to stabilize the active species present. Lifetime studies revealed that whilst the systems containing *O* or *N* donors

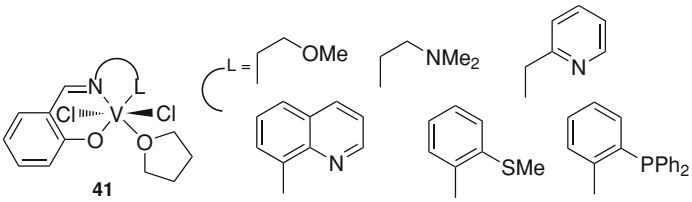


**Fig. 4.30** Pro-catalysts of the type **41**

**Fig. 4.31** Pro-catalysts of the type **42** and **43**

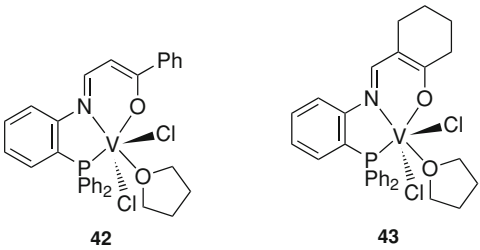


lost in excess of 70% of their activity over 30 min, those containing the softer *S* or *P* donors lost only around 30% [41].

Co-polymerizations of ethylene with 1-hexene or with norbornene, in the presence of $Et_2AlCl$, were also investigated. As for the homo-polymerization of ethylene, high activity and a uni-modal molecular weight distribution of products was evident. Structure–activity relationships were also noted, for example, complexes bearing a nitrogen donor led to high molecular weight products ($M_w$ up to 138,000) for ethylene/1-hexene co-polymerization. The ethylene/1-hexene co-polymer microstructure was determined using $^{13}C$ NMR spectroscopy in $o$-$C_6D_4Cl_2$ at 135 °C. At 3 mol% co-monomer incorporation, the hexene units were isolated between ethylene units, whereas once the incorporation level reached 12.9 mol%, a block sequence of hexene (labeled $\alpha\alpha$) was present. In the case of ethylene/norbornene co-polymerization, the highest activity (17,280 g/mmol h bar) was observed for the type **41** system bearing the phosphorus donor. All ethylene/norbornene co-polymers were of high molecular weight ($M_w$ up to 164,000), with the highest molecular weights obtained using those pro-catalysts bearing a soft donor atom.

### 4.4.1.3 Tetra-Dentate Salicylaldiminato/Phenoxyimines

The tetra-dentate [*O*,*N*,*N*,*O*] salen ligands $\mathbf{L^3H_2}$ (Fig. 4.32), for which the backbone was either ethylene ($-CH_2CH_2-$) or cyclohexylene ($-C_6H_{10}-$), suspended in dichloromethane, were treated with one equivalent of $VCl_4$ to afford dark green 6-coordinate vanadium(IV) dichloride products [$VCl_2(L^3)$] (**44**) [42]. Subsequent screening for ethylene polymerization of these *trans*-dichloride pro-catalysts using

the co-catalysts $EtAlCl_2$, $Et_2AlCl$, $Et_3Al$ or MAO, revealed that the most efficient (activity ≤1,000 g/mmol) systems were accessible when using $EtAlCl_2$ as co-catalyst, the proposed reasons (nature of the ion-pairing) for which were akin to those described by Wang and Nomura for their (arylimido)(aryloxo)vanadium systems (Fig. 4.33) [43].

The presence of a cyclohexylene bridge in the parent ligand set (**46**, Fig. 4.34, right) led to enhanced activity (cf. **45**, 4.34, left), but made little difference to the polymer properties. In all cases, high molecular weight, linear polyethylene was obtained, with very broad molecular weight distribution (≤28.9), which was indicative of multiple active species. Variation of the *ortho* and *para* substituents on the phenolic ring of the ligand set also led to the observation of structure–activity relationships. In particular, the presence of electron withdrawing groups at the *para* position (e.g. Br or Cl) or electron donating substituents at the *ortho* position (e.g. *tert*-butyl, OMe) generally led to enhanced activity.

Comparison with the Fujita FI (phenoxyimine) systems revealed similar activities which suggested that the tetra-dentate-based systems must undergo a rearrangement of the *trans*-disposed chlorines to afford a system which is more catalytically favorable [44–46].

$^1$H NMR (and FTIR) analysis of the polymer produced from **45**/$Et_2AlCl$ revealed only vinyl end groups, consistent with $\beta$-hydrogen transfer to the metal or monomer. For **46**/$EtAlCl_2$, there was also a small methylenoxy peak ($\delta$ 3.57 ppm), suggesting that the increased Lewis acidity of this co-catalyst was also allowing some chain transfer to aluminum to occur [47].

The salen-type complex ethylene(5-chlorosalicylideneiminato)vanadium dichloride **45** has been supported on $MgCl_2(THF)_2$ or $MgCl_2(THF)_2/Et_nAlCl_{3-n}$ ($n = 1$–3; [Mg]:[Al] molar ratio 1:2). Ethylene polymerization screening, conducted in the presence of a variety of organoaluminum co-catalysts, revealed that for the Mg-immobilized system, co-catalyst efficiency followed the order $Et_2AlCl$ > MAO > $EtAlCl_2$. The Mg-supported system was six times more active in *n*-hexane than in toluene with either $Et_2AlCl$ or MAO. The magnesium support was thought to improve the resistance of vanadium to reduction. In the case of the Mg/Al support,

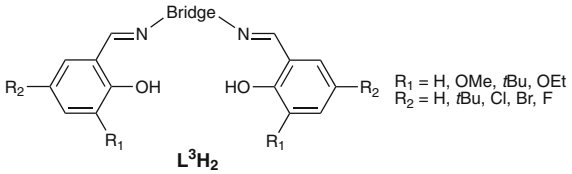


**Fig. 4.32** Salen ligands of the type $\mathbf{L^3H_2}$

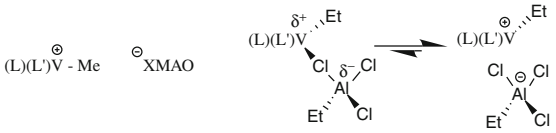


**Fig. 4.33** Nature of the ion-pairing for different co-catalysts

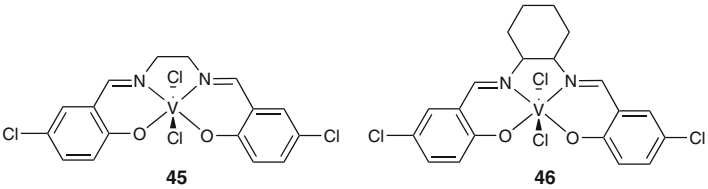


**Fig. 4.34** Pro-catalysts **45** and **46**

MAO was the preferred co-catalyst. Despite being the most favored co-catalyst for the non-immobilized system, $EtAlCl_2$ proved to be the worst co-catalyst for both supported systems. Each type of support also had a different response to an increase in the temperature of the polymerization run. For the Mg-supported system, a decrease in activity was observed, whereas the Mg/Al-supported system showed an increase, peaking at 60 °C. Both an increase in the pressure and the [Al]:[V] molar ratio, led to improved activity, and both systems exhibited extended lifetimes, with activity being observed well beyond 2 h. The polyethylene product was linear (M. Pt > 135 °C), and had broad PDI (≥15). Particle size distribution was bi-modal for the Mg/Al-supported catalyst at 60 °C, with the majority of particle sizes at 0.3 (46%) and 0.6 mm (34%).

The related 1,2-cyclohexylene(5-chlorosalicylideneiminato)vanadium dichloride **46** when supported (via a co-milling procedure) on magnesium chloride (formed on addition of $Et_2AlCl$ to the adduct $MgCl_2 \cdot 3.4$ethanol) was highly active for ethylene polymerization and ethylene/1-octene co-polymerization at 50 °C. Highest activity was obtained using MAO as co-catalyst. As in the previously mentioned ethylene system **45**, use of halogenated co-catalysts in conjunction with the supported system led to disappointing results. Both supported and unsupported systems yielded linear polyethylene, with a wider spread of molecular weights noted for the former. Polyethylene grain size for the supported system varied with co-catalyst. Over 70 wt% of the grains measured over 2 mm when trialkylaluminums were used, whereas grains of either 0.3 or 0.4 mm were in excess with MAO. As for **45**, use of a support led to increased thermal stability and higher observed activity values, though these were at the expense of molecular weight, which followed the reverse trend.

This supported system was also shown to be capable of ethylene/1-octene co-polymerization, with a maximum of about 4.5 mol% co-monomer incorporation achieved at a co-monomer concentration of 1.82 mol/L Both the polymer molecular weight and the crystallinity thereof, decreased with increasing co-monomer concentration. SEM micrographs of the supported vanadium pro-catalyst particles revealed a regular, though not spherical structure, for which the particle surface was porous.

Use of 0.5 equivalents of the diamine (Fig. 4.35) led to a bis-imine bridged ligand set $\mathbf{L^4H_6}$, which on further reaction with an equimolar amount of $[VO(O\mathit{n}Pr)_3]$ led to the complex $[VO(\mathbf{L^4H_4})]$ **47** (Fig. 4.36, left), possessing a

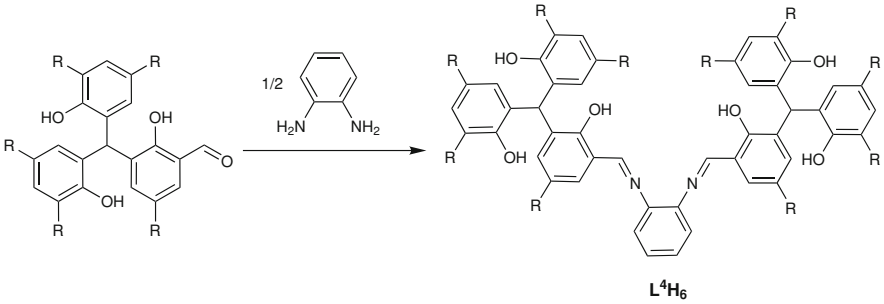


**Fig. 4.35** Preparation of the bis-imine bridged ligand $\mathbf{L^4H_6}$

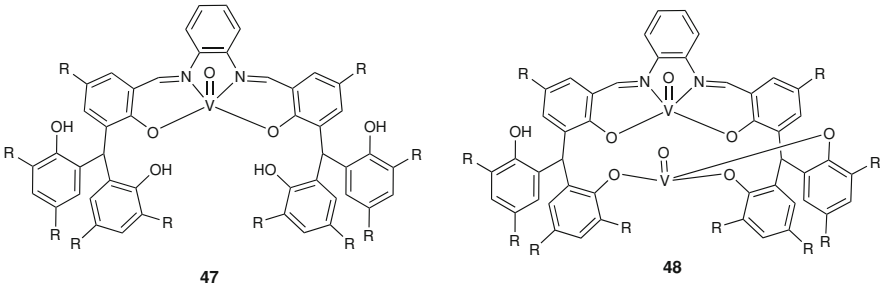


**Fig. 4.36** Pro-catalysts **47** and **48**

square-based pyramidal vanadium(IV) centre. The phenoxyimine groups bind in a *cis* fashion due to the constraints imposed by the ligand, leaving four uncoordinated phenolic groups. The activity of this pro-catalyst (using DMAC/ETA) was about 2,500 g/mmol h bar, with a corresponding polymer molecular weight ($M_w$) of 245,000 and an $M_w/M_n$ of 2.4.

If the amount of [VO(O*n*Pr)$_3$] was increased such that the reaction was now 1:2 ($\mathbf{L^4H_6}$:V), the product isolated contained two vanadyl centres, see **48** (Fig. 4.36, right). The second vanadyl group was bound to three of the previously uncoordinated phenolic groups affording a tetrahedral geometry at vanadium. Screening of this pro-catalyst under the same conditions as for **47** led to an activity of 4,200 g/mmol h bar ($M_w$ 293,000; $M_w/M_n$ of 2.2), which was suggestive of a possible cooperative effect (cf. **47**) [39].

## *4.4.2 β-Enaminoketonato*

Reaction of [VCl$_3$(THF)$_3$] with one equivalent of the lithium salt of the parent *β*-enaminoketonate ligand led to the isolation of the essentially octahedral

**Fig. 4.37** Pro-catalysts **49–51**

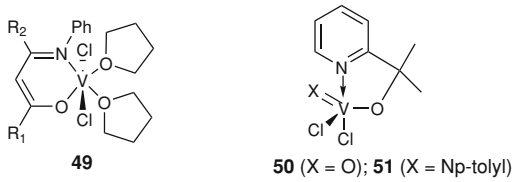


a) R1 = Ph, R2 = $CF_3$; b) R1 = tBu, R2 = $CF_3$;
c) R1 = $CF_3$, R2 = $CH_3$; d) R1 = Ph, R2 = $CH_3$;
e) R1 = Ph, R2 = H

complexes **49a–e** (Fig. 4.37, left). Ethylene polymerization screening conducted using $Et_2AlCl$ as co-catalyst and ETA as re-activator led to activities in the order **b** > **d** ≈ **a** > **c** ≈ **e**. All the polymers isolated were of high molecular weight with little branching and PDIs in the range 2.3–3.0. Varying the [Al]:[V] molar ratio affected the observed activity, with the peak activity attained at a ratio of ca. 4,000:1. The polymer molecular weight decreased almost linearly with increasing [Al]:[V] molar ratio. Similarly, increasing the temperature of the polymerization run led to a peak in activity at 50 °C, whilst polymer molecular weight decreased in an almost linear fashion [48].

These pro-catalysts are also capable of co-polymerizations. For ethylene/norbornene (NBE), pro-catalyst **e** exhibited the highest activity (6,840 g/mmol h), and **c** the lowest (2,760 g/mmol h); the NBE content remained constant. If the NBE level in the feed was raised; however, then the degree of incorporation increases and a maximum incorporation of 39.43% was observed. This increased incorporation though was at the expense of a decrease in activity. Variation of the [Al]:[V] molar ratio had little affect on the NBE incorporation, but did affect the activity. The temperature also affected activity with maximum observed activity at 50 °C, whilst slight decreases in NBE content were noted as the temperature was raised. Polymer analyses revealed a uni-modal distribution of molecular weight of high molecular weight products, for which the NBE was incorporated either in isolation or in alternation with ethylene units.

In the case of ethylene/1-hexene co-polymerization, the pro-catalyst **a** exhibited the highest activity (5,820 g/mmol h); however, this was lower than that observed for $[VCl_3(THF)_3]$ (6,000 g/mmol) under the same conditions. Pro-catalysts **49a–e** showed no obvious differences in the degree of 1-hexene incorporation, though the incorporations (and the molecular weights) were far higher than that observed for $[VCl_3(THF)_3]$. Increasing the 1-hexene concentration in the feed led to an initial increase and then a dramatic decrease in activity, whilst the 1-hexene incorporation increased in an essentially linear fashion over the range studied. Variation of the [Al]:[V] molar ratio led to a maximum activity of 2,640 g/mmol h at an [Al]:[V] ratio of 3,000:1. The degree of 1-hexene incorporation, molecular weights and the molecular weight distributions remained constant. Polymer analysis revealed that no hexene block sequences were present.

### 4.4.3 Pyridine Alkoxide

The oxo and organomido pro-catalysts **50** and **51** (Fig. 4.37, right) were prepared by treatment of the appropriate vanadium(V) trihalide [V(X)$Cl_3$] (X = O, N*p*-tolyl) and the lithium salt of the pyridylalkoxide. $^1$H NMR data suggested that for both **50** and **51**, the chelate ligand binds in $\eta^2$-*O*,*N* fashion to the metal center. Ethylene polymerization screening was conducted (30 or 50 °C, 6 bar ethylene) using $Et_2AlCl$ (20 equivalents) as co-catalyst. The oxo pro-catalyst **50** exhibited moderate activity (88 g/mmol h bar at 50 °C); however, this was somewhat lower than that observed under the same conditions for the chelate-free complex [$VOCl_2$(O*i*Pr)] (182 g/mmol h bar). It was suggested that the presence of the donor *N* either contributes to increased electron density at vanadium thereby stabilizing the complex or that it blocks/occupies a required coordination site [49]. The performance of the organoimido complex **51** was far poorer (<2 g/mmol h bar), which was ascribed to its inability to form a Lewis adduct with aluminum akin to that often postulated for oxo species.

## 4.5 *N*,*O*,*S*-Penta-/Hexa-Dentate Salicylaldiminato/Phenoxyimines

The softer second row donor sulfur has proved beneficial when employed in the backbone of a number of chelate ligands for group IV systems [50–53]. Further, Miyatake and more recently Sabota et al. have reported the use of similar chelate ligands in vanadium-based systems [54, 55]. The combination of an imine and a sulfur donor within one ligand set was thus an attractive target. With this in mind, the ligand $\mathbf{L^5H_2}$ (Fig. 4.38, left) was synthesized by an adaptation of the method of Rajeskhar et al. [56]. When $\mathbf{L^5H_2}$ was treated with [V(X)$(OR)_3$] (X = O,

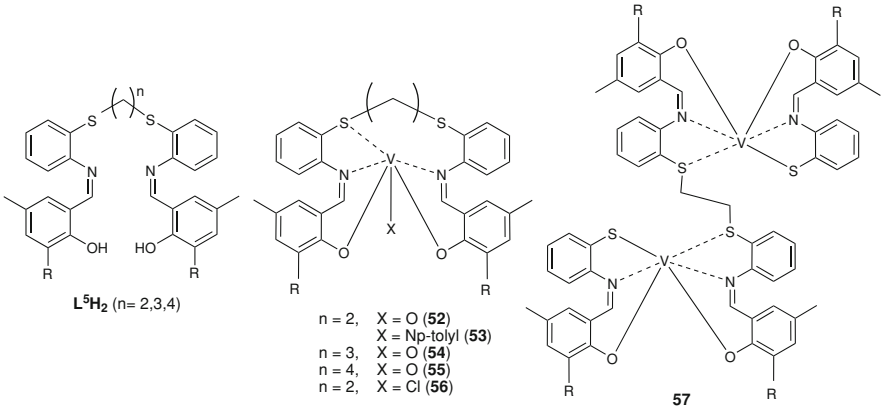


**Fig. 4.38** Ligand $L^5H_2$ and pro-catalysts **52–57**

R = *n*Pr; X = N*p*-tolyl, R = Et), complexes of the form [V(X)$\mathbf{L^5}$] (**52**–**55**) were isolated (Fig. 4.38, middle). Crystallographic studies revealed octahedral coordination at vanadium, with the sixth site occupied by one of the bridging thioether groups. In the case of $n = 2$, carrying out the reaction in the presence of DMAC led to the formation of the vanadium(III) complex **56**. Prolonged reaction of $\mathbf{L^5}H_2$ with [V(N*p*-tolyl)$(OEt)_3$] led, via oxidative cleavage of the C–S bond, to the bimetallic complex **57** (Fig. 4.38, right). Complex **57** was also accessible, in higher yield, via use of the reduced form of $\mathbf{L^5H_2}$ (i.e. a bis(phenoxyamine)) and [VO(O*n*Pr)$_3$] [57].

For comparative purposes, these pro-catalysts were screened alongside the Fujita type phenoxyimine-based pro-catalysts **29** and **30** (see Sect. 4.4.1.1, Fig. 4.18). Both **29** and [V(Cl)'$\mathbf{L^5}$] exhibited similar catalytic activity (ca. 11,000 g/mmol h bar), whereas comparison with **30** (8,000 g/mmol h bar) suggested the higher activity of [V(Cl)'$\mathbf{L^5}$] could be attributed to the additional $\pi$-donation from the bridging sulfur. Variation of n revealed a preference for a 1,3-propanediyl (i.e.$n = 3$) bridge in terms of observed activity. Polymer molecular weights were in the range 160,000–206,000. The use of TMA or MAO as co-catalyst instead of DMAC proved to be ineffective. Rather surprisingly, the presence of ETA did not improve the performance of this catalyst system.

These pro-catalysts were also capable of ethylene/1-hexene co-polymerization with activities of up to 1,200 g/mmol h bar, and $C_6$ incorporation of between 5.1 and 13.6 mol%. In the case of pro-catalyst **52** (Fig. 4.38, middle), it was noted that a minimum of 3,200 equivalents of 1-hexene (to vanadium) was needed to simply prevent only polyethylene formation. Any increase in the amount of 1-hexene above the 3,200 equivalents level was found to be detrimental to polymer molecular weight, whilst at 8,000 equivalents, no material was recovered. Activity and molecular weight were also found to decrease by an order of magnitude on increasing the temperature from 25 to 45 °C. Co-polymer analysis by $^{13}C$ NMR spectroscopy and microstructure assignment using the method of Hsieh and Randell, [58] was consistent with long chains of polyethylene with isolated hexane units (1 unit of hexane per 10 units of ethylene).

## 4.6 Other

### *4.6.1 Ketimide*

1-Adamantylimido vanadium ketimide complexes, unlike their arylimido counterparts, can be readily isolated from $VOCl_3$, the isocyanate and the lithium salt of the ketimide. Evaluation of type **58** complexes (Fig. 4.39) as pro-catalysts for the polymerization of ethylene in the presence of MAO, led to an observed catalytic activity order of N = C*t*Bu$_2$ (516 g/mmol h) > N = C(*t*Bu)Ph (300 g/mmol h) > N = CPh$_2$ (105 g/mmol h) > N = C(*t*Bu)CH$_2$SiMe$_3$ (70.8 g/mmol h). The general trend for these moderate activities suggested an influence from the electronic

properties of the ketimide ligand. The polymer products possessed bi-modal molecular weight distributions [59].

A crystal structure determination (see Fig. 4.40) of the N = C*t*Bu$_2$ analogue confirmed the distorted tetrahedral geometry at the metal. Purification of the N = CPh$_2$ derivative required extraction into dichloromethane, however this was accompanied by a gradual decomposition to the dimeric complex [N(Ad)H$_3$] [V$_2$($\mu_2$-Cl)$_3$Cl$_2$(NAd)$_2$(N=CPh$_2$)$_2$].

### 4.6.2 Tris(3,5-dimethylpyrazolyl)borato (Tp*)

The tris(3,5-dimethylpyrazolyl)borato (Tp*) arylimido complex [Tp*V(NAr)Cl$_2$] (**59**, Ar = 2,6-*i*Pr$_2$C$_6$H$_3$), prepared via the addition of ArNCO to [VOCl$_3$] and subsequent treatment with KTp*, was characterized by X-ray crystallography. The Tp* ligand was bound *facially* to a distorted octahedral vanadium centre. The ligands *cis* to the bulky imido group were all found to bend away somewhat (towards N(7)) such that the vanadium centre was 0.1,871(3) Å out of the Cl(1), Cl(2), N(1) and N(6) plane. This pro-catalyst was active for ethylene as well as propylene polymerization. Screening using MAO (1,000 equivalents) at ambient temperature and 1 bar pressure led to an activity (for ethylene) of 14 g/mmol h, and a product with $M_w$ 47,000 and $M_w/M_n$ 3.0. In the case of propylene (7 bar),

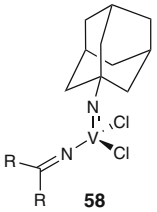


**Fig. 4.39** Pro-catalysts of the type **58**

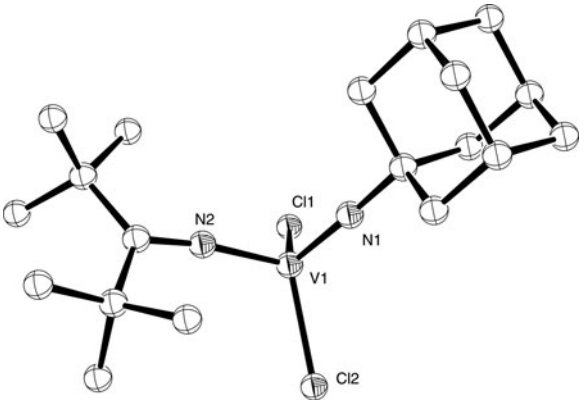


**Fig. 4.40** Crystal structure of pro-catalyst **58** (R = *t*Bu). Reproduced with permission from Ref [59]

the product formed was mostly atatic, with a slight excess of *r* diads consisting of low molecular weight ($M_w$ 3,800, $M_w/M_n$ 2.0) regio-regular chains. Isopropyl end groups were suggestive of 1–2 insertions of propylene into the V–Me groups. The activity for propylene polymerization though was low at 1 g/mmol h bar [60].

The bulky (3-Ms-pyrazolyl)$_2$(5-Ms-pyrazolyl)borate *tert*-butylimido vanadium(V) complex **60** (Ms = 2,4,6-trimethylphenyl) has been immobilized on a number of different inorganic supports such as $SiO_2$, MAO modified $SiO_2$, MgO, $MgCl_2$, $SiO_2$–$Al_2O_3$ and MCM-41 (an aluminosilicate possessing weak acidity) [61]. The V-content in these supported systems was found to be in the range 0.054–0.098 mmolV/g.support, with the highest value observed when using the $SiO_2$–$Al_2O_3$ or MCM-41 support. Given that the MAO-modified support used still possessed unreacted silanol groups, immobilization of vanadium was possible at both silanol as well as MAO sites, for example as depicted in Fig. 4.41. Analysis by XRF showed that such an MAO-modified surface possessed a higher preference for type **60** complexes than did unmodified $SiO_2$.

Screening (30 °C in hexane) of these supported systems using MAO or MAO/TiBA (1:1) ([Al]:[V] = 1,000:1) resulted in activities in the range 8–88 g/mmol h. In the case of MAO, the highest activity was achieved using $SiO_2$. Use of MAO/TiBA (1:1) further increased activity; the TiBA increases the aliphatic solvent polarity and enhances the solubility through modification of the MAO. In general, the use of acidic or basic supports led to less active systems. In all cases, the activities are far lower than those observed for their homogenous counterparts.

For example, pro-catalyst **60** and the 2,6-diisopropylphenylimido derivative **61** were screened for ethylene polymerization using MAO or MAO/TiBA as co-catalysts, using either hexane or toluene as solvent. Results in toluene were poor, which was ascribed to the competitive coordination of the toluene versus ethylene. In hexane, pro-catalyst **60** was most active (1,460 g/mmol h), with optimum conditions of 30 °C and 2,000 equivalents of MAO/TiBA as co-catalyst. The product as measured via viscosity-averaged molecular weights in decaline at 165 °C, was ultra high molecular weight polyethylene [62].

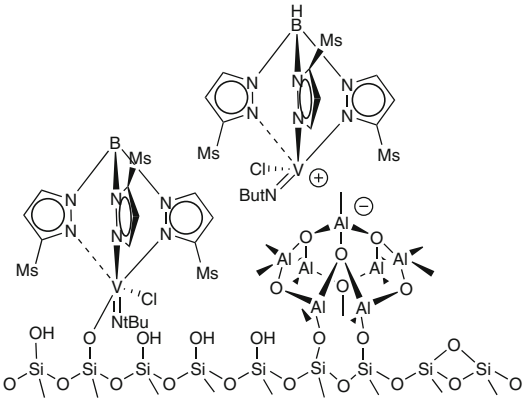


**Fig. 4.41** Immobilization of **60** on MAO-modified silica

In the case of the supported systems, the lack of a favorable correlation between high activity and increased V content was thought to be due to likely bi-molecular deactivation when high concentrations of V are present. However, in the case of the $SiO_2$–$Al_2O_3$ support, X-ray emission spectra (used to measure the spatial distribution of V) depicted a non-uniform V distribution, which taken together with the XRF measurements (which showed a comparable V-content for the $SiO_2$/MAO-4.5 wt% Al and $SiO_2$–$Al_2O_3$ supports) suggested the acidic nature of the support was the likely culprit of the poor activity. Lower vanadium loadings, of the order of 0.05 wt%, also disfavored bi-molecular deactivation reactions. In situ immobilization resulted in activity values of up to five times higher (as high as 352 g/mmol h) when using $SiO_2$/MAO as support. No such increase was obtained when using only an $SiO_2$ support. DSC measurements gave melting points in the range 132–140 °C, whilst GPC data showed the polyethylene to be ultra-high molecular weight. Scanning electron microscopy (SEM) of the various supported systems showed near retention of the spherical particle morphology.

Tris(3,5-dimethylpyrazolyl)methane ($Tp^{/}$) vanadium(IV) complexes **62** (Fig. 4.42) are accessible via treatment of the imido precursors $[V(NR)Cl_2(NHMe_2)_2]$ (R = 2,6-$C_6H_3$*i*$Pr_2$, 2-$C_6H_4$*t*Bu, 2-$C_6H_4CF_3$, *t*Bu, adamantyl) with $Tp^{/}$ in benzene at 80 °C for 6 h. The products $[Tp^{/}V(NR)Cl_2]$ are monomeric with *facially* bound $Tp^{/}$ ligands and near linear imido groups.

Screening in the presence of MAO (1,500 equivalents) at ambient temperature afforded activities ≤30 g/mmol h bar. There was no sign of activity when $Et_2AlCl$ (1,000 equivalents) was employed as co-catalyst. Within the series, some structure–activity trends were observable, for example, those complexes bearing an arylimido substituent were three to five times more productive than the *tert*-butylimido derivative. The bulkiest 2-$C_6H_4$*t*Bu derivative performed best, and the resulting polymer had a bi-modal molecular weight distribution. The majority (80 wt/mol%) was a low molecular weight fraction, which had a narrow distribution ($M_w/M_n$ 1.3), whereas that at higher molecular weight was broader ($M_w/M_n$ 5.3). $^1H$ NMR analysis of the low molecular weight fraction was consistent with an $M_n$ of about 800. From this, and the observation that 35% of the chains were terminated by vinyl groups, it was concluded that whilst chain transfer to monomer is significant; transfer to aluminum is dominant [63].

**Fig. 4.42** $Tp^{/}$ pro-catalyst **62**

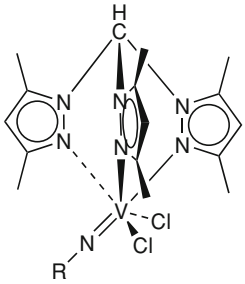


**62**

### 4.6.3 Phthalocyanine

Vanadyl phthalocyanine and porphyrin complexes of the type **63** and **64** (Fig. 4.43) have been screened for α-olefin polymerization in the presence of either MAO or $EtAlCl_2$. The better performance of the napthalocyanine complex **63** compared with **64** was thought to be due to favorable solubility of the former in the polymerization medium. Although a number of alkenes were screened using **63**, it proved possible only to polymerize ethylene at room temperature. The product formed was linear polyethylene as evidenced by $^1$H NMR and DSC. At higher reaction temperatures (120 °C) with MAO as co-catalyst, co-polymerization with propylene or 1-decene proved possible, with co-monomer incorporations of 13 and 7.4%, respectively. Other experiments suggested that complete dissociation of the phthalocyanine ligand does not occur in these polymerizations [64].

### 4.6.4 (2-Anilidomethyl)pyridine

Arylimidovanadium(V) dichlorides of the type **65** (Fig. 4.44, left) were shown to adopt a distorted trigonal bipyramidal geometry at vanadium with the nitrogen atoms of the pyridine and imido group occupying the axial positions. Screening at 25 °C in toluene using MAO (from which $Me_3Al$ had been removed), revealed that the [Al]:[V] molar ratio played an important role in the observed catalytic activity. For the R = Me or *i*Pr derivatives, activity was optimized at 300 equivalents of MAO, whereas for the R = F derivative, 1,000 equivalents was the preferred option. In the case of the R = F derivative, a lowering of the temperature to 0 °C also favored higher activity, whereas elevation of the temperature above 50 °C was detrimental in terms of activity and catalyst stability. Use of $Et_2AlCl$ as

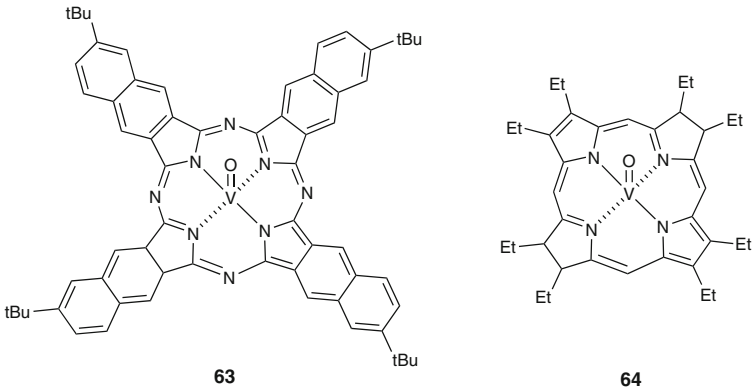


**Fig. 4.43** Vanadyl phthalocyanine and porphyrin complexes of the type **63** and **64**

co-catalyst at 0 °C produced a lower activity for the R = F derivative (156 g/mmol h) compared to the R = Me (840 g/mmol h) and R = *i*Pr (3,780 g/mmol h) derivatives. The optimized activity (0 °C, 200 equivalents of co-catalyst) for the R = Me derivative was 6,000 g/mmol h [65].

In the case of MAO as co-catalyst, the polymer products possessed high molecular weights with $M_w$ in the range 1,000,000–3,000,000 with mono-modal molecular weight distributions. The $M_w$ values for the 2,6-$F_2C_6H_3$ derivative were found not to change on varying the [Al]:[V] molar ratio, but were affected by changing the anilide substituents. High molecular weight polymers also resulted from the use of $Et_2AlCl$ as co-catalyst, with molecular weights in the range 1,720,000–3,520,000 at 0 °C.

The imidovanadium(V) complexes **66** (Fig. 4.44, right) bearing (2-anilidomethyl)pyridine ligation, are readily available via the reaction of $[V(NL)Cl_3]$ with $Li[2\text{-}ArNCH_2(C_5H_4N)]$. Each adopts a distorted trigonal bipyramidal geometry at vanadium, for which the mutually *trans* pyridine and imido nitrogens are axial. In the presence of MAO, the adamantyl derivatives with R = Me or *i*Pr exhibited excellent activities for ethylene dimerization, leading to 1-butene with high selectivity. Changes to the [Al]:[V] molar ratio impacted on the activity of the system as did the pressure, though variation of neither parameter significantly affected selectivity. The system performed best at near ambient temperatures, whereas activity decreased at either 0 or 50 °C. Under optimized conditions, an observed activity of 76,500 g/mmol h (TOF: 2,730,000 $h^{-1}$ or 758 $s^{-1}$) was achieved with a 97.0% selectivity for 1-butene. Use of methylisobutylaluminoxane (MMAO) as co-catalyst also led to appreciable activity and selectivity. The introduction of an *ortho*-methyl group on the arylimido substituent produced a system which, under the same conditions, only afforded trace amounts of products. For such a system, it proved necessary to increase the catalyst concentration, whereupon a mixture of 1-butene and polyethylene was isolated. Use of cyclohexyl- or phenylimido derivatives also led to high activity systems, affording predominantly 1-butene. The activity for this family of pro-catalyst followed the trend adamantyl > cyclohexyl > phenyl for the substituent at the imido group. By contrast, use of the 2,6-dimethylphenylimido derivative led to the isolation of only polyethylene [66].

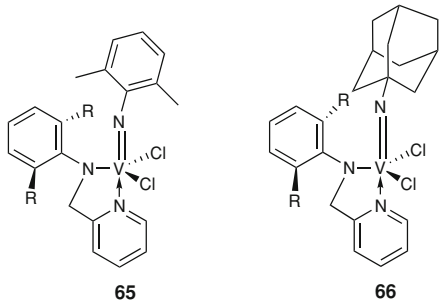


**Fig. 4.44** Pro-catalysts **65** and **66**

### 4.6.5 Quinolinolato

The reaction of imido trichlorides of the form [V(NR)$Cl_3$] with 2-methyl-8-quinolinol (HÔN) afforded the black solids [V(NR)(ÔN)$Cl_2$] (**67**, Fig. 4.45, left), where R = *n*-hexyl (yield ca. 90%) or R = $C_6H_3$*i*$Pr_2$-2,6 (yield ca. 55%). Using MMAO as co-catalyst led to moderate activities (ca. 20 g/mmol h bar) for R = $C_6H_3$*i*$Pr_2$-2,6, producing polymer with a bi-modal distribution of molecular weight. Under similar conditions, for R = *n*-hexyl the observed activity was only ca. 7 g/mmol h bar, but the polymer had a higher molecular weight with a mono-modal molecular weight distribution. The activity of the R = *n*-hexyl was increased by the use of MAO as co-catalyst, or even better by using dried MAO. An [Al]:[V] ratio of only 50:1 proved to be sufficient to bring about activation. Activities were lower when either $Et_2AlCl$ or $Me_3Al$ were employed as co-catalyst. Polymer melting points were in the range 142–147 °C, indicative of highly linear polyethylene [67].

The R = *n*-hexyl derivative also proved to be capable of polymerizing propylene in the presence of MAO or dried MAO, whereas $Et_3Al$ or $Me_3Al$ were ineffective. At ambient temperature, with a ratio of [Al]:[V] of 50:1, the activity was 0.24 g/mmol h bar with an $M_n$ of 172,000 for the atactic polypropylene and $M_w/M_n$ 1.4.

### 4.6.6 Lutidene

The bi-metallic complex **68** (Fig. 4.45, right), prepared from [$VOCl_3$] and the ligand [{calix[4]arene$(OH)_2$($\mu$-OpyO)}$_2$], possesses two trigonal bipyramidal vanadyl centres, for which both vanadyl groups are orientated in the same direction with respect to the lutidene bridge. In the presence of DMAC/ETA, an activity of 10,400 g/mmol h bar was achieved, producing polymer with $M_w$ 113,000 and a narrow molecular weight distribution ($M_w/M_n$ 2.5) with a melting point (135 °C) typical of linear polyethylene [68].

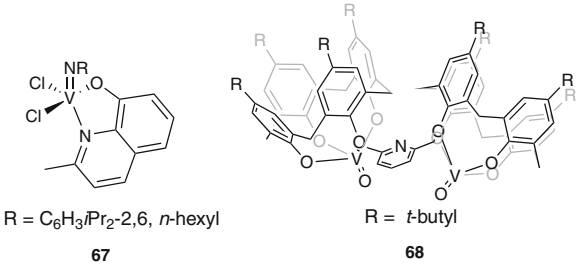


**Fig. 4.45** Pro-catalysts of the type **67** and **68**

## 4.7 Concluding Remarks

Vanadium-based systems are now achieving the kind of catalytic activities at elevated temperatures which make them intriguing academic targets, though they still have some way to go before they can compete industrially with the more established Ziegler–Natta and Phillips catalysts The coordination environment about the vanadium plays a crucial role, and the ease of synthesis and tune-ability of many of the ligand sets allows for systematic studies on the effect of the steric and electronic properties of the ligands and their resulting effect on the reactivity of the corresponding pro-catalysts. From the many pro-catalysts described in this chapter, it is clear that imine-containing ligand sets play a central role, and impact on the polymerization catalysis principally by stabilizing the catalytically active metal centre. The products obtained cover a wide range, for example imidovanadium(V) complexes bearing (2-anilidomethyl)pyridine ligation show a selectivity for 1-butene (via ethylene dimerization), whereas other systems such as phenoxyimines supported on $MgCl_2/Et_mAl(OR)_n$ led to ultra high molecular weight ($M_w > 5{,}000{,}000$) polyethylene. Many of the systems are capable of co-polymerizations, and products resulting from the co-polymerization of ethylene with propylene, 1,3-butadiene, 1-hexene, 1-octene, norbornadiene amongst others have been reported. Quantitative immobilization at low catalyst loadings has also proved possible, and this together with the performances noted at high temperatures, suggests that vanadium-based systems are truly emerging as a promising class of catalysts for α-olefin polymerization.

**Acknowledgments** Dr Simon Lancaster (UEA) is thanked for useful discussions.

## References

1. Sinclair KB, Wilson RB (1994) Metallocene catalysts: a revolution in olefin polymerization. Chem Ind 21:857–862
2. McDaniel MP (1988) Controlling polymer properties with the Phillips chromium catalysts. Ind Eng Chem Res 27(9):1559–1564. doi:10.1021/ie00081a001
3. Hirsekorn KF, Hulley EB, Wolczanski PT, Cundari TR (2008) Olefin substitution in $(silox)_3M(olefin)$ (silox = $tBu_3SiO$; M = Nb, Ta): The role of density of states in second vs third row transition metal reactivity. J Am Chem Soc 130:1183–1196. doi:10.1021/ja074972j
4. Nomura K (2005) Design of new generation vanadium complex catalysts offering new possibilities for controlled olefin polymerization. In: Bevy LP (ed) New developments in catalysis research. Nova Science Publishers Inc 7:199–217. ISBN: 1-59454-440-9
5. See for example, Redshaw C (2010) Vanadium procatalysts bearing chelating aryloxides: structure-activity trends in ethylene polymerization. Dalton Trans 5595–5604. doi:10.1039/b924088h
6. Raspolli Galletti AM, Pampaloni G (2010) Niobium complexes as catalytic precursors for the polymerization of olefins. Coord Chem Rev 254:525–536. doi:10.1016/j.ccr.2009.07.026
7. Milione S, Cavallo G, Tedesco C, Grassi A (2002) Synthesis of α-diimine V(III) complexes and their role as ethylene polymerisation catalysts. Dalton Trans 1839–1846. doi: 10.1039/b105931a

8. Xu, B-C, Hu T, Wu J-Q, Hu N-H, Li Y-S (2009) Novel vanadium(III) complexes with bidentate *N*,*N*-chelating iminopyrrolide ligands: synthesis, characterization and catalytic behaviour of ethylene polymerization and copolymerization with 10-undecen-1-ol. Dalton Trans 8854-8863. doi: 10.1039/b909495d
9. Kim W-K, Fevola MJ, Liable-Sands LM, Rheingold AL, Theopold KH (1998) [$(Ph)_2$nacnac] $MCl_2(THF)_2$ (M = Ti, V, Cr): A new class of homogeneous olefin polymerization catalysts featuring $\beta$-diiminate ligands. Organometallics 17:4541–4543. doi:10.1021/om9806545
10. Brussee EAC, Meetsma A, Hessen B, Teuben JH (1998) Electron-deficient vanadium(III) alkyl and allyl complexes with amidinate ancillary ligands. Organometallics 17:4090–4095. doi:10.1021/om980431e
11. Brussee EAC, Meetsma A, Hessen B, Teuben JH (2000) The *N*,*N'*-bis(trimethylsilyl)pentafluorobenzamidinate ligand: enhanced ethane oligomerisation with a neutral V(III) bis(benzamidinate) alkyl catalyst. Chem Commun 497–498. doi: 10.1039/b000397m
12. Shmulinson M, Pilz A, Eisen MS (1997) Carbon–fluorine bond activation in perfluorobenzonitrile by $LiN(SiMe_3)_2$. Synthesis of $(Me_3Si)_2NC_6F_4CN$-4 and crystal structure of $LiN(C_6F_4CN\text{-}4)_2 \cdot 2C_4H_8O$. Dalton Trans 2483–2486. doi:10.1039/a700682i
13. Liguori D, Centore R, Csok Z, Tuzi A (2004) Polymerization of propene and 1, 3-butadiene with vanadyl(V) monoamidinate precatalysts and MAO or dialkylaluminium chloride cocatalysts. Macromol Chem Phys 205:1058–1063. doi:10.1002/macp.200300234
14. Brandsma MJR, Brussee EAC, Meetsma A, Hessen B, Teuben JH (1998) An amidinate ligand with a pendant amine functionality: synthesis of a vanadium(III) complex and ethene polymerization catalysis. Eur J Inorg Chem 1867–1870. doi: 10.1002/(SICI)1099-0682(199812)1998:12
15. Severn JR, Duchateau R, Chadwick JC (2005) Immobilization and activation of vanadium(III) and titanium(III) single-site catalysts for ethylene polymerization using $MgCl_2$-based supports. Polym Int 54:837–841. doi:10.1002/pi.1779
16. Aharonovich S, Botoshansky M, Tumanskii B, Nomura K, Waymouth RM, Eisen MS (2010) Mono- and bis-amidinate 2,6-xylylimido vanadium chlorides: synthesis, structure and reactivity. Dalton Trans 5643–5649. doi: 10.1039/b925974k
17. Gibson VC, Redshaw C, Solan GA (2007) Bis(imino)pyridines: surprisingly reactive ligands and a gateway to new families of catalysts. Chem Rev 107:1745–1776. doi:10.1021/cr068437y
18. Hanton MJ, Tenza K (2008) Bis(imino)pyridine complexes of the first-row transition metals: alternative methods of activation. Organometallics 27:5712–5716. doi:10.1021/om800744j
19. Colamarco E, Milione S, Cuomo C, Grassi A (2004) Homo- and copolymerization of butadiene catalyzed by an bis(imino)pyridyl vanadium complex. Macromol Rapid Commun 25:450–454. doi:10.1002/marc.200300022
20. Reardon D, Conan F, Gambarotta S, Yap G, Wang Q (1999) Life and death of an active ethylene polymerization catalyst. Ligand involvement in catalyst activation and deactivation. Isolation and characterization of two unprecedented neutral and anionic vanadium(I) alkyls. J Am Chem Soc 121:9318–9325. doi:10.1021/ja990263x
21. Schmidt R, Welch MB, Knudsen RD, Gottfried S, Alt HG (2004) N, N, N-Tridentate iron(II) and vanadium(III) complexes Part I. Synthesis and characterization. J Mol Catal 222:9–15. doi:10.1016/j.molcata.2004.07.014
22. Schmidt R, Welch MB, Knudsen RD, Gottfried S, Alt HG (2004) N, N, N-Tridentate iron(II) and vanadium(III) complexes Part II. Catalytic behaviour for the oligomerization and polymerization of ethene and characterization of the resulting products. J Mol Catal 222:17–25. doi:10.1016/j.molcata.2004.07.015
23. Schmidt R, Welch MB, Palackal SJ, Alt HG (2002) Heterogenized iron(II) complexes as highly active ethene polymerization catalysts. J Mol Catal 179:155–173. doi:10.1016/S1381-1169(01)00333-8
24. Schmidt R, Welch MB, Knudsen RD, Gottfried S, Alt HG (2004) N, N, N-Tridentate iron(II) and vanadium(III) complexes Part III. UV–Vis spectroscopic studies of reactions of ethene-

oligomerization and polymerization catalysts with methyl aluminoxane cocatalyst. J Mol Catal 222:27–45. doi:10.1016/j.molcata.2004.06.026
25. Romero J, Carrillo-Hermosilla F, Antiñolo A, Otero A (2009) Homogeneous and supported bis(imino)pyridyl vanadium(III) catalysts. J Mol Catal A Chem 304:180–186. doi:10.1016/j.molcata.2009.02.010
26. Lang JRV, Denner CE, Alt HG (2010) Homogeneous catalytic dimerization of propylene with bis(imino)pyridine vanadium(III) complexes. J Mol Catal A Chem 222:45–49. doi:10.1016/j.molcata.2010.02.013
27. Al-Benna S, Sarsfield MJ, Thornton-Pett M, Ormsby DL, Maddox PJ, Brès P, Bochmann M (2000) Sterically hindered iminophosphorane complexes of vanadium, iron, cobalt and nickel: a synthetic and catalytic study. J Chem Soc Dalton Trans 4247–4257. doi: 10.1039/b006329k
28. Abbo HS, Mapolie SF, Darkwa J, Titinchi SJJ (2007) Bis(pyrazolyl)pyridine vanadium(III) complexes as highly active ethylene polymerization catalysts. J Organomet Chem 692: 5327–5330. doi:10.1016/j.organchem.2007.08.035
29. Tomov AK, Gibson VC, Zaher D, Elsegood MRJ, Dale SH (2004) Bis(benzimidazole)amine vanadium catalysts for olefin polymerisation and co-polymerisation: thermally robust, single-site catalysts activated by simple alkylaluminium reagents. Chem Commun 1956–1957. doi:10.1039/b407065h
30. Nakayama Y, Bando H, Sonobe Y, Suzuki Y, Fujita T (2003) Highly active, thermally robust v-based new olefin polymerization catalyst system. Chem Lett 32:766–767. doi:10.1246/cl.2003.766
31. Nakayama Y, Bando H, Sonobe Y, Fujita T (2004) Development of single-site new olefin polymerization catalyst systems using $mgcl_2$-based activators: MAO-free $MgCl_2$-supported FI catalyst systems. Bull Chem Soc Jpn 77:617–625. doi:10.1246/bcsj.77.617
32. Nakayama Y, Bando H, Sonobe Y, Fujita T (2004) Olefin polymerization behavior of bis(phenoxy-imine) Zr, Ti and V complexes with $MgCl_2$-based cocatalysts. J Mol Catal A Chem 213:141–150. doi:10.1016/j.molcata.2003.11.025
33. Nakayama Y, Saito J, Bando H, Fujita T (2006) $MgCl_2/R'_nAl(OR)_{3-n}$: an excellent activator/support for transition-metal complexes for olefin polymerization. Chem Eur J 12:7546–7556. doi:10.1002/chem.200600355
34. Wu J-Q, Pan L, Hu N-H, Li Y-S (2008) Synthesis, structural characterization and ethylene polymerization behavior of the vanadium(III) complexes bearing salicylaldiminato ligands. Organometallics 27:3840–3848. doi:10.1021/om8000097b
35. Wu J-Q, Pan L, Liu S-R, He L-P, Li Y-S (2009) Ethylene polymerization and ethylene/hexane copolymerization with vanadium(III) catalysts bearing heteroatom-containing salicylaldiminato ligands. Polym Sci A Polym Chem 47:3573–3582. doi:10.1002/pola.23441
36. Houghton J, Simonovic S, Whitwood AC, Douthwaite RE, Carabineiro SA, Yuan J-C, Marques MM, Gomes PT (2008) Transition-metal complexes of phenoxy-imine ligands modified with pendant imidazolium salts: synthesis, characterization and testing as ethylene polymerization catalysts. J Organomet Chem 693:717–724. doi:10.1016/j.organchem.2007.11.060
37. Onishi Y, Katao S, Fujiki M, Nomura K (2008) Synthesis and structural analysis of (arylimido)vanadium(V) complexes containing phenoxyimine ligands: new, efficient catalyst precursors for ethylene polymerization. Organometallics 27:2590–2596. doi:10.1021/om800177g
38. Scott MJ, Cottone A, Morales D, Lecuivre JL (2002) Synthesis and reactivity of bi-, tri-, and hexametallic and zwitterionic methyl aluminum complexes containing a phenoxide/imine ligand system. Organometallics 21:418–428. doi:10.1021/om010773b
39. Homden D, Redshaw C, Wright JA, Hughes DL, Elsegood MRJ (2008) Early transition metal complexes bearing a *C*-capped tris(phenolate) ligand incorporating a pendant imine arm: synthesis, structure and ethylene polymerization behavior. Inorg Chem 47:5799–5814. doi:10.1021/ic702506w
40. Soshnikov IE, Semikolenova NV, Bryliakov KP, Shubin AA, Zakharov VA, Redshaw C, Talsi EP (2009) An EPR study of the V(IV) species formed upon activation of a vanadyl

phenoxyimine polymerization catalyst with $AlR_3$ and $AlR_2Cl$ (R = Me, Et). Macromol Chem Phys 210:542–548. doi:10.1002/macp.200800556
41. Wu J-G, Pan L, Li Y-G, Liu S-R, Li Y-S (2009) Synthesis, structural characterization and olefin polymerization behavior of vanadium(III) complexes bearing tridentate Schiff base ligands. Organometallics 28:1817–1825. doi:10.1021/om801028g
42. Bialek M, Czaja K (2008) Dichlorovanadium(IV) complexes with Salen-type ligands for ethylene polymerization. Polym Sci A Polym Chem 46:6940–6949. doi:10.1002/pola.23003
43. Wang W, Nomura K (2006) Notable effects of aluminum alkyls and solvents for highly efficient ethylene (co)polymerizations catalyzed by (arylimido)-(aryloxo)vanadium complexes. Adv Synth Catal 348:743–750. doi:10.1002/adsc.200505446
44. Bialek M, Czaja K, Szydlo E (2009) Transition metal complexes of tetradentate and bidentate Schiff bases as catalysts for ethylene polymerization: effect of transition metal and cocatalyst. Polym Sci A Polym Chem 47:565–575. doi:10.1002/pola.23173
45. Bialek M, Pietuszka A (2009) Ethylene(5-chlorosalicylideneiminato)vanadium dichloride immobilized on $MgCl_2$-based supports as a highly effective precursor for ethylene polymerization. J Polym Sci A Polym Chem 47:3480–3489. doi:10.1002/pola.23426
46. Bialek M, Liboska O (2010) Vanadium complex with tetradentate [O, N, N, O] ligand supported on magnesium type carrier for ethylene homopolymerization and copolymerization. J Polym Sci A Polym Chem 48:471–478. doi:10.1002/pola.23808
47. Bialek M (2010) Effect of catalyst composition on chain-end-group of polyethylene produced by salen-type complexes of titanium, zirconium and vanadium. J Polym Sci A Polym Chem 48:3209–3214. doi:10.1002/pola.24096
48. Tang L-M, Wu J-Q, Duan Y-Q, Pan L, Li Y-G, Li Y-S (2008) Ethylene polymerizations, and the copolymerizations of ethylene with hexene or norbornene with highly active mono ($\beta$-enaminoketonato) vanadium(III) catalysts. J Polym Sci A Polym Chem 46:2038–2048. doi:10.1002/pola.22538
49. Hagen H, Bezemer C, Boersma J, Kooijman H, Lutz M, Spek AL, van Koten G (2000) Vanadium(IV) and (V) complexes with O, N-chelating aminophenolate and pyridylalkoxide ligands. Inorg Chem 39:3970–3977. doi:10.1021/ic991415s
50. Mulhaupt R, Sernetz FG, Fokken S, Okuda J (1997) Copolymerization of ethene with styrene using methylaluminoxane-activated bis(phenolate) complexes. Macromolecules 30:1562–1569. doi:10.1021/ma961443j
51. Schaverien CJ, Vanderlinden A, Meijboom N, Ganter C, Orpen AG (1995) Polymerization of $\alpha$-olefins and butadiene and catalytic cyclotrimerization of 1-alkynes by a new class of group IV catalysts. Control of molecular weight and polymer microstructure via ligand tuning in sterically hindered chelating phenoxide titanium and zirconium species. J Am Chem Soc 117:3008–3021. doi:10.1021/ja00116a006
52. Sobota P, Janas Z, Jerzykiewicz LB, Przybylak K, Szczegot K (2004) Titanium complexes stabilized by a sulfur-bridged chelating bis(aryloxo) ligand as active catalysts for olefin polymerization. Eur J Inorg Chem 1639–1645. doi: 10.1002/ejic.200300768
53. Janas Z (2010) Well-defined single-site thiobis(phenolate) Group 4 metal catalysts for heterogeneous olefin polymerization. Coord Chem Rev. doi:10.1016/j.ccr.2010.05.008
54. Takaoki K, Miyatake T (2000) Titanium and vanadium based non-metallocene catalysts for olefin polymerization. Macromol Symp 157:251–257. doi:10.1002/1521-3900(200007)157:1<251
55. Janas Z, Wisniewska D, Jerzykiewicz LB, Sobota P, Drabent K, Szczegot, K. (2007) Synthesis, structural studies and reactivity of vanadium complexes with tridentate (OSO) ligand. Dalton Trans 2065–2069. doi: 10.1039/b616961a
56. Rajsekhar G, Rao CP, Saarenketo P, Nattinen K, Rissanen K (2004) Complexation behaviour of hexadentate ligands possessing $N_2O_4$ and $N_2O_2S_2$ cores: differential reactivity towards Co(II), Ni(II) and Zn(II) salts and structures of the products. New J Chem 28:75–84. doi: 10.1039/b305313j
57. Homden DM, Redshaw C, Hughes DL (2007) Vanadium complexes possessing $N_2O_2S_2$-based ligands: highly active procatalysts for the homopolymerization of ethylene and

copolymerization of ethylene/1-hexene. Inorg Chem 46:10827–10839. doi:10.1021/ic701461b
58. Hsieh ET, Randell JC (1982) Monomer sequence distributions in ethylene-1-hexene copolymers. Macromolecules 15:1402–1406. doi:10.1021/ma00233a036
59. Zhang W, Nomura K (2008) Synthesis of (1-adamantylimido)vanadium(V) complexes containing aryloxo, ketimide ligands: effect of ligand substituents in olefin insertion/metathesis polymerization. Inorg Chem 47:6482–6492. doi:10.1021/ic800347n
60. Scheuer S, Fischer J, Kress J (1995) Synthesis, structure and olefin polymerization activity of vanadium(V) catalysts stabilized by Imido and Hydrotris(pyrazolyl)borato ligands. Organometallics 14:2627–2629. doi:10.1021/om00006a006
61. Casagrande ACA, Tavares TT da R, Kuhn MCA, Casagrande Jr OL, dos Santos JHZ, Teranishi T (2004) Tris(pyrazolyl)borate imido vanadium(V) compound immobilzed on inorganic supports and its use in ethylene polymerization. J Mol Cat A Chem 212:267–275. doi:10.1016/j.molcata.2003.11.005
62. Casagrande ACA, Gil MP, Casagrande OL Jr (2005) Titanium and vanadium ethylene polymerization catalysts containing tris(pyrazolyl)borate ligand: effects of polymerization parameters on activity and polymer properties. J Braz Chem Soc 16:1283–1289. doi:10.1590/S0103-50532005000700029
63. Bigmore HR, Zuideveld MA, Kowalczyk RM, Cowley AR, Kraenburg M, McInnes EJL, Mountford P (2006) Synthesis, structures and olefin polymerization capability of vanadium(4 +) imido compounds with *fac*-$N_3$ donor ligands. Inorg Chem 45:6411–6423. doi:10.1021/ic060454i
64. Long GS, Snedeker B, Bartosh K, Werner ML, Sen A (2001) Transition metal phthalocyanine and porphyrin complexes as catalysts for the polymerization of alkenes. Can J Chem 79:1026–1029. doi:10.1139/cjc-79-5/6-1026
65. Zhang S, Katao S, Sun W-H, Nomura K (2009) Synthesis of (arylimido)vanadium(V) complexes containing (2-anilidomethyl)pyridine ligands and their use as the catalyst precursors for olefin polymerization. Organometallics 28:5925–5933. doi:10.1021/om900633u
66. Zhang S, Normura K (2010) Highly efficient dimerization of ethylene by (imido)vanadium complexes containing (2-anilidomethyl)pyridine ligands: notable ligand effect toward activity and selectivity. J Am Chem Soc 132:4960–4965. doi:10.1021/ja100573d
67. Sato Y, Nakayama Y, Yasuda H (2005) Synthesis of pentavalent imidovanadium complexes and their catalyses for the polymerization of ethylene and propylene. J Appl Polym Sci 97:1008–1015. doi:10.1002/app.21826
68. Redshaw C, Rowan MA, Warford L, Homden DM, Arbaoui A, Elsegood MRJ, Dale SH, Yamato T, Casas CP, Matsui S, Matsuura S (2007) Oxo- and Imidovanadium complexes incorporating methylene- and dimethylene-bridged calix[3]- and –[4]arenes: synthesis, structures and ethylene polymerisation catalysis. Chem Eur J 13:1090–1107. doi:10.1002/chem.200600679

# Chapter 5
# Imino- and Amido-Pyridinate *d*-Block Metal Complexes in Polymerization/ Oligomerization Catalysis

**Giuliano Giambastiani, Lapo Luconi, Roger L. Kuhlman and Phillip D. Hustad**

**Abstract** This contribution is aimed at providing an overview of the oligomerization/polymerization catalysis mediated by early and late transition metal complexes stabilized by imino- and amidopyridinate ligands. While late metals are often coordinated by *imino*-pyridyl moieties, earlier metals are generally stabilized by *amido*-pyridyl systems. The ability of the complexes described within this chapter at catalytic olefin upgrading is quite remarkable, ranging from the well-controlled olefin oligomerization to the production of high molecular weight isotactic polypropylene in high polymerization temperature processes. Particular attention has been paid to the ligand and complex syntheses as well as to unveil the role of the ligand substituents on the catalyst activity and selectivity.

## List of Abbreviations

| | |
|---|---|
| AAC | Azide-alkyne cycloaddition |
| acac | Acetylacetonate |
| Anth | Anthracenyl |
| Ap | N,6-dimesitylpyridin-2-amine |

G. Giambastiani (✉) · L. Luconi
Institute of Chemistry of OrganoMetallic Compounds – ICCOM-CNR,
10-Sesto F.no – 50019 Florence, Italy
e-mail: giuliano.giambastiani@iccom.cnr.it

L. Luconi
e-mail: lapo.luconi@iccom.cnr.it

R. L. Kuhlman (✉) · P. D. Hustad
The Dow Chemical Company, 2301 N. Brazosport Blvd.- B-1603 - Freeport,
TX 77541, USA
e-mail: kuhlmarl@dow.com

P. D. Hustad
e-mail: pdhustad@dow.com

G. Giambastiani and J. Cámpora (eds.), *Olefin Upgrading Catalysis by Nitrogen-based Metal Complexes I*, Catalysis by Metal Complexes, 35
DOI: 10.1007/978-90-481-3815-9_5, 

| | |
|---|---|
| Ap′ | N-(2,6-diisopropylphenyl)-6-(2,6-dimethylphenyl)pyridin-2-amine |
| Ap+ | N,6-bis(2,6-dimethylphenyl)pyridin-2-amine |
| Ap- | N-mesityl-6-(2,4,6-triisopropylphenyl)pyridin-2-amine |
| Ap* | N-(2,6-diisopropylphenyl)-6-(2,4,6-triisopropylphenyl)pyridin-2-amine |
| ATRP | Atom-transfer radical polymerization |
| BBF | Butyl branching frequency |
| BHE | $\beta$-hydride elimination |
| BHT | $\beta$-hydride transfer to monomer |
| BIMP | Bis(imino)pyridine |
| Bip | Biphenyl |
| BM | Bohr magneton |
| CGC | Constrained geometry catalyst |
| CRP | Controlled radical polymerization |
| dba | Dibenzylideneacetone |
| DFT | Differential Fourier transform |
| DIBAL | Di-isobutylaluminum hydride, $i$Bu$_2$AlH |
| dme | 1,2-dimethoxyethane |
| DMF | N,N-dimethylformamide |
| DSC | Differential scanning calorimetry |
| EPR | Electron paramagnetic resonance |
| LLDPE | Linear-low density polyethylene |
| LRP | Living radical polymerization |
| MAO | Methylaluminoxane |
| MMA | Methyl methacrylate |
| MMAO | Modified methylaluminoxane |
| MWCNT | Multi-walled carbon nanotubes |
| Nap | Naphthyl |
| NB | Norbornene, bicyclo[2,2,1]hept-2-ene |
| NIR | Near-infrared |
| NMR | Nuclear magnetic resonance |
| NP-acac | 3-$n$-pentyl-acetylacetonate |
| PDI | Polydispersity index ($M_w/M_n$) |
| PE | Polyethylene |
| PFT | Polymerization filling technique |
| Phen | Phenanthrenyl |
| PIM | (imino)pyridine |
| PMAO-IP | Polymethylaluminoxane (available from AkzoNobel) |
| PMMA | Polymethyl methacrylate |
| Py | Pyridine |
| rds | Rate determining step |
| SANS | Small-angle neutron scattering |
| SEC | Size exclusion chromatography |
| $T_g$ | Glass transition temperature |

| | |
|---|---|
| TS | Transition state |
| TIBA | Tri-isobutylaluminum, Al(*i*Bu)$_3$ |
| TIBAO | Tetraisobutylaluminoxane |
| TOF | Turnover frequency |
| ULDPE | Ultra-low density polyethylene |
| Xantphos | (9,9-dimethyl-9H-xanthene-4,5-diyl)bis(diphenylphosphine) |
| $\mu_{eff}$ | Effective magnetic moment |

## 5.1 Introduction

The discovery and commercialization of new oligomerization/polymerization technologies based on single-site catalysts still represents one of the most dynamic areas of organometallic chemistry, homogeneous catalysis and polymer science. Through a simple insertion reaction, inexpensive and abundant olefins are transformed into polymeric materials for a wide range of applications, including plastics, fibers, and elastomers [1–3]. The extremely large number of tailored transition metal complexes (catalyst precursors) and main-group organometallic compounds (co-catalysts or activators) [4] has paved the way towards the development of new polymerization processes and properly tailored polymer architectures. The intense industrial activity in the field of polyolefins production and single-site catalysts commercialization (multibillion dollars per year) [5], have deeply stimulated fundamental academic research, in turn strengthened by new and fruitful collaborations between research groups coming from both industry and academia. Although heterogeneous polymerization systems traditionally represent the workhorse of the polymer industry, offering many important advantages over their homogeneous counterparts in commercial production, they suffer from a number of significant drawbacks. In particular, the control of either the polymer molecular weight distribution, comonomer incorporation, or the relative/absolute polymer stereochemistry is inevitably linked to the precise identity of the catalyst active species. In contrast to heterogeneous systems, the readily tunable metal center coordination environment of homogeneous catalysts facilitates the control over all these polymerization features. Homogeneous catalysts can be commercially employed in solution-phase polymerization or heterogenized on solid supports for gas-phase or slurry polymerization processes.

Early- and late- transition metal complexes based on nitrogen-containing ligands occupy an important position in the field of modern homogeneous catalysis applied to highly efficient and selective oligomerization/polymerization processes [3, 6, 7]. In particular, *N*,*N*-bidentate systems of the type discussed throughout this chapter have represented a real breakthrough in the field of olefin polymerization catalysis, as witnessed by the impressive number of papers and patents appearing in the last few years. The key feature of these organometallics is the facile tuning

of their polymerization/oligomerization activity and selectivity by means of simple modifications of their ligand architecture. All these systems are to be considered *pre*-catalysts, which require a preliminary activation with a co-catalyst, typically an organoaluminum or organoboron compound.

The catalysts described in this chapter are grouped into two major classes: (1) imino-pyridine ligands and related late-transition metals complexes and (2) amino-pyridinate ligands and related amido-pyridinate early-transition metal systems. This review will concentrate on the description of the state-of-the-art oligomerization/polymerization catalytic processes, focusing on Group 8–10 metals for imino-based systems and Group 3–4 metals for amido-based ones.

## 5.2 Synthesis of Iminopyridyl Ligands

Iminopyridyl ligands are commonly prepared by simple condensation reactions between 2-acetyl or 2-formyl-pyridine fragments with an equimolar amount of the proper amine [8–13] or aniline [11, 14–30], generally in the presence of an acid co-catalyst (Scheme 5.1). The synthesis of variably substituted iminopyridyl ligands, particularly those containing aryl or heteroaryl substituents on the 6-position of the pyridine ring, generally requires a more complex procedure which employs the Schiff-base condensation step at the end of the synthetic path. Although most of these ligands are prepared in multigram scale and typically purified by crystallization, iminopyridyl systems containing either keto or ester pendant arms, such as 2-keto-6-iminopyridyl and 2-alkylcarboxylate-6-iminopyridyl ligands, prepared from 2,6-diacetylpyridine [31] and 2-alkylcarboxylate-6-acetylpyridine [21, 22, 32], respectively, generally require a more careful purification step to remove 2,6-bis(imino)pyridine by-products or the 2,6-diacetylpyridine precursor.

Palladium catalyzed C–C bond coupling is a widely used approach for the introduction of aryl or heteroaryl moieties on the 6-position of the pyridine ring. A Suzuki reaction [33, 34] or a Stille protocol [34, 35] on α-Br-pyridine derivatives has been conveniently adopted for preparing 6-aryl [27–29, 36, 37] or

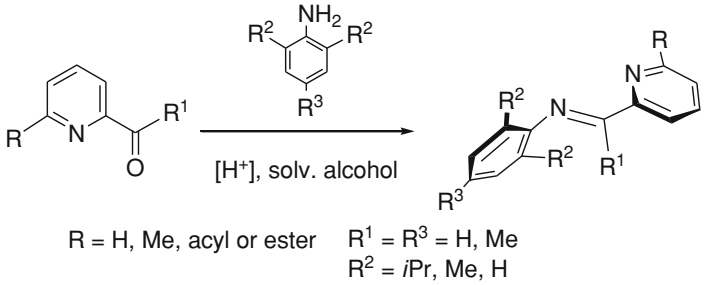


**Scheme 5.1** Synthetic procedures to iminopyridyl ligands

heteroaryl-2-iminopyridyl ligands [27–30, 36, 37] under mild conditions from good to high yields (Scheme 5.2).

A number of sterically demanding and multidentate ligands have also been proposed as effective supports for the preparation of mononuclear or binuclear $Fe^{II}$, $Co^{II}$, $Ni^{II}$ and $Zn^{II}$-based catalyst precursors. Forcing two different metal centers within the same molecular architecture is a topic of much current interest. Indeed, the possibility to accommodate two catalytic centers in close proximity to each other is expected to generate improved catalytic structures capable of (1) producing unconventional mixtures of PEs and/or α-olefins, (2) exhibiting increased activity due to favorable steric and electronic metal–metal interactions, and/or (3) producing tailored materials via chain transfer from one metal to the other with or without a shuttling agent. To date, however, the complexity of the ligand design and synthesis has allowed only marginal progress toward these goals. The majority of homo- or hetero-polynuclear catalyst precursors prepared so far present their active centers at the extremities of the manifold ligand, thus limiting any potential cooperative metal–metal interaction. Novel molecular architectures, coupling two iminopyridyl moieties (PIM) (Fig. 5.1a) [23] or combining an iminopyridyl fragment with a bis(imino)pyridine unit (BIMP) (Fig. 5.1b,c) [24, 25], have been recently proposed as effective scaffolds for the preparation of mono- and/or bi-nuclear oligomerization/polymerization catalysts. Redox-active ferrocenyl-based mono- and bis(iminopyridyl) ligands have been straightforwardly prepared by Gibson et al. (Fig. 5.1d) for the preparation of mono- and binuclear nickel pre-catalysts [10]. Redox-active ligands offer exciting potential within homogeneous transition metal catalysis, since the oxidation of a redox-active substituent induces a higher system electrophilicity ultimately perturbing the catalytic properties of the metal centers coordinated to the $N_2$ and $N_4$-type frameworks [38, 39]. Finally, mono-, bis- and tetra(imino)pyridyl ligands containing long alkyl chain substituents at the imino nitrogens (Fig. 5.1e) have been proposed by Mapolie et al. [9, 40, 41]. All the free ligands reported in Fig. 5.1, are presented in their generally unfavorable s-*cis* configuration (or *U*-

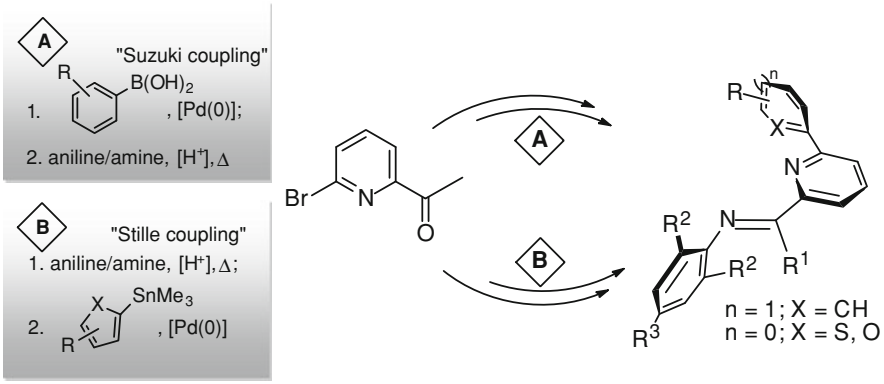


**Scheme 5.2** Synthetic procedures to 6-aryl or heteroaryl-2-iminopyridyl ligands

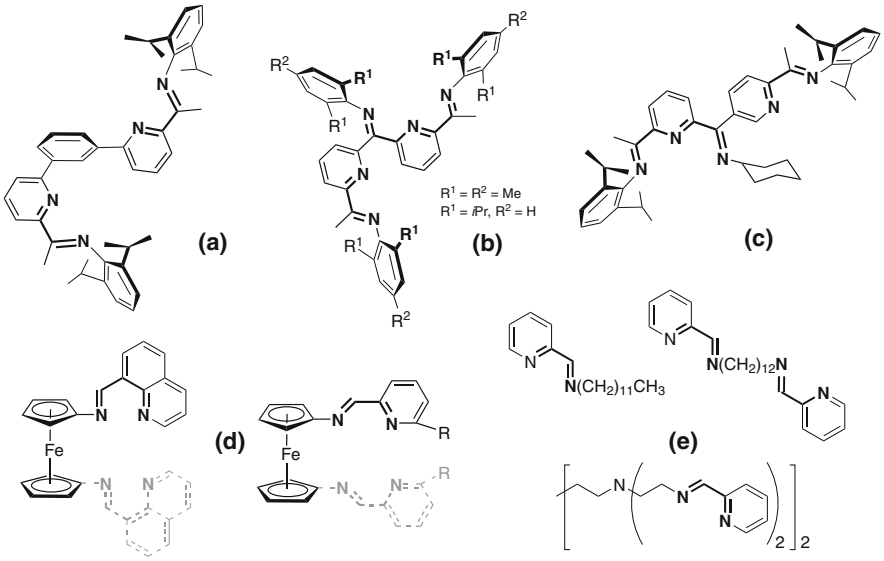


**Fig. 5.1** Typical iminopyridyl polydentate ligands. Chelating U-shaped configured arms are in bold

shaped configuration), experimentally observed in their metal complexes [6], with the arylimino moiety lying orthogonal to the N=C–C=$N_{py}$ plane.

(Imino)pyridyl ligands can exhibit a rich chemistry on their own, particularly at the imine unit, leading to (1) vinylaniline derivatives in almost quantitative yields by ligand treatment with strong non-nucleophilic bases (Giambastiani G, Bianchini C, Guerrero Rios I, Meli A, unpublished results) or (2) reductive alkylation products by treatment of the keto- or aldoimine moiety with an excess of an aluminum alkyl ($AlMe_3$ or $AlEt_3$) [42]. Notably, the reaction of aminopyridine or $\alpha$-diimino ligands with $AlMe_3$ in toluene at elevated temperatures has been found to generate highly crystalline aluminum pyridineamido complexes [43] whose molecular structures have been reported independently by Gibson [44] and Erker [45].

## 5.3 Synthesis of Iminopyridyl-Based Late Transition Metal Complexes

The preparation of metal catalyst precursors (basically from the first transition row) is straightforwardly achieved by addition of the solid ligands to a solution (*n*-BuOH, thf, toluene or $CH_2Cl_2$) of either anhydrous or hydrated metal dihalides (Scheme 5.3) [3, 6, 9, 10, 15–17, 21, 22, 32, 33, 42, 43, 46–53]. Improved solubility in aromatic hydrocarbons is generally exhibited by metal dihalide solvent

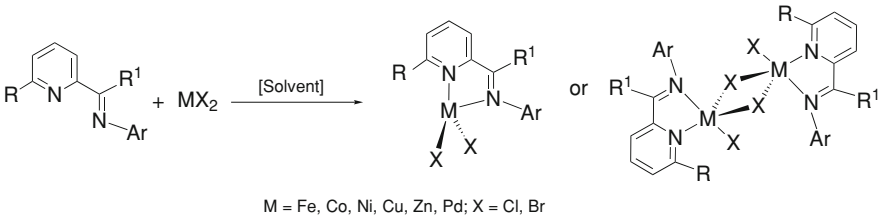


**Scheme 5.3** General scheme for the synthesis of late transition metal dihalide complexes

adducts $MX_2(solv)_y$ [8, 54–56]. Complexes are generally obtained as microcrystalline air-stable solids, while decomposition occurs in solution when they are left to stand for prolonged times unless protected by an inert atmosphere. Depending on both metal halides and degree of substitution at the pyridine ring, they can be isolated as mononuclear complexes or centrosymmetric dimers [8, 16, 18, 24, 51, 57–59]. In all cases, their IR spectra show red shifts of $\nu$(C=N) by ca. 50–60 $cm^{-1}$ as compared with the corresponding free ligand, which reflects the coordination of the imine N atom to the metal center.

### 5.3.1 $Fe^{II}$-(imino)pyridinate Complexes

(Imino)pyridinate-$Fe^{II}$ complexes are prepared by reacting anhydrous iron-dihalide with the proper ligand in either thf or an alcohol to give paramagnetic [23, 60] red to dark-brown microcrystalline solids with coordination geometries around the metal center ranging from tetrahedral to trigonal–bipyramidal with various degrees of distortion from the idealized geometries [8, 18, 20, 21, 23, 26, 31]. Less sterically demanding iminopyridyl ligands often result in the formation of halo-bridged dimers with each metal center lying within a distorted trigonal–bipyramidal structure [8, 18], while more sterically crowded ligands favor pseudo-tetrahedral coordination geometries [18] (Scheme 5.3). Table 5.1 lists a series of $Fe^{II}$ dihalide complexes stabilized by variably substituted iminopyridyl ligands (Fig. 5.2).

### 5.3.2 $Co^{II}$-(imino)pyridinate Complexes

Iminopyridinate $Co^{II}$ complexes are prepared by reacting anhydrous $Co^{II}$ dihalide with the proper ligand in ethers to give green microcrystalline paramagnetic solids with magnetic moment ($\mu_{eff}$) values at room temperature ranging from 4.6 to 5.1 BM, consistent with $d^7$ high-spin $Co^{II}$ configurations [21, 23–25, 27, 29, 60, 63]. The coordination geometry around the metal center is quite flexible, varying from tetrahedral to trigonal–bipyramidal with various distortions depending on the substitution degree at the pyridine unit. Similarly to $Fe^{II}$ derivatives, less sterically demanding ligands result in the formation of chloro-bridged dimers with a

**Table 5.1** $Fe^{II}$ complexes stabilized by (imino)pyridinate ligands

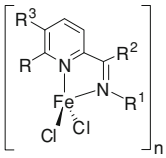

| n | R | $R^1$ | $R^2$ | $R^3$ | References |
|---|---|---|---|---|---|
| 2 | H | 2,6-*i*$Pr_2(C_6H_3)$ | H | H | [8] |
| 1 | $COCH_3$ | 2,6-*i*$Pr_2(C_6H_3)$ | Me | H | [31, 61] |
| 1 | $COCH_3$ | 2,6-$Me_2(C_6H_3)$ | Me | H | [61] |
| 1 | $COCH_3$ | 3-$CF_3(C_6H_4)$ | Me | H | [20] |
| 1 | $CO_2Et$ | 2,6-$Me_2(C_6H_3)$ | Me | H | [21, 62] |
| 1 | $CO_2Et$ | 2,6-$Et_2(C_6H_3)$ | Me | H | [21] |
| 1 | $CO_2Et$ | 2,6-*i*$Pr_2(C_6H_3)$ | Me | H | [21] |
| 1 | $CO_2Et$ | 2,6-$F_2(C_6H_3)$ | Me | H | [21] |
| 1 | $CO_2Et$ | 2,6-$Cl_2(C_6H_3)$ | Me | H | [21] |
| 1 | $CO_2Et$ | 2,6-$Br_2(C_6H_3)$ | Me | H | [21] |
| 1 | $C_6H_5$ | 2,6-*i*$Pr_2(C_6H_3)$ | Me | H | [27] |
| 1 | 2,6-$Me_2(C_6H_3)$ | 2,6-*i*$Pr_2(C_6H_3)$ | H | H | [26] |
| 1 | 2,4,6-*i*$Pr_3(C_6H_2)$ | 2,6-*i*$Pr_2(C_6H_3)$ | H | H | [26] |
| 1 | H | *n*-propyl | H | H | [8] |
| 1 | H | *c*-$C_6H_{11}$ | H | H | [8] |
| 1 | H | *c*-$C_{12}H_{23}$ | H | H | [8] |
| 1 | Me | *n*-propyl | H | H | [8] |
| 1 | Me | *c*-$C_{12}H_{23}$ | H | H | [8] |
| 1 | 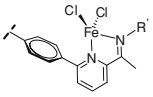 R' = 2,6-*i*$Pr_2(C_6H_3)$ | 2,6-*i*$Pr_2(C_6H_3)$ | Me | H | [23] |
| 1 | 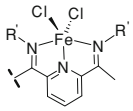 R' = 2,4,6-$Me_3(C_6H_2)$ | 2,4,6-$Me_3(C_6H_2)$ | Me | H | [24] |
| 1 | 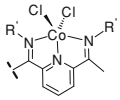 R' = 2,4,6-$Me_3(C_6H_2)$ | 2,4,6-$Me_3(C_6H_2)$ | Me | H | [24] |
| 1 | H | 2,6-*i*$Pr_2(C_6H_3)$ | Me | 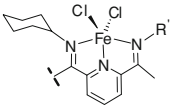 R' = 2,6-*i*$Pr_2(C_6H_3)$ | [25] |

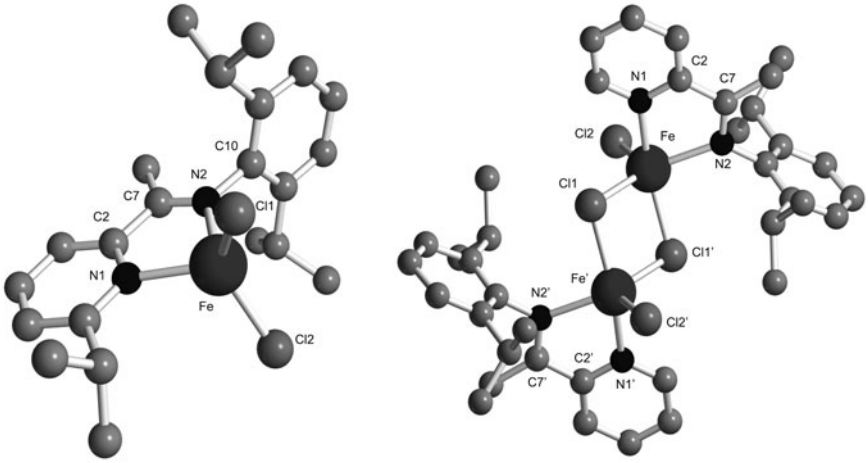


**Fig. 5.2** *Left ball and stick* drawing of the crystal structure of $FeCl_2\{2\text{-}(2,6\text{-}i\text{Pr}_2C_6H_3N{=}CH)\text{-}6\text{-}(i\text{Pr})C_5H_3N\}$ (hydrogen atoms and a thf molecule omitted) [18]. Selected distances (Å) and angles (°): Fe-N1 2.108(3), Fe-N2 2.111(3), Fe-Cl1 2.209(1), Fe-Cl2 2.223(1), C2-C7 1.479(5), C7-N2 1.271(5), N1-Fe-N2 77.3(1), Cl1-Fe-Cl2 118.68(5). *Right ball and stick* drawing of the crystal structure of $[FeCl_2\{2\text{-}(2,6\text{-}i\text{Pr}_2C_6H_3N{=}CMe)C_5H_3N\}]_2$ (hydrogen atoms omitted) [18]. Selected distances (Å) and angles (°): Fe-N1 2.126(7), Fe-N2 2.201(6), N1-Fe-N2 74.8(2), Cl1-Fe-Cl2 105.3(1), Cl1-Fe-Cl1' 84.9(1)

distorted trigonal–bipyramidal coordination geometry [18, 19], while 6-aryl substituted derivatives [29] show highly distorted tetrahedral coordination geometries (Fig. 5.3). Solution and solid state visible/NIR spectra of the mononuclear $Co^{II}$ complexes display three d–d absorption bands at 1,800–1,640, 1,430–1,330, 1,050–990 nm, respectively, and two or three higher intensity bands in the region between 690 and 550 nm, typical for high-spin $Co^{II}$-ions in a tetrahedral coordination geometry (Fig. 5.4, left) [29, 60, 63]. With three unpaired electrons ($S = 3/2$), these $Co^{II}$ complexes are EPR silent at room temperature in both the solid state and $CH_2Cl_2$ solution [64, 65]. In spite of their paramagnetic nature, $Co^{II}$ bis-halide precursors have also been characterized via $^1$H-NMR spectroscopy in a relatively large spectral window. Unambiguous signal assignment has been also achieved on the basis of the isotropic shifts, essentially attributable to a Fermi contact contribution [66–68]. Table 5.2 summarizes a series of $Co^{II}$ dihalide complexes stabilized by variably substituted iminopyridyl ligands.

### *5.3.3 $Ni^{II}$- and $Pd^{II}$-(imino)pyridinate Complexes*

$Ni^{II}$-dihalide (imino)pyridinate complexes are generally prepared by reacting the ligand with $NiBr_2$(dme) or $NiCl_2{\cdot}xH_2O$ in an ether or alcohol, respectively, to give green to orange–yellow solids. Dialkyl $Ni^{II}$-iminopyridinate systems have also

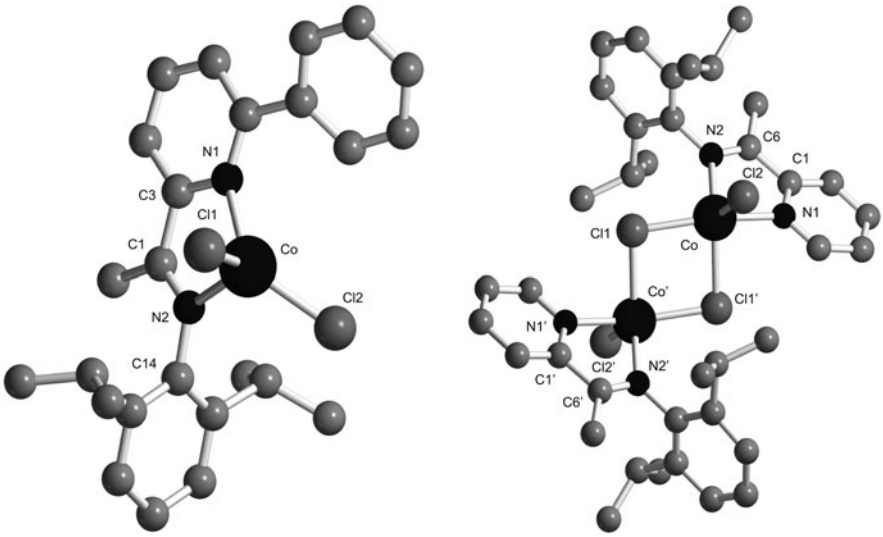


**Fig. 5.3** *Left ball and stick* drawing of the crystal structure of $CoCl_2\{2\text{-}(2,6\text{-}i\text{Pr}_2C_6H_3N{=}CMe)\text{-}6\text{-}(C_6H_5)C_5H_3N\}$ (hydrogen atoms omitted) [29]. Selected distances (Å) and angles (°): Co-N1 2.084(4), Co-N2 2.049(4), Co-Cl1 2.206(2), Co-Cl2 2.205(2), N1-Co-N2 80.71, N1-Co-Cl2 129.78. *Right ball and stick* drawing of the crystal structure of $[CoCl_2\{2\text{-}(2,6\text{-}i\text{Pr}_2C_6H_3N{=}CMe)C_5H_3N\}]_2$ (hydrogen atoms omitted) [18]. Selected distances (Å) and angles (°): C1-C6 1.482(2), C6-N2 1.290(2), Co1-N1 2.093(1), Co1-N2 2.123(1), Co1-Cl1 2.3419(5), Co1-Cl2 2.2878(6), Co1-Cl1' 2.4589(5), N1-Co1-N2 76.64(5), Cl1-Co1-Cl2 103.42(2), Cl1-Co1-Cl1' 86.01(2)

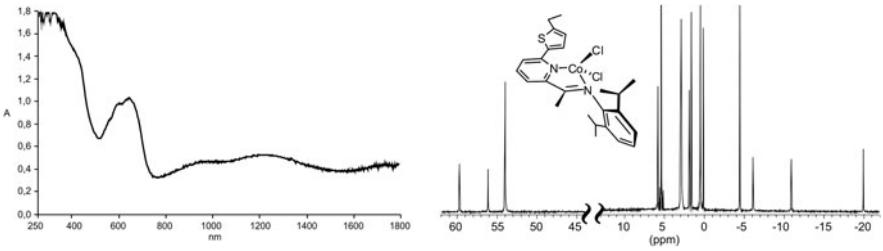


**Fig. 5.4** *Left* Diffuse reflectance spectrum of $CoCl_2\{2\text{-}(2,6\text{-}i\text{Pr}_2C_6H_3N{=}CMe)\text{-}6\text{-}(C_6H_5)C_5H_3N\}$. *Right* $^1$H-NMR spectrum ($CD_2Cl_2$, 22 °C) of $CoCl_2\{2\text{-}(2,6\text{-}i\text{Pr}_2C_6H_3N{=}CMe)\text{-}6\text{-}(2\text{-}C_4H_2S\text{-}5\text{-}C_2H_5)C_5H_3N)\}$. Figures reprinted "in part" with permission from [27]. Copyright 2007 American Chemical Society

been prepared by ligand exchange reactions from $NiR_2Py_2$ adducts [76]. The coordination geometries around the metal centers vary from trigonal–bipyramidal to tetrahedral with various distortions from the idealized geometries depending on the substitution degree at the pyridine moiety, which ultimately influence their magnetic properties. While tetrahedral [10, 14–16, 23, 32] and trigonal–bipyramidal $Ni^{II}$ complexes [18, 58, 59] have $\mu_{eff}$ values ranging from 2.8 to 3.4 BM,

**Table 5.2** $Co^{II}$ complexes stabilized by (imino)pyridyl ligands

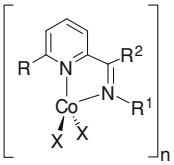

| n | R | $R^1$ | $R^2$ | X | References |
|---|---|---|---|---|---|
| 2 | H | 2,6-*i*$Pr_2(C_6H_3)$ | H | Br | [58] |
| 2 | Br | 2,6-*i*$Pr_2(C_6H_3)$ | Me | Cl | [27, 69] |
| 1 | $CO_2Et$ | 2,6-$Me_2(C_6H_3)$ | Me | Cl | [21, 62] |
| 1 | $CO_2Et$ | 2,6-$Et_2(C_6H_3)$ | Me | Cl | [21, 70] |
| 1 | $CO_2Et$ | 2,6-*i*$Pr_2(C_6H_3)$ | Me | Cl | [21] |
| 1 | $CO_2Et$ | 2,6-$F_2(C_6H_3)$ | Me | Cl | [21] |
| 1 | $CO_2Et$ | 2,6-$Cl_2(C_6H_3)$ | Me | Cl | [21] |
| 1 | $CO_2Et$ | 2,6-$Br_2(C_6H_3)$ | Me | Cl | [21] |
| 1 | $(CH_2)O_2CCH{=}CH_2$ | 2,6-*i*$Pr_2(C_6H_3)$ | H | Cl | [50] |
| 1 | Ph | 2,6-*i*$Pr_2(C_6H_3)$ | Me | Cl | [27–29, 36, 37, 47, 71–73] |
| 1 | Ph | 2,6-$Me_2(C_6H_3)$ | Me | Cl | [37] |
| 1 | Ph | 2-$Me_2(C_6H_4)$ | Me | Cl | [37] |
| 1 | 2,6-$Me_2(C_6H_3)$ | 2,6-*i*$Pr_2(C_6H_3)$ | H | Cl | [26] |
| 1 | 2,4,6-*i*$Pr_3(C_6H_2)$ | 2,6-*i*$Pr_2(C_6H_3)$ | H | Cl | [26] |
| 1 | 2-naph | 2,6-*i*$Pr_2(C_6H_3)$ | Me | Cl | [27, 28] |
| 1 |  | 2,6-*i*$Pr_2(C_6H_3)$ | Me | Cl | [27–30, 36, 37, 47, 74, 75] |
| 1 |  | 2,6-*i*$Pr_2(C_6H_3)$ | Me | Cl | [27, 47] |
| 1 | 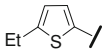 | 2,6-*i*$Pr_2(C_6H_3)$ | Me | Cl | [27–30, 72, 73] |
| 1 |  | 2,6-*i*$Pr_2(C_6H_3)$ | Me | Cl | [27–29, 37] |
| 1 | 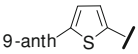 | 2,6-*i*$Pr_2(C_6H_3)$ | Me | Cl | [30, 69] |
| 1 | 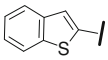 | 2,6-*i*$Pr_2(C_6H_3)$ | Me | Cl | [27, 28, 30, 36, 37, 46, 72, 73] |
| 1 | 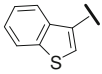 | 2,6-*i*$Pr_2(C_6H_3)$ | Me | Cl | [27] |
| 1 | 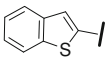 | 2,6-*i*$Pr_2(C_6H_3)$ | $(CH_2)_3OH$ | Cl | [30] |
| 1 | 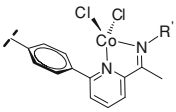 R' = 2,6-*i*$Pr_2(C_6H_3)$ | 2,6-*i*$Pr_2(C_6H_3)$ | Me | Cl | [23] |

(continued)

**Table 5.2** (continued)

| n | R | $R^1$ | $R^2$ | X | References |
|---|---|---|---|---|---|
| 1 | 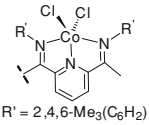 R' = 2,4,6-$Me_3(C_6H_2)$ | 2,4,6-$Me_3(C_6H_2)$ | Me | Cl | [24] |
| 1 | 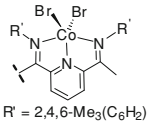 R' = 2,4,6-$Me_3(C_6H_2)$ | 2,4,6-$Me_3(C_6H_2)$ | Me | Br | [24] |
| 1 | H | 2,6-*i*$Pr_2(C_6H_3)$ | Me | Cl | [25] |

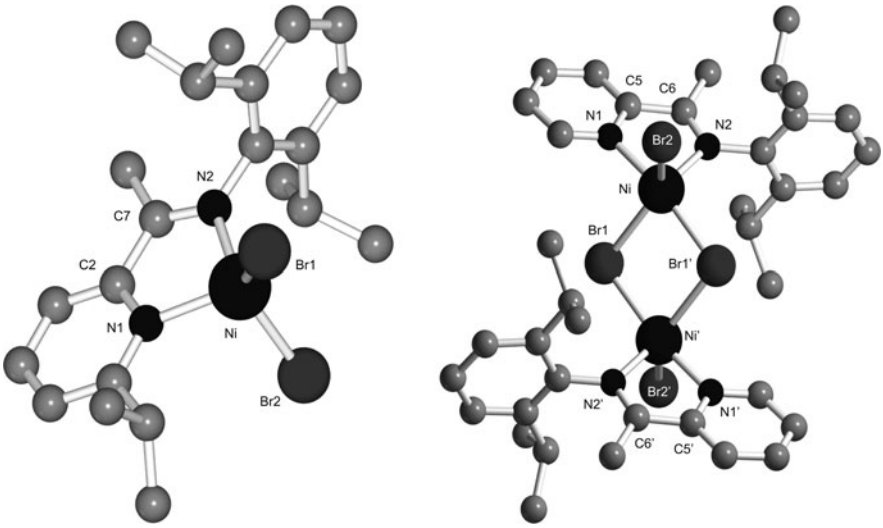


**Fig. 5.5** *Left ball and stick* drawing of crystal structure of $NiBr_2\{2\text{-}(2,6\text{-}iPr_2C_6H_3N{=}CMe)\text{-}6\text{-}(iPr)C_5H_3N\}$ (hydrogen atoms omitted) [18]. Selected distances (Å) and angles (°): Ni-N2 1.995(2), Ni-N1 1.994(2), Ni-Br1 2.3577(5), Ni-Br2 2.3169(5), N1-Co-N2 81.7(1), Br1-Ni-Br2 123.64(2). *Right ball and stick* drawing of the crystal structure of $[NiBr_2\{2\text{-}(2,6\text{-}iPr_2C_6H_3N{=}C\text{-}Me)C_5H_3N\}]_2$ (hydrogen atoms omitted) [59]. Selected distances (Å) and angles (°): C5-C6 1.452(8), Ni'-N1 2.069(5), Ni-N2 2.042(5), Ni-Br1 2.4759(12), Ni'-Br2 2.4139(18), Ni-Br1' 2.5479(12), N1-Ni'-N2 79.4(2), Br1-Ni'-Br2 132.06(6), Br1-Ni'-Br1' 86.63(4)

typical for paramagnetic $d^8$ high-spin species [23, 60], the square-planar $Ni^{II}$ derivatives [27, 60] are diamagnetic [16, 27] (Fig. 5.5).

$Pd^{II}$-dihalide complexes stabilized by (imino)pyridine ligands are generally mononuclear, diamagnetic yellow–orange solids with square-planar coordination geometry around the metal center [9, 10, 19, 22, 26, 40, 41, 51, 59, 76–78]

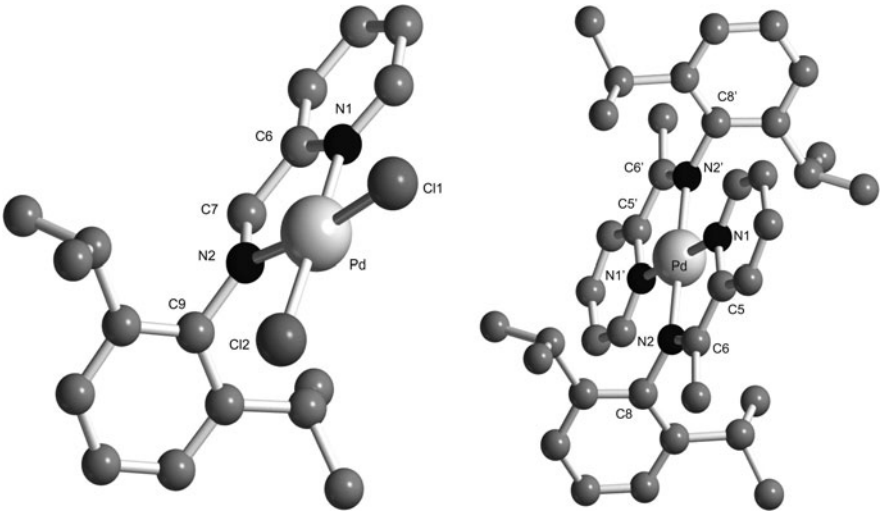


**Fig. 5.6** *Left ball and stick* drawing of the crystal structure of $PdCl_2\{2\text{-}(2,6\text{-}i\text{Pr}_2C_6H_3N{=}CH)C_5H_3N\}$ (hydrogen atoms omitted) [19]. Selected distances (Å) and angles (°): Pd-N1 2.028(3), Pd-N2 2.022(3), Pd-Cl1 2.2809(11), Pd-Cl2 2.2768(10), C6-C7 1.457(5), C7-N2 1.279(4), N1-Pd-N2 80.08(11), N1-Pd-Cl1 94.33(9), N1-Pd-Cl2 174.51(9). *Right ball and stick* drawing of the crystal structure of $Pd\{2\text{-}(2,6\text{-}i\text{Pr}_2C_6H_3N{=}CMe)C_5H_3N\}_2$ (hydrogen atoms and $2(BAr_4)^-$ omitted) [51]. Selected distances (Å) and angles (°): Pd-N1 2.054(4), Pd-N2 2.052(4), N1-Pd-N2 78.3(2), N1-Pd-N1'=N2-Pd-N2' 180.00

(Fig. 5.6, left). Asymmetric $Pd^{II}$-haloalkyl complexes maintain distorted square-planar geometries around the metal center and a favorable *cis* orientation of the alkyl group with respect to the imino nitrogen atom [51, 77]. Dicationic derivatives of the type $[Pd(N\text{–}N)_2]X_2$ ($2X^- = 2BF_4^-$, $2BAr_4^-$ or $2Bar_4^{F-}$) can accommodate up to two iminopyridyl units with a mutually *trans* arrangement of the two imino and pyridyl nitrogen atoms, with the palladium ion lying on a crystallographic center of symmetry [51]. Table 5.3 lists a series of $Ni^{II}$ and $Pd^{II}$ complexes stabilized by variably substituted iminopyridyl ligands.

## 5.4 Principal Activators and Mechanistic Considerations

Many (imino)pyridine $Co^{II}$, $Fe^{II}$, $Ni^{II}$ and $Pd^{II}$ dihalides can be converted into active olefin polymerization/oligomerization catalyst systems by treatment of toluene solutions/suspensions of the pre-catalysts with an excess of co-catalyst such as methylaluminoxane (MAO) or modified methylaluminoxane (MMAO) [MMAO, MAO containing 20–25% $Al(i\text{Bu})_3$] and exposure of the activated species to olefin solutions/atmosphere. Some proposed structures for MAO include one-dimensional linear chains and cyclic rings containing three-coordinate Al

**Table 5.3** $Ni^{II}$ and $Pd^{II}$ complexes stabilized by (imino)pyridyl ligands

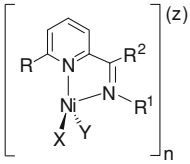


| n | R | $R^1$ | $R^2$ | X | Y | (z) | References |
|---|---|---|---|---|---|---|---|
| 2 | H | 2,6-*i*$Pr_2(C_6H_3)$ | H | Cl | Cl | – | [58] |
| 2 | H | 2,6-*i*$Pr_2(C_6H_3)$ | H | Br | Br | – | [52, 58] |
| 2 | H | 2,6-$Me_2(C_6H_3)$ | H | Br | Br | – | [59] |
| 2 | Me | 2,6-*i*$Pr_2(C_6H_3)$ | H | Br | Br | – | [59] |
| 2 | H | 2,6-*i*$Pr_2(C_6H_3)$ | Me | Br | Br | – | [59] |
| 2 | H | 2,6-*i*$Pr_2(C_6H_3)$ | Ph | Br | Br | – | [59] |
| 1 | H | 2,6-$Me_2(C_6H_3)$ | H | Br | Br | – | [14] |
| 1 | H | 2,6-$Me_2(C_6H_3)$ | Me | Br | Br | – | [14] |
| 1 | H | 2-*i*Pr$(C_6H_3)$ | H | Br | Br | – | [14] |
| 1 | H | 2-*i*Pr$(C_6H_3)$ | Me | Br | Br | – | [14] |
| 1 | H | 2,6-*i*$Pr_2(C_6H_3)$ | H | Br | Br | – | [14] |
| 1 | H | 2,6-*i*$Pr_2(C_6H_3)$ | Me | Br | Br | – | [14] |
| 1 | H | 2,6-*i*$Pr_2(C_6H_3)$ | H | Br | Br | – | [15] |
| 1 | Me | 2,6-*i*$Pr_2(C_6H_3)$ | H | Br | Br | – | [15] |
| 1 | H | 2,6-*i*$Pr_2(C_6H_3)$ | H | $Et_2O$ | Me | $(BAr_4^F)$ | [15] |
| 1 | H | 4-$OSiMe_3(C_6H_4)$ | H | Br | Br | – | [16] |
| 1 | H | 2,5-$Me_2$-4-$OSiMe_3(C_6H_2)$ | H | Br | Br | – | [16] |
| 1 | Me | 2,5-$Me_2$-4-$OSiMe_3(C_6H_2)$ | H | Br | Br | – | [16] |
| 2 | H | 4-$OH(C_6H_4)$ | H | ½Br | ½Br | – | [16] |
| – | H | 2,6-*i*$Pr_2(C_6H_3)$ | H | Allyl | – | $(BAr_4^F)$ | [17] |
| 1 | $CO_2Et$ | 2,6-$Me_2(C_6H_3)$ | Me | Cl | Cl | – | [32] |
| 1 | $CO_2Et$ | 2,6-$Et_2(C_6H_3)$ | Me | Cl | Cl | – | [32] |
| 1 | $CO_2Et$ | 2,6-*i*$Pr_2(C_6H_3)$ | Me | Cl | Cl | – | [32] |
| 1 | $CO_2Et$ | 2,6-$F_2(C_6H_3)$ | Me | Br | Br | – | [32] |
| 1 | $CO_2Et$ | 2,6-$Cl_2(C_6H_3)$ | Me | Br | Br | – | [32] |
| 1 | $CO_2Et$ | 2,6-$Br_2(C_6H_3)$ | Me | Br | Br | – | [32] |
| 1 | $(CH_2)O_2CCH{=}CH_2$ | 2,6-*i*$Pr_2(C_6H_3)$ | H | Br | Br | – | [50] |
| 1 | Ph | 2,6-*i*$Pr_2(C_6H_3)$ | Me | Cl | Cl | – | [27] |
| 1 | 2,6-$Me_2(C_6H_3)$ | 2,6-*i*$Pr_2(C_6H_3)$ | H | Cl | Cl | – | [26] |
| 1 | 2,4,6-*i*$Pr_3(C_6H_2)$ | 2,6-*i*$Pr_2(C_6H_3)$ | H | Cl | Cl | – | [26] |
| 1 | H | 1-naph | H | Br | Br | – | [14] |
| 1 | H | 1-naph | Me | Br | Br | – | [14] |
| 1 | H |  | H | Br | Br | – | [10] |
| 1 | Me |  | H | Br | Br | – | [10] |

(continued)

**Table 5.3** (continued)

| n | R | $R^1$ | $R^2$ | X | Y | (z) | References |
|---|---|---|---|---|---|---|---|
| 1 | 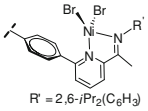 R' = 2,6-*i*Pr$_2$(C$_6$H$_3$) | 2,6-*i*Pr$_2$(C$_6$H$_3$) | Me | Br | Br | – | [23] |
| 1 | 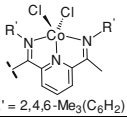 R' = 2,4,6-Me$_3$(C$_6$H$_2$) | 2,4,6-Me$_3$(C$_6$H$_2$) | Me | Br | Br | – | [24] |

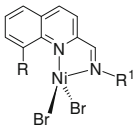


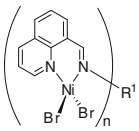


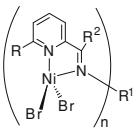


| Complex | n | R | $R^1$ | $R^2$ | References |
|---|---|---|---|---|---|
| A | – | H | 2,6-*i*Pr$_2$(C$_6$H$_3$) | – | [14] |
| A | – | Me | 2,6-*i*Pr$_2$(C$_6$H$_3$) | – | [14] |
| A | – | H | 2,6-*i*Pr$_2$(C$_6$H$_3$) | – | [14] |
| A | – | Me | 2,6-*i*Pr$_2$(C$_6$H$_3$) | – | [14] |
| A | – | H | 2,6-*i*Pr$_2$(C$_6$H$_3$) | – | [14, 15] |
| A | – | Me | 2,6-*i*Pr$_2$(C$_6$H$_3$) | – | [14] |
| A | – | *i*-Pr | 2,6-*i*Pr$_2$(C$_6$H$_3$) | – | [14] |
| B | 1 | – | 2,6-*i*Pr$_2$(C$_6$H$_3$) | – | [15] |
| B | 1 | – |  | – | [10] |
| B | 2 | – |  | – | [10] |
| C | 2 | H |  | H | [10] |
| C | 2 | Me |  | H | [10] |

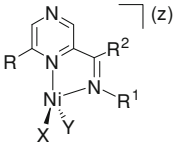

| R | $R^1$ | $R^2$ | X | Y | (z) | References |
|---|---|---|---|---|---|---|
| H | 2,6-*i*Pr$_2$(C$_6$H$_3$) | H | Br | Br | – | [15] |
| Me | 2,6-*i*Pr$_2$(C$_6$H$_3$) | H | Et$_2$O | Br | (BAr$_4^F$) | [15] |

(continued)

**Table 5.3** (continued)

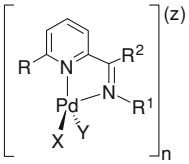


| n | R | $R^1$ | $R^2$ | X | Y | (z) | References |
|---|---|---|---|---|---|---|---|
| 1 | H | 2,6-*i*$Pr_2(C_6H_3)$ | Me | Cl | Me | – | [51] |
| 1 | H | 2,6-*i*$Pr_2(C_6H_3)$ | Me | $CH_3CN$ | Me | $(BAr_4)$ | [51] |
| 2 | H | 2,6-*i*$Pr_2(C_6H_3)$ | Me | – | – | $(BAr_4)_2$ | [51] |
| 1 | H | 2,6-*i*$Pr_2(C_6H_3)$ | H | Cl | Cl | – | [59] |
| 1 | H | 2,6-$Me_2(C_6H_3)$ | H | Cl | Cl | – | [59] |
| 1 | Me | 2,6-*i*$Pr_2(C_6H_3)$ | H | Cl | Cl | – | [59] |
| 1 | H | 2,6-*i*$Pr_2(C_6H_3)$ | H | $CH_3CN$ | $CH_3CN$ | $(BF_4)_2$ | [59] |
| 1 | Me | 2,6-*i*$Pr_2(C_6H_3)$ | H | $CH_3CN$ | $CH_3CN$ | $(BF_4)_2$ | [59] |
| 1 | $CO_2Et$ | 2,6-$Me_2(C_6H_3)$ | Me | Cl | Cl | – | [22] |
| 1 | $CO_2Et$ | 2,6-$Et_2(C_6H_3)$ | Me | Cl | Cl | – | [22] |
| 1 | $CO_2Et$ | 2,6-*i*$Pr_2(C_6H_3)$ | Me | Cl | Cl | – | [22] |
| 1 | $CO_2Et$ | 2,4,6-$Me_3(C_6H_2)$ | Me | Cl | Cl | – | [22] |
| 1 | $CO_2Et$ | 2,6-$F_2(C_6H_3)$ | Me | Br | Br | – | [22] |
| 1 | $CO_2Et$ | 2,6-$Cl_2(C_6H_3)$ | Me | Br | Br | – | [22] |
| 1 | $CO_2Et$ | 2,6-$Br_2$-4-$Me(C_6H_2)$ | Me | Br | Br | – | [22] |
| 1 | $(CH_2)O_2CCH{=}CH_2$ | 2,6-*i*$Pr_2(C_6H_3)$ | H | Cl | Cl | – | [50] |
| 1 | 2,6-$Me_2(C_6H_3)$ | 2,6-*i*$Pr_2(C_6H_3)$ | H | Cl | Cl | – | [26] |
| 1 | 2,4,6-*i*$Pr_3(C_6H_2)$ | 2,6-*i*$Pr_2(C_6H_3)$ | H | Cl | Cl | – | [26] |

**complex A**

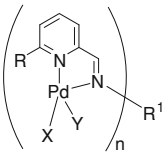


**complex B**

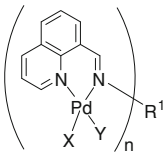


| complex | n | R | $R^1$ | References |
|---|---|---|---|---|
| A | 1 | H | $(CH_2)_2CH_3$ | [11] |
| A | 1 | H | $(CH_2)_4CH_3$ | [12] |
| A | 1 | H | $(CH_2)_7CH_3$ | [12] |
| A | 1 | H | $(CH_2)_{11}CH_3$ | [9, 12] |
| A | 1 | H | $(CH_2)CH{=}CH_2$ | [11] |
| A | 1 | H | $(C_6H_4)$-4-$CH{=}CH_2$ | [11] |
| A | 1 | H | Ph | [11] |
| A | 1 | H | $(C_6H_4)$-4-OH | [11] |
| A | 1 | H | $(C_6H_4)$-4-OH | [10] |
| A | 1 | H | $(C_6H_4)$-4-OH | [10] |
| A | 1 | Me | $(C_6H_4)$-4-OH | [10] |
| A | 2 | H | $(C_6H_4)$-4-OH | [10] |

(continued)

**Table 5.3** (continued)

| complex | n | R | $R^1$ | References |
|---|---|---|---|---|
| A | 2 | H | $(C_6H_4)$-4-OH | [10] |
| A | 2 | H | $\vert-(CH_2)_{12}-\vert$ | [9] |
| A | 2 | H | 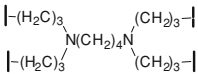 | [41] |
| B | 1 | – |  | [10] |
| B | 2 | – |  | [10] |
| B | 2 | – |  | [10] |

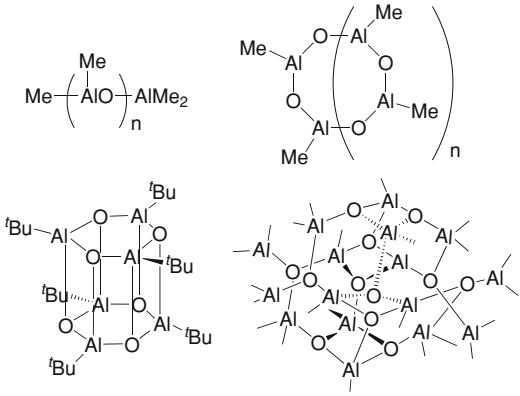

**Fig. 5.7** Principal structures proposed for aluminoxanes

centers, two-dimensional structures, and three-dimensional clusters, all formed from methyl aluminoxane subunits during the controlled hydrolysis of trimethyl aluminum [79–81] (Fig. 5.7). A three-dimensional structure has been proposed by Sinn on the basis of structural similarities with *tert*-butylaluminoxanes [82], which form isolable cage structures [83]. Although its effective structure is still a matter of debate [84], for the sake of simplicity, it is often considered as a linear chain of general formula $[\text{-Al(Me)-O-}]_n$.

The generally accepted mechanism by which MAO can activate late-metal halide complexes for alkene insertion is outlined in Scheme 5.4. MAO is expected to replace halide ligands with methyl groups and ultimately create an ion pair made of a coordinatively unsaturated complex cation and anions derived from MAO [4].

Heterogeneous co-catalysts such as silica gel supported partially hydrolyzed trimethylaluminum (PHT) [14] or physico-chemical supported methylaluminoxanes

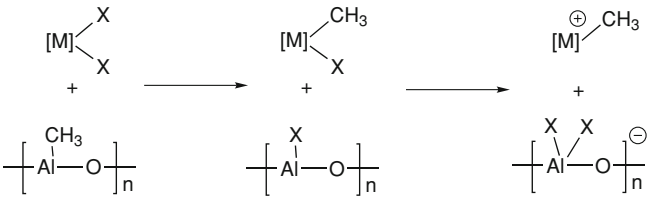


**Scheme 5.4** Proposed mechanism for the activation of [M]-dihalide catalyst precursors

[74, 75] (s-MAO or s-MMAO) have also been proposed as activators for imino-pyridyl dihalide complexes. However, MAO and MMAO remain the most commonly reported co-catalysts in ethylene polymerization/oligomerization for this class of catalysts.

In general, there are several similarities between cobalt and iron bis(imino) pyridine-based complexes and their unsymmetrical mono(imino)pyridine (PIM) counterparts, both in their activation pathways and in the nature of the propagating species. Previous studies on $Co^{II}$ and $Fe^{II}$ bis(imino)pyridine complexes demonstrate that cobalt complexes usually display much lower productivity than their iron counterparts [21, 85–87]. On the contrary, unsymmetrical bidentate $Co^{II}$-(imino)pyridine-based systems exhibit remarkably higher olefin oligomerization activities than their ferrous analogues [7, 21, 27, 88]. Moreover, in contrast to the high molecular weight polymer formed by either sterically demanding α-diimine or bis(imino)pyridine catalysts, (imino)pyridine (PIM) systems provide only half of the axial steric protection and tend to generate low molecular weight branched polyethylenes or light oligomers [7]. The reduced axial steric hindrance generally leads to a higher catalyst activity and a reduced activation barrier in the chain transfer process, in line with previous reports regarding bis(imino)pyridyl iron catalysts [6, 7, 89, 90]. However, the reduction of the steric protection of the metal center also leads to a more rapid active species decomposition [15, 21].

Product analysis and studies on the dependence of the activity and Schulz–Flory α values on the ethylene pressure have been used to elucidate the propagation and chain transfer mechanisms operating in 6-aryl-substituted $Co^{II}$ (imino)pyridine oligomerization catalysts [27, 37]. It has been established that propagation occurs via a classical Cossee-Arlman mechanism and chain transfer proceeds by *β*-H elimination to the metal (BHE), although the concomitant occurrence of alternative termination processes [such as *β*-H transfer to the monomer (BHT)] cannot be ruled out by the authors. Scheme 5.5 illustrates the overall reaction path for ethylene oligomerization by a series of $N_2^{Ar}CoCl_2$/MAO systems. Ethylene oligomerization experiments have shown a linear dependence of activity with monomer pressure while the α factor is independent from the pressure, indicating that the propagation and chain transfer rates are first order in ethylene concentration [29].

The authors therefore propose that the catalyst resting state is a cobalt alkyl species, and the rate determining step (rds) is the monomer coordination to the

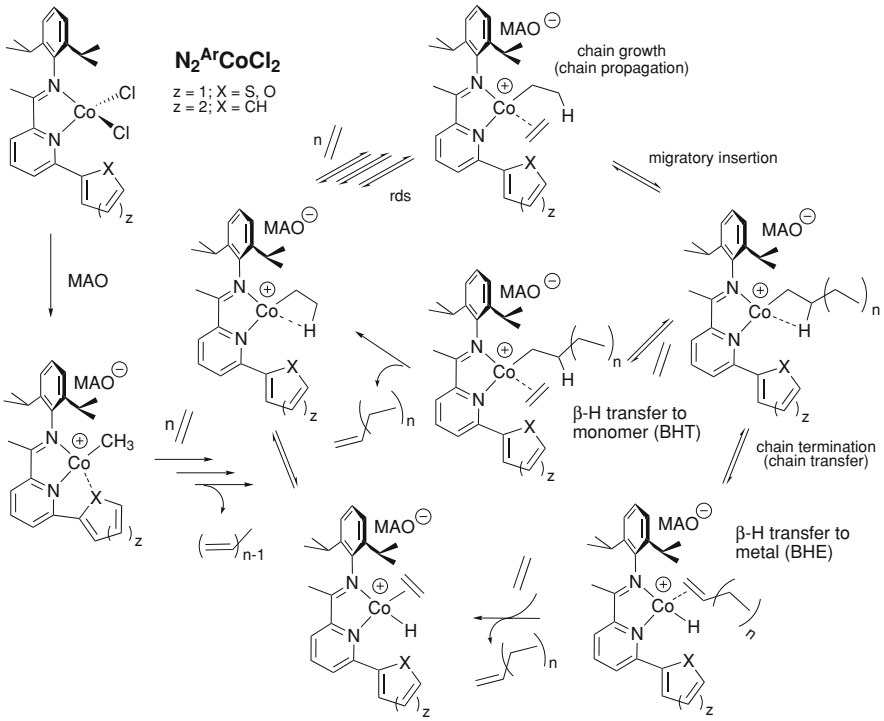


**Scheme 5.5** Reaction mechanism for ethylene oligomerization catalyzed by $N_2^{Ar}CoCl_2$/MAO systems

metal center. In situ and *operando* electron paramagnetic resonance (EPR) experiments have provided useful insights on the nature of the propagating alkyl $Co^{II}$ species involved in the oligomerization process. All high-spin $Co^{II}$ precursors of this series undergo a spin state changeover with formation of paramagnetic square-planar low-spin $Co^{II}$ propagating alkyls of the general formula $[CoN_2^{Ar}(alkyl)]$, where the aryl or heteroaryl group on the 6-position of the pyridine ring is expected to regulate both activity and selectivity of the active species acting as an hemilabile ligand. Density functional theory (DFT) calculations carried out on the latter compounds are consistent with the experimental results, highlighting the importance of the ligand hemilability in assisting olefin insertion by cobalt catalysis [27, 91] and, more generally, stressing the significant influence of the ligand environment on catalyst activity and selectivity.

Other relevant roles of MAO, such as reducing agent, hydrogen abstractor, C-alkylating agent and O-ligand, have also been reported in the literature [4, 92]; nonetheless, we are not aware of any published reports describing these functions on these $Co^{II}$-iminopyridinate systems.

Similar arguments regarding chain growth/chain termination paths and the role of the ligand environment apply to $Pd^{II}$ and $Ni^{II}$ iminopyridinate catalyst precursors

as well. Like α-diimine systems, the catalyst resting state in the catalytic cycle of $Pd^{II}$ iminopyridinate complexes is an alkyl-olefin complex [9, 15, 93], and the rate determining step is represented by the olefin migratory insertion into the metal alkyl bond. Therefore, the rate of propagation for $Pd^{II}$ iminopyridine catalyst systems shows a zero order dependence on ethylene concentration. The same resting state applies in the $Ni^{II}$ systems at low temperature [94]. Metal migration (chain running) along the growing alkyl chain can occur in these species via *β*-H elimination/re-addition reactions without chain transfer (Scheme 5.6). While successive ethylene migratory insertions lead to a linear polymer, insertion following chain running leads to the introduction of branching in the polymer chain (chain propagation/chain running competition). As a result, a fine tuning of the ethylene pressure, reaction temperature, and ligand framework [10–12, 14, 16, 40, 41, 59] allows access to ethylene homopolymers and oligomers, whose structures vary from highly branched to linear semicrystalline materials [88, 95].

### *5.4.1 Olefin Polymerization by 8–10 Group Metal (imino)pyridyl-Based Catalysts*

Unlike sterically demanding α-diimine or bis(imino)pyridine catalysts for the production of high molecular weight polymers, less axially crowded (imino)pyridine

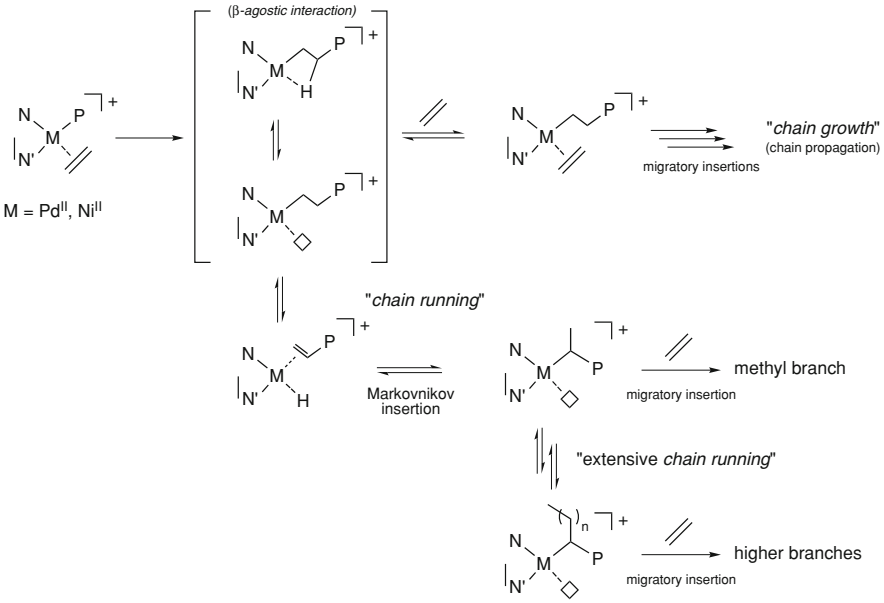


**Scheme 5.6** Proposed mechanism of chain propagation/chain running for the production of branched polymers using $Ni^{II}$ or $Pd^{II}$ iminopyridinate systems

systems (PIM), upon activation with the proper co-catalysts, generate, with rare exceptions, low molecular weight, branched polymeric materials. The production of low molecular weight polymers is generally ascribed to the reduced axial steric protection of these unsymmetrical bidentate systems, which translates into a reduction of the activation barrier for the chain transfer process (see Sect. 5.4).

Mono- and di-nuclear $Ni^{II}$ dihalide (imino)pyridine complexes of the type shown in Scheme 5.7 exhibit, upon activation by MAO, from moderate to fairly good productivity in ethylene polymerization [up to $1.57 \times 10^3$ $kg_{PE}$ ($mol_{Ni}$ h · bar)$^{-1}$], leading to predominantly methyl-branched waxy polymeric materials [15, 17, 58, 59]. Polymer molecular weights as well as type and degree of branching in the polymer depend on several factors, including: (1) ethylene pressure, (2) reaction temperature and (3) ligand environment. Although highly dependent on the polymerization temperature (most of the catalysts of this type undergo irreversible decomposition over 40 °C in toluene), the molecular weights of the materials produced by these $Ni^{II}$ complexes ($M_w$ in the range 300–45,000) remain remarkably lower than those obtained with analogous α-diimine systems under similar conditions [96]. Complex mixtures of olefins in a Schulz–Flory distribution in combination with hyper-branched low molecular weight PEs are often obtained with productivity from low to moderate [16]. Although the origin of this dual activity still remains unclear, it is most likely ascribable to the unsymmetrical nature of the catalyst precursors [97].

$Ni^{II}$ complexes containing quinoline fragments or alkyl arms at the 6-position of the pyridine ring lying on the $N_2$ plane only show very modest activities or, in some cases, complete inactivity for olefin upgrading [14, 16, 59]. Tuning the steric bulk at either the *ortho* positions of the iminoaryl ring or at the imino carbon atom generally translates into differently branched materials. Similarly to α-diimine catalysts [98], a decreased steric bulk at the iminoaryl moiety (isopropyl groups vs. methyl groups) generally produces more linear polymers, while bulky groups (H vs. Me vs. Ph) at the imino carbon atom lead to higher branching degrees [14, 59] (predominantly methyl branching, 9–237 branches per 1,000 carbon atoms). Reported polymerization activities by $Co^{II}$-analogues are fairly negligible and clearly lower than those observed for the corresponding $Ni^{II}$-based systems [58, 96].

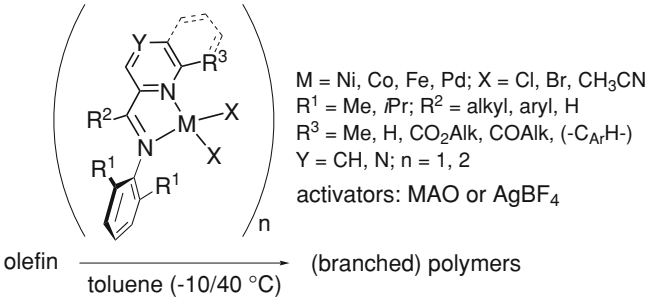


**Scheme 5.7** Polymerization by $Ni^{II}$, $Co^{II}$, $Fe^{II}$ and $Pd^{II}$ (imino)pyridyl/activator catalysis

Upon MAO activation, mononuclear (imino)pyridyl $Pd^{II}$ dihalide complexes of the type shown in Scheme 5.7 form active species for the bicyclo[2,2,1]hept-2-ene (norbornene, NB) polymerization, whereas their dicationic counterparts, prepared from neutral palladium species by treatment with $AgBF_4$, generate polymerization systems with low activity [59]. Like $Ni^{II}$ congeners, activity and selectivity of $Pd^{II}$ (imino)pyridyl systems is sensitive to the ligand environment. Mono-, bi- and tetra-nuclear $Pd^{II}$ complexes with medium-long alkyl chain substituents at the imino nitrogen atom have been prepared and evaluated for ethylene polymerization to linear high molecular weight polyethylenes with moderate productivity [up to 44 $kg_{PE}$ $(mol_{Pd}$ h bar$)^{-1}$] [9, 12, 40, 41]. Higher polymerization activities [up to 134 $kg_{PE}$ $(mol_{Pd}$ h bar$)^{-1}$] have been reported for $Pd^{II}$ iminopyridine systems containing 4-phenol groups at the imino nitrogen atom [11].

$Ni^{II}$ [32], $Pd^{II}$ [22] and $Co^{II}$ dihalide [21] complexes stabilized by 2-alkoxycarbonyl-6-(imino)pyridyl ligands generate rather modest ethylene polymerization catalysts, in most cases providing complex mixtures of light olefins and polyethylene materials. Iron(II) congeners exhibit the highest activities in ethylene polymerization, with productivity up to 95 $kg_{PE}$ $(mol_{Fe}$ h bar$)^{-1}$ and always provide complex mixtures of low molecular weight polyethylenes and short chain α-olefins in a Schulz–Flory distribution [21, 62]. The bonding versatility of the alkoxycarbonyl substituent makes the final coordination geometry around the metal center quite unpredictable. As a result, clear-cut structure/selectivity relationships can be only roughly outlined. Curiously, switching from $Fe^{II}$ 2-alkoxycarbonyl-6-iminopyridyl to 2-acetyl-6-iminopyridyl systems results in an impressive increase of the catalyst productivity for ethylene polymerization [31, 61, 99] [up to $13 \times 10^3$ $kg_{PE}$ $(mol_{Fe}$ h bar$)^{-1}$]. The improved productivity in the latter case is most likely the result of contamination with traces of $Fe^{II}$ 2,6-bis(imino)pyridyl complexes.

### *5.4.2 Olefin Oligomerization by Group 8–10 Metal (imino)pyridinato Catalysts*

Oligomers are produced as a consequence of a highly competitive chain transfer process relative to chain propagation [100]. It is generally established that the chain transfer activation barrier is increased in the presence of axially crowded systems, thus favoring the production of high molecular weight oligomers or polymers. Unlike bis(arylimino)pyridyl or α-diimino complexes, unsymmetrical (imino)pyridine systems (PIM), which provide only half of the axial steric protection at the metal center, constitute excellent and to some extent unique candidates for the efficient production of light oligomers. Ligand stereo-electronic features and reaction temperature are the key factors controlling catalyst activity and selectivity.

Cationic $Pd^{II}$ complexes of the type shown in Scheme 5.8 have been reported to catalyze the oligomerization of ethylene with productivity in light hyper-branched

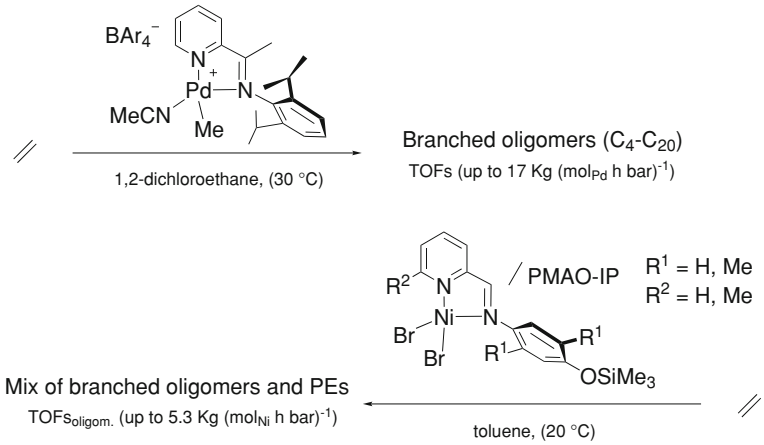


**Scheme 5.8** Oligomerization catalysis by $Ni^{II}$ and $Pd^{II}$ iminopyridine complexes

internal olefins ($C_4$–$C_{20}$) up to 18 kg $(mol_{Pd}\ h\ bar)^{-1}$ [51]. Aldimine $Ni^{II}$ complexes from the same series [16] (Scheme 5.8), although less active than their ketimine Pd congeners, still produce branched olefins together with small portions of insoluble PE fractions. Carbosilane dendritic compounds containing up to 16 terminal pyridylimine $Ni^{II}$ complexes of this type have also been evaluated, in combination with MAO, for the production of mixtures of branched oligomers that follow a Schulz–Flory distribution and highly branched low molecular weight PEs ($M_W = 2{,}000$–$177{,}000$) [16].

2-Alkoxycarbonyl-6-(imino)pyridyl ligands in combination with $Fe^{II}$, $Pd^{II}$, $Ni^{II}$ or $Co^{II}$ ions have been reported to oligomerize ethylene with moderate to fairly good productivity (Fig. 5.8a). $Pd^{II}$ dihalide complexes of this type, upon activation with MAO, generate ethylene dimers with TOFs up to 19 kg $(mol_{Pd}\ h\ bar)^{-1}$ and a small fraction of PE materials [22]. Mixtures of branched light oligomers ($C_4$–$C_8$) in a non-Schulz–Flory distribution and insoluble PE materials have been obtained with the 2,6-dihaloaryl-substituted $Ni^{II}$ congeners too, with productivity in the oligomeric fraction up to 213 kg $(mol_{Ni}\ h\ bar)^{-1}$ [32]. Significantly improved activity [TOFs over 797 kg $(mol_{Ni}\ h\ bar)^{-1}$] and selectivity towards ethylene oligomerization (i.e., when light olefins are produced without traces of PE) have been obtained with the latter $Ni^{II}$ compound when $PPh_3$ is employed as an auxiliary ligand. Although the role of $PPh_3$ has not been definitively addressed, the authors suggest that the temporary coordination of the $PPh_3$ to the vacant coordination site at the metal center improves the active species lifetime [32].

Simultaneous ethylene oligomerization and polymerization have also been documented for 2-alkoxycarbonyl $Fe^{II}$ and $Co^{II}$-dihalo complexes [21, 62, 70]; while ferrous complexes exhibit higher activity towards ethylene polymerization, under similar reaction conditions, their cobalt counterparts present higher activity towards light oligomers [from $C_4$–$C_8$ $\alpha$-olefins in a Schulz–Flory distribution with

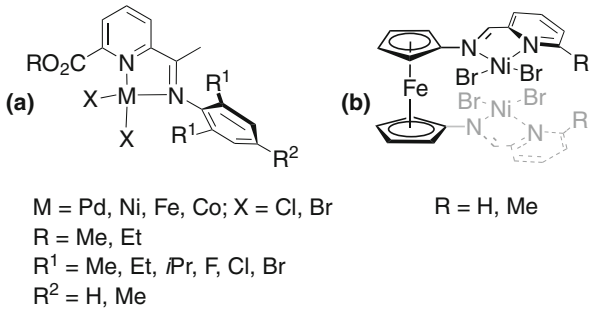


**Fig. 5.8** **a** 2-Alkoxycarbonyl iminopyridyl $Pd^{II}$, $Ni^{II}$, $Fe^{II}$ and $Co^{II}$ oligomerization catalysts; **b** Mono- or di-nuclear $Ni^{II}$-dibromo complexes containing ferrocenyl N,N ligands

productivity up to 72 kg $(mol_{Fe}\ h\ bar)^{-1}$ to almost exclusively 1-butenes with TOFs over $1.35 \times 10^3$ kg $(mol_{Co}\ h\ bar)^{-1}$].

Relatively modest productivity in light oligomers (mainly butenes and hexenes) with a Schulz–Flory distribution [up to 30 kg $(mol_{Fe}\ h\ bar)^{-1}$] have also been reported for 2-acetyl-6-(imino)pyridyl $Fe^{II}$-complex bearing electron withdrawing groups (e.g., *m*-$CF_3$) at the arylimino fragment [20]. Compared to $Ni^{II}$ systems containing bulky *ortho*-substituted aryl groups at the imino nitrogen atom that produce branched oligomers and PEs or mixture thereof [14–16, 58, 59], mono- and/or di-nuclear $Ni^{II}$ dibromo complexes stabilized by iminopyridyl ligands containing a ferrocenyl substituent at the imino moiety (Fig. 5.8b) have been found to generate almost exclusively ethylene dimers with TOFs up to 536 kg $(mol_{Ni}\ h\ bar)^{-1}$ [10].

Iminopyridine ligands bearing aryl or heteroaryl substituents on the 6-position of the pyridine ring have been used to develop a new class of highly active and selective tetrahedral $Co^{II}$-dihalide complexes for ethylene, propylene and norbornene oligomerization and co-oligomerization. On activation with MAO, these $Co^{II}$ catalyst precursors generate active species for ethylene conversion into short-chain α-olefins in a Schulz–Flory distribution with turnover frequencies as high as $5.2 \times 10^3$ kg $(mol_{Co}\ h\ bar)^{-1}$ and selectivity in 1-olefins up to 95% [27–29].

A crucial role in controlling both activity and selectivity for these $Co^{II}$-systems is played by the nature of the substituent on the 6-position of the pyridine ring. Among the various systems investigated, $Co^{II}$ precursors bearing 2-thienyl fragments show higher activity leading to α-olefins with a Schulz–Flory distribution in the $C_4$–$C_{12}$ range. Notably, catalysis by $Co^{II}$ complexes containing 6-aryl or 6-heteroaryl groups of comparable steric size but with no pendant 2-thienyl arms (furanyl, phenyl, naphthyl or 3-thiophenyl) leads almost exclusively to ethylene dimers with slightly lower productivity (Scheme 5.9) [27–29].

In situ and in *operando* EPR experiments conducted on the MAO-activated complexes have highlighted the central role exerted by the 6-organyl group in steering ethylene oligomerization activity and selectivity [27] (see Sect. 5.4). The higher activity observed for the 2-thienyl-substituted catalysts is ascribed to the sulfur atom coordination/detachment at the cobalt center in the activated species, which is expected to stabilize the transition state for migratory insertion and, at the same time, retard the chain transfer process [27].

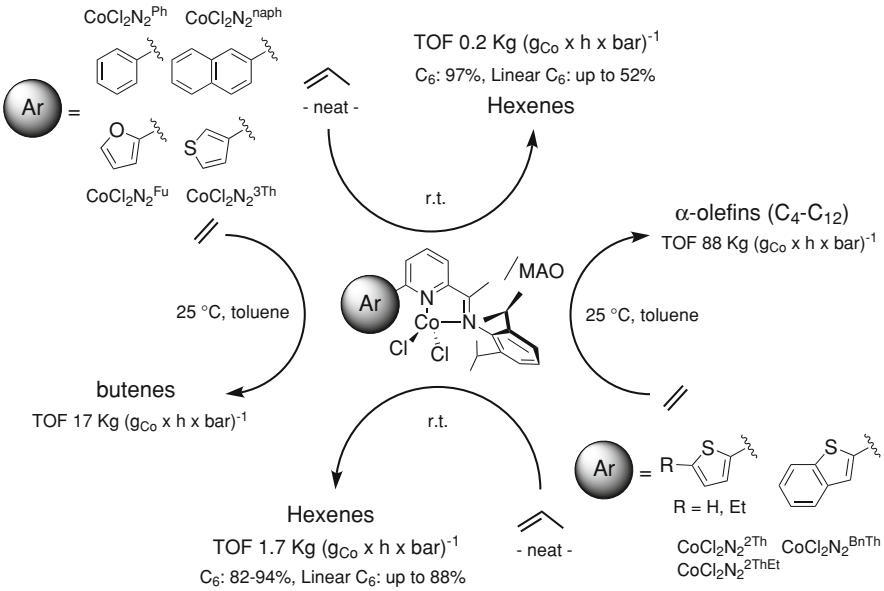


**Scheme 5.9** Ethylene and propylene oligomerization catalysis by $Co^{II}$ 6-aryl substituted iminopyridine complexes

Similar activity and selectivity arguments on these MAO-activated 6-aryl substituted $Co^{II}$-iminopyridinate systems have been reported for propylene oligomerization [36]. While the $CoCl_2N_2^{2Th}$/MAO system promotes the highly regioselective and efficient formation of linear propylene dimers in the presence of a small amount of higher oligomers (trimers and tetramers), a higher selectivity towards dimers (up to 97%), and a lower productivity and regioselectivity (linear hexenes and methyl branched pentenes are produced in comparable yields) is obtained with the $CoCl_2N_2^{Ph}$/MAO system (Scheme 5.9). The latter system has also been found to generate active species that catalyze the unprecedented diastereoselective enchainment of one norbornene molecule (NB) with two ethylene molecules to give *exo*-2,*exo*-3 ethyl-vinyl norbornane with extremely high activity [up to $6.3 \times 10^3$ $kg_{NB\ conv.}$ $(mol_{Co}\ h\ bar)^{-1}$] and selectivity (Scheme 5.10, top) [37, 71].

Although the thien-2-yl $Co^{II}$-complex generates a more efficient system for the NB conversion into the ethyl-vinylated derivative than the phenyl substituted one, it suffers from a lower selectivity. Indeed, its greater ability to generate ethylene oligomers higher than 1-butene results in complex mixtures of ethyl–vinyl norbornane, $C_6$–$C_{12}$ α-olefins, and detectable amounts of hetero-tetramers and pentamers (Scheme 5.10, top) [37]. Notably, the hetero-trimerization protocol has also been accomplished by the same authors with NB monomers containing polar functional groups, such as norbornene-methanol and norbornene-carboxylic acid, with activities up to 17 kg $(mol_{Co}\ h\ bar)^{-1}$ and complete diastereoselectivity. To this purpose, polar monomers are previously protected in situ by treatment with

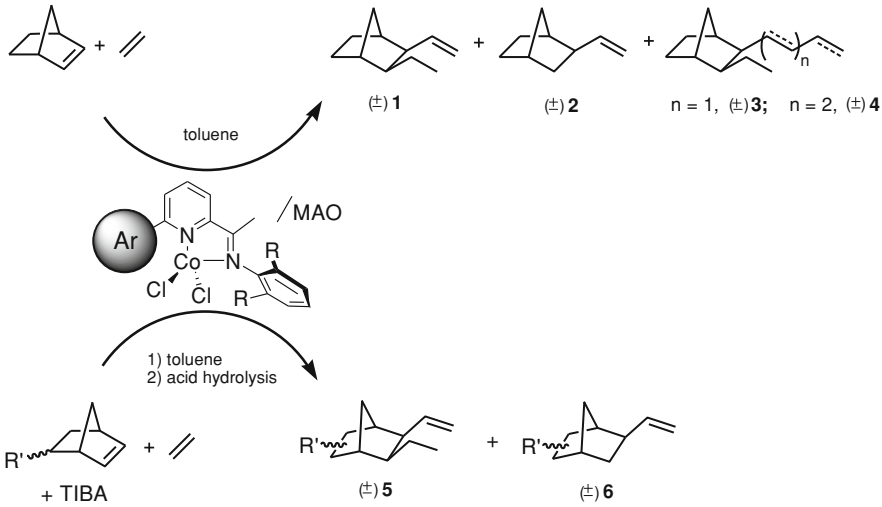


| pre-catalyst | R | R' | (±) 1 | (±) 2 | (±) 3 | (±) 4 | (±) 5 | (±) 6 |
|---|---|---|---|---|---|---|---|---|
| Ar = Ph | *i*Pr | - | 97% d.e.> 99% | 2% | 1% | - | - | - |
| Ar = Th | *i*Pr | - | 82% d.e.> 99% | 3% | 9% | 6% | - | - |
| Ar = Ph | Me | $CH_2OH$ | - | - | - | - | 94% d.e.> 99% | 6% |
| Ar = Ph | Me | $CO_2H$ | - | - | - | - | 92% d.e.> 99% | 8% |

**Scheme 5.10** Co-oligomerization catalysis by $Co^{II}$-iminopyridinato/MAO systems; ethylene-norbornene hetero-trimerization protocol (*top*) and hetero-trimerization protocol on norbornenes containing polar functionalities (*bottom*)

triisobutyl aluminum (TIBA) [101–104] to avoid both catalyst poisoning effects and undesired side-reactions with MAO. A less sterically demanding complex ($CoCl_2N_2^{Ph/Me2}$) has also been found to provide better activity and selectivity in the hetero-trimerization process (Scheme 5.10, bottom) [37].

Cobaltous systems of this type bearing 6-heteroaryl groups capable of a stronger $\sigma$-ligating character to the metal center (as for 2-pyridyl groups) result in the formation of completely inactive oligomerization/co-oligomerization catalysts [27]. In spite of that, pentacoordinate $Co^{II}$-dihalide complexes bearing a quinoxalinyl fragment on the 6-position of the pyridine ring are found to generate, upon activation with MMAO, relatively active systems for ethylene dimerization [167 kg $(mol_{Co}\ h\ bar)^{-1}$] [105]. Finally, neither the tetrahedral high-spin $d^6$ $Fe^{II}$ catalysts ($FeCl_2N_2^{Ph}$ and $FeCl_2N_2^{2Th}$) nor the square-planar diamagnetic $d^8$ $Ni^{II}$ congeners ($NiCl_2N_2^{Ph}$ and $NiCl_2N_2^{2Th}$) generate active oligomerization/polymerization catalysts upon treatment with MAO [27].

Related $Co^{II}$ and $Ni^{II}$-iminopyridinate complexes bearing more sterically demanding aryl groups on the 6-position of the pyridine ring [xylyl or 2,4,6-$iPr_3(C_6H_2)$] have also been proposed as efficient precursors for ethylene oligomerization to light α-olefins (mainly butenes) with productivity up to 472 kg $(mol_{Co}\ h\ bar)^{-1}$ [26]. Bulkier ligands of this type are not found to affect the selectivity of the resulting $Co^{II}$ and $Ni^{II}$-iminopyridinate systems significantly. Short-chain α-olefins are produced almost exclusively, although small amounts of polymeric materials are somehow generated depending on the catalyst activator employed ($AlEt_3$ vs. MAO). While $Fe^{II}$ catalysts of this type turn out to be virtually inactive towards ethylene oligomerization/polymerization, $Pd^{II}$ congeners provide only polymeric materials with productivity comparable to those reported for the less sterically hindered $Pd^{II}$-iminopyridinate systems [9, 12, 40, 41]. Two $Co^{II}$ and $Ni^{II}$-dihalo iminopyridinate fragments have been combined within a unique molecular structure by means of an aryl linker fixed at the 6-position of the respective pyridine rings to give novel homo-dinuclear catalyst precursors (Scheme 5.11) [23]. Both complexes, once activated with MAO, show fairly low activity [up to 20 kg $(mol_{Ni}\ h\ bar)^{-1}$ and 1 kg $(mol_{Co}\ h\ bar)^{-1}$] in ethylene oligomerization with no apparent M-M cooperative effect, providing mixtures of linear α-olefins and internal isomers (Co) or methyl branched ethylene oligomers (Ni).

Pentadentate ligands joining 2-iminopyridyl and 2,6-bis(imino)pyridyl moieties capable of accommodating one or two metal centers with different coordination geometries have been used to prepare mono- and homodi-nuclear $Fe^{II}$ and $Co^{II}$-dihalo complexes (Scheme 5.12) [25]. On activation by MAO in toluene, all these systems have been found to generate effective catalysts for ethylene oligomerization to α-olefins with productivity and Schulz–Flory parameters depending on the type and number of coordinated metals. Although only negligible M–M magnetic interactions have been measured in the dinuclear systems, the occurrence of some M–M cooperative effect is invoked by the authors to explain why the dinuclear derivative $CyAr_2N_5Co_2Cl_4$ is four times more active than its mononuclear analogue $CyAr_2N_5CoCl_2$ [25].

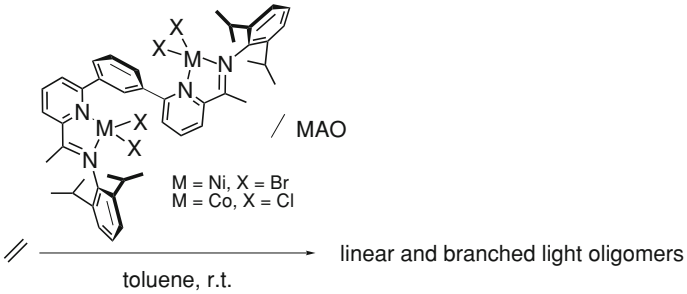


**Scheme 5.11** $Ni^{II}$ and $Co^{II}$ catalysis by homodinuclear iminopyridinate complexes

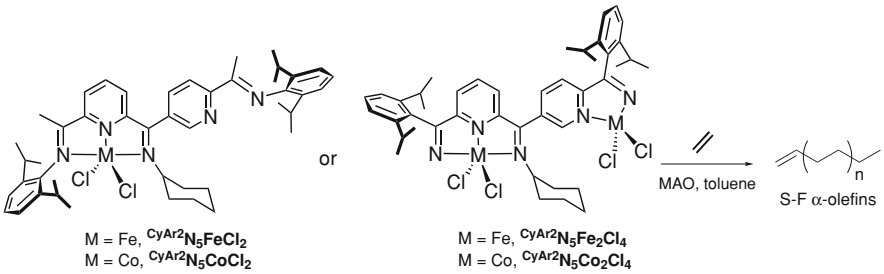


**Scheme 5.12** $Fe^{II}$ and $Co^{II}$ catalysis by mono- and homodi-nuclear complexes

### *5.4.3 $Ni^{II}$ and $Co^{II}$-iminopyridine Systems in* Tandem *Co-polymerization Catalysis*

Short-chain branched linear low-density polyethylenes (LLDPEs) are traditionally produced on industrial scale by ethylene/α-olefin co-polymerization catalyzed by either heterogeneous Ziegler–Natta type or homogeneous single-site catalysts [106–108]. Catalytic systems based on homogeneous Group 4 constrained-geometry catalysts (CGCs) offer the possibility of incorporating higher α-olefins in the PE microstructure and thus can produce long-chain branched polyethylenes [109–111].

*Tandem* co-polymerization catalysis is a relatively recent technique for the production of branched PE from ethylene feedstock [112–114]. Since an early report by Bazan and Barnhart in 1998 [112], a great variety of combinations of early and late transition metal catalyst precursors have been successfully employed to prepare a variety of PEs spanning from LLDPE up to completely amorphous, ultra-low density polyethylenes (ULDPE).

The ability of iminopyridinate late transion metal complexes to act as oligomerization systems in *tandem* co-polymerization protocols, together with their excellent compatibility towards a wide range of polymerization systems and activators, is well documented in a number of contributions appearing on iminopyridinate-based *tandem* co-polymerization processes for the production of variably branched PEs and composites. Silica-supported co-polymerization $Ti^{IV}$ CGC/MMAO systems, in combination with a $Ni^{II}$-dibromo iminopyridine/MMAO oligomerization system, have been reported by Okuda and co-workers as a *tandem* approach to ethylene/α-olefin co-polymerization for the production of moderately branched PEs (up to 21 br/1,000 C) with a good control on the polymer microstructure (Scheme 5.13) [52].

6-Aryl-substituted $Co^{II}$ iminopyridinate oligomerization catalysts for the production of highly linear α-olefins with a Schulz-Flory distribution, in combination with the CGC, $TiCl_2[(\eta^5\text{-}C_5Me_4)SiMe_2(t\text{BuN})]$, have been found to generate, upon activation with MAO, a class of homogeneous *tandem* systems for the effective conversion of ethylene into variably branched PE materials [46, 72, 73]. An appropriate choice of both Co/Ti molar ratio ($\chi_{Co}$) and experimental conditions,

leads to polymers ranging from slightly branched semicrystalline LLDPEs ($C_2$ br. 83%; $C_4$ br. 17%; tot. br. 27 per 1,000 $C_{atoms}$) to hyper-branched, amorphous PEs ($C_2$ br. 85%; $C_4$ br. 13%; $C_6$ br. ≥2% tot. br. 254 per 1,000 $C_{atoms}$) with *T*g as low as −60 °C and productivity up to $1.5 \times 10^3$ kg $(mol_{Ti}\ h\ bar)^{-1}$ (Scheme 5.14) [46].

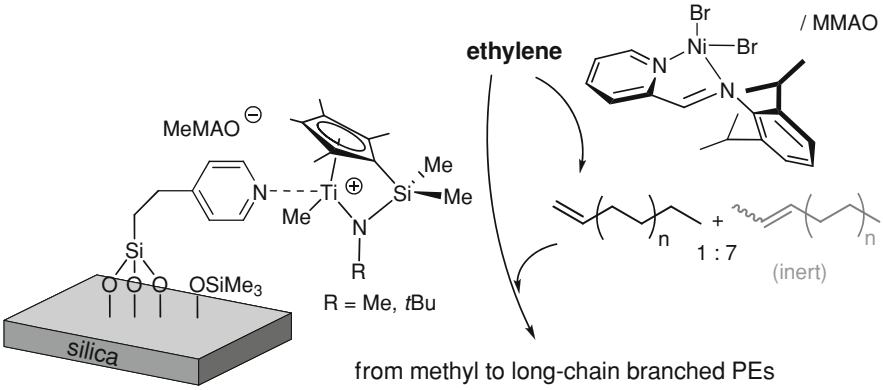


**Scheme 5.13** $Ni^{II}$-iminopyridinate/supported-$Ti^{IV}$-CGC *tandem* co-polymerization catalysis

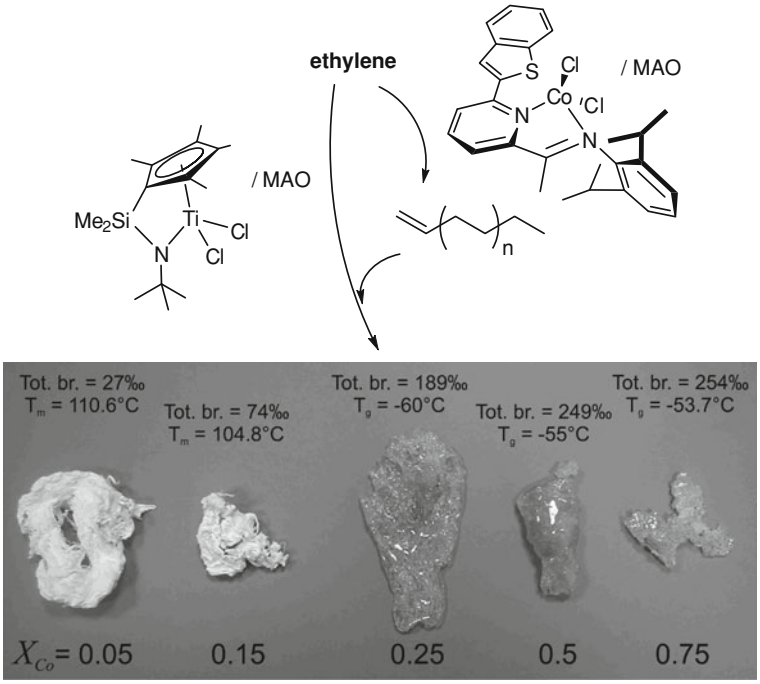


**Scheme 5.14** Homogeneous $Co^{II}/Ti^{IV}$ *tandem* co-polymerization protocol for producing polymers ranging from LLDPEs to amorphous PEs [46]. (Picture under copyright Wiley–VCH Verlag GmbH & Co. KGaA. Reproduced with permission)

A metallocene ($Cp_2ZrCl_2$) as co-polymerization catalyst has also been employed by the same authors to set up, in combination with $Co^{II}$-iminopyridinate oligomerization systems from the same series, a novel *tandem* protocol for the production of almost exclusively ethyl-branched (tot. br. up to 56‰) materials. In spite of a higher productivity compared with $Ti^{IV}$-CGC [over $12.7 \times 10^3$ $Kg_{LLDPE}$ $(mol_{Zr}\ h\ bar)^{-1}$], only semicrystalline off-white solids exhibiting melting points between 87 and 121 °C were obtained with this *tandem* protocol [47].

Lower polymer branching degrees and different α-olefin incorporation kinetics, as a function of the α-olefin length, highlight the superior ability of CGCs at incorporating higher α-olefins than metallocenes. The combination of these co-polymerization *tandem* protocols with the *polymerization filling technique* (PFT) has recently enabled a procedure for the textured surface coating of multi-walled carbon nanotubes (MWCNTs) with moderately branched LLDPEs (from 3.5 br to 34.5 br/1,000 C) (Scheme 5.15) [74, 75]. This approach to the preparation of structurally tailored composite materials using homogeneous single-site oligomerization/co-polymerization catalysts activated at the surface of a heterogeneous co-catalyst provides an effective and original way to control PE branching and morphology at the nanofiller surface.

In order to increase the catalytic efficiency of *tandem* systems [115–118] as to improve the comonomer enchainment efficiency into the PE microstructures, Osakada and co-workers have proposed an efficient and clean method to prepare new heterodinuclear early-late transition metal catalysts accommodating the two

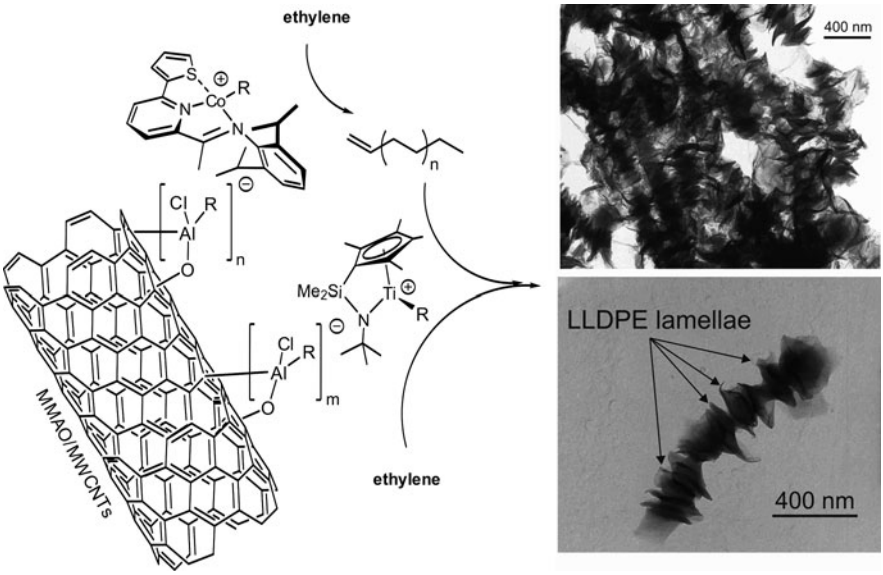


**Scheme 5.15** *Tandem* co-polymerization catalysis/polymerization filling technique for the preparation of structurally tailored MWCNTs/LLDPEs composites. Figure partially reprinted with permission from [75]. Copyright 2008 American Chemical Society

active centers in close proximity to each other. (Scheme 5.16) [50, 119]. Activity and selectivity of the new heterobinuclear early-late precursors have been compared with those observed for the separate mononuclear complexes, thus highlighting the occurrence of a positive synergic effect between the two metal centers (Scheme 5.16).

### *5.4.4 Atom Transfer Radical Polymerization by $Cu^{I}$ and $Fe^{II}$ Iminopyridinate Catalysts*

Atom transfer radical polymerization (ATRP) is an exceptionally robust way to uniformly and precisely control the chemical composition and architecture of polymers, as well as the uniform growth of every polymer chain, while employing a broad range of monomers. Since its discovery in the mid-1990s, this controlled radical polymerization (CRP) method has allowed scientists to form structurally tailored polymers comprising vinyl monomers (styrenic, methacrylic, acrylic, just to mention a few) in a controlled, piece-by-piece fashion, thus leading to polymeric materials with well-defined $M_n$ and narrow molecular weight distributions [120–123].

Bidentate pyridyl-2-aldimino ligands in combination with $Cu^{I}$-ions generate very efficient catalysts for ATRP because of their ability to stabilize the metal ions in low oxidation states [124] and produce soluble $Cu^{I}$ species for homogeneous processes. Pyridyl-2-(*N*-propyl-aldimine) $Cu^{I}$ complexes of the type shown in Scheme 5.17a have been used as efficient catalyst precursors, in conjunction with ethyl 2-bromoisobutyrate as initiator, for ATRP of methyl methacrylate (MMA) in either a homogeneous [125–127] or heterogeneous phase (silica or polystyrene supported catalysts) [13]. $Cu^{I}$-complexes of this type bearing *n*-alkyl substituents at the imine nitrogen atom have shown superior catalytic performance towards polymerization of MMA compared with those containing branched N-alkyl groups, which exhibit slow reaction rates and broad polydispersity indexes (PDIs) [128]. It is generally demonstrated that longer alkyl arms at the imine nitrogen atom (from propyl to octyl) generate more soluble ATRP catalysts, resulting in more controlled polymerizations as evidenced by the narrow molecular weight distributions [128, 129].

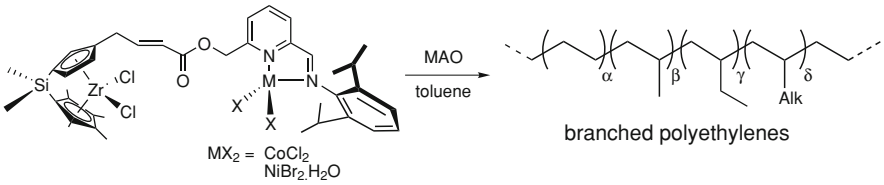


**Scheme 5.16** Homogeneous $Ni^{II}/Zr^{IV}$ and $Co^{II}/Zr^{IV}$ intramolecular *tandem* co-polymerization protocols for the production of highly branched PEs

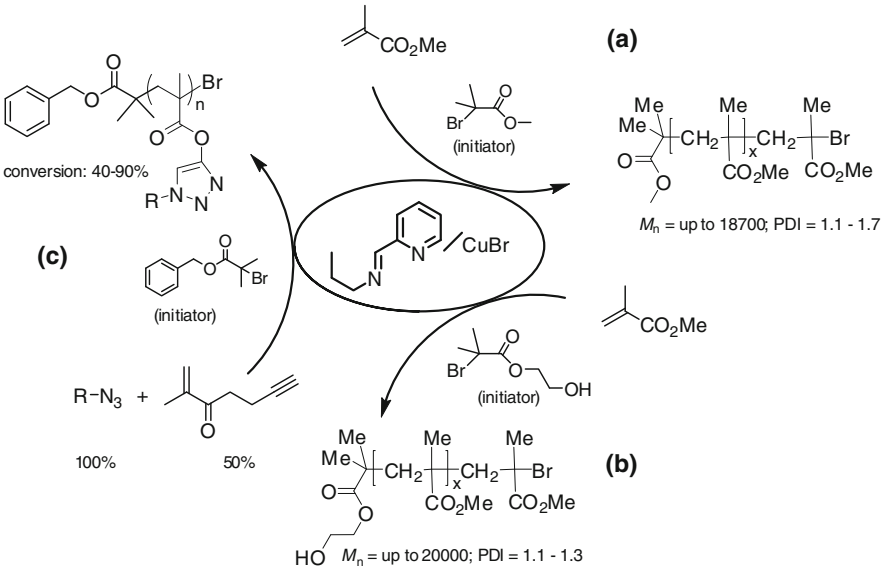


**Scheme 5.17** **a** and **b** ATRP by $Cu^I$-iminopyridinate complexes; **c** Sequential one-pot CuAAC/LRP by $Cu^I$-iminopyridinate catalysis

α-Hydroxy functionalized PMMAs have also been prepared using the same $Cu^I$-catalysts in combination with an hydroxyl alkyl bromide as initiator with no apparent effect on the control of the molecular weights ($M_n$) and PDI of the monohydroxy terminated PMMAs (Scheme 5.17b) [57]. Furthermore, the $Cu^IBr$/iminopyridine catalytic system has been reported to promote the sequential, one-pot azide-alkyne cycloaddition [CuAAC -Huisgens type reaction)/living radical polymerization (LRP) process, providing a novel and original synthetic tool for the production of functional molecular materials (Scheme 5.17c) [130, 131].

Relatively fast and controlled ATRP of styrene and MMA by mono- and di-nuclear $Fe^{II}$ iminopyridyl catalysis have been reported by Gibson et al. [8]. Mononuclear species obtained with bulky imine substituents and a methyl group on the pyridine 6-position generate relatively active catalysts for the controlled polymerization of styrene and MMA. On the contrary, a reduced steric hindrance on the N atom, which favors dinuclear derivatives formation, produces less efficient catalytic systems.

## 5.5 Synthesis of Group(IV) Metal Amidoalkylpyridinate Complexes

While iminopyridyl ligands are well suited for stabilizing late transition metal complexes, early metals are much more electrophilic and prone to react at the imine moiety. Thus, the chemistry of early- and some mid-transition metals is

**Table 5.4** Amidoalkylpyridinato Group IV metal complexes

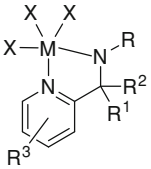


| R | $R^1$ | $R^2$ | $R^3$ | M | X | References |
|---|---|---|---|---|---|---|
| 2,6-*i*$Pr_2C_6H_3$ | Me | Ph | H | Zr | Bn | [132] |
| 2,6-*i*$Pr_2C_6H_3$ | Me | Me | H | Zr | Bn | [45, 132] |
| 2,6-*i*$Pr_2C_6H_3$ | $=CH_2$ | | H | Zr | Bn | [132] |
| *N*-2,5-$Me_2$pyrrole | Me | Me | H | Zr | Bn | [133] |
| *N*-2,5-$Me_2$pyrrole | Me | Bn | H | Zr | Bn | [133] |
| *N*-2,6-$Me_2$piperidine | Me | Me | H | Zr | Bn | [133] |
| *N*-2,6-$Me_2$piperidine | Me | Bn | H | Zr | Bn | [133] |
| 2,6-*i*$Pr_2C_6H_3$ | H | H | H | Zr | Bn | [45] |
| 2,6-*i*$Pr_2C_6H_3$ | H | H | H | Hf | $Me_2N$ | [45] |
| 2,6-*i*$Pr_2C_6H_3$ | H | Me | H | Zr | $Me_2N$ | [45] |
| 2,6-*i*$Pr_2C_6H_3$ | Me | Me | H | Zr | $Me_2N$ | [45] |
| 2,6-*i*$Pr_2C_6H_3$ | H | H | 4,6-*t*$Bu_2$ | Zr | $Me_2N$ | [45] |
| 2,6-*i*$Pr_2C_6H_3$ | H | H | 4,6-*t*$Bu_2$ | Hf | $Me_2N$ | [45] |
| 2,6-*i*$Pr_2C_6H_3$ | H | Me | Benzo[*e*] | Zr | $Me_2N$ | [45] |
| 2,6-*i*$Pr_2C_6H_3$ | H | Me | 6-*i*Pr | Zr | $Me_2N$ | [45] |
| 2,6-*i*$Pr_2C_6H_3$ | H | Me | 6-*i*Pr | Hf | $Me_2N$ | [45] |

more widely described by amidoalkylpyridyl ligation. Group IV amidopyridinate complexes are one of the first reported classes of soluble high-activity post-metallocene polymerization catalysts. Many of these complexes have demonstrated success as olefin oligomerization and/or polymerization catalysts, and some have played essential roles in the development of new polyolefin materials. The complexes discussed in this section are summarized in Table 5.4.

Olefin polymerization using these catalysts was first reported by Murray in 1999 [132]. At least three methods for generating catalytically active complexes of this type are reported. One approach involves a simple reaction of an iminopyridyl ligand precursor with $Zr(CH_2Ph)_4$, generating a zirconium-amido linkage in situ via reductive imine benzylation (Scheme 5.18a). Alternatively, the imine ligand can be reductively alkylated in advance with $Me_3Al$ and quenched with aqueous base to generate an aminoalkylpyridyl ligand; the subsequent reaction with $Zr(CH_2Ph)_4$ generates the expected {N, $N^-$}-ligated complex via protonolysis of a benzyl fragment (Scheme 5.18b). In a third method, a catalyst solution can be generated by adding ether-free benzyl Grignard to a slurry of $ZrCl_4$ and the iminopyridyl ligand precursor (Scheme 5.18c).

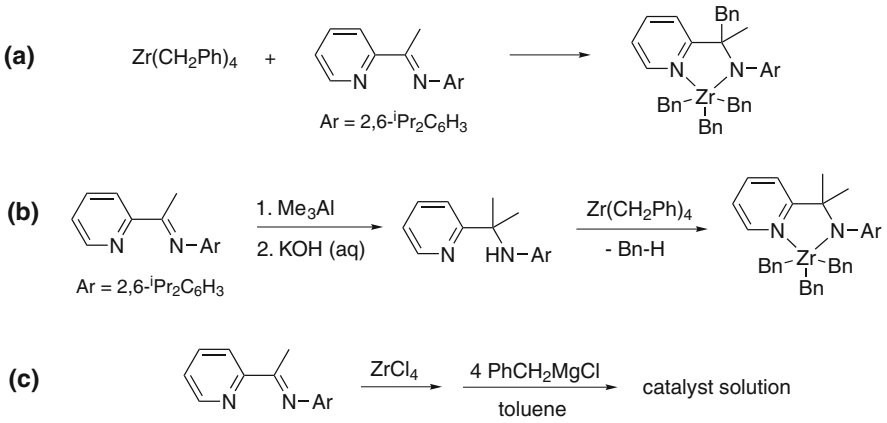


**Scheme 5.18** Synthetic methods for the preparation of Group IV amidoalkylpyridinato complexes

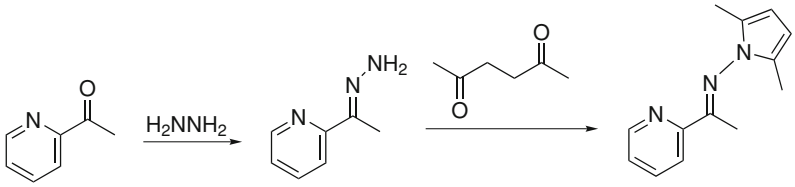


**Scheme 5.19** Synthesis of an iminopyridine ligand comprising an N-2,5-dimethylpyrrole substituent

While the most widely reported substituent at either the imino or amino N-atom is 2,6-*i*$Pr_2C_6H_3$, Murray has also reported the use of N-heterocycles in this position, such as 2,5-dimethylpyrrole or 2,6-dimethylpiperidine. The imine intermediates in the ligand syntheses can be prepared either by direct condensation of an acetyl-substituted pyridine compound with an N-amino-heterocycle, or by condensation of hexane-2,5-dione with 2-(1-hydrazonoethyl)pyridine, as shown in Scheme 5.19.

Further elaboration of this ligand family has been reported by Erker et al. [45] focusing primarily on the introduction of alkyl substituents on the pyridine ring (Table 5.5). The acetyl-substituted pyridine precursors containing an alkyl substituent at the 6-position of the pyridine ring have been prepared following a relatively complex synthetic procedure outlined in Scheme 5.20a. 2-Isopropyl- and 2-*t*Bu-pyridine are prepared by successive α-methylations of 2-ethylpyridine. Subsequent conversion to 2-acetyl derivatives is accomplished by *ortho*-cyanation followed by reductive alkylation with MeLi. An entirely different approach is used to prepare the 4,6-*t*$Bu_2$-disubstituted 2-formylpyridine derivative, involving a pyrylium intermediate of the type shown in Scheme 5.20b. Selenium dioxide

**Table 5.5** Structural variants of aminoalkylpyridyl ligands [45]

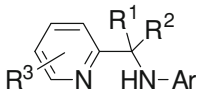


| $R^1$ | $R^2$ | $R^3$ |
|---|---|---|
| H | H | H |
| H | H | 4,6-*t*$Bu_2$ |
| Me | H | H |
| Me | H | Benzo[e] |
| Me | Me | H |
| H | Me | 6-*i*Pr |
| H | Me | 6-*t*Bu |
| Me | Me | 6-*i*Pr |
| Me | Me | 6-*t*Bu |

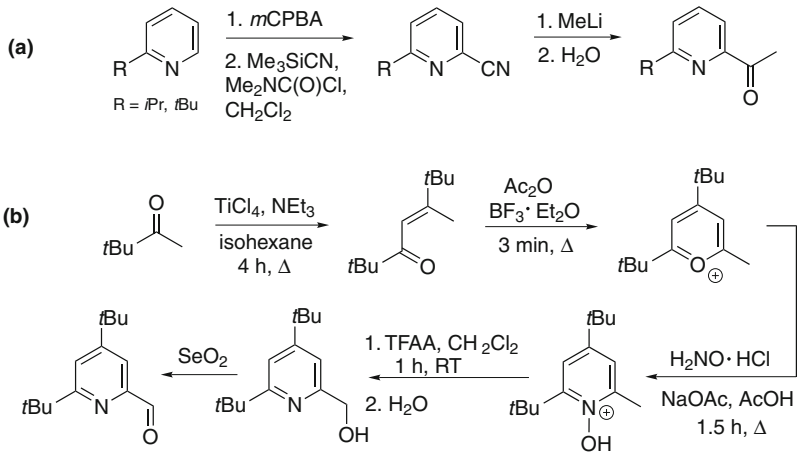


**Scheme 5.20** Key synthetic steps for aminoalkylpyridyl ligands with bulky substituents at the pyridine ring

oxidation is ultimately used to convert the 2-hydroxymethylpyridine into 2-formylpyridine intermediate.

The same authors report the synthesis of $Zr^{IV}$ and $Hf^{IV}$ complexes generated via protonolysis reaction with either $M(NMe_2)_4$ or $M(Bn)_4$ to give the corresponding tris(dimethylamido) or tris(benzyl) complexes, respectively (see also Scheme 5.18b). An $Al^{III}$-dimethyl complex has also been isolated and characterized while reducing the iminopyridine ligands with $Al(Me)_3$ (imine reductive alkylation; see also Scheme 5.18a). However, the authors have been able to synthesize only a limited number of zirconium and hafnium variants bearing the very bulky *tert*-butyl group in the 6-position of the pyridine ring (only when $R^1 = R^2 = H$).

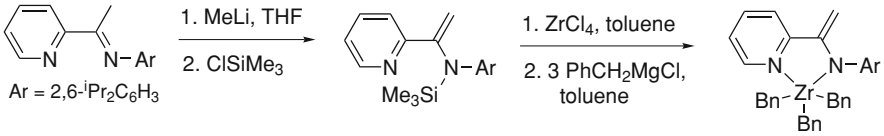


**Scheme 5.21** Synthesis of a pyridyl-enamide $Zr^{IV}$ complex

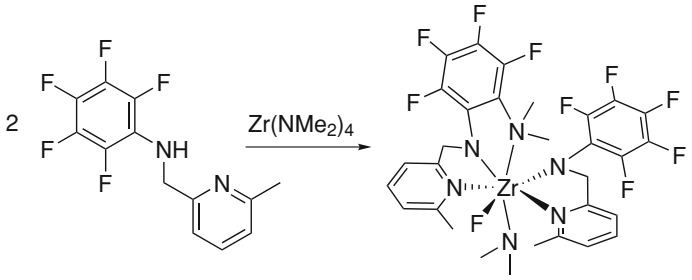


**Scheme 5.22** Net reaction of a perfluorophenyl-substituted aminomethylpyridyl ligand with $Zr(NMe_2)_4$

An unusual example of a ligand having an unsaturated group bridging the pyridine and the amido moieties was reported by Murray [132] (Scheme 5.21). The silyl enamine is isolated after deprotonation of the methyl group of the ketoimine fragment with MeLi followed by $ClSiMe_3$ quench. The synthesis of the enamido-pyridinato $Zr^{IV}$ complex is then accomplished by reaction with $ZrCl_4$ followed by treatment with BnMgCl, similar to the procedure outlined in Scheme 5.18c.

Pellecchia et al. have reported the synthesis of a zirconium complex derived from an aminomethylpyridyl ligand containing a perfluorophenyl substituent at the amine nitrogen atom [134]. The ligand is prepared by condensation of the formyl-substituted pyridine with the perfluorophenyl aniline followed by $NaBH_3CN$ reduction. The relatively small (e.g., compared with *i*Pr groups) arylamido substituents allow two ligand units to bind to the zirconium certer, yielding $L_2ZrCl_2$ complexes in reaction with $ZrCl_4$. Reaction with $Zr(NMe_2)_4$ yields a complex with two amidopyridyl ligands as well, but the product undergoes further modification by reactions with a pentafluoroaryl group. More specifically, a fluorine atom migrates to the metal center, and is replaced by a dimethylamido group, the latter mantaining the N-coordination to the metal center as shown in Scheme 5.22.

### *5.5.1 Olefin Polymerization Behavior of Group(IV) Metal Amidoalkylpyridinate Complexes*

Results for ethylene-hexene copolymerizations are summarized in Table 5.6 [132]. Catalysts have been generated in situ prior to activation by combining the

**Table 5.6** Ethylene-hexene co-polymerization data [132] for amidoalkylpyridinato complexes

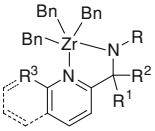


| R | $R^1$ | $R^2$ | $R^3$ | Act[a] | $I_{21}^b$ | BBF[c] |
|---|---|---|---|---|---|---|
| Cy | Me | Bn | H | 5 | | |
| Ph | Me | Bn | H | 1 | | |
| 2,6-$Me_2C_6H_3$ | Me | Bn | H | 23 | 0.511 | 9.23 |
| 2-*i*Pr-6-$MeC_6H_3$ | Me | Bn | H | 68 | Slow | 6.85 |
| 2-*t*$BuC_6H_4$ | Me | Bn | H | 26 | 9.83 | 10.51 |
| 2-*t*Bu-6-$MeC_6H_3$ | Me | Bn | H | 25 | 0.897 | 4.37 |
| 2,4,6-*t*$Bu_3C_6H_2$ | H | Bn | H | 2 | | |
| 2,6-*i*$Pr_2C_6H_3$ | H | H | H | 23 | 5.39 | 13.64 |
| 2,6-*i*$Pr_2C_6H_3$ | Me | Me | H | 183 | Slow | 8.68 |
| 2,6-*i*$Pr_2C_6H_3$ | H | Bn | H | 39 | 1.04 | 12.49 |
| 2,6-*i*$Pr_2C_6H_3$ | Me | Bn | H | 115 | | 7.16 |
| 2-*i*Pr-6-$MeC_6H_3$ | Me | Bn | Benzo[e] | 10 | | 5.86 |
| 2,6-*i*$Pr_2C_6H_3$ | Me | Bn | Benzo[e] | 41 | 2.42 | 13.36 |
| 2-*t*Bu-6-$MeC_6H_3$ | H | Bn | Benzo[e] | 6 | | |
| 2,6-*i*$Pr_2C_6H_3$ | H | Bn | Me | 16 | | 5.96 |
| 2,6-*i*$Pr_2C_6H_3$ | $=CH_2$ | | H | 28 | 0.512 | 12.26 |

*Conditions* 85 °C, 600 mL hexane, 43 mL 1-hexene, MMAO Al/Zr = 1,000, 85 psi ethylene
[a] Activity in units $kg_{pol}$ $(mol_{Zr}\ h\ 100\ psig)^{-1}$
[b] $I_{21}$ is the flow index (dg/min) at 190 °C
[c] BBF = butyl branch frequency, butyl branches/1,000 main chain carbon atoms

appropriate ligand or ligand precursor with $ZrBn_4$. More specifically, catalysts may be generated either via benzyl alkylation of the C=N moiety of an iminopyridyl precursor or via protonolysis of a benzyl group by an aminopyridyl ligand. Within the data set reported in Table 5.6, the catalysts bearing 2,6-*i*$Pr_2C_6H_3$ substituents on nitrogen (R-position) provide the best catalytic performances, and higher efficiencies are obtained for catalysts that are further substituted with non-hydrogen groups at both the $R^1$ and $R^2$ positions. Ethylene-hexene polymerization results obtained with systems containing N-heterocycle substituents (R), are shown in Table 5.7 [135]. Erker et al. report ethylene homopolymerization data (Table 5.8), which demonstrate the effects of the larger alkyl substituents at the 6-position of the pyridine ring on the final catalyst performance [45]. Indeed, the 6-*i*Pr-substituted catalyst makes polymer with a relatively low melting point, which the authors attribute to very low molecular weight. Ethylene polymerization data are reported for the perfluorophenyl-derived complexes as well (Table 5.9), with very high molecular weight polyethylenes produced. Very little or no polymer is produced with these complexes in propylene or hexene polymerization tests.

**Table 5.7** Ethylene-hexene polymerization data [135] for amidoalkylpyridinato complexes with R = N-heterocycle

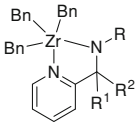


| R | $R^1$ | $R^2$ | μmol | Act[a] | $I_{21}^b$ | BBF[c] |
|---|---|---|---|---|---|---|
| *N*-2,5-$Me_2$pyrrole | Me | Bn | 1 | 8 | 4.16 | 15.08 |
| *N*-2,5-$Me_2$pyrrole | Me | Me | 0.5 | 31 | 0.839 | 17.38 |
| *N*-2,6-$Me_2$piperidine | Me | Bn | 0.5 | 18 | 27.79 | 4.06 |
| *N*-2,6-$Me_2$piperidine | Me | Me | 0.5 | 34 | 4.49 | 3.22 |

*Conditions*: 65 °C, 600 mL hexane, 43 mL 1-hexene, MMAO Al/Zr = 1000, 85 psi ethylene
[a] Activity in units $Kg_{pol}$ ($mol_{Zr}$ h 100 psig)$^{-1}$
[b] $I_{21}$ is the flow index (dg/min) at 190 °C
[c] BBF = butyl branch frequency, butyl branches/1,000 main chain carbon atoms

**Table 5.8** Ethylene polymerization data [45] for amidoalkylpyridinato complexes containing bulky alkyl substituent at the pyridine ring

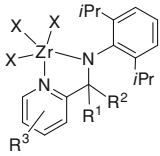


| $R^1$ | $R^2$ | $R^3$ | X | Act[a] | Tm[b] |
|---|---|---|---|---|---|
| H | H | H | Bn | 438 | 122 |
| Me | Me | H | Bn | 1,905 | 121 |
| H | H | 4,6-*t*$Bu_2$ | $NMe_2$ | – | – |
| Me | H | H | $NMe_2$ | 42 | 120 |
| Me | H | Benzo[*e*] | $NMe_2$ | 77 | 122 |
| Me | Me | H | $NMe_2$ | 170 | 122 |
| Me | H | 6-*i*Pr | $NMe_2$ | 70 | 117 |

*Conditions* Toluene, 25 °C, 2 bar ethylene, MAO activator with Al/Zr > 1,000
[a] Activity in units $kg_{pol}$ ($mol_{Zr}$ h bar)$^{-1}$
[b] Melting points measured by DSC

## 5.6 Synthesis of 6-Aryl(heteroaryl)-substituted Aminoalkylpyridyl Ligands

Aminoalkylpyridyl ligands bearing aryl or heteroaryl substituents at the 6-position of the pyridine ring are prepared by simple reduction or reductive alkylation of the corresponding imines (Scheme 5.23). While imine reduction can be conveniently conducted using $LiAlH_4$ or $NaBH_3CN$ [136–141], substituents at the bridging methylene fragment are generally introduced by reductive alkylation of the imine fragment with either an organolithium, organomagnesium or organoaluminum

**Table 5.9** Ethylene polymerization data [134] for amidoalkylpyridinato complexes derived from perfluoroaniline

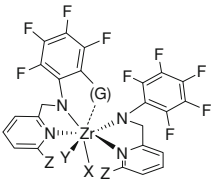

| G | X | Y | Z | Act[a] | $T_m^b$ | $M_w$ (kg/mol)[c] | $M_w/M_n^d$ |
|---|---|---|---|---|---|---|---|
| F | Cl | Cl | Me | 22.6 | 135.8 | 2,486 | 128.9 |
| $\mu$-$NMe_2$ | $NMe_2$ | F | Me | 83.2 | 134.3 | 550 | 69.7 |
| $\mu$-$NMe_2$ | Cl | Cl | Me | 72.7 | 133.9 | n.d.[d] | n.d.[d] |
| F | Bn | Bn | Me | 18.6 | 134.9 | 172 | 78.2 |
| F | $NMe_2$ | $NMe_2$ | Br | 20.0 | 133.5 | 268 | 53.3 |

*Conditions* 90 mL toluene solvent, $T = 50$ °C, 6 atm ethylene, 20 μmol cat, DIBAL/Zr = 30, MAO activator with Al/Zr = 1,000, $t = 60$ min

[a] Activity in units $kg_{pol}$ $(mol_{Zr}$ h atm$)^{-1}$

[b] Melting points measured by DSC

[c] Molecular weight data measured by GPC

[d] Not determined

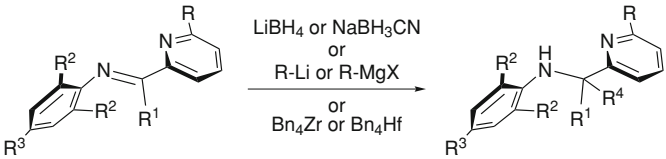


R = Ph, 1-naphthyl, thiophenyl, furyl, *o*-xylyl, etc.
$R^1$ = H, Me

$R^2$ = Me, *i*Pr, etc
$R^3$ = H, Me, Cl

$R^4$ = H, Me, Ph, 2-*i*Pr$C_6H_4$, Bn, etc

**Scheme 5.23** General synthetic procedures for 6-aryl or heteroaryl-2-aminoalkylpyridyl ligands

compound, or by treatment of the iminopyridyl ligand with a tetrabenzyl Group IV metal precursor [42, 136–146] (Scheme 5.23). A simplified synthesis of an aminoalkylpyridyl ligand has been proposed recently by Hagadorn et al. The authors use a pyridyllithium reagent to alkylate an imine fragment and generate the corresponding alkylamino ligand in one step (Scheme 5.24) [146]. Most ligands are conveniently prepared on a multigram scale and are generally purified by crystallization.

Most examples of 6-aryl substituted aminoalkylpyridyl ligands incorporate simple aryl functionalities such as phenyl or naphthyl, but a few examples bearing more complex heteroaryl systems have also been reported (Fig. 5.9). Examples bearing thiophenes and benzofurans have been prepared using a Suzuki-type coupling, [27, 30, 42, 143, 144, 147] and ligands bearing ferrocene substituents in the 6-position of the pyridine ring have also been prepared using this synthetic

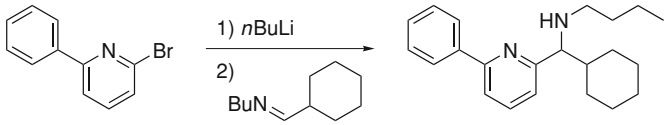


**Scheme 5.24** Synthesis of aminoalkylpyridyl ligands via a pyridyllithium intermediate

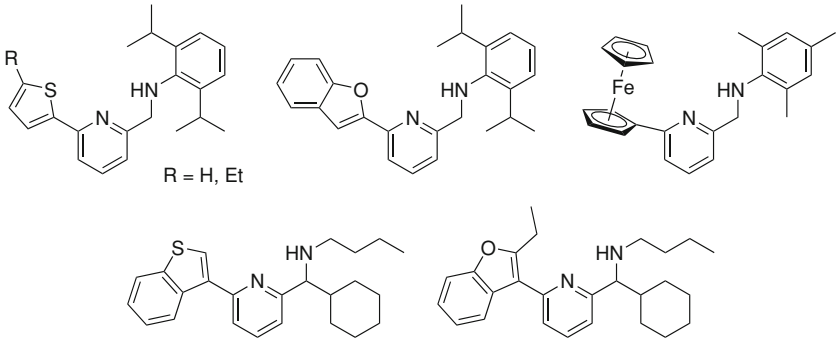


**Fig. 5.9** Selected examples of 6-heteroaryl-2-aminoalkylpyridyl ligands

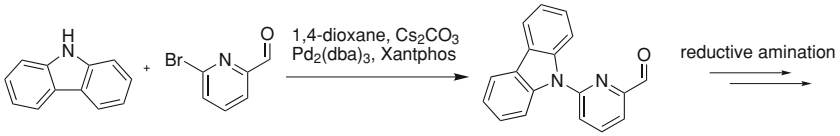


**Scheme 5.25** Key synthetic step in the synthesis of carbazole- or indole-functionalized amidopyridyl ligands

approach [141]. The synthesis of ligands bearing either carbazole or indole fragments at the same position of the pyridine moiety have also been prepared by a Buchwald–Hartwig amination protocol [148, 149] (Scheme 5.25), followed by reductive amination as described above (see Scheme 5.18) [144, 146].

The majority of aminoalkylpyridyl ligands are either unsubstituted or monosubstituted at the bridging carbon between the pyridine and the amine, but a few examples of α,α'-disubstituted versions have also been reported [42, 142]. These ligands have been prepared by condensation of an aniline with a pyridylketone, followed by reductive alkylation of the resulting ketimine with $Me_3Al$ (Scheme 5.26).

Compared to the ligands described above having secondary amine substitution, a smaller number of aminoalkylpyridyl ligands containing tertiary amino groups have also been reported (Scheme 5.27) [141, 146]. These compounds have been prepared by condensation of the aldehyde with a dialkylamine using benzotriazole to generate a stabilized iminium salt which undergoes nucleophilic attack by a

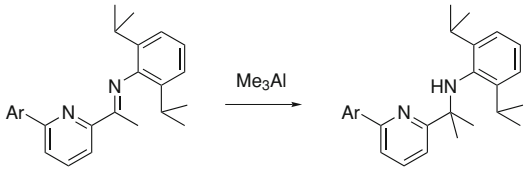


Ar = Ph, 2,6-$Me_2C_6H_3$, 2-(5-Et-thiophene), 2-Benzofuran, 2-Thiophene, 2-Vinylnaphthyl

**Scheme 5.26** Synthesis of α,α'-disubstituted 6-aryl-aminoalkylpyridyl ligands

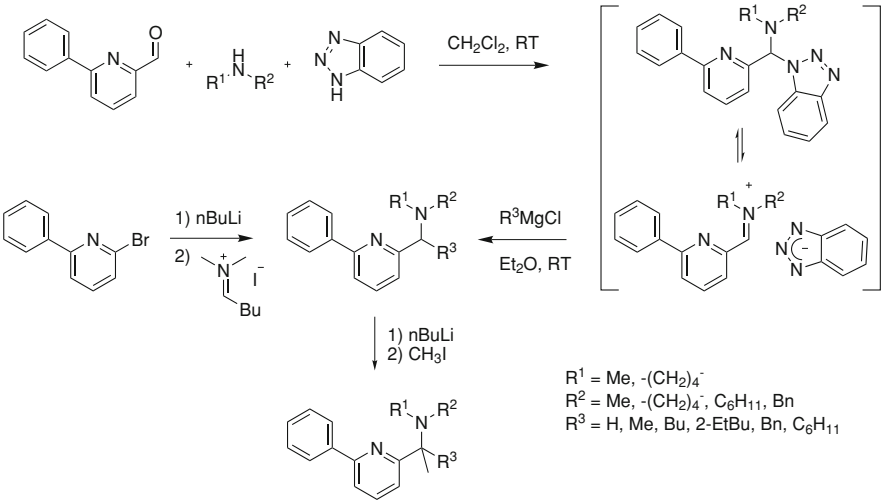


**Scheme 5.27** Synthetic routes to 6-aryl-aminoalkylpyridyl ligands containing tertiary amine groups

**Scheme 5.28** A synthetic route to a silyl-bridged 6-aryl-aminopyridyl ligand

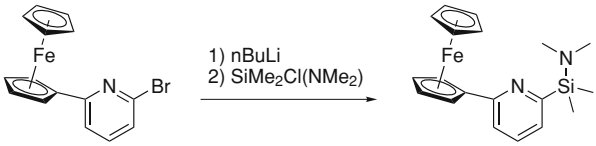


Grignard reagent [146]. Alternatively, alkylation of an aminium iodide by a lithiated pyridine also can provide the desired ligands [146]. These compounds can optionally be further elaborated to α,α'-disubstituted compounds by deprotonation with *n*BuLi and quenching with $CH_3I$ [146]. Additionally, aminoalkylpyridyl ligands bearing silicon bridges in place of the usual carbon atom bridges have been reported by Hagadorn (Scheme 5.28) [141]. These ligands are prepared by 2-bromo-6-ferrocenylpyridine metallation with *n*BuLi followed by reaction with $SiMe_2Cl(NMe_2)$.

### 5.6.1 Synthesis of 6-Aryl(heteroaryl)-substituted Amidoalkylpyridinato Group IV Metal Complexes

Several examples of amido, alkyl, and halo Group IV metal complexes stabilized with 6-aryl(heteroaryl) aminoalkylpyridyl ligands have been isolated and investigated with respect to their catalytic performance in olefin polymerization under different conditions. A representative series of $Hf^{IV}$ complexes is listed in Table 5.10, and the various synthetic methods applied to their preparation are summarized below.

Most of these complexes are generated by transamination/protonolysis reactions leading to either mono-anionic bidentate $\{N^-,N\}$- or di-anionic tridentate $\{N^-,N,C^-\}$-ligated complexes (Scheme 5.29) [137–140, 147, 150]. For ligands bearing an unsubstituted phenyl substituent at the 6-position of the pyridine ring (Scheme 5.29 top), the reactions with $Hf(NMe_2)_4$ liberate two equivalents of $NHMe_2$. The first equivalent is released by a transamination reaction and the second by *ortho*-metallation at the phenyl group, the latter producing a M–C(aryl) $\sigma$-bond. The X-ray structure in Fig. 5.10a reveals a $C_1$-symmetric complex with highly distorted trigonal–bipyramidal geometry at the metal center. The pyridine and activated phenyl group are almost coplanar, and the dimethylamido ligands occupy diastereotopic equatorial sites.

Under the same conditions, ligands bearing bulkier 6-aryl substituents, such as 1-naphthyl, liberate only one equivalent of $NHMe_2$ to give a bidentate monoanionic $\{N^-,N\}$-*tris*-dimethylamido complex (Scheme 5.29 bottom). The crystal structure of the latter complex (Fig. 5.10b) reveals a much less distorted trigonal–bipyramidal geometry with the bidentate ligand occupying two of the axial positions. The naphthyl group is twisted away from the pyridine at a dihedral angle of nearly $\sim 90°$. The *tris*-dimethylamido complex is presumably stabilized toward amine elimination due to unfavorable steric interactions hindering naphthyl/pyridine coplanarity.

Giambastiani et al. have recently reported the synthesis of Zr- and Hf-dimethylamido complexes bearing variably 6-aryl(heteroaryl) substituted aminomethylpyridyl ligands (Scheme 5.30) [147]. A careful variable-temperature $^1H$ NMR analysis of all prepared $Zr^{IV}$ and $Hf^{IV}$ complexes has revealed a dramatic change occurring at the metal coordination sphere upon temperature variations. Indeed, the initially-formed *tris*-dimethylamido complexes undergo completely reversible temperature-controlled $\sigma$-bond metathesis/protonolysis reactions that complicate solution characterization of the complexes. The cyclometallated *bis*-dimethylamido complexes are finally isolated after prolonged heating to completely remove the $NHMe_2$ from the metal coordination sphere (Scheme 5.30).

Dialkyl Group IV metal complexes have been prepared by a number of methods, which are summarized in Schemes 5.29 and 5.31. The *bis*-dimethylamido complexes can be converted to dimethyl species by treatment with excess $Me_3Al$ [137–140, 150]. As shown in Scheme 5.29, *tris*-dimethylamido monoanionic $\{N^-,N\}$-ligated complexes are converted to dimethyl species bearing a

**Table 5.10** 6-Aryl-substituted amidoalkylpyridinato $Hf^{IV}$ complexes

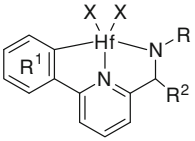


| R | $R^1$ | $R^2$ | X | References |
|---|---|---|---|---|
| Bn | 1-Nap | H | $NMe_2$, Bn | [137–140, 150] |
| 4-*i*Pr($C_6H_4$) | Ph | H | $NMe_2$, Bn | [137–140, 150] |
| 4-*i*Pr($C_6H_4$) | Ph | Bn | $NMe_2$, Bn | [137–140, 150] |
| 4-*i*Pr($C_6H_4$) | Ph | Ph | $NMe_2$, Bn | [137–140, 150] |
| 4-*i*Pr($C_6H_4$) | Ph | 2-Bip | $NMe_2$, Bn | [137–140, 150] |
| 4-*i*Pr($C_6H_4$) | Ph | 1-Anth | $NMe_2$, Bn | [137–140, 150] |
| 4-*i*Pr($C_6H_4$) | 1-Nap | H | $NMe_2$, Bn | [137–140, 150] |
| 4-*i*Pr($C_6H_4$) | 1-Nap | Ph | $NMe_2$, Bn | [137–140, 150] |
| 4-*i*Pr($C_6H_4$) | 1-Nap | 2-Bip | $NMe_2$, Bn | [137–140, 150] |
| 1-Nap | Ph | Bn | $NMe_2$, Bn | [137–140, 150] |
| 1-Nap | Ph | Ph | $NMe_2$, Bn | [137–140, 150] |
| 1-Nap | 1-Nap | Ph | $NMe_2$, Bn | [137–140, 150] |
| 2-Me-naphthyl | Ph | H | $NMe_2$, Bn | [137–140, 150] |
| 2-Me-naphthyl | Ph | Ph | $NMe_2$, Bn | [137–140, 150] |
| 2-Me-naphthyl | 1-Nap | H | $NMe_2$, Bn | [137–140, 150] |
| 2-Me-naphthyl | 1-Nap | Ph | $NMe_2$, Bn | [137–140, 150] |
| 2-Me-naphthyl | 1-Nap | 1-Anth | $NMe_2$, Bn | [137–140, 150] |
| 3,5-$(CF_3)_2C_6H_3$ | Ph | 2-Bip | $NMe_2$, Bn | [137–140, 150] |
| 3,5-$(CF_3)_2C_6H_3$ | 1-Nap | 2-Bip | $NMe_2$, Bn | [137–140, 150] |
| 2-Bip | Ph | H | $NMe_2$, Bn | [137–140, 150] |
| 2-Bip | Ph | Ph | $NMe_2$, Bn | [137–140, 150] |
| 2-Me-4-(MeO)$C_6H_3$ | Ph | Ph | $NMe_2$, Bn | [137–140, 150] |
| 2,6-$Me_2C_6H_3$ | Ph | H | $NMe_2$, Bn | [137–140, 150] |
| 2,6-$Me_2C_6H_3$ | Ph | Bn | $NMe_2$, Bn | [137–140, 150] |
| 2,6-$Me_2C_6H_3$ | Ph | 1-Anth | $NMe_2$, Bn | [137–140, 150] |
| 2,6-$Me_2C_6H_3$ | 1-Nap | H | $NMe_2$, Bn | [137–140, 150] |
| 2,6-$Me_2C_6H_3$ | 1-Nap | Bn | $NMe_2$, Bn | [137–140, 150] |
| 2,6-$Me_2C_6H_3$ | 1-Nap | Ph | $NMe_2$, Bn | [137–140, 150] |
| 2,6-$Me_2C_6H_3$ | 1-Nap | 1-Nap | $NMe_2$, Bn | [137–140, 150] |
| 2,6-*i*$Pr_2C_6H_3$ | Ph | H | $NMe_2$, Bn, Me | [136–140, 150, 151] |
| 2,6-*i*$Pr_2C_6H_3$ | Ph | Ph | $NMe_2$, Bn, Me | [136–140, 150] |
| 2,6-*i*$Pr_2C_6H_3$ | 1-Nap | H | Me | [151] |
| 2,6-*i*$Pr_2C_6H_3$ | 1-Nap | Ph | $NMe_2$, Bn, Me | [137–140, 150] |
| 2,6-*i*$Pr_2C_6H_3$ | 1-Nap | 2-*i*Pr$C_6H_4$ | Me, Cl, $CH_2SiMe_3$ | [145] |
| 2,6-*i*$Pr_2C_6H_3$ | 1-Nap | 2-($C_6H_{11}$)$C_6H_4$ | Me | [145] |
| 2,6-*i*$Pr_2C_6H_3$ | 1-Nap | 2-*t*Bu$C_6H_4$ | Me | [145] |
| 2,6-*i*$Pr_2$4-Cl-$C_6H_2$ | 4-Cl-$C_6H_4$ | 2-($C_6H_{11}$)$C_6H_4$ | Me | [145] |

(continued)

**Table 5.10** (continued)

| R | $R^1$ | $R^2$ | X | References |
|---|---|---|---|---|
| 2,6-*i*$Pr_2$4-Cl-$C_6H_2$ | 1-Nap | 2-*i*$PrC_6H_4$ | Me | [145] |
| 2,6-*i*$Pr_2$4-Cl-$C_6H_2$ | 1-Nap | 2-$(C_6H_{11})C_6H_4$ | Me | [145] |
| 2,6-{CHMe(4-*t*$BuC_6H_4$)}$_2$-4-$MeC_6H_2$ | Ph | H | Me | [136] |

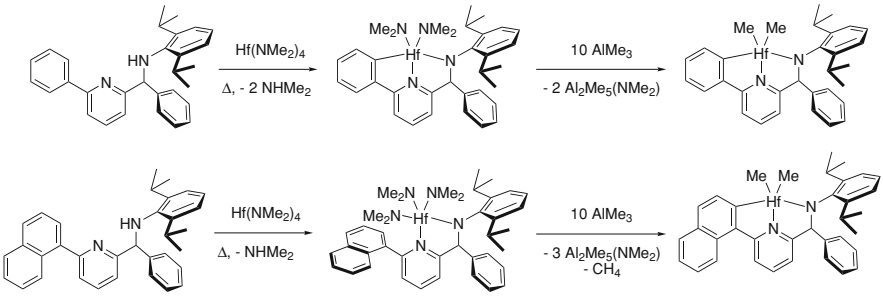


**Scheme 5.29** Synthesis of dimethylamido- and dimethyl $Hf^{IV}$ complexes stabilized by mono-anionic bidentate {$N^-$,N}- or di-anionic tridentate {$N^-$,N,$C^-$} ligands

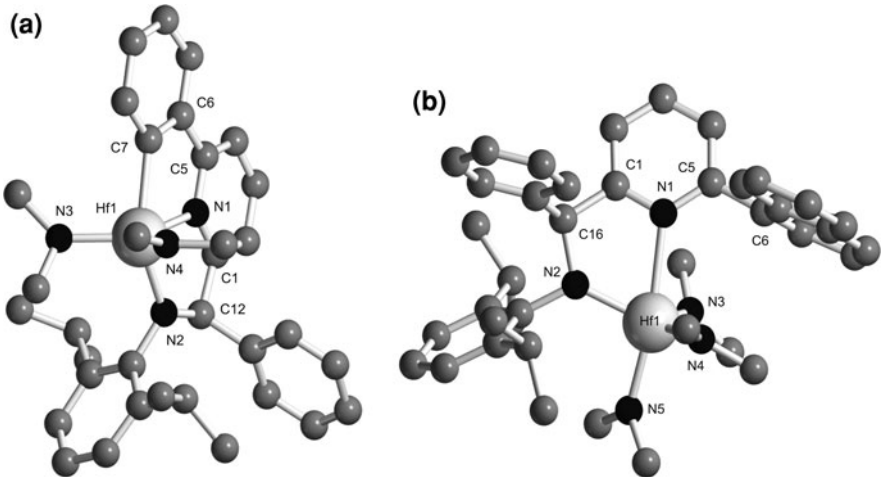


**Fig. 5.10** **a** *Ball and stick* drawing of the crystal structure of {$\eta^3$-($N^-$,N,$C^-$)-L}$Hf(NMe_2)_2$} (hydrogen atoms omitted) [150]. Selected distances (Å) and angles (°): Hf1-N1 2.340(5), Hf1-N2 2.130(4), Hf1-C7 2.298(6), Hf1-N4 2.028(5), Hf1-N3 2.008(5), N1-Hf1-N2 69.68(17), N1-Hf1-C7 70.1(2), N1-C5-C6-C7 -5.23. **b** *Ball and stick* drawing of the crystal structure of {$\eta^2$-($N^-$,N,)-L}$Hf(NMe_2)_3$} (hydrogen atoms omitted) [150]. Selected distances (Å) and angles (°): Hf1-N1 2.472(5), Hf1-N2 2.113(5), Hf1-N3 2.021(5), Hf1-N4 2.073(5), Hf1-N5 2.050(6), N1-Hf1-N2 71.87(17)

**Scheme 5.30** Synthesis of tautomeric mixtures of $Hf^{IV}$ and $Zr^{IV}$ complexes stabilized by 6-aryl(heteroaryl) amidomethylpyridinate ligands

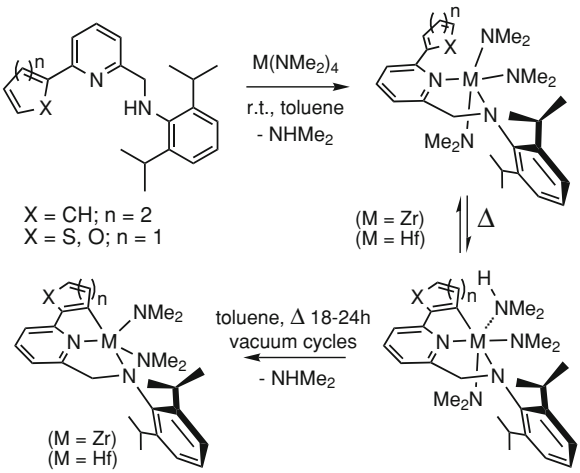


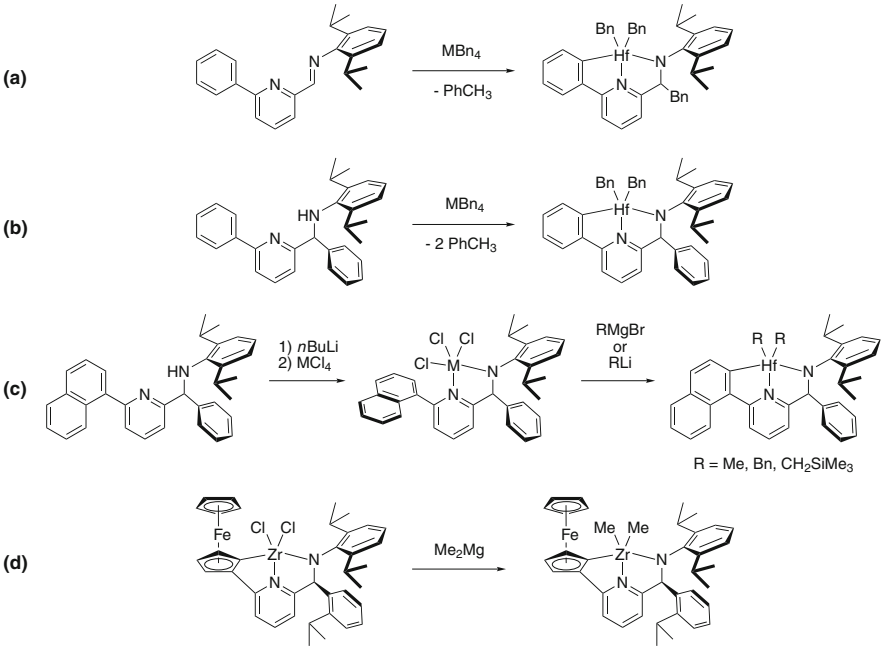


**Scheme 5.31** Synthetic approaches to the preparation of tridentate dianionic 6-aryl(heteroaryl) amidoalkylpyridinato metal-alkyl complexes

dianionic $\{N^-,N,C^-\}$ ligand, which indicates that the driving force for liberating one further equivalent of methane is enough to overcome the steric crowding (eclipsing hydrogens) of coplanar naphthyl and pyridine rings.

A simple method for the preparation of dialkyl complexes involves alkylation of an imine ligand precursor with $MBn_4$ (M = Zr, Hf) with the concomitant liberation of one molecule of toluene to give the L-$MBn_2$ complexes (Scheme 5.31a) [137–141, 150]. Likewise, the reaction of a free aminopyridyl compound with $MBn_4$ gives L-$MBn_2$ complexes with release of two toluene molecules (Scheme 5.31b) [137–141, 150]. L-$MR_2$ complexes have also been synthesized by reaction of a lithiated ligand with $MCl_4$ (salt metathesis) to give the trichloride intermediates, which undergo alkylation upon treatment with organolithium or organomagnesium compounds (Scheme 5.31c) [136, 145, 151]. Similarly, Hagadorn has reported the synthesis of a L-$ZrMe_2$ complex by treating the L-$ZrCl_2$ species with $Me_2Mg$ (Scheme 5.31d) [141]. Trialkyl complexes, potential intermediates in these reactions, are typically not observed, as the electrophilic metal readily activates a C–H group of the aryl substituent on the pyridine ring.

Representative crystal structures of the achiral and chiral (racemic) L-$HfMe_2$ complexes are shown in Fig. 5.11. The complex bearing the achiral ligand in Fig. 5.11a is $C_2$-symmetric with a mirror plane defined by the pyridine and phenyl rings and a trigonal–bipyramidal geometry around the metal center. The structural features of the chiral racemic species in Fig. 5.11b are nearly identical to those of the dimethylamido complex bearing the same ligand (see Fig. 5.10a).

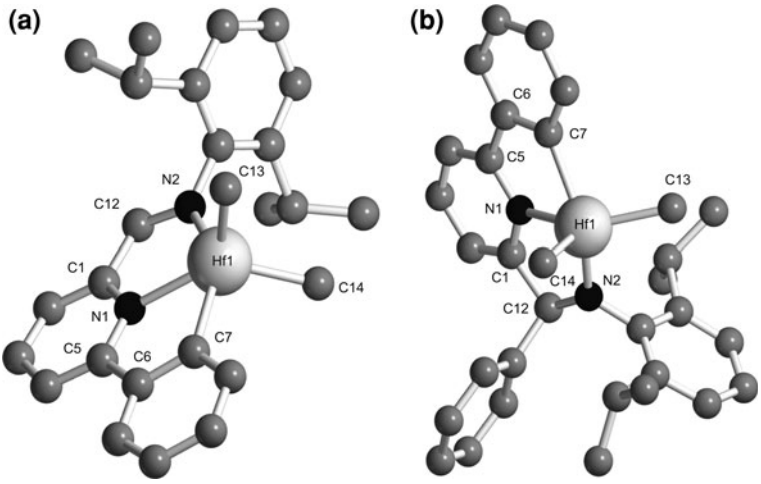


**Fig. 5.11** **a** *Ball and stick* drawing of the crystal structure of $\{\eta^3\text{-}(N^-,N,C^-)\text{-}L_{achiral}\}Hf(Me)_2\}$ (hydrogen atoms and a toluene molecule are omitted) [136]. Selected distances (Å) and angles (°): Hf1-N1 2.2985(13), Hf1-N2 2.0830(11), Hf1-C7 2.2693(15), Hf1-C13 2.1986(16), Hf1-C14 2.2116(17), N1-Hf1-N2 70.96(4), N1-Hf1-C7 70.11(5), N1-C5-C6-C7 -0.29. **b** *Ball and stick* drawing of the crystal structure of $\{\eta^3\text{-}(N^-,N,C^-)\text{-}L_{chiral}\}Hf(Me)_2\}$ (hydrogen atoms omitted) [136]. Selected distances (Å) and angles (°): Hf1-N1 2.3039(10), Hf1-N2 2.0826(10), Hf1-C7 2.2725(13), Hf1-C13 2.2067(14), Hf1-C14 2.2038(15), N1-Hf1-N2 70.72(4), N1-Hf1-C7 69.88(4), N1-C5-C6-C7-4.47

**Table 5.11** $Zr^{IV}$ and $Hf^{IV}$ 6-ferrocenyl substituted amidoalkylpyridinate complexes [141]

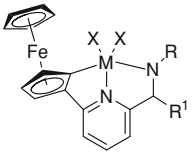


| R | $R^1$ | M | X |
|---|---|---|---|
| 2,4,6-$Me_3C_6H_2$ | H | Zr, Hf | Bn |
| 2,4,6-$Me_3C_6H_2$ | $CH_2SiMe_3$ | Zr | Bn |
| 2,6-*i*$Pr_2C_6H_3$ | H | Zr | Cl, Bn |
| 2,6-*i*$Pr_2C_6H_3$ | Bn | Zr, Hf | Bn |
| 2,6-*i*$Pr_2C_6H_3$ | 2-$MeC_6H_4$ | Zr | Me |
| 2,6-*i*$Pr_2C_6H_3$ | 2-*i*$PrC_6H_4$ | Zr | Me |

Hagadorn has described the synthesis of $Zr^{IV}$ and $Hf^{IV}$ complexes bearing a ferrocenyl unit in place of the typical phenyl or naphthyl groups at the 6-position of the pyridine ring [141]. Details of these Group IV metal complexes are collected in Table 5.11. These species also undergo C–H activation at the ferrocene fragment to give complexes stabilized by dianionic tridentate {$N^-$,N,$C^-$} ligands. A representative X-ray structure of a dibenzyl $Zr^{IV}$-complex is shown in Fig. 5.12. The complex is $C_1$-symmetric due to the cyclometallated ferrocene substituent. Again, the geometry at the metal center is trigonal–bipyramidal, and one of the benzyl groups is $\eta^2$-coordinated to the Zr atom.

A few examples of $Hf^{IV}$ and $Zr^{IV}$-dihalo complexes have been reported in the literture, and their synthetic paths are outlined in Scheme 5.32. A L-$HfCl_2$ complex is synthesized by treatment of the corresponding L-$HfMe_2$ intermediate with [$HNEt_3$]Cl (Scheme 5.32a) [145, 152, 153]. Hagadorn has also reported a L-$ZrCl_2$ species formed by reaction of a ferrocenyl-substituted aminopyridyl ligand with $ZrBn_2Cl_2(OEt_2)$ (Scheme 5.32b) [141].

Kuhlman and Whiteker have recently described "snap shut" catalysts containing an insertable pendant arm on the aryl substituent at the 6-position of the pyridine ring [154]. In the example shown in Scheme 5.33, the ligand is designed to direct metallation to the C–H bond *ortho* to the tethered vinyl fragment. The $Hf^{IV}$ complex has been synthesized by salt metathesis/alkylation. $^1H$ NMR analysis of the reaction mixture prior to heating at 70 °C shows a mixture of products with signals for vinylic hydrogens, the latter disappearing in the $^1H$ NMR spectrum of the final product. This behavior can be explained by the complex undergoing a "snap shut" reaction, the insertion of the vinyl group into the Hf–aryl bond to give the cyclometallated dianionic $Hf^{IV}$–dimethyl complex shown in Scheme 5.33. Notably, the product is a metal complex supported by a {$N^-$, N, $C^-$} ligand with an $sp^3$-hybridized carbon bound to hafnium. This catalyst shows a negligible induction period in octene polymerization, which bears on the mechanism discussed in Sect. 5.7.4.

Coates et al. have described the synthesis of a $Hf^{IV}$-dimethyl complex bearing a ligand with a 2-vinylnaphthyl substituent (Scheme 5.34) [155]. Treatment of the trichloro species with MeMgBr at room temperature produces the corresponding

trimethyl complex. Upon heating to 80 °C, the latter complex undergoes an intramolecular insertion of the appended vinyl moiety into the Hf–alkyl bond to give a new metal complex supported by a tridentate dianionic ligand containing an $sp^3$-C donor. The X-ray structure of this unusual $Hf^{IV}$ complex is depicted in Fig. 5.13.

## 5.7 Olefin Polymerization Using 6-Aryl(heteroaryl)-substituted Amidoalkylpyridinato Group IV Metal Complexes

These complexes have shown tremendous versatility in olefin polymerization catalysis, setting the way for the synthesis of new polymer classes. In this section,

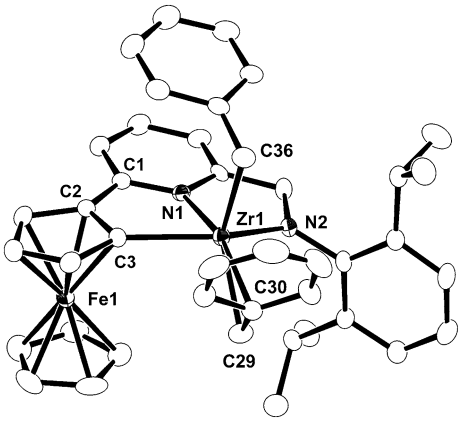


**Fig. 5.12** Crystal structure of $\{\eta^3\text{-}(N^-,N,C^-)\text{-}L_{ferrocenyl}\}Zr(Bn)_2\}$ [141]. Thermal ellipsoids are drawn at the 30% probability level. Hydrogen atoms are omitted. Selected distances (Å) and angles (°): Zr1-N1 2.332(3), Zr1-N2 2.091(4), Zr1-C3 2.300(4), Zr1-C29 2.273(5), Zr1-C30 2.653(4), Zr1-C36 2.264(5), N1-Zr1-N2 69.93(14), N1-Zr1-C3 70.65(14), N1-C1-C2-C3 7.4(6). (reproduced with permission)

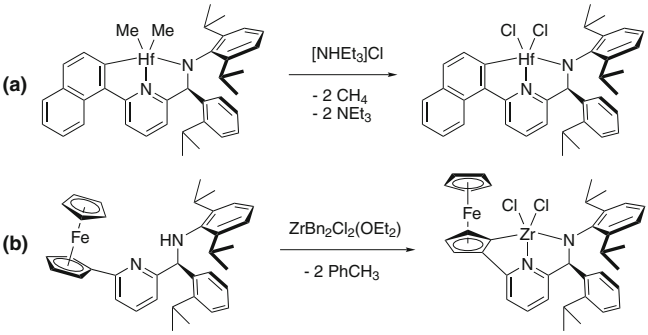


**Scheme 5.32** Synthesis of $Hf^{IV}$ and $Zr^{IV}$-dihalo complexes

some of these polymerization results are tabulated and discussed, although it is not intended to be an exhaustive review of every reported polymerization reaction. Series of experiments that demonstrate relationships between catalyst structure and polymerization performance are generally included, while those that are more focused on the usage of different catalyst activators and/or polymerization conditions are only partially outlined. While an effort has been made to create tables for which polymerization experiments are performed under identical or very similar conditions, there are some exceptions which must be carefully interpreted. Many different units have been used for reporting polymerization efficiencies in the literature, and there is currently no standardized unit of measure. Herein, units used in the original literature are maintained, and they can vary from table to table. For this reason and because different laboratories generally perform polymerization tests under different conditions, table-to-table comparisons of catalyst efficiencies are generally not useful.

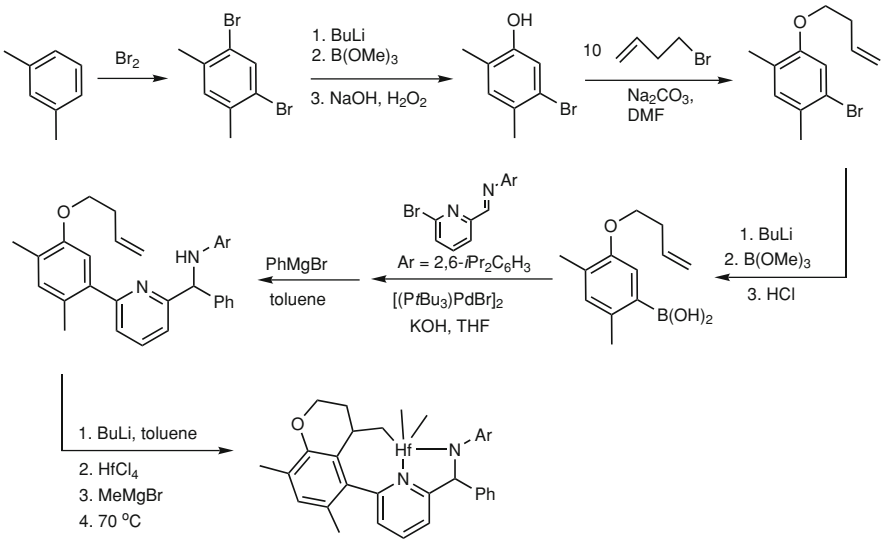


**Scheme 5.33** Synthesis of a "snap shut" catalyst

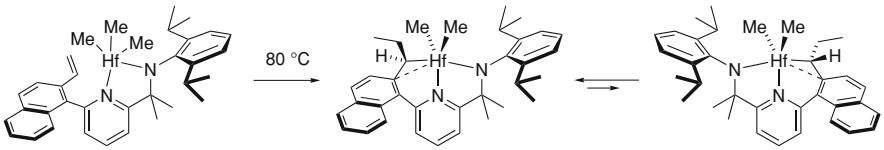


**Scheme 5.34** Synthesis of a $Hf^{IV}$-dimethyl complex bearing a $\{N^-,N,C^-\}$-ligand with an $sp^3$-carbon donor

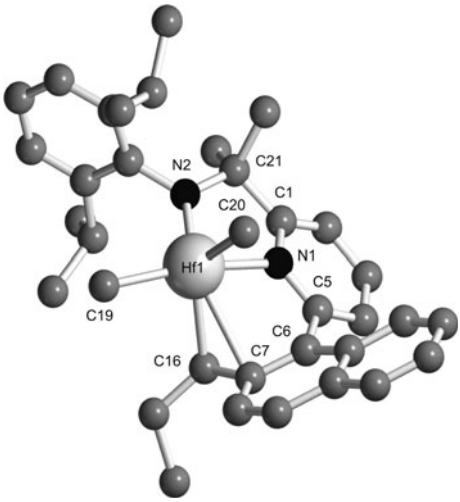


**Fig. 5.13** *Ball and stick* drawing of the crystal structure of $\{\eta^3\text{-}(N^-,N,C^-_{sp3})\text{-}L\}Hf(Me)_2\}$ (hydrogen atoms and a toluene molecule are omitted) [155]. Selected distances (Å) and angles (°): Hf1-N1 2.292(5), Hf1-N2 2.050(6), Hf1-C7 2.684(7), Hf1-C16 2.329(7), Hf1-C19 2.261(6), Hf1-C20 2.238(8), N1-Hf1-N2 71.35(19), N1-Hf1-C16 74.5(2), N1-C5-C6-C7 57.07

### *5.7.1 Polymerization of Propylene*

High-throughput experimentation has played a significant role in the development of this catalyst class for propylene polymerization. Due to the relative ease of handling liquids, octene polymerization screens have been initially used to identify promising candidates for high-efficiency polymerization of α-olefins. These candidates were further tested for propylene polymerization using Symyx parallel pressure reactor (PPR) technology. As the program developed, the focus centered on three key ligand substituents, labeled R, $R^1$ and $R^2$ as in the figure of Table 5.12. Of the dozens of variants tested, most of them produce amorphous (stereoirregular) polymers, but the combination of R = 2,6-*i*$Pr_2C_6H_3$; $R^1$ = phenyl or 1-naphthyl; and $R^2$ = aryl was found to produce crystalline polypropylenes. Subsequently, complexes of this sub-class received the most extensive study. Using high-throughput synthesis and screening, [156] this family of catalysts was developed to find candidates with high polymerization efficiency, high molecular weight, and high melting point (indicative of tacticity) [150]. This combination of capabilities was unprecedented, and led to commercialization of a new product in less than four years after the launch of the catalyst discovery program [157] (Table 5.12).

Boussie et al. [150] have compared the polymerization capabilities of two amidopyridinate complexes with the more conventional $C_2$-symmetric metallocene *rac*-[$Me_2Si$(2-Me-4-Ph-1-indenyl)$_2$Zr($\eta^4$-1,4-$Ph_2$-1,3-butadiene)] (see Table 5.12). Although the new complexes show lower catalytic activity, they produce polypropylene with a similar melting point (indicator of isotacticity), and much higher molecular weight. It is this remarkable capability to make high

**Table 5.12** Propylene polymerization [150] using either the $C_2$-symmetric metallocene *rac*-[$Me_2Si$(2-Me-4-Ph-1-indenyl)$_2$Zr($\eta^4$-1,4-$Ph_2$-1,3-butadiene)] or {$\eta^3$-($N^-$,N,$C^-$)-L}Hf$(Me)_2$} catalysts

| | complex A | | | complex B | | | |
|---|---|---|---|---|---|---|---|
| Complex | R | $R^1$ | $R^2$ | Act[a] | $M_w$ (kg/mol) | $M_w/M_n$ | $T_m$ |
| A | 2,6-*i*$Pr_2C_6H_3$ | Ph | Ph | 1.9 | 300 | 2.1 | 127 |
| A | 2,6-*i*$Pr_2C_6H_3$ | 1-Nap | Ph | 0.3 | 710 | 3.2 | 141 |
| B | – | – | – | 9.2 | 95 | 2.0 | 142 |

*Conditions* 90 °C, toluene solvent, 1.1 equivalent [$PhNMe_2H$][$B(C_6F_5)_4$], 10–30 equivalents DIBAL, 100 psi propylene

[a] Activity is reported as $kg_{pol}$ $(mmol_M\ min)^{-1}$

molecular weight polypropylenes, even at high polymerization temperatures, that has created new opportunities for propylene-based polymers made in a solution process.

An extensive series of propylene polymerization experiments has been reported by Boussie et al. [137–140, 150] and a subset of the results are given below. These results were obtained using parallel pressure reactor (PPR$^{TM}$) technology in glass reaction vessels of approximately 7 mL size. The table is not a complete reproduction of all achieved results but it is rather an attempt to report the effects of ligand variations on the catalyst performance in analytical way to facilitate a rapid examination to the readership. The two favored methods for catalyst preparation in the high-throughput studies are protonolysis reaction with $M(CH_2Ph)_4$ (Scheme 5.31b) or protonolysis with $M(NMe_2)_4$ followed by treatment with $AlMe_3$ (Scheme 5.29). Groups labeled R, $R^1$ and $R^2$ in the figure of Table 5.13 are varied extensively and polymerization results are reported hereafter.

In a set of experiments with the hafnium catalyst derived from the ligand with $R/R^1/R^2$ = 2,6-*i*$Pr_2C_6H_3$/1-Nap/Ph, the effects of the catalyst activation on the catalyst polymerization performance and polymer properties have been examined. Either the *tris*-dimethylamide complex $LHf(NMe_2)_3$ or the dimethyl complex $LHfMe_2$ has been activated with [$PhNMe_2H$][$B(C_6F_5)_4$] and either a mixture of DIBAL/$BEt_3$ or $Me_3Al$. Activities are high in all cases using $Me_3Al$, but the crystallinity index (as measured by *infrared* spectroscopy) is relatively invariant and shows no clearly discernable trends, ranging from 0.74 to 0.81. The molecular weights are consistently lower for $Me_3Al$-activated catalyst systems. Temperature effects on the polymerization reactions are also investigated, with the expected trend observed that higher polymerization temperature produces lower activity, molecular weight and crystallinity index.

**Table 5.13** Propylene polymerization data [137–140, 150] for $\{\eta^3\text{-}(N^-,N,C^-)\text{-}L\}Hf(Me)_2\}$ catalysts

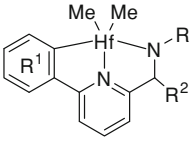


| R | $R^1$ | $R^2$ | Act[a] | Cryst index[b] | $M_w$ (kg/mol) |
|---|---|---|---|---|---|
| 2,6-*i*$Pr_2C_6H_3$ | 4-$FC_6H_4$ | Ph | 41 | 0.72 | 90 |
| 2,6-*i*$Pr_2C_6H_3$ | 4-$(CF_3)C_6H_4$ | Ph | 43 | 0.66 | 109 |
| 2,6-*i*$Pr_2C_6H_3$ | 2-$(CF_3)C_6H_4$ | Ph | 67 | 0.70 | 93 |
| 2,6-*i*$Pr_2C_6H_3$ | 1-Nap | Ph | 41 | 0.79 | 106 |
| 2,6-*i*$Pr_2C_6H_3$ | 1-Nap | 2-$MeC_6H_4$ | 320[c] | 0.84 | 161 |
| 2,6-*i*$Pr_2C_6H_3$ | 1-Nap | 3,5-$Me_2C_6H_3$ | 348[c] | 0.84 | 218 |
| 2,6-*i*$Pr_2C_6H_3$ | 1-Nap | 9-Phen | 624[c] | 0.86 | 177 |
| 2,6-*i*$Pr_2C_6H_3$ | 1-Nap | Nap | 518[c] | 0.86 | 154 |
| 2,6-*i*$Pr_2C_6H_3$ | 1-Nap | *n*Bu | 3 | n.d. | n.d. |
| 2,6-*i*$Pr_2C_6H_3$ | 1-Nap | *s*Bu | 2 | n.d. | n.d. |
| 2,6-*i*$Pr_2C_6H_3$ | 1-Nap | *t*Bu | 1 | n.d. | n.d. |
| 2,6-*i*$Pr_2C_6H_3$ | 1-Nap | Bn | 6 | n.d. | n.d. |
| 2,6-*i*$Pr_2C_6H_3$ | 1-Nap | 3,5-$Me_2C_6H_3$ | 158 | 0.84 | 165 |
| 2,6-*i*$Pr_2C_6H_3$ | 1-Nap | 2-$MeC_6H_4$ | 50 | 0.84 | 106 |
| 2,6-*i*$Pr_2C_6H_3$ | 1-Nap | 1-Nap | 191 | 0.87 | 124 |
| 2,6-*i*$Pr_2C_6H_3$ | 1-Nap | 9-Phen | 258 | 0.86 | 124 |
| 2,6-$Et_2C_6H_3$ | Ph | 9-Anth | 230[c,d] | 0.38 | 64 |
| 2,6-$Et_2C_6H_3$ | 1-Nap | 9-Anth | 716[c,d] | 0.56 | 94 |
| 2,6-$Et_2C_6H_3$ | Ph | 9-Phen | 79[c,d] | 0.53 | 67 |
| 2,6-$Et_2C_6H_3$ | 4-$FC_6H_4$ | 9-Phen | 47[c,d] | 0.30 | 76 |
| 2,6-*i*$Pr_2C_6H_3$ | Ph | 9-Phen | 2511[c,d] | 0.92 | 86 |
| 2,6-*i*$Pr_2C_6H_3$ | 1-Nap | 9-Phen | 825[c,d] | 0.91 | 100 |
| 2,6-*i*$Pr_2C_6H_3$ | 1-Nap | Ph | 779[c,d] | 0.88 | 90 |
| 2,6-*i*$Pr_2C_6H_3$ | Ph | Ph | 1466[c,d] | 0.88 | 89 |
| 2-*t*$BuC_6H_4$ | 1-Nap | Ph | 1 | n.d. | n.d. |
| 2,5-*t*$Bu_2C_6H_3$ | 1-Nap | Ph | 2 | n.d. | n.d. |
| 2-*i*Pr-6-$MeC_6H_3$ | 1-Nap | Ph | 188 | 0.52 | 97 |
| 2-*t*Bu-6-$MeC_6H_3$ | 1-Nap | Ph | 1 | n.d. | n.d. |
| 2,6-$Et_2C_6H_3$ | 1-Nap | Ph | 33 | 0.56 | 62 |
| 2-*s*-Bu-6-$EtC_6H_3$ | 1-Nap | Ph | 21 | 0.63 | 46 |

n.d. = not determined

*Conditions* 0.1 μmol $Hf(NMe_2)_4$, Ligand/Hf = 1/1, DIBAL/Hf = 30/1, octene/Hf = 20/1, $[PhNMe_2H][B(C_6F_5)_4]$/Hf = 1.1/1, 100 psi propylene, 110 °C

[a] Activity is reported as kg polymer $(mol_M\ min)^{-1}$

[b] Height ratio of IR bands at 995 and 972 $cm^{-1}$

[c] 0.060 μmol of $LHf(NMe_2)_3$ complex with no 1-octene

[d] $Me_3Al$ (Al/M = 30/1) instead of DIBAL

Additional propylene polymerization data have been reported by Frazier et al. [145] for complexes containing bulkier (relative to 2-$MeC_6H_4$) $R^2$ substituents, such as 2-*i*$PrC_6H_4$, 2-$CyC_6H_4$ or 2-*t*$BuC_6H_4$ groups (Table 5.14). These high-efficiency catalysts produce high molecular weight, high-$T_m$ polypropylenes. The highest melting point is observed for the *t*Bu-substituted version, albeit with a significant decline of both catalyst efficiency and polymer molecular weight. An increase in the polymer molecular weight is observed when a 4-Cl-2,6-*i*$Pr_2C_6H_2$ substituent is incorporated at the R position, although the catalyst efficiency is slightly reduced. One zirconium example is also reported; it shows lower performance by all three metrics when compared to its Hf analog.

While the polypropylene produced is predominantly isotactic, these catalysts sometimes generate slightly more regioerrors than typically found with the highest-performing $C_2$-symmetric metallocene systems. Furthermore, the stereochemistry of the former regioerrors is found to be the opposite of that generally observed in polypropylenes generated by $C_2$-symmetric metallocenes (Fig. 5.14). The unique microstructure is confirmed and further elaborated [158] using the 2D-NMR INADEQUATE pulse sequences enabled by an NMR instrument equipped with a cryoprobe [159].

**Table 5.14** Propylene polymerization [145] using 6-aryl-amidomethylpyridinato $Hf^{IV}$ and $Zr^{IV}$ $\{\eta^3\text{-}(N^-,N,C^-)\text{-}L\}M(Me)_2\}$ catalysts containing bulky $R^2$ substituents

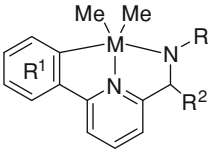


| M | R | $R^1$ | $R^2$ | Act[a] | $T_m$ | $M_w$ (kg/mol) | $M_w/M_n$ |
|---|---|---|---|---|---|---|---|
| Hf | 2,6-*i*$Pr_2C_6H_3$ | 1-Nap | 2-*i*$PrC_6H_4$ | 294 | 153.2 | 229 | 2.22 |
| Hf | 2,6-*i*$Pr_2C_6H_3$ | 1-Nap | 2-$CyC_6H_4$ | 293 | 151.8 | 234 | 2.20 |
| Hf | 4-Cl-2,6-*i*$Pr_2C_6H_2$ | 4-$ClC_6H_5$ | 2-$CyC_6H_4$ | 190 | 150 | 558 | 2.78 |
| Hf | 4-Cl-2,6-*i*$Pr_2C_6H_2$ | 1-Nap | 2-*i*$PrC_6H_4$ | 194 | 153.2 | 281 | 2.14 |
| Hf | 4-Cl-2,6-*i*$Pr_2C_6H_2$ | 1-Nap | 2-$CyC_6H_4$ | 201 | 151.8 | 296 | 2.21 |
| Zr | 4-Cl-2,6-*i*$Pr_2C_6H_2$ | 1-Nap | 2-*i*$PrC_6H_4$ | 77 | 147.5 | 52 | 2.12 |
| Hf | 2,6-*i*$Pr_2C_6H_3$ | 1-Nap | 2-*t*$BuC_6H_4$ | 85 | 155.4 | 77 | n.d. |
| Hf[b] | 2,6-*i*$Pr_2C_6H_3$ | 1-Nap | 2-*i*$PrC_6H_4$ | 379 | 150.3 | n.d. | n.d. |

n.d. = not determined

*Conditions* 90 °C, 1.8 L reaction volume, 667 g mixed alkanes solvent, 286 g propylene, 1.0 μmol catalyst, 1.2 equivalent of an ammonium borate with approximate molecular formula $[(C_{18}H_{37})_2NMeH][B(C_6F_5)_4]$, 30 equivalents of PMAO-IP, 10 min run time

[a] Activity is reported as $kg_{poly}\ (g_M)^{-1}$

[b] *bis*-Trimethylsilylmethyl (not dimethyl) hafnium complex

Propylene–ethylene copolymers (those that have crystallinity derived from polypropylene sequences interrupted by ethylene monomers) have also been prepared [160, 161] using $Hf^{IV}$-dimethyl complexes with ligands having the following substitution pattern: $R/R^1/R^2$ = 2,6-*i*$Pr_2C_6H_3$/1-Nap/Ph or 2,6-*i*$Pr_2C_6H_3$/1-Nap/9-Phen. The use of $Hf^{IV}$ dimethyl or dichloro complexes stabilized with a similarly substituted ligand ($R/R^1/R^2$ = 2,6-*i*$Pr_2C_6H_3$/1-Nap/2-$MeC_6H_4$) supported on inorganic materials such as MAO-modified silica have also been reported for the gas-phase propylene polymerization [162].

## 5.7.2 Ethylene/α-Olefin Copolymerization

These complexes can be very highly active catalysts for ethylene-co-α-olefin polymer synthesis, using a variety of α-olefins. Polymerization data for ethylene-*co*-octene polymers have been reported in Symyx patents using the $Hf(NMe_2)_3$ complex having $R/R^1/R^2$ = 2-MeNap/1-Nap/9-Anth as ligand substituents [137–140]. Froese et al. have reported data for a $Hf^{IV}$-dimethyl complex bearing a ligand with $R/R^1/R^2$ = 2,6-*i*$Pr_2C_6H_3$/1-Nap/2-*i*$PrC_6H_4$ substituents at different octene molar fractions ($f_{oct}$ = [octene]/([ethylene] + [octene]) [163] (Table 5.15). The GPC traces have been deconvoluted into high and low molecular weight fractions. The authors

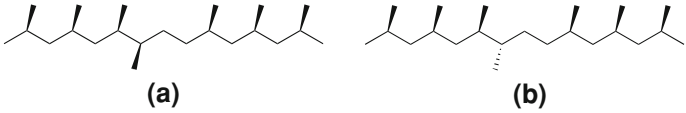


**Fig. 5.14** Regioerrors typically observed for: **a** {$\eta^3$-($N^-$,N,$C^-$)-L}$M(Me)_2$} catalysts; **b** $C_2$-symmetric metallocenes

**Table 5.15** Ethylene-octene copolymerization at variable octene molar fractions using a {$\eta^3$-($N^-$,N,$C^-$)-L}$Hf(Me)_2$} catalyst

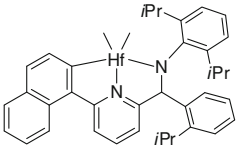


| $f_{oct}$ | Act[a] | $M_w$(LMW) (kg/mol) | wt%(LMW) | $M_w$(HMW) (kg/mol) | wt%(HMW) |
|---|---|---|---|---|---|
| 0.16 | 4,400 | 194 | 59 | 936 | 41 |
| 0.31 | 2,000 | 121 | 34 | 1,140 | 66 |
| 0.75 | 3,300 | 133 | 17 | 1,190 | 83 |

*Conditions* Isopar-E solvent, 120 °C, 450 psi ethylene, 1.2 equivalent of an ammonium borate with approximate molecular formula $[(C_{18}H_{37})_2NMeH][B(C_6F_5)_4]$, MMAO with Al/Hf = 5, hydrogen, 10 min run time

[a] Activity is reported as $kg_{poly}(mol_M\ h\ bar)^{-1}$

note that the higher molecular weight fraction becomes dominant for higher octene molar fractions ($f_{oct}$). These results are explained in detail in Sect. 5.7.4.

Hagadorn has reported ethylene–octene polymerization results for amidoalkylpyridinato complexes containing a ferrocenyl substituent [141]. The results are summarized in Table 5.16.

Ethylene–styrene copolymerizations have been reported by Boussie et al. [138] and the results are summarized in Tables 5.17 and 5.18. Hafnium catalysts consistently make ethylene–styrene copolymers with both higher polymerization efficiencies and more styrene incorporated into the polymer microstructure, relative to the zirconium analogs.

Symyx also has reported the copolymerization of ethylene and the relatively unreactive comonomer isobutylene [137–140]. Only one example is mentioned, which is performed using a $Hf^{IV}$ complex prepared by mixing $HfBn_4$ with a ligand characterized by the substituents $R/R^1/R^2$ = 2,4-$Me_2C_6H_3$/H/H.

### 5.7.3 Chain Shuttling Polymerization

One of the most outstanding properties of these catalysts is their ability to participate in chain shuttling polymerization processes. Chain shuttling is the

**Table 5.16** Ethylene-octene copolymerization results for ferrocenyl-substituted amidoalkylpyridinato $Zr^{IV}$ and $Hf^{IV}$ complexes

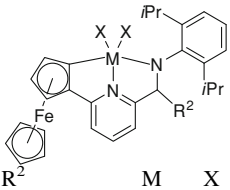


| $R^2$ | M | X | Activator | Act[a] | wt% C8 | $M_w$ (kg/mol) | $M_w/M_n$ |
|---|---|---|---|---|---|---|---|
| Bn | Zr | Bn | $[PhNMe_2H][B(C_6F_5)_4]$[b] | 45 | 2 | 3,712 | 1.7 |
| 2-*i*Pr$C_6H_4$ | Zr | Me | $[PhNMe_2H][B(C_6F_5)_4]$[b] | 65 | 1 | 2,004 | 1.9 |
| 2-Me$C_6H_4$ | Zr | Me | $[PhNMe_2H][B(C_6F_5)_4]$[b] | 40 | 2 | 1,848 | 1.9 |
| Bn | Hf | Bn | $[PhNMe_2H][B(C_6F_5)_4]$[b] | 25 | 3 | 1,974 | 3.1 |
| H | Zr | Bn | $[PhNMe_2H][B(C_6F_5)_4]$[b] | 5 | 3 | n.d. | n.d. |
| Bn | Zr | Bn | MAO[c] | 55 | 1 | 245 | 4 |
| 2-*i*Pr$C_6H_4$ | Zr | Me | MAO[c] | 4,880 | 3 | 97 | 1.6 |
| 2-Me$C_6H_4$ | Zr | Me | MAO[c] | 4,540 | 3 | 94 | 1.5 |
| Bn | Hf | Bn | MAO[c] | 37 | 5 | 473 | 2 |
| H | Zr | Bn | MAO[c] | 33 | 3 | 376 | 1.8 |

*Conditions* Toluene solvent, 5 mL, 80 nmol catalyst, 200 psig ethylene
[a] Activity is reported as kg polymer $(mol_M\ h\ bar)^{-1}$
[b] One equivalent of activator and 0.1 mL $Oct_3Al$
[c] Al/M = 500

**Table 5.17** Ethylene–styrene copolymerization using $Hf^{IV}$ and $Zr^{IV}$ $\{\eta^3\text{-}(N^-,N,C^-)\text{-}L\}M(Bn)_2\}$ catalysts

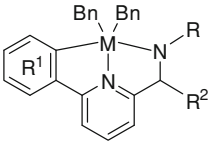


| R | $R^1$ | $R^2$ | M | Yield[a] | wt% Sty[b] |
|---|---|---|---|---|---|
| *p*-Cumyl | 1-Nap | 1-Bip | Zr | 152 | 6 |
| *p*-Cumyl | 1-Nap | 1-Bip | Hf | 469 | 14 |
| *p*-Cumyl | Ph | Ph | Zr | 209 | 7 |
| *p*-Cumyl | Ph | Ph | Hf | 326 | 15 |
| *p*-Cumyl | Ph | 1-Bip | Zr | 138 | 7 |
| *p*-Cumyl | Ph | 1-Bip | Hf | 295 | 15 |
| *p*-Cumyl | Ph | Bn | Zr | 163 | 7 |
| *p*-Cumyl | Ph | Bn | Hf | 278 | 10 |
| $3,5\text{-}(CF_3)_2C_6H_3$ | 1-Nap | H | Zr | 134 | 6 |
| $3,5\text{-}(CF_3)_2C_6H_3$ | 1-Nap | H | Hf | 153 | 15 |

*Conditions* 15 μmol TIBA, catalyst prepared from 1.5 μmol ligand + 1.5 μmol $MBn_4$ + 30 μmol 1-octene, 100 psi ethylene, 0.5 mL styrene

[a] Polymer yield in mg

[b] Weight % of styrene in the polymer determined by IR

rapid and reversible exchange of a polymeryl chain among active catalyst sites, mediated by a chain shuttling agent (CSA), typically a main group metal alkyl. This process enables the production of olefin block copolymers mediated by coordination polymerization catalysts without stoichiometric limitations, and it has been the subject of a recent review [164]. The $\{\eta^3\text{-}(N^-,N,C^-)\text{-}L\}Hf(Me)_2\}$ catalyst with $R/R_1/R_2 = iPr_2C_6H_3/1\text{-}Nap/2\text{-}iPrC_6H_4$ ligand substituents (see Fig. 5.15) has been shown to exhibit chain shuttling behavior in the presence of diethylzinc as CSA. [165, 166] This capability has been employed in the production of linear multi-block [165–167] and linear di-block [168, 169] copolymers.

To make linear multi-block copolymers, the amidopyridinato complex is used in tandem with a second catalyst having different ethylene-octene selectivity (Fig. 5.15). A single reactor is used, but different block types are generated because of the different monomer selectivities of the two catalysts. The CSA transports chains among different catalyst types on the timescale of the lifetime of the polymer chain, creating an alternating linear block copolymer with a distribution of block lengths and number of blocks per chain.

The same amidopyridinato complex (Fig. 5.15) has been used to produce di-block copolymers. Unlike the single-reactor/multi-catalyst approach to making multiblocks, production of diblock copolymers by chain shuttling employs a two-reactor/single catalyst system. The two reactors are controlled at different relative monomer concentrations to generate the different block types.

**Table 5.18** Ethylene–styrene copolymerization using either $\{\eta^3\text{-}(N^-,N,C^-)\text{-}L\}Hf(Bn)_2\}$ or $\{\eta^2\text{-}(N^-,N)\text{-}L\}Hf(NMe_2)_3\}$ catalysts

**complex A**

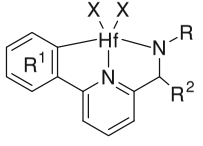


X = Bn

**complex B**

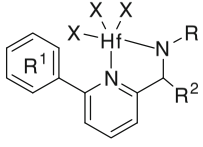


X = $NMe_2$

| Complex | R | $R^1$ | $R^2$ | Act[a] | wt% Sty[b] | $M_w$ (kg/mol) |
|---|---|---|---|---|---|---|
| A | p-Cumyl | Ph | Ph | 23[d] | 3.3 | 42 |
| A | p-Cumyl | Ph | o-Bip | 23[d] | 3.6 | 34 |
| A | p-Cumyl | 1-Nap | o-Bip | 61[d] | 3.3 | 49 |
| A | 2,4,6-$Me_3C_6H_2$ | 1-Nap | H | 44[d] | 4.7 | 259 |
| B | 2,6-*i*$Pr_2C_6H_3$ | 1-Nap | 2-$MeC_6H_4$ | 180 | 4.5 | 571 |
| B | 2,6-*i*$Pr_2C_6H_3$ | 1-Nap | 3,5-$Me_2C_6H_3$ | 155 | 3.6 | 384 |
| B | 2,6-*i*$Pr_2C_6H_3$ | 1-Nap | 9-Phen | 139 | 4.6 | 652 |
| B | 2,6-*i*$Pr_2C_6H_3$ | 1-Nap | 1-Nap | 144 | 4.8 | 512 |

*Conditions* 0.50 μmol catalyst, DIBAL/Hf = 10/1, $[PhNMe_2H][B(C_6F_5)_4]$/Hf = 1.1/1, 100 psi ethylene, 0.10 mL styrene, 110 °C

[a] Activity is reported as $Kg_{poly}$ $(mol_M\ min)^{-1}$

[b] Weight % of styrene in the polymer determined by IR

[c] TIBA/Hf = 10/1 instead of DIBAL, and 0.25 mL of styrene

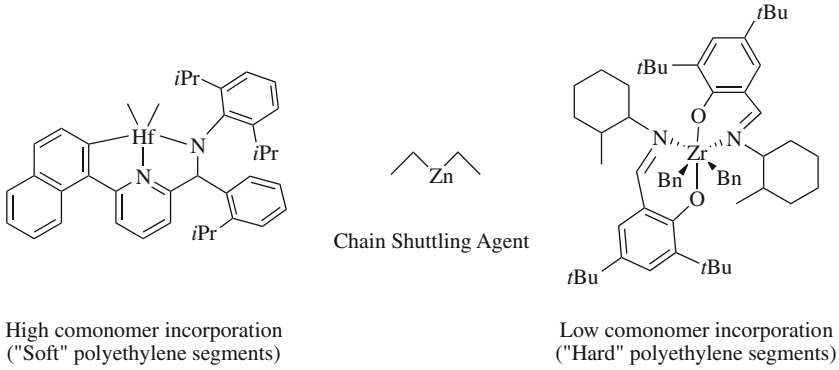


**Fig. 5.15** Combination of catalysts and chain shuttling agent utilized for preparing linear olefin block copolymers

The ethylene-octene diblock copolymers reported have soft (high octene content) blocks attached to hard (low octene content) blocks. When no CSA is used, a blend is produced since each catalyst center generally produces hundreds of polymer chains. However, when a CSA is employed, the CSA transfers live polymer chains from the first reactor to the second, creating a diblock architecture.

This same catalyst has been used with $AlOct_3$ as a CSA in ethylene–hexene copolymerizations and quenched with $D_2O$ [170]. The $^2H$ label is shown to be attached almost exclusively to the linear endgroups of the polymer, indicating that chain shuttling occurs faster after ethylene insertion than after α-olefin insertion. Additionally, the experiments reveal a significant decrease in molecular weight distribution ($M_w/M_n$) even though less than half of the available aluminum valences are occupied by polymeryl chains.

Busico and Stevens et al. have recently reported on the polypropylene chain shuttling polymerization using the same $Hf^{IV}$ catalyst shown in Fig. 5.15, and comparing it with its enantiopure form [171, 172]. As reported above, the predominant type of stereoerror observed for $C_2$-symmetric metallocenes operating under site control is $m_x$(r)(r)$m_y$, indicative of an isolated methyl group of opposite stereochemistry (see Fig. 5.14). On the contrary, the *rac*-$Hf^{IV}$ catalyst shown in Fig. 5.15 generates stereoblock isotactic polypropylenes joined by a $m_x$(r)$m_y$ stereoerror in which methyl groups along the backbone instantly switch from one alignment to the other [173, 174]. Notably, this stereoerror is absent when an enantiopure catalyst is employed. These results are reasonably explained by a chain shuttling process. Chain shuttling produces the stereoerror when a chain is shuttled from one enantiomeric catalyst center to the other. Of course, chain shuttling among enantiopure catalyst centers does not produce any error. The authors also have found a significant enhancement in shuttling rate when a polar solvent such as difluorobenzene is employed rather than the less polar toluene.

### *5.7.4 Olefin Polymerization Mechanism*

*When Ziegler and Natta first started at it,*
*They never could have foreseen*
*The storied legacy and subtle treachery*
*Of this wicked polymer machine.*

*Shuttling effective, it's isoselective!*
*The polymer straight as an arrow.*
*But we must not forget the best feature yet:*
*The new stereoregioerror.*

*The metal is tight, the aryl quite right,*
*But between them the normalcy stops.*
*Is there a bond? First off then it's on,*
*Next…in the monomer pops.*

*The naphthyl swings the electrons it brings*
*From the front, or the side, or the back.*
*And the metal may find an amine to bind,*
*Or a ligand C–H to attack.*

*If ever one thinks he is on the brink*
*Of placing the clinching piece,*
*The final test does not match with the rest,*
*And the puzzle's depth is increased.*

*The catalyst is magic; to study it, tragic,*
*And the mania won't be denied:*
*Wizened gray chemists, fists raised to the heavens,*
*Wail "Curse you, pyridyl-amide!"*

The conventional approach to the design of new catalysts active for the highly isotactic propylene polymerization has been dominated for a long time by $C_2$-symmetric metallocene catalysts [175]. However, high-throughput screening methods have enabled the development of a new class of $C_1$-symmetric post-metallocene systems of the type described above (amidoalkylpyridinato complexes, see Sects. 5.7.1 and 5.7.2). This new class of complexes has been found to produce highly isotactic polymers with high efficiency and molecular weight, even at high reaction temperatures. Initial efforts can be described as serendipity by design, maximizing chances for unexpected discovery. The remarkable performance of this new class of catalysts challenges the field for mechanistic description. If the unconventional catalyst structure portended mechanistic complexity or originality, the field of investigation has not been disappointed.

The mechanistic groundwork has been laid by Murphy, Stevens and Busico et al. [150]. The authors analyzed the variable-temperature propylene polymerization for the $Hf^{IV}$ dimethyl catalyst inset in Fig. 5.16, by plotting $\ln[\sigma/(1-\sigma)]$ versus 1/RT (Fig. 5.16). The straight line and zero intercept resemble typical behavior for $C_2$-symmetric metallocene catalysts, and therefore reasonably imply

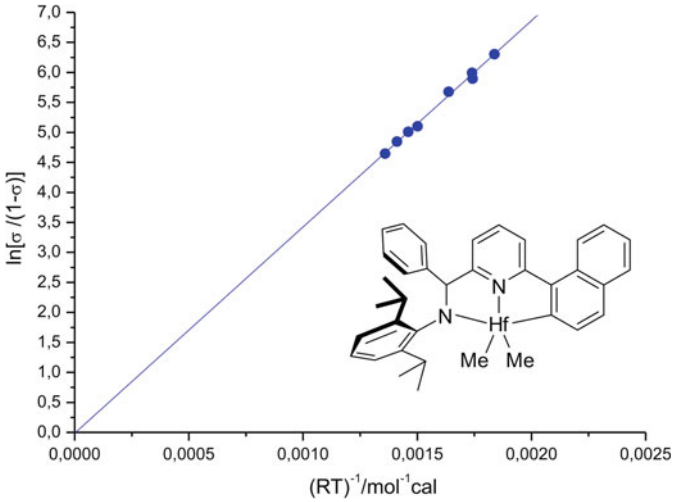


**Fig. 5.16** Plot of variable-temperature propylene polymerization for the catalyst shown in figure using $Ph_3C[B(C_6F_5)_4]$ as catalyst activator. $\sigma$ = probability of propylene insertion in one enantioface, $1-\sigma$ = probability for insertion at the other enantioface. It is reasoned that one diastereotopic "side" of the catalyst is highly favored for insertions

highly selective insertions at one of the two possible diastereomeric faces. Furthermore, the authors have observed the isoselectivity to be insensitive to propylene concentration, indicating very high epimerization rate relative to propagation rate. Density functional theory (DFT) calculations also are reported, and they are found to be consistent with the experimental observations. However, the authors point out that in situ ligand modification by monomer may also affect the mechanistic path.

A mechanism involving ligand modification by monomer was presented in significant detail by Froese [163]. While investigating ethylene–octene copolymerizations, the authors noted a multi-modal molecular weight distribution of the produced polymeric materials that shifts toward the higher molecular weight fraction(s) as the reactor composition becomes richer in octene (Fig. 5.17). This highly unusual behavior is explained according to a mechanism involving the first monomer insertion into the Hf–*naphthyl* bond, which permanently modifies the catalyst structure. In a simplistic view, the polymer composition can be considered as bimodal, with one fraction derived from an ethylene-modified catalyst and the other obtained by an octene-modified catalyst. This idea is supported by DFT calculations, which show a lower barrier for the Hf–*naphthyl* bond insertion by about 0.4–2.2 kcal/mol relative to the insertion into the Hf–alkyl bond. While this energy difference is about the same as the error in calculation, a simple kinetic consideration discounts this unconventional insertion as a deactivation mechanism, because the catalyst performs several hundred thousand conventional insertions during polymer generation. Therefore, this ligand modification reaction must occur

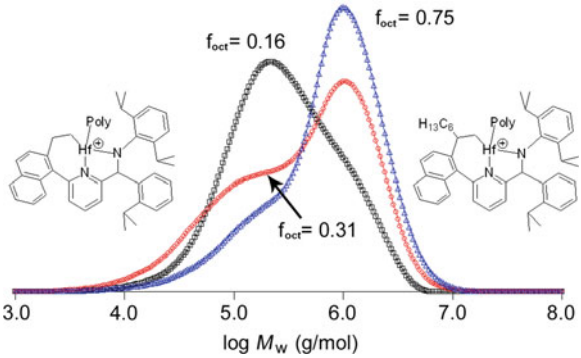


**Fig. 5.17** GPC traces for copolymers prepared at variable $f_{oct}$ and interpreted in terms of ligand modification by monomer. $f_{oct} = [C_8H_{16}]/([C_2H_4] + [C_8H_{16}])$

in a reaction step prior to the start of polymerization. The driving forces for the insertion are relief of an eclipsing H–H interaction of the naphthalene and pyridine rings, and formation of a stabilizing interaction between the metal center and the naphthalene $\pi$ cloud. No $\alpha$- or $\beta$-agostic interactions are found by DFT calculations for the olefin-modified complex (facilitating chain epimerization), olefin binding is relatively weak, and transition state energies for polymerization differ by more than 4 kcal/mol for the diastereotopic faces. This energetic profile is generally consistent with the observations and inferences outlined in Ref. [150] for insertions at a single side of the catalyst and a stereospecificity in the olefin insertion which is independent of propylene concentration.

A thorough NMR investigation of the activation path for amidopyridinate $Hf^{IV}$-dimethyl complexes containing R = 2,6-*i*$Pr_2C_6H_3$, $R^1$ = 1-Nap or Ph, and $R^2$ = 2-*i*$PrC_6H_4$ ligand substituents, has been reported by Macchioni et al. [176]. While activation of the naphthyl complex with $B(C_6F_5)_3$ leads to abstraction of a methyl group and formation of a single inner-sphere diastereoisomeric ion pair (with a bridging methyl group), activation with $Ph_3C[B(C_6F_5)_4]$ yields a 1:1 mixture of the two possible outer-sphere diastereomeric ion pairs. When the Brønsted acid $[PhNMe_2H][B(C_6F_5)_4]$ is used as activator instead of a Lewis acid, the complex activation path is remarkably sensitive to the nature of the $R^1$ substituent (Scheme 5.35). In either case (phenyl or naphthyl), the cyclometallated aryl group is initially protonolyzed to generate a bidentate $\{N^-,N\}$-chelated complex. The phenyl ring re-metallates to release methane and regenerate the tridentate $\{N^-,N,C^-\}$-chelated complex, which then binds $PhNMe_2$. In contrast, the naphthyl congener does not immediately re-metallate under the conditions tested, but can participate in reactions involving dimethylaniline as shown in Scheme 5.35. An X-ray crystal structure of the protonolyzed naphthyl $[\{N^-,N\}$-$Hf(Me_2)][B(C_6F_5)_4]$ complex is provided in Fig. 5.18. The latter species is found to undergo different reaction paths: (a) it can react with a second equivalent of the Brønsted acid activator to form the dicationic complex $[\{N^-,N\}$-Hf(Me)N-$Me_2C_6H_4][B(C_6F_5)_4]_2$; (b) it can bind and *ortho*-metallate the formed N,N-dimethyl aniline with methane elimination ultimately re-arranging, over time, into an aniline-bound complex cation stabilized by a tetradentate trianionic ligand,

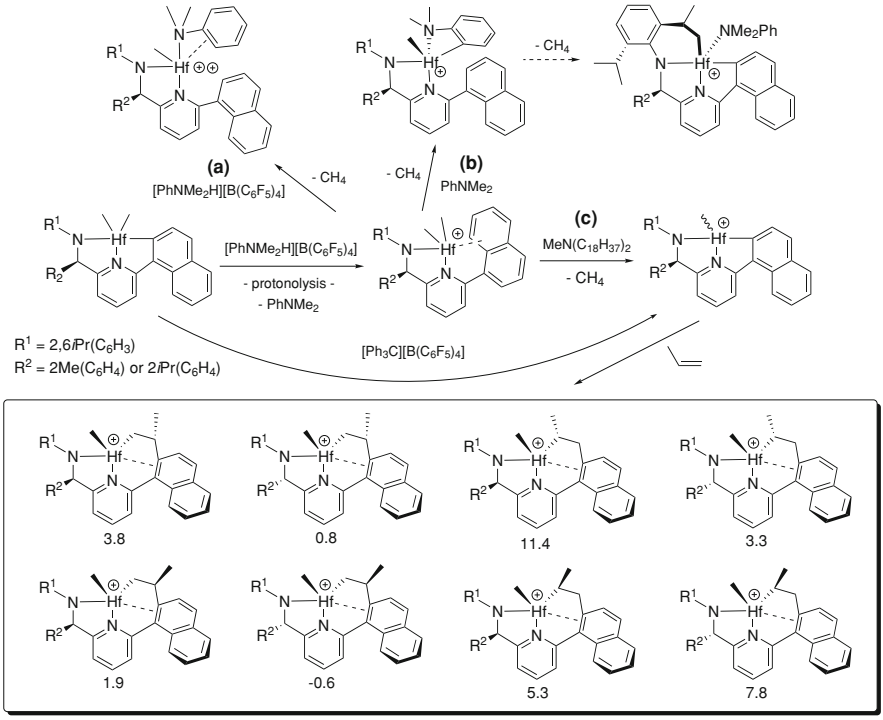


**Scheme 5.35** Possible catalyst activation paths resulting from the treatment of $\{\eta^3\text{-}(N^-,N,C^-)\text{-}L\}Hf(Me)_2\}$ pre-catalysts with either Brønsted or Lewis acid activators [176]. Possible permanent catalyst modifications by propylene insertion into the Hf–$C_{Nap}$ bond are highlighted, with numbers reported below each propylene-modified cation structure representing relative energies (kcal/mol) for transition states (TS) according to DFT calculations [163]

$[\{N^-,N,C^-,C^-\}\text{-}Hf(NMe_2Ph)][B(C_6F_5)_4]$ (a similar result is observed for the phenyl substituted complex); (c) it can re-metallate the naphthyl ring upon treatment with one equivalent of $CH_3N(C_{18}H_{37})_2$, liberating a further methane equivalent.

This difference in reactivity between the phenyl- and naphthyl-substituted systems can be explained by the $\eta^2$-coordination of the cationic metal center to the naphthyl ring at the 8- and 9-carbons, an interaction which is clearly not possible when $R^1$ = Ph. This metastable intermediate is proposed to cause an induction period that is observed in octene polymerization tests with naphthyl-containing $Hf^{IV}$-complexes once activated by protic co-catalysts. On the contrary, no appreciable induction period is observed for the same catalyst when activated by Lewis acids or the phenyl congener when activated by either co-catalyst types.

Hustad et al. have reported a mechanistic evaluation of the propylene polymerization with a catalyst having a symmetrically-substituted backbone ($R^3$ = H) [151]. These $C_s$-symmetric catalysts simplify the consideration of olefin insertion into the Hf–aryl bond since there are only four possible isomers rather than eight.

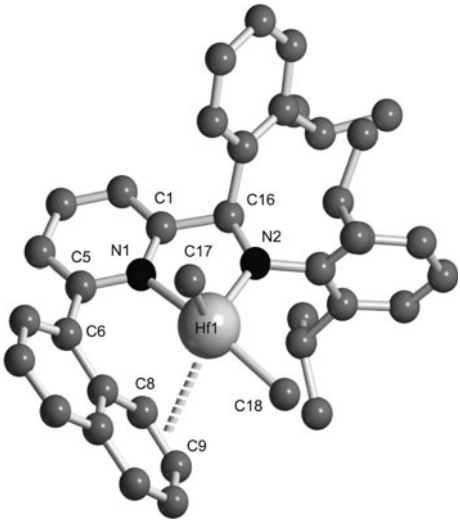


**Fig. 5.18** *Ball and stick* drawing of the crystal structure of $\{\eta^2\text{-}(N^-,N)\text{-}L\}Hf(Me)_2\}$ (hydrogen atoms and $B(C_6F_5)_4^-$ anion are omitted) [176]. Selected distances (Å) and angles (°): Hf1-N1 2.2983(17), Hf1-N2 2.0108(18), Hf1-C8 2.612(2), Hf1-C9 2.737(2), Hf1-C17 2.190(2), Hf1-C18 2.297(2), N1-Hf1-N2 72.70(7), N1-C5-C6-C7 -43.45

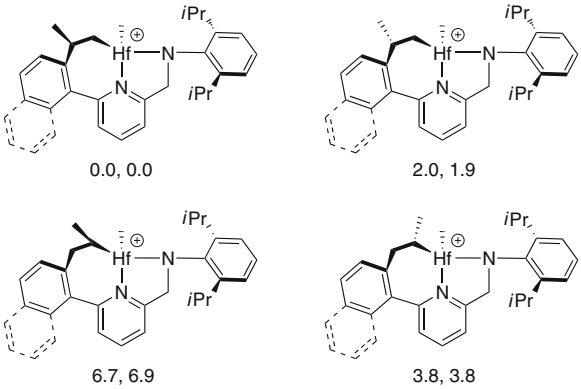


**Fig. 5.19** Possible propylene insertion products into the Hf–$C_{aryl}$ bond and relative transition state energies (kcal/mol) for systems containing an aryl = phenyl or naphthyl, respectively

Remarkably, even with this more symmetric system, polypropylene GPC traces are well described by a trimodal distribution. The authors hypothesize that this result can be explained by assuming a catalyst mixture comprising three of the four potential propylene-modified catalytic species. This hypothesis is consistent with DFT calculations, which place one transition state significantly higher than the other three (Fig. 5.19). The polymer obtained is moderately isotactic, consistent with polymerization by asymmetric (not $C_s$-symmetric) catalysts. Polyethylene made with this catalyst has narrow molecular weight distribution, as expected.

Allgaier et al. have reported the in situ and/or time-resolved investigation of octene polymerization by hafnium dimethyl catalyst with $R/R^1/R^2$ = 2,6-*i*$Pr_2C_6H_3$/Ph/H [177]. The authors deconvolute the molecular weight distribution of GPC traces with refractive index detection into two peaks. A small amount of a third, higher molecular weight fraction becomes more apparent when light

scattering detection is used. The authors' conclusions are that three catalyst species are operative, at least, in the polymerization process, one of them being present in low concentration but responsible for the higher polymerization rate. They observe first order disappearance of octene by $^1$H NMR analysis when the polymerization is conducted in an NMR tube from −10 to 20 °C. Only single, non-aggregated chains are observed by SANS measurements.

Coates et al. have obtained isoenriched poly-(1-hexene)s from polymerization using a $C_s$-symmetric pre-catalysts of the same type [136]. They report very narrow molecular weight distributions, and characterize the polymerization behavior as living.

Further direct and indirect evidence for the first insertion of these catalysts occurring at the metal–aryl bond is reported by Zuccaccia et al. [178]. Reactions of activated catalyst with 2-vinylpyridine or 3-ethoxy-1-propylene lead to products derived from insertion of the olefinic portion into the Hf–$C_{aryl}$ bond. Furthermore, low-temperature treatment of activated catalyst with 173 equivalent of hexene enables direct NMR detection of a catalyst modified by hexene insertion at the expected Hf–$C_{aryl}$ reactive site.

The mechanistic investigations are summarized graphically in Scheme 5.35. Possible permanent catalyst modifications from the regio- and stereo-insertion of propylene into the Hf–$C_{Nap}$ bond are shown, with energies calculated for each TS reported under each structure [163]. More recently, Zuccaccia et al. have revisited these DFT calculations with an additional level of complexity, including the complex counterion [178]. Including the counterion in the calculations generally leads to higher (more realistic) energy barriers to insertion. With or without including anion, energy differences for transition states and for the products of various Hf–$C_{aryl}$ insertions are relatively small, and multiple olefin-modified catalyst species are expected.

### *5.7.5 6-Aryl(heteroaryl)-substituted Amidoalkylpyridinato Yttrium Complexes*

Giambastiani, Trifonov et al. have prepared a series of $Y^{III}$-alkyl or hydrido complexes stabilized by 6-aryl- or heteroaryl-substituted amidoalkylpyridyl ligands [42, 143]. Metal alkyl complexes are prepared by reactions of an equimolar amount of the ligand with $[Y(CH_2SiMe_3)_3(thf)_2]$, which proceed cleanly at 0 °C with the release of two equivalents of $Me_4Si$, to give the corresponding $\{N^-,N,C^-\}$-ligated monoalkyl complexes (Scheme 5.36). *ortho*-Metallation of the aryl or heteroayl group rapidly occurs at a $C_{sp2}$–H bond, while for the 2,6-dimethylphenyl-substituted ligand, the activation unexpectedly occurs at the $C_{sp3}$–H bond of one methyl fragment. Complexes with simple aryl substituents form mono-thf adducts, while those bearing activated heteroaryl groups bind two equivalents of thf. Addition of $PhSiH_3$ to these monoalkyl complexes results in the

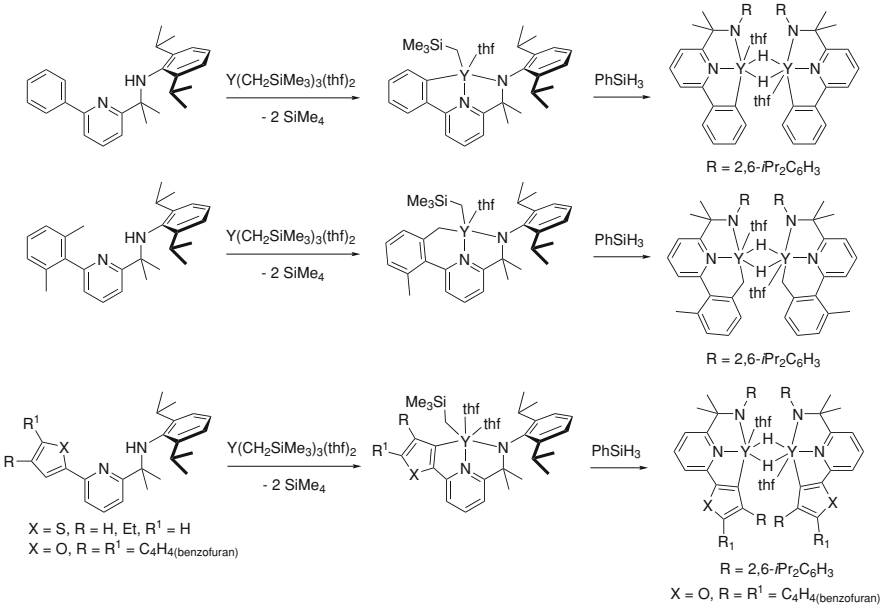


**Scheme 5.36** Synthesis of amidopyridinate $Y^{III}$ complexes

highly selective protonolysis of the Y-alkyl bond to give a series of hydride-bridged dinuclear $Y^{III}$-complexes with unconventional structures (Scheme 5.36).

Representative crystal structures of selected $Y^{III}$-alkyl and hydrido complexes are shown in Fig. 5.20 [42]. The alkyl complex in Fig. 5.20a reveals a coordination environment including a tridentate dianionic amidoalkylpyridyl ligand $\{N^-,N,C^-_{sp3}\}$, one further $sp^3$ carbon atom from the residual "benzylic" group, and one oxygen atom from a thf molecule. Moreover, a close contact between the metal center and the *ipso* carbon on the "benzylic" residue is observed, which increases the coordination number to six. The structure of a binuclear $Y^{III}$–H species is shown in Fig. 5.20b. This complex contains two six-coordinate yttrium atoms, each coordinated by a thf molecule; two bridging hydrido atoms; and a nearly planar dianionic tridentate amidoalkylpyridinate ligand $\{N^-,N,C^-_{sp2}\}$.

These $Y^{III}$-alkyl and -hydrido complexes have been investigated in ethylene polymerization under a variety of reaction conditions [143]. The complexes are inactive in the absence of a cocatalyst/activator, but addition of MAO (excess) generates active polymerization species with activity as high as 3.1 $kg_{PE}$ $(mol_Y\ bar\ h)^{-1}$. Complexes containing $sp^3$-carbon donors at the ligand framework show much lower activity, producing only 0.3 $kg_{PE}$ $(mol_Y\ bar\ h)^{-1}$. Activation with $[PhNMe_2H][B(C_6F_5)_4]$ and $iBu_3Al$ at 65 °C also results in formation of PE, but with rather modest activities (0.8 and 0.4 $kg_{PE}$ $(mol_Y\ bar\ h)^{-1}$).

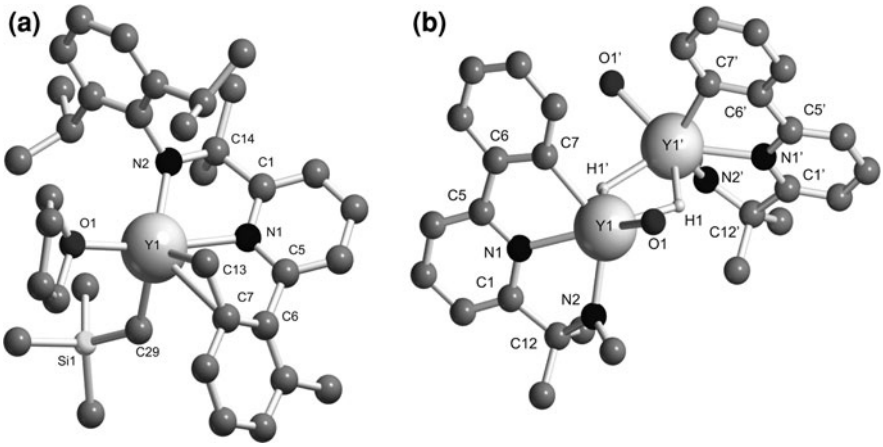


**Fig. 5.20** **a** *Ball and stick* drawing of the crystal structure of $\{\eta^3\text{-}(N^-,N,C^-_{sp3})\text{-}L\}Y(CH_2SiMe_3)(THF)\}$ (hydrogen atoms are omitted) [42]. Selected distances (Å) and angles (°): Y1-N1 2.4200(14), Y1-N2 2.2015(14), Y1-C7 2.9421(17), Y1-C13 2.4520(18), Y1-C29 2.4139(17), N1-Y1-N2 70.00(5), N1-C5-C6-C7 -52.57. **b** *Ball and stick* drawing of the crystal structure of $\{(\eta^3\text{-}(N^-,N,C^-_{sp2})\text{-}L\}YH(thf))_2\}$ (hydrogen atoms omitted) [42]. Selected distances (Å) and angles (°): Y1-N1 2.4252(17), Y1-N2 2.2205(18), Y1-C7 2.469(2), Y1-H 2.15(2), Y1-Y1' 3.5780(4), N1-Y1-N2 68.24(6), N1-Y1-C7 68.43(7), N1-C5-C6-C7-7.52

### *5.7.6 6-Aryl(heteroaryl)-substituted Aminoalkylpyridinato Chromium Complexes*

In addition to stabilizing Group IV metals as amido ligands, 6-(hetero)aryl aminopyridinate compounds have also been used to form chromium complexes containing monoanionic tridentate ligating systems. Selected chromium complexes of this type are listed in Table 5.19 [144] and Table 5.20 [141]. The dichloride complexes are formed by reaction of the amino ligand with $CrMeCl_2(thf)_3$ at 60 °C (Scheme 5.37). The reactions proceed by release of one methane equivalent through the $C_{sp2}$–H activation of the ligand aryl group to give a monoanionic tridentate $\{N,N,C^-\}$ complex. Select examples of these complexes have been diversified by metathesis reactions with Li[acetylacetonate] (Li-acac), K[3-$n$C$_5$H$_{11}$-acetylacetonate] (K-NP-acac), or $Ag(O_2CCF_3)_2$, respectively (Scheme 5.37).

Representative structures of L-$CrCl_2$ and L-CrCl(acac) complexes are shown in Fig. 5.21. Both species possess octahedral coordination geometry around the chromium centers, and the L-$CrCl_2$ species is coordinated by *trans* chloride atoms and a thf molecule O-coordinated *trans* to the pyridine ring.

These $Cr^{III}$ complexes have been found to be active and selective catalysts for ethylene oligomerization [141, 144]. Oligomerizations were initially conducted in a 48-well parallel polymerization reactor [179, 180]. The chromium precatalysts

**Table 5.19** Select examples of $Cr^{III}$ complexes stabilized by 6-aryl-aminoalkylpiridyl ligands [144]

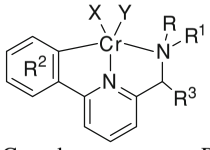


| Complex | R | $R^1$ | $R^2$ | $R^3$ | $X^a$ | $Y^a$ |
|---|---|---|---|---|---|---|
| Cr-1 | H | 4-*i*Pr$C_6H_4$ | Ph | Ph | Cl | Cl |
| Cr-2 | H | 4-(*n*$C_{12}H_{25}$)$C_6H_4$ | Ph | 4-*n*Bu$C_6H_4$ | Cl | Cl |
| Cr-3 | H | 4-(*n*$C_{12}H_{25}$)$C_6H_4$ | Ph | Bn | Cl | Cl |
| Cr-4 | H | *n*Bu | Ph | $C_6H_{11}$ | Cl | Cl |
| Cr-5 | H | *n*Bu | Ph | $C_6H_{11}$ | Cl | acac |
| Cr-6 | H | *n*Bu | Ph | $C_6H_{11}$ | $O_2CCF_3$ | $O_2CCF_3$ |
| Cr-7 | H | *n*Bu | Ph | $C_6H_{11}$ | Cl | NP-acac |
| Cr-8 | H | *n*Bu | Ph | $C_6H_{11}$ | NP-acac | NP-acac |
| Cr-9 | H | 4-*n*Bu$C_6H_4$ | Ph | 4-*n*Bu$C_6H_4$ | Cl | Cl |
| Cr-10 | H | nBu | 3-benzothiophene | $C_6H_{11}$ | Cl | Cl |
| Cr-11 | H | nBu | 3,5-$Me_2C_6H_3$ | $C_6H_{11}$ | Cl | acac |
| Cr-12 | Me | Me | Ph | *n*Bu | Cl | Cl |
| Cr-13 | Me | Me | Ph | *n*Bu | Cl | acac |
| Cr-14 | Me | Me | Ph | *n*Bu | Cl | NP-acac |
| Cr-15 | Me | Me | Ph | *n*Bu | NP-acac | NP-acac |
| Cr-16 | Me | Me | Ph | 2-EtBu | Cl | acac |
| Cr-17 | Me | Me | 4-*t*Bu$C_6H_4$ | *n*Bu | Cl | Cl |
| Cr-18 | Me | Me | 4-*t*Bu$C_6H_4$ | *n*Bu | Cl | acac |
| Cr-19 | Me | Me | 4-*t*Bu$C_6H_4$ | *n*Bu | NP-acac | NP-acac |
| Cr-20 | Me | $C_6H_{11}$ | Ph | H | Cl | acac |
| Cr-21 | Me | Me | Ph | Me | Cl | acac |
| Cr-22 | -$(CH_2)_4$- | | Ph | Bn | Cl | acac |

(continued)

**Table 5.19** (continued)

| Complex | R | $R^1$ | $R^2$ | $R^3$ | $X^a$ | $Y^a$ |
|---|---|---|---|---|---|---|
| Cr-23 | $-(CH_2)_4-$ | | Ph | $C_6H_{11}$ | Cl | acac |
| Cr-24 | Me | Me | 4-$(NMe_2)C_6H_4$ | *n*Bu | Cl | acac |
| Cr-25 | Me | Bn | Ph | Bn | Cl | acac |
| Cr-26 | Me | $C_6H_{11}$ | Ph | H | Cl | acac |
| Cr-27 | Me | $C_6H_{11}$ | Ph | H | NP-acac | NP-acac |
| Cr-28 | Me | Me | Ph | Bn | Cl | acac |
| Cr-29 | Me | Me | 4-*t*Bu$C_6H_4$ | 2-EtBu | Cl | acac |
| Cr-30 | $-(CH_2)_4-$ | | 4-*t*Bu$C_6H_4$ | *n*Bu | Cl | acac |
| Cr-31 | Me | Me | Ph | $C_6H_{11}$ | Cl | acac |
| Cr-32 | Me | Me | 3,4,5-$(MeO)_3C_6H_2$ | *n*Bu | Cl | acac |
| Cr-33 | Me | Et | Ph | *n*Bu | Cl | acac |
| Cr-34 | Me | Me | 4-$(SiMe_3)C_6H_4$ | 2-EtBu | Cl | acac |
| Cr-35 | Me | Me | 4-(BnO)$C_6H_4$ | *n*Bu | Cl | Cl |
| Cr-36 | Me | Me | 4-(BnO)$C_6H_4$ | *n*Bu | Cl | acac |
| Cr-37 | Me | Me | 4-(BnO)$C_6H_4$ | *n*Bu | NP-acac | NP-acac |
| Cr-38 | Me | Me | 3,4-$(MeO)_2C_6H_2$ | *n*Bu | Cl | acac |

[a] acac = acetylacetonate, NP-acac = 3-*n*-pentyl-acetylacetonate

**Table 5.20** 6-Ferrocenyl-substituted aminopyridinate $Cr^{III}$ complexes [141]

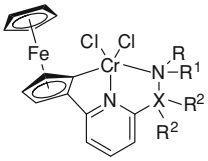

| Complex | R | $R^1$ | $R^2$ | X |
|---|---|---|---|---|
| Cr-39 | *n*Bu | H | H | C |
| Cr-40 | Ph | H | H | C |
| Cr-41 | Me | Me | H | C |
| Cr-42 | Me | Me | Me | Si |

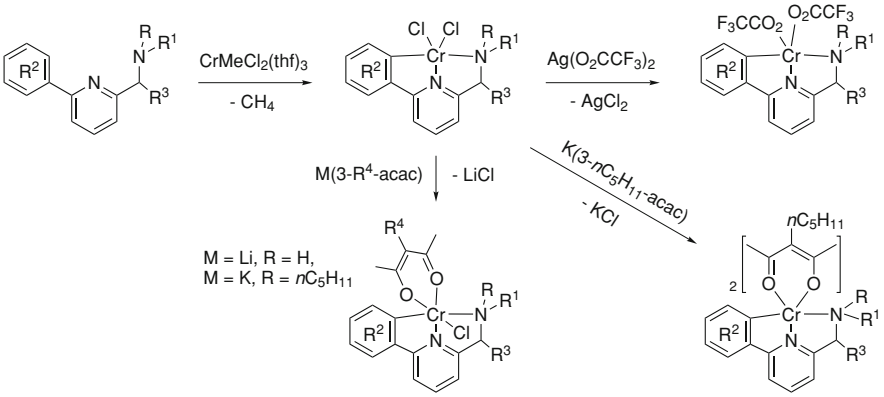


**Scheme 5.37** Synthesis of chromium complexes supported by amidoalkylpyridyl ligands. Refer to Table 5.18 for $R/R^1/R^2/R^3$ substituent codes

were activated with a combination of MMAO and either $i$Bu$_2$AlH or Me$_3$Al. Representative results captured in Table 5.21 were obtained from tests conducted at 80 °C and 400 psi of ethylene using heptane as solvent. Complexes bearing simple aryl substituents in the 6-position of the pyridine ring display high 1-hexene selectivities (>99.9% in one case) and turnover frequencies higher than $5 \times 10^5$ (h)$^{-1}$. Precatalyst Cr-20 shows the highest 1-hexene selectivity (>99.9%), while Cr-16 has the highest turnover frequency ($5.84 \times 10^5$ (h)$^{-1}$). In all presented examples, some fractions of PE are produced although the 1-hexene/PE ratio always remains relatively high (>130 g of 1-hexene/g PE). In comparison, complexes bearing 6-ferrocenyl-pyridyl ligands are much less active and selective, although a direct comparison between the two systems is complicated by other differences in the ligand substituents [141].

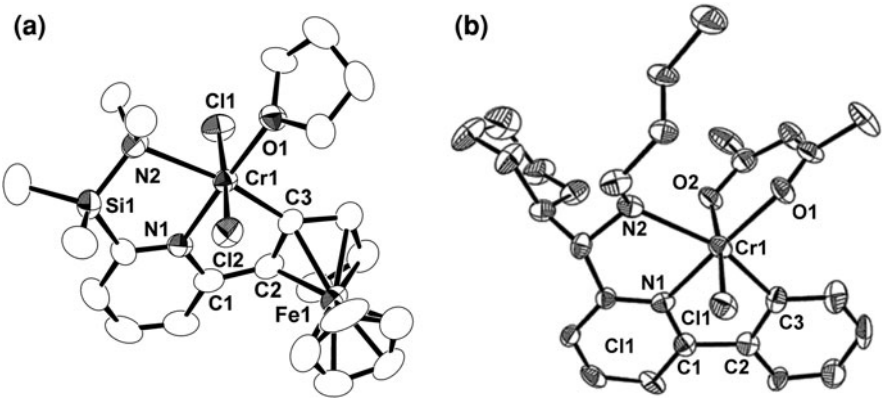


**Fig. 5.21** **a** Crystal structure of $\{\eta^3\text{-(N,N,C}^-)\text{-L}_{\text{ferrocenyl}}\}\text{CrCl}_2\text{(thf)}\}$ [141] (see also entry Cr-42 in Table 5.19). Thermal ellipsoids are drawn at the 50% probability level. Hydrogen atoms are omitted. Selected distances (Å) and angles (°): Cr1-N1 2.061(3), Cr1-N2 2.415(3), Cr1-C3 2.054(3), Cr1-Cl1 2.342(1), Cr1-Cl2 2.337(1), N1-Cr1-N2 85.98(12), N1-Cr1-C3 81.36(14), N1-C1-C2-C3 4.9(5). **b** Crystal structure of $\{\eta^3\text{-(N,N,C}^-)\text{-L}\}\text{CrCl(acac)}\}$ [144] (see also entry Cr-5 in Table 5.17). Thermal ellipsoids are drawn at the 50% probability level. Hydrogen atoms are omitted. Selected distances (Å) and angles (°): Cr1-N1 2.025(2), Cr1-N2 2.237(2), Cr1-C3 2.045(2), Cr1-Cl1 2.3409(5), Cr1-O1 1.972(1), Cr1-O2 1.964(1), N1-Cr1-N2 78.12(6), N1-Cr1-C3 80.42(7), N1-C1-C2-C3 3.6(5). (reproduced with permission)

**Table 5.21** Ethylene oligomerization by either 6-aryl- or 6-ferrocenyl-substituted $Cr^{III}$ aminoalkylpiridinate complexes

| Cat. | μmol Cr | MMAO (Al/Cr) | 1-Hex TOF[c] ($10^3$ $h^{-1}$) | 1-Hex Sel[d] | PE (g) | 1-Hex/PE[e] (g/g) |
|---|---|---|---|---|---|---|
| Cr-5 | 0.05 | 300[a] | 571 | 97.9 | 2.4 | 259 |
| Cr-6 | 0.05 | 300[a] | 318 | 97.5 | 2.4 | 152 |
| Cr-7 | 0.05 | 500[a] | 306 | 98.0 | 2.3 | 211 |
| Cr-8 | 0.05 | 500[a] | 312 | 97.7 | 2.0 | 233 |
| Cr-13 | 0.05 | 300[a] | 531 | 98.3 | 0.8 | 700 |
| Cr-14 | 0.05 | 500[a] | 281 | 98.7 | 3.0 | 158 |
| Cr-15 | 0.05 | 500[a] | 219 | 98.8 | 2.5 | 191 |
| Cr-16 | 0.05 | 300[a] | 584 | 98.3 | 2.1 | 297 |
| Cr-17 | 0.1 | 300[a] | 192 | 97.9 | 2.7 | 162 |
| Cr-20 | 0.2 | 550[b] | 99.9 | >99.9 | 1.3 | 136 |
| Cr-39 | 0.04 | 600 | 9.21 | >80 | 1.6 | n.r.[f] |
| Cr-40 | 0.04 | 600 | 0.246 | Low | 4.1 | n.r.[f] |
| Cr-41 | 0.04 | 600 | 0.085 | Low | 1.4 | n.r.[f] |

*Conditions* 48-well parallel polymerization reactor, $T = 80$ °C, 400 psi ethylene, heptane solvent
[a] 10 equivalents of $i\text{Bu}_2\text{AlH}$
[b] 10 equivalents of $\text{Me}_3\text{Al}$
[c] 1-hexene turnover frequency (TOF) = [μmol hexene]/([μmol Cr] [time]/60)
[d] 1-hexene selectivity = 100 [μmol hexene]/[sum of μmol $C_6$–$C_{16}$ olefins]
[e] 1-hexene/PE mass ratio
[f] Insufficient data to determine

## 5.8 Aminopyridyl Ligands and Related Group III–IV Metal Complexes

### *5.8.1 Synthesis of 6-Aryl-Aminopyridyl Ligands*

A related class of ligands without a carbon or silicon bridging atom between the pyridine and amine unit have been extensively explored by the group of Kempe [181]. Initial reports on these aminopyridyl (Ap) ligands describe plain amido-pyridinato species, [182, 183] but the majority of examples refer to Ap systems bearing aryl substituents at the pyridine 6-position. These ligands are generally synthesized in a two-step procedure involving a Kumada–Corriu nickel-catalyzed Grignard coupling [184, 185] followed by a palladium-catalyzed Buchwald–Hartwig amination [148, 149] (Scheme 5.38). The ligands are generally prepared in high yields and purified via crystallization.

### *5.8.2 Synthesis of 6-Aryl-Amidopyridinato Complexes*

#### 5.8.2.1 Group III and Rare Earth Metal Complexes

Several examples of Group III and Lanthanide complexes bearing sterically hindered Ap-ligands (for Ap nomenclature refer to the ligand table in Scheme 5.38) have been reported by the group of Kempe. Metal-alkyl complexes have been prepared by reaction of the free Ap ligands with either $[M(CH_2SiMe_3)_3(thf)_2]$ or $[MBn_3(thf)_3]$ metal precursors (Scheme 5.39) [186–189]. Amido complexes of scandium and rare earth metals have also been prepared by reaction of the proper Ap-ligand with $[M\{N(SiHMe_2)_2\}_3(thf)]$ [186]. Finally, metal-halide complexes can be obtained by reaction of the ligand potassium salt with $MX_3(thf)_x$ (M = Y, Sm, Nd), and for different sterically-demanding ligands, either mono- or bis-ligated complexes may be obtained [190, 191].

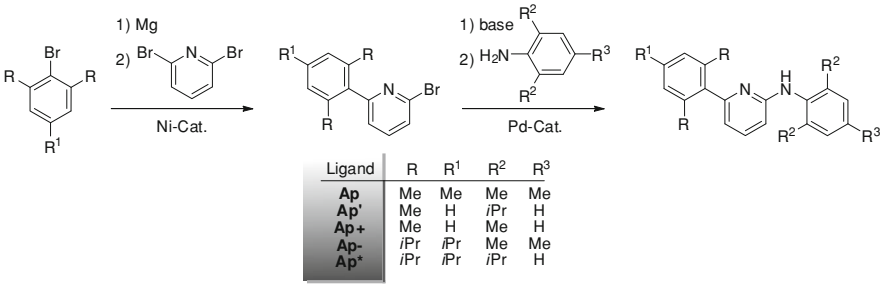


| Ligand | R | $R^1$ | $R^2$ | $R^3$ |
|---|---|---|---|---|
| **Ap** | Me | Me | Me | Me |
| **Ap'** | Me | H | *i*Pr | H |
| **Ap+** | Me | H | Me | H |
| **Ap-** | *i*Pr | *i*Pr | Me | Me |
| **Ap*** | *i*Pr | *i*Pr | *i*Pr | H |

**Scheme 5.38** Synthesis of bulky 6-aryl-substituted amidopyridyl ligands. Readers are asked to refer to the above mentioned **Ap** nomenclature, while reading the following sections

A representative structure of $Ap^*ScBn_2(thf)$ shown in Fig. 5.22a reveals a coordination number of five with the $\eta^2$-{N⁻,N}-coordinated Ap* ligand, two benzyl groups, and one thf molecule filling the metal coordination sphere.

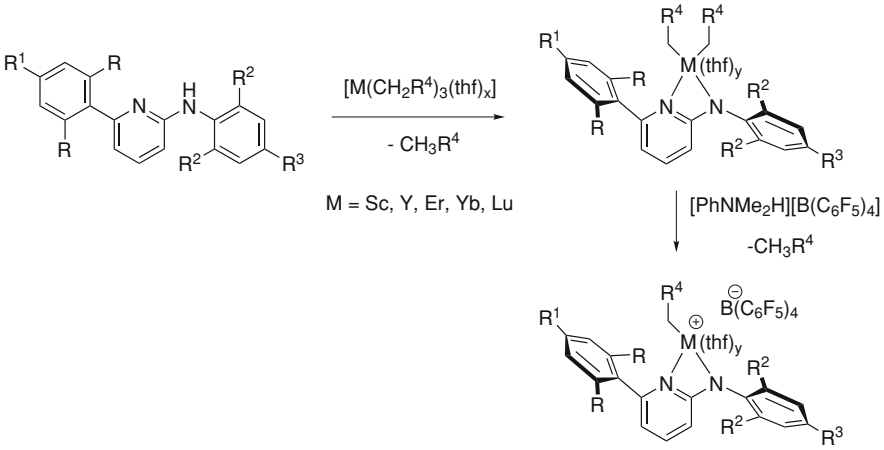


**Scheme 5.39** Synthesis of neutral and cationic Group III and lanthanide complexes bearing Ap-ligands

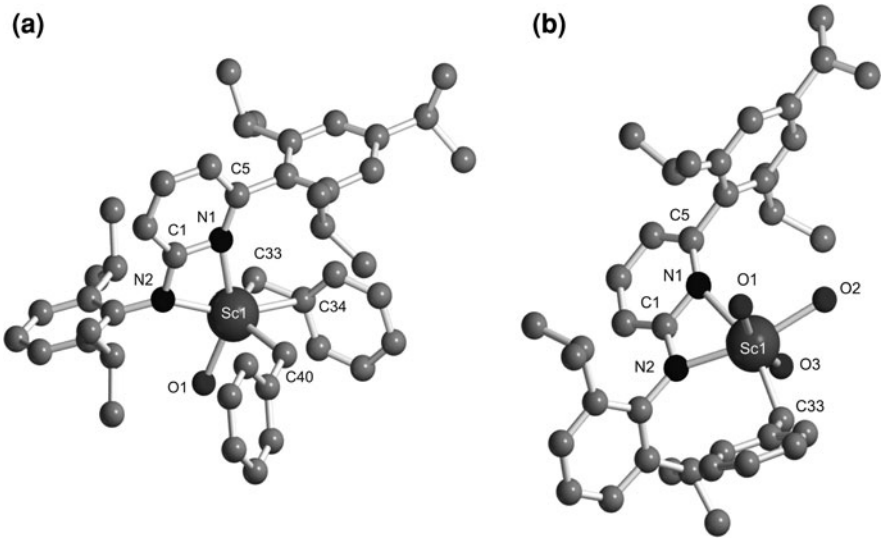


**Fig. 5.22** **a** *Ball and stick* drawing of the crystal structure of $\{\eta^2$-(N⁻,N)-Ap*}Sc(Bn)$_2$(thf)} (hydrogen atoms and a molecule of pentane are omitted) [186]. Selected distances (Å) and angles (°): Sc1-N1 2.286(2), Sc1-N2 2.129(19), Sc1-C33 2.256(3), Sc1-C34 2.657(2), Sc1-C40 2.245(3), N1-Sc1-N2 61.31(7). **b** *Ball and stick* drawing of the crystal structure of $\{\eta^2$-(N⁻,N,)-Ap*}ScBn(thf)$_3\}^+$ (hydrogen atoms and $B(C_6F_5)_4^-$ are omitted) [186]. Selected distances (Å) and angles (°): Sc1-N1 2.358(4), Sc1-N2 2.188(4) Sc1-C33 2.234(6), Sc1-O1 2.192(3), Sc1-O2 2.217(3), Sc1-O3 2.177(3), N1-Sc1-N2 59.77

One benzyl shows $\eta^1$-coordination while the other is bound in $\eta^2$-fashion. Select examples of these alkyl complexes were also transformed to hydrido species by addition of $PhSiH_3$ or $H_2$ [192]. Aluminum alkyl complexes have also been generated by reaction of Ap ligands with either $i$Bu$_3$Al [189] or $Me_3Al$ [193].

Yttrium-alkyl complexes bearing two Ap' ligands can be prepared by a salt metathesis reactions of a halide precursor with $LiCH_2SiMe_3$ (Scheme 5.40) [191]. An $(Ap')_2YCH_2SiMe_3$(thf) complex undergoes, over time, an intramolecular C–H bond activation at the methyl group of one of the Ap'-ligands. The reaction proceeds slowly with first-order kinetics but it is dramatically accelerated by conversion of the alkyl species into a $Y^{III}$-hydride derivative upon addition of $PhSiH_3$. Comparative kinetic experiments indicate that activation of the transient $Y^{III}$–H bond is roughly 500 times faster than that of the alkyl congener. Interestingly, the $(Ap^+)_2ScCH_2SiMe_3$(thf) species shows no signs of C–H activation even in the presence of $PhSiH_3$ [194].

Ap-scandium complexes have also been activated with anilinium borates to give stable ion pairs, several of which have been crystallographically characterized [186, 188]. A representative structure of an Ap*-scandium ion is shown in Fig. 5.22b [186]. The metal center shows a distorted octahedral geometry with three coordinated thf molecules and one benzyl with $\eta^1$-coordination. For further details on related lanthanide complexes, the reader is referred to Chap. 3 of this book.

#### 5.8.2.2 Group IV Metal Complexes

$Zr^{IV}$ and $Hf^{IV}$ complexes bearing bulky Ap-ligands have also been reported, including both mono- and bis-ligated species [193, 195]. *Bis*-ligated $(Ap)_2ZrCl_2$ complexes are formed by reaction of the Ap-ligand potassium salt with $ZrCl_4$ (Scheme 5.41, top). Representative structures of $(Ap')_2ZrCl_2$ and $(Ap^*)_2ZrCl_2$ complexes are shown in Fig. 5.23. Both $Zr^{IV}$ species present distorted octahedral coordination geometries aound the metal center with the chlorine atoms *cis* in the less sterically crowded $(Ap')_2ZrCl_2$ system yet closer to *trans* in the bulkier $(Ap^*)_2ZrCl_2$ species. The treatment of the dichloride complexes with MeLi produces the $(Ap)_2ZrMe_2$ species [193]. Despite their asymmetry, $^1H$ and $^{13}C$ NMR spectra for these $(Ap)_2Zr^{IV}$ complexes show only one set of ligand resonances at

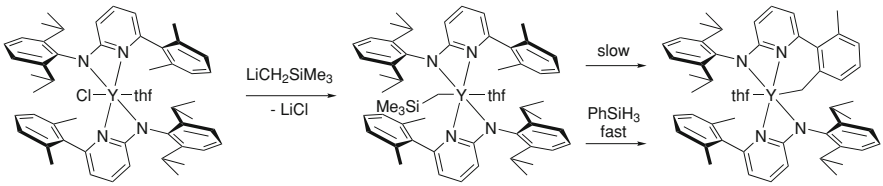


**Scheme 5.40** Intramolecular C–H activation of a *bis*-Ap'-yttrium alkyl complex, accelerated by conversion to the transient hydrido species by $PhSiH_3$ addition

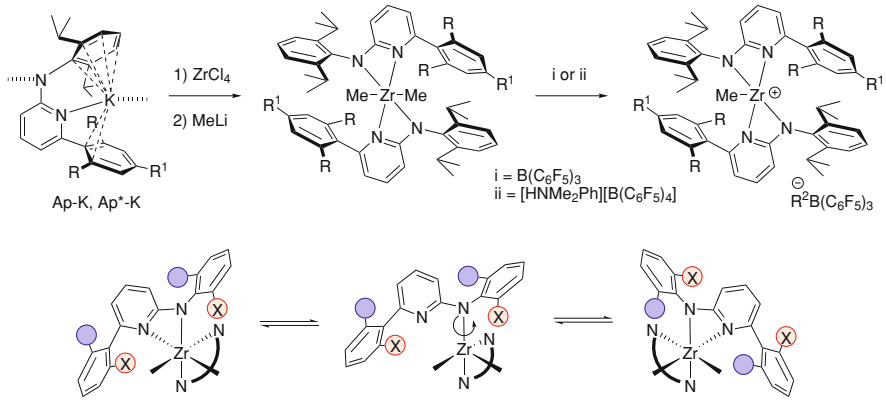


**Scheme 5.41** Synthesis of neutral and cationic $(Ap)_2$-$Zr^{IV}$ amidopyridinate complexes (*top*) and proposed mechanism for a dissociative ligand interconversion (*bottom*)

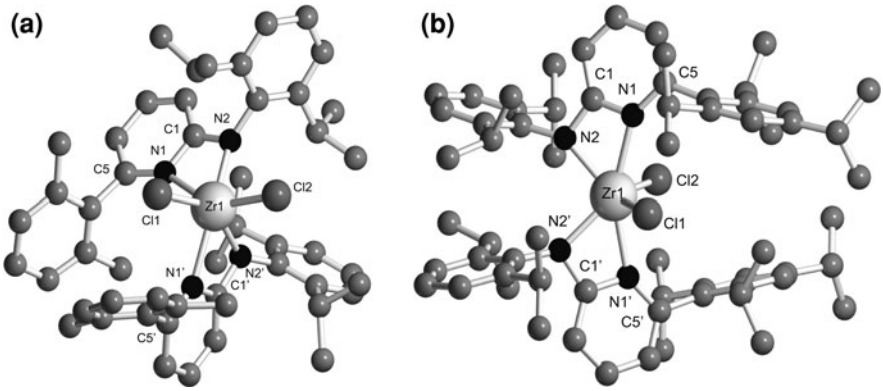


**Fig. 5.23** **a** *Ball and stick* drawing of the crystal structure of $\{\eta^2\text{-}(N^-,N)\text{-Ap'}\}_2ZrCl_2$ (hydrogen atoms and two molecule of benzene are omitted) [193]. Selected distances (Å) and angles (°): Zr1-N1 2.348(3), Zr1-N1' 2.355(3), Zr1-N2' 2.145(3), Zr1-N2 2.123(3), N1-Zr1-N2 60.04(11), N1'-Zr1-N2' 59.44(11), Cl1-Zr1-Cl2 96.47(4). **b** *Ball and stick* drawing of the crystal structure of $\{\eta^2\text{-}(N^-,N,)\text{-Ap*}\}_2ZrCl_2$ (hydrogen atoms and one molecule of hexane are omitted) [193]. Selected distances (Å) and angles (°): Zr1-N1 2.358(4), Zr1-N1' 2.338(4), Zr1-N2' 2.184(4), Zr1-N2 2.154(4), N1-Zr1-N2 59.52(14), N1'-Zr1-N2' 59.40(14), Cl1-Zr1-Cl2 123.08(6)

room temperature, indicative of a fast ligand interconversion on the NMR time-scale that the authors propose to occur via pyridine dissociation (Scheme 5.41, bottom) [193].

The syntheses of several mono-ligated $(Ap)Zr^{IV}$ and $Hf^{IV}$ benzyl complexes have also been accomplished by reacting one Ap ligand equivalent with $M(Bn)_4$ to give the desired mono-ligated complexes in almost quantitative yields [195] (Scheme 5.42). Their treatment with $B(C_6F_5)_3$ generates Zwitterionic complexes as reflected in the $^{19}F$ NMR spectra, by the large $\Delta\delta[(p\text{-F})\text{-}(m\text{-F})]$ values

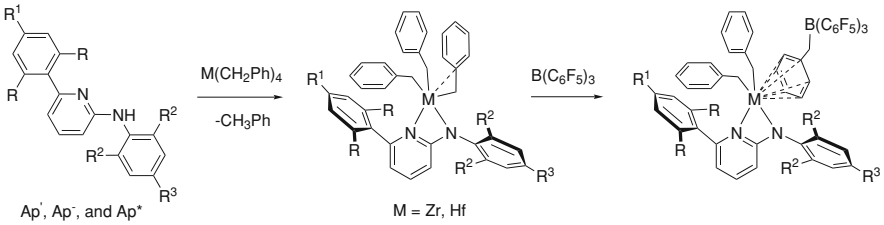


**Scheme 5.42** Synthesis of neutral and cationic Ap-Zr$^{IV}$ and Hf$^{IV}$ benzyl complexes stabilized by Ap', Ap$^{-}$ and Ap* ligands [195]

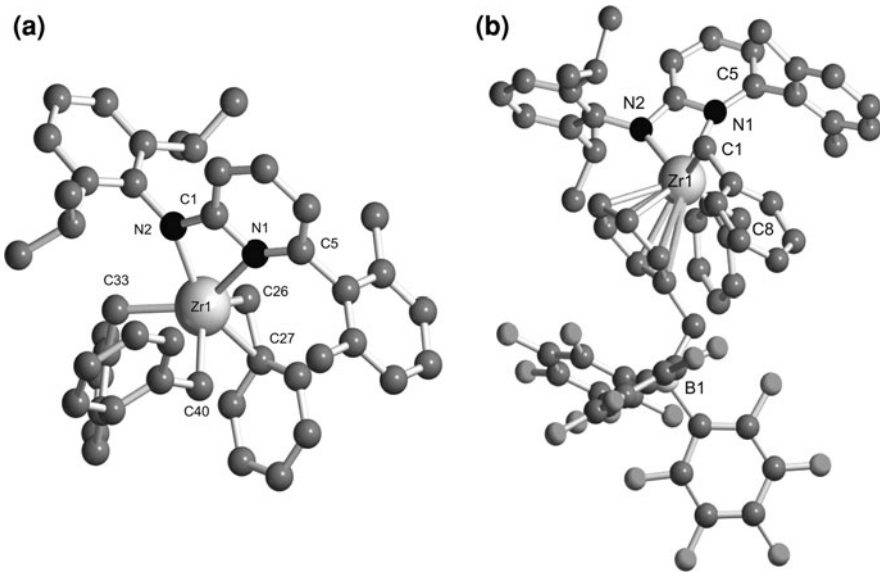


**Fig. 5.24** **a** *Ball and stick* drawing of the crystal structure of {$\eta^2$-(N$^{-}$,N)-Ap'Zr(Bn)$_3$} (hydrogen atoms and one molecule of benzene are omitted) [195]. Selected distances (Å) and angles (°): Zr1-N1 2.359(11), Zr1-N2 2.180(12), Zr1-C26 2.268(16), Zr1-C27 2.629(15), Zr1-C33 2.260(16), Zr1-C40 2.273(15), N1-Zr1-N2 58.70(4). b *Ball and stick* drawing of the crystal structure of {$\eta^2$-(N$^{-}$,N,)-Ap'Zr(Bn)$_2$}{$\eta^6$-Bn[B(C$_6$F$_5$)$_3$]} (hydrogen atoms and one molecule of toluene are omitted) [195]. Selected distances (Å) and angles (°): Zr1-C1 2.258(5), Zr1-C8 2.267(5), N1-Zr1-N2 59.00(14)

[196–201] (Scheme 5.42). A representative structure of (Ap')ZrBn$_3$, shown in Fig. 5.24a, reveals two $\eta^1$-benzyl groups with the third benzyl substituent coordinated in $\eta^2$-fashion. A crystal structure of the Zwitterionic [(Ap')ZrBn$_2$][BnB(C$_6$F$_5$)$_3$] complex is also shown in Fig. 5.24b. The latter species displays a [Ap'ZrBn$_2$]$^+$ cation and a $\pi$-coordinated Bn-moiety from the [BnB(C$_6$F$_5$)$_3$]$^-$ anion. The two residual benzyl groups remaining on the cation are $\eta^1$-coordinated.

## 5.8.3 Polymerization Activity of 6-Aryl-substituted Amidopyridyl (Ap) Complexes

### 5.8.3.1 Polymerization by Group III and Rare Earth Metal Complexes

Kempe et al. have tested various Ap-supported scandium, yttrium, and rare earth complexes for ethylene and isoprene polymerization. (Ap)Y($CH_2SiMe_3$)$_2$ systems have been found to be active for ethylene polymerization upon activation with ammonium borates in the presence of aluminum alkyls; select polymerization results are summarized in Table 5.22 [189]. As shown in entries 1–3, the bulkier Ap* complex presents higher activity compared to Ap' and $Ap^-$ species. All of these systems produce bimodal polyethylenes at 80 °C.

Further studies with the Ap* organoyttrium compound have revealed an interesting temperature dependence on the molecular weight distribution, with an increase in the $M_w$ at higher temperatures and uncharacteristically narrow polydispersities, with $M_w/M_n$ values as low as 1.3 [189]. These results indicate that a coordinative chain transfer polymerization (CCTP) mechanism might be operating in the system [202]. This hypothesis has been validated by varying the Al/Y ratio in the polymerization tests, as shown in Table 5.22 (entries 1 and 4–7). Increasing the Al/Y ratio leads to a decrease in the polyethylene $M_w$ and narrower polydispersities (Fig. 5.25). A linear relationship of $M_n$ versus monomer conversion was also observed up to $M_n$ values of ca. 4,000 g/mol, which is the $M_n$ at which the HDPE begins to precipitate from the solution. Similar rare earth metal complexes are discussed in Chap. 3 of this book.

Ap-supported scandium and rare earth cations generated by reaction of the alkyl complexes with anilinium borates have also been found to generate active species for isoprene polymerization [186, 188]. Ap*-scandium cations have been reported to polymerize isoprene in a controlled fashion with high 3,4-selectivity [186]. Among the polymerization conditions examined, the (Ap)*$ScBn_2$(thf)/

**Table 5.22** Ethylene polymerization with select (Ap)Y($CH_2SiMe_3$)$_2$ complexes

| Entry | Ligand | Al/M | T (°C) | Activity[a] | $M_w$ (kg/mol) | $M_w/M_n$ |
|---|---|---|---|---|---|---|
| 1 | Ap* | 20 | 80 | 1,070 | 66.5[b] | 3.2 |
| 2 | Ap' | 20 | 80 | 400 | 46.1[b] (10.8) | 4.3 (1.5) |
| 3 | $Ap^-$ | 20 | 80 | 432 | 264[b] (16.3) | 28.8 (2.4) |
| 4 | Ap* | 0 | 80 | 0 | n.d. | n.d. |
| 5 | Ap* | 5 | 80 | 1,080 | 88.1 | 2.3 |
| 6 | Ap* | 50 | 80 | 376 | 3.94 | 1.09 |
| 7 | Ap* | 100 | 80 | 168 | 1.46 | 1.05 |

*General conditions* 260 mL toluene, 5 bar ethylene, $t = 15$ min, 10 μmol M, 1.1 equivalent [$R_2NMeH$][$B(C_6F_5)_4$], where R = $C_{16}H_{33}$–$C_{18}H_{37}$, 20 equivalents tetraisobutylalumoxane (TIBAO) as scavenger

[a] Activity reported in units of $kg_{PE}$ ($mol_{ca}$ h bar)$^{-1}$

[b] Bimodal $M_w$ distribution, $M_w$ and $M_w/M_n$ of the main peak (>90%) are reported in parentheses

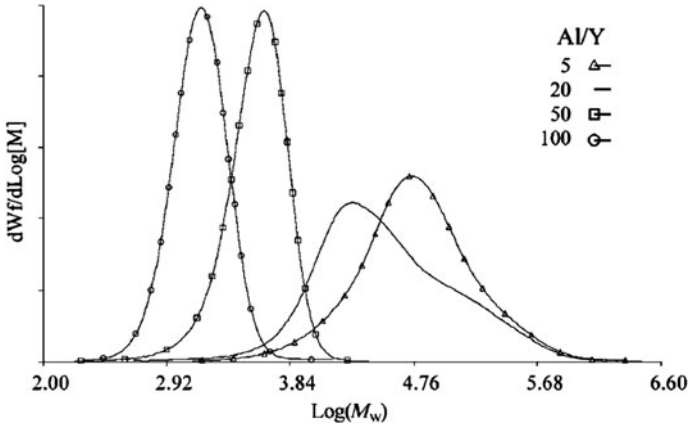


**Fig. 5.25** Molecular weight distributions (SEC) for PEs prepared with the $\{\eta^2$-$(N^-,N,)$-Ap*$Y(CH_2SiMe_3)_2\}$/$[R_2NMeH][B(C_6F_5)_4]$/TIBAO catalyst system at different Al/Y ratio. (Copyright Wiley–VCH Verlag GmbH & Co. KGaA. Reproduced with permission)

$[Ph_3C][B(C_6F_5)_4]$ catalyst system has shown the most regio- and stereoselective performance, producing a polyisoprene with 95% 3,4-content and [*mm*] = 100%. The addition of alkylaluminum species modifies the catalyst reactivity and selectivity in the isoprene polymerization. An increase in size of the rare earth metals also results in a shift toward *cis*-1,4-selectivity [188].

### 5.8.3.2 Polymerization by Group IV Metal Complexes

(Ap)$Zr^{IV}$ and $Hf^{IV}$ benzyl complexes have been reported as catalyst precursors for olefin homo- and copolymerizations [195]. Selected ethylene polymerization results using (Ap)$MBn_3$ complexes are summarized in Table 5.23. Activation of (Ap*)$ZrBn_3$ with $B(C_6F_5)_3$ generates from low to moderately active systems capable of producing PEs with narrow polydispersities, indicative of single polymerization sites. The low activity is likely the result of formation of the aforementioned Zwitterionic complex (see Fig. 5.24b) blocking the active coordination site. Alternatively, the activation of the same catalyst precursor with an ammonium borate cocatalyst leads to a more active catalyst system at the expense of the single site behavior, producing a PE with a trimodal molecular weight distribution [195]. The corresponding $Hf^{IV}$ complex shows lower activity but produces PE with much higher $M_w$ than the $Zr^{IV}$ analog. Zirconium complexes supported by less bulky Ap' and $Ap^-$ ligands show similar activities and broad multimodal molecular weight distributions. Both (Ap*)$ZrBn_3$ and (Ap*)$HfBn_3$ show very low activity in propylene polymerization but are active in ethylene/propylene copolymerizations, with the (Ap*)$ZrBn_3$/borate system displaying activities up to 6,200 $kg_{poly}$ $(mol_{cat}\ bar\ h)^{-1}$. Under the reaction conditions

employed, the $Hf^{IV}$ species produces a highly alternating ethylene/propylene copolymer with no evidence of consecutive propylene insertions.

Kempe et al. have also demonstrated ethylene polymerization with $(Ap)_2ZrX_2$ complexes [193]. Select results from ethylene polymerizations conducted at 80 °C are summarized in Table 5.24. The $(Ap)_2ZrCl_2$ complexes were activated by treatment with an excess of MAO, while an ammonium borate cocatalyst was employed to activate the $(Ap)_2ZrMe_2$ species. The ligand's steric bulk stabilizes the complexes to ligand redistribution processes but causes induction periods with the dichloro species, presumably due to slow alkylation paths. Nevertheless, all species examined generate highly active polymerization catalysts under proper activation conditions. Interesting activator/co-catalyst effects are observed for the different species; $(Ap')_2ZrCl_2$/MAO produces a high molecular weight PE, while the $(Ap')_2ZrMe_2$/borate system gives low molecular weight α-olefins. In contrast, both $(Ap^*)_2ZrX_2$ species (X = Cl, Me) produce high molecular weight PEs, often with multimodal molecular weight distributions. The authors attribute the broad molecular weight distributions to precipitation of the PE

**Table 5.23** Ethylene polymerization with select $(Ap)MBn_3$ complexes

| Run | Cat. | Co-cat.[a] | T (°C) | Act.[b] | $M_w$ (kg/mol) | $M_w/M_n$ |
|---|---|---|---|---|---|---|
| 1 | $(Ap^*)ZrBn_3$ | Borane | 50 | 20 | n.r.[c] | n.r.[c] |
| 2 | $(Ap^*)ZrBn_3$ | Borane | 80 | 120 | 1,130 | 1.9 |
| 3 | $(Ap^*)ZrBn_3$ | Borate | 50 | 920 | 72.9 | 21.1 |
| 4 | $(Ap^*)ZrBn_3$ | Borate | 80 | 1,120 | 71.8 | 21.6 |
| 5 | $(Ap^*)HfBn_3$ | Borate | 80 | 533 | 212 | 5.5 |
| 6 | $(Ap')ZrBn_3$ | Borate | 50 | 640 | 328 | 62.3 |
| 7 | $(Ap^-)ZrBn_3$ | Borate | 50 | 480 | 45.2 | 14.2 |

*General conditions* 260 mL toluene, 5 bar ethylene, $t = 15$ min, 1.1 equivalent cocatalyst, 50 μmol TIBAO scavenger

[a] Co-catalysts: Borane = $B(C_6F_5)_3$, Borate = $[R_2NMeH][B(C_6F_5)_4]$, where R = $C_{16}H_{33}$–$C_{18}H_{37}$

[b] Activity reported in units of $kg_{PE}$ $(mol_{cat}$ h bar$)^{-1}$

[c] n.r. = not reported

**Table 5.24** Ethylene polymerization with select $(Ap)_2ZrX_2$ complexes

| Run | Cat. | Cocat. | Act.[a] | $M_w$ (kg/mol) | $M_w/M_n$ |
|---|---|---|---|---|---|
| 1 | $(Ap')_2ZrCl_2$ | MAO[b] | 320 | 675 | 14.6 |
| 2 | $(Ap^*)_2ZrCl_2$ | MAO[b] | 2,760 | 536 | 2.0 |
| 3 | $(Ap')_2ZrMe_2$ | Borate[c,d] | 4,440 | 9.67 | 1.9 |
| 4 | $(Ap^*)_2ZrMe_2$ | Borate[c,d] | 3,160 | 1,063 | 394 |

*General conditions* 2 μmol Zr, 260 mL toluene, 5 bar ethylene, $T = 80$ °C, $t = 15$ min, 1.1 equivalent cocatalyst

[a] Activity units $kg_{PE}$ $(mol_{Zr}$ h bar$)^{-1}$

[b] Al/Zr = 500

[c] Borate = $[R_2NMeH][B(C_6F_5)_4]$, where R = $C_{16}H_{33}$–$C_{18}H_{37}$, B/Zr = 1.1, mixed prior to injection

[d] 50 equivalent TIBAO scavenger added

during chain growth, which generates a heterogeneous diffusion-controlled polymerization environment.

The *bis*-ligated (Ap) complexes are reported to be almost inactive for propylene polymerization, likely due to the sterically-hindered nature of the active site which makes them highly ethylene selective in mixtures of ethylene and propylene. Even at relatively high partial pressure of propylene, the catalysts produce polymers containing less than 1 mol% of propylene. Finally, the $(Ap^*)_2ZrMe_2$ species shows characteristics of living polymerization at 50 °C when polymerizations are conducted in the absence of additional chain transfer agents.

## 5.9 Conclusions

Despite its long history, the polyolefin industry keeps growing steadily and remains technologically driven because of new discoveries of catalysts, processes, and applications. In this respect, one of the major challenges of modern organometallic chemistry deals with the development of highly efficient, selective and stable oligomerization/polymerization systems. Imino- and amino-pyridinate ligands, in combination with late and early-transition metals, respectively, have provided excellent and to some extent unique results in the field of olefin polymerization catalysis, and constitute some of the most active systems known in the market to date. This chapter is intended to provide the readership with a comprehensive review of the most important developments in olefin catalysis based on imino- and amido-pyridinate *d*-block metal complexes in recent years. To this purpose, the authors' effort was to bring together the academic and industrial point-of-view on a highly fascinating and attracting research topic. Reading through this chapter, it seems that the number of possible ways through which a metal-alkyl fragment can be engaged in consecutive C–C bond formation for olefin upgrading to oligomers and polymers is only limited by the chemist's imagination. This leads us to believe that more and more efficient and selective transformations are still to come!

## References

1. Alt HG, Köppl A (2000) Chem Rev 100:1205
2. Coates GW (2000) Chem Rev 100:1223
3. Ittel SD, Johnson LK, Brookhart M (2000) Chem Rev 100:1169
4. Chen EY, Marks TJ (2000) Chem Rev 100:1391
5. Polyolefins planning service: executive report global commercial analysis (2010) Nexant, Inc, London
6. Bianchini C, Giambastiani G, Guerrero Rios I, Mantovani G, Meli A, Segarra AM (2006) Coord Chem Rev 250:1391
7. Bianchini C, Giambastiani G, Luconi L, Meli A (2010) Coord Chem Rev 254:431

8. Gibson VC, O'Reilly RK, Wass DF, White AJP, Williams DJ (2003) Dalton Trans 2824
9. Chen R, Mapolie SF (2003) J Mol Catal A Chem 193:33
10. Gibson VC, Halliwell CM, Long NJ, Oxford PJ, Smith AM, White AJP, Williams DJ (2003) Dalton Trans 918
11. Cloete J, Mapolie SF (2006) J Mol Catal A Chem 243:221
12. Chen R, Bacsa J, Mapolie SF (2003) Polyhedron 22:2855
13. Haddleton DM, Kukulj D, Radigue AP (1999) Chem Commun 99
14. Köppl A, Alt HG (2000) J Mol Catal A Chem 154:45
15. Britovsek GJP, Baugh SPD, Hoarau O, Gibson VC, Wass D, White AJP, Williams DJ (2003) Inorg Chim Acta 345:279
16. Benito JM, de Jesús E, de la Mata JF, Flores JC, Gómez R, Gómez-Sal P (2006) Organometallics 25:3876
17. Johnson L, Feldman J, Kreutzer KA, McLain SJ, Bennett AMA, Coughlin EB, Donald DS, Nelson JLT, Parthasarathy A, Shen X, Tam W, Wang Y (1998) US Patent Publication 5,714,556
18. Nienkemper K, Kotov VV, Kehr G, Erker G, Fröhlich R (2006) Eur J Inorg Chem 366–379
19. Laine TV, Klinga M, Leskelä M (1999) Eur J Inorg Chem 6:959–964
20. Bluhm ME, Folli C, Döring M (2004) J Mol Catal A Chem 212:13
21. Sun W-H, Tang X, Gao T, Wu B, Zhang W, Ma H (2004) Organometallics 23:5037
22. Zhang W, Sun W-H, Wu B, Zhang S, Ma H, Li Y, Chen J, Hao P (2006) J Organomet Chem 691:4759
23. Champouret YDM, Fawcett J, Nodes WJ, Sing K, Solan GA (2006) Inorg Chem 45:9890
24. Barbaro P, Bianchini C, Giambastiani G, Guerrero Rios I, Meli A, Oberhauser W, Segarra AM, Sorace L, Toti A (2007) Organometallics 26:4639
25. Bianchini C, Giambastiani G, Guerrero Rios I, Meli A, Oberhauser W, Sorace L, Toti A (2007) Organometallics 26:5066
26. Irrgang T, Keller S, Maisel H, Kretschmer W, Kempe R (2007) Eur J Inorg Chem 4221
27. Bianchini C, Gatteschi D, Giambastiani G, Guerrero Rios I, Ienco A, Laschi F, Mealli C, Meli A, Sorace L, Toti A, Vizza F (2007) Organometallics 26:726
28. Bianchini C, Giambastiani G, Mantovani G, Meli A, Mimeau D (2004) J Organomet Chem 689:1356
29. Bianchini C, Mantovani G, Meli A, Migliacci F (2003) Organometallics 22:2545
30. Bianchini C, Sommazzi A, Mantovani G, Santi R, Masi F (2005) US Patent Publication 6,916,931 B2
31. Fernandes S, Bellabarba RM, Ribeiro AFG, Gomes PT, Ascenso JR, Mano JF, Dias AR, Marques MM (2002) Polym Int 51:1301
32. Tang X, Sun W-H, Gao T, Hou J, Chen J, Chen W (2005) J Organomet Chem 690:1570
33. Espinet P, Echavarren AM (2004) Angew Chem Int Ed 43:4704
34. Tsuji J (1996) Palladium reagents and catalysts: innovation in organic synthesis. Wiley, New York
35. Miyaura N, Suzuki A (1995) Chem Rev 95:2457
36. Bianchini C, Giambastiani G, Guerrero Rios I, Meli A, Segarra AM, Toti A, Vizza F (2007) J Mol Catal A Chem 277:40
37. Toti A, Giambastiani G, Bianchini C, Meli A, Luconi L (2008) Adv Synth Catal 350:1855
38. Allgeier AM, Mirkin CA (1998) Angew Chem Int Ed 37:894
39. Lorkovic IM, Duff JRR, Wrighton (1995) J Am Chem Soc 117:3617
40. Chen R, Bacsa J, Mapolie SF (2002) Inorg Chem Commun 5:724
41. Smith G, Chen R, Mapolie SF (2003) J Organomet Chem 673:111
42. Lyubov DM, Fukin GK, Cherkasov AV, Shavyrin AS, Trifonov AA, Luconi L, Bianchini C, Meli A, Giambastiani G (2009) Organometallics 28:1227
43. van Koten G, Jastrzebski JTBH, Vrieze K (1983) J Organomet Chem 250:49
44. Gibson VC, Redshaw C, White AJP, Williams DJ (1998) J Organomet Chem 550:453
45. Nienkemper K, Kehr G, Kehr S, Fröhlich R, Erker G (2008) J Organomet Chem 693:1572

46. Bianchini C, Frediani M, Giambastiani G, Kaminsky W, Meli A, Passaglia E (2005) Macromol Rapid Commun 26:1218
47. Bianchini C, Giambastiani G, Meli A, Guerrero Rios I, Toti A, Passaglia E, Frediani M (2008) Top Catal 48:107
48. Gibson VC, Wass DF (1999) Angew Chem Int Ed 38:419
49. Gómez J, Garcia-Herbosa G, Cuevas JV, Arnáiz A, Carbayo A, Muñoz A, Falvello L, Fanwick PE (2006) Inorg Chem 45:2483
50. Kuwabara J, Takeuchi D, Osakada K (2006) Chem Commun 3815
51. Meneghetti SP, Lutz PJ, Kress J (1999) Organometallics 18:2734
52. Musikabhumma K, Spaniol TP, Okuda J (2003) J Polym Sci Part A Polym Chem 41:528
53. Small BL, Brookhart M (1999) Macromolecules 32:2120
54. Kern RJ (1962) J Inorg Nucl Chem 24:1105
55. Vallarino LM, Hill WE, Quagliano JV (1965) Inorg Chem 4:1598
56. Cotton FA, Luck RL, Son K-A (1991) Inorg Chim Acta 179:11
57. Haddleton DM, Waterson C, Derrick PJ, Jasieczek CB, Shooter AJ (1997) Chem Commun 683
58. Laine TV, Lappalainen K, Liimatta J, Aitola E, Löfgren B, Leskelä M (1999) Macromol Rapid Commun 20:487
59. Laine TV, Piironen U, Lappalainen K, Klinga M, Aitola E, Leskelä M (2000) J Organomet Chem 606:112
60. Cotton FA, Wilkinson G, Murillo CA, Bochmann M (1999) Advanced inorganic chemistry, 6th edn. Wiley, New York
61. Jiang T, Ning Y, Hu W, Wang L, Huang Z, Liu X (2006) Chin Sci Bull 51:2197
62. Su B-Y, Zhao J-S (2006) Polyhedron 25:3289
63. Morassi R, Sacconi L (1971) J Chem Soc A 492
64. Bencini A, Gatteschi D (1982) Transition metal chemistry. M Dekker, New York
65. Pilbrow JR (1990) Transition ion electron paramagnetic resonance. Clarendon Press, Oxford
66. Holm RH, Phillips WD, Averill BA, Mayerle JJ, Herskovitz JJ (1974) J Am Chem Soc 96:2109
67. Jesson JP (1973) NMR of paramagnetic molecules: principles and applications. Academic Press, New York
68. McConnell HM (1972) Proc Natl Acad Sci USA 69:335
69. Mantovani G (2000) ICCOM, PhD dissertation, Florence, Italy
70. Su B-Y, Zhao J-S, Gao Q-C (2007) Chin J Chem 25:121
71. Bianchini C, Giambastiani G, Meli A, Toti A (2007) Organometallics 26:1303
72. Frediani M, Bianchini C, Kaminsky W (2006) Kinet Catal 47:207
73. Frediani M, Piel C, Kaminsky W, Bianchini C, Rosi L (2006) Macromol Symp 236:124
74. Bredeau S, Bonduel D, Alexandre M, Boggioni L, Tritto I, Giambastiani G, Toti A, Meli A, Bianchini C, Dubois P (2008) Polymer Preprints 49:289
75. Toti A, Giambastiani G, Bianchini C, Meli A, Bredeau S, Dubois P, Bonduel D, Claes M (2008) Chem Mater 20:3092
76. Cámpora J, del Mar Conejo M, Mereiter K, Palma P, Pérez C, Reyes ML, Ruiz C (2003) J Organomet Chem 683:220
77. Rülke RE, Delis JGP, Groot AM, Elsevier CJ, van Leeuwen PWNM, Vrieze K, Goubitz K, Schenk H (1996) J Organomet Chem 508:109
78. Bacchi A, Carcelli M, Pelizzi C, Pelizzi G, Pelagatti P, Ugolotti S (2002) Eur J Inorg Chem 2179
79. Bryant PL, Harwell CR, Mrse AA, Emery EF, Gan Z, Caldwell T, Reyes AP, Kuhns P, Hoyt DW, Simeral LS, Hall RW, Butler LG (2001) J Am Chem Soc 123:12009
80. Reddy SS, Sivaran S (1995) Prog Polym Sci 20:309
81. Sinn H, Kaminsky W, Hoker (1995) Alumoxanes; Macromolecular Symposia 97. Hutig & Wepf, Heidelberg, Germany
82. Sinn H (1995) Macromol Symp 97:27
83. Mason MR, Smith JM, Bott SG, Barron AR (1993) J Am Chem Soc 115:4971

84. Hackmann M, Rieger B (1997) CATTECH 1:79
85. Bianchini C, Mantovani G, Meli A, Migliacci F, Zanobini F, Laschi F, Sommazzi A (2003) Eur J Inorg Chem 1620
86. Britovsek GJP, Mastroianni S, Solan GA, Baugh SPD, Redshaw C, Gibson VC, White AJP, Williams DJ, Elsegood MRJ (2000) Chem Eur J 6:2221
87. Chen YF, Chen RF, Qian CT, Dong XC, Sun J (2003) Organometallics 22:4312
88. Giambastiani G, Bianchini C, Luconi L (2010) Late transition metal complexes in olefin oligomerization. In: Seminars in organic synthesis. Società Chimica Italiana, Gargnano (BS), Italy, p 199
89. Britovsek GJP, Bruce M, Gibson VC, Kimberley BS, Maddox PJ, Mastroianni S, McTavish SJ, Redshaw C, Solan GA, Strömberg S, White AJP, Williams DJ (1999) J Am Chem Soc 121:8728
90. Deng L, Margl P, Ziegler T (1999) J Am Chem Soc 121:6479
91. Daugulis O, Brookhart M, White PS (2003) Organometallics 22:4699
92. Humphries MJ, Tellmann KP, Gibson VC, White AJP, Williams DJ (2005) Organometallics 24:2039
93. Gates DP, Svejda SA, Oñate E, Killian CM, Johnson LK, White PS, Brookhart M (2000) Macromolecules 33:2320
94. Svejda SA, Johnson LK, Brookhart M (1999) J Am Chem Soc 121:10634
95. Guan Z, Cotts PM, McCord EF, McLain SJ (1999) Science 283:2059
96. Laine TV, Klinga M, Maaninen A, Aitola E, Leskelä M (1999) Acta Chem Scand 53:968
97. Bianchini C, Giambastiani G, Guerrero Rios I, Meli A, Passaglia E, Gragnoli E (2004) Organometallics 23:6087
98. Johnson LK, Killian CM, Brookhart M (1995) J Am Chem Soc 117:6414
99. Sommazzi A, Milani B, Proto A, Corso G, Mestroni G, Masi F (2001) WO Patent 0110875 A1
100. Skupinska J (1991) Chem Rev 91:613
101. Goretzki R, Fink G (1999) Macromol Chem Phys 200:881
102. Turunen J, Pakkanen TT, Löfgren B (1997) J Mol Catal A: Chemical 123:35
103. Wendt RA, Fink G (2000) Macromol Chem Phys 201:1365
104. Wendt RA, Fink G (2002) Macromol Chem Phys 203:1071
105. Sun W-H, Hao P, Li G, Zhang S, Wang W, Yi J, Asma M, Tang N (2007) J Organomet Chem 692:4506
106. James DE (1985) Encyclopedia of polymer science and engineering. Wiley-Interscience, New York
107. Stevens JC (1996) Studies in surface science and catalysis. Elsevier Science, Amsterdam
108. Weckhuysen BM, Schoonheydt RA (1999) Catal Today 51:215
109. Lai SY, Wilson JR, Knight GW, Stevens JC (1997) US Patent Publication 5,665,800
110. Lai SY, Wilson JR, Knight GW, Stevens JC, Chum PWS (1993) US Patent Publication 5,272,236
111. Wang WJ, Yahn D, Zhu S, Hamielec AE (1998) Macromolecules 31:8677
112. Barnhard RW, Bazan GC (1998) J Am Chem Soc 120:1082
113. Komon ZJA, Bazan GC (2001) Macromol Rapid Commun 22:467
114. Bianchini C, Miller H, Ciardelli F (2004) Combinations of Transition Metal Catalysts for Reactor Blending. Kluwer, The Netherlands
115. Abramo GP, Li L, Marks TJ (2002) J Am Chem Soc 124:13966
116. Li H, Li L, Schwartz DJ, Metz MV, Marks TJ, Liable-Sands L, Rheingold AL (2005) J Am Chem Soc 127:14756
117. Li L, Metz MV, Li H, Chen M-C, Marks TJ, Liable-Sands L, Rheingold AL (2002) J Am Chem Soc 124:12725
118. Wang J, Li H, Guo N, Li L, Stern CL, Marks TJ (2004) Organometallics 23:5112
119. Bianchini C, Giambastiani G, Toti A (2007) ChemTracts Inorg Chem 20:107
120. Kato M, Kamigaito M, Sawamoto M, Higashimura T (1995) Macromolecules 28:1721
121. Matyjaszewski K, Wang J-S (1995) Macromolecules 28:7901

122. Perced V, Barboui B (1995) Macromolecules 28:7970
123. Perced V, Barboui B, Neumann A, Ronda JC, Zhao M (1996) Macromolecules 29:3665
124. van Koten G, Vrieze K (1982) Adv Organomet Chem 21:157
125. Haddleton DM, Jasieczek CB, Hannon MJ, Shooter AJ (1997) Macromolecules 30:2190
126. Haddleton DM (1997) WO Patent 9747661 A1
127. Perrier S, Jackson SG, Haddleton DM, Améduri B, Boutevin B (2003) Macromolecules 36:9042
128. Haddleton DM, Duncalf DJ, Kukulj D, Crossman MC, Jackson SG, Bon SAF, Clark AJ, Shooter AJ (1998) Eur J Inorg Chem 1799
129. Amass AJ, Wyres CA, Colclough E, Marcia Hohn I (2000) Polymer 41:1697
130. Geng J, Lindqvist J, Mantovani G, Haddleton DM (2008) Angew Chem Int Ed 47:4180
131. Mantovani G, Ladmiral V, Tao L, Haddleton DM (2005) Chem Commun 2089
132. Murray RE (1999) WO Patent Application 99/01460
133. Murray RE (2003) US Patent Application 20030166454
134. Annunziata L, Pappalardo D, Tedesco C, Pellecchia C (2009) Organometallics 28:688
135. Annunziata L, Pappalardo D, Tedesco C, Pellecchia C (2009) Macromolecules 42:5572
136. Domski GJ, Lobkovsky EB, Coates GW (2007) Macromolecules 40:3510
137. Boussie TR, Diamond GM, Goh C, Hall KA, LaPointe AM, Leclerc MK, Lund C, Murphy V (2002) PCT Int Appl WO 046249; PCT Int Appl WO 038628
138. Boussie TR, Diamond GM, Goh C, Hall KA, LaPointe AM, Leclerc MK, Lund C, Murphy V (2004) US Patent 6,706,829; US Patent Publication 6,713,577
139. Boussie TR, Diamond GM, Goh C, LaPointe AM, Hall KA, Leclerc MK, Lund C, Murphy V (2006) US Patent Publication 7,157,400
140. Boussie TR, Diamond GM, Goh C, LaPointe AM, Leclerc MK, Lund C, Murphy V (2004) US Patent Publication 6,750,345
141. Hagadorn JR (2009) PCT Int Appl WO 114209
142. Domski GJ, Edson JB, Keresztes I, Lobkovsky EB, Coates GW (2008) Chem Commun 6137
143. Luconi L, Lyubov DM, Bianchini C, Rossin A, Faggi C, Fukin GK, Cherkasov AV, Shavyrin AS, Trifonov AA, Giambastiani G (2010) Eur J Inorg Chem 2010:608
144. McConville DH, Ackerman LJ, Li RT, Bei X, Kuchta MC, Boussie TR, Walzer JF Jr, Diamond GM, Rix FC, Hall KA, La PAM, Longmire JM, Murphy VJ, Sun P, Verdugo D, Schofer S, Dias E (2008) US Patent 7,425,661 B2
145. Frazier KA, Boone H, Vosejpka PC, Stevens JC (2004) US Patent Publication 6,953,764
146. Hagadorn JR, Boller TM, Brown SD, Diamond GM, Hall KA, Longmire JM, Ackerman LJ, Schofer SJ, Dias ELK, Cottone A, III, Whittle CE (2009) US Patent Publication 0082573
147. Luconi L, Giambastiani G, Rossin A, Bianchini C, Lledós A (2010) Inorg Chem 49:6811
148. Wolfe JP, Buchwald SL (2004) Org Synth 10:423
149. Paul F, Patt J, Hartwig JF (1994) J Am Chem Soc 116:5969
150. Boussie TR, Diamond GM, Goh C, Hall KA, LaPointe AM, Leclerc MK, Murphy V, Shoemaker JAW, Turner H, Rosen RK, Stevens JC, Alfano F, Busico V, Cipullo R, Talarico G (2006) Angew Chem Int Ed 45:3278
151. Busico V, Cipullo R, Pellecchia R, Rongo L, Talarico G, Macchioni A, Zuccaccia C, Froese RDJ, Hustad PD (2009) Macromolecules 42:4369
152. Coalter JN, III, Van Egmond JW, Fouts LJ Jr, Painter RB, Vosejpka PC (2004) US Patent 7,115,689
153. Coalter JN, III, Van Egmond JW, Fouts LJ Jr, Painter RB, Vosejpka PC (2006) US Patent 7,598,328
154. Kuhlman RL, Whiteker GT (2010) US Patent Application 0227990
155. Domski GJ, Edson JB, Keresztes I, Lobkovsky EB, Coates GW (2008) Chem Commun 46:6137
156. Boussie TR, Diamond GM, Goh C, Hall KA, LaPointe AM, Leclerc M, Lund C, Murphy V, Shoemaker JAW, Tracht U, Turner H, Zhang J, Uno T, Rosen RK, Stevens JC (2003) J Am Chem Soc 125:4306

157. For details see: http://www.dow.com/versify
158. Zhou Z, Stevens JC, Klosin J, Kümmerle R, Qiu X, Redwine D, Cong R, Taha A, Mason J, Winniford B, Chauvel P, Montañez N (2009) Macromolecules 42:2291
159. Zhou Z, Kümmerle R, Stevens JC, Redwine D, He Y, Qiu X, Cong R, Klosin J, Montañez N, Roof G (2009) J Magn Reson 200:328
160. Tau L-M, Cheung YW, Diehl CF, Hazlitt LG (2004) US Patent Publication 10/429651
161. Stevens JC, Vanderlende DD (2003) WO Patent Publication 2003/040201
162. Coalter JN, III, Van Egmond JW, Painter RB, Fouts LJ Jr, Vosejpka PC (2003) WO Patent Publication 040195
163. Froese RDJ, Hustad PD, Kuhlman RL, Wenzel TT (2007) J Am Chem Soc 129:7831
164. Wenzel TT, Arriola DJ, Carnahan EM, Hustad PD, Kuhlman RL (2009) Chain shuttling catalysis and olefin block copolymers (OBCs). In: Metal catalysts in olefin polymerization. Topics in organometallic chemistry. Springer, Berlin, p 65
165. Arriola DJ, Carnahan EM, Hustad PD, Kuhlman RL, Wenzel TT (2006) Science 312:714
166. Arriola DJ, Carnahan EM, Cheung YW, Devore DD, Graf DD, Hustad PD, Kuhlman RL, Li Pi Shan C, Poon BC, Roof GR, Stevens JC, Stirn PJ, Wenzel TT (2005) US Patent Publication 090427
167. Kuhlman RL, Klosin J (2010) Macromolecules 43:7903
168. Hustad PD, Kuhlman RL, Arriola DJ, Carnahan EM, Wenzel TT (2007) Macromolecules 40:7061
169. Hustad PD, Marchand GR, Garcia-Meitin EI, Roberts PL, Weinhold JD (2009) Macromolecules 42:3788
170. Kuhlman RL, Wenzel TT (2008) Macromolecules 41:4090
171. Alfano F, Boone HW, Busico V, Cipullo R, Stevens JC (2007) Macromolecules 40:7736
172. Busico V, Boone HW, Stevens JC, Alfano F, Cipullo R (2008) US Patent Publication 137524
173. Busico V, Cipullo R (2001) Prog Polym Sci 26:443
174. Busico V, Cipullo R, Talarico G, Van Axel Castelli V (2002) Isr J Chem 42:295
175. Resconi L, Cavallo L, Fait A, Piemontesi F (2000) Chem Rev 100:1253
176. Zuccaccia C, Macchioni A, Busico V, Cipullo R, Talarico G, Alfano F, Boone HW, Frazier KA, Hustad PD, Stevens JC, Vosejpka PC, Abboud KA (2008) J Am Chem Soc 130:10354
177. Niu A, Stellbrink Jr, Allgaier Jr, Richter D, Hartmann R, Domski GJ, Coates GW, Fetters LJ (2009) Macromolecules 42:1083
178. Zuccaccia C, Busico V, Cipullo R, Talarico G, Froese RDJ, Vosejpka PC, Hustad PD, Macchioni A (2009) Organometallics 28:5445
179. Dales GC, Diamond G, Frank TG, Freitag JC, Higashihara KS, Huffman D, Troth JR (2005) US Patent 6,913,934 B2
180. Dales GC, Troth JR, Higashihara KS, Diamond G, Murphy V, Chandler WHJ, Frank TG, Freitag JC (2004) US Patent 6,759,014 B2
181. Kempe R (2010) Z Anorg Allg Chem 636:2135
182. Noor A, Kretschmer W, Kempe R (2006) Eur J Inorg Chem 2683
183. Polamo MT, Talja M, Piironen AJ (2005) Z Kristallogr NCS 220:41
184. Corriu RJP, Masse JP (1972) J Chem Soc Chem Commun 144
185. Tamao K, Sumitani K, Kumada M (1972) J Am Chem Soc 94:4374
186. Döring C, Kretschmer WP, Bauer T, Kempe R (2009) Eur J Inorg Chem 4255
187. Döring C, Kempe R (2009) Eur J Inorg Chem 412
188. Döring C, Kretschmer WP, Kempe R (2010) Eur J Inorg Chem 2853
189. Kretschmer WP, Meetsma A, Hessen B, Schmalz T, Qayyum S, Kempe R (2006) Chem Eur J 12:8969
190. Scott NM, Kempe R (2005) Eur J Inorg Chem 1319
191. Skvortsov GG, Fukin GK, Trifonov AA, Noor A, Döring C, Kempe R (2007) Organometallics 26:5770
192. Lyubov DM, Döring C, Fukin GK, Cherkasov AV, Shavyrin AS, Kempe R, Trifonov AA (2008) Organometallics 27:2905

193. Kretschmer WP, Hessen B, Noor A, Scott NM, Kempe R (2007) J Organomet Chem 692:4569
194. Qayyum S, Skvortsov GG, Fukin GK, Trifonov AA, Kretschmer WP, Döring C, Kempe R (2010) Eur J Inorg Chem 248
195. Noor A, Kretschmer WP, Glatz G, Meetsma A, Kempe R (2008) Eur J Inorg Chem 5088
196. Horton AD, de With J (1996) Chem Commun 1375
197. Horton AD, de With J, van der Linden AJ, van de Weg H (1996) Organometallics 15:2672
198. Pellecchia C, Grassi A, Immirzi A (1993) J Am Chem Soc 115:1160
199. Pellecchia C, Grassi A, Zambelli A (1993) J Mol Catal 82:57
200. Pellecchia C, Immirzi A, Grassi A, Zambelli A (1993) Organometallics 12:4473
201. Pellecchia C, Immirzi A, Pappalardo D, Peluso A (1994) Organometallics 13:3773
202. Kempe R (2007) Chem Eur J 13:2764

# Subject Index

**W**



**Y**



**Z**